ANL/EVS/TM/07-1
DOE/HS-0005
NUREG/CR-6937

User's Manual for RESRAD-OFFSITE Version 2

Environmental Science Division

ANL/EVS/TM/07-1
DOE/HS-0005
NUREG/CR-6937

User's Manual for RESRAD-OFFSITE Version 2

by
C. Yu, E. Gnanapragasam, B.M. Biwer, S. Kamboj, J.-J. Cheng, T. Klett, D. LePoire,
A.J. Zielen, S.Y. Chen, W.A. Williams,* A. Wallo,* S. Domotor,* T. Mo,* and A. Schwartzman*
Environmental Science Division, Argonne National Laboratory

work sponsored by the U.S. Department of Energy,
Offices of Environmental Management and Health, Safety and Security,
and the U.S. Nuclear Regulatory Commission

June 2007

*Williams, Wallo, and Domotor are affiliated with the U.S. Department of Energy and
Mo and Schwartzman with the U.S. Nuclear Regulatory Commission.

CONTENTS

CONTENTS (Cont.)

CONTENTS (Cont.)

CONTENTS (Cont.)

CONTENTS (Cont.)

CONTENTS (Cont.)

FIGURES

TABLES

NOTATION

The following is a list of the acronyms, initialisms, and abbreviations (including units of measure) used in this document.

ACRONYMS, INITIALISMS, AND ABBREVIATIONS

BIOMOVS	Biosphere Model Validation Study
ICRP	International Commission on Radiological Protection
NRC	U.S. Nuclear Regulatory Commission
QA	quality assurance
QC	quality control

UNITS OF MEASURE

cm	centimeter(s)
d	day(s)
g	gram(s)
h	hour(s)
K	degree(s) Kelvin
kg	kilogram(s)
m	meter(s)
m^2	square meter(s)
m^3	cubic meter(s)
mm	millimeter(s)
pCi	picocurie(s)
s	second(s)
s^2	square second(s)
yr	year(s)

USER'S MANUAL FOR RESRAD-OFFSITE VERSION 2

by

C. Yu, E. Gnanapragasam, B.M. Biwer, S. Kamboj, J.-J. Cheng, T. Klett,
D. LePoire, A.J. Zielen, S.Y. Chen, W.A. Williams, A. Wallo,
S. Domotor, T. Mo, and A. Schwartzman

ABSTRACT

The RESRAD-OFFSITE code is an extension of the RESRAD (onsite) code, which has been widely used for calculating doses and risks from exposure to radioactively contaminated soils. The development of RESRAD-OFFSITE started more than 10 years ago, but new models and methodologies have been developed, tested, and incorporated since then. Some of the new models have been benchmarked against other independently developed (international) models. The databases used have also expanded to include all the radionuclides (more than 830) contained in the International Commission on Radiological Protection (ICRP) 38 database. This manual provides detailed information on the design and application of the RESRAD-OFFSITE code. It describes in detail the new models used in the code, such as the three-dimensional dispersion groundwater flow and radionuclide transport model, the Gaussian plume model for atmospheric dispersion, and the deposition model used to estimate the accumulation of radionuclides in offsite locations and in foods. Potential exposure pathways and exposure scenarios that can be modeled by the RESRAD-OFFSITE code are also discussed. A user's guide is included in Appendix A of this manual. The default parameter values and parameter distributions are presented in Appendix B, along with a discussion on the statistical distributions for probabilistic analysis. A detailed discussion on how to reduce run time, especially when conducting probabilistic (uncertainty) analysis, is presented in Appendix C of this manual.

1 INTRODUCTION

The RESRAD-OFFSITE code is an extension of the original RESRAD code, which was designed for evaluation of radiological doses to an onsite receptor from exposure to RESidual RADioactive materials in soil (Yu et al. 1993, 2001). To prevent potential confusion of these two code names, the "original" RESRAD code is denoted as RESRAD (onsite) where appropriate, although RESRAD-OFFSITE can model both onsite and offsite receptors as discussed later in this report.

The methodology and formulations, exposures and scenarios, and parameter values and distributions used in the RESRAD-OFFSITE code are discussed in detail in this report. Additional modules included in RESRAD-OFFSITE that were not part of RESRAD (onsite) permit modeling of both the transport of radionuclides to locations that are outside the footprint of the primary contamination and their accumulation at those offsite locations. The general information contained in Chapters 1, 2, and the first section of Chapter 3 of the RESRAD (onsite) manual (Yu et al. 2001) apply to RESRAD-OFFSITE as well. However, many of the formulations used in RESRAD-OFFSITE differ from those in RESRAD (onsite), particularly those relating to fate and transport. Although the underlying principles used to calculate exposure are the same, the methodology is different in that in RESRAD-OFFSITE, the concentrations of radionuclides in various media (soil, water, air, plants, and animals) are directly calculated and used in dose and risk calculations; while the RESRAD (onsite) uses the environmental transport factors method (Yu et al. 2001).

Brief descriptions of the RESRAD (onsite) and RESRAD-OFFSITE codes are presented in Sections 1.1 and 1.2. Section 1.3 describes the same or similar models used in both the RESRAD (onsite) and RESRAD-OFFSITE codes. A more detailed comparison of RESRAD (onsite) and RESRAD-OFFSITE is documented in the *Benchmarking of RESRAD-OFFSITE* report (Yu et al. 2006).

1.1 RESRAD (ONSITE)

The RESRAD (onsite) computer code evaluates the radiological dose and excess cancer risk to an individual who is exposed while residing and/or working in an area where the soil is contaminated with radionuclides (Yu et al. 2001). RESRAD was developed by the Environmental Assessment Division of Argonne National Laboratory (Argonne) in the 1980s and has been widely used to perform assessments of contaminated sites since its release in 1989. Since then, the RESRAD (onsite) code has undergone continuous improvement in response to feedback from users and sponsors. The RESRAD team has participated in many national and international model intercomparison studies in which both hypothetical and actual contaminated site-based scenarios were analyzed using RESRAD (onsite). The evolution of the RESRAD-OFFSITE code from RESRAD (onsite) began in the 1990s during the Biosphere Modeling Validation Study II (BIOMOVS II), in which models were compared (Gnanapragasam and Yu 1997).

1.2 RESRAD-OFFSITE

The RESRAD-OFFSITE code was first formed by the addition of an offsite soil accumulation submodel (BIOMOVS II 1995) to the basic RESRAD (onsite) code and then by the inclusion of an advective-dispersive groundwater transport submodel (BIOMOVS II 1996). The ability to accept a time series for the release from the contaminated soil was also added during this study. The advective-dispersive groundwater transport submodel was improved to better predict the transport of progeny produced in transit during participation in the multimedia model comparison study (Gnanapragasam et al. 2000). Since then, an atmospheric transport submodel and a surface water body accumulation submodel have been added. Many of the submodels in RESRAD (onsite) were also modified during the addition of these new submodels to RESRAD-OFFSITE. The computational algorithm of the RESRAD-OFFSITE code also changed from that of RESRAD (onsite). RESRAD (onsite) numerically evaluates the analytical expressions for concentration, dose, and risk at any desired time since the site survey. RESRAD-OFFSITE uses numerical methods to compute the concentration, dose, and risk progressively over time.

The RESRAD-OFFSITE computer code evaluates the radiological dose and excess cancer risk to an individual who is exposed while located within or outside the area of initial (primary) contamination. The primary contamination, which is the source of all the releases modeled by the code, is assumed to be a layer of soil. The releases of contaminants from the primary contamination to the atmosphere, to surface runoff, and to groundwater are considered. The code models the movement of the contaminants from the primary contamination to agricultural areas, pastures, a dwelling area, a well, and a surface water body. It also models the accumulation of the contaminants at those locations where appropriate. Any contribution of the contaminants from the water sources to the land-based locations is also modeled. As shown in Figure 1.1, the water sources and the land-based locations can be outside the boundary of the primary contamination. These locations are referred to as offsite locations in RESRAD-OFFSITE.

Nine exposure pathways are considered in RESRAD-OFFSITE: direct exposure from contamination in soil, inhalation of particulates, inhalation of radon, ingestion of plant food (i.e., vegetables, grain, and fruits), ingestion of meat, ingestion of milk, ingestion of aquatic foods, ingestion of water, and ingestion (incidental) of soil.

1.3 SAME OR SIMILAR SUBMODELS IN RESRAD (ONSITE) AND RESRAD-OFFSITE

This section identifies the submodels in RESRAD-OFFSITE that are essentially the same as the corresponding ones in RESRAD (onsite). The differences, if any, in those submodels are also described.

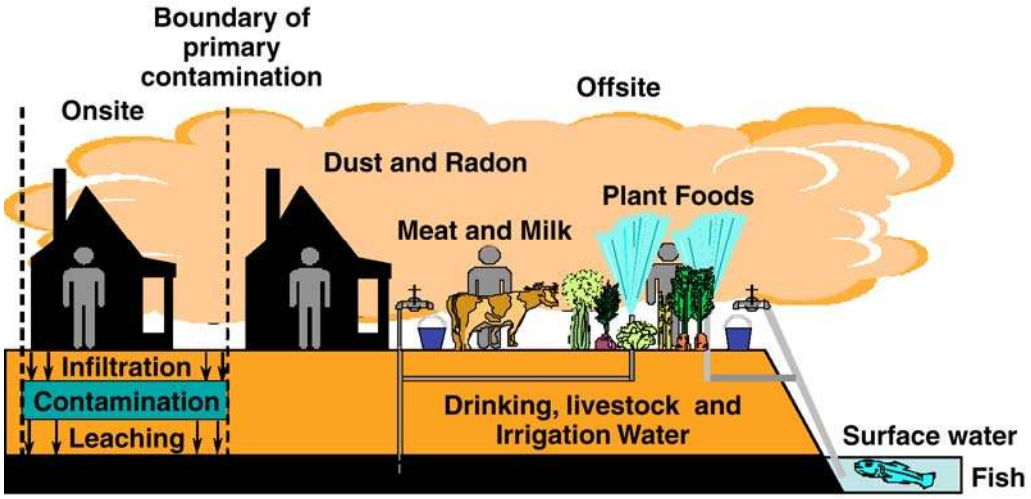

FIGURE 1.1 Locations of Primary and Secondary Contamination in RESRAD-OFFSITE

1.3.1 Groundwater Release Submodel

The release to groundwater is the only release that RESRAD (onsite) explicitly considers. This is a first-order release model in which the flux of radionuclides released to the infiltrating water at any time is in direct proportion to the radionuclide inventory in the contaminated soil at that time. The same model was retained in RESRAD-OFFSITE, although the radionuclide inventory at any time is adjusted differently because of the modifications to the surface soil mixing submodel.

1.3.2 Surface Soil Mixing Submodel

The surface soil mixing submodel in RESRAD (onsite) ignores the contaminants that were removed by erosion of the initially uncontaminated mixing zone. Although this model is appropriate for RESRAD (onsite) because that code does not address the surface soil release to offsite locations, it is not suitable for RESRAD-OFFSITE, which models the accumulation of the eroded material in a surface water body and offsite soils. The new model in RESRAD-OFFSITE maintains a mass balance of contaminants.

1.3.3 Dust Release Model

Although RESRAD (onsite) does not explicitly model a release to the atmosphere, it does model the effects of a dust release (inhalation, foliar deposition) by using the concept of a mass loading factor. In RESRAD-OFFSITE, this concept has been extended to provide a release to the atmospheric transport model.

1.3.4 Exposure Models

All the exposure models in RESRAD (onsite) — direct external radiation; inhalation of dust and radon; and ingestion of vegetables, meat, milk, aquatic food, and soil — were retained in RESRAD-OFFSITE, with minor changes. In RESRAD-OFFSITE, these exposure models are applied at more locations and more contamination pathways — on primary contamination and agricultural and farmed areas because of contamination by irrigation and deposition of dust. The exposure models were changed to accommodate the numerical nature of the RESRAD-OFFSITE code and also to facilitate their application to the offsite locations.

1.3.5 Advective Groundwater Transport Model

The groundwater transport model in RESRAD (onsite) considers the effects of the different transport rates of the progeny nuclides that are produced in transit. The option of using this advective transport model was retained in RESRAD-OFFSITE, in addition to the option of considering the effects of dispersive transport. Although the basic concepts are the same for both codes, each code implements them differently. The concentrations of nuclides in well and surface water at any time are expressed analytically in RESRAD (onsite), although these expressions are evaluated numerically. In RESRAD-OFFSITE, the nuclide transport is modeled zone by zone (each unsaturated zone and then the saturated zone) by numerically calculating the flux across each zone progressively over time.

1.4 INTEGRATED MODULES IN RESRAD-OFFSITE

The computational modules for primary contamination (source), atmospheric transport, groundwater transport, offsite accumulation, and exposure; the input modules to process the information from the user interface and to manage the single parameter sensitivity analysis; the module to generate the text reports; and the probabilistic/uncertainty module are all integrated in the RESRAD-OFFSITE computational program.

The models and formulations used in the computational modules are described in detail in Chapters 2 through 7 of this manual. A user's guide that describes the user interface is included in Appendix A of this manual, and the parameters used in the code are discussed in detail in Appendix B. The transfer of information from the interface to the computational program occurs when the user issues the "run" or "Run RESRAD-OFFSITE" command in the interface. The text reports produced by the program are described in the user's guide

(Appendix A). The procedures for performing probabilistic/uncertainty and sensitivity analysis are described in the user's guide (Appendix A). The run time for probabilistic analysis can be long if a large number of samples/realizations are selected. The ways to reduce run time are discussed in Appendix C.

The information presented in this manual is organized as follows:

- Primary contamination and the source term – Chapter 2,
- Groundwater transport model – Chapter 3,
- Atmospheric transport model – Chapter 4,
- Accumulation of radionuclides at offsite locations and in food – Chapter 5,
- Exposure pathways and exposure scenarios – Chapter 6,
- Time points for numerical computations – Chapter 7,
- Verification and validation of RESRAD-OFFSITE – Chapter 8,
- References cited in the report – Chapter 9,
- User's guide for the RESRAD-OFFSITE code – Appendix A,
- Parameter distributions and default values – Appendix B, and
- How to reduce run time – Appendix C.

2 PRIMARY CONTAMINATION AND THE SOURCE TERM

This chapter consists of four sections. The first (Section 2.1) describes the manner in which RESRAD-OFFSITE conceptualizes the primary contamination, specifically its physical dimensions; the concentration of radionuclides in it; and the releases to the atmosphere, to surface erosion, and to groundwater as a function of time. Section 2.2 derives the expressions that result from the conceptual model, and Section 2.3 deals with the implementation of the solution or the evaluation of these expressions in the computational code. Section 2.4 describes the method overriding the source term model used in the RESRAD-OFFSITE code.

2.1 CONCEPTUALIZATION OF THE PRIMARY CONTAMINATION

The initial contamination is assumed to be distributed uniformly throughout a soil layer. This contaminated layer is of uniform thickness and can have a clean cover of uniform thickness above it. The clean cover and the primary contamination may be eroded by surface runoff, and their thicknesses can decrease over time. Erosion occurs from a well-mixed surface layer. The thickness of the primary contamination is not affected until the thickness of the cover erodes to the thickness of this surface layer. The primary contamination is situated above the water table; it can be just above and in contact with the water table, or there can be up to five different intervening partially saturated soil layers. The assumptions about the shape of the conceptual primary contamination vary across exposure and transport models. The atmospheric and groundwater transport modules assume rectangular shapes, although the shape specified for the use by the two transport modes need not be identical. The external exposure module assumes either a circular shape or a polygonal shape for the primary contamination.

The current version of RESRAD-OFFSITE uses a rate-controlled model to compute the release to groundwater. The radionuclides are released (leached) to groundwater uniformly over the depth of the primary contamination under the rate-controlled model. Thus, the release to groundwater affects the concentration in the primary contamination, but not its physical dimensions. Equilibrium-controlled (i.e., solubility or adsorption) groundwater release models in which contaminants are removed from the top of the layer, leading to nonuniform concentration profiles in the vertical direction, are not built into this version of the code.

The release of dust to the atmosphere and the release of contaminated soil to surface runoff occur from the well-mixed surface layer at the top of the primary contamination. Thus, these releases decrease the total quantity of the radionuclides in primary contamination, but not the concentration in the primary contamination below the surface layer. The release of H-3, and C-14 by evasion can occur from over the whole depth of the contamination; it is modeled in RESRAD-OFFSITE as being uniform over the entire depth of the primary contamination and affects the concentration in the primary contamination, but not its physical dimensions.

2.2 DERIVITION OF MATHEMATICAL EXPRESSIONS FOR THE CONCEPTUAL PRIMARY CONTAMINATION MODEL

The conceptual model has to be translated into mathematical expressions before it can be used in the computational code. The idealized descriptions of the previous section are expressed in mathematical terms in this section.

2.2.1 Thickness of the Primary Contamination

The thickness of the primary contamination is computed as a function of time on the basis of the values of the initial thicknesses and erosion rates of the cover and the primary contamination as follows:

$$T_{pc}(t) = T_{pc}(0) \text{ when } t \le t_{cv}, \text{ and} \tag{2.1}$$

$$T_{pc}(t) = T_{pc}(0) - \varepsilon_{pc}(t - t_{cv}) \text{ when } t > t_{cv} \ ,$$

where

$T_{pc}(t)$ = thickness of the primary contamination at time t (m),

$T_{pc}(0)$ = initial thickness of the primary contamination (m),

t = time since the site was characterized (yr),

t_{cv} = $T_{cv}(0)/\varepsilon_{cv}$ = time to erode the cover (yr),

$T_{cv}(0)$ = initial thickness of the cover (m),

ε_{cv} = rate at which the cover is eroded (m yr^{-1}), and

ε_{pc} = rate at which the primary contamination is eroded (m yr^{-1}).

The erosion rate is computed using the Universal Soil Loss Equation. Section 12.10 of the *Handbook of Hydrology* (Shen and Julien 1993) has figures and tables for the first five factors in the following expression for erosion rate,

$$\varepsilon = 224 \times R \times K \times LS \times C \times P / (\rho \times 10^6) \tag{2.2}$$

where

ε = erosion rate (m yr^{-1}),

R = annual rainfall erosion index, the rainfall erosivity factor, or the rainfall and runoff factor (yr^{-1}),

K = soil erodibility factor (tons/acre),

LS = slope length-steepness factor (dimensionless),

C = cropping-management factor or the cover and management factor (dimensionless),

P = conservation practice factor or the support practice factor (dimensionless),

224 = to convert tons per acre to gram per square meter (g m^{-2} $[tons/acre]^{-1}$),

ρ = dry bulk density of the soil (g $[cm]^{-3}$), and

10^6 = to convert per cubic centimeter to per cubic meter ($[cm]^3$ m^{-3}).

2.2.2 Concentration of Radionuclides in the Primary Contamination

Radiological transformations and leaching diminish the concentration of radionuclides in soil in the primary contamination over time. The concentration of progeny nuclides can increase over time if the transformation of the parent nuclide produces more progeny nuclides than are lost by leaching and by transformation of the progeny. Because both rate-controlled leaching and radiological transformations occur uniformly over the entire primary contamination, the activity concentration of the nuclide remains uniform over the primary contamination. Under these conditions, the activity concentrations of the initially present radionuclide and its progeny are obtained by solving the series of equations,

$$\frac{dA_1}{dt} = -(\lambda_1 + \mu_1)A_1, \text{ and} \qquad (2.3)$$

$$\frac{dA_k}{dt} = \lambda_k A_{k-1} - (\lambda_k + \mu_k)A_k \text{ for } 2 \le k \le n,$$

where

$A_k(t)$ = activity concentration of the k^{th} radionuclide of the transformation chain (pCi g^{-1}),

t = time since the site was characterized (yr),

λ_k = radiological transformation constant of the k^{th} radionuclide (yr^{-1}), and

μ_k = leach rate constant[1] of the k^{th} radionuclide (yr^{-1}).

The solutions obtained by multiplying the equation by $e^{(\lambda_k+\mu_k)t}$ and evaluating the integral $\int_0^t e^{(\lambda_k+\mu_k)t} A_{k-1}(t)dt$ are of the form,

$$A_k(t) = \sum_{i=1}^{k} a_{k,i} \exp(-\lambda_i t - \mu_i t), \tag{2.4}$$

where

$a_{k,i}$ = set of coefficients defined by $a_{1,1} = A_1(0)$,

$a_{k,i} = \dfrac{\lambda_k a_{k-1,i}}{\lambda_k + \mu_k - \lambda_i - \mu_i}$ for all $1 \le i < k$, and

$a_{k,k} = -\sum_{i=1}^{k-1} a_{k,i}$.

For H-3 and C-14, the activity concentration is given by the equation,

$$A(t) = A(0) \exp(-\lambda t - \mu t - \varepsilon v(t)t), \tag{2.5}$$

where

$\varepsilon v(t)$ = evasion rate at time t (yr^{-1}) (See Appendix L of the User's Manual for RESRAD Version 6 [Yu et al. 2001] for the time-dependent evasion rate and for a discussion of the H-3 and C-14 models).

2.2.3 Surface Soil Mixing Model

The releases to the atmosphere and to surface runoff occur from the surface soil layer. The concentration of radionuclides in surface soil differs from the concentration in the primary contamination because of mixing with any uncontaminated cover or with soil below the primary

---

1 If the user does not input a leach rate, RESRAD-OFFSITE will estimate a leach rate by equating the initial release rate to the equilibrium desorption release rate, computed using the user-specified distribution coefficient of the radionuclide in the region of primary contamination.

contamination. Because the contaminant concentrations are expressed in terms of mass of soil (and not in terms of the volume of soil), it is necessary to account for any differences in density among the different layers of soil.

2.2.3.1 Density of Soil in the Mixing Zone

The density of the mixing zone is computed by assuming that mixing occurs continuously (over time) over the specified mixing depth. If the thickness of the cover exceeds the depth of mixing, the mixing zone will be uncontaminated, and the density is not computed for this condition. The cover can erode with time, and the mixing zone will then penetrate the primary contamination. The density of the mixing zone for this condition is computed as follows:

When $T_{cv}(t) < d_{mix} \le T_{cv}(t) + T_{pc}(t)$, the density is obtained by solving the equation $d_{mix}\dfrac{d\rho_{mix}}{dt} = \varepsilon(\rho_{pc} - \rho_{mix})$ with the appropriate initial condition; the term on the left is the change in mass within the mixing zone, the terms on the right, in order, are the mass entering the mixing zone from the primary contamination and the mass leaving the mixing zone due to erosion.

The initial conditions are

$$\rho_{mix}(0) = \rho_{cv} \text{ if } T_{cv}(0) \ge d_{mix}, \text{ and} \tag{2.6}$$

$$\rho_{mix}(0) = \rho_{pc} + \frac{T_{cv}(0)}{d_{mix}}\left(\rho_{cv} - \rho_{pc}\right) \text{ if } T_{cv}(0) < d_{mix}.$$

The solution is easier to understand and is more compact when expressed as a function of the depth of penetration of mixing zone into the primary contamination since initial mixing, rather than as a function of time. The expression for the density of the mixing zone is

$$\rho_{mix}(d_{pc}) = \rho_{pc} + \left(\rho_{mix}(0) - \rho_{pc}\right)\exp\left(-d_{pc}/d_{mix}\right), \tag{2.7}$$

where

$T_{cv}(t)$ = thickness of the cover after time t (m),

d_{mix} = depth of the mixing zone (m),

$\rho_{mix}(d_{pc})$ = density of the mixing zone (g [cm]$^{-3}$),

ρ_{pc} = density of the primary contamination (g [cm]$^{-3}$),

ρ_{cv} = density of the clean cover (g [cm]$^{-3}$), and

d_{pc} = depth of penetration of the mixing zone into the primary contamination since initial mixing (m).

Eventually the cover and primary contamination will be eroded so that their combined thickness will be less than the depth of the mixing zone. Then the soil underlying the primary contamination will enter the mixing zone. Because it is too cumbersome to track the layers (first any unsaturated zones and then the saturated zone) that can enter the mixing zone over time, density changes are not modeled after the mixing zone penetrates the bottom of the primary contamination. However, if the initial thicknesses of the clean cover and the primary contamination are less than the post-release mixing depth, the code does compute the density at initial mixing, including consideration of the densities of the underlying layers that enter the mixing zone at time zero.

2.2.3.2 Volume Fraction of Soil from the Primary Contamination in the Mixing Zone

The quantity of radionuclides in the mixing zone is directly proportional to the volume of soil in the mixing zone that originated from the primary contamination. The mixing zone is uncontaminated as long as its depth is less than the thickness of the clean cover. The volume fraction of soil from the primary contamination in the mixing zone is evaluated when the depth of the mixing zone exceeds the thickness of the clean cover. It is evaluated by assuming that mixing occurs continuously (over time) over the specified mixing depth and that the volume fraction in the eroded soil is the same as the volume fraction in surface soil.

When $T_{cv}(t) < d_{mix} \le T_{cv}(t) + T_{pc}(t)$, the volume fraction of primary contamination in the mixing zone is obtained by solving the equation $d_{\min} \dfrac{df_{vm}}{dt} = \varepsilon\left(1 - f_{vm}\right)$, with the appropriate initial condition. The term on the left is the change in the volume of soil from the primary contamination in the mixing zone, and the terms on the right, in order, are the volume of soil that enters the mixing zone from the primary contamination and the volume of soil from the primary contamination that leaves the mixing zone due to erosion. The initial conditions are

$$f_{vm}(0) = 0 \text{ if } T_{cv}(0) \ge d_{mix}, \text{ and} \tag{2.8}$$

$$f_{vm}(0) = 1 - \frac{T_{cv}(0)}{d_{mix}} \text{ if } T_{cv}(0) < d_{mix}.$$

As in the case with the density in the preceding section (Section 2.2.3.1), the solution is easier to understand and is more compact when expressed as a function of the depth of penetration of the mixing zone into the primary contamination since initial mixing, rather than as a function of time. The expression for the volume fraction of primary contamination in the mixing zone is

$$f_{vm}(d_{pc}) = 1 - \left(1 - f_{vm}(0)\right)\exp\left(-d_{pc} / d_{mix}\right), \tag{2.9}$$

where

$f_{vm}(d_{pc})$ = volume fraction of primary contamination in the mixing zone.

As the cover erodes, the mixing layer penetrates deeper into the primary contamination, and the volume fraction increases asymptotically towards unity as long as the bottom of the mixing zone stays within the primary contamination.

When the bottom of the mixing zone moves out of the primary contamination and into the underlying layers, the volume fraction will decrease. The volume fraction is computed under the assumption that the underlying soil is uncontaminated.[2]

When $d_{mix} > T_{cv}(t) + T_{pc}(t)$, the volume fraction of contamination in the mixing layer is obtained by solving the equation $d_{mix}\dfrac{df_{vm}}{dt} = -\varepsilon f_{vm}$ with the appropriate initial condition. The initial conditions are

$$f_{vm}^{p} = 1 - \exp\left(-T_{pc}(0) / d_{mix}\right) \text{ if } T_{cv}(0) \geq d_{mix},$$

$$f_{vm}^{p} = 1 - \frac{T_{cv}(0)}{d_{mix}}\exp\left(-\frac{T_{cv}(0) + T_{pc}(0) - d_{mix}}{d_{mix}}\right) \text{ if } T_{cv}(0) < d_{mix} < T_{cv}(0) + T_{pc}(0), \text{ and}$$

$$f_{vm}^{p} = \frac{T_{pc}(0)}{d_{mix}} \text{ if } d_{mix} \geq T_{cv}(0) + T_{pc}(0). \tag{2.10}$$

The expression for the volume fraction of primary contamination in the mixing zone, now in terms of the depth of penetration below the primary contamination for clarity and simplicity, is

$$f_{vm}(d_{upc}) = f_{vm}^{p}\exp\left(-d_{upc} / d_{mix}\right), \tag{2.11}$$

where

d_{upc} = depth of penetration of the mixing zone into the layers underlying the primary contamination since initial mixing (m).

The algorithms in the code can accommodate a situation where there is no mixing layer. In such a situation, the combined modification factor is zero while there is a cover and unity when there is no cover.

---

2 Because the code calculates only the flux of contaminants across the partially saturated zone boundaries and across the water table, and not the concentration profile in those layers, it is not possible to account for the contaminants in the underlying layer in this calculation and in the calculation of external direct radiation.

2.2.3.3 Concentration of Radionuclides in the Surface Soil above the Primary Contamination

The concentration of radionuclides in surface soil is computed by applying two modification factors to the concentration in the primary contamination: the first considers the volumetric mixing within the mixing layer, and the other accounts for the differences in density. These modification factors are independent of the concentration in the primary contamination and can be treated separately.

$$A_{sc}(t) = f_{vm}(t) A_{pc}(t) \rho_{pc} / \rho_{mix}(t) , \tag{2.12}$$

where

$A_{sc}(t)$ = activity concentration in surface soil after time t (pCi g^{-1}), and

$A_{pc}(t)$ = activity concentration in primary contamination after time t (pCi g^{-1}).

2.2.3.4 Three-Layer Model

The mixing model conceptualizes three layers for the source: (1) a clean cover, (2) the unmixed portion of the initial primary contamination, and (3) a mixing layer that is contaminated to a lesser extent than the primary contamination. From the preceding sections (2.2.3.1, 2.2.3.2, and 2.2.3.3) that discuss the surface layer mixing model, it can be seen that no more than two of these layers can exist at any particular time. While the depth of the mixing zone is less than the depth of the primary cover, there will not be a contaminated mixing zone. Conversely, after the cover thickness decreases to the depth of the mixing zone, there will be no clean cover. With time, erosion could also lead to a situation where the mixing zone breaks through the layer of initial contamination; then there would not be any initial contamination that is unmixed. These conditions are summarized below.

$$\text{When } T_{cv}(t) \geq d_{mix} \text{, then} \tag{2.13}$$

$$T_{cv}^{c}(t) = T_{cv}(t) \text{ , } T_{mix}^{c}(t) = 0 \text{, and } T_{pc}^{um}(t) = T_{pc}(0) ,$$

where

$T_{cv}^{c}(t)$ = thickness of the clean cover (m),

$T_{mix}^{c}(t)$ = thickness of the contaminated mixing layer (m), and

$T_{pc}^{um}(t)$ = thickness of the unmixed portion of the primary contamination (m).

When $T_{cv}(t) < d_{mix} \le T_{cv}(t) + T_{pc}(t)$, then (2.14)

$$T_{cv}^{c}(t) = 0,\ T_{mix}^{c}(t) = d_{mix}, \text{ and } T_{pc}^{um}(t) = T_{pc}(t) + T_{cv}(t) - d_{mix}.$$

When $T_{cv}(t) + T_{pc}(t) < d_{mix}$, then

$$T_{cv}^{c}(t) = 0,\ T_{mix}^{c}(t) = d_{mix}, \text{ and } T_{pc}^{um}(t) = 0.$$

2.2.4 Release by Surface Runoff

The activity of radionuclide released to surface water by the erosion of the surface soil above the primary contamination per unit of time is given by the product of the activity concentration in surface soil and the surface erosion rate. It is more easily computed as the product of the mass of primary contamination that is eroded per unit time and the activity concentration in the primary contamination. The rate (g yr^{-1}) at which soil from the primary contamination is eroded is given by

$$m_{pc}(t) = \varepsilon A f_{vm}(t) \rho_{pc} 10^{6} \tag{2.15}$$

where

A = area of the primary contamination (m^2), and

10^6 = to convert per cubic centimeter to per cubic meter ($[cm]^3\ m^{-3}$).

Then

$$R_k^{sr}(t) = m_{pc}(t) A_k(t), \tag{2.16}$$

where

$R_k^{sr}(t)$ = rate (activity per time) at which the k^{th} radionuclide of the transformation chain is released by erosion (pCi yr^{-1}).

2.2.5 Release to Groundwater

The activity of radionuclide released by rate-controlled leaching to groundwater per unit of time is given by the product of the total activity in soil and the release rate,

$$R_k^{gw}(t) = \mu_k A_k(t) \rho_{pc} A\left(f_{vm} T_{mix}^{c}(t) + T_{pc}^{um}(t)\right) 10^{6}, \tag{2.17}$$

where

$R_k^{gw}(t)$ = rate (activity per time) at which the k^{th} radionuclide of the transformation chain is released to groundwater (pCi y^{-1}), and

10^6 = to convert per cubic centimeter to per cubic meter ($[cm]^3$ m^{-3}).

2.2.6 Release to the Atmosphere in the Form of Dust

The activity of radionuclide released to the atmosphere per unit of time is given by the product of the activity concentration in surface soil and the rate at which dust is released from the area of primary contamination. The conceptual model assumes that there is no net change in the mass loading of dust above the region of primary contamination. Under this assumption, the rate at which dust is released from the primary contamination is equal to the rate at which dust settles out of the air onto the region of primary contamination:

$$R_k^{du}(t) = f_{vm}(t)\frac{\rho_{pc}}{\rho_{mix}(t)} A_k(t) m_{du} A v_{du} 3.15576 \times 10^7, \qquad (2.18)$$

where

$R_k^{du}(t)$ = rate (activity per time) at which the k^{th} radionuclide of the transformation chain is released to the atmosphere as dust (pCi y^{-1}),

m_{du} = concentration of dust in air above the area of primary contamination (g m^{-3}), and

v_{du} = deposition velocity of dust in the area of primary contamination (m s^{-1}), and 3.15576×10^7 is to convert per second to per year (s yr^{-1}).

2.3 IMPLEMENTATION OF THE MODELS FOR THE PRIMARY CONTAMINATION

This section describes how the conceptual model (Section 2.1) or the expressions derived from the conceptual model (Section 2.2) are implemented in the computational code.

2.3.1 Shape and Dimensions of the Primary Contamination

The shape of the conceptual primary contamination in the horizontal plane depends on the exposure or transport model. The dimensions and orientation of the rectangular shape for the atmospheric transport model are specified in the site layout form or the map interface as described in Sections 4.3 and 4.4 of the user's guide. The area of primary contamination is computed by the computational code as the product of the two dimensions.

The groundwater transport model assumes that the primary contamination is rectangular in shape and with one pair of sides parallel to the direction of groundwater flow. The length of one of these sides is specified in the primary contamination form as described in Section 4.14 of the user's guide. The length of the other pair of sides is computed by the computational code using the area of the primary contamination.

Either a circular shape or a polygonal shape can be specified for the calculation of direct external radiation from the primary contamination, as described in Section 4.27 of the user's guide. The polygon can have as many sides as necessary to approximate the shape of the actual contamination. Polygonal-shaped primary contaminations and circular-shaped ones involving a nonconcentric receptor are analyzed by finding the fractions of the areas of a set of 16 annular regions, concentric with the receptor, that are covered by the primary contamination. The computation of the fraction of the annular regions that contain the primary contamination is preformed in the interface and not in the computational code.

2.3.2 Thicknesses of the Primary Contamination, Cover, Clean Cover, Contaminated Mixing Zone, and Undisturbed Primary Contamination

The thickness of the cover is computed at each intermediate time on the basis of the values of the initial thickness and erosion rate of the cover as follows:

$$T_{cv}(t) = T_{cv}(0) - \varepsilon_{cv} t \text{ when } t \le t_{cv} = T_{cv}(0)/\varepsilon_{cv} \text{, and}$$

$$T_{cv}(t) = 0 \text{ when } t > t_{cv}. \tag{2.19}$$

The thickness of the primary contamination is computed at each intermediate time on the basis of the values of the initial thicknesses and erosion rates of the cover and the primary contamination as follows:

$$T_{pc}(t) = T_{pc}(0) \text{ when } t \le t_{cv},$$

$$T_{pc}(t) = T_{pc}(0) - \varepsilon_{pc}(t - t_{cv}) \text{ when } t_{cv} < t \le t_{cv} + t_{pc} = T_{cv}(0)/\varepsilon_{cv} + T_{pc}(0)/\varepsilon_{pc} \text{, and}$$

$$T_{pc}(t) = 0 \text{ when } t > t_{cv} + t_{pc}. \tag{2.20}$$

The thicknesses of the clean cover, the unmixed portion of the initial primary contamination, and the contaminated mixing zone are computed at each intermediate time on the basis of the thicknesses of the cover and the primary contamination at that time and the depth of the mixing zone, as follows:

$$T_{cv}^{c}(t) = T_{cv}(t),\ T_{mix}^{c}(t) = 0,\ T_{pc}^{um}(t) = T_{pc}(0) \text{ when } T_{cv}(t) \ge d_{mix}, \tag{2.21}$$

$$T_{cv}^{c}(t) = 0\,,\ T_{mix}^{c}(t) = d_{mix}\,,\ \text{and}\ T_{pc}^{um}(t) = T_{pc}(t) + T_{cv}(t) - d_{mix}$$

$$\text{when}\ T_{cv}(t) < d_{mix} \le T_{cv}(t) + T_{pc}(t)\,,\ \text{and}$$

$$T_{cv}^{c}(t) = 0\,,\ T_{mix}^{c}(t) = d_{mix}\ \text{and}\ T_{pc}^{um}(t) = 0\ \text{when}\ T_{cv}(t) + T_{pc}(t) < d_{mix}\,.$$

2.3.3 Concentration of Radionuclides in the Primary Contamination

The activity concentrations of the radionuclides are computed at each of the intermediate time points on the bases of the initial activity of the parent nuclides and on the leach rates and transformation constants of the nuclides in the transformation chain with the following analytical expression:

$$A_k(t) = \sum_{i=1}^{k} a_{k,i} \exp(-\lambda_i t - \mu_i t)\,, \tag{2.22}$$

where

$a_{k,i}$ = set of coefficients defined by $a_{1,1} = A_1(0)$,

$$a_{k,i} = \frac{\lambda_k a_{k-1,i}}{\lambda_k + \mu_k - \lambda_i - \mu_i}\ \text{for all}\ 1 \le i < k\,,\ \text{and}$$

$$a_{k,k} = -\sum_{i=1}^{k-1} a_{k,i}\ .$$

2.3.4 Depth of Penetration of the Mixing Zone

The expressions developed in Section 2.2 for the density of the mixing layer and for the volume fraction of soil from the primary contamination in the mixing zone were compact and easier to understand when stated in terms of the depth of penetration of the mixing zone, instead of in terms of time. The depth of penetration into the primary contamination following initial mixing is computed at each intermediate time as the difference between the sums of the thicknesses of the cover and primary contamination at the time of initial mixing and at the intermediate time. This algorithm is simple and has to deal with only two conditions:

$$d_{pc}(t) = T_{cv}(t_{im}) + T_{pc}(t_{im}) - \left[T_{cv}(t) + T_{pc}(t)\right] \ge 0\,,\ \text{while}\ d_m \le T_{cv}(t) + T_{pc}(t)\,, \tag{2.23}$$

where

$$T_{cv}(t_{im}) + T_{pc}(t_{im}) = T_{pc}(0) + d_m \text{ if } d_m \le T_{cv}(0),$$

$$T_{cv}(t_{im}) + T_{pc}(t_{im}) = T_{pc}(0) + T_{cv}(0) \text{ if } d_m > T_{cv}(0), \text{ and}$$

t_{im} = denotes the time of initial mixing, which does not need to be determined but is used for identification purposes.

The depth of penetration of the mixing zone below the primary contamination is also computed in a similar manner using the following algorithm:

$$d_{upc}(t) = T_{cv}(t_{pm}) + T_{pc}(t_{pm}) - \left[T_{cv}(t) + T_{pc}(t)\right] \text{ when } d_m > T_{cv}(t) + T_{pc}(t), \tag{2.24}$$

where

$$T_{cv}(t_{pm}) + T_{pc}(t_{pm}) = d_m \text{ if } d_m \le T_{cv}(0) + T_{pc}(0),$$

$$T_{cv}(t_{pm}) + T_{pc}(t_{pm}) = T_{pc}(0) + T_{cv}(0) \quad \text{if } d_m > T_{cv}(0) + T_{pc}(0), \text{ and}$$

t_{pm} = time at which the mixing layer contains the highest amount of soil from the primary contamination, which does not need to be determined but is used for identification purposes.

2.3.5 Density of Soil in the Mixing Zone

The algorithms in the code consider two possible initial conditions for the mixing zone. Typically the depth (or thickness) of the mixing zone will be smaller than the thickness of the clean cover; the mixing zone has the same properties as the cover under these conditions. If the depth of the mixing zone is specified to be greater than the depth of the clean cover, the code assumes immediate mixing of the material within the mixing zone at time zero. The initial density (at time zero) is calculated as follows:

$$\rho_{mix}(0) = \rho_{cv} \text{ if } T_{cv}(0) \ge d_{mix}, \tag{2.25}$$

$$\rho_{mix}(0) = \rho_{pc} + \frac{T_{cv}(0)}{d_{mix}}\left(\rho_{cv} - \rho_{pc}\right) \text{ if } T_{cv}(0) < d_{mix} \le T_{cv}(0) + T_{pc}(0), \text{ and}$$

$$\rho_{mix}(0) = \rho_{pc} + \frac{T_{cv}(0)}{d_{mix}}\left(\rho_{cv} - \rho_{pc}\right) + \sum_{is}^{N_s} \frac{H_{dm}(is)}{d_{mix}}\left(\rho_{us}(is) - \rho_{pc}\right) + \frac{T_{dm}^{sat}}{d_{mix}}\left(\rho_{sat} - \rho_{pc}\right)$$

$$\text{if } T_{cv}(0) + T_{pc}(0) < d_{mix},$$

where

N_s = number of partially saturated zones,

$H_{dm}(is)$ = thickness of each partially saturated zone that is within the mixing zone at time zero,

$\rho_{us}(is)$ = dry bulk density of the partially saturated zone,

T_{dm}^{sat} = thickness of the saturated zone that is within the mixing layer at time zero, and

ρ_{sat} = dry bulk density of the saturated zone.

The density of the mixing layer is computed at each intermediate time; the algorithm used was greatly simplified by the use of the depth of penetration instead of time as the independent variable. The density of the mixing layer is computed by using the following algorithm:

$$\rho_{mix}(d_{pc}) = \rho_{pc} + \left(\rho_{mix}(0) - \rho_{pc}\right)\exp\left(-d_{pc} / d_{mix}\right) \text{ while } d_{pc} \le T_{cv}(t) + T_{pc}(t). \qquad (2.26)$$

2.3.6 Volume Fraction of Soil from the Primary Contamination in the Mixing Zone

The algorithms in the code consider two possible initial conditions for the mixing zone. If, as is the typical case, the depth (or thickness) of the mixing zone is less than the thickness of the clean cover, the mixing zone has the same properties as the cover. If the depth of the mixing zone is specified to be greater than that of the clean cover, the code assumes immediate mixing of the material within the mixing zone at time zero. The initial volume fraction of soil from the primary contamination in the mixing zone is calculated as follows:

$$f_{vm}(0) = 0 \text{ if } T_{cv}(0) \ge d_{mix}, \qquad (2.27)$$

$$f_{vm}(0) = 1 - \frac{T_{cv}(0)}{d_{mix}} \text{ if } T_{cv}(0) < d_{mix} \le T_{cv}(0) + T_{pc}(0), \text{ and}$$

$$f_{vm}(0) = \frac{T_{pc}(0)}{d_{mix}} \text{ if } T_{cv}(0) + T_{pc}(0) < d_{mix}.$$

The volume fraction of soil from the primary contamination in the mixing zone is computed with the following algorithms at each intermediate time point:

$$f_{vm}(d_{pc}) = 1 - \left(1 - f_{vm}(0)\right)\exp\left(-d_{pc} / d_{mix}\right) \text{ when } d_{mix} \le T_{cv}(t) + T_{pc}(t) \text{, and} \tag{2.28}$$

$$f_{vm}(d_{upc}) = f_{vm}^{p} \exp\left(-d_{upc} / d_{mix}\right) \text{ when } d_{mix} > T_{cv}(t) + T_{pc}(t) \text{,}$$

where

$$f_{vm}^{p} = 1 - \exp\left(-T_{pc}(0) / d_{mix}\right) \text{ if } T_{cv}(0) \ge d_{mix} \text{,}$$

$$f_{vm}^{p} = 1 - \frac{T_{cv}(0)}{d_{mix}} \exp\left(-\frac{T_{cv}(0) + T_{pc}(0) - d_{mix}}{d_{mix}}\right) \text{ if } T_{cv}(0) < d_{mix} \le T_{cv}(0) + T_{pc}(0) \text{, and}$$

$$f_{vm}^{p} = \frac{T_{pc}(0)}{d_{mix}} \text{ if } T_{cv}(0) + T_{pc}(0) < d_{mix} \text{.}$$

The algorithms in the code can also accommodate a situation where there is no mixing zone. In such a situation, the combined modification factor is zero while there is a cover and unity when there is no cover.

2.3.7 Concentration of Radionuclides in the Surface Soil above the Primary Contamination

The concentration of radionuclides in surface soil is computed at each intermediate time by using the concentration in the primary contamination, the volume fraction of soil from the primary contamination in the mixing zone, and the dry bulk densities of the mixing zone and the primary contamination:

$$A_{sc}(t) = f_{vm}(t) A_{pc}(t) \rho_{pc} / \rho_{mix}(t) \text{.} \tag{2.29}$$

2.3.8 Release by Surface Runoff

The rate at which soil from the primary contamination is eroded is computed at each intermediate time as the product of the rate of erosion of the surface soil, the area of the primary contamination, the volume fraction of soil from the primary contamination in the mixing zone, and the dry bulk density of the primary contamination.

$$m_{pc}(t) = \varepsilon A f_{vm}(t) \rho_{pc} 10^{6} \text{,} \tag{2.30}$$

where

$\varepsilon = \varepsilon_{cv}$ when $T_{cv}(t) > 0$, and

$\varepsilon = \varepsilon_{pc}$ when $T_{cv}(t) = 0$.

The rate at which the radionuclide is released to surface water by the erosion of the surface soil above the primary contamination is computed at each intermediate time as the product of the mass of primary contamination that is eroded per unit time and the activity concentration in the primary contamination:

$$R_k^{sr}(t) = m_{pc}(t) A_k(t) . \tag{2.31}$$

2.3.9 Release to Groundwater

The rate at which the radionuclide is released to groundwater by rate-controlled leaching is computed at each intermediate time as the product of the total activity in soil and the release rate:

$$R_k^{gw}(t) = \mu_k A_k(t) \rho_{pc} A\left(f_{vm} T_{mix}^{c}(t) + T_{pc}^{um}(t)\right) 10^6 . \tag{2.32}$$

2.3.10 Release to the Atmosphere in the Form of Dust

The rate at which the radionuclide is released to the atmosphere is given by the product of the activity concentration in surface soil and the rate at which dust is released from the area of primary contamination:

$$R_k^{du}(t) = f_{vm}(t) \frac{\rho_{pc}}{\rho_{mix}(t)} A_k(t) m_{du} A v_{du} 3.15576 \times 10^7 . \tag{2.33}$$

2.4 OVERRIDING THE RESRAD-OFFSITE SOURCE TERM MODEL

If all the information that is computed by the RESRAD-OFFSITE source term model is available either from a more sophisticated model or from a series of measurements, the computational code can be flagged to suppress its source term module and to read in the time series of the information. The temporal series of source term and release information has to be in the format that is useable by the RESRAD-OFFSITE computational code. The names of the files containing the temporal source term and release data and their contents are described in Table 2.1.

The data files are structured on the basis of the number of parent progeny combinations at the site. They contain a column of data for each parent-progeny combination. The order of the columns is determined as follows. The initially present nuclides are sorted first alphabetically by their chemical symbol and then by the nominal atomic weight in the case of isotopes. The first column of data pertains to the first nuclide in the sorted list. If that nuclide has principal radionuclide progeny, there must be a column of data for each progeny in the order in which they occur in the transformation chain. If the nuclide has more than one transformation thread, there

must be additional columns of data for each transformation thread. Then there must be a column of data for the second initially present radionuclide in the sorted list, followed by a column each for its progeny in the order in which they occur in its transformation chain, and so on for each nuclide in the sorted list. The number of times at which data are available determines the number of rows in the different files — there must be a row for each time at which data are available.

The computational code uses a linear interpolation between the specified times when performing the calculations. The input interface does not at present have a form to bypass the source module and accept these inputs because of the complexity of the format required for these input files.

TABLE 2.1 Input Files Used to Specify the Source Characteristics and Releases to the Code

File name	Contents
SFSIN.DAT	Temporal data of the concentration (Section 2.2.2), in pCi g^{-1}, of each initially present radionuclide and its principal nuclide progeny in the unmixed region of the primary contamination.
CZTHICK3.DAT	Temporal data of the composite modification factor for the concentration of nuclides in the mixing zone (Section 2.2.3.3) and of the thicknesses, in m, of clean cover, contaminated mixing zone, and the unmixed portion of the contaminated zone (Section 2.3.3.4).
AQFLUXIN.DAT	Temporal data of the flux, in pCi $year^{-1}$, of each initially present radionuclide and its principal nuclide progeny, to the groundwater pathway.
SWFLUXIN.DAT	Temporal data of the eroded flux, in pCi $year^{-1}$, of each initially present radionuclide and its principal nuclide progeny and the mass of eroded soil, in g $year^{-1}$, to surface runoff.
AIFLUXIN.DAT	Temporal data of the flux, in pCi $year^{-1}$, of each initially present radionuclide and its principal nuclide progeny, to the atmosphere.

3 GROUNDWATER TRANSPORT MODEL

Section 3.1 describes the manner in which RESRAD-OFFSITE conceptualizes the groundwater transport pathway, specifically the unsaturated and saturated zones and the transport through these zones. Section 3.2 discusses derivation of the expressions that result from the conceptual model. Section 3.3 deals with the implementation of the solution or the evaluation of these expressions in the computational code.

3.1 CONCEPTUALIZATION OF GROUNDWATER TRANSPORT

The conceptual model for the groundwater pathway consists of zero to five horizontal layers of partially saturated zones and one unconfined saturated zone; Figure 3.1 illustrates a situation with two partially saturated zones. Flow in the partially saturated zone is in the downward vertical direction; convective and dispersive transport in the vertical direction are modeled. The flow in the saturated zone is in the horizontal direction; convective and dispersive transport in the direction of flow and dispersive transport in the two directions perpendicular to the flow are modeled.

The plane view of the primary contamination (its shape in the horizontal plane) is assumed to be rectangular, with one pair of sides being parallel to the direction of groundwater flow. The contaminant plume in the partially saturated zone maintains this rectangular shape because transport in the partially saturated zone is assumed to occur only in the vertical direction.

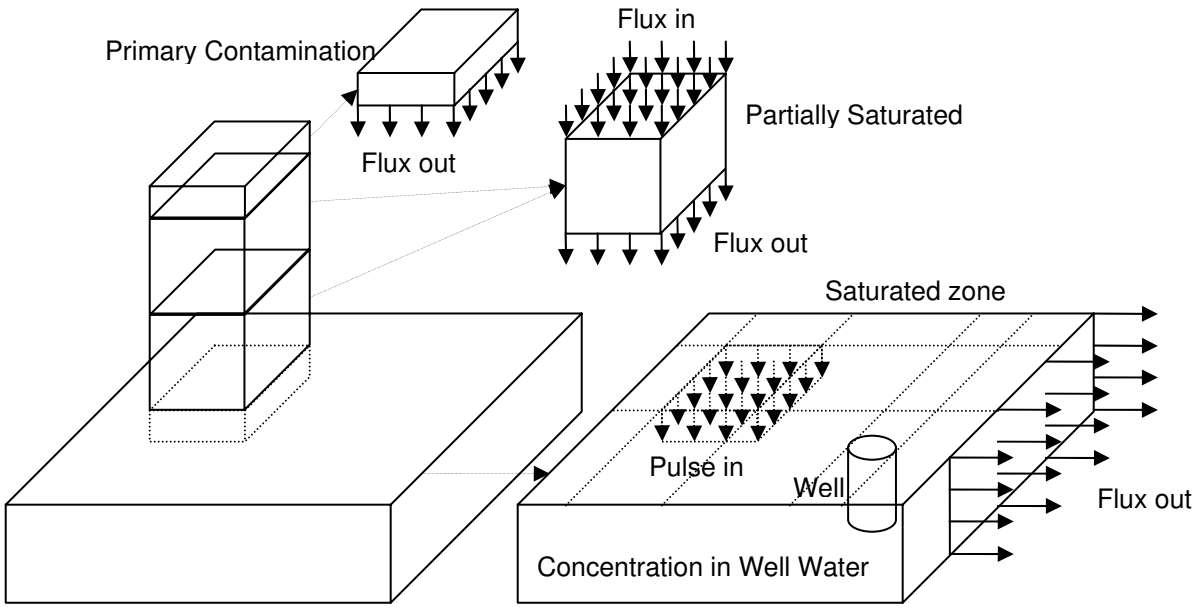

FIGURE 3.1 Conceptualization of Groundwater Transport in RESRAD-OFFSITE

The transport zones are treated as homogenous layers; the specified properties (density, porosities, hydraulic conductivity, dispersivities, and hydraulic gradient) are assumed to be constant over a transport zone. Only the pores that are interconnected are of concern in modeling the transport of nuclides in groundwater, because isolated pores do not affect the movement of the nuclides. The conceptual model differentiates between two kinds of interconnected pores: mobile pores and immobile pores (Figure 3.2). The water in mobile pores is free to move and contributes to the advective transport of nuclides. The moisture in the immobile pores is held in place either because it is in dead-end pores or because it is tightly bound to the solid phase and does not contribute to the advective transport of nuclides. The total porosity is the measure of all the moisture-filled connected pores (both mobile and immoble) into which the nuclide can enter by either advection or diffusion. The effective porosity is the measure of the moisture-filled pores that are effective in the advective transport of the nuclide. Moisture in pores that lead to dead ends and moisture that is tightly bound to the solid phase of the soil and is thus immobile are two reasons why the total porosity can be greater than the effective porosity. In the derivation that follows in Section 3.2.1, it is assumed that immobile pores are due to dead ends.

3.2 DERIVATION OF MATHEMATICAL EXPRESSIONS FOR THE CONCEPTUAL GROUNDWATER TRANSPORT MODEL

The conceptual model has to be translated into mathematical expressions before it can be used in the computational code. The idealized descriptions of Section 3.1 are expressed in mathematical terms in this section.

Each partially saturated zone is idealized in the conceptual model as a rectangular prism. The flux of nuclide that exits the contaminated zone is known as a function of time — at the intermediate time points — as discussed in Chapter 2. This is the flux that crosses the upper boundary of the uppermost partially saturated zone. The groundwater transport model computes the flux that crosses the lower boundary of each partially saturated layer.

When a large number of atoms of a radionuclide travel across a transport layer, some of them will undergo radiological transformations and will exit the layer as one of the progeny of the radionuclide that entered the layer. The remainder, which did not transform, will exit the layer in the same form. The equations developed in this section, for the output flux as a function of the input flux, consider the effects of longitudinal dispersion on the transport of a radionuclide, if it travels through an entire transport layer in the same form. Two solutions are developed for the transport of a progeny nuclide that entered the layer as one of its parents and then transformed within the layer. One considers the effects of nuclide-specific distribution coefficients of the nuclides in the transformation chain from the parent to the progeny and ignores the effects of longitudinal dispersion; the other considers the effects of longitudinal dispersion and ignores the effects of nuclide-specific distribution coefficients. A method for modeling both processes is discussed in Section 3.3.13.

The idealized saturated zone that is conceptualized by the code is depicted in Figure 3.3. The flux out of the last unsaturated zone, or in the absence of any unsaturated zone, the flux out of the primary contamination, is treated as pulse distributed over a rectangular prism within the

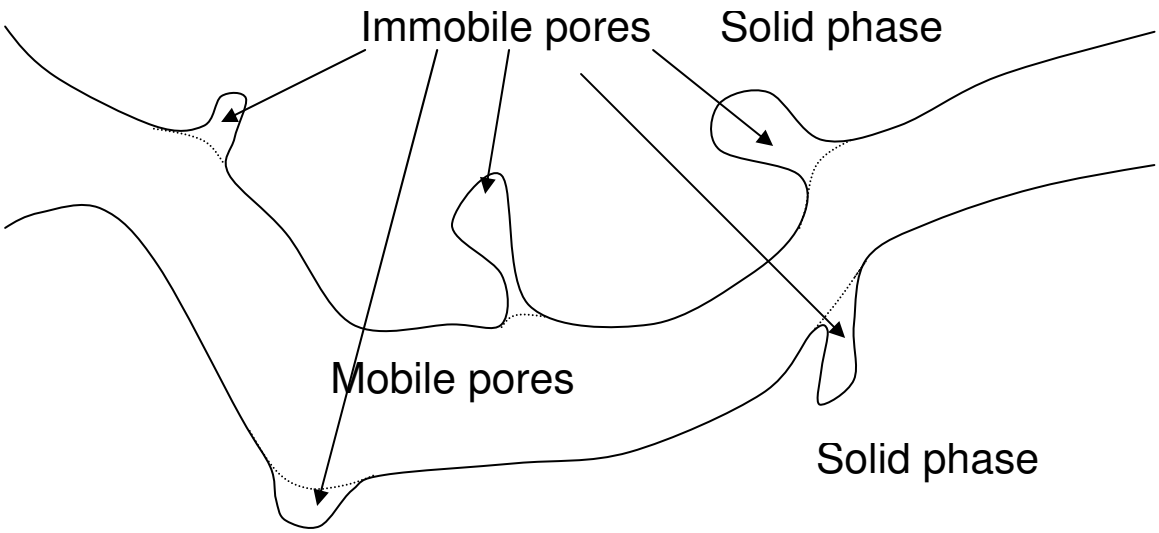

FIGURE 3.2 Conceptualization of Mobile and Immobile Pores

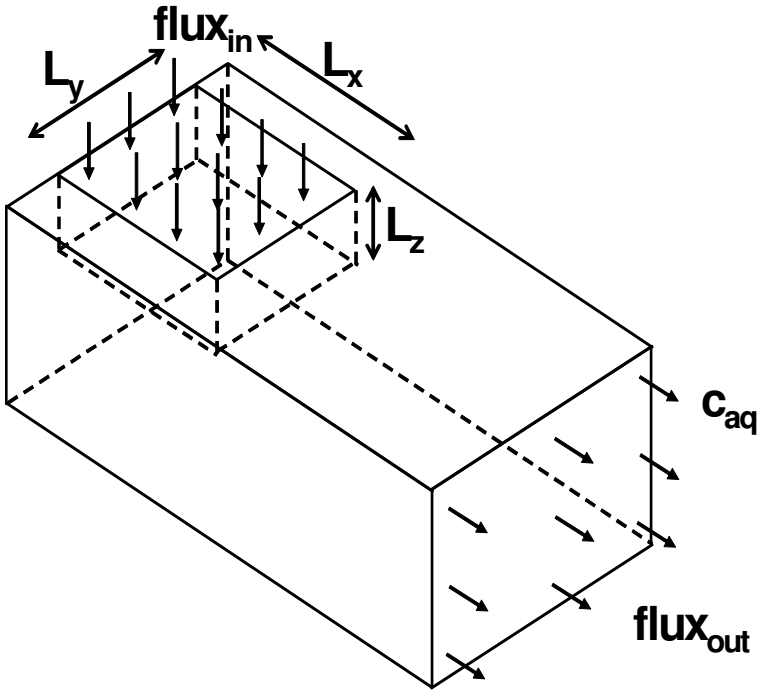

FIGURE 3.3 Idealized Saturated Zone Modeled by RESRAD-OFFSITE

saturated zone. The length and width of this rectangular prism is the same as that of the primary contamination. The depth is determined by the depth of advective penetration.

The groundwater transport model computes the spatial profile of the flux across a vertical plane in the aquifer or the spatial profile of the concentration in water over a vertical plane in the aquifer. Consideration of transverse and lateral dispersion is separated out from the consideration of longitudinal dispersion for ease of computation. As with the case for the flux input, two expressions are developed to model the transport of those atoms that transformed within the transport zone; one considers longitudinal dispersion while the other considers the nuclide-specific distribution coefficients.

3.2.1 Governing Equation for the Transport of Nuclides in Soil

The equation governing the transport of nuclides in porous media is obtained by expressing each of the processes being modeled in mathematical form. The processes considered are the losses and gains resulting from radiological transformations, advective transport by water as it flows through the porous medium, and dispersive transport caused by concentration gradients. The net result of these processes is a change in storage in the surface of the solid phase and in the aqueous phase of the soil. The mathematical representations of the process are written considering an elemental volume (Figure 3.4) of dimensions δx (m), δy (m), and δz (m) over a time period of δt (y).

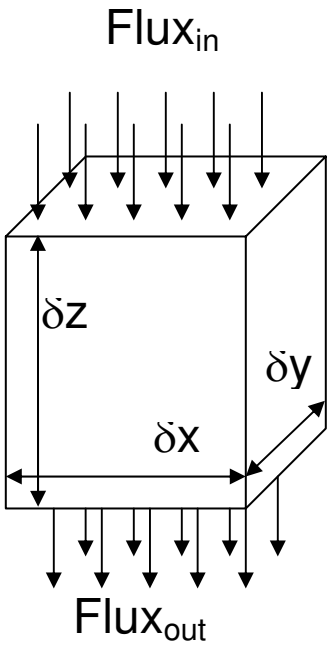

FIGURE 3.4 Elemental Volume of Soil

3.2.1.1 Volume of Connected Moisture-Filled Pores and the Soil in Contact with the Pores

The porosities of the two types of pores (Figure 3.2) are related by the following expression:

$$\theta_m + \theta_{im} = \theta_t \ , \tag{3.1}$$

where

θ_m = mobile porosity, the porosity that allows or contributes to the movement of water;

θ_{im} = immobile porosity, the porosity that does not contribute to the movement of water; and

θ_t = sum of the two porosities; i.e., the total connected porosity.

Although the nuclides are adsorbed to the surface of the solids in the soil, their concentration in soil is expressed in terms of the mass of the solids. The volume fractions of the soil associated with the mobile and immobile pores are assumed to be in the same ratio as the porosities of those two phases:

$$v_m : v_{im} = \theta_m : \theta_{im} \ . \tag{3.2}$$

3.2.1.2 Partitioning of Nuclides between the Aqueous and Solid Phases of Soil

The partitioning of nuclides between the aqueous phase in the pores and the solid phase adsorbed to the surface is dynamic. The nuclides are adsorbed at a rate that depends on the concentration of the nuclides in the aqueous phase. Conversely, the nuclides that were adsorbed on the surface desorb at a rate that depends on the concentration of nuclides in the solid (adsorbed) phase. Over time, the two phases achieve equilibrium, and the partitioning of nuclides between the aqueous and solid phases is characterized by the equilibrium distribution coefficient:

$$K_d = \frac{s_m}{c_m} 10^6 = \frac{s_{im}}{c_{im}} 10^6 \ , \tag{3.3}$$

where

K_d = distribution coefficient ($[\text{cm}]^3$ pCi g^{-1});

s_m, s_{im} = concentrations of the nuclides in soil associated with the mobile and immobile pores, respectively (pCi g^{-1});

c_m, c_{im} = concentrations of the nuclides in the mobile and immobile pores, respectively (pCi m^{-3}); and

10^6 = unit conversion factor ($[cm]^3$ m^{-3}).

3.2.1.3 Quantity of Nuclides in a Unit Volume of Soil

The quantity of nuclides in a unit volume of soil is the sum of the quantities in the mobile and immobile pores and in the solid phase associated with theses pores.

$$\theta_m c_m + \theta_{im} c_{im} + \upsilon_m \rho_b 10^6 s_m + \upsilon_{im} \rho_b 10^6 s_{im}$$

$$\begin{aligned}
&= \theta_m c_m + \theta_{im} c_{im} + \frac{\upsilon_m}{\upsilon_m + \upsilon_{im}} \rho_b 10^6 s_m + \frac{\upsilon_{im}}{\upsilon_m + \upsilon_{im}} \rho_b 10^6 s_{im} \\
&= \theta_m c_m + \theta_{im} c_{im} + \frac{\theta_m}{\theta_m + \theta_{im}} \rho_b K_d c_m + \frac{\theta_{im}}{\theta_m + \theta_{im}} \rho_b K_d c_{im} \\
&= \theta_m c_m + \frac{\rho_b K_d}{\theta_t} \theta_m c_m + \theta_{im} c_{im} + \frac{\rho_b K_d}{\theta_t} \theta_{im} c_{im} \\
&= \left(1 + \frac{\rho_b K_d}{\theta_t}\right) \theta_m c_m + \left(1 + \frac{\rho_b K_d}{\theta_t}\right) \theta_{im} c_{im} \\
&= \frac{\theta_m c_m + \theta_{im} c_{im}}{\theta_t} \left(\theta_t + \rho_b K_d\right) \\
&= c_{av} \left(\theta_t + \rho_b K_d\right)
\end{aligned} \tag{3.4}$$

where

c_{av} = average concentration of the nuclide in the connected pores (pCi m^{-3}).

3.2.1.4 Change in Quantity of Nuclides Stored in the Elemental Volume Due to Radiological Transformations

This change in the quantity of nuclides in the elemental volume of soil over time as a result of radiological transformations follows from the expression for the quantity of nuclides in a unit volume of soil derived in Section 3.2.1.3:

$$\text{Change} = -\lambda c_{av} \left(\theta_t + \rho_b K_d\right) \delta x \delta y \delta z \ . \tag{3.5}$$

3.2.1.5 Change in Quantity of Nuclides Stored in the Elemental Volume Due to Advective Transport

This change is the difference between the amount of nuclides carried in by water flowing in through the mobile pores at the upgradient face of the elemental volume and the amount of nuclides carried out by water flowing out through the mobile pores at the downgradient face of the elemental volume:

$$\text{Change} = -V_m \theta_m \delta x \delta y \frac{\partial c_m}{\partial z} \delta z \ , \tag{3.6}$$

where

V_m = average velocity of the water flowing through the mobile pores (m year^{-1}).

3.2.1.6 Change in Quantity of Nuclides Stored in the Elemental Volume Due to Longitudinal Dispersion

This change is the difference between the amount of nuclides dispersing in through the mobile pores across the upgradient face of the elemental volume and the amount of nuclides dispersing out through the mobile pores across the downgradient face of the elemental volume:

$$\text{Change} = \theta_m \delta x \delta y D_z^m \frac{\partial^2 c_m}{\partial z^2} \delta z \ , \tag{3.7}$$

where

D_z^m = dispersion coefficient of the nuclides in the mobile pores (m^2 year^{-1}).

3.2.1.7 Net Change in Quantity of Nuclides Stored in the Elemental Volume

This net change in the quantity of nuclides in the elemental volume of soil over time follows from the expression for the quantity of nuclides in a unit volume of soil derived in Section 3.2.1.3:

$$\text{Net Change} = \left(\theta_t + \rho_b K_d\right) \frac{\partial c_{av}}{\partial t} \delta x \delta y \delta z \ . \tag{3.8}$$

3.2.1.8 Mass Balance Equation

Mass balance requires that the sum of changes represented by Equations 3.5, 3.6, and 3.7 be equal to the net change represented by Equation 3.8:

$$\left(\theta_t + \rho_b K_d\right)\frac{\partial c_{av}}{\partial t} = -\lambda\left(\theta_t + \rho_b K_d\right)c_{av} - V_m\theta_m\frac{\partial c_m}{\partial z} + D_z^m\theta_m\frac{\partial^2 c_m}{\partial z^2} \ . \tag{3.9}$$

Rearranging the above equation gives

$$\frac{\partial c_{av}}{\partial t} = -\lambda c_{av} + \frac{\theta_m}{\left(\theta_t + \rho_b K_d\right)}\left(-V_m\frac{\partial c_m}{\partial z} + D_z^m\frac{\partial^2 c_m}{\partial z^2}\right) . \tag{3.10}$$

This equation has to be solved with appropriate initial and boundary conditions to model the transport of the nuclides in the unsaturated and saturated zones. Some of these conditions (e.g., the boundary condition for transport in the unsaturated zone, Equation 3.25) are expressed in terms of the concentration in the mobile pores, c_m. Other conditions (e.g., the initial condition for transport in the saturated zone, Equation 3.34) are expressed in terms of the average concentration in the connected pores, c_{av}. A relationship between these two concentrations is therefore needed to model the transport.

3.2.1.9 Concentration of Nuclides in the Mobile Pores and Immobile Pores

As the contaminant plume moves, the water entering the mobile pores contains the nuclides. The nuclides in the mobile pores are transferred into the immobile pores at a rate that depends on the concentration of the nuclides in the mobile pores. Conversely, the nuclides in the immobile pores are transferred to the mobile pores at a rate that depends on the concentration of nuclides in the immobile pores. Over time, the concentration in the immobile pores increases to a level at which equilibrium between the two (mobile and immobile pores) is achieved. Two limiting assumptions are used to obtain the relationships among the concentrations in the mobile, immobile, and total pores. If the time needed to travel through a region of soil is much shorter than the time needed for the mobile and immobile pores to achieve equilibrium, then the concentration in the immobile pores will be negligible compared to the concentration in the mobile pores. Under these conditions, the average concentration in the total pores is given by the following equation:

$$c_{av} = \frac{\theta_m c_m + \theta_{im} c_{im}}{\theta_t} \approx \frac{\theta_m}{\theta_t} c_m \ . \tag{3.11}$$

If the time needed to travel through a region of soil is much greater than the time needed by the mobile and immobile pores to achieve equilibrium, then the concentration in the immobile pores will be equal to the concentration in the mobile pores. Under these conditions, the average concentration in the total pores is given by the following equation:

$$c_{av} = \frac{\theta_m c_m + \theta_{im} c_{im}}{\theta_t} \approx \frac{\theta_t}{\theta_t} c_m = c_m \ . \tag{3.12}$$

3.2.1.10 Governing Equation for Transport

Combining Equations 3.10 and 3.11 gives the following:

$$\frac{\theta_m}{\theta_t}\frac{\partial c_m}{\partial t} = -\lambda\frac{\theta_m}{\theta_t}c_m + \frac{\theta_m}{(\theta_t + \rho_b K_d)}\left(-V_m\frac{\partial c_m}{\partial z} + D_z^m\frac{\partial^2 c_m}{\partial z^2}\right)$$

$$\frac{\partial c_m}{\partial t} = -\lambda c_m + \frac{\theta_t}{(\theta_t + \rho_b K_d)}\left(-V_m\frac{\partial c_m}{\partial z} + D_z^m\frac{\partial^2 c_m}{\partial z^2}\right) \qquad (3.13)$$

$$= -\lambda c_m - V_c\frac{\partial c_m}{\partial z} + D_z^c\frac{\partial^2 c_m}{\partial z^2}\ ,$$

where

$V_c = V_m\dfrac{\theta_t}{\theta_t + \rho_b K_d}$ = average velocity of contaminants in the soil (m year^{-1}) and

$D_z^c = D_z^m\dfrac{\theta_t}{\theta_t + \rho_b K_d}$ = dispersion coefficient of contaminants in the soil (m^2 year^{-1}).

Combining Equations 3.10 and 3.12 gives

$$\frac{\partial c_m}{\partial t} = -\lambda c_m + \frac{\theta_m}{(\theta_t + \rho_b K_d)}\left(-V_m\frac{\partial c_m}{\partial z} + D_z^m\frac{\partial^2 c_m}{\partial z^2}\right)$$

$$= -\lambda c_m - V_c\frac{\partial c_m}{\partial z} + D_z^c\frac{\partial^2 c_m}{\partial z^2}\ , \qquad (3.14)$$

where

$V_c = V_m\dfrac{\theta_m}{\theta_t + \rho_b K_d}$ = average velocity of contaminants in the soil (m year^{-1}) and

$D_z^c = D_z^m\dfrac{\theta_m}{\theta_t + \rho_b K_d}$ = dispersion coefficient of the contaminant in the soil (m^2 year^{-1}).

3.2.1.11 Retardation Factor

The ratio between the average velocity of water in the mobile pores and the average velocity of the contaminants is called the retardation factor:

$$R_d = \frac{V_m}{V_c} \ . \tag{3.15}$$

When the travel time through a region of soil is much shorter than the time needed for the mobile and immobile pores to achieve equilibrium, the governing equation (3.13) contains a retardation factor of

$$R_d = \frac{\theta_t + \rho_b K_d}{\theta_t} = 1 + \frac{\rho_b K_d}{\theta_t} \ . \tag{3.16}$$

When the travel time through a region of soil is much longer than the time needed for the mobile and immobile pores to achieve equilibrium, the governing equation (3.14) contains a retardation factor of

$$R_d = \frac{\theta_t + \rho_b K_d}{\theta_m} = \frac{\theta_t}{\theta_m} + \frac{\rho_b K_d}{\theta_m} \ . \tag{3.17}$$

Equation 3.16 is used as the default retardation factor in RESRAD-OFFSITE code because it gives a faster breakthrough time and higher radionuclide concentrations than Equation 3.17 does. See further discussion at the end of Section 3.2.1.12.

3.2.1.12 Pore Water Velocity

The volumetric flow rate through a unit cross section is called the Darcy velocity or apparent velocity of flow. The Darcy velocity of flow in the partially saturated zone is the infiltration rate, which is computed by using the following expression:

$$V_d = I = \left(1 - C_e\right)\left[\left(1 - C_r\right)P_r + I_{rr}\right] , \tag{3.18}$$

where

V_d = Darcy velocity (m year^{-1}),

I = infiltration rate (m year^{-1}),

C_e = evapotranspiration coefficient,

C_r = runoff coefficient,

P_r = precipitation rate (m year^{-1}), and

I_{rr} = annual irrigation applied over the primary contamination (m year^{-1}).

The Darcy velocity of flow in the saturated zone is the ground water flow rate, which is computed by using the following expression:

$$V_d = K_{hc} i_{hg} \ , \tag{3.19}$$

where

K_{hc} = saturated hydraulic conductivity (m year^{-1}) and

i_{hg} = hydraulic gradient.

The pore water velocity of the mobile pores is related to the Darcy velocity by the following expression:

$$V_d = \theta_m V_m \ . \tag{3.20}$$

Equation 3.20 is combined with Equations 3.18 and 3.19, respectively, to compute the pore water velocities in the unsaturated and saturated zones.

The average velocity of the nuclides in soil is computed in the code by using the following expression:

$$V_c = \frac{V_d}{\theta_m R_d} \ . \tag{3.21}$$

Equation 3.21 is combined with the equation for the retardation factor (3.16 or 3.17) and with Equations 3.18 and 3.19, respectively, to compute the nuclide transport velocities in the unsaturated and saturated zones.

Using Equation 3.16 and Equation 3.21 gives a faster average nuclide velocity and hence an earlier breakthrough time for radionuclides. Because Equation 3.16 predicts a shorter breakthrough time and consequently a higher concentration in water, it is used as the default retardation factor definition in the RESRAD-OFFSITE code. For derivation of cleanup criteria and for dose/risk assessment, the default retardation factor (i.e., Equation 3.16) provides more conservative results. The use of Equation 3.16 also is consistent with the retardation factor definition used in the RESRAD (onsite) code. (Note that Equation 3.17 was used in beta versions of the RESRAD-OFFSITE code.)

3.2.1.13 Dispersivity

This is the ratio between the dispersion coefficient of the nuclide in soil and the velocity of the nuclide in soil:

$$d = \frac{D_z^c}{V_c} = \frac{D_z^m}{V_m} \ , \tag{3.22}$$

where

d = dispersivity of the nuclide (m).

The dispersion coefficient of the nuclide in soil is computed in the code by using the following expression:

$$D_z^c = \frac{dV_d}{\theta_m R_d} \ . \tag{3.23}$$

3.2.2 Output Flux and Concentration Resulting from an Input Flux for Radionuclides That Entered and Exited the Transport Layer in the Same Form

The governing equation is solved for an instantaneous unit flux across the upper boundary, assuming a layer of unbounded thickness. The governing equation to be solved is as follows:

$$\frac{\partial c_m(z,t)}{\partial t} + \lambda c_m(z,t) + V_c \frac{\partial c_m(z,t)}{\partial z} - D_z^c \frac{\partial^2 c_m(z,t)}{\partial z^2} = 0 \, . \tag{3.24}$$

The instantaneous unit flux across the upper boundary can be expressed by the equation:

$$V_m \theta_m c_m(z,t) - \theta_m D_z^m \frac{\partial c_m(z,t)}{\partial z} = V_c R_d \theta_m c_m(z,t) - D_z^c R_d \theta_m \frac{\partial c_m(z,t)}{\partial z} = \delta(z,t) \ , \tag{3.25}$$

where

$\delta(z,t)$ = a delta function.

The assumption of a layer of unbounded thickness allows the global mass balance equation to be written as $\int_{z=0}^{z=\infty} (\theta_t + \rho_b K_d) c_{av}(z,t) dz = R_d \theta_m \int_{z=0}^{z=\infty} c_m(z,t) dz = e^{-\lambda t}$.

Starting with the solution of Lindstrom et al. (1967) for a “flux-plug type of input at the surface” and considering the limit where the duration of the flux plug tends to zero while the

total flux goes to unity, and then modifying for a transforming solute, we obtain (after fixing a typo in the reference):

$$c_m(z,t) = \frac{e^{-\lambda t}}{\theta_m R_d}\left[\frac{2}{\sqrt{4\pi D_z^c t}}\exp\left(-\frac{(z-V_c t)^2}{4D_z^c t}\right) - \frac{V_c}{2D_z^c}\exp\left(\frac{zV_c}{D_z^c}\right) erfc\left(\frac{z+V_c t}{\sqrt{4D_z^c t}}\right)\right]. \quad (3.26)$$

The flux at a distance z at time t is given by

$$f(z,t) = \frac{z}{t}\sqrt{\frac{1}{4\pi D_z^c t}}\exp\left(-\frac{(z-V_c t)^2}{4D_z^c t} - \lambda t\right). \quad (3.27)$$

If the flux entering a partially saturated layer is known as a function of time, it can be convolved with the above expression (for output flux from an instantaneous unit input flux) to obtain the flux exiting the layer:

$$f(z,t) = \int_0^t f(0,t-\tau)\frac{z}{\tau}\sqrt{\frac{1}{4\pi D_z^c \tau}}\, exp\left(-\frac{(z-V_c\tau)^2}{4D_z^c \tau} - \lambda\tau\right) d\tau\,. \quad (3.28)$$

3.2.3 Output Flux and Concentration Resulting from an Input Flux for Radionuclides That Were Produced by Radiological Transformations within the Transport Layer

Ingrowth from the parent nuclides needs to be considered in addition to the processes discussed in Section 3.2.1 when modeling the transport of progeny that are produced in transit. The governing equation then becomes

$$\lambda c_m(z,t) + \frac{\partial c_m(z,t)}{\partial t} + V_c\frac{\partial c_m(z,t)}{\partial z} - D_z^c\frac{\partial^2 c_m(z,t)}{\partial z^2} = \lambda c_m^p(z,t)\frac{\theta_t + K_d^p\rho_b}{\theta_t + K_d\rho_b}, \quad (3.29)$$

where

c_m^p = concentration of the parent radionuclide in water (pCi m^{-3}), and

K_d^p = soil-water distribution coefficient of the parent radionuclide ([cm]^3 g^{-1}).

An exact solution involves solving this equation for each nuclide of the chain using the solution for the previous member of the chain and is complex, especially for the later members of a transport chain. RESRAD-OFFSITE provides two simpler solutions; one that is applicable when longitudinal dispersion is dominant and the other for cases where the differences in the distribution coefficients of the parent and progeny are significant. Situations where both processes are of comparable importance can be modeled by subdividing the transport layer as discussed in Section 3.3.13.

3.2.3.1 Concentration and Flux of Radionuclides That Were Produced by Radiological Transformations within the Transport Layer from a Flux Input When Dispersion Is Dominant

The solutions in this case are obtained under the assumption that the nuclides in the transformation chain, from the parent that enters the zone to the progeny that exit the zone, all travel at the same velocity and partition to the same extent between the solid and aqueous phases of the soil. The transport can then be separated out from the ingrowth and the flux of the k^{th} progeny resulting from an instantaneous unit flux of the parent is given by

$$f_k(z,t) = \sum_{i=1}^{k} a_{k,i} \frac{z}{t} \sqrt{\frac{1}{4\pi D_z^c t}} \exp\left(-\frac{(z - V_c t)^2}{4 D_z^c t} - \lambda_i t \right), \tag{3.30}$$

where

$f_{k(z,t)}$ = flux of the k^{th} radionuclide of the transformation chain (pCi yr^{-1}) and $a_{k,i}$ is a set of coefficients defined by $a_{1,1} = 1$,

$$a_{k,i} = \frac{\lambda_k a_{k-1,i}}{\lambda_k - \lambda_i} \text{ for all } 1 \le i < k, \text{ and}$$

$$a_{k,k} = -\sum_{i=1}^{k-1} a_{k,i} \ .$$

The concentration is given by

$$c_k(z,t) = \frac{\dfrac{2}{\sqrt{4\pi D_z^c t}} e^{-\frac{(z - V_c t)^2}{4 D_z^c t}} - \dfrac{V_c}{2 D_z^c} e^{\frac{z V_c}{D_z^c}} erfc\left(\dfrac{z + V_c t}{4 D_z^c t} \right)}{\theta_m R_d} \sum_{i=1}^{k-1} a_{k,i} \exp(-\lambda t) \, . \tag{3.31}$$

3.2.3.2 Concentration and Flux of Radionuclides That Were Produced by Radiological Transformations within the Transport Layer from a Flux Input When Differences in Their Distribution Coefficients Are Dominant

The solution in this case is obtained by ignoring longitudinal dispersion. The derivation of the solution for the first three members of a transport chain is discussed in Appendix I of the User's Manual for RESRAD Version 6 (Yu et al. 2001). The solutions are expressed in terms of the contaminant travel times, $T_i = z/v_i$. Subscripts i, j, k, l, and m are used to describe the nuclides of the transport chain in the order in which they occur in the transformation chain, while subscripts 1, 2, 3, 4, and 5 are used to describe the nuclides sorted in ascending order of the travel time. The transfer functions for advective flux are all of the form

$$f_k(z,t) = \frac{\lambda_k}{\lambda_i} \sum \gamma \exp\left(\alpha_{i,j} t + \beta_{i,j} T_1\right), \tag{3.32}$$

where

$\gamma, \alpha_{i,j}, \beta_{i,j}$ = all functions of the radiological transformation constants, the ratios of the travel times of the radionuclides, and the travel time of the fastest radionuclide of the transport chain, and

T_1 = travel time of the fastest radionuclide of the transport chain.

The concentration is obtained by dividing the advective flux by the volumetric flow rate in this case.

3.2.4 Concentration and Flux of Radionuclides That Traversed the Transport Layer in the Same Form, from a Pulse Input

The governing equation for longitudinal transport is the same as the one for the partially saturated zone; as stated earlier, the transverse transport due to transverse dispersion is considered separately for ease of computation. The boundary condition, however, is different. Unlike in the partially saturated zone where the input flux entered from the upgradient face of the transport zone, the input flux for the saturated zone is from the top side of the horizontal transport zone. The contaminant can, under the appropriate conditions, disperse out of the upgradient face of the transport zone.

The solution for a volume source is obtained by integrating the solution for a plane source along the longitudinal axis. The governing evaluation for transport in the saturated zone is:

$$\lambda c_m + \frac{\partial \alpha_m}{\partial t} + V_c \frac{\partial \alpha_m}{\partial x} - D_x^c \frac{\partial^2 c_m}{\partial^2 x} = 0, \tag{3.33}$$

The boundary condition of a unit pulse across a vertical plane can be written as

$$L_y L_z \left(\theta_t + \rho_b K_d\right) c_{av}(x, t=0) = L_y L_z \theta_m R_d c_m(x, t=0) = \delta(x), \tag{3.34}$$

where

L_y = width of the primary contamination (m),

$L_z = L_x \frac{I}{V_d}$ = depth of advective penetration of the contamination into the saturated zone (m),

L_x = length of the primary contamination in the direction of groundwater flow (m), and

I = infiltration rate through the primary contamination (m yr^{-1}).

Assuming that the saturated zone is infinite in length, the global mass balance equation can be written as $L_y L_z\left(\theta_t + \rho_b K_d\right)\int_{x=0}^{x=\infty} c_{av}(x,t)dx = L_y L_z R_d \theta_m \int_{x=0}^{x=\infty} c_m(x,t)dx = e^{-\lambda t}$.

The solution to the governing equation (Equation 3.33) under the mass balance and boundary conditions is

$$c_m(x,t) = \frac{1}{L_y L_z \theta_m R_d}\sqrt{\frac{1}{4\pi D_x^c t}}\exp\left(-\frac{\left(x - V_c t\right)^2}{4D_x^c t} - \lambda t\right). \tag{3.35}$$

The flux is given by[3]

$$f\left(x,t\right) = \frac{1}{2L_y L_z}\left(V_c + \frac{x}{t}\right)\sqrt{\frac{1}{4\pi D_x^c t}}\exp\left(-\frac{\left(x - V_c t\right)^2}{4D_x^c t} - \lambda t\right). \tag{3.36}$$

The solution for an instantaneous unit release over the rectangular prism is obtained by integrating over the appropriate length of the saturated zone. The concentration at a distance x from the center of the rectangular prism is

$$c_m(x,t) = \frac{1}{L_x L_y L_z\left(\theta_m R_d\right)}\sqrt{\frac{1}{4\pi D_x^c t}}\int_{x-L_x/2}^{x+L_x/2}\exp\left(-\frac{\left(\hat{x} - V_x^c t\right)^2}{4D_x^c t} - \lambda t\right)d\hat{x}, \tag{3.37}$$

which, upon integration, yields[4]

---

[3] $f\left(x,t\right) = \theta_m V_m c_m - \theta_m D_m \frac{\partial c_m}{\partial x}$, substituting for the concentration gives

$$f\left(x,t\right) = \frac{1}{L_y L_z}\left[\frac{V_m}{R_d} - \frac{D_x}{R_d}\left(\frac{V_c t - x}{2D_x^c t}\right)\right]\sqrt{\frac{1}{4\pi D_x^c t}}e^{\left(-\frac{\left(x - V_c t\right)^2}{4D_x^c t} - \lambda t\right)}.$$

[4] Transforming the variable to recognize the error function yields

$$c_m(x,t) = \frac{1}{L_x L_y L_z\left(\theta_m R_d\right)}\frac{e^{-\lambda t}}{2}\frac{2}{\sqrt{\pi}}\int_{\frac{x-\frac{L_x}{2}-V_c t}{\sqrt{4D_x^c t}}}^{\frac{x+\frac{L_x}{2}-V_c t}{\sqrt{4D_x^c t}}}\exp\left[-\left(\frac{\hat{x} - V_c t}{\sqrt{4D_x^c t}}\right)^2\right]d\left(\frac{\hat{x} - V_c t}{\sqrt{4D_x^c t}}\right).$$

$$c_m(x,t) = \frac{\exp(-\lambda t)}{L_x L_y L_z (\theta_m R_d)} \frac{erf\left(\frac{x + L_x/2 - V_c t}{\sqrt{4D_x^c t}}\right) - erf\left(\frac{x - L_x/2 - V_c t}{\sqrt{4D_x^c t}}\right)}{2}. \quad (3.38)$$

The flux at distance x from the center of the rectangular prism is

$$f(x,t) = \frac{V_c e^{-\lambda t}}{2L_x L_y L_z}\left[erf\left(\frac{x + \frac{L_x}{2} - V_c t}{\sqrt{4D_x^c t}}\right) - erf\left(\frac{x - \frac{L_x}{2} - V_c t}{\sqrt{4D_x^c t}}\right)\right] \quad (3.39)$$

$$-\sqrt{\frac{D_x^c}{4\pi t}}\frac{e^{-\lambda t}}{L_x L_y L_z}\left[e^{-\frac{\left(x+\frac{L_x}{2}-V_c t\right)^2}{4D_x^c t}} - e^{-\frac{\left(x-\frac{L_x}{2}-V_c t\right)^2}{4D_x^c t}}\right].$$

Now include the effect of lateral dispersion. The simplified equations to be solved are

$$\frac{\partial c_m}{\partial t} - \frac{\partial^2 c_m}{\partial y^2} = 0 \text{ and } \frac{\partial c_m}{\partial t} - \frac{\partial^2 c_m}{\partial x^2} = 0. \quad (3.40)$$

By using the analogy between these equations and the equation for longitudinal transport,

$$c_m(x,y,z,t) = \frac{\exp(-\lambda t)}{8L_x L_y L_z (\theta_m R_d)}\left[erf\left(\frac{x + L_x/2 - V_c t}{\sqrt{4D_x^c t}}\right) - erf\left(\frac{x - L_x/2 - V_c t}{\sqrt{4D_x^c t}}\right)\right] \times \left[erf\left(\frac{y + L_y/2}{\sqrt{4D_y^c t}}\right) - erf\left(\frac{y - L_y/2}{\sqrt{4D_y^c t}}\right)\right]\left[erf\left(\frac{z + L_z}{\sqrt{4D_z^c t}}\right) - erf\left(\frac{z - L_z}{\sqrt{4D_z^c t}}\right)\right]. \quad (3.41)$$

A reflection will occur when the vertical concentration profile reaches the boundary of the impermeable layer underlying the aquifer. This is modeled by including a mirror source at twice the depth of the aquifer, $2H_{aq}$. Additional mirror sources are introduced each time the reflected profile reaches the water table or the lower impermeable boundary:

$$-2H_{aq}, 4H_{aq}, -4H_{aq}, 6H_{aq}, \ldots. \quad (3.42)$$

Now consider a well that obtains water from a depth d_w of the aquifer over a pumping diameter of $\phi_w = U_w/(d_w V_d)$, and is situated at a distance x_w along the plume centerline and a distance y_w perpendicular to the plume centerline from the center of the prism.

The concentration in the water extracted from the well is obtained by integrating over the region of the aquifer defined by the depth d_w and width ϕ_w:

$$c_w(x_w, y_w, t) = \frac{1}{d_w}\int_0^{d_w}\frac{1}{\varphi_w}\int_{y_w-\frac{\varphi_w}{2}}^{y_w+\frac{\varphi_w}{2}} c_m(x_w, y, z, t)\,dy\,dz\,, \tag{3.43}$$

$$c_w(x_w, y_w, t) = \frac{\exp(-\lambda t)}{2L_x L_y L_z(\theta_m R_d)}\frac{\sqrt{D_y^c t}}{\phi_w}\frac{\sqrt{D_z^c t}}{d_w}\left[erf\left(\frac{x_w + L_x/2 - V_c t}{\sqrt{4D_x^c t}}\right) - erf\left(\frac{x_w - L_x/2 - V_c t}{\sqrt{4D_x^c t}}\right)\right] \tag{3.44}$$
$$\times \int_{y_w-\frac{\phi_w}{2}}^{y_w+\frac{\phi_w}{2}}\left[erf\left(\frac{y + L_y/2}{\sqrt{4D_y^c t}}\right) - erf\left(\frac{y - L_y/2}{\sqrt{4D_y^c t}}\right)\right]\frac{dy}{\sqrt{4D_y^c t}}\int_0^{d_w}\left[erf\left(\frac{z + L_z}{\sqrt{4D_z^c t}}\right) - erf\left(\frac{z - L_z}{\sqrt{4D_z^c t}}\right)\right]\frac{dz}{\sqrt{4D_z^c t}}.$$

The integral of the error function is evaluated by using the following series for the error function, which is useful for arguments in the range -4.0 to +4.0:

$$erf(x) = \frac{2}{\sqrt{\pi}}\sum_{n=0}^{\infty}(-1)^n\frac{x^{2n+1}}{(2n+1)n!}. \tag{3.45}$$

Thus, $Interf(x) = \int_0^x erf(\hat{x})\,d\hat{x} = \frac{2}{\sqrt{\pi}}\sum_{n=0}^{\infty}\frac{x^{2n+2}}{(2n+2)(2n+1)n!}$.

The concentration in well water may be written as the product of three factors:

$$c_w(x_w, y_w, t) = c_{w,x}(x_w, t)\; c_{w,y}(y_w, t)\; c_{w,z}(t)\,, \tag{3.46}$$

where

$$c_{w,x}(x_o, t) = \frac{exp(-\lambda t)}{2L_z}\frac{V_c}{V_d L_x L_y}\left[erf\left(\frac{x + L_x/2 - V_c t}{\sqrt{4D_x^c t}}\right) - erf\left(\frac{x - L_x/2 - V_c t}{\sqrt{4D_x^c t}}\right)\right] \quad \text{and}$$

$$c_{w,y}(y_w, t) = \frac{\sqrt{D_y^c t}}{\varphi_w}\left(Interf\frac{2y_w + \varphi_w + L_y}{\sqrt{16D_y^c t}} - Interf\frac{2y_w + \varphi_w - L_y}{\sqrt{16D_y^c t}} - Interf\frac{2y_w - \varphi_w + L_y}{\sqrt{16D_y^c t}} + Interf\frac{2y_w - \varphi_w - L_y}{\sqrt{16D_y^c t}}\right),$$

with additional terms in $c_{w,z}(t)$ for reflections off the impermeable layer and the water table if necessary.

The concentration in well water can be computed by convolving the above expression for the concentration in well water due to a unit pulse input into the saturated zone, with the time-dependent input pulse obtained from the unsaturated zone transport calculations. RESRAD-OFFSITE, however, uses a further approximation to simplify the calculations in order

to (1) reduce run time, (2) to generate the transverse cross-sectional concentration profile in the aquifer at the location of the well without excessive demand on memory, and (3) to implement the subdivision of the saturated zone to better predict the transport of the progeny.

The previous expressions pertained to an instantaneous source in the shape of a rectangular prism; we now consider a point source. The concentration due to an instantaneous point source is

$$c_p(x,y,z,t) = \frac{\exp\left[-\lambda t - \frac{(x-V_c t)^2}{4D_x^c t} - \frac{y^2}{4D_y^c t} - \frac{z^2}{4D_y^c t}\right]}{(\theta_m R_d)\sqrt{4\pi D_x^c t}\sqrt{4\pi D_y^c t}\sqrt{4\pi D_z^c t}}. \quad (3.47)$$

The peak concentration at any location occurs at a time given by[5]

$$t_p = \left[-\frac{3}{2} + \sqrt{\left(\frac{3}{2}\right)^2 + \left(\lambda + \frac{V_c^2}{4D_x^c}\right)\left(\frac{x^2}{D_x^c} + \frac{y^2}{D_x^c} + \frac{z^2}{D_x^c}\right)}\right] \div \left[2\left(\lambda + \frac{V_c^2}{4D_x^c}\right)\right]. \quad (3.48)$$

More generally, the peak concentration at the centerline occurs at

$$t_p = \frac{-nD_x^c + \sqrt{\left(nD_x^c\right)^2 + \left(4\lambda D_x^c + V_c^2\right)x^2}}{\left(4\lambda D_x^c + V_c^2\right)}, \quad (3.49)$$

where n is the number of directions in which dispersion is active. Dispersion is considered to be inactive in the vertical direction, if the concentration profile in the vertical direction becomes essentially uniform because of repeated reflection of the plume by the lower impermeable layer and the water table. It is also inactive if a zero value is specified for the vertical-lateral dispersivity.

If there were no dispersion in the longitudinal direction, contaminants would show up at a point x distance away along the plume center line at a time x/V_c following an instantaneous point release. Longitudinal dispersion spreads out the contaminants and they arrive over a period of time, with the peak occurring at time t_p. The transverse profile of the concentration will vary somewhat over this period of time. In RESRAD-OFFSITE, the transverse concentration profile at time t_p is used in place of the range of profiles. The expression used by RESRAD-OFFSITE

---

5 $$\left.\frac{\partial c_p(x,y,z,t)}{\partial t}\right|_{t=t_p} = 0$$

$$\left[-\frac{3}{2t} - \lambda - \frac{V_c^2}{4D_x^c} + \frac{x^2}{4D_x^c t^2} + \frac{y^2}{4D_y^c t^2} + \frac{z^2}{4D_z^c t^2}\right] c_p(x,y,z,t)\Big|_{t=t_p} = 0.$$

for concentration in water extracted from the water sources due to an instantaneous pulse input over a region in the shape of a rectangular prism is

$$c_w(x_w, y_w, t) = c_{w,x}(x_w, t) c_{w,y}(y_w) c_{w,x}, \tag{3.50}$$

where

$$c_{w,x}(x_w, t) = \frac{\exp(-\lambda t)}{2L_x} \frac{V_c}{V_d L_y L_z} \left[erf\left(\frac{x_w + L_x/2 - V_c t}{\sqrt{4D_x^c t}} \right) - erf\left(\frac{x_w - L_x/2 - V_c t}{\sqrt{4D_x^c t}} \right) \right],$$

$$c_{w,y}(y_w) = \frac{\sqrt{D_y^c t_p}}{\phi_w} \left(Interf \frac{2y_w + \phi_w + L_y}{\sqrt{16 D_y^c t_p}} - Interf \frac{2y_w + \phi_w - L_y}{\sqrt{16 D_y^c t_p}} - Interf \frac{2y_w - \phi_w + L_y}{\sqrt{16 D_y^c t_p}} + Interf \frac{2y_w - \phi_w - L_y}{\sqrt{16 D_y^c t_p}} \right), \text{ and}$$

$$c_{w,z} = \frac{\sqrt{D_z^c t_p}}{d_w} \left(Interf \frac{d_w + L_z}{\sqrt{4 D_z^c t_p}} - Interf \frac{d_w - L_z}{\sqrt{4 D_z^c t_p}} - Interf \frac{L_z}{\sqrt{4 D_z^c t_p}} + Interf \frac{-L_z}{\sqrt{4 D_z^c t_p}} \right),$$

with additional terms in $c_{w,z}$ for reflections off the lower impermeable layer and the water table if necessary.

The above expression for concentration due to a unit pulse input into the saturated zone is convolved numerically with the time-dependent input pulse obtained from the unsaturated zone transport calculations to compute the concentration in the well water. Under the peak time approximation, the shapes of the lateral profiles are independent of time; *cw*,*y*(*yo*)and *cw*,*z* are computed once outside the convolution.

When the user chooses to model vertical transverse dispersion, the code does not consider the effects of any clear infiltration along the length of offsite transport. On the other hand, if the user chooses not to model vertical transverse dispersion, the effects of clean infiltration along the length of offsite transport is modeled by using the following expression:

$$c_{w,z} = \max\left(0, \min\left(d_w, \frac{(x + L_x) I}{V_d} \right) - \frac{xI}{V_d} \right) \Big/ d_w . \tag{3.51}$$

The effect of lateral dispersion on the radionuclide flux entering the surface water body is modeled in a similar manner. The flux into a surface water body is

$$f_s(x_s, y_n, y_f, t) = f_{s,x}(x_s, t) f_{s,y}(y_n, y_f) f_{s,z}, \tag{3.52}$$

where

$$f_{s,x}(x_s,t)=\frac{V_c e^{-\lambda t}}{2L_xL_yL_z}\left[erf\left(\frac{x_s+\frac{L_x}{2}-V_ct}{\sqrt{4D_x^ct}}\right)-erf\left(\frac{x_s-\frac{L_x}{2}-V_ct}{\sqrt{4D_x^ct}}\right)\right]-\sqrt{\frac{D_x^c}{4\pi t}}\frac{e^{-\lambda t}}{L_xL_yL_z}\left[e^{-\frac{\left(x_s+\frac{L_x}{2}-V_ct\right)^2}{4D_x^ct}}-e^{-\frac{\left(x_s-\frac{L_x}{2}-V_ct\right)^2}{4D_x^ct}}\right],$$

$$f_{s,y}(y_n,y_f)=\sqrt{D_y^ct_p}\left(Interf\frac{2y_f+L_y}{\sqrt{16D_y^ct_p}}-Interf\frac{2y_f-L_y}{\sqrt{16D_y^ct_p}}-Interf\frac{2y_n+L_y}{\sqrt{16D_y^ct_p}}+Interf\frac{2y_n-L_y}{\sqrt{16D_y^ct_p}}\right),$$

$$f_{s,z}=\sqrt{D_z^ct_p}\left(Interf\frac{d_s+L_z}{\sqrt{4D_z^ct_p}}-Interf\frac{d_s-L_z}{\sqrt{4D_z^ct_p}}-Interf\frac{L_z}{\sqrt{4D_z^ct_p}}+Interf\frac{-L_z}{\sqrt{4D_z^ct_p}}\right),$$

x_S = distance along the plume centerline from the center of the rectangular prism source to the center of the surface water body (m),

y_n = distance from the plume center line to the near edge of the surface water body (m),

y_f = distance from the plume center line to the far edge of the surface water body (m), and

d = depth of the aquifer contributing to the surface water body (m).

The above expression for flux due to a unit pulse input into the saturated zone is convolved numerically with the time-dependent input pulse obtained from the unsaturated zone transport calculations to compute the flux to the surface water body. Under the peak time approximation, the shapes of the lateral profiles are independent of time; $f_{s,y}(y_n, y_f)$ and $f_{s,z}$ are computed once outside the convolution.

3.2.5 Concentration and Flux of Radionuclides That Were Produced by Radiological Transformations within the Transport Layer from a Pulse Input

As in the case of the flux input (Section 3.2.3), RESRAD-OFFSITE contains two solutions for the transport of progeny produced in transit. One is applicable when longitudinal dispersion is dominant, and the other is for cases where the differences in the distribution coefficients of the parent and progeny are significant. Situations where both processes are of comparable importance can be modeled by subdividing the transport layer as discussed in Section 3.3.13.

3.2.5.1 Concentration and Flux of Radionuclides That Were Produced by Radiological Transformations within the Transport Layer When Dispersion Is Dominant, from a Pulse Input

The solution in this case is obtained under the assumption that the nuclides in the transformation chain form the parent that enters the zone to the progeny that exits the zone, all travel at the same velocity, and that they partition between the aqueous and solid phases of the soil in the same proportion. The transport can then be separated out from the ingrowth, and the concentration of the k^{th} progeny in well water, resulting from an instantaneous unit flux of the parent is given by

$$c_w^k(x_o, y_o, t) = c_{w,x}^k(x_o, t) c_{w,y}(y_o) c_{w,z}, \tag{3.53}$$

where

$$c_{w,x}^k(x_o, t) = \sum_{i=1}^{k} a_{k,i} \frac{e^{-\lambda_i t}}{2L_x} \frac{V_c}{V_d L_y L_z} \left[erf\left(\frac{x + L_x/2 - V_c t}{\sqrt{4D_x^c t}} \right) - erf\left(\frac{x - L_x/2 - V_c t}{\sqrt{4D_x^c t}} \right) \right]$$

$c_{w,y}(y_O)$, $c_{w,z}$ = same as in Equations 3.50 and 3.51,

$a_{k,i}$ = a set of coefficients defined by $a_{1,1} = 1$,

$$a_{k,i} = \frac{\lambda_k a_{k-1,i}}{\lambda_k - \lambda_i} \text{ for all } 1 \le i < k \text{, and}$$

$$a_{k,k} = -\sum_{i=1}^{k-1} a_{k,i} .$$

The flux of the k^{th} progeny to the surface water body is given by

$$f_s^k(x_s, y_n, y_f, t) = f_{s,x}^k(x_s, t) f_{s,y}(y_n, y_f) f_{s,z}, \tag{3.54}$$

where

$$f_{s,x}^k(x_s, t) = \sum_{i=1}^{k} \frac{a_{k,i} e^{-\lambda t}}{L_x L_y L_z} \left[\frac{V_c}{2} \left\{ erf\left(\frac{x_s + \frac{L_x}{2} - V_c t}{\sqrt{4D_x^c t}} \right) - erf\left(\frac{x_s - \frac{L_x}{2} - V_c t}{\sqrt{4D_x^c t}} \right) \right\} - \sqrt{\frac{D_x^c}{4\pi t}} \left\{ e^{-\frac{\left(x_s + \frac{L_x}{2} - V_c t\right)^2}{4D_x^c t}} - e^{-\frac{\left(x_s - \frac{L_x}{2} - V_c t\right)^2}{4D_x^c t}} \right\} \right],$$

$f_{s,y}(y_n, y_f)$, $f_{s,z}$ = same as in Equation 3.52.

The above expressions for concentration and flux due to a unit pulse input into the saturated zone is convolved numerically with the time-dependent input pulse obtained from the unsaturated

zone transport calculations to compute the concentration in well water and the flux to the surface water body. Under the peak time approximation, the shapes of the lateral profiles are independent of time; the expressions for the effects of lateral dispersion are computed once outside the convolution.

3.2.5.2 Concentration and Flux of Radionuclides That Were Produced by Radiological Transformations within the Transport Zone When Differences in Their Distribution Coefficients Are Dominant, from a Pulse Input

The solution in this case is obtained by ignoring longitudinal dispersion. The derivation of the solution for the first three members of a transport chain is discussed in Appendix I of the User's Manual for RESRAD Version 6 (Yu et al. 2001). The solutions are expressed in terms of the onsite and offsite contaminant travel times, $T_{i,on}$ and $T_{i,off}$. Subscripts i, j, k, l, m are used to describe the nuclides of the transport chain in the order in which they occur in the transformation chain, while subscripts 1, 2, 3, 4, 5 are used to describe the nuclides sorted in ascending order of the travel time. The transfer functions are all of the form

$$f_k(z,t) = \frac{\lambda_k}{\lambda_i} \sum \gamma \exp\left(\alpha_{i,j} t + \beta_{i,j} T_{i,off} + \beta_{i,j} T_{1,on} y(t)\right) , \quad (3.55)$$

where

$\gamma, \alpha_{i,j}, \beta_{i,j}$ = all functions of the radiological transformation constants and the ratios of the travel times of the radionuclides and the travel time of the fastest radionuclide of the transport chain,

$T_{i,off}$ = offsite travel time of the fastest radionuclide of the transport chain,

$T_{i,on}$ = onsite travel time of the fastest radionuclide of the transport chain, and

$y(t)$ = onsite travel distance.

The above expression for flux due to a unit pulse input into the saturated zone is convolved numerically with the time-dependent input pulse obtained from the unsaturated zone transport calculations to compute the advective flux. The concentration, in this case, is obtained by dividing the advective flux by the volumetric flow rate.

3.3 IMPLEMENTATION OF THE GROUNDWATER TRANSPORT MODELS

This section describes how the expressions derived from the conceptual model (Section 3.2) are implemented in the computational code. As shown in Figure 3.1, modeling the transport in the partially saturated zone involves predicting the flux out of the zone that is a result

of the known flux into the zone. The implementation of the expressions for output flux resulting from an input flux is discussed in Sections 3.3.1 through 3.3.3. Section 3.3.1 deals with those atoms that traveled across the transport zone without undergoing any radioactive transformations, while Sections 3.3.2 and 3.3.3 give the two alternative formulations for those atoms that underwent radioactive transformations during their travel across the transport zone. Sections 3.3.4 through 3.3.9 deal with the implementation of the expressions for the output flux or the concentration in well water resulting from a pulse input. Sections 3.3.10, 3.3.11, and 3.3.12 deal with the implementation of the expressions for the concentration in well water that results from an input flux. Although the concentration from a flux input is not necessary for the conceptual model depicted in Figure 3.1, it is utilized in Section 3.3.13, where a method for improving the modeling of progeny produced in transit is discussed.

3.3.1 Output Flux Resulting from an Input Flux for Radionuclides That Traversed the Layer in the Same Form

In RESRAD-OFFSITE, the fluxes entering a layer are known at each of a series of times. Assuming that the fluxes entering a layer vary linearly between those times, an analytical solution for the flux exiting the layer can be obtained as follows.

Let the input fluxes at times t_1 and t_2 be $f(0,t_1)$ and $f(0,t_2)$, respectively.

Applying the expression developed in Section 3.2.2, the output flux at a distance z at time $t_n > t_2 > t_1$ due to the input flux entering between times t_1 and t_2 is obtained by the convolution:

$$f_{t_1}^{t_2}(z,t_n) = \int_{t_n-t_2}^{t_n-t_1} f(0,t_n-\tau)\frac{z}{\tau}\sqrt{\frac{1}{4\pi D_z^c \tau}}\exp\left(-\frac{(z-V_c\tau)^2}{4D_z^c\tau}-\lambda\tau\right)d\tau\,. \tag{3.56}$$

Approximate the input flux during that time interval by linear interpolation:

$$f(0,t_1 \le t_n-\tau \le t_2) = f(0,t_1)\frac{t_2-(t_n-\tau)}{t_2-t_1} + f(0,t_2)\frac{(t_n-\tau)-t_1}{t_2-t_1}\,. \tag{3.57}$$

By rearranging in terms of τ,

$$f(0,t_1 \le t_n-\tau \le t_2) = a + b\tau\,,$$

where

$$a = f(0,t_1)\frac{t_2-t_n}{t_2-t_1} + f(0,t_2)\frac{t_n-t_1}{t_2-t_1}\,, \text{ and}$$

$$b = \frac{f(0,t_1)-f(0,t_2)}{t_2-t_1}\,.$$

Substituting the linear interpolation in the convolution gives

$$f_{t_1}^{t_2}(z,t_n) = \int_{t_n-t_2}^{t_n-t_1} (a+b\tau)\frac{z}{\tau}\sqrt{\frac{1}{4\pi D_z^c \tau}}\exp\left(-\frac{(z-V_c\tau)^2}{4D_z^c\tau} - \lambda\tau\right)d\tau\,. \tag{3.58}$$

The convolution can be performed analytically[6] to give

$$f_{t_1}^{t_2}(z,t_n) = \frac{1}{2}\left(a+\frac{bz}{\sqrt{V_c^2+4D_z^c\lambda}}\right)exp\left(\frac{z\left(V_c-\sqrt{V_c^2+4D_z^c\lambda}\right)}{2D_z^c}\right)\left[erf\left(\frac{z-\sqrt{V_c^2+4D_z^c\lambda}(t_n-t_2)}{\sqrt{4D_z^c(t_n-t_2)}}\right)-erf\left(\frac{z-\sqrt{V_c^2+4D_z^c\lambda}(t_n-t_1)}{\sqrt{4D_z^c(t_n-t_1)}}\right)\right] \tag{3.59}$$

$$+\frac{1}{2}\left(a-\frac{bz}{\sqrt{V_c^2+4D_z^c\lambda}}\right)exp\left(\frac{z\left(V_c+\sqrt{V_c^2+4D_z^c\lambda}\right)}{2D_z^c}\right)\left[erf\left(\frac{z+\sqrt{V_c^2+4D_z^c\lambda}(t_n-t_2)}{\sqrt{4D_z^c(t_n-t_2)}}\right)-erf\left(\frac{z+\sqrt{V_c^2+4D_z^c\lambda}(t_n-t_1)}{\sqrt{4D_z^c(t_n-t_1)}}\right)\right].$$

The flux exiting the layer at the n^{th} time point is obtained by summing the contributions of the input fluxes over the preceding $n-1$ time intervals.

---

6 First recognize that the exponent of the exponential part of the integrand can be written as

$$\frac{(z-V_c\tau)^2}{4D_z^c\tau}+\lambda\tau = \frac{\left(z-\sqrt{V_c^2+4D_z^c\lambda}\tau\right)^2}{4D_z^c\tau} - \frac{zV_c}{2D_z^c} + \frac{z\sqrt{V_c^2+4D_z^c\lambda}}{2D_z^c} = \frac{\left(z+\sqrt{V_c^2+4D_z^c\lambda}\tau\right)^2}{4D_z^c\tau} - \frac{zV_c}{2D_z^c} - \frac{z\sqrt{V_c^2+4D_z^c\lambda}}{2D_z^c}\,,$$

and write the nonexponential part of the integrand as

$$(a+b\tau)\frac{z}{\tau}\frac{1}{\sqrt{4\pi D_z^c\tau}} = \frac{-1}{\sqrt{\pi}}\left(a+\frac{bz}{\sqrt{V_c^2+4D_z^c\lambda}}\right)\left(\frac{z}{\sqrt{4D_z^c\tau}}\frac{-1}{2\tau}-\sqrt{\frac{\left(V_c^2+4D_z^c\lambda\right)\tau}{4D_z^c}}\frac{1}{2\tau}\right)$$

$$+\frac{-1}{\sqrt{\pi}}\left(a-\frac{bz}{\sqrt{V_c^2+4D_z^c\lambda}}\right)\left(\frac{z}{\sqrt{4D_z^c\tau}}\frac{-1}{2\tau}+\sqrt{\frac{\left(V_c^2+4D_z^c\lambda\right)\tau}{4D_z^c}}\frac{1}{2\tau}\right)$$

in order to transform the variables to $\dfrac{z\pm\sqrt{V_c^2+4D_z^c\lambda}\tau}{\sqrt{4D_z^c\tau}}$ for the two components. Then the convolution can be expressed as the sum of two integrals that are recognizable as error functions, namely,

$$\frac{1}{2}\left(a+\frac{bz}{\sqrt{V_c^2+4D_z^c\lambda}}\right)\exp\frac{z\left(V_c-\sqrt{V_c^2+4D_z^c\lambda}\right)}{2D_z^c}\int\frac{2}{\sqrt{\pi}}\exp\left[-\left(\frac{z-\sqrt{V_c^2+4D_z^c\lambda}\tau}{\sqrt{4D_z^c\tau}}\right)^2\right]d\left(\frac{z-\sqrt{V_c^2+4D_z^c\lambda}\tau}{\sqrt{4D_z^c\tau}}\right)$$

and

$$\frac{1}{2}\left(a-\frac{bz}{\sqrt{V_c^2+4D_z^c\lambda}}\right)\exp\frac{z\left(V_c+\sqrt{V_c^2+4D_z^c\lambda}\right)}{2D_z^c}\int\frac{2}{\sqrt{\pi}}\exp\left[-\left(\frac{z+\sqrt{V_c^2+4D_z^c\lambda}\tau}{\sqrt{4D_z^c\tau}}\right)^2\right]d\left(\frac{z+\sqrt{V_c^2+4D_z^c\lambda}\tau}{\sqrt{4D_z^c\tau}}\right).$$

$$f(z,t_n) = \sum_{m=1}^{n-1}\frac{1}{2}\left(a_m + \frac{b_m z}{\sqrt{V_c^2+4D_z^c\lambda}}\right)exp\frac{z\left(V_c-\sqrt{V_c^2+4D_z^c\lambda}\right)}{2D_z^c}\left[erf\left(\frac{z-\sqrt{V_c^2+4D_z^c\lambda}(t_n-t_{m+1})}{\sqrt{4D_z^c(t_n-t_{m+1})}}\right)-erf\left(\frac{z-\sqrt{V_c^2+4D_z^c\lambda}(t_n-t_m)}{\sqrt{4D_z^c(t_n-t_m)}}\right)\right] \quad (3.60)$$

$$+\sum_{m=1}^{n-1}\frac{1}{2}\left(a_m - \frac{b_m z}{\sqrt{V_c^2+4D_z^c\lambda}}\right)exp\frac{z\left(V_c+\sqrt{V_c^2+4D_z^c\lambda}\right)}{2D_z^c}\left[erf\left(\frac{z+\sqrt{V_c^2+4D_z^c\lambda}(t_n-t_{m+1})}{\sqrt{4D_z^c(t_n-t_{m+1})}}\right)-erf\left(\frac{z+\sqrt{V_c^2+4D_z^c\lambda}(t_n-t_m)}{\sqrt{4D_z^c(t_n-t_m)}}\right)\right],$$

with

$$a_m = f(0,t_m)\frac{t_{m+1}-t_n}{t_{m+1}-t_m} + f(0,t_{m+1})\frac{t_n-t_m}{t_{m+1}-t_m} \text{ and } b_m = \frac{f(0,t_m)-f(0,t_{m+1})}{t_{m+1}-t_m}.$$

This expression is semianalytical, that is, part of this analytical expression, specifically the error function, has to be evaluated numerically. The error functions in this expression are dependent only on the length of the transport zone, the contaminant transport velocity, contaminant dispersion coefficient, the radiological transformation rate, and on the time intervals between the intermediate times; they are independent of the (time dependent) flux coefficients a_m and b_m. If the intermediate time points are spaced linearly, then the time interval $(t_n - t_m)$ depends only on the difference $n-m$ and not on the value of n. For example, the time interval between the first and the 20th intermediate time point will be same as the time interval between the 21st and 40th intermediate time points. Thus when the linear spacing option is chosen, the error function for all the appropriate time intervals can be computed once and stored in memory for subsequent use, thus reducing the run time.

3.3.2 Output Flux Resulting from an Input Flux for Radionuclides That Were Produced by Radiological Transformations within the Transport Layer When Dispersion Is Dominant

Let the input fluxes of the parent nuclide entering the transport layer be $f_1(0, t_1)$ and $f(0, t_2)$, respectively, at times t_1 and t_2.

Applying the expression developed in Section 3.2.3.1, the output flux of the k^{th} progeny at a distance z at time $t_n > t_2 > t_1$, due to the input flux of the parent nuclide between times t_1 and t_2, is obtained by the convolution:

$$f_{k\,t_1}^{t_2}(z,t_n) = \sum_{i=1}^{k} a_{k,i}\int_{t_n-t_2}^{t_n-t_1} f_1(0,t_n-\tau)\frac{z}{\tau}\sqrt{\frac{1}{4\pi D_z^c\tau}}\exp\left(-\frac{(z-V_c\tau)^2}{4D_z^c\tau}-\lambda_i\tau\right)d\tau\,. \quad (3.61)$$

The flux of the k^{th} nuclide of the transformation chain exiting the layer at the end of the n^{th} time point is obtained by summing the contributions of the input fluxes over the preceding $n-1$ time intervals as in Section 3.3.1:

$$f_k(z,t_n) = \sum_{m=1}^{n-1}\sum_{i=1}^{k}\frac{a_{k,i}}{2}\left(a_m + \frac{b_m z}{\sqrt{V_c^2 + 4D_z^c\lambda_i}}\right) exp\frac{z\left(V_c - \sqrt{V_c^2 + 4D_z^c\lambda_i}\right)}{2D_z^c}\left[erf\left(\frac{z - \sqrt{V_c^2 + 4D_z^c\lambda_i}\,(t_n - t_{m+1})}{\sqrt{4D_z^c(t_n - t_{m+1})}}\right) - erf\left(\frac{z - \sqrt{V_c^2 + 4D_z^c\lambda_i}\,(t_n - t_m)}{\sqrt{4D_z^c(t_n - t_m)}}\right)\right] \quad (3.62)$$

$$+ \sum_{m=1}^{n-1}\sum_{i=1}^{k}\frac{a_{k,i}}{2}\left(a_m - \frac{b_m z}{\sqrt{V_c^2 + 4D_z^c\lambda_i}}\right) exp\frac{z\left(V_c + \sqrt{V_c^2 + 4D_z^c\lambda_i}\right)}{2D_z^c}\left[erf\left(\frac{z + \sqrt{V_c^2 + 4D_z^c\lambda_i}\,(t_n - t_{m+1})}{\sqrt{4D_z^c(t_n - t_{m+1})}}\right) - erf\left(\frac{z + \sqrt{V_c^2 + 4D_z^c\lambda_i}\,(t_n - t_m)}{\sqrt{4D_z^c(t_n - t_m)}}\right)\right].$$

The code uses this solution if all the nuclides in the transformation chain from the parent entering the transport zone to the progeny exiting the zone have the same distribution coefficient. In this case, all these nuclides under consideration will have the same transport velocity and the same dispersion coefficient. Even in cases where these nuclides have different distribution coefficients, it is possible to instruct the code to use this equation to model the transport of the progeny produced in transit. When this choice is made, it is also necessary to make a choice of whether to use the distribution coefficient of the parent or the distribution coefficient of the progeny to calculate the transport velocity and the dispersion coefficient of these nuclides. When the linear spacing option is chosen for the intermediate time points, the error function for all the appropriate time intervals is computed once and stored in memory for subsequent use for the reasons mentioned previously.

3.3.3 Output Flux Resulting from an Input Flux for Radionuclides That Were Produced by Radiological Transformations within the Transport Layer When Differences in Their Distribution Coefficients Are Dominant

In RESRAD-OFFSITE, the fluxes entering a layer are known at each of a series of times. Assuming that the fluxes entering a layer vary linearly between the fluxes at the intermediate times and applying the expression developed in Section 3.2.3.2, an analytical solution for the output flux of the k^{th} progeny at a distance z at time $t_n > t_2 > t_1$, due to the input flux of the parent nuclide between times t_1 and t_2 , is obtained by the convolution:

$$f_{k\,t_1}^{t_2}(z,t_n) = \int_{t_n - t_2}^{t_n - t_1}(a + b\tau)\frac{\lambda_k}{\lambda_1}\sum_{i,j}\gamma\exp\left(\alpha_{i,j}\tau + \beta_{i,j}T_1\right)d\tau\,. \quad (3.63)$$

The convolution can be performed analytically[7] to give

$$f_{k\,t_1}^{\,t_2}(z,t_n)=\frac{\lambda_k}{\lambda_1}\sum_{i,j}\gamma\left[\frac{\alpha_{i,j}a-b}{\alpha_{i,j}^2}\left(e^{\alpha_{i,j}(t_n-t_1)+\beta_{i,j}T_1}-e^{\alpha_{i,j}(t_n-t_2)+\beta_{i,j}T_1}\right)\right.$$
$$\left.+\frac{b(t_n-t_1)}{\alpha_{i,j}}e^{\alpha_{i,j}(t_n-t_1)+\beta_{i,j}T_1}-\frac{b(t_n-t_2)}{\alpha_{i,j}}e^{\alpha_{i,j}(t_n-t_2)+\beta_{i,j}T_1}\right]. \quad (3.64)$$

The flux exiting the layer at the end of the n^{th} time point is obtained by summing the contributions of the input fluxes over the preceding $n-1$ time intervals.

$$f_k(z,t_n)=\frac{\lambda_k}{\lambda_1}\sum_{m=1}^{n-1}\sum_{i,j}\gamma\left[\frac{\alpha_{i,j}a_m-b_m}{\alpha_{i,j}^2}\left(e^{\alpha_{i,j}(t_n-t_m)+\beta_{i,j}T_1}-e^{\alpha_{i,j}(t_n-t_{m+1})+\beta_{i,j}T_1}\right)\right.$$
$$\left.+\frac{b_m(t_n-t_m)}{\alpha_{i,j}}e^{\alpha_{i,j}(t_n-t_m)+\beta_{i,j}T_1}-\frac{b_m(t_n-t_{m+1})}{\alpha_{i,j}}e^{\alpha_{i,j}(t_n-t_{m+1})+\beta_{i,j}T_1}\right]. \quad (3.65)$$

This expression is a linear function of the time-dependent flux coefficients a_m and b_m, the rest of the expression consists of the advective travel times, T_i, of the nuclides in the transformation chain, the coefficients $\alpha_{i,j}$, $\beta_{i,j}$, which are functions of the ratios of the advective travel times, and the radiological transformation constants of the nuclides in the transformation chain, and the time intervals between the intermediate times. If the intermediate time points are spaced linearly, then the time interval $(t_n - t_m)$ depends only on the difference $n - m$ and not on the value of n. Thus when the linear spacing option is chosen, the output flux from a unit input flux can be computed once for all the appropriate time intervals and stored in memory for subsequent use with the appropriate flux, thus reducing the run time.

3.3.4 Output Flux Resulting from a Pulse Input for Radionuclides That Traversed the Layer in the Same Form

In RESRAD-OFFSITE, the fluxes entering the water table across the footprint of the primary contamination are known at each of a series of times. The spatially integrated flux across a vertical plane in the saturated zone, at a distance x downgradient of the center of the primary contamination, is obtained as follows.

---

7 $f_{k\,t_1}^{\,t_2}(z,t_n)=\frac{\lambda_k}{\lambda_1}\sum_{i,j}\gamma\int_{t_n-t_2}^{t_n-t_1}(a+b\tau)\exp(\alpha_{i,j}t+\beta_{i,j}T_1)d\tau$ and

$$f_{k\,t_1}^{\,t_2}(z,t_n)=\frac{\lambda_k}{\lambda_1}\sum_{i,j}\gamma\left[\frac{a+b\tau}{\alpha_{i,j}}\exp(\alpha_{i,j}\tau+\beta_{i,j}T_1)-\frac{b}{\alpha_{i,j}^2}\exp(\alpha_{i,j}\tau+\beta_{i,j}T_1)\right]_{t_n-t_2}^{t_n-t_1}.$$

Let the spatially integrated flux at the water table at time t be $F_{wt}(t)$.

By applying the expression developed in Section 3.2.4, the spatially integrated output flux at time t_n is obtained by the convolution:

$$F(x,t_n) = L_y L_z \int_0^{t_n} F_{wt}(t_n - \tau) \left\{ \begin{array}{l} \dfrac{V_c e^{-\lambda\tau}}{2L_x L_y L_z} \left[erf\left(\dfrac{x + \dfrac{L_x}{2} - V_c\tau}{\sqrt{4D_x^c \tau}} \right) - erf\left(\dfrac{x - \dfrac{L_x}{2} - V_c\tau}{\sqrt{4D_x^c \tau}} \right) \right] \\ \\ - \sqrt{\dfrac{D_x^c}{4\pi t}} \dfrac{e^{-\lambda\tau}}{L_x L_y L_z} \left[e^{-\frac{\left(x + \frac{L_x}{2} - V_c\tau\right)^2}{4D_x^c\tau}} - e^{-\frac{\left(x - \frac{L_x}{2} - V_c\tau\right)^2}{4D_x^c\tau}} \right] \end{array} \right\} d\tau \,. \quad (3.66)$$

This is evaluated numerically by using either Simpson's (parabolic) formula or Romberg's method (Section 3.3.14), assuming that the flux to the water table varies linearly between the values at the intermediate times.

As in the previous cases, substantial savings in computation time can be achieved if the intermediate times are in a linear series. Two transfer functions are computed for each time interval. The first is for a flux that increases linearly from zero at time t_{m-1} to one at time t_m, and the second is for a flux that decreases linearly from one at time t_{m-1} to zero at time t_m.

$$f_1(x, t_n - t_m) = \int_{t_n - t_m}^{t_n - t_{m-1}} \left(\frac{t_n - t_{m-1} - \tau}{t_m - t_{m-1}} \right) \left\{ \begin{array}{l} \dfrac{V_c e^{-\lambda\tau}}{2L_x} \left[erf\left(\dfrac{x + \dfrac{L_x}{2} - V_c\tau}{\sqrt{4D_x^c \tau}} \right) - erf\left(\dfrac{x - \dfrac{L_x}{2} - V_c\tau}{\sqrt{4D_x^c \tau}} \right) \right] \\ \\ - \sqrt{\dfrac{D_x^c}{4\pi t}} \dfrac{e^{-\lambda\tau}}{L_x} \left[e^{-\frac{\left(x + \frac{L_x}{2} - V_c\tau\right)^2}{4D_x^c\tau}} - e^{-\frac{\left(x - \frac{L_x}{2} - V_c\tau\right)^2}{4D_x^c\tau}} \right] \end{array} \right\} d\tau \,. \quad (3.67)$$

$$f_2(x, t_n - t_{m-1}) = \int_{t_n - t_m}^{t_n - t_{m-1}} \left(\frac{\tau - t_n + t_m}{t_m - t_{m-1}} \right) \left\{ \begin{array}{l} \dfrac{V_c e^{-\lambda\tau}}{2L_x} \left[erf\left(\dfrac{x + \dfrac{L_x}{2} - V_c\tau}{\sqrt{4D_x^c \tau}} \right) - erf\left(\dfrac{x - \dfrac{L_x}{2} - V_c\tau}{\sqrt{4D_x^c \tau}} \right) \right] \\ \\ - \sqrt{\dfrac{D_x^c}{4\pi t}} \dfrac{e^{-\lambda\tau}}{L_x} \left[e^{-\frac{\left(x + \frac{L_x}{2} - V_c\tau\right)^2}{4D_x^c\tau}} - e^{-\frac{\left(x - \frac{L_x}{2} - V_c\tau\right)^2}{4D_x^c\tau}} \right] \end{array} \right\} d\tau \,. \quad (3.68)$$

Both of these are evaluated numerically by using either Simpson's (parabolic) formula or Romberg's method (Section 3.3.14) and stored in memory for subsequent use with the appropriate flux.

Then the spatially integrated flux across the vertical plane is obtained by summing the contributions of all the relevant time intervals,

$$F(x,t_n) = \sum_{m=1}^{n-1} F_{wt}(t_m)\left(f_1(x,t_n - t_m) + f_2(x,t_n - t_m)\right) . \tag{3.69}$$

The nuclide enters the surface water body through a rectangle of finite dimensions, a subsection of the vertical plane. This is accounted for by using the expressions derived in Section 3.2.4, as follows:

$$F_{sw}(x,t_n) = F(x,t_n)\frac{f_{s,y}(y_n, y_f)}{L_y}\frac{f_{s,z}}{L_z} , \tag{3.70}$$

where

$$f_{s,y}(y_n, y_f) = \sqrt{D_y^c t_p}\left(Interf\frac{2y_f + L_y}{\sqrt{16D_y^c t_p}} - Interf\frac{2y_f - L_y}{\sqrt{16D_y^c t_p}} - Interf\frac{2y_n + L_y}{\sqrt{16D_y^c t_p}} + Interf\frac{2y_n - L_y}{\sqrt{16D_y^c t_p}}\right) ,$$

and

$$f_{s,z} = \sqrt{D_z^c t_p}\left(Interf\frac{d_s + L_z}{\sqrt{4D_z^c t_p}} - Interf\frac{d_s - L_z}{\sqrt{4D_z^c t_p}} - Interf\frac{L_z}{\sqrt{4D_z^c t_p}} + Interf\frac{-L_z}{\sqrt{4D_z^c t_p}}\right) ,$$

or

$$f_{s,z} = \max\left(0, \min\left(d_s, \frac{(x + L_x)I}{V_d}\right) - \frac{xI}{V_d}\right),$$

depending on whether the dispersivity in the vertical direction is nonzero or not. The expression for $f_{s,z}$ will contain additional terms for every reflection of the dispersion plume at the lower impervious boundary and at the water table.

3.3.5 Concentration in Well Water Resulting from a Pulse Input for Radionuclides That Traversed the Layer in the Same Form

In RESRAD-OFFSITE, the fluxes entering the water table across the footprint of the primary contamination are known at each of a series of times. The concentration in well water is obtained as follows.

Let the spatially integrated flux at the water table at time t be $F_{wt}(t)$.

By applying the expression developed in Section 3.2.4, the concentration in well water at time t_n is obtained by the convolution:

$$c_{well}(x_w, y_w, t_n) = c_{w,z} c_{w,y}(y_w) \frac{V_c}{2V_d L_y L_z L_x} \int_0^{t_n} F_{wt}(t_n - \tau) e^{-\lambda\tau} \left[\begin{array}{l} erf\left(\dfrac{x_w + L_x/2 - V_c\tau}{\sqrt{4D_x^c \tau}} \right) \\ \\ - erf\left(\dfrac{x_w - L_x/2 - V_c\tau}{\sqrt{4D_x^c \tau}} \right) \end{array} \right] d\tau , \qquad (3.71)$$

where

$$c_{w,y}(y_w) = \frac{\sqrt{D_y^c t_p}}{\varphi_w} \left(\begin{array}{l} Interf \dfrac{2y_w + \varphi_w + L_y}{\sqrt{16 D_y^c t_p}} - Interf \dfrac{2y_w + \varphi_w - L_y}{\sqrt{16 D_y^c t_p}} \\ \\ - Interf \dfrac{2y_w - \varphi_w + L_y}{\sqrt{16 D_y^c t_p}} + Interf \dfrac{2y_w - \varphi_w - L_y}{\sqrt{16 D_y^c t_p}} \end{array} \right) ,$$

and

$$c_{w,z} = \frac{\sqrt{D_z^c t_p}}{d_w} \left(\begin{array}{l} Interf \dfrac{d_w + L_z}{\sqrt{4 D_z^c t_p}} - Interf \dfrac{d_w - L_z}{\sqrt{4 D_z^c t_p}} \\ \\ - Interf \dfrac{L_z}{\sqrt{4 D_z^c t_p}} + Interf \dfrac{-L_z}{\sqrt{4 D_z^c t_p}} \end{array} \right) ,$$

or

$$c_{w,z} = \max\left(0, \min\left(d_w, \frac{(x + L_x) I}{V_d} \right) - \frac{xI}{V_d} \right) \Big/ d_w \ ,$$

depending on whether the dispersivity in the vertical direction is nonzero or not, with additional terms in $c_{w,z}$ for reflections off the lower impermeable layer and the water table if necessary.

This is evaluated numerically using either the Simpson's (parabolic) formula or Romberg's method (Section 3.3.14), assuming that the flux to the water table varies linearly between the values at the intermediate times.

As in the previous cases, substantial savings in computational time can be achieved if the intermediate times are in a linear series. Two transfer functions are computed for each time interval. The first is for a flux that increases linearly from zero at time $t_{m\text{-}1}$ to one at time t_m, and the second is for a flux that decreases linearly from one at time $t_{m\text{-}1}$ to zero at time t_m.

$$f_1(x,t_n - t_m) = \int_{t_n - t_m}^{t_n - t_{m-1}} \left(\frac{t_n - t_{m-1} - \tau}{t_m - t_{m-1}} \right) \frac{V_c e^{-\lambda\tau}}{2L_x V_d L_y L_z} \left[erf\left(\frac{x + L_x/2 - V_c\tau}{\sqrt{4D_x^c \tau}} \right) - erf\left(\frac{x - L_x/2 - V_c\tau}{\sqrt{4D_x^c \tau}} \right) \right] d\tau \qquad (3.72)$$

$$f_2(x,t_n - t_{m-1}) = \int_{t_n - t_m}^{t_n - t_{m-1}} \left(\frac{\tau - t_n + t_m}{t_m - t_{m-1}} \right) \frac{V_c e^{-\lambda\tau}}{2L_x V_d L_y L_z} \left[erf\left(\frac{x + L_x/2 - V_c\tau}{\sqrt{4D_x^c \tau}} \right) - erf\left(\frac{x - L_x/2 - V_c\tau}{\sqrt{4D_x^c \tau}} \right) \right] d\tau \ . \qquad (3.73)$$

Both of these are evaluated numerically using either the Simpson's (parabolic) formula or Romberg's method (Section 3.3.14) and stored in memory for subsequent use with the appropriate flux.

Then the concentration in well water is obtained by summing the contributions of all the relevant time intervals,

$$c_{well}(x_w, y_w, t_0) = c_{w,z} c_{w,y}(y_w) \sum_{m=1}^{n-1} F_{wt}(t_m) \left(f_1(x, t_0 - t_m) + f_2(x, t_0 - t_m) \right) \ . \qquad (3.74)$$

3.3.6 Output Flux Resulting from a Pulse Input for Radionuclides That Were Produced by Radiological Transformations within the Transport Layer When Dispersion Is Dominant

In RESRAD-OFFSITE, the fluxes entering the water table across the footprint of the primary contamination are known at each of a series of times. The spatially integrated flux of the k^{th} progeny across a vertical plane in the saturated zone, at a distance x downgradient of the center of the primary contamination, is obtained as follows.

Let the spatially integrated flux of the parent nuclide across the water table at time t be $F_{wt}(t)$. By applying the expression developed in Section 3.2.5.1, the spatially integrated output flux at time t_n is obtained by the convolution:

$$F_k(x,t_0) = L_y L_z \sum_{j=1}^{k} a_{k,j} \int_0^{t_n} F_{wt}(t_n - \tau) \left\{ \begin{array}{l} \dfrac{V_c e^{-\lambda_j \tau}}{2 L_x L_y L_z} \left[erf\left(\dfrac{x + \frac{L_x}{2} - V_c\tau}{\sqrt{4 D_x^c \tau}} \right) - erf\left(\dfrac{x - \frac{L_x}{2} - V_c\tau}{\sqrt{4 D_x^c \tau}} \right) \right] \\ \quad - \sqrt{\dfrac{D_x^c}{4\pi t}} \dfrac{e^{-\lambda_j \tau}}{L_x L_y L_z} \left[e^{-\frac{\left(x + \frac{L_x}{2} - V_c\tau\right)^2}{4 D_x^c \tau}} - e^{-\frac{\left(x - \frac{L_x}{2} - V_c\tau\right)^2}{4 D_x^c \tau}} \right] \end{array} \right\} d\tau \quad . \quad (3.75)$$

This is evaluated numerically using either the Simpson's (parabolic) formula or Romberg's method (Section 3.3.14), assuming that the flux to the water table varies linearly between the values at the intermediate times.

As in the previous cases, substantial savings in computational time can be achieved if the intermediate times are in a linear series. Two transfer functions are computed for each time interval. The first is for a flux that increases linearly from zero at time t_{m-1} to one at time t_m, and the second is for a flux that decreases linearly from one at time t_{m-1} to zero at time t_m.

$$f_1^{1\to k}(x, t_n - t_m) = \int_{t_n - t_m}^{t_n - t_{m-1}} \left(\frac{t_n - t_{m-1} - \tau}{t_m - t_{m-1}} \right) \sum_{j=1}^{k} a_{k,j} e^{-\lambda_j \tau} \frac{1}{L_x} \left\{ \begin{array}{l} \dfrac{V_c}{2} \left[erf\left(\dfrac{x + \frac{L_x}{2} - V_c\tau}{\sqrt{4 D_x^c \tau}} \right) - erf\left(\dfrac{x - \frac{L_x}{2} - V_c\tau}{\sqrt{4 D_x^c \tau}} \right) \right] \\ \quad - \sqrt{\dfrac{D_x^c}{4\pi t}} \left[e^{-\frac{\left(x + \frac{L_x}{2} - V_c\tau\right)^2}{4 D_x^c \tau}} - e^{-\frac{\left(x - \frac{L_x}{2} - V_c\tau\right)^2}{4 D_x^c \tau}} \right] \end{array} \right\} d\tau \quad . \quad (3.76)$$

$$f_2^{1\to k}(x, t_n - t_{m-1}) = \int_{t_n - t_m}^{t_n - t_{m-1}} \left(\frac{\tau - t_n + t_m}{t_m - t_{m-1}} \right) \sum_{j=1}^{k} a_{k,j} e^{-\lambda_j \tau} \frac{1}{L_x} \left\{ \begin{array}{l} \dfrac{V_c}{2} \left[erf\left(\dfrac{x + \frac{L_x}{2} - V_c\tau}{\sqrt{4 D_x^c \tau}} \right) - erf\left(\dfrac{x - \frac{L_x}{2} - V_c\tau}{\sqrt{4 D_x^c \tau}} \right) \right] \\ \quad - \sqrt{\dfrac{D_x^c}{4\pi t}} \left[e^{-\frac{\left(x + \frac{L_x}{2} - V_c\tau\right)^2}{4 D_x^c \tau}} - e^{-\frac{\left(x - \frac{L_x}{2} - V_c\tau\right)^2}{4 D_x^c \tau}} \right] \end{array} \right\} d\tau \quad . \quad (3.77)$$

Both of these are evaluated numerically using either the Simpson's (parabolic) formula or Romberg's method (Section 3.3.14) and stored in memory for subsequent use with the appropriate flux.

Then the spatially integrated flux of the k^{th} progeny across the vertical plane is obtained by summing the contributions of all the relevant time intervals:

$$F_k(x,t_n) = \sum_{m=1}^{n-1} F_{wt}(t_m)\left(f_1^{1\to k}(x,t_n - t_m) + f_2^{1\to k}(x,t_n - t_m)\right) . \tag{3.78}$$

As in Section 3.3.4, the lateral dispersion factors $f_{s,y}(y_n,y_f)$ and $f_{s,z}$ are used to account for the size and location of the rectangular subsection of the plane through which the flux must pass to enter the surface water body.

$$F_{sw}(x,t_n) = F_k(x,t_n)\frac{f_{s,y}(y_n,y_f)}{L_y}\frac{f_{s,z}}{L_z} , \tag{3.79}$$

where

$$f_{s,y}(y_n,y_f) = \sqrt{D_y^c t_p}\left(\begin{array}{c} Interf\dfrac{2y_f + L_y}{\sqrt{16D_y^c t_p}} - Interf\dfrac{2y_f - L_y}{\sqrt{16D_y^c t_p}} \\ - Interf\dfrac{2y_n + L_y}{\sqrt{16D_y^c t_p}} + Interf\dfrac{2y_n - L_y}{\sqrt{16D_y^c t_p}} \end{array}\right) ,$$

and

$$f_{s,z} = \sqrt{D_z^c t_p}\left(\begin{array}{c} Interf\dfrac{d_s + L_z}{\sqrt{4D_z^c t_p}} - Interf\dfrac{d_s - L_z}{\sqrt{4D_z^c t_p}} - Interf\dfrac{L_z}{\sqrt{4D_z^c t_p}} \\ + Interf\dfrac{-L_z}{\sqrt{4D_z^c t_p}} \end{array}\right) ,$$

or

$$f_{s,z} = \max\left(0, \min\left(d_s, \frac{(x+L_x)I}{V_d}\right) - \frac{xI}{V_d}\right) ,$$

if the dispersivity in the vertical direction is set to zero. The expression for $f_{s,z}$ will contain additional terms for every reflection of the dispersion plume at the lower impervious boundary and at the water table.

The code uses this solution if all the nuclides in the transformation chain from the parent entering the transport zone to the progeny exiting the zone have the same distribution coefficient. In this case, all these nuclides under consideration will have the same transport velocity and the same dispersion coefficient. Even in cases where these nuclides have different distribution

coefficients, it is possible to instruct the code to use this equation to model the transport of the progeny produced in transit. When this choice is made, it is also necessary to make a choice of whether to use the distribution coefficient of the parent or the distribution coefficient of the progeny to calculate the transport velocity and the dispersion coefficient of these nuclides.

3.3.7 Concentration in Well Water Resulting from a Pulse Input for Radionuclides That Were Produced by Radiological Transformations within the Transport Layer When Dispersion Is Dominant

In RESRAD-OFFSITE, the fluxes entering the water table across the footprint of the primary contamination are known at each of a series of times. The concentration of the k^{th} progeny in well water is obtained as follows.

Let the spatially integrated flux of the parent nuclide across the water table at time t be $F_{wt}(t)$. By applying the expression developed in Section 3.2.5.1, the concentration of the k^{th} progeny in well water at time t_n is obtained by the convolution:

$$c_{well,k}(x_w, y_w, t_n) = c_{w,z}c_{w,y}(y_w)\frac{V_c}{2V_d L_y L_z L_x}\int_0^{t_0} F_{wt}(t_n-\tau)\sum_{j=1}^{k} a_{k,j}e^{-\lambda_j \tau}\left[\begin{array}{l} erf\left(\dfrac{x_w + L_x/2 - V_c\tau}{\sqrt{4D_x^c\tau}}\right) \\ \\ -erf\left(\dfrac{x_w - L_x/2 - V_c\tau}{\sqrt{4D_x^c\tau}}\right)\end{array}\right]d\tau, \qquad (3.80)$$

where

$$c_{w,y}(y_w) = \frac{\sqrt{D_y^c t_p}}{\varphi_w}\left(\begin{array}{l} Interf\dfrac{2y_w + \varphi_w + L_y}{\sqrt{16D_y^c t_p}} - Interf\dfrac{2y_w + \varphi_w - L_y}{\sqrt{16D_y^c t_p}} - Interf\dfrac{2y_w - \varphi_w + L_y}{\sqrt{16D_y^c t_p}} \\ \\ \quad + Interf\dfrac{2y_w - \varphi_w - L_y}{\sqrt{16D_y^c t_p}}\end{array}\right),$$

and

$$c_{w,z} = \frac{\sqrt{D_z^c t_p}}{d_w}\left(Interf\frac{d_w + L_z}{\sqrt{4D_z^c t_p}} - Interf\frac{d_w - L_z}{\sqrt{4D_z^c t_p}} - Interf\frac{L_z}{\sqrt{4D_z^c t_p}} + Interf\frac{-L_z}{\sqrt{4D_z^c t_p}}\right),$$

or

$$c_{w,z} = \max\left(0, \min\left(d_w, \frac{(x+L_x)I}{V_d}\right) - \frac{xI}{V_d}\right)\Big/ d_w \ ,$$

depending on whether the dispersivity in the vertical direction is nonzero or not, with additional terms in $c_{w,z}$ for reflections off the lower impermeable layer and the water table if necessary.

This is evaluated numerically using either the Simpson's (parabolic) formula or Romberg's method (Section 3.3.14), assuming that the flux to the water table varies linearly between the values at the intermediate times.

As in the previous cases, substantial savings in computational time can be achieved if the intermediate times are in a linear series. Two transfer functions are computed for each time interval. The first is for a flux that increases linearly from zero at time t_{m-1} to one at time t_m, and the second is for a flux that decreases linearly from one at time t_{m-1} to zero at time t_m.

$$f_1^{1\to k}(x,t_n-t_m)=\int_{t_n-t_m}^{t_n-t_{m-1}}\left(\frac{t_n-t_{m-1}-\tau}{t_m-t_{m-1}}\right)\sum_{j=1}^{k}a_{k,j}e^{-\lambda_j\tau}\frac{V_c}{2L_xV_dL_yL_z}\left[\begin{array}{l}erf\left(\dfrac{x+L_x/2-V_c\tau}{\sqrt{4D_x^c\tau}}\right)\\ \\ -erf\left(\dfrac{x-L_x/2-V_c\tau}{\sqrt{4D_x^c\tau}}\right)\end{array}\right]d\tau\ . \qquad (3.81)$$

$$f_2^{1\to k}(x,t_n-t_{m-1})=\int_{t_n-t_i}^{t_n-t_{i-1}}\left(\frac{\tau-t_n+t_m}{t_m-t_{m-1}}\right)\sum_{j=1}^{k}a_{k,j}e^{-\lambda_j\tau}\frac{V_c}{2L_xV_dL_yL_z}\left[\begin{array}{l}erf\left(\dfrac{x+L_x/2-V_c\tau}{\sqrt{4D_x^c\tau}}\right)\\ \\ -erf\left(\dfrac{x-L_x/2-V_c\tau}{\sqrt{4D_x^c\tau}}\right)\end{array}\right]d\tau\ . \qquad (3.82)$$

Both of these are evaluated numerically by using either Simpson's (parabolic) formula or Romberg's method (Section 3.3.14) and stored in memory for subsequent use with the appropriate flux.

Then the concentration in well water is obtained by summing the contributions of all the relevant time intervals:

$$c_{well}(x_w,y_w,t_n)=c_{w,z}c_{w,y}(y_w)\sum_{m=1}^{n-1}F_{wt}(t_m)\left(f_1^{1\to k}(x,t_n-t_m)+f_2^{1\to k}(x,t_n-t_m)\right)\ . \qquad (3.83)$$

3.3.8 Output Flux Resulting from a Pulse Input for Radionuclides That Were Produced by Radiological Transformations within the Transport Layer When Differences in Their Distribution Coefficients Are Dominant

In RESRAD-OFFSITE, the fluxes entering the water table across the footprint of the primary contamination are known at each of a series of times. The spatially integrated flux of the k^{th} progeny across a vertical plane in the saturated zone, at a distance x downgradient of the center of the primary contamination, is obtained as follows.

Let the spatially integrated flux of the parent nuclide across the water table at time t be $F_{wt}(t)$. By applying the expression developed in Section 3.2.5.2, the spatially integrated output flux at time t_n is obtained by the convolution:

$$F_k(x,t_n) = \int_0^{t_n} F_{wt}(t_n - \tau)\frac{\lambda_k}{\lambda_1}\sum_{i,j}\gamma \exp\left(\alpha_{i,j}\tau + \beta_{i,j}T_{1,off} + \beta_{i,j}T_{1,on}y(\tau)\right)d\tau \,. \tag{3.84}$$

This is evaluated numerically by using either Simpson's (parabolic) formula or Romberg's method (Section 3.3.14), assuming that the flux to the water table varies linearly between the values at the intermediate times.

As in the previous cases, substantial savings in computational time can be achieved if the intermediate times are in a linear series. Two transfer functions are computed for each time interval. The first is for a flux that increases linearly from zero at time t_{m-1} to one at time t_m, and the second is for a flux that decreases linearly from one at time t_{m-1} to zero at time t_m.

$$f_1^{1\to k}(x,t_n - t_m) = \frac{\lambda_k}{\lambda_1}\int_{t_n - t_m}^{t_n - t_{m-1}}\left(\frac{t_n - t_{m-1} - \tau}{t_m - t_{m-1}}\right)\sum_{i,j}\gamma \exp\left(\alpha_{i,j}\tau + \beta_{i,j}T_{1,off} + \beta_{i,j}T_{1,on}y(\tau)\right)d\tau \,. \tag{3.85}$$

$$f_2^{1\to k}(x,t_n - t_{m-1}) = \frac{\lambda_k}{\lambda_1}\int_{t_n - t_m}^{t_n - t_{m-1}}\left(\frac{\tau - t_n + t_m}{t_m - t_{m-1}}\right)\sum_{i,j}\gamma \exp\left(\alpha_{i,j}\tau + \beta_{i,j}T_{1,off} + \beta_{i,j}T_{1,on}y(\tau)\right)d\tau \,. \tag{3.86}$$

Both of these are evaluated numerically by using either Simpson's (parabolic) formula or Romberg's method (Section 3.3.14) and stored in memory for subsequent use with the appropriate flux.

Then the spatially integrated flux of the k^{th} progeny across the vertical plane is obtained by summing the contributions of all the relevant time intervals:

$$F_k(x,t_n) = \sum_{m=1}^{n-1} F_{wt}(t_m)\left(f_1^{1\to k}(x,t_n - t_m) + f_2^{1\to k}(x,t_n - t_m)\right) \,. \tag{3.87}$$

As in Section 3.3.4, the lateral dispersion factors $f_{s,y}(y_n,y_f)$ and $f_{s,z}$ are used to account for the size and location of the rectangular subsection of the plane through which the radionuclide must pass to enter the surface water body.

$$F_{sw}(x,t_n) = F_k(x,t_n)\frac{f_{s,y}(y_n,y_f)}{L_y}\frac{f_{s,z}}{L_z} \,, \tag{3.88}$$

where

$$f_{s,y}(y_n, y_f) = \sqrt{D_y^c t_p}\left(Interf\frac{2y_f + L_y}{\sqrt{16D_y^c t_p}} - Interf\frac{2y_f - L_y}{\sqrt{16D_y^c t_p}} - Interf\frac{2y_n + L_y}{\sqrt{16D_y^c t_p}} + Interf\frac{2y_n - L_y}{\sqrt{16D_y^c t_p}} \right),$$

and

$$f_{s,z} = \sqrt{D_z^c t_p}\left(Interf\frac{d_s + L_z}{\sqrt{4D_z^c t_p}} - Interf\frac{d_s - L_z}{\sqrt{4D_z^c t_p}} - Interf\frac{L_z}{\sqrt{4D_z^c t_p}} + Interf\frac{-L_z}{\sqrt{4D_z^c t_p}} \right),$$

or

$$f_{s,z} = \max\left(0, \min\left(d_s, \frac{(x + L_x)I}{V_d}\right) - \frac{xI}{V_d}\right),$$

if the dispersivity in the vertical direction is set to zero. The expression for $f_{s,z}$ will contain additional terms for every reflection of the dispersion plume at the lower impervious boundary and at the water table.

3.3.9 Concentration in Well Water Resulting from a Pulse Input for Radionuclides That Were Produced by Radiological Transformations within the Transport Layer When Differences in Their Distribution Coefficients Are Dominant

In RESRAD-OFFSITE, the fluxes entering the water table across the footprint of the primary contamination are known at each of a series of times. The concentration of the k^{th} progeny in well water is obtained as follows.

Let the spatially integrated flux of the parent nuclide across the water table at time t be $F_{wt}(t)$. By applying the expression developed in Section 3.2.5.2, the concentration of the k^{th} progeny in well water at time t_n is obtained by the convolution:

$$c_{well,k}(x_w, y_w, t_n) = c_{w,z}c_{w,y}(y_w)\frac{1}{V_d L_y L_z}\int_0^{t_n} F_{wt}(t_n - \tau)\frac{\lambda_k}{\lambda_1}\sum_{i,j}\gamma\, exp\left(\alpha_{i,j}\tau + \beta_{i,j}T_{1,off} + \beta_{i,j}T_{1,on}y(\tau)\right)d\tau, \quad (3.89)$$

where

$$c_{w,y}(y_w) = \frac{\sqrt{D_y^c t_p}}{\varphi_w}\left(\begin{array}{l} Interf\frac{2y_w + \varphi_w + L_y}{\sqrt{16D_y^c t_p}} - Interf\frac{2y_w + \varphi_w - L_y}{\sqrt{16D_y^c t_p}} - Interf\frac{2y_w - \varphi_w + L_y}{\sqrt{16D_y^c t_p}} \\ \qquad + Interf\frac{2y_w - \varphi_w - L_y}{\sqrt{16D_y^c t_p}} \end{array} \right),$$

and

$$c_{w,z} = \frac{\sqrt{D_z^c t_p}}{d_w}\left(Interf\frac{d_w + L_z}{\sqrt{4D_z^c t_p}} - Interf\frac{d_w - L_z}{\sqrt{4D_z^c t_p}} - Interf\frac{L_z}{\sqrt{4D_z^c t_p}} + Interf\frac{-L_z}{\sqrt{4D_z^c t_p}}\right),$$

or

$$c_{w,z} = \max\left(0, \min\left(d_w, \frac{(x+L_x)I}{V_d}\right) - \frac{xI}{V_d}\right) \Big/ d_w \ ,$$

depending on whether the dispersivity in the vertical direction is nonzero or not, with additional terms in $c_{w,z}$ for reflections off the lower impermeable layer and the water table if necessary.

This is evaluated numerically by using either Simpson's (parabolic) formula or Romberg's method (Section 3.3.14), assuming that the flux to the water table varies linearly between the values at the intermediate times.

As in the previous cases, substantial savings in computational time can be achieved if the intermediate times are in a linear series. Two transfer functions are computed for each time interval. The first is for a flux that increases linearly from zero at time t_{m-1} to one at time t_m, and the second is for a flux that decreases linearly from one at time t_{m-1} to zero at time t_m.

$$f_1^{1\to k}(x, t_n - t_m) = \frac{1}{V_d L_y L_z}\frac{\lambda_k}{\lambda_1}\int_{t_n - t_m}^{t_n - t_{m-1}}\left(\frac{t_n - t_{m-1} - \tau}{t_m - t_{m-1}}\right)\sum_{i,j}\gamma\, exp\left(\alpha_{i,j}\tau + \beta_{i,j}T_{1,off} + \beta_{i,j}T_{1,on}y(\tau)\right)d\tau \ . \quad (3.90)$$

$$f_2^{1\to k}(x, t_n - t_{m-1}) = \frac{1}{V_d L_y L_z}\frac{\lambda_k}{\lambda_1}\int_{t_n - t_{m+1}}^{t_n - t_m}\left(\frac{\tau - t_n + t_m}{t_m - t_{m-1}}\right)\sum_{i,j}\gamma\exp\left(\alpha_{i,j}\tau + \beta_{i,j}T_{1,off} + \beta_{i,j}T_{1,on}y(\tau)\right)d\tau \ . \quad (3.91)$$

Both of these are evaluated numerically using either the Simpson's (parabolic) formula or Romberg's method (Section 3.3.14) and stored in memory for subsequent use with the appropriate flux.

Then the concentration in well water is obtained by summing the contributions of all the relevant time intervals:

$$c_{well}(x_w, y_w, t_n) = c_{w,z}c_{w,y}(y_w)\sum_{m=1}^{n-1}F_{wt}(t_m)\left(f_1^{1\to k}(x, t_n - t_m) + f_2^{1\to k}(x, t_n - t_m)\right) . \quad (3.92)$$

3.3.10 Concentration in Well Water Resulting from a Flux Input for Radionuclides That Traversed the Layer in the Same Form

In RESRAD-OFFSITE, the fluxes entering a layer are known at each of a series of times. Assuming that the fluxes entering a layer vary linearly between those times, the concentration in well water can be obtained as follows.

Let the spatially integrated input fluxes at times t_1 and t_2 be $F(0,t_1)$ and $F(0,t_1)$, respectively. Let the length of the layer be x. By applying the expression developed in Section 3.2.2, the concentration in well water at time t_n is obtained by the convolution:

$$c_{well}(x_w, y_w, t_n) = c_{w,z} c_{w,y}(y_w) \frac{V_c}{V_d L_y L_z} \int_0^{t_n} F(0, t_n - \tau) e^{-\lambda\tau} \left[\begin{array}{l} \dfrac{2}{\sqrt{4\pi D_x^c \tau}} exp\left(-\dfrac{(x - V_c\tau)^2}{4 D_x^c \tau} \right) \\ \qquad - \dfrac{V_c}{2 D_x^c} exp\left(\dfrac{x V_c}{D_x^c} \right) erfc\left(\dfrac{x + V_c \tau}{4 D_x^c \tau} \right) \end{array} \right] d\tau \quad , \qquad (3.93)$$

where

$$c_{w,y}(y_w) = \frac{\sqrt{D_y^c t_p}}{\varphi_w} \left(\begin{array}{l} Interf \dfrac{2y_w + \varphi_w + L_y}{\sqrt{16 D_y^c t_p}} - Interf \dfrac{2y_w + \varphi_w - L_y}{\sqrt{16 D_y^c t_p}} - Interf \dfrac{2y_w - \varphi_w + L_y}{\sqrt{16 D_y^c t_p}} \\ \qquad + Interf \dfrac{2y_w - \varphi_w - L_y}{\sqrt{16 D_y^c t_p}} \end{array} \right),$$

and

$$c_{w,z} = \frac{\sqrt{D_z^c t_p}}{d_w} \left(Interf \frac{d_w + L_z}{\sqrt{4 D_z^c t_p}} - Interf \frac{d_w - L_z}{\sqrt{4 D_z^c t_p}} - Interf \frac{L_z}{\sqrt{4 D_z^c t_p}} + Interf \frac{-L_z}{\sqrt{4 D_z^c t_p}} \right),$$

or

$$c_{w,z} = \max\left(0, \min\left(d_w, \frac{(x + L_x) I}{V_d} \right) - \frac{x I}{V_d} \right) \Big/ d_w \quad ,$$

depending on whether the dispersivity in the vertical direction is nonzero or not, with additional terms in $c_{w,z}$ for reflections off the lower impermeable layer and the water table if necessary.

This is evaluated numerically by using either Simpson's (parabolic) formula or Romberg's method (Section 3.3.14), assuming that the flux to the water table varies linearly between the values at the intermediate times.

As in the previous cases, substantial savings in computational time can be achieved if the intermediate times are in a linear series. Two transfer functions are computed for each time interval. The first is for a flux that increases linearly from zero at time t_{m-1} to one at time t_m, and the second is for a flux that decreases linearly from one at time t_{m-1} to zero at time t_m.

$$f_1(x,t_n-t_m)=\int_{t_n-t_m}^{t_n-t_{m-1}}\left(\frac{t_n-t_{m-1}-\tau}{t_m-t_{m-1}}\right)\frac{V_c e^{-\lambda\tau}}{V_d L_y L_z}\left[\begin{array}{l}\dfrac{2}{\sqrt{4\pi D_x^c\tau}}exp\left(-\dfrac{(x-V_c\tau)^2}{4D_x^c\tau}\right)\\ \qquad -\dfrac{V_c}{2D_x^c}exp\left(\dfrac{xV_c}{D_x^c}\right)erfc\left(\dfrac{x+V_c\tau}{4D_x^c\tau}\right)\end{array}\right]d\tau\ . \qquad (3.94)$$

$$f_2(x,t_n-t_{m-1})=\int_{t_n-t_m}^{t_n-t_{m-1}}\left(\frac{\tau-t_n+t_m}{t_m-t_{m-1}}\right)\frac{V_c e^{-\lambda\tau}}{V_d L_y L_z}\left[\begin{array}{l}\dfrac{2}{\sqrt{4\pi D_x^c\tau}}exp\left(-\dfrac{(x-V_c\tau)^2}{4D_x^c\tau}\right)\\ \qquad -\dfrac{V_c}{2D_x^c}exp\left(\dfrac{xV_c}{D_x^c}\right)erfc\left(\dfrac{x+V_c\tau}{4D_x^c\tau}\right)\end{array}\right]d\tau\ . \qquad (3.95)$$

Both of these are evaluated numerically by using either Simpson's (parabolic) formula or Romberg's method (Section 3.3.14) and stored in memory for subsequent use with the appropriate flux.

Then the concentration in well water is obtained by summing the contributions of all the relevant time intervals:

$$c_{well}(x_w,y_w,t_n)=c_{w,z}c_{w,y}(y_w)\sum_{m=1}^{n-1}F(t_m)\left(f_1(x,t_n-t_m)+f_2(x,t_n-t_m)\right)\ . \qquad (3.96)$$

3.3.11 Concentration in Well Water Resulting from a Flux Input for Radionuclides That Were Produced by Radiological Transformations within the Transport Layer When Dispersion Is Dominant

In RESRAD-OFFSITE, the fluxes entering a layer are known at each of a series of times. Assuming that the fluxes entering a layer vary linearly between those times, the concentration of the k^{th} progeny in well water can be obtained as follows.

Let the spatially integrated input fluxes of the parent nuclide at times t_1 and t_2 be $F_1(0,t_1)$ and $F_1(0,t_2)$, respectively. Let the length of the layer be x. By applying the expression developed in Section 3.2.3.1, the concentration in well water at time t_n is obtained by the convolution:

$$c_{well}(x_w, y_w, t_n) = c_{w,z} c_{w,y}(y_w) \frac{V_c}{V_d L_y L_z} \int_0^{t_n} F_1(0, t_n - \tau) \sum_{i=1}^{k} a_{k,i} e^{-\lambda_i \tau} \left[\begin{array}{l} \dfrac{2}{\sqrt{4\pi D_x^c \tau}} \exp\left(-\dfrac{(x - V_c\tau)^2}{4 D_x^c \tau} \right) \\ \\ -\dfrac{V_c}{2 D_x^c} \exp\left(\dfrac{x V_c}{D_x^c} \right) erfc\left(\dfrac{x + V_c \tau}{4 D_x^c \tau} \right) \end{array} \right] d\tau , \quad (3.97)$$

where

$$c_{w,y}(y_w) = \frac{\sqrt{D_y^c t_p}}{\varphi_w} \left(\begin{array}{l} Interf \dfrac{2y_w + \varphi_w + L_y}{\sqrt{16 D_y^c t_p}} - Interf \dfrac{2y_w + \varphi_w - L_y}{\sqrt{16 D_y^c t_p}} - Interf \dfrac{2y_w - \varphi_w + L_y}{\sqrt{16 D_y^c t_p}} \\ \\ \quad + Interf \dfrac{2y_w - \varphi_w - L_y}{\sqrt{16 D_y^c t_p}} \end{array} \right),$$

and

$$c_{w,z} = \frac{\sqrt{D_z^c t_p}}{d_w} \left(Interf \frac{d_w + L_z}{\sqrt{4 D_z^c t_p}} - Interf \frac{d_w - L_z}{\sqrt{4 D_z^c t_p}} - Interf \frac{L_z}{\sqrt{4 D_z^c t_p}} + Interf \frac{-L_z}{\sqrt{4 D_z^c t_p}} \right),$$

or

$$c_{w,z} = \max\left(0, \min\left(d_w, \frac{(x + L_x) I}{V_d} \right) - \frac{x I}{V_d} \right) \Big/ d_w ,$$

depending on whether the dispersivity in the vertical direction is nonzero or not, with additional terms in $c_{w,z}$ for reflections off the lower impermeable layer and the water table if necessary.

This is evaluated numerically by using either Simpson's (parabolic) formula or Romberg's method (Section 3.3.14), assuming that the flux to the water table varies linearly between the values at the intermediate times.

As in the previous cases, substantial savings in computational time can be achieved if the intermediate times are in a linear series. Two transfer functions are computed for each time interval. The first is for a flux that increases linearly from zero at time t_{m-1} to one at time t_m, and the second is for a flux that decreases linearly from one at time t_{m-1} to zero at time t_m.

$$f_1^{1\to k}(x, t_n - t_m) = \int_{t_n - t_m}^{t_n - t_{m-1}} \left(\frac{t_n - t_{m-1} - \tau}{t_m - t_{m-1}} \right) \sum_{i=1}^{k} a_{k,i} e^{-\lambda_i \tau} \frac{V_c}{V_d L_y L_z} \left[\begin{array}{l} \dfrac{2}{\sqrt{4\pi D_x^c \tau}} exp\left(-\dfrac{(x - V_c\tau)^2}{4 D_x^c \tau} \right) \\ \\ -\dfrac{V_c}{2 D_x^c} exp\left(\dfrac{x V_c}{D_x^c} \right) erfc\left(\dfrac{x + V_c \tau}{4 D_x^c \tau} \right) \end{array} \right] d\tau . \quad (3.98)$$

$$f_2^{1\to k}(x,t_n-t_{m-1})=\int_{t_n-t_m}^{t_n-t_{m-1}}\left(\frac{\tau-t_n+t_m}{t_m-t_{m-1}}\right)\sum_{i=1}^{k}a_{k,i}e^{-\lambda_i\tau}\frac{V_c}{V_dL_yL_z}\left[\begin{array}{l}\frac{2}{\sqrt{4\pi D_x^c\tau}}exp\left(-\frac{(x-V_c\tau)^2}{4D_x^c\tau}\right)\\ \qquad -\frac{V_c}{2D_x^c}exp\left(\frac{xV_c}{D_x^c}\right)erfc\left(\frac{x+V_c\tau}{4D_x^c\tau}\right)\end{array}\right]d\tau \quad . \qquad (3.99)$$

Both of these are evaluated numerically by using either Simpson's (parabolic) formula or Romberg's method (Section 3.3.14) and stored in memory for subsequent use with the appropriate flux.

Then the concentration in well water is obtained by summing the contributions of all the relevant time intervals:

$$c_{well}(x_w,y_w,t_n)=c_{w,z}c_{w,y}(y_w)\sum_{m=1}^{n-1}F_1(t_m)\left(f_1^{1\to k}(x,t_n-t_m)+f_2^{1\to k}(x,t_n-t_m)\right). \qquad (3.100)$$

3.3.12 Concentration in Well Water Resulting from a Flux Input for Radionuclides That Were Produced by Radiological Transformations within the Transport Layer When Differences in Their Distribution Coefficients Are Dominant

In RESRAD-OFFSITE, the fluxes entering a layer are known at each of a series of times. Assuming that the fluxes entering a layer vary linearly between those times, the concentration of the k^{th} progeny in well water can be obtained as follows.

Let the spatially integrated input fluxes of the parent nuclide at times t_1 and t_2 be $F_1(0,t_1)$ and $F_1(0,t_2)$, respectively. Let the length of the layer be x. By applying the expression developed in Section 3.2.3.2, the concentration in well water at time t_n is obtained by the convolution:

$$c_{well}(x_w,y_w,t_n)=c_{w,z}c_{w,y}(y_w)\frac{1}{V_dL_yL_z}\int_0^{t_n}F_1(0,t_n-\tau)\frac{\lambda_k}{\lambda_1}\sum_{i,j}\gamma\exp\left(\alpha_{i,j}\tau+\beta_{i,j}T_1\right)d\tau\,, \qquad (3.101)$$

where

$$c_{w,y}(y_w)=\frac{\sqrt{D_y^ct_p}}{\varphi_w}\left(\begin{array}{l}Interf\frac{2y_w+\varphi_w+L_y}{\sqrt{16D_y^ct_p}}-Interf\frac{2y_w+\varphi_w-L_y}{\sqrt{16D_y^ct_p}}-Interf\frac{2y_w-\varphi_w+L_y}{\sqrt{16D_y^ct_p}}\\ \qquad +Interf\frac{2y_w-\varphi_w-L_y}{\sqrt{16D_y^ct_p}}\end{array}\right),$$

and

$$c_{w,z} = \frac{\sqrt{D_z^c t_p}}{d_w}\left(Interf\frac{d_w + L_z}{\sqrt{4D_z^c t_p}} - Interf\frac{d_w - L_z}{\sqrt{4D_z^c t_p}} - Interf\frac{L_z}{\sqrt{4D_z^c t_p}} + Interf\frac{-L_z}{\sqrt{4D_z^c t_p}} \right),$$

or

$$c_{w,z} = \max\left(0, \min\left(d_w, \frac{(x+L_x)I}{V_d}\right) - \frac{xI}{V_d}\right) \Big/ d_w \ ,$$

depending on whether the dispersivity in the vertical direction is nonzero, or not, with additional terms in $c_{w,z}$ for reflections off the lower impermeable layer and the water table if necessary.

This is evaluated numerically by using either Simpson's (parabolic) formula or Romberg's method (Section 3.3.14), assuming that the flux to the water table varies linearly between the values at the intermediate times.

As in the previous cases, substantial savings in computational time can be achieved if the intermediate times are in a linear series. Two transfer functions are computed for each time interval. The first is for a flux that increases linearly from zero at time t_{m-1} to one at time t_m, and the second is for a flux that decreases linearly from one at time t_{m-1} to zero at time t_m.

$$f_1^{1\to k}(x, t_n - t_m) = \frac{1}{V_d L_y L_z}\frac{\lambda_k}{\lambda_1}\int_{t_n - t_m}^{t_n - t_{m-1}} \left(\frac{t_n - t_{m-1} - \tau}{t_m - t_{m-1}}\right) \sum_{i,j} \gamma \exp\left(\alpha_{i,j}\tau + \beta_{i,j} T_1\right) d\tau \ . \qquad (3.102)$$

$$f_2^{1\to k}(x, t_n - t_{m-1}) = \frac{1}{V_d L_y L_z}\frac{\lambda_k}{\lambda_1}\int_{t_n - t_m}^{t_n - t_{m-1}} \left(\frac{\tau - t_n + t_m}{t_m - t_{m-1}}\right) \sum_{i,j} \gamma \exp\left(\alpha_{i,j}\tau + \beta_{i,j} T_1\right) d\tau \ . \qquad (3.103)$$

Both of these are evaluated numerically by using either Simpson's (parabolic) formula or Romberg's method (Section 3.3.14) and stored in memory for subsequent use with the appropriate flux.

Then the concentration in well water is obtained by summing the contributions of all the relevant time intervals:

$$c_{well}(x_w, y_w, t_n) = c_{w,z} c_{w,y}(y_w) \sum_{m=1}^{n-1} F_1(t_m)\left(f_1^{1\to k}(x, t_n - t_m) + f_2^{1\to k}(x, t_n - t_m)\right) . \qquad (3.104)$$

3.3.13 Improving the Modeling of the Transport of Progeny Produced in Transit by Subdividing the Transport Zone

Consider a situation that requires the modeling of the flux or concentration in the aquifer of a progeny of a nuclide that was initially present in the primary contamination. Assume that

there is an unsaturated layer between the primary contamination and the aquifer. The progeny atoms in the saturated zone can be classified into three groups on the basis of the zone in which the radiological transformation of the parent atom produced that atom of the progeny as shown in Figure 3.5. Some of the atoms would have transformed in the primary contamination and traveled both the partially saturated zone and the saturated zone as a progeny. The second group consists of those atoms that exited the primary contamination and traveled part of the unsaturated zone in the form of parent atoms, transformed to the progeny in the unsaturated zone and traveled the rest of the unsaturated zone and the saturated zone as progeny atoms. The last group consists of those atoms that exited and traveled the unsaturated zone and part of the saturated zone in the form of the parent, transformed to the progeny in the saturated zone, and traveled the rest of the saturated zone as a progeny.

The code uses the expressions in Sections 3.2.2 and 3.2.4 to model the transport of the first group of nuclides that traverse the unsaturated and saturated transport zones as progeny atoms without transformation. The transport of the second group of atoms is modeled by using one of the expressions in Sections 3.2.3.1 or 3.2.3.2 for the unsaturated zone and the expression in Section 3.2.4 for the saturated zone. Modeling the transport of the third group of atoms involves the expression in Section 3.2.2 for the unsaturated zone and one of the expressions in Section 3.2.5.1 or Section 3.2.5.2 for the saturated zone. The code will model the effects of longitudinal dispersion and will ignore the differences in the distribution coefficients of the nuclides in the zone in which the transformation occurred by using the first of the pair of expressions, or it will model the effects of the differences in the distribution coefficients of the nuclides and ignore the effects of longitudinal dispersion by using the second expression according to the users preference specified in the input interface. Such a choice may not be acceptable when both processes are of comparable importance. Both processes can be modeled over a greater part of the transport zone by dividing the transport zone into a number of smaller transport zones. This is illustrated in Figure 3.6, where the unsaturated and saturated zones have been divided into two for groundwater transport calculations. Now one of the processes (longitudinal dispersion or nuclide-specific distribution coefficient) will have to be ignored over either half the length of the unsaturated zone or half the length of the saturated zone when modeling the transport of any progeny nuclide produced in transit.

The code-suggested default is to model the nuclide-specific distribution coefficients in the subzones in which each atom undergoes radiological transformations and to ignore longitudinal dispersion in those subzones. This choice is appropriate in most cases for the following reasons:

1. If the subzones are small enough, longitudinal dispersion in a subzone will be small and ignoring it for that one zone would not cause a significant change in the result.

2. The distribution coefficient affects both the partitioning of the nuclide between the water and the solid phases of soil, and the nuclide's transport velocity. The differences in the partitioning are not affected by the size of the subzone and will still be significant even in a small subzone.

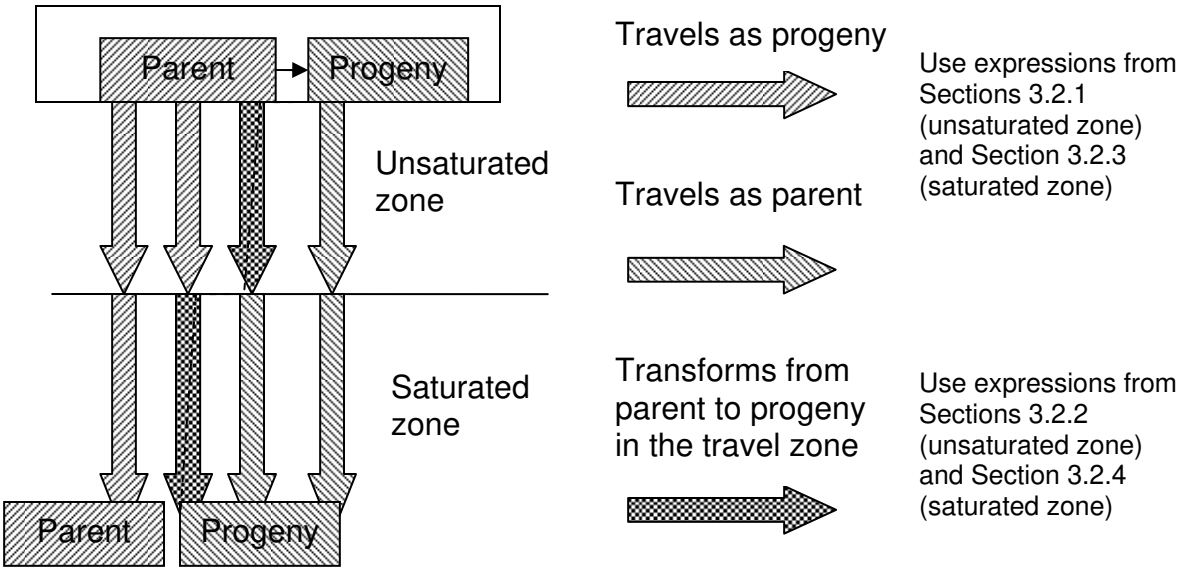

FIGURE 3.5 Progeny in the Aquifer Due to a Parent Nuclide in Primary Contamination

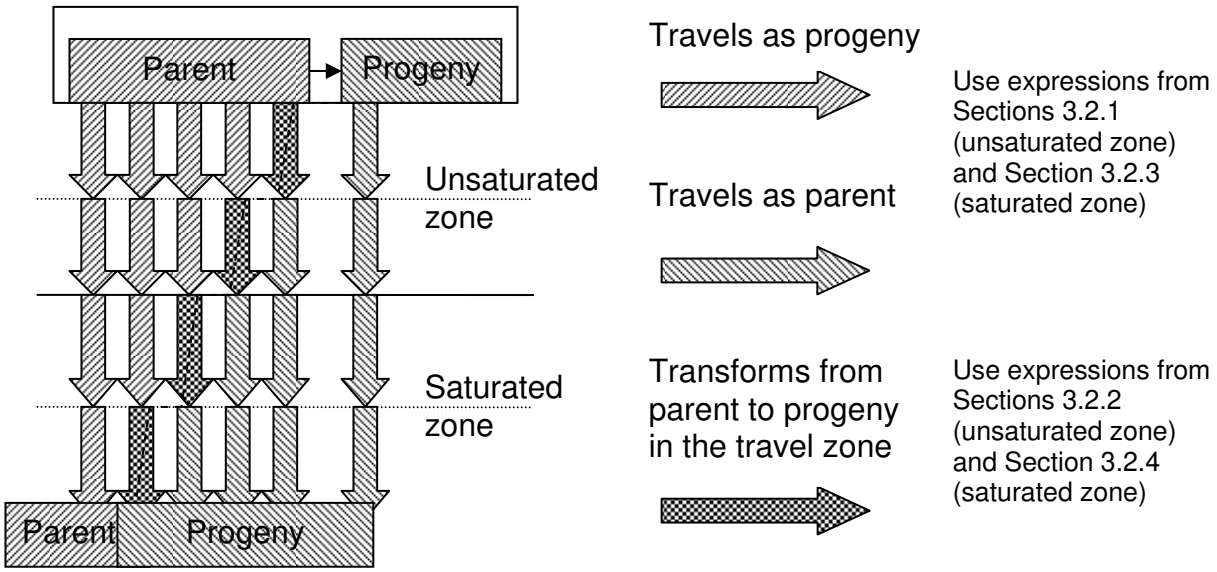

FIGURE 3.6 Progeny in Aquifer Due to Parent Nuclide in Primary Contamination, with Subdivided Transport Zones

However, in situations where longitudinal dispersion overwhelms longitudinal transport, it would be better to ignore the effects of differences in the distribution coefficients and to model the effects of longitudinal dispersion in the zones of transformations and to use the distribution coefficient of the progeny for all nuclides.

The input and output for the subdivided zones in the partially saturated layers are the flux entering the upgradient face and the flux exiting the downgradient face, the same as for the undivided partially saturated zone. The formulations in Sections 3.3.1 through 3.3.3 are repeatedly applied for each subzone. Furthermore, because the subzones are identical the transfer factors computed for the first subzone can be saved and used for all the subsequent subzones, thereby reducing the computation time, this is practical only when the intermediate time points are spaced uniformly, Section 7.3.

Only the part of the saturated transport zone that is outside the footprint of the primary contamination, called the offsite transport distance, can be subdivided. The first subzone of the saturated zone consists of the saturated zone within the footprint of the primary contamination and the first subdivision of the offsite transport distance. The input for this first subzone is the pulse flux at the water table, and the output is the flux at the downgradient face of the subzone. Thus the formulations discussed in Sections 3.3.4, 3.3.6, and 3.3.8 for the flux output are used for the first subzone of the saturated zone. The input for each of the remaining subzones is the flux entering at the upgradient face. The ouput for all but the last subzone is the flux exiting the downgradient face. The formulations in Sections 3.3.1 through 3.3.3 are used for all but the first and last subzones of the saturated zone. The output of the last subzone depends on the water source; it is the flux exiting the downgradient face for the surface water body, and the concentration for the well. The formulations for flux discussed in Sections 3.3.1 through 3.3.3 are applicable for the last subzone to the surface water body. The expressions for concentration discussed in Sections 3.3.10 through 3.3.12 are applicable for the last subzone to the well.

3.3.14 Simpson's and Romberg Numerical Integration

The computational code uses the numerical integration method described in Press et al. (1989) to evaluate the integral $\int_a^b f(x)dx$ when the analytical solution is not known.

A series of trapezoidal integrals is first computed as follows:

$$T_1 = (b-a)\frac{f(a)+f(b)}{2} \tag{3.105}$$

is the first trapezoidal estimate using only the endpoints.

$$T_2 = \frac{b-a}{2}\frac{f(a)+f\left(\frac{a+b}{2}\right)}{2} + \frac{b-a}{2}\frac{f\left(\frac{a+b}{2}\right)+f(b)}{2}$$
$$T_2 = \frac{b-a}{2}\left[\frac{f(a)}{2}+\frac{f(b)}{2}+f\left(\frac{a+b}{2}\right)\right] = \frac{T_1}{2}+\frac{b-a}{2}f\left(\frac{a+b}{2}\right) \tag{3.106}$$

is the second trapezoidal estimate using the endpoints and the midpoint.

$$T_3 = \frac{b-a}{4}\left[\frac{f(a)+f\left(\frac{3a+b}{4}\right)}{2}+\frac{f\left(\frac{3a+b}{4}\right)+f\left(\frac{a+b}{2}\right)}{2}+\frac{f\left(\frac{a+b}{2}\right)+f\left(\frac{a+3b}{4}\right)}{2}+\frac{f\left(\frac{a+3b}{4}\right)+f(b)}{2}\right] \tag{3.107}$$
$$T_3 = \frac{b-a}{4}\left[\frac{f(a)}{2}+\frac{f(b)}{2}+f\left(\frac{a+b}{2}\right)+f\left(\frac{3a+b}{4}\right)+f\left(\frac{a+3b}{4}\right)\right] = \frac{T_2}{2}+\frac{b-a}{4}\left[f\left(\frac{3a+b}{4}\right)+f\left(\frac{a+3b}{4}\right)\right]$$

is the third trapezoidal estimate using the endpoints and the quarter points.

The succeeding trapezoidal estimates using values of the function at 1/8 of the interval, at 1/16 of the interval, etc., are computed in a similar fashion. Then a series of parabolic estimates (Simpson's method) can be obtained from the successive trapezoidal estimates as follows:

$$S_1 = \frac{b-a}{6}\left[f(a)+4f\left(\frac{a+b}{2}\right)+f(b)\right] = \frac{4T_2-T_1}{3} \tag{3.108}$$

is the 3-point parabolic integral.

$$S_2 = \frac{b-a}{12}\left[f(a)+4f\left(\frac{3a+b}{4}\right)+f\left(\frac{a+b}{2}\right)\right]+\frac{b-a}{12}\left[f\left(\frac{a+b}{2}\right)+4f\left(\frac{a+3b}{4}\right)+f(b)\right]$$
$$S_2 = \frac{b-a}{12}\left[f(a)+f(b)+2f\left(\frac{a+b}{2}\right)+4f\left(\frac{3a+b}{4}\right)+4f\left(\frac{a+3b}{4}\right)\right] = \frac{4T_3-T_2}{3} \tag{3.109}$$

is the 5-point parabolic integral.

In a similar fashion, the 9-point (1/8 interval) parabolic estimate is $S_3 = \frac{4T_4-T_3}{3}$, the 17-point (1/16 interval) parabolic estimate is $S_4 = \frac{4T_5-T_4}{3}$, and the 33-point (1/32 interval) parabolic estimate is $S_5 = \frac{4T_6-T_5}{3}$.

If the 17-point and 33-point parabolic estimates agree within the user-specified criterion, the 33-point parabolic estimate is used. Otherwise, successive 4^{th} order interpolations of the trapezoidal estimates (Romberg Integration) are obtained until they agree within the user-specified criterion. If the 4^{th} order Romberg estimates with 16,385 points and 32,769 points do not agree within the criterion, the 32,769-point estimate is used.

4 ATMOSPHERIC TRANSPORT MODEL

The atmospheric transport model used in RESRAD-OFFSITE is a Gaussian plume dispersion model based on an area source release. Radionuclides released from a contaminated area are transported by the wind and are dispersed as a result of atmospheric turbulence. The area source is characterized as a rectangular area with a time-dependent emission rate and located upwind of a receptor location. A plume-rise model developed by Briggs (1969) is used to estimate the buoyancy induced rise of the release, if applicable. Depending on the circumstances, either the standard Pasquill-Gifford dispersion coefficients (Slade 1968, Eimutis and Konicek 1972) or the Briggs (1974) dispersion coefficients can be used. The former are suitable for ground-level releases; the latter are better for elevated releases. For vapor or particulate radionuclides, deposition of plume content by dry and wet deposition is also considered for any user-specified receptor location. Air and ground concentrations of radionuclides are calculated for the estimation of exposure via various pathways.

The primary contamination and the offsite receptor locations are all treated as rectangles oriented parallel to a set of common Cartesian axes. The code performs a spatial integration of the atmospheric transport by subdividing the primary contamination and the receptor regions into small squares based on the grid spacing. The transport from each subdivision of the primary contamination to each subdivision of the receptor region is computed by the model, and these results are combined to obtain the spatially integrated value. The atmospheric transport calculations to a receptor region are performed only if that region and the primary contamination do not overlap.

Transport of the radionuclides in particulate form, transport of C-12 and H-3 in vapor or gaseous form, and the transport of the radon isotopes Rn-220 and Rn-222 and their short-lived progeny are modeled by the code. The decay and ingrowth of radon isotopes and their short-lived progeny during the transport are also modeled.

4.1 EFFECTIVE RELEASE HEIGHT

Material released from a contaminated area may rise above the release point as a result of thermal buoyancy. The thermal buoyancy could be related to solar heating of the ground or a local heat source, such as underground steam lines. An effective release height, H, is used in the atmospheric dispersion equations to account for the additional height of the release. The effective release height is the sum of the actual physical release height, h, and the thermally induced plume rise, Δh, with an adjustment for terrain height:

$$H = h + \Delta h - (1 - P_c)[min(h + \Delta h, E_r - E_p)], \quad (4.1)$$

where

H = effective release height (m),

h = physical release height (m),

Δh = plume rise (m),

P_c = plume-path coefficient (unitless),

E_r = receptor elevation (m), and

E_p = release elevation, the reference point for the release height (m).

4.2 PLUME RISE

Plume rise is estimated in RESRAD-OFFSITE with the formulas derived by Briggs (1969) for buoyant plumes. The rise from thermal buoyancy is seen to be dependent on stability class, wind speed, and receptor distance. For stability classes A, B, C, and D, the plume rise is given by

$$\Delta h = \frac{1.6F^{1/3}x^{2/3}}{u_H}, \text{ for } x \le 10\ h, \tag{4.2}$$

$$\Delta h = \frac{1.6F^{1/3}(10h)^{2/3}}{u_H}, \text{ for } x > 10\ h, \tag{4.3}$$

where

F = $3.7 \times 10^{-5}\ Qh$ (m^4/s^3),

Q_h = heat flux from radionuclide release area (cal/s),

x = downwind receptor distance from release area (m), and

u_H = wind speed at effective release height (m/s).

For stability classes E and F, the plume rise is calculated according to

$$\Delta h = \frac{1.6F^{1/3}x^{2/3}}{u_H}, \textit{ for } x \le 2.4\frac{u_H}{\sqrt{s}}, \tag{4.4}$$

$$\Delta h = 2.9\left(\frac{F}{u_H s}\right)^{1/3}, \; for \; x > 2.4\frac{u_H}{\sqrt{s}}, \tag{4.5}$$

except when the wind is so light that the plume rises vertically. Under such conditions, the final plume rise is given by Briggs (1969) as

$$\Delta h = \frac{5.0F^{1/4}}{s^{3/8}}, \text{ when } u_H \le u_{test}, \tag{4.6}$$

where

$$s = \frac{g}{T_a}\left(\frac{\partial T_a}{\partial z} + l\right), \tag{4.7}$$

$$u_{test} = 0.195F^{1/4}s^{1/8}, \tag{4.8}$$

s = stability parameter,

g = gravitational acceleration (9.80665 m/s^2),

T_a = ambient air temperature (K),

l = normal adiabatic lapse rate of the atmosphere (0.0098 K/m),

$\frac{\partial T_a}{\partial z} + l$ = potential temperature lapse rate (0.002 and 0.035 for stability classes E and F, respectively), and

z = vertical distance above the release point (m).

As recommended by Briggs (1969), Equations 4.2 through 4.5 contain wind speed in the denominator, which would produce unrealistically high values for very low wind speeds. Because the Briggs equations are applicable only to windy conditions, a minimum wind speed of 0.1 m/s is imposed in the above plume-rise calculations.

4.3 TERRAIN HEIGHT ADJUSTMENT

The presence of rising terrain downwind from an area emission source requires that the release height derived for flat terrain be adjusted accordingly. Stability-dependent plume-path coefficients are used in RESRAD-OFFSITE to estimate the effects of terrain elevation on the height of the plume centerline. The correction to the release height for downwind elevations involves the third term in Equation 4.1, as given in Ross et al. (1985).

An increase in receptor elevation downwind effectively reduces the release height if the release height is greater than zero. This condition is embodied in the $\min(h + \Delta h, E_r - E_p)$ portion of Equation 4.1. On the other hand, the plume will not travel straight into a hillside but will follow air currents part way up the hill on its approach. The portion of Equation 4.1 with the plume-path coefficient $(1 - P_C)$ partially defines the amount of the effective reduction in release height and ensures that the terrain height adjustment is not too extreme. For neutral and unstable conditions (stability classes A, B, C, and D), P_c is set to 0.5 so that the plume height remains at least one-half the distance aboveground as it would be if no adjustment was made. Similarly for stable conditions (stability classes E and F), P_c is set to 0.3 so that the plume height remains at least one-third the height above the ground as it would be if no adjustments were made. A plume-path coefficient of 1 represents a non-terrain-lifted plume.

4.4 WIND POWER-LAW ADJUSTMENT

For atmospheric dispersion calculations, the measured average wind speed at the effective release height, u_H, is not always available. RESRAD-OFFSITE uses a power-law function with the following form to estimate the wind speed at the desired height:

$$\frac{u_H}{u_a} = \left(\frac{H}{z_a}\right)^p , \tag{4.9}$$

where

u_a = wind speed at measurement height (m/s),

z_a = height of anemometer for wind speed measurement (m), and

p = power for height ratio (unitless).

The wind speed of u_a from the measurement height z_a is adjusted to the effective release height H of the plume for the dispersion calculations. Values for the exponent p as presented in Table 4.1 were taken from Irwin (1979), as modified by Hanna et al. (1982) for the different population zones and stability classes.

TABLE 4.1 Estimates of the Power (*p*) in Equation 4.9 for Population Zones as a Function of Stability Class

	Stability Class					
Population Zone	A	B	C	D	E	F
Rural	0.07	0.07	0.10	0.15	0.35	0.55
Suburban/urban	0.15	0.15	0.20	0.25	0.40	0.60

4.5 ATMOSPHERIC DISPERSION

A Gaussian plume atmospheric dispersion model is used in RESRAD-OFFSITE to evaluate the downwind transport of radionuclide contaminants released to the atmosphere from a continuous (chronic) area source. The model preserves mass balance and accounts for depletion of the plume from dry and wet deposition processes. Radioactive decay is not considered because transport times are relatively short, on the order of minutes.

4.5.1 Gaussian Plume

For a discrete puff generated from a point source with an effective release height H above ground level, the Gaussian time-dependent dispersion equation can be written as, assuming Gaussian symmetry, that is, $\sigma_x = \sigma_y$ (m^2) (Pasquill 1974),

$$C_a(i,x,y,z,t) = \frac{Q_{x_i}}{(2\pi)^{3/2}\sigma_y^2\sigma_z} exp\left(\frac{-r^2}{2\sigma_y^2}\right)\left[exp\left(\frac{-(z-H)^2}{2\sigma_z^2}\right) + exp\left(\frac{-(z+H)^2}{2\sigma_z^2}\right)\right], \quad (4.10)$$

where

$C_a(i,x,y,z,t)$ = air concentration of radionuclide i at x,y,z from a release at $0,0,H$ at time t after release (Ci/m^3),

Q_{xi} = depleted source strength of nuclide i at distance x (Ci) [Equation 4.31],

σ_y = horizontal dispersion coefficient [Equation 4.39],

σ_z = vertical dispersion coefficient [Equation 4.37],

r^2 = $(x - u_H t)^2 + y^2$,

x = downwind receptor distance from the release point (m),

y = crosswind distance from the plume centerline (m),

u_H = average wind speed at the effective release height (m/s) [Equation 4.9],

t = time following release (s), and

H = effective release height (m) [Equation 4.1].

The ground-level air concentration (Ci/m^3) for a discrete puff is obtained by setting $z = 0$ in Equation 4.10.

$$C_a(i,x,y,0,t) = \frac{2Q_{x_i}}{(2\pi)^{3/2}\sigma_y^2\sigma_z}\left\{\exp-\left(\frac{r^2}{2\sigma_y^2}+\frac{H^2}{2\sigma_z^2}\right)\right\}. \quad (4.11)$$

A continuous point source can be considered to be a series of overlapping puff emissions. Thus, integration of Equation 4.11 over time yields the downwind air concentration (Ci/m^3):

$$\overline{C}_a(i,x,y) = \int_0^\infty C_a(i,x,y,0,t)dt\ , \quad (4.12)$$

which can be shown to be (Slade 1968)

$$\overline{C}_a(i,x,y) = \frac{Q_{x_i}}{\pi\sigma_y\sigma_z u_H}\left[exp-\left(\frac{y^2}{2\sigma_y^2}+\frac{H^2}{2\sigma_z^2}\right)\right], \quad (4.13)$$

where Q_{x_i} is the initial source term for radionuclide i (now in units of Ci/s for a continuous source), corrected for wet and dry deposition from the plume, as shown later in Equation 4.31. Because of the short times involved during air transport, this treatment does not consider radioactive decay.

4.5.2 Plume Reflection

The existence of a stable air layer at higher altitudes under unstable and neutral atmospheric conditions affects atmospheric dispersion at great distances from the release point. The upward dispersion of the plume is eventually restricted when the plume encounters an elevated stable layer (or lid) or a mixing layer at some height L. In RESRAD-OFFSITE, the plume is assumed to be reflected by this stable layer at these distances. With vertical distribution limited by reflection, integration of Equation 4.10 over z (0 to L) as well as integration over time yields

$$\overline{C}_a(i,x,y) = \frac{Q_{x_i}}{\sqrt{2\pi}\sigma_y u_H L}\exp-\left(\frac{y^2}{2\sigma_y^2}\right), \quad (4.14)$$

where

L = mixing layer height, sometimes referred to as the lid height (m).

The following conditions (Powell et al. 1979) are used to determine whether Equation 4.13 or 4.14 is used for the dispersion calculation.

Equation 4.13 is used for distances where σ_z is small compared to L, when

$$\frac{\sigma_z}{L} \le \frac{\sqrt{1-\frac{H}{L}}}{1.2}. \tag{4.15}$$

Equation 4.14 is used when σ_z is of the same order as L and a uniform distribution can be assumed; that is, it is used when

$$0 \le H/L < 0.5$$

and

$$\frac{\sigma_z}{L} \ge -2.37\left(\frac{H}{L}\right)^2 + 0.489\left(\frac{H}{L}\right) + 0.756, \tag{4.16}$$

or it is used when

$$0.5 \le H/L < 1.0$$

and

$$\frac{\sigma_z}{L} \ge -2.37\left(\frac{H}{L}\right)^2 + 4.25\left(\frac{H}{L}\right) - 1.13. \tag{4.17}$$

At downwind distances between the no-mixing (Equation 4.15) and the total-mixing (Equations 4.16 and 4.17) conditions, the concentration is determined by a linear interpolation between Equations 4.13 and 4.14.

4.5.3 Chronic Release

Equations 4.13 and 4.14 are valid for unchanging weather conditions when the period of release exceeds the time necessary for the airborne material to travel downwind from the release point to the receptor location. However, weather conditions will fluctuate with time (generally on the order of minutes or longer), causing the plume to meander within a sector when the wind is

blowing in a particular direction. Thus, it is more appropriate to evaluate the sector-average air concentration for use in estimating human health impacts under such conditions.

The air dispersion model in RESRAD-OFFSITE uses a polar grid with 16 sectors to specify the wind direction. The sector-average air concentration at a receptor location that is a distance of x m from the release point (see Figure 4.1) can be estimated as the integral of Equation 4.13 or 4.14 over y, from minus infinity to plus infinity, divided by the width of the sector ($2y_{sec}$) at distance x from the release point. Because of the symmetry of the Gaussian equation, this sector-average concentration for the case where there is no plume reflection can be written as

$$\overline{C_{\text{sec}}}(i,x) = \frac{1}{y_{\text{sec}}}\int_0^{\infty} \overline{C_a}(i,x,y)dy = \frac{1}{y_{\text{sec}}}\int_0^{\infty} \frac{Q_{x_i}}{\pi\sigma_y\sigma_z u_H}\left[\exp-\left(\frac{y^2}{2\sigma_y^2}+\frac{H^2}{2\sigma_z^2}\right)\right]dy, \quad (4.18)$$

where

$$y_{\text{sec}} = x\tan\left(11.25^{\circ}\right). \quad (4.19)$$

Equation 4.18 can be rewritten as

$$\overline{C_{\text{sec}}}(i,x) = \frac{Q_{x_i}}{\pi\sigma_y\sigma_z u_H y_{\text{sec}}}\exp\left(\frac{-H^2}{2\sigma_z^2}\right)\int_0^{\infty}\exp\left(\frac{-y^2}{2\sigma_y^2}\right)dy. \quad (4.20)$$

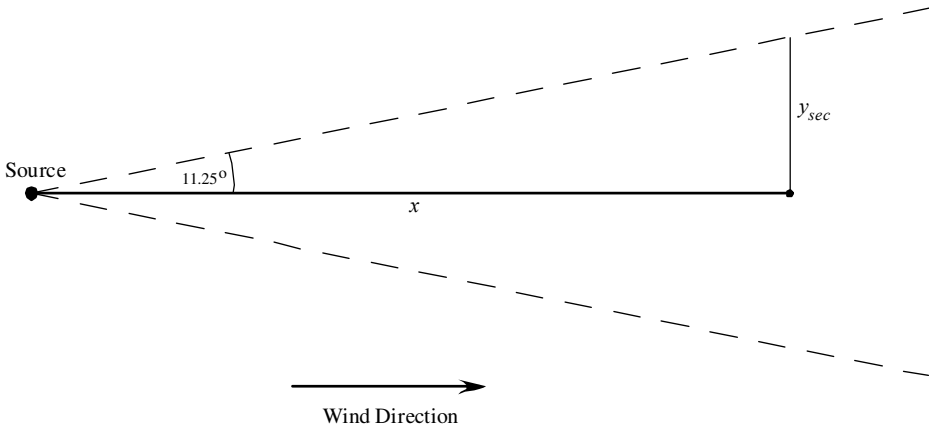

FIGURE 4.1 Relationships Used in Sector-Average Air Concentration Calculations

By using the identity

$$\int_0^\infty \exp\left(-a^2x^2\right)dx = \frac{1}{2a}\sqrt{\pi}, \tag{4.21}$$

Equation 4.20 reduces to

$$\overline{C_{\text{sec}}}(i,x) = \frac{Q_{x_i}}{\sqrt{2\pi}\sigma_z u_H y_{\text{sec}}} \exp\left(\frac{-H^2}{2\sigma_z^2}\right), \tag{4.22}$$

to give the sector-averaged air concentration at a distance x m from the source when there is no plume reflection. In the case when there is plume reflection with total uniform mixing, the sector-average air concentration is given as

$$\overline{C_{\text{sec}}}(i,x) = \frac{1}{y_{\text{sec}}}\int_0^\infty \frac{Q_{x_i}}{\sqrt{2\pi}\sigma_y u_H L}\left[\exp\left(\frac{-y^2}{2\sigma_y^2}\right)\right]dy. \tag{4.23}$$

By using Equation 4.21, Equation 4.23 can be simplified to give

$$\overline{C_{\text{sec}}}(i,x) = \frac{Q_{x_i}}{2y_{\text{sec}}u_H L}. \tag{4.24}$$

In both cases, with and without plume reflection (Equations 4.24 and 4.22, respectively), the integration of y to infinity and averaging using the sector width result in the compression of the plume to within the sector boundaries.

4.5.4 Area Source Model

RESRAD-OFFSITE assumes rectangular source and receptor areas. No area source approximations are used. Rather, a series of point-to-point calculations are performed using Equation 4.22 or 4.24, depending on distance.

The source and receptor areas are first partitioned into grids of 1-m square resolution or greater. The center point of each grid square is used as the source or receptor point representing that small area. Air concentration calculations are performed for each receptor grid square for emissions from every source grid square, with an average chronic air concentration then calculated for each receptor grid square. The average air concentration over the entire receptor area is then taken to be the average value over all receptor grid squares. Each point-to-point calculation uses the appropriate wind direction and frequency for the specific points involved.

While this method avoids any area source approximations, it does increase computation time. "Point" sources (the size of a grid square [the grid spacing]) larger than 1 m^2 may be specified to reduce computation time at the sacrifice of some accuracy.

4.6 DEPLETION CORRECTION

As a radioactive plume travels downwind, its radionuclide content decreases as the result of ground deposition. Two deposition mechanisms, dry and wet, account for this radionuclide depletion from the plume. This section describes the methods used by RESRAD-OFFSITE to calculate plume depletion from radionuclide deposition.

4.6.1 Dry Deposition

With the exception of inert gases, most radioactive material emitted from area sources will be in particulate form. Those particulates with dimensions on the order of a few micrometers or less have vertical movements largely dependent on the vertical turbulence and mean motion of the air; settling of the particles by gravity is minimal. Deposition of such small particles on the ground surface is the result of turbulent diffusion and Brownian motion. Chemical absorption, impaction, and other physical and chemical processes cause the material to be retained at the surface. Such a deposition mechanism depletes the amount of radioactivity in the plume, causing ground contamination, and thus affects potential radiological hazards as the plume travels farther downwind. Radiological hazards to individuals occur by way of either direct exposure from the ground or indirect exposure via the ingestion of contaminated foodstuff.

Calculation of the dry deposition rate involves the concept of deposition velocity, that is, the ratio of the deposition rate to the air concentration expressed in units of velocity. The deposition velocity is determined from either field measurements or laboratory measurements of air and ground concentrations. When plume depletion by dry deposition is considered, the initial source term, Q_{o_i}, at the release point can be replaced by a depleted source term, Q_{x_i}, along the downwind sector. In this approach, known as the source depletion model, it is assumed that the depletion reduces only the effective source strength and that the vertical Gaussian profile remains unchanged. In this derivation, total activity has been conserved.

The reduced source strength Q_{xi} as the result of deposition is calculated from the following equation (Slade 1968):

$$Q_{x_i} = Q_{0_i}\, exp\left[-\frac{V_{d_i}}{\sqrt{\frac{\pi}{2}}u_H} \int_0^x F(x)dx \right], \tag{4.25}$$

where

Q_{xi} = depleted source strength of nuclide i at distance x (Ci/s),

Q_{0i} = initial amount of radionuclide i released (Ci/s),

V_{d_i} = deposition velocity for radionuclide i (m/s),

$F(x)$ = Equation 4.26 or 4.27 (1/m), and

u_H = average wind speed at effective release height (m/s) [Equation 4.9].

At downwind distances not affected by the presence of a mixing layer,

$$F(x) = \frac{\exp\left(\frac{-H^2}{2\sigma_z^2}\right)}{\sigma_z}, \tag{4.26}$$

where

H = effective release height (m) [Equation 4.1], and

σ_z = vertical dispersion coefficient [Equation 4.37].

At downwind distances where total mixing by the presence of a mixing layer can be assumed (Powell et al. 1979),

$$F(x) = \frac{1}{L}, \tag{4.27}$$

where

L = mixing layer height sometimes referred to as lid height (m).

At downwind distances between the no-mixing (Equation 4.15) and total-mixing (Equations 4.16 and 4.17) conditions, $F(x)$ is determined by a linear combination of Equations 4.26 and 4.27.

4.6.2 Wet Deposition

Radionuclides can also be removed from a plume by rain or snowfall. In wet deposition, the depletion mechanism of radionuclides is such that the plume is "washed out" by rain or snow. Thus, the wet deposition rate is dependent on the total amount of radioactivity contained in the plume, in contrast to dry deposition, for which the depletion is closely related to the air

concentration at ground level. The fraction of material removed per unit time by wet deposition is known as the "washout coefficient," V_W, and is defined as

$$V_w = -\frac{1}{C_a}\frac{dC_a}{dt}, \tag{4.28}$$

where

V_W = washout coefficient (1/s), and

C_a = local air concentration (Ci/m^3).

Calculated and measured values of the washout coefficient range from about 1.0×10^{-5} to 1.0×10^{-2} per second (Ritchie et al. 1978, McMahon and Dennison 1979). The value of the washout coefficient increases with an increasing rainfall rate and is linearly dependent on the rainfall rate:

$$V_w = W_c R, \tag{4.29}$$

where

W_C = 1×10^{-3} (1/s)(mm/h)$^{-1}$ for stability classes A to D and

1.0×10^{-4} (1/s)(mm/h)$^{-1}$ for stability classes E and F [Ritchie et al. 1978], and

R = rainfall rate (mm/h).

The depleted source strength from wet deposition, assuming a steady rainfall rate and wind speed, is given by

$$Q_{WET_{x_i}} = Q_{0_i} \exp\left(-\frac{V_w x}{u_H}\right). \tag{4.30}$$

4.6.3 Dry and Wet Deposition

Dry deposition is always considered in RESRAD-OFFSITE. When wet deposition is also considered, the depleted source strength at a distance x downwind becomes a function of both dry and wet deposition. The depleted source strength becomes a combination of Equations 4.25 and 4.30 and is calculated according to

$$Q_{x_i} = Q_{0_i}\, exp\left\{-\left[\frac{V_w x}{u_H} + \frac{V_{d_i}}{\sqrt{\frac{\pi}{2}}u_H}\int_0^x F(x)dx\right]\right\}. \quad (4.31)$$

4.7 MIXING HEIGHT

The value of the mixing height (L) is estimated from the annual average input values for morning and afternoon (Holzworth 1972). The mixing height is estimated from the following:

$L = 1.5\ L_{pm}$ for an extremely unstable atmosphere (stability class A) (4.32)

$= 0.5\ (L_{am} + L_{pm})$ for a neutral atmosphere (stability class D),

where

L_{am} = mean annual morning mixing height (m), and

L_{pm} = mean annual afternoon mixing height (m).

For other unstable situations (stability classes B and C), L is taken to be equal to L_{pm}. The mixing height does not apply to stable atmospheric conditions.

4.8 METEOROLOGICAL CONDITIONS

As presented in the previous sections, the dispersion model in RESRAD-OFFSITE requires the following meteorological data:

1. Stability class (A through F),
2. Wind speed (m/s),
3. Mixing height (m) (for stability classes A through D),
4. Ambient temperature (K), and
5. Rainfall rate (mm/h).

Either a single stability class and wind speed can be used, or joint frequency data on weather conditions over a period of time (e.g., annual data) can be input manually or read from a STability ARray (STAR) format data file.

Atmospheric stabilities are classified into six categories (A, B, C, D, E, and F) in order of increasing stability on the basis of criteria established by Pasquill (1974). The dispersion equations in the models used are generic to all stability categories and empirical in nature. For each stability category, a set of dispersion coefficients, σ_y and σ_z, are initially calculated on the basis of the Pasquill-Gifford curves (Eimutis and Konicek 1972) and later adjusted for buoyancy induced dispersion, as discussed in the next section. The Pasquill-Gifford dispersion coefficients are calculated according to

$$\sigma'_y = \left(0.000246\sigma_\theta^2 + 0.00576\sigma_\theta + 0.066\right)x^{0.9031} \tag{4.33}$$

and

$$\sigma'_z = ax^b + c\,. \tag{4.34}$$

Table 4.2 contains the values for the unitless dispersion parameters σ_θ, a, b, and c as a function of stability class.

Briggs (1974) developed formulas for the dispersion coefficients on the basis of data collected from elevated releases:

$$\sigma'_y \text{ or } \sigma'_z = ax\left(1+bx\right)^c. \tag{4.35}$$

In addition, Briggs coefficients have been derived for rural and urban population zones. The urban values are also used in suburban zone calculations in RESRAD-OFFSITE. Table 4.3 gives values of a, b, and c.

4.9 BUOYANCY INDUCED DISPERSION

Buoyancy induced dispersion is considered in RESRAD-OFFSITE because emitted plumes undergo a certain amount of growth during the plume-rise phase as a result of turbulent motions associated with plume release conditions and turbulent entrainment of ambient air. Pasquill (1976) suggests that this induced dispersion, σ_{zb}, can be approximated by the following equation:

$$\sigma_{zb} = \frac{\Delta h}{3.5}, \tag{4.36}$$

where

σ_{zb} = buoyancy induced vertical dispersion (m).

TABLE 4.2 Pasquill-Gifford Dispersion Parameters for Ground-Level Releases

Applicable Range (downwind distance, m)	Stability Class	Coefficients			
		σ_θ	a	b	c
$x > 1{,}000$	A	25	0.00024	2.094	–9.6
	B	20	0.055	1.098	2.0
	C	15	0.133	0.911	0.0
	D	10	1.26	0.516	–13.0
	E	5	6.73	0.305	–34.0
	F	1.5	18.05	0.18	–48.6
$100 \leq x \leq 1{,}000$	A	25	0.00066	1.941	9.27
	B	20	0.0382	1.149	3.3
	C	15	0.113	0.911	0.0
	D	10	0.222	0.725	–1.7
	E	5	0.211	0.678	–1.3
	F	1.5	0.086	0.74	–0.35
$x < 100$	A	25	0.192	0.936	0.0
	B	20	0.156	0.922	0.0
	C	15	0.116	0.905	0.0
	D	10	0.079	0.881	0.0
	E	5	0.063	0.871	0.0
	F	1.5	0.053	0.814	0.0

Source: Data from Eimutis and Konicek (1972).

The effective dispersion coefficient used in RESRAD-OFFSITE calculations can then be determined by adding variances, such as

$$\sigma_z = \left(\sigma_{zb}^2 + \sigma_z'^2\right)^{1/2}. \tag{4.37}$$

At the distance of final plume rise and beyond, σ_{zb} becomes constant.

Because the plume can be assumed to be symmetrical about its centerline in the initial growth phases of release, the calculation assumes that buoyancy induced dispersion in the horizontal direction is equal to that in the vertical direction:

$$\sigma_{yb} = \frac{\Delta h}{3.5}, \tag{4.38}$$

where

σ_{yb} = buoyancy induced horizontal dispersion (m).

TABLE 4.3 Briggs Dispersion Coefficients for Elevated Releases

		σ_y					
		Rural			Urban		
Weather Conditions	Stability Class	a	b	c	a	b	c
Extremely unstable	A	0.22	0.0001	–0.5	0.32	0.0004	–0.5
Moderately unstable	B	0.16	0.0001	–0.5	0.32	0.0004	–0.5
Slightly unstable	C	0.11	0.0001	–0.5	0.22	0.0004	–0.5
Neutral	D	0.08	0.0001	–0.5	0.16	0.0004	–0.5
Moderately stable	E	0.06	0.0001	–0.5	0.11	0.0004	–0.5
Very stable	F	0.04	0.0001	–0.5	0.11	0.0004	–0.5
		σ_z					
		Rural			Urban		
Weather Conditions	Stability Class	a	b	c	a	b	c
Extremely unstable	A	0.20	0.0	0.0	0.24	0.001	0.5
Moderately unstable	B	0.12	0.0	0.0	0.24	0.001	0.5
Slightly unstable	C	0.08	0.0002	–0.5	0.20	0.0	0.0
Neutral	D	0.06	0.0015	–0.5	0.14	0.0003	–0.5
Moderately stable	E	0.03	0.0003	–1.0	0.08	0.00015	–0.5
Very stable	F	0.016	0.0003	–1.0	0.08	0.00015	–0.5

Source: Briggs (1974).

This expression is combined with that for dispersion resulting from ambient turbulence, in the same manner described above for the vertical direction, to give the horizontal dispersion coefficient used in the RESRAD-OFFSITE calculations for estimating air and ground concentrations:

$$\sigma_y = \left(\sigma_{yb}^2 + \sigma_y'^2\right)^{1/2}. \tag{4.39}$$

5 ACCUMULATION OF RADIONUCLIDES AT OFFSITE LOCATIONS AND IN FOOD

This chapter describes the manner in which RESRAD-OFFSITE conceptualizes the accumulation of contaminants in offsite agricultural areas, in a surface water body, and in the plants and animals that live off those areas. The methods and expressions used to compute the concentration of contaminants in surface soil, surface water, plants, meat, milk, and aquatic food are presented.

The accumulation of contaminants in offsite surface soil due to irrigation with contaminated water and due to deposition of contaminated dust is considered. Radiological transformations, mixing of soil in the surface layer, erosion of the surface layer, and equilibrium desorption release are considered in computing the concentration in surface soil.

Accumulation of contaminants in plants due to root uptake from offsite soil and onsite soil, and foliar uptake from overhead irrigation and deposition of contaminated dust on plants are considered.

Transfer and accumulation of contaminants in meat and milk due to ingestion of contaminated plant material, incidental ingestion of soil with plant feed, and consumption of contaminated water are considered.

The code considers three modes of contamination of an offsite surface water body: (1) the influx of contaminated soil removed from the primary contamination by surface erosion, (2) the contribution of contaminated groundwater entering a surface water body (lake), and (3) the deposition of dust from atmospheric transport. Radiological transformations, equilibrium adsorption desorption between the deposited material and water, and removal of contaminants in the outflow from the lake are considered in computing the contaminant inventory in the lake. Concentration in aquatic food is computed using equilibrium bioaccumulation factors.

5.1 ACCUMULATION IN OFFSITE SURFACE SOIL

The processes that are considered in modeling the accumulation of a radionuclide are represented as follows. The mathematical representations of the processes are written considering the activity of the nuclide in the mixing zone of the offsite receptor location over a time period of δt.

Deposition: The deposition into the mixing zone is given by

$$D_i(t)A^o\delta t, \tag{5.1}$$

where

$D_i(t)$ = time-dependent deposition rate of the radionuclide (pCi m^{-2}), and

A^o = area of the offsite receptor region (m^2).

Radioactive Transformations: The ingrowth within the mixing zone is given by

$$\lambda_i s_j^o(t)\rho_b^o d_{mix}^o A^o \delta t\,, \tag{5.2}$$

where

$s_j^o(t)$ = concentration of the parent nuclide in offsite soil (pCi g^{-1}),

ρ_b^o = dry bulk density of soil at the offsite location (g $[cm]^{-3}$), and

$d_{mix}^o t$ = mixing depth at the offsite location (m).

The decay within the mixing layer is given by

$$\lambda_i s_i^o(t)\rho_b^o d_{mix}^o A^o \delta t\,. \tag{5.3}$$

Surface Erosion: The erosion loss from the mixing layer is given by

$$s_i^o(t)\rho_b^o \varepsilon^o A^o \delta t = s_i^o(t)\rho_b^o E^o d_{mix}^o A^o \delta t\,, \tag{5.4}$$

where

ε^o = rate of erosion soil at the offsite location (m yr^{-1}), and

E^o = fraction of the mixing zone that is eroded each year (yr^{-1}).

Adsorption-Desorption Equilibrium Leaching: Let $c_i(t)$ and $s_i'(t)$ denote the activity concentration of nuclide *i* in the aqueous and solid phases of the mixing layer at time *t*. Then combining the expressions for mass balance, $c_i(t)\theta_c^o + s_i'(t)\rho_b^o = s_i^o(t)\rho_b^o$, and linear adsorption, $s_i'(t) = c_i(t)K_{d_i}^o$, yields

$$c_i(t) = \frac{s_i^o(t)\rho_b^o}{\theta_c^o + \rho_b^o K_{d_i}^o}\,. \tag{5.5}$$

The loss due to leaching is given by

$$c_i(t)A^oI^o\delta t = \frac{s_i^o(t)\rho_b^o}{\theta_c^o + \rho_b^o K_{d_i}^o} A^oI^o\delta t = L_i^o s_i^o(t)\rho_b^o d_{mix}^o A^o\delta t\,, \tag{5.6}$$

where

$K_{d_i}^o$ = soil-water distribution coefficient of radionuclide at the offsite location ([cm]^3 g^{-1}),

θ_c^o = contaminated porosity in soil at the offsite location (dimensionless),

I^o = infiltration rate at the offsite location (m yr^{-1}), and

L_i^o = rate at which the nuclide is leached out of the mixing layer (yr^{-1})

$= L_i^o = \dfrac{I^o / d_{mix}^o}{\theta_c^o + \rho_b^o K_{d_i}^o}$.

The net effect of these processes is the change in the activity in the mixing layer given by

$$\rho_b^o d_{mix}^o A^o \frac{ds_i^o(t)}{dt}\delta t\,. \tag{5.7}$$

By equating the combined effect of the processes to the net change, we get the mass balance equation:

$$\begin{aligned}\rho_b^o d_{mix}^o A^o \frac{ds_i^o(t)}{dt} \quad &= D_i(t)A^o + \lambda_i s_j^o(t)\rho_b^o d_{mix}^o A^o - \lambda_i s_i^o(t)\rho_b^o d_{mix}^o A^o \\ &\quad - s_i^o(t)\rho_b^o E^o d_{mix}^o A^o - L_i^o s_i^o(t)\rho_b^o d_{mix}^o A^o\end{aligned}\,. \tag{5.8}$$

This simplifies to

$$\frac{ds_i^o(t)}{dt} + \left(\lambda_i + E^o + L_i^o\right)s_i^o(t) = \frac{D_i(t)}{\rho_b^o d_{mix}^o} + \lambda_i s_j^o(t)\,. \tag{5.9}$$

This can be integrated from time 0 to t to obtain

$$\begin{aligned}s_i^o(t) = s_i^o(0)e^{-\left(\lambda_i + E^o + L_i^o\right)t} &+ \frac{e^{-\left(\lambda_i + E^o + L_i^o\right)t}}{\rho_b^o d_{mix}^o}\int_0^t D_i(t)e^{\left(\lambda_i + E^o + L_i^o\right)t}dt \\ &+ \lambda_i e^{-\left(\lambda_i + E^o + L_i^o\right)t}\int_0^t s_j^o(t)e^{\left(\lambda_i + E^o + L_i^o\right)t}dt\,.\end{aligned} \tag{5.10}$$

The form of $D_i(t)$ needs to be known to solve this equation.

5.1.1 Deposition Due to Contaminated Irrigation Water

Depending on the distribution of potential evapotranspiration and rainfall over the year, it will be necessary to irrigate the land only during part of the year. It is possible to integrate the above equation for two time periods — first for the part of the year when irrigation is applied, and then with no deposition for the rest of the year. However, given the assumption of uniform mixing throughout the year rather than the once-a-year mixing that occurs during plowing, it is appropriate to model the accumulation by assuming that the quantity of irrigation water is applied uniformly over the year. The rate at which the contaminant is deposited on the ground is then given by

$$D_i(t) = q_{ir} w_i^{ir}(t) \left[1 - f_{\text{int}} \frac{1 - \exp\left(-\lambda_w t_g\right)}{\lambda_w t_g} \right], \tag{5.11}$$

where

q_{ir} = quantity of irrigation water that is applied to a unit area of the agricultural field during a year (m),

$w_i^{ir}(t)$ = concentration of the radionuclide in the irrigation water (pCi m^{-3}),

f_{int} = foliar interception factor (dimensionless),

λ_w = weathering constant (yr^{-1}), and

t_g = growing period when the crop is assumed to be irrigated throughout the growing period (yr).

The last term adjusts for the fraction of deposition that is intercepted and retained by the plant (see Section 5.3.3). The activity concentration of the radionuclide in irrigation water is known at a series of time points and is assumed to vary linearly between these time points. Thus, the deposition of the radionuclide by irrigation water is approximated by a linear function of time; that is,

$$D_i(t) = \alpha_i + \beta_i t, \tag{5.12}$$

where α_i and β_i are constants between each pair of the time points.

5.1.2 Deposition of Particulates from the Atmosphere

The rate at which the contaminant is deposited on the ground from the atmosphere is given by

$$D_i(t) = V_{dep} a_i(t) \left[1 - f_{\text{int}} \frac{1 - \exp\left(-\lambda_w t_g\right)}{\lambda_w} \right], \tag{5.13}$$

where

V_{dep} = deposition velocity of the particulate that is contaminated (m yr^{-1}), and

$a_i(t)$ = concentration of the radionuclide in the atmosphere (pCi m^{-3}).

The last term adjusts for the fraction of deposition that is intercepted and retained by the plant (see Section 5.3.4). The activity concentration of the radionuclide in air is known at a series of time points and is assumed to vary linearly between these time points. Thus, deposition of the radionuclide associated with particulates is approximated by a linear function of *t*ime.

5.1.3 Concentration in Offsite Soil of the First Member of the Transformation Chain

Replacing the time-dependent deposition rate by a linear function of time and integrating[8] yields

$$s_1^o(t) = s_1^o(0) e^{-\left(\lambda_1 + E^o + L_1^o\right)t} + \frac{\left(\alpha_1 - \dfrac{\beta_1}{\lambda_1 + E^o + L_1^o} \right)\left(1 - e^{-\left(\lambda_1 + E^o + L_1^o\right)t}\right) + \beta_1 t}{\rho_b^o d_{mix}^o \left(\lambda_1 + E^o + L_1^o\right)}. \tag{5.14}$$

Collect the terms to obtain

$$s_1^o(t) = A_1^0 + A_1^1 t + C_1^1 e^{-\left(\lambda_1 + E^o + L_1^o\right)t}, \tag{5.15}$$

8
$$\begin{aligned} s_1^o(t) &= s_1^o(0) e^{-\left(\lambda_1 + E^o + L_1^o\right)t} + \frac{e^{-\left(\lambda_1 + E^o + L_1^o\right)t}}{\rho_b^o d_{mix}^o} \int_0^t \left(\alpha_1 + \beta_1 t\right) e^{\left(\lambda_1 + E^o + L_1^o\right)t} dt \\ &= s_1^o(0) e^{-\left(\lambda_1 + E^o + L_1^o\right)t} + \frac{e^{-\left(\lambda_1 + E^o + L_1^o\right)t}}{\rho_b^o d_{mix}^o} \alpha_i \frac{e^{\left(\lambda_1 + E^o + L_1^o\right)t} - 1}{\lambda_1 + E^o + L_1^o} \\ &\quad + \frac{e^{-\left(\lambda_1 + E^o + L_1^o\right)t}}{\rho_b^o d_{mix}^o} \beta_i \left(\frac{t e^{\left(\lambda_1 + E^o + L_1^o\right)t} - 0}{\lambda_1 + E^o + L_1^o} - \frac{e^{\left(\lambda_1 + E^o + L_1^o\right)t} - 1}{\left(\lambda_1 + E^o + L_1^o\right)^2} \right) \end{aligned}$$

where

$$A_1^1 = \frac{\beta_1}{\rho_b^o d_{mix}^o \left(\lambda_1 + E^o + L_1^o\right)},$$

$$A_1^0 = \frac{\alpha_1 - \dfrac{\beta_1}{\lambda_1 + E^o + L_1^o}}{\rho_b^o d_{mix}^o \left(\lambda_1 + E^o + L_1^o\right)} = \frac{\alpha_1}{\rho_b^o d_{mix}^o \left(\lambda_1 + E^o + L_1^o\right)} - \frac{A_1^1}{\lambda_1 + E^o + L_1^o} \text{ , and}$$

$$C_1^1 = s_1^o(0) - \frac{\alpha_1 - \dfrac{\beta_1}{\lambda_1 + E^o + L_1^o}}{\rho_b^o d_{mix}^o \left(\lambda_1 + E^o + L_1^o\right)} = s_1^o(0) - A_1^0 \text{ .}$$

5.1.4 Concentration in Soil of the Second Member of the Transformation Chain

An analogy with the expression for the first member, Section 5.1.3, gives

$$s_2^o(t) = s_2^o(0)e^{-\left(\lambda_2 + E^o + L_2^o\right)t} + \frac{\left(\alpha_2 - \dfrac{\beta_2}{\lambda_2 + E^o + L_2^o}\right)\left(1 - e^{-\left(\lambda_2 + E^o + L_2^o\right)t}\right) + \beta_2 t}{\rho_b^o d_{mix}^o \left(\lambda_2 + E^o + L_2^o\right)} + \lambda_2 e^{-\left(\lambda_2 + E^o + L_2^o\right)t} \int_0^t s_1^o(t) e^{\left(\lambda_2 + E^o + L_2^o\right)t} dt \quad . \qquad (5.16)$$

Substituting for the concentration of the first member and integrating[9] gives

$$s_2^o(t) = s_2^o(0)e^{-\left(\lambda_2 + E^o + L_2^o\right)t} + \frac{\left(\alpha_2 - \dfrac{\beta_2}{\lambda_2 + E^o + L_2^o}\right)\left(1 - e^{-\left(\lambda_2 + E^o + L_2^o\right)t}\right) + \beta_2 t}{\rho_b^o d_{mix}^o \left(\lambda_2 + E^o + L_2^o\right)} + \lambda_2 \frac{\left(A_1^0 - \dfrac{A_1^1}{\lambda_2 + E^o + L_2^o}\right)\left(1 - e^{-\left(\lambda_2 + E^o + L_2^o\right)t}\right) + A_1^1 t}{\lambda_2 + E^o + L_2^o} + \lambda_2 C_1^1 \frac{e^{-\left(\lambda_1 + E^o + L_1^o\right)t} - e^{-\left(\lambda_2 + E^o + L_2^o\right)t}}{\lambda_2 + L_2^o - \lambda_1 - L_1^o} \quad . \qquad (5.17)$$

$$\int_0^t \left(A_1^0 + A_1^1 t + C_1^1 e^{-\left(\lambda_1 + E^o + L_1^o\right)t}\right) e^{\left(\lambda_2 + E^o + L_2^o\right)t} dt = A_1^0 \frac{e^{\left(\lambda_2 + E^o + L_2^o\right)t} - 1}{\lambda_2 + E^o + L_2^o}$$

9

$$+ A_1^1 \frac{t e^{\left(\lambda_2 + E^o + L_2^o\right)t}}{\lambda_2 + E^o + L_2^o} - A_1^1 \frac{e^{\left(\lambda_2 + E^o + L_2^o\right)t} - 1}{\left(\lambda_2 + E^o + L_2^o\right)^2} + C_1^1 \frac{e^{\left(\lambda_2 + L_2^o - \lambda_1 - L_1^o\right)t} - 1}{\lambda_2 + L_2^o - \lambda_1 - L_1^o}$$

Collecting the terms yields

$$s_2^o(t) = A_2^0 + A_2^1 t + C_2^1 e^{-\left(\lambda_1 + E^o + L_1^o\right)t} + C_2^2 e^{-\left(\lambda_2 + E^o + L_2^o\right)t}, \tag{5.18}$$

where

$$A_2^1 = \frac{\beta_2}{\rho_b^o d_{mix}^o \left(\lambda_2 + E^o + L_2^o\right)} + \frac{\lambda_2 A_1^1}{\lambda_2 + E^o + L_2^o},$$

$$A_2^0 = \frac{\alpha_2 - \dfrac{\beta_2}{\lambda_2 + E^o + L_2^o}}{\rho_b^o d_{mix}^o \left(\lambda_2 + E^o + L_2^o\right)} + \lambda_2 \frac{A_1^0 - \dfrac{A_1^1}{\lambda_2 + E^o + L_2^o}}{\lambda_2 + E^o + L_2^o}$$

$$= \frac{\alpha_2}{\rho_b^o d_{mix}^o \left(\lambda_2 + E^o + L_2^o\right)} + \frac{\lambda_2 A_1^0}{\lambda_2 + E^o + L_2^o} - \frac{A_2^1}{\lambda_2 + E^o + L_2^o}$$

$$C_2^1 = \frac{\lambda_2 C_1^1}{\lambda_2 + L_2^o - \lambda_1 - L_1^o}, \text{ and}$$

$$C_2^2 = s_2^o(0) - A_2^0 - C_2^1.$$

5.1.5 Concentration in Soil of the *j*th Member of the Transformation Chain

Using the form of the expressions for the first and second members of the chains, the expression for the j^{th} member of the chain is obtained by induction. Assume that the concentration of the i^{th} member of the transformation chain in offsite soil is

$$s_i^o(t) = A_i^0 + A_i^1 t + \sum_{k=1}^{i} C_i^k e^{-\left(\lambda_k + E^o + L_k^o\right)t}. \tag{5.19}$$

Then the concentration of the next member, j, of the transformation chain is given by

$$s_j^o(t) = s_j^o(0) e^{-\left(\lambda_j + E^o + L_j^o\right)t} + \frac{\left(\alpha_j - \dfrac{\beta_j}{\lambda_j + E^o + L_j^o}\right)\left(1 - e^{-\left(\lambda_j + E^o + L_j^o\right)t}\right) + \beta_j t}{\rho_b^o d_{mix}^o \left(\lambda_j + E^o + L_j^o\right)} + \lambda_j e^{-\left(\lambda_j + E^o + L_j^o\right)t} \int_0^t \left(A_i^0 + A_i^1 t + \sum_{k=1}^{i} C_i^k e^{-\left(\lambda_k + E^o + L_k^o\right)t}\right) e^{\lambda_j + E^o + L_j^o t} dt. \tag{5.20}$$

Integration gives

$$s_j^o(t) = s_j^o(0)e^{-\left(\lambda_j + E^o + L_j^o\right)t} + \lambda_j \sum_{k=1}^{i} C_i^k \frac{e^{-\left(\lambda_k + E^o + L_k^o\right)t} - e^{-\left(\lambda_j + E^o + L_j^o\right)t}}{\lambda_j + L_j^o - \lambda_k - L_k^o}$$

$$+ \frac{\left(\frac{\alpha_j}{\rho_b^o d_{mix}^o} + \lambda_j A_i^0 - \frac{\beta_j \big/ \rho_b^o d_{mix}^o + \lambda_j A_i^1}{\lambda_j + E^o + L_j^o}\right)\left(1 - e^{-\left(\lambda_j + E^o + L_j^o\right)t}\right) + \left(\frac{\beta_j}{\rho_b^o d_{mix}^o} + \lambda_j A_i^1\right)t}{\lambda_j + E^o + L_j^o} \quad . \qquad (5.21)$$

$$s_j^o(t) = s_j^o(0)e^{-\left(\lambda_j + E^o + L_j^o\right)t} + \frac{\left(\alpha_j - \frac{\beta_j}{\lambda_j + E^o + L_j^o}\right)\left(1 - e^{-\left(\lambda_j + E^o + L_j^o\right)t}\right) + \beta_j t}{\rho_b^o d_{mix}^o \left(\lambda_j + E^o + L_j^o\right)}$$

$$+ \lambda_j \frac{\left(A_i^0 - \frac{A_i^1}{\lambda_j + E^o + L_j^o}\right)\left(1 - e^{-\left(\lambda_j + E^o + L_j^o\right)t}\right) + A_i^1 t}{\lambda_j + E^o + L_j^o} + \lambda_j \sum_{k=1}^{i} C_i^k \frac{e^{-\left(\lambda_k + E^o + L_k^o\right)t} - e^{-\left(\lambda_j + E^o + L_j^o\right)t}}{\lambda_j + L_j^o - \lambda_k - L_k^o} \qquad (5.22)$$

Collecting the terms yields

$$s_j^o(t) = A_j^0 + A_j^1 t + \sum_{k=1}^{j} C_j^k e^{-\left(\lambda_k + E^o + L_k^o\right)t} ,$$

where

$$A_j^1 = \frac{\beta_j}{\rho_b^o d_{mix}^o \left(\lambda_j + E^o + L_j^o\right)} + \frac{\lambda_j A_{j-1}^1}{\lambda_j + E^o + L_j^o} ,$$

$$A_j^0 = \frac{\alpha_j - \frac{\beta_j}{\lambda_j + E^o + L_j^o}}{\rho_b^o d_{mix}^o \left(\lambda_j + E^o + L_j^o\right)} + \lambda_j \frac{A_{j-1}^0 - \frac{A_{j-1}^1}{\lambda_j + E^o + L_j^o}}{\lambda_j + E^o + L_j^o} \quad ,$$

$$= \frac{\alpha_j}{\rho_b^o d_{mix}^o \left(\lambda_j + E^o + L_j^o\right)} + \frac{\lambda_j A_{j-1}^0}{\lambda_j + E^o + L_j^o} - \frac{A_j^1}{\lambda_j + E^o + L_j^o}$$

$$C_j^k = \frac{\lambda_j C_{j-1}^k}{\lambda_j + L_j^o - \lambda_k - L_k^o} \text{ for all } k \neq j \text{, and}$$

$$C_j^j = s_j^o(0) - A_j^0 - \sum_{k=1}^{j-1} C_j^k \ .$$

5.2 ACCUMULATION OF RADIONUCLIDES IN SURFACE WATER

The processes that are considered in modeling the accumulation of a radionuclide are represented as follows. The mathematical representations of the processes are written by considering the change in the activity of the nuclide in the surface water body over a time period of δt.

Input of Radionuclides in Sediments from Surface Erosion: The quantity of radionuclide *i* resulting from the erosion of the primary contamination is

$$R_i^{sr}(t) SDR \delta t \ , \tag{5.23}$$

where

$R_i^{sr}(t)$ = release rate of nuclide *i* due to erosion of the surface soil above the primary contamination, Section 2.5 (pCi y^{-1}), and

SDR = sediment delivery ratio.

The sediment delivery ratio can be estimated by using the regression equation given in Section 12.10 of Shen and Julien (1993), which after changing the units of the drainage area to m^2 is $SDR = 26A^{-0.3}$.

Input of Radionuclides from Groundwater: The quantity of radionuclide *i* transported by groundwater flow is

$$f_s(t) \delta t \ , \tag{5.24}$$

where $f_s(t)$ is the flux of radionuclide *i* carried by groundwater entering the surface water body, Section 3.2 (pCi yr^{-1}).

Input of Radionuclides from Atmospheric Transport: The quantity of radionuclide *i* transported by wind is

$$a_i(t) V_{dep} A^{sw} \delta t \ , \tag{5.25}$$

where

$a_i(t)$ = concentration of the radionuclide *i* in the atmosphere (pCi m^{-3}),

V_{dep} = deposition velocity of the particulate that is contaminated (m yr^{-1}), and

A^{sw} = surface area of the surface water body (m^2).

Radioactive Transformations: The quantity of radionuclide *i* added due to ingrowth from parent radionuclide *i-1* is

$$\lambda_i V^{sw} w_{i-1}^{sw}(t)\delta t + \lambda_i m^{sd}(t) s_{i-1}^{sd}(t)\delta t\,, \tag{5.26}$$

where

V^{sw} = volume of water in the surface water body (m^3),

$w_{i-1}^{sw}(t)$ = concentration of the parent nuclide in water (pCi m^{-3}),

$m^{sd}(t)$ = cumulative mass of contaminated soil deposited into surface water body (g), and

$s_{i-1}^{sd}(t)$ = concentration of the parent nuclide in the contaminated soil deposited into the surface water (pCi g^{-1}).

The quantity of radionuclide *i* removed due to radiological transformations is

$$\lambda_i V^{sw} w_i^{sw}(t)\delta t + \lambda_i m^{sd}(t) s_i^{sd}(t)\delta t\,. \tag{5.27}$$

By using the relationship between the aqueous phase and adsorbed phase concentrations, $s_i^{sd}(t) = 10^{-6} K_d^i w_i^{sw}(t)$, these expressions become

$$\lambda_i \left(V^{sw} + 10^{-6} m^{sd}(t) K_d^{i-1}\right) w_{i-1}^{sw}(t)\delta t - \lambda_i \left(V^{sw} + 10^{-6} m^{sd}(t) K_d^{i}\right) w_i^{sw}(t)\delta t\,. \tag{5.28}$$

By defining an equivalent volume of the surface water body for nuclide *i* by the equation

$$V_i^{sw}(t) = V^{sw} + m^{sd}(t) K_d^i / 10^6\,, \tag{5.29}$$

this reduces to

$$\lambda_i V_{i-1}^{sw}(t) w_{i-1}^{sw}(t)\delta t - \lambda_i V_i^{sw}(t) w_i^{sw}(t)\delta t\,. \tag{5.30}$$

Removal of Contaminated Lake Water: The quantity of radionuclide *i* removed from the surface water body by the outflow of contaminated water is

$$q_{sw} w_i^{sw}(t)\delta t\,. \tag{5.31}$$

Net Change in the Lake: The net effect of all the changes discussed above leads to a change in the concentration of radionuclide *i* in the water and eroded soil contained in the surface water body. This is represented by

$$
\begin{aligned}
& V^{sw}\frac{dw_i^{sw}(t)}{dt}\delta t + \frac{dm^{sd}(t)s_i^{sd}(t)}{dt}\delta t \\
& = V^{sw}\frac{dw_i^{sw}(t)}{dt}\delta t + m^{sd}(t)\frac{ds_i^{sd}(t)}{dt}\delta t + s_i^{sd}(t)\frac{dm^{sd}(t)}{dt}\delta t \\
& = \left(V^{sw} + 10^{-6} m^{sd}(t)K_d^i\right)\frac{dw_i^{sw}(t)}{dt}\delta t + 10^{-6} K_d^i w_i^{sw}(t)\frac{dm^{sd}(t)}{dt}\delta t \\
& = V_i^{sw}(t)\frac{dw_i^{sw}(t)}{dt}\delta t + 10^{-6} K_d^i w_i^{sw}(t)\frac{dm^{sd}(t)}{dt}\delta t
\end{aligned}
\quad . \tag{5.32}
$$

Equating the combined effect of these process to the net change gives the mass balance equation:

$$
\begin{aligned}
V_i^{sw}(t)\frac{dw_i^{sw}(t)}{dt} + 10^{-6} K_d^i w_i^{sw}(t)\frac{dm^{sd}(t)}{dt} &= R_i^{sr}(t)SDR + f_s(t) + a_i(t)V_{dep}A^{sw} \\
&\quad + \lambda_i V_{i-1}^{sw}(t)w_{i-1}^{sw}(t) - \lambda_i V_i^{sw}(t)w_i^{sw}(t) - q_{sw}w_i^{sw}(t)
\end{aligned}
\tag{5.33}
$$

Dividing by the equivalent volume of the surface water body for nuclide *i* and defining the rates of removal, change, and inflow, yields

$$
\frac{dw_i^{sw}(t)}{dt} + \left(\lambda_i + \lambda_i^{sw} + \lambda_i^{sd}\right)w_i^{sw}(t) = I_i^{sw}(t) + \lambda_i \frac{V_{i-1}^{sw}(t)}{V_i^{sw}(t)} w_{i-1}^{sw}(t), \tag{5.34}
$$

where

$\lambda_i^{sw} = \dfrac{q_{sw}}{V_i^{sw}(t)}$ = rate constant for the removal of nuclide *i* with the water flowing out of the surface water body (yr^{-1}),

$\lambda_i^{sd} = \dfrac{10^{-6} K_d^i}{V_i^{sw}(t)}\dfrac{dm^{sd}(t)}{dt}$ = equivalent rate constant for the change in partitioning caused by the additional mass of eroded soil into the surface water body (yr^{-1}), and

$$I_i^{sr}(t) = \frac{R_i^{sr}(t)SDR + f_s(t) + a_i(t)V_{dep}A^{sw}}{V_i^{sw}(t)}$$ = rate at which nuclide *i* enters the surface water body per unit equivalent volume (pCi yr^{-1}).

This can be integrated from time 0 to *t* assuming that the ratio $\frac{V_{i-1}^{sw}(t)}{V_i^{sw}(t)}$ is a constant during this time interval. Integration yields

$$\begin{aligned} w_i^{sw}(t) = w_i^{sw}(0)e^{-\left(\lambda_i+\lambda_i^{sw}+\lambda_i^{sd}\right)t} + e^{-\left(\lambda_i+\lambda_i^{sw}+\lambda_i^{sd}\right)t}\int_0^t I_i^{sw}(t)e^{\left(\lambda_i+\lambda_i^{sw}+\lambda_i^{sd}\right)t}dt \\ + \lambda_i e^{-\left(\lambda_i+\lambda_i^{sw}+\lambda_i^{sd}\right)t}\frac{V_{i-1}^{sw}(t)}{V_i^{sw}(t)}\int_0^t w_{i-1}^{sw}(t)e^{\left(\lambda_i+\lambda_i^{sw}+\lambda_i^{sd}\right)t}dt. \end{aligned} \tag{5.35}$$

The form of $I_i^{sw}(t)$ needs to be known to solve this equation.

5.2.1 Inflow of Radionuclides into the Surface Water Body

The rates at which a radionuclide enters the surface water body from surface erosion, groundwater flow, and atmospheric deposition of dust are each known at a series of times. The nuclide-specific equivalent volume of the lake is also known at those times. Hence, the nuclide input per equivalent lake volume can be computed at each of those times and is assumed to vary linearly between these time points. Thus, it is approximated by a linear function of *t*, that is, $I_i^{sw}(t) = \alpha_i + \beta_i t$, where α_i and β_i are constants between each pair of time points and are determined by the contaminant input time pairs bracketing the time of interest.

5.2.2 Concentration of the First Member of the Transformation Chain in the Surface Water Body

Replacing the time-dependant inflow by a linear function of time and integrating, as in Section 5.1.3, yields

$$w_1^{sw}(t) = w_1^{sw}(0)e^{-\left(\lambda_1+\lambda_1^{sw}+\lambda_1^{sd}\right)t} + \frac{\left(\alpha_1 - \frac{\beta_1}{\lambda_1+\lambda_1^{sw}+\lambda_1^{sd}}\right)\left(1-e^{-\left(\lambda_1+\lambda_1^{sw}+\lambda_1^{sd}\right)t}\right)+\beta_1 t}{\lambda_1+\lambda_1^{sw}+\lambda_1^{sd}}. \tag{5.36}$$

Collect the terms to obtain

$$w_1^{sw}(t) = A_1^0 + A_1^1 t + C_1^1 e^{-\left(\lambda_1+\lambda_1^{sw}+\lambda_1^{sd}\right)t}, \tag{5.37}$$

where

$$A_1^1 = \frac{\beta_1}{\lambda_1 + \lambda_1^{sw} + \lambda_1^{sd}},$$

$$A_1^0 = \frac{\alpha_1 - \dfrac{\beta_1}{\lambda_1 + \lambda_1^{sw} + \lambda_1^{sd}}}{\lambda_1 + \lambda_1^{sw} + \lambda_1^{sd}} = \frac{\alpha_1 - A_1^1}{\lambda_1 + \lambda_1^{sw} + \lambda_1^{sd}} \text{ and}$$

$$C_1^1 = w_1^{sw}(0) - \frac{\alpha_1 - \dfrac{\beta_1}{\lambda_1 + \lambda_1^{sw} + \lambda_1^{sd}}}{\lambda_1 + \lambda_1^{sw} + \lambda_1^{sd}} = w_1^{sw}(0) - A_1^0.$$

5.2.3 Concentration of the Second Member of the Transformation Chain in the Surface Water Body

An analogy with the expression for the first member, Section 5.2.2, gives

$$w_2^{sw}(t) = w_2^{sw}(0)e^{-\left(\lambda_2+\lambda_2^{sw}+\lambda_2^{sd}\right)t} + \frac{\left(\alpha_2 - \dfrac{\beta_2}{\lambda_2 + \lambda_2^{sw} + \lambda_2^{sd}}\right)\left(1 - e^{-\left(\lambda_2+\lambda_2^{sw}+\lambda_2^{sd}\right)t}\right) + \beta_2 t}{\lambda_2 + \lambda_2^{sw} + \lambda_2^{sd}} + \lambda_2 e^{-\left(\lambda_2+\lambda_2^{sw}+\lambda_2^{sd}\right)t} \frac{V_1^{sw}(t)}{V_2^{sw}(t)} \int_0^t w_1^{sw}(t) e^{\left(\lambda_2+\lambda_2^{sw}+\lambda_2^{sd}\right)t} dt \quad (5.38)$$

Substituting for the concentration of the first member and integrating as in Section 5.1.4 gives

$$w_2^{sw}(t) = w_2^{sw}(0)e^{-\left(\lambda_2+\lambda_2^{sw}+\lambda_2^{sd}\right)t} + \frac{V_1^{sw}(t)}{V_2^{sw}(t)} \frac{\lambda_2 C_1^1 \left(e^{-\left(\lambda_1+\lambda_1^{sw}+\lambda_1^{sd}\right)t} - e^{-\left(\lambda_2+\lambda_2^{sw}+\lambda_2^{sd}\right)t}\right)}{\lambda_2 + \lambda_2^{sw} + \lambda_2^{sd} - \lambda_1 - \lambda_1^{sw} - \lambda_1^{sd}}$$

$$+ \frac{\left(\alpha_2 + \lambda_2 \frac{V_1^{sw}(t)}{V_2^{sw}(t)} A_1^0 - \dfrac{\beta_2 + \lambda_2 A_1^1 V_1^{sw}(t)/V_2^{sw}(t)}{\lambda_2 + \lambda_2^{sw} + \lambda_2^{sd}}\right)\left(1 - e^{-\left(\lambda_2+\lambda_2^{sw}+\lambda_2^{sd}\right)t}\right) + \left(\beta_2 + \lambda_2 \frac{V_1^{sw}(t)}{V_2^{sw}(t)} A_1^1\right)t.}{\lambda_2 + \lambda_2^{sw} + \lambda_2^{sd}} \quad (5.39)$$

Collecting the terms yields

$$w_2^{sw}(t) = A_2^0 + A_2^1 t + C_2^1 e^{-\left(\lambda_1+\lambda_1^{sw}+\lambda_1^{sd}\right)t} + C_2^2 e^{-\left(\lambda_2+\lambda_2^{sw}+\lambda_2^{sd}\right)t}, \quad (5.40)$$

where

$$A_2^1 = \left(\beta_2 + \frac{V_1^{sw}(t)}{V_2^{sw}(t)} \lambda_2 A_1^1 \right) \Big/ \left(\lambda_2 + \lambda_2^{sw} + \lambda_2^{sd} \right),$$

$$A_2^0 = \frac{\alpha_2 + \lambda_2 \dfrac{V_1^{sw}(t)}{V_2^{sw}(t)} A_1^0 - \dfrac{\beta_2 + \lambda_2 A_1^1 V_1^{sw}(t) / V_2^{sw}(t)}{\lambda_2 + \lambda_2^{sw} + \lambda_2^{sd}}}{\lambda_2 + \lambda_2^{sw} + \lambda_2^{sd}},$$

$$= \left(\alpha_2 + \frac{V_1^{sw}(t)}{V_2^{sw}(t)} \lambda_2 A_1^0 - A_2^1 \right) \Big/ \left(\lambda_2 + \lambda_2^{sw} + \lambda_2^{sd} \right)$$

$$C_2^1 = \frac{V_1^{sw}(t)}{V_2^{sw}(t)} \frac{\lambda_2 C_1^1}{\lambda_2 + \lambda_2^{sw} + \lambda_2^{sd} - \lambda_1 - \lambda_1^{sw} - \lambda_1^{sd}}, \text{ and } C_2^2 = w_2^{sw}(0) - A_2^0 - C_2^1.$$

5.2.4 Concentration of the *j^th^* Member of the Transformation Chain in the Surface Water Body

Using the form of the expressions for the first and second members of the chains, the expression for the *j^th^* member of the chain is obtained by induction. The expression is developed along the lines of Section 5.1.5 and is given by

$$w_j^{sw}(t) = w_j^{sw}(0) e^{-\left(\lambda_j + \lambda_j^{sw} + \lambda_j^{sd}\right)t} + \frac{\left(\alpha_j - \dfrac{\beta_j}{\lambda_j + \lambda_j^{sw} + \lambda_j^{sd}} \right)\left(1 - e^{-\left(\lambda_j + \lambda_j^{sw} + \lambda_j^{sd}\right)t}\right) + \beta_j t}{\lambda_j + \lambda_j^{sw} + \lambda_j^{sd}}$$

$$+ \lambda_j e^{-\left(\lambda_j + \lambda_j^{sw} + \lambda_j^{sd}\right)t} \frac{V_i^{sw}(t)}{V_j^{sw}(t)} \int_0^t \left(A_{j-1}^0 + A_{j-1}^1 t + \sum_{k=1}^{j-1} C_{j-1}^k e^{-\left(\lambda_k + \lambda_k^{sw} + \lambda_k^{sd}\right)t} \right)(t) e^{\left(\lambda_j + \lambda_j^{sw} + \lambda_j^{sd}\right)t} dt \tag{5.41}$$

Collecting the terms yields

$$w_j^{sw}(t) = A_j^0 + A_j^1 t + \sum_{k=1}^{j} C_j^k e^{-\left(\lambda_k + \lambda_k^{sw} + \lambda_k^{sd}\right)t}, \tag{5.42}$$

where

$$A_j^1 = \left(\beta_j + \frac{V_{j-1}^{sw}(t)}{V_j^{sw}(t)} \lambda_j A_{j-1}^1 \right) \Big/ \left(\lambda_j + \lambda_j^{sw} + \lambda_j^{sd} \right),$$

$$A_j^0 = \frac{\alpha_j}{\lambda_j + \lambda_j^{sw} + \lambda_j^{sd}} + \frac{V_{j-1}^{sw}(t)}{V_j^{sw}(t)} \frac{\lambda_j A_{j-1}^0}{\lambda_j + \lambda_j^{sw} + \lambda_j^{sd}} - \frac{A_j^1}{\lambda_j + \lambda_j^{sw} + \lambda_j^{sd}},$$

$$C_j^k = \frac{V_{j-1}^{sw}(t)}{V_j^{sw}(t)} \frac{\lambda_j C_{j-1}^k}{\lambda_j + \lambda_j^{sw} + \lambda_j^{sd} - \lambda_k - \lambda_k^{sw} + \lambda_k^{sd}} \text{ for all } k \neq j, \text{ and}$$

$$C_j^j = w_j^{sw}(0) - A_j^0 - \sum_{k=1}^{j-1} C_j^k .$$

5.3 ACCUMULATION IN PLANTS

The processes that are considered in modeling the contamination on plants and the expressions used to model these processes are discussed in the following subsections. The concentration of the radionuclide in plant material is obtained by summing the four components discussed below.

5.3.1 Root Uptake from Onsite Soil

If part (or all) of the agricultural area lies above the primary contamination, the roots of the plants could penetrate the primary contamination and take up the contaminants. This is computed as follows:

$$p_i^{onsoil}(t) = f_a f_{cd}(t) rtf_i s_i(t), \tag{5.43}$$

where

$p_i^{onsoil}(t)$ = activity concentration of radionuclide *i* in the edible portion of the plant resulting from uptake by root from the primary contamination (pCi g^{-1}),

f_a = fraction of the agricultural area that lies directly above the primary contamination,

rtf_i = root uptake factor of radionuclide *i* for the plant,

$s_i(t)$ = activity concentration of radionuclide *i* in onsite soil (pCi g^{-1}),

$f_{cd}(t)$ = cover and depth factor, which is the fraction of the root length exposed to the primary contamination given by

$$f_{cd}(t) = 0 \text{ when } T_{cv}^c(t) \geq d_{root},$$

$$f_{cd}(t) = f_{vm}(t) \frac{\rho_{pc}}{\rho_{mix}} \text{ when } T_{mix}^c(t) \geq d_{root},$$

$$f_{cd}(t) = \frac{f_{vm}(t)\frac{\rho_{pc}}{\rho_{mix}} T^{c}_{mix}(t) + d_{root} - T^{c}_{cv}(t) - T^{c}_{mix}(t)}{d_{root}} \text{ when } T^{c}_{cv}(t) + T^{c}_{mix}(t) + T^{um}_{pc}(t) \geq d_{root}, \text{ and}$$

$$f_{cd}(t) = \frac{f_{vm}(t)\frac{\rho_{pc}}{\rho_{mix}} T^{c}_{mix}(t) + T^{um}_{cz}(t)}{d_{root}} \text{ when } T^{c}_{cv}(t) + T^{c}_{mix}(t) + T^{um}_{pc}(t) < d_{root}$$

where

d_{root} = length of the root (m), and the remaining quantities are as defined and described in Section 2.2.

5.3.2 Root Uptake from Offsite Soil

The activity concentration of radionuclide *i* in the edible portion of the plant resulting from uptake by roots from the offsite soil is computed using

$$p^{offsoil}_{i}(t) = rtf_{i}s^{o}_{i}(t). \tag{5.44}$$

Adjustments are not made for the situation where the depth of root might exceed the thickness of the mixing layer because the code only models the concentration of radionuclides in the mixing zone, not in the soil below.

5.3.3 Foliar Uptake from Overhead Irrigation

This uptake is computed by using

$$p^{oi}_{i}(t) = \frac{f_{\text{int}} f_{tl}}{Y} \frac{1 - \exp(-\lambda_{w} t_{g})}{\lambda_{w}} \frac{q_{ir}}{t_{g}} w^{ir}_{i}(t), \tag{5.45}$$

where

$p^{oi}_{i}(t)$ = activity concentration of radionuclide *i* in the edible portion of the plant resulting from foliar interception of overhead irrigation (pCi g^{-1}),

$= f_{tl}$ = fraction of contaminant that is translocated from the foliage to the edible part of the plants, and

Y = wet weight crop yield (kg m^{-2}).

This expression is derived by assuming that the concentration of radionuclide in the irrigation water is constant during the growing season. Consider the changes in the quantity of the radionuclide in the plant over a time period of δt. The quantity of the radionuclide intercepted and retained by the plant is given by

$$f_{\text{int}} \frac{q_{ir}}{t_g} w_i^{ir} \delta t \,. \tag{5.46}$$

The quantity of the radionuclide lost from the plant due to weathering is given by

$$\lambda_w P_i^{oi}(t) \delta t \,, \tag{5.47}$$

where

$P_i^{oi}(t)$ = quantity of radionuclide in the plant grown in a unit area of land, resulting from overhead irrigation.

The change in the quantity of the radionuclide in the plant is represented by

$$\frac{dP_i^{oi}(t)}{dt} \delta t \,. \tag{5.48}$$

Equating the change to the net change gives the mass balance equation:

$$\frac{dP_i^{oi}(t)}{dt} = f_{\text{int}} \frac{q_{ir}}{t_g} w_i^{ir} - \lambda_w P_i^{oi}(t). \tag{5.49}$$

Integration over the growing period gives

$$P_i^{oi}(t) = f_{\text{int}} \frac{q_{ir}}{t_g} w_i^{ir} \frac{1 - \exp(-\lambda_w t_g)}{\lambda_w} \,. \tag{5.50}$$

This is the factor applied in Section 5.1.1 to account for the quantity of the radionuclide that is retained by the plant. The concentration in the edible portion of the plant is obtained by applying the translocation factor and the yield.

5.3.4 Foliar Uptake of Dust

This uptake is computed by using

$$p_i^{dust}(t) = \frac{f_{\text{int}} f_{tl}}{Y} \frac{1 - \exp(-\lambda_w t_g)}{\lambda_w} V_{dep} a_i(t), \tag{5.51}$$

where $p_i^{dust}(t)$ is the activity concentration of radionuclide *i* in the edible portion of the plant resulting from foliar interception of dust (pCi g^{-1}). It is derived by assuming that the concentration of radionuclides in dust is constant over the growing period. The derivation is analogous to that for foliar interception of overhead irrigation.

5.4 ACCUMULATION IN MEAT AND MILK

Transfer and accumulation of contaminants in meat and milk due to ingestion of contaminated plant material, incidental ingestion of soil with plant feed, and consumption of contaminated livestock water are considered. This process is computed by using

$$m_i(t) = imf_i \left[q_{ing}^p p_i(t) + q_{ing}^s \left(s_i^o(t) + f_a f_{vm} \frac{\rho_{cz}}{\rho_{mix}} s_i(t) \right) + q_{ing}^w w_i^{lf}(t) \right], \tag{5.52}$$

where

imf_i = concentration of the nuclide in meat or milk at the time of slaughter or milking due to a uniform intake of unit activity of radionuclide per day ([pCi {kg}$^{-1}$]/[pCi d^{-1}]),

q_{ing}^p = rate of ingestion of plant derived feed by the livestock (kg d^{-1}),

q_{ing}^s = rate of ingestion of soil with plant derived feed by the livestock (kg d^{-1}), and

q_{ing}^w = rate of ingestion of water by the livestock (L d^{-1}).

5.5 ACCUMULATION IN FISH AND AQUATIC FOODS

Equilibrium transfer of contaminants from lake water to the aquatic food is used. The concentration in aquatic food is computed by using

$$aqf_i(t) = baf_i w_i^{sw}(t), \tag{5.53}$$

where

$aqf_i(t)$ = activity concentration of nuclide *i* in aquatic food (pCi $[kg]^{-1}$), and

baf_i = bioaccumulation factor or the equilibrium concentration ratio between aquatic food and lake water ($[pCi\ \{kg\}^{-1}]/[pCi\ L^{-1}]$).

6 EXPOSURE PATHWAYS AND EXPOSURE SCENARIOS

In RESRAD-OFFSITE, the general principles for computing exposure are the same as for the RESRAD (onsite) code (Yu et al. 2001). The primary difference between the two codes is that media concentrations at the time of exposure, not environmental transfer factors, are used in RESRAD-OFFSITE. The dose or risk resulting directly from the primary contamination and from the particulates and gases released from the primary contamination are summed and reported together. Likewise, the dose and risk resulting from the releases to groundwater and to surface runoff are summed and reported together.

6.1 EXTERNAL RADIATION FROM CONTAMINATION IN SOIL

The code models the external radiation from contamination in soil for the following situations:

- Exposure to radiation from the primary contamination while located indoors and outdoors in an onsite dwelling above the primary contamination.
- Exposure to radiation from the primary contamination while located indoors and outdoors in an offsite dwelling that is outside the perimeter of the primary contamination.
- Exposure to radiation from the accumulation in the soil in the offsite dwelling site while located indoors and outdoors in the offsite dwelling site.
- Exposure to radiation from the accumulation in the soil in an offsite agricultural area while located outdoors in that offsite agricultural area.

The exposures resulting from all four situations are summed and reported as a single quantity.

As discussed in Appendix A of the user's manual for RESRAD (onsite) code (Yu et al. 2001), the exposure for each of the above situations is computed as the product of the following:

- The dose conversion factor or slope factor for external radiation, for a volume source of infinite thickness and infinite area, from the chosen dose factor library ([mrem yr^{-1}]/[pCi g^{-1}] or [risk yr^{-1}]/[pCi g^{-1}]),
- The concentration of the radionuclide in the soil (pCi g^{-1}),
- An occupancy and indoor shielding factor to account for the time spent at the location and for the shielding from any building components while indoors,

- A cover and depth factor to account for the finite thickness of the contamination and for any intervening clean cover between the contamination and the receptor, and

- An area and shape factor to account for the finite area and shape of the contaminated soil and for the position (location) of the receptor in relation to the contaminated area.

All but the occupancy factor depend on the radionuclide. The shape of the primary contamination can be specified to be circular or polygonal. The location of the onsite and offsite dwellings in relation to the primary contamination can also be specified. The offsite areas (dwelling and agricultural areas) are assumed to be circular in shape, with the receptor located at the center of the circle, when calculating the exposure from external radiation.

6.2 INHALATION OF CONTAMINATED DUST

The code models the effects of inhalation of contaminated particulates for the following situations:

- Inhalation of particulate matter released from the primary contamination, while located indoors and outdoors in an onsite dwelling above the primary contamination.

- Inhalation of particulate matter released from the primary contamination and transported to the offsite dwelling site by the atmosphere, while located indoors and outdoors in an offsite dwelling that is outside the perimeter of the primary contamination.

- Inhalation of particulate matter released from the primary contamination and transported to the offsite agricultural area while located outdoors in that offsite agricultural area.

The exposures resulting from all these situations are summed and reported as a single quantity.

Following the general principles discussed in Appendix B of the user's manual for RESRAD (onsite) (Yu et al. 2001), the exposure for each of the above situations is computed as the product of the following:

- The dose conversion factor or slope factor for the radionuclide from the chosen dose factor library ([mrem pCi^{-1}] or [risk pCi^{-1}]),

- An occupancy and indoor filtration factor to account for the time spent at the location and for the filtration of dust by any building components while indoors,

- The inhalation rate (m^3 yr^{-1}), and
- The concentration of the radionuclide in air at the exposure location (pCi m^{-3}).

The concentration in air at an onsite location is obtained as the product of the following:

- The concentration in the primary contamination (pCi g^{-1}),
- The factor for volumetric mixing of the surface soil (Section 2.2.3),
- The ratio of the density of primary contamination to the density of the mixing zone (Section 2.2.3),
- The concentration of respirable dust particles in air above the primary contamination (g m^{-3}), and
- The area factor to account for the dilution of the dust derived from the primary contamination by the dust blown in from uncontaminated areas (Chang et al. 1998).

The concentration in air at an offsite location is obtained as the product of

- The Chi/Q atmospheric transport factor for that offsite location (s m^{-3}),
- The rate of release of radionuclides to the atmosphere (pCi yr^{-1}), and
- A factor to convert seconds to years.

The inhalation of gaseous C-14 (CO_2) and H-3 in vapor form (H_2O) is also computed and reported under this exposure pathway. Thus, the inhalation exposure reported for C-14 includes exposure from both the particulate form and the gaseous form. Different dose conversion factors can be used for the two forms of C-14. The inhalation exposure reported for H-3 is for the vapor form and includes a 50% increase to account for the absorption of ^3HHO through the skin at a rate equal to 50% of the breathing rate (ICRP 1979–1982).

6.3 INHALATION OF RADON AND SHORT-LIVED PROGENY

The RESRAD-OFFSITE code models the effects of inhalation of radon and its short-lived progeny for the following situations:

- Inhalation of radon and progeny released from contaminated water used inside a dwelling (both onsite and offsite dwellings).

- Inhalation of radon that emanated from the primary contamination and its progeny while indoors and outdoors at the onsite dwelling location.

- Inhalation of radon that emanated from the primary contamination and was transported to the offsite dwelling site by the atmosphere, and its short-lived progeny that were produced during the transport, while indoors and outdoors at the offsite dwelling location.

- Inhalation of radon that emanated from the primary contamination and was transported to the agricultural areas by the atmosphere, and its short-lived progeny that were produced during the transport, while outdoors in the offsite agricultural area.

The methodology used for the first two situations is as described in Appendix C of the user's manual for RESRAD (onsite) (Yu et al. 2001). The exposure for the remaining two situations is modeled by using the concentration of radon and progeny at those locations. The concentrations are computed from the flux of radon released from the primary contamination and the ingrowth- and decay-adjusted Chi/Q factors for radon and its short-lived progeny, computed from the atmospheric transport model.

6.4 INGESTION OF WATER, PLANT-DERIVED FOOD, MEAT, MILK, AQUATIC FOOD, AND INCIDENTAL INGESTION OF SOIL

The exposure from the ingestion of water, plant-derived food, meat, milk, and aquatic food is computed as the product of the following:

- The dose conversion factor or slope factor for the radionuclide and food type from the chosen dose factor library ([mrem pCi^{-1}]) or [risk pCi^{-1}]),

- The ingestion rate (kg yr^{-1} or l yr^{-1}),

- The fraction of the food that was obtained from the contaminated areas, and

- The concentration of the radionuclide in the food (pCi $[kg]^{-1}$, pCi L^{-1}).

The exposure from the incidental ingestion of soil is computed by summing the product of the following at the onsite location and at each of the offsite locations:

- The dose conversion factor or slope factor for the radionuclide from the chosen dose factor library ([mrem pCi^{-1}] or [risk pCi^{-1}],

- The incidental ingestion rate of soil (g yr^{-1}),

- The fraction of time spent at the onsite or offsite location, and

- The concentration of the radionuclide in the soil at the onsite or offsite location (pCi g^{-1}).

6.5 EXPOSURE SCENARIOS FOR RESRAD-OFFSITE

This section describes the principal exposure scenarios that can be modeled by RESRAD-OFFSITE. They are based on the exposure scenarios developed for RESRAD (onsite). Additional potential scenarios that require refinements and additional components for the code are also discussed where appropriate. The four main current scenarios are rural resident farmer, urban resident, worker, and recreationist. The principal exposure scenarios can give rise to specific subscenarios, such as office worker, industrial worker, or construction worker. These possibilities are listed in Sections 6.5.1 through 6.5.4. The pathways considered in the various scenarios are summarized in Tables 6.1 through 6.10 at the end of this chapter.

As described in Attachment 6 to *Results of Evaluations for Realistic Exposure Scenarios* (Travers 2003), the exposure scenarios that need to be considered for each site can be arrived at by determining the potential land use of that specific site and then considering the exposure groups that are relevant to each of those potential land uses.

Different combinations of land use and exposure group can lead to the same generic exposure scenario. For example, a maintenance worker in a pubic park or golf course and a resident maintenance worker in a large apartment complex would both fall under the generic maintenance worker scenario. These exposure scenarios would each have different input parameters to reflect the differences in land use and in activities performed. Thus, the land use/exposure group approach is necessary for conducting site-specific analyses and developing input values for the exposure scenarios.

This report focuses on the exposure scenarios that can be modeled by RESRAD-OFFSITE. It does not deal with the selection of exposure scenarios or parameter development for them. Thus, it does not use the land use/exposure group approach. Instead, it provides an overview of the main generic exposure scenarios that can be modeled with the code. Because it is not practical to provide an exhaustive list of all the exposure scenarios that can be modeled, information about RESRAD-OFFSITE that is useful in deciding whether this code can be used to model other exposure scenarios is presented in Section 2. Methods for developing site-specific scenarios and for modifying generic scenarios based on site characteristics are given in Chapter 5 and Appendix I of NUREG-1757 (Schmidt et al. 2003). The general scenarios given in Table I.3 of NUREG-1757, Volume 2, for sites with contamination in soil can be modeled using either the main generic scenarios listed in Sections 6.5.1 through 6.5.4 or as a subscenario of one of the main generic scenarios.

6.5.1 Rural Resident Farmer Scenario

The primary case would be a self-sufficient resident farmer-survivalist who produces all food to meet his dietary needs in the affected area. All exposure pathways would be active. A

TABLE 6.1 Exposure Pathways Considered for a Rural Resident Farmer Scenario

Exposure Pathway	Location of Contamination: Dwelling Site	Agricultural Land and Pasture	Surface Water Body	Well
External gamma from accumulation in soil or water	Yes	Yes	No	NA[a]
Inhalation of dust blown in from primary contamination	Yes	Yes	No	NA
Inhalation of radon from primary contamination	No[b]	No[b]	No	NA
Inhalation of radon from water used at home	NA	NA	No[b]	No[b]
Ingestion of vegetables, fruit, and grain	NA	Yes	NA	NA
Ingestion of meat	NA	Yes	NA	NA
Ingestion of milk	NA	Yes	NA	NA
Ingestion of aquatic food	NA	NA	Yes	NA
Ingestion of soil	Yes	Yes	NA	NA
Ingestion of water	NA	NA	Yes	Yes

[a] NA = not applicable.

[b] The radon pathway should be excluded under the U.S. Nuclear Regulatory Commission's (NRC's) license termination rule for decommissioning of contaminated facilities and sites.

more likely variation would be the subscenario of a semi-self-sufficient resident farmer who purchases some food to meet his dietary needs from outside the affected area. While it is expected that all the pathways would still be active, the ingestion parameters would reflect the reduced reliance on food from the affected area. Depending on the location and topography, water could be obtained primarily from a well or from a surface water body. The contaminant transport pathways to a surface water body might also have to be deactivated, depending on whether the water body was upgradient of the primary contamination. It is also possible that some portion or all of the farmed areas and the dwelling would be located directly above the primary contamination.

A second variation of the main scenario would arise if the extent of the area that was impacted was large. In this case, a significant portion of the food to meet dietary needs would be produced in the affected area, although not by the same individual. The occupancy factor would

TABLE 6.2 Contamination Pathways Considered for a Rural Resident Farmer Scenario

	Location of Contamination				
Contamination Pathway	Dwelling Site	Agricultural Land and Pasture	Surface Water Body	Well	Primary Contamination
Deposition of dust	Yes	Yes	Yes	NA[a]	NA
Source of contamination	No	No	NA	NA	Yes
Interception of groundwater	NA	NA	Yes	Yes	NA
Source of contamination	No	No	NA	NA	Yes
Surface runoff	NA	No	Yes	NA	NA
Source of contamination	No	No	NA	NA	Yes
Irrigation water	Yes	Yes	NA	NA	No
Source of contamination	NA	NA	Yes	Yes	NA

[a] NA = not applicable.

need to be reduced to reflect the applicable situation. For example, the food might be picked at a cooperative farm or purchased from a roadside stand or farmer's market.

6.5.2 Urban Resident Scenario

It is likely that the meat, milk, and aquatic food pathways would be inactive and that input appropriate for the location of the affected area would be used to model the urban resident scenario. Depending on the location of the water supply and type of water treatment process, the drinking water and household water pathways might have to be deactivated. If the dwelling was a house, seasonal vegetable consumption from a home garden would be a possibility. If the dwelling was an apartment or town home, the vegetable pathway might also be inactive. It is possible that the urban resident might work at a different location that was also in the affected area. Direct modeling of this variation is not currently possible, but an informed user can adjust the occupancy in the unused agricultural area to model this subscenario. The code can be expanded to include an offsite work area at a location different from the offsite dwelling when the dwelling model is refined.

6.5.3 Worker Scenario

The drinking water, vegetables, meat, milk, and aquatic food pathways would be inactive for the worker scenario. The occupancy, shielding, inhalation, and incidental soil ingestion parameters would be different for the different workers — office worker, industrial worker, and

TABLE 6.3 Exposure Pathways Considered for an Urban Resident Scenario

Exposure Pathway	Location of Contamination: Dwelling Site	Agricultural Land and Pasture	Surface Water Body	Well
External gamma from accumulation in soil or water	Yes	NA[a]	No	NA
Inhalation of dust blown in from primary contamination	Yes	NA	No	NA
Inhalation of radon from primary contamination	No[b]	NA	No	NA
Inhalation of radon from water used at home	NA	NA	No[b]	No[b]
Ingestion of vegetables, fruit, and grain	Maybe[c]	NA	NA	NA
Ingestion of meat	NA	NA	NA	NA
Ingestion of milk	NA	NA	NA	NA
Ingestion of aquatic food	NA	NA	Maybe	NA
Ingestion of soil	Yes	NA	NA	NA
Ingestion of water	NA	NA	Maybe	Maybe

[a] NA = not applicable.

[b] The radon pathway should be excluded under the NRC's license termination rule for decommissioning of contaminated facilities and sites.

[c] Maybe = not suggested for the default scenario, can be considered if appropriate.

construction worker. Either the offsite or onsite dwelling location could be appropriate for these worker scenarios. The relevant agricultural area would be used to model a farm worker. As discussed in Section 6.5.2, a combined urban resident worker subscenario would be necessary if the worker also resided in an affected area.

6.5.4 Recreationist Scenario

Numerous recreational use scenarios are possible, ranging from an avid sportsperson/outdoorsperson who would obtain a significant portion of his meat and fish from the affected area to a person who would hike in an affected area for only a few hours in a year.

TABLE 6.4 Contamination Pathways Considered for an Urban Resident Scenario

	Location of Contamination				
Contamination Pathway	Dwelling Site	Agricultural Land and Pasture	Surface Water Body	Well	Primary Contamination
Deposition of dust	Yes	NA[a]	Maybe[b]	NA	NA
Source of contamination	No	No	NA	NA	Yes
Interception of groundwater	NA	NA	Maybe	Maybe	NA
Source of contamination	No	No	NA	NA	Yes
Surface runoff	NA	NA	Maybe	NA	NA
Source of contamination	No	No	NA	NA	Yes
Irrigation water	Maybe	Maybe	NA	NA	No
Source of contamination	NA	NA	Maybe	Maybe	NA

[a] A = not applicable.

[b] Maybe = not suggested for the default scenario, can be considered if appropriate.

The vegetable, milk, and drinking water pathways would be turned off for the sportsperson/outdoorsperson scenario, although the ingestion of some wild berries, mushrooms, and springwater would be plausible. The ingestion rates for meat and aquatic food would depend on the available game and aquatic organisms at the location. All the water used by livestock would probably come from the surface water body. The irrigation rate should be set to reflect the situation being modeled, since the foraging area would likely be unirrigated.

A person who trains or exercises routinely in an affected playfield or park, or a person who regularly spends time in a park is another likely candidate for recreational exposure. The vegetable, meat, milk, aquatic food, and drinking water pathways would be turned off for this scenario. The park or playfield could be modeled as the outdoor occupancy of the offsite dwelling, since the park/playfield option is not available.

The RESRAD-OFFSITE code is not currently equipped to model a swimmer or boater scenario. A module to compute the direct exposure from the contaminants in the lake would have to be added. A more detailed lake model, which considers potential stratification and turnover of the lake and the rate-controlled release from the sediments, might also be necessary.

TABLE 6.5 Exposure Pathways Considered for the Worker Scenario

	Location of Contamination			
Exposure Pathway	Work Site[a]	Agricultural Land[b]	Surface Water Body	Well
External gamma from accumulation in soil or water	Yes	Yes	NA[c]	NA
Inhalation of dust blown in from primary contamination	Yes	Yes	NA	NA
Inhalation of radon from primary contamination	No[d]	No[d]	NA	NA
Inhalation of radon from water used at home	NA	NA	NA	NA
Ingestion of vegetables, fruit, and grain	NA	NA	NA	NA
Ingestion of meat	NA	NA	NA	NA
Ingestion of milk	NA	NA	NA	NA
Ingestion of aquatic food	NA	NA	NA	NA
Ingestion of soil	Yes	Yes	NA	NA
Ingestion of water	NA	NA	Maybe[e]	Maybe

[a] For office worker, industrial worker, and construction worker scenarios.

[b] For agricultural worker scenario.

[c] NA = not applicable.

[d] The radon pathway should be excluded under the NRC's license termination rule for decommissioning of contaminated facilities and sites.

[e] Maybe = not suggested for the default scenario, can be considered if appropriate.

TABLE 6.6 Contamination Pathways Considered for the Worker Scenario

	Location of Contamination				
Contamination Pathway	Work Site[a]	Agricultural Land[b]	Surface Water Body	Well	Primary Contamination
Deposition of dust	Yes	Yes	Yes	NA[c]	NA
Source of contamination	No	No	NA	NA	Yes
Interception of groundwater	NA	NA	Yes	Yes	NA
Source of contamination	No	No	NA	NA	Yes
Surface runoff	NA	No	Yes	NA	NA
Source of contamination	No	No	NA	NA	Yes
Irrigation water	NA	Yes	NA	NA	No
Source of contamination	NA	NA	Yes	Yes	NA

[a] For office worker, industrial worker, and construction worker scenarios.

[b] For agricultural worker scenario.

[c] NA = not applicable.

TABLE 6.7 Exposure Pathways Considered for a Sportsperson/Outdoorsperson Recreational Scenario

Exposure Pathway	Location of Contamination			
	Dwelling Site	Agricultural Land and Pasture (for forest)	Surface Water Body	Well (for spring)
External gamma from accumulation in soil or water	NA[a]	Yes	No	NA
Inhalation of dust blown in from primary contamination	NA	Yes	No	NA
Inhalation of radon from primary contamination	NA	No[b]	No	NA
Inhalation of radon from water used at home	NA	NA	NA	NA
Ingestion of vegetables, fruit, and grain	NA	Maybe[c]	NA	NA
Ingestion of meat	NA	Yes	NA	NA
Ingestion of milk	NA	NA	NA	NA
Ingestion of aquatic food	NA	NA	Yes	NA
Ingestion of soil	NA	Yes	NA	NA
Ingestion of water	NA	NA	Maybe	Maybe

[a] NA = not applicable.

[b] The radon pathway should be excluded under the NRC's license termination rule for decommissioning of contaminated facilities and sites.

[c] Maybe = not suggested for the default scenario, can be considered if appropriate.

TABLE 6.8 Contamination Pathways Considered for a Sportsperson/Outdoorsperson Recreational Scenario

	Location of Contamination				
Contamination Pathway	Dwelling Site	Agricultural Land and Pasture (for forest)	Surface Water Body	Well (for spring)	Primary Contamination
Deposition of dust	NA[a]	Yes	Yes	NA	NA
Source of contamination	No	No	NA	NA	Yes
Interception of groundwater	NA	NA	Yes	Maybe[b]	NA
Source of contamination	No	No	NA	NA	Yes
Surface runoff	NA	No	Yes	NA	NA
Source of contamination	No	No	NA	NA	Yes
Irrigation water	NA	NA	NA	NA	NA
Source of contamination	NA	NA	NA	NA	NA

[a] NA = not applicable.

[b] Maybe = not suggested for the default scenario, can be considered if appropriate.

TABLE 6.9 Exposure Pathways Considered for the Park or Playfield Recreational Scenario

Exposure Pathway	Location of Contamination			
	Dwelling Site	Agricultural Land and Pasture (for park or playfield)	Surface Water Body	Well
External gamma from accumulation in soil or water	NA[a]	Yes	NA	NA
Inhalation of dust blown in from primary contamination	NA	Yes	NA	NA
Inhalation of radon from primary contamination	NA	No[b]	NA	NA
Inhalation of radon from water used at home	NA	NA	NA	NA
Ingestion of vegetables, fruit, and grain	NA	NA	NA	NA
Ingestion of meat	NA	NA	NA	NA
Ingestion of milk	NA	NA	NA	NA
Ingestion of aquatic food	NA	NA	NA	NA
Ingestion of soil	NA	Yes	NA	NA
Ingestion of water	NA	NA	Maybe[c]	Maybe

[a] NA = not applicable.

[b] The radon pathway should be excluded under the NRC's license termination rule for decommissioning of contaminated facilities and sites.

[c] Maybe = not suggested for the default scenario, can be considered if appropriate.

TABLE 6.10 Contamination Pathways Considered for a Park or Playfield Recreational Scenario

	Location of Contamination				
Contamination Pathway	Dwelling Site	Agricultural Land and Pasture (for park or playfield)	Surface Water Body	Well	Primary Contamination
Deposition of dust	NA[a]	Yes	Yes	NA	NA
Source of contamination	No	No	NA	NA	Yes
Interception of groundwater	NA	NA	Yes	Yes	NA
Source of contamination	No	No	NA	NA	Yes
Surface runoff	NA	No	Yes	NA	NA
Source of contamination	No	No	NA	NA	Yes
Irrigation water	NA	Maybe[b]	NA	NA	NA
Source of contamination	NA	NA	Maybe[b]	Maybe[b]	NA

[a] NA = not applicable.

[b] Maybe = not suggested for the default scenario, can be considered if appropriate.

7 TIME POINTS FOR NUMERICAL COMPUTATIONS

All of the expressions for the releases from the primary contamination that were developed in Chapter 2 can be evaluated analytically. One feature of the code, although it is not yet fully implemented (Section 2.4), is the ability to accept user-specified releases and even media concentrations. These inputs, which could be from historical measurements or the predictions of other models, cannot be expected to be in the form of analytical expressions; they would likely be in the form of measured or predicted values at a series of times.

The expressions for flux and concentration under dispersive transport (Chapter 3) can only be convolved analytically with a limited set of analytical input fluxes. In the development in Chapter 3, they were convolved by assuming that the input fluxes were known at a series of time points and that the input fluxes varied linearly between the values at those times. They could have been convolved numerically with a general analytical expression for the flux, but the result (i.e., the flux out of the zone) would not have been analytical. Thus, if the groundwater transport involved more than the saturated zone, an analytical approach would not be feasible. An important feature of the RESRAD-OFFSITE code is its ability to model a number of partially saturated zones, each with properties that are distinct from the properties of the others. The code also needs to be able to allow subdivision of the partially saturated zones and the saturated zone to make better predictions of the transport of the progeny produced in transit (Section 3.3.13). While the very first subdivision of the topmost partially saturated zone could have been treated analytically, the code-calculated flux out of this transport zone would not have been an analytical expression but rather a series of fluxes at a series of times. Thus, the calculations for the remaining zones would have inputs that are not analytical but are fluxes at a series of times.

Finally, the expressions for accumulation in both offsite soil and in the surface water body use inputs that are available only as values at a series of times and not as analytical expressions. Even if they had been in the form of analytical expressions, deriving analytical expressions for the accumulation would have been possible for only a limited number of cases.

For these reasons, a numerical approach was used in the RESRAD-OFFSITE code. This approach involves computing the releases, fluxes, and concentrations at a series of times. The computed quantities are assumed to vary linearly between each pair of times in the series. The fluxes computed for a transport zone depend on the calculations performed for the preceding transport zones. In the case of accumulation (Chapter 5), the value computed at any particular time depends on the accumulation calculated for the preceding times, as well as the fluxes and concentrations calculated for the transport zones. The accuracy of the calculations depends on the choice of the series of time points. The time horizon over which predictions are to be made, the number of time points to be used over this time horizon, and the manner in which the time points are to be spaced over the time horizon must be chosen with care in order to obtain meaningful predictions.

7.1 FORECAST TIME HORIZON

Model calculations are performed to make predictions of exposure, risk, and concentration over a period of time ranging from the present, time zero, to an exposure duration beyond the greatest time at which the predictions are required (Section 4.9 of the User's Guide in Appendix A). This is the forecast time horizon.

7.2 NUMBER OF TIME POINTS

The number of time points should be sufficient to capture the variation in the computed fluxes and concentrations. This is especially important when the groundwater transport zones are subdivided (Section 3.3.13). The time points should be close enough to represent the temporal variation of the flux across each subdivided zone to prevent the buildup of numerical errors (Chapter 4 of Yu et al. 2006). The code provides the following choices for the number of time points: 32, 64, 128, 256, ...16,384 and 22,000; all but the last is a power of 2. The next power of 2 — 32,768 — and higher are not provided in the list of choices because the graphing program used in the code for deterministic graphics cannot handle that many points.

7.3 SPACING OF TIME POINTS

The code offers two choices for the spacing of the time points. The time points may be spaced uniformly from 0 to the forecast time horizon, or they can be spaced in a geometric series (log spacing). The first time point is time zero under both choices. When the log spacing is selected, the second time point is set to the user-specified minimum time increment because a zero value cannot be a part of a geometric series. The remaining time points are placed in a geometric series between the minimum time increment and the forecast time horizon. If this results in time points that are spaced at less than the minimum time increment, a possibility at the beginning of the geometric series, those time points will be placed in an arithmetic series with a spacing of the minimum time increment until the rest of the time points can be placed in a geometric series with a larger interval between time points.

It is preferable to use the uniformly spaced linear spacing option. This choice allow the groundwater transport transfer factors to be saved and reused for all points that have the same travel time, leading to a shorter execution time (Section 2.1.3 of Appendix C).

7.4 STORAGE TIME CONSIDERATIONS

The food products, water, and livestock feed might not always be consumed immediately upon harvest or extraction. The concentration of the radionuclides in these products at the time of harvest or extraction is needed in order to account for the radiological transformations that take place during the time that these products are stored prior to consumption. The code computes the concentrations at harvest or extraction by linear interpolation of the concentration at the series of time points discussed above.

7.5 TIME-INTEGRATED DOSE AND RISK

The radiological doses and risks reported by the code in textual and graphical form are all time-integrated quantities. The dose reported for a particular time is the dose over a period of one year beginning at that time. Likewise, the risk reported for a particular time is the value over an exposure duration beginning at that time. The code performs a trapezoidal integration using the value at the reporting time, the values at all the time points that fall within the integration period, and the value at the end of the integration period. If the integration period ends between two time points, the value at the end of the time period is found by linear interpolation between those two time points.

8 VERIFICATION AND VALIDATION

The RESRAD-OFFSITE code was developed following the RESRAD program quality assurance (QA) and quality control (QC) procedures. Some components of the code were verified by separately developed spreadsheets, or benchmarked against the RESRAD (onsite) code for most of the equations used in the code.

As previously indicated, the RESRAD-OFFSITE code is an extension of the RESRAD (onsite) code, and the two codes share the same database and many models and modules. The RESRAD (onsite) code has already been extensively tested, verified, and validated as documented in Chapter 5 of the RESRAD User's Manual and other documents (Yu et al. 2001; Halliburton NUS 1994; Cheng et al. 1995; Gnanapragasam et al. 2000; Mills et al. 1997; Whelan et al. 1999a,b).

The beta versions of RESRAD-OFFSITE have been in existence for many years, and the code has been tested by users who downloaded it. Many users provided comments that resulted in improvement of the code over the years.

Many parameter values used in the RESRAD-OFFSITE code were taken from the RESRAD (onsite) database. These parameters include soil-plant transfer factors, meat and milk transfer factors, bioaccumulation factors, dose conversion factors, decay half-lives, and scenario-specific occupancy factors. The RESRAD (onsite) database is well documented and verified (Yu et al. 2000, 2001, 2003).

Argonne recently conducted a benchmarking of RESRAD-OFFSITE and RESRAD (onsite) for an onsite exposure scenario. This study was documented in a separate report (Yu et al. 2006). The results indicated that although there are differences between some models used in the two codes, by adjusting the input parameters, the RESRAD-OFFSITE can reproduce the RESRAD (onsite) results for an onsite exposure scenario.

Additional benchmarking of the RESRAD-OFFSITE code against other peer codes was performed over the past several years. Some of the results were documented in the benchmarking report (Yu et al. 2006) and in other reports and peer-reviewed articles (Gnanapragasam and Yu 1997, Gnanapragasam et al. 2000; BIOMOVS II 1995, 1996).

Currently, the RESRAD-OFFSITE code is being used by the International Atomic Energy Agency's Environmental Modeling for Radiation Safety Program's Naturally Occurring Radioactive Material Working Group for testing scenarios such as "Area Source" and "Area Source + River." Additional testing and validation of RESRAD-OFFSITE are planned when data sets are available.

9 REFERENCES

BIOMOVS (Biosphere Model Validation Study) II, 1995, *Long-Term Contaminant Migration and Impacts from Uranium Mill Tailings — Comparison of Computer Models Using a Hypothetical Dataset*, BIOMOVS II Technical Report No. 4, Biosphere Model Validation Study Steering Committee, Swedish Radiation Protection Institute, Stockholm, Sweden.

BIOMOVS II, 1996, *Long-Term Contaminant Migration and Impacts from Uranium Mill Tailings — Comparison of Computer Models Using a Realistic Dataset*, BIOMOVS II Technical Report No. 5, Biosphere Model Validation Study Steering Committee, Swedish Radiation Protection Institute, Stockholm, Sweden.

Briggs, G.A., 1969, *Plume Rise*, U.S. Atomic Energy Commission Critical Review Series, prepared for Nuclear Safety Information Center, Oak Ridge National Laboratory, reprinted by the National Technical Information Service, Springfield, Va.

Briggs, G.A., 1974, *Diffusion Estimation for Small Emissions*, Environmental Research Laboratories Atmospheric Turbulence and Diffusion Laboratory 1973 Annual Report, Report No. ATDL-106, National Oceanic and Atmospheric Administration, Washington, D.C.

Chang, Y.-S., et al., 1998, *Evaluation of the Area Factor Used in the RESRAD Code for the Estimation of Airborne Contaminant Concentrations of Finite Area Sources*, ANL/EAD/TM-82, Argonne National Laboratory, Argonne, Ill., July.

Cheng, J.J., et al., 1995, *Benchmarking Analysis of Three Multimedia Models: RESRAD, MMSOILS, and MEPAS*, DOE/ORO-2033, U.S. Department of Energy, Washington, D.C.

Eimutis, E.C., and M.G. Konicek, 1972, "Derivation of Continuous Functions for the Lateral and Vertical Dispersion Coefficients," *Atmospheric Environment* 6:859–863.

Gnanapragasam, E., and C. Yu, 1997, *Analysis of BIOMOVS II Uranium Mill Tailings Scenario 1.07 with the RESRAD Computer Code*, ANL/EAD/TM-66, Argonne National Laboratory, Argonne, Ill.

Gnanapragasam, E., et al., 2000, "Comparison of Multimedia Model Predictions for a Contaminant Plume Migration Scenario," *J. Contaminant Hydrology* 46(1–2):17–38.

Halliburton NUS Corporation, 1994, *Verification of RESRAD. A Code for Implementing Residual Radioactive Material Guidelines, Version 5.03*, HNUS-ARPD-94-174, Gaithersburg, Md.

Hanna, S.R., et al., 1982, *Handbook on Atmospheric Diffusion*, DOE/TIC-11223, Technical Information Center, U.S. Department of Energy, Washington, D.C.

Holzworth, G., 1972, *Mixing Heights, Wind Speeds, and Potential for Urban and Air Pollution throughout the Contiguous United States*, AP-101, U.S. Environmental Protection Agency, Washington, D.C.

ICRP (International Commission on Radiological Protection), 1979–1982, *Limits for Intakes of Radionuclides by Workers*, ICRP Publication 30, Part 1 (and Supplement), Part 2 (and Supplement), Part 3 (and Supplements A and B), and Index, a report by Committee 2 of the International Commission on Radiological Protection, adopted by the Commission in July 1978, Annals of the ICRP, Pergamon Press, New York, N.Y.

Irwin, J.S., 1979, "A Theoretical Variation of the Wind Profile Power-Law Exponent as a Function of Surface Roughness and Stability," *Atmospheric Environment* 13:191–194.

Lindstrom F.T., et al., 1967, "Theory on the Movement of Some Herbicides in Soils: Linear Diffusion and Convection of Chemicals in Soils," *Environmental Science and Technology* 1(7):561–565.

McMahon, T.A., and P.J. Dennison, 1979, "Empirical Atmospheric Deposition Parameters — A Survey," *Atmospheric Environment* 13:571–585.

Mills, W.B., et al., 1997, "Multimedia Benchmarking Analysis for Three Risk Assessment Models: RESRAD, MMSOILS, and MEPAS," *Risk Analysis* 17(2):187–201.

Pasquill, F., 1974, *Atmospheric Diffusion*, 2nd ed., John Wiley & Sons, New York, N.Y.

Pasquill, F., 1976, *Atmospheric Dispersion Parameters in Gaussian Plume Modeling. Part II. Possible Requirements for Change in the Turner Workbook Values*, EPA-600/4-76-03b, U.S. Environmental Protection Agency, Washington, D.C.

Powell, D.C., et al., 1979, *MESODIF-II: A Variable Trajectory Plume Segment Model to Assess Ground-Level Air Concentrations and Deposition of Effluent Releases from Nuclear Power Facilities*, NUREG/CR-0523, U.S. Nuclear Regulatory Commission, Washington, D.C.

Press, W.H., et al., 1989, *Numerical Recipes, the Art of Scientific Computing (Fortran Version)*, Cambridge University Press, New York, N.Y.

Ritchie, L.T., et al., 1978, "Effects of Rainstorms and Runoff on Consequences of Atmospheric Releases from Nuclear Reactor Accidents," *Nuclear Safety* 19:200–238.

Ross, D.G., et al., 1985, *CITPUFF: A Gaussian Puff Model for Estimating Pollutant Concentrations in Complex Terrain*, RM-261, U.S. Department of Agriculture, Rocky Mountain Forest and Range Experimentation Station, Ft. Collins, Colo., July.

Schmidt, D.W., et al., 2003, *Consolidated NMSS Decommissioning Guidance*, NUREG-1757, Vol. 2, U.S. Nuclear Regulatory Commission, Washington, D.C., Sept.

Shen, H.W., and P.Y. Julien, 1993, "Erosion and Sediment Transport" in *Handbook of Hydrology*, D.R. Maidment (editor), McGraw-Hill Inc.

Slade, D.H. (ed.), 1968, *Meteorology and Atomic Energy*, NTIS TID-24190, prepared by the Air Resources Laboratories, Research Laboratories, Environmental Science Service Administration, U.S. Department of Commerce, for Division of Reactor Development and Technology, U.S. Atomic Energy Commission, July.

Travers, W.D., 2003, "Results of Evaluations for Realistic Exposure Scenarios," Attachment 6 to *Results of the License Termination Rule Analysis*, Paper SECY-03-0069, U.S. Nuclear Regulatory Commission, Washington, D.C., May 2.

Whelan, et al., 1999a, "Benchmarking of the Saturated-Zone Module Associated with Three Risk Assessment Models: RESRAD, MMSOILS, and MEPAS," *Environmental Engineering Science* 16(1):67–80.

Whelan, G., et al., 1999b, "Benchmarking of the Vadose-Zone Module Associated with Three Risk Assessment Models: RESRAD, MMSOILS, and MEPAS," *Environmental Engineering Science* 16(1):81–91.

Yu, C., et al., 1993, *Manual for Implementing Residual Radioactive Material Guidelines Using RESRAD, Version 5.0*, ANL/EAD/LD-2, Argonne National Laboratory, Argonne, Ill., Sept.

Yu, C., et al., 2001, *User's Manual for RESRAD Version 6*, ANL/EAD-4, Argonne National Laboratory, Argonne, Ill., July.

Yu, C., et al., 2003, *User's Manual for RESRAD-BUILD Version 3*, ANL/EAD/03-1, Argonne National Laboratory, Argonne, Ill., June.

Yu, C., et al., 2006, *Benchmarking of RESRAD-OFFSITE: Transition from RESRAD (onsite) to RESRAD-OFFSITE and Comparison of RESRAD-OFFSITE Predictions with Peer codes,* ANL/EVS/TM/06-03, DOE/EH-0708, Argonne National Laboratory, Argonne, Ill., May.

APPENDIX A:

USER'S GUIDE FOR RESRAD-OFFSITE

VERSION 2

CONTENTS

CONTENTS (Cont.)

1 PURPOSE OF USER'S GUIDE

RESRAD-OFFSITE for Windows has many features to help users understand and use the software. This user's guide describes those features and provides additional information about the input parameters to increase understanding of the code. This information is organized into the following major sections:

- Section 2. Installation: Installation procedures and system requirements are discussed.
- Section 3. Navigation: Instructions for moving around the interface to accomplish various tasks and to save input and output are presented.
- Section 4. Input Forms: Each input form is described, information on how to use each form is presented, and the parameters in the input forms are described.
- Section 5. Outputs: Instructions on finding results in the textual and graphical output are provided.
- Section 6. Enhancements: The probabilistic/uncertainty analysis and sensitivity analysis features are explained.
- Section 7. Help: Various sources for obtaining help are discussed.

2 INSTALLATION

2.1 REQUIREMENTS

- Windows 2000 or XP operating system
- Pentium class processor
- 128 MB of RAM
- 100 MB of disk space
- A display resolution of 1280 × 1024 or finer

2.2 INSTALLING FROM THE RESRAD WEB SITE

1. Connect to the Web site at www.evs.anl.gov/resrad.
2. Click on "Download Codes."
3. Fill in the requested information and download the installation program.
4. When the installation program launches, enter the information requested by the standard installation program.
5. After installation, a new RESRAD-OFFSITE icon will appear in the RESRAD group. Double-clicking on this icon will start RESRAD-OFFSITE.

2.3 INSTALLING FROM COMPACT DISK

1. Insert RESRAD-OFFSITE installation CD into appropriate drive.
2. If the setup program does not launch itself, run the SETUP.EXE program from the drive (for example, D:SETUP). This can be done through the Start/Run sequence or though Explorer.
3. Enter the information requested by the standard installation program.
4. After installation, a new RESRAD-OFFSITE icon will appear in the RESRAD group. Double-clicking on this icon will start RESRAD-OFFSITE.

2.4 UNINSTALLING

1. Use the Add or Remove Programs utility in the Widows control panel.

3 NAVIGATION

Four independent ways are available to access information through the RESRAD-OFFSITE interface:

1. **Menu and Toolbars:** These are the standard Windows tools used to manipulate files, input forms (i.e., screens), and output forms; shortcut keys are included for advanced users. These are described in Section 3.1.

2. **Linked Input Forms:** All relevant input forms are linked together by two buttons in each input form that save the data in that input form and then open either the next input form or the previous one (Section 3.4). Start by pressing the "New user, Chain through all Input Screens" button in the About RESRAD-OFFSITE popup window that displays upon starting RESRAD-OFFSITE. The About screen can also be accessed via the Help menu [Alt h, a].

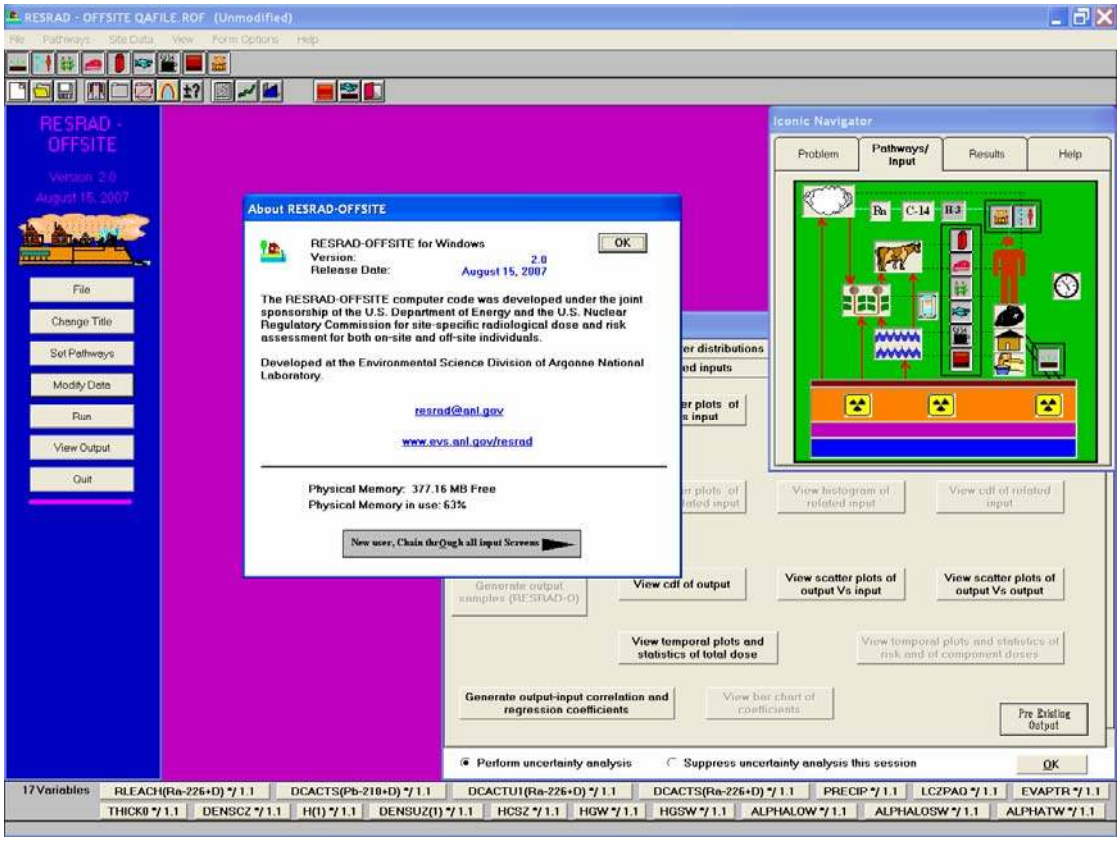

3. **RESRAD-DOS Emulator:** This set of textual command buttons is similar to buttons used in the RESRAD for DOS interface (Section 3.2).

4. **Iconic Navigator Window:** This tabbed window allows access to the information through more graphical cues (Section 3.3).

3.1 MENUS AND TOOLBARS

3.1.1 Menus

The menu on the main RESRAD-OFFSITE window (i.e., Main Menu) gives complete access to all the forms, functions, and features of the code. The Main Menu and the submenus that branch from it are shown above. The menu operations can be preformed by clicking the mouse, by pressing the hot (underlined) keys after activating them with the Alt key, or by using the shortcut keys shown next to the submenu commands.

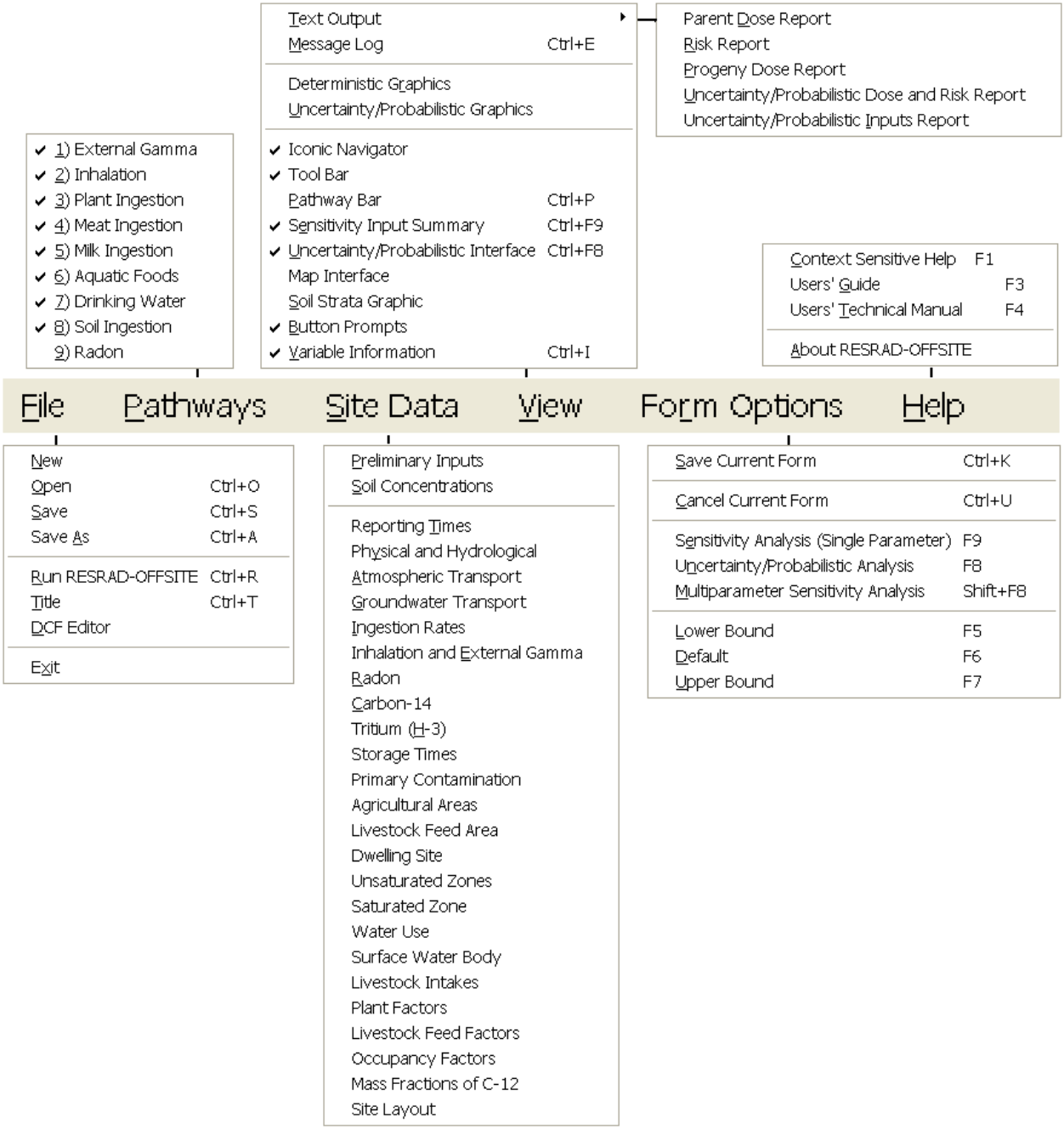

File submenu: The first block of four commands performs common file operations: New to start afresh with a set of default or place holder values for all the parameters; Save to save the current input file; Open to open a previously saved input file; and Save As to save the current inputs under a different file name.

The file submenu can also be used to perform an analysis by using the current inputs (Run RESRAD-OFFSITE), access the Title window (Title), or launch the dose conversion factor editor (Dose factors).

Pathways submenu: This is used to activate, deactivate, or verify the status of each exposure pathway. A checkmark next to a pathway indicates that it is currently active.

Site Data submenu: All but four of the forms that are needed to specify the situation to be modeled are directly accessible from this submenu. The shape and area factor form for external radiation is accessible from the inhalation and external gamma form, and the nuclide-dependent property forms (the source release and atmospheric transport form, the distribution coefficients form, and the transfer factors form) are accessible after the nuclides have been selected from the source form. Any forms that are currently open (i.e., being displayed) are indicated by a checkmark on the submenu.

View submenu: This submenu has two functions. It provides access to the various output windows, and it is used to set the display options for a number of features of the code. The first two subgroups display the textual and graphical outputs of a RESRAD-OFFSITE analysis. The outputs are discussed in Section 5. The last group of commands on this submenu is used to set the user's preference to display (indicated by a checkmark) or hide (no checkmark) the following functions of the code:

- **Iconic Navigator:** This is the Iconic Navigator window, which can also be used to access the forms, to perform the analysis, and to view the output. This is discussed in Section 3.3.

- **Tool Bar:** This is the primary toolbar, shown in Section 3.1.2.

- **Pathway Bar:** This is the pathways toolbar, shown in Section 3.1.2.

- **Sensitivity Input Summary:** This is the sensitivity analysis (one parameter at a time) information bar, shown in Section 3.1.2.

- **Uncertainty/Probabilistic Interface:** This is the form detailing any probabilistic analysis that is to be performed for the current site, discussed in Section 6.2. This form can also be used to perform step-by-step probabilistic analysis and to view plots of the results.

- **Map Interface:** This is the form displaying the plan view of the locations of the primary and secondary contamination. Section 4.4 describes the map interface. Unlike in the other cases where the user's preference is a simple

show or hide, there are three possibilities in this case. The user may indicate a preference to see the map only when the site layout form is displayed in the sequence of forms (set the preference to view map or not while the layout form is displayed to set this), to see the map at all times (set the preference to view map or not when the layout form is not being displayed to set this), or never see the map.

- **Soil Strata Graphics:** This is a sketch of the cross section of the ground below the primary contamination.

- **Button Prompts:** A button prompt is a short descriptive name for a control on the toolbar or on the Pathways/Inputs tab of the Iconic Navigator window. A prompt is displayed when the mouse cursor moves over the control and lingers there for a short while. The descriptions of the objects in the map interface are also displayed as the mouse lingers over the different objects in the map interface.

- **Variable Information:** This is the variable information bar, shown in Section 3.1.2.

Form Options submenu: The first two commands on the Form Options submenu, Save current form and Cancel current form, are used to save or cancel the changes made to an open form (Section 4). The remaining six commands perform operations on the input boxes contained in the forms, as follows:

- **Sensitivity Analysis (Single parameter):** This is used to activate "one parameter at a time sensitivity analysis" (Section 6.1) on the input parameter and to set the range of the parameter for the analysis.

- **Uncertainty/Probabilistic Analysis:** This is used to include the input parameter in the probabilistic or uncertainty analysis (Section 6.2). It also can be used to display the uncertainty/probabilistic analysis form if it is not visible.

- **Multi-parameter Sensitivity Analysis:** This is used to include the input parameter in the probabilistic or uncertainty analysis with a uniform distribution of 0.9 to 1.1 of its current value and to display the uncertainty/probabilistic analysis form if it is not visible.

- **Lower Bound:** This is used to set the input to the lowest value accepted by RESRAD-OFFSITE. The lowest value may be a physical bound (i.e., the lowest value that is applicable for the parameter because of physical considerations) or simply a numerical bound imposed to prevent the code from crashing.

- **Default:** This is used to set the input to the default value assigned in the RESRAD-OFFSITE code. While some default values (e.g., ingestion rates, inhalation rates) are generally accepted values, others (e.g., field capacity, distribution coefficient) are merely placeholder values because of the site-specific nature of these parameters.

- **Upper Bound:** This is used to set the input to the highest value accepted by RESRAD-OFFSITE. The highest value may be a physical bound (i.e., the highest value that is applicable for the parameter because of physical considerations) or simply a numerical bound imposed to prevent the code from crashing.

Help submenu: This submenu is used to obtain context-sensitive information about the inputs, forms, and features in RESRAD-OFFSITE, to access pdf versions of this users' guide and of the users' technical manual, and to display the about RESRAD-OFFSITE form, as follows:

- **Context Sensitive Help:** Information about a specific input parameter, form, or feature in RESRAD can be obtained by pressing the F1 function key while the input control is in focus (box, option buttons, dropdown box, etc.). The input control is in focus when the cursor is in the field of the control.

- **Users' Guide:** This opens the pdf version of this document.

- **Users' Manual:** This opens the pdf version of the users' manual.

- **About RESRAD-OFFSITE:** This displays the About RESRAD-OFFSITE form (i.e., the About form). This form shows the version and release date of the RESRAD-OFFSITE software installed on the computer, the amount of physical memory that is available on the computer, and the e-mail contact for the RESRAD team. It also provides a link to access the RESRAD Web site.

3.1.2 Toolbars

Primary Toolbar

The primary toolbar below is displayed if the user preference is set to display it in the View submenu (Section 3.1.1) (the default is to show this toolbar). The operations that can be performed by clicking on the icons on the primary toolbar are shown below. A message prompt appears as the cursor lingers over an icon to display what the icon means if the Button Prompts option was selected from the View submenu on the Main Menu.

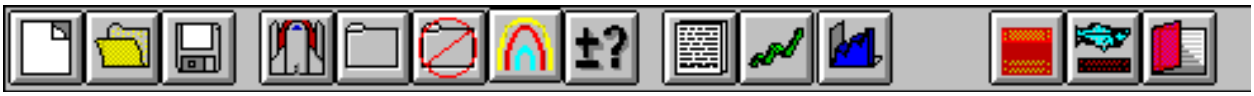

Files **Input** **Results** **Display Feedback**

- Files
  - Reset all input parameters to default values
  - Open an existing input file
  - Save data currently in all input forms to a file

- Input
  - Perform calculations
  - Save changes to current input form
  - Cancel changes to current input form
  - Display/hide sensitivity analysis input form
  - Display/hide uncertainty analysis input form

- Results
  - View summary report
  - View deterministic graphics
  - View uncertainty/probabilistic graphics

- Display Feedback
  - Display/hide soil strata graphics
  - Display/hide pathway button bar
  - Display/hide variables for sensitivity analysis

Pathways Toolbar

The pathways toolbar below is displayed if the user preference is set to display it in the View submenu (Section 3.1.1) (the default is to hide this toolbar). The pathways toolbar is used to toggle each pathway between active and inactive, and it displays the status of the pathways.

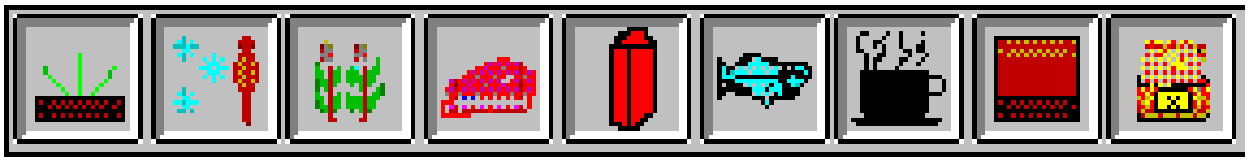

Sensitivity Analysis Input Summary Bar

The sensitivity analysis input summary bar shown in the upper half of the figure below is displayed if the user preference is set to display it in the View submenu (Section 3.1.1) (the default is to show this interactive summary bar). It shows the number of variables selected for one-parameter-at-a-time sensitivity analysis (Section 6.1) and contains a button for each of those variables. The buttons display the FORTRAN variable name and the range factor for the sensitivity analysis on the variable. Left click the mouse with the cursor on the sensitivity button to access the Sensitivity Analysis form for the variable. Right click the mouse with the cursor on the sensitivity button to remove that variable from sensitivity analysis. The height of the bar depends on the number of variables selected for sensitivity analysis and should not be adjusted by the user.

Variable Information Bar

The variable information bar shown in the lower half of the figure above is displayed if the user preference is set to display it in the View submenu (Section 3.1.1) (the default is to show this information bar). This bar displays information (FORTRAN name, default, and bounds) about the current input.

3.2 RESRAD-DOS EMULATOR

All applicable input fields can be accessed by following the command buttons in the RESRAD-DOS Emulator found on the left side of the interface. Some of the command buttons are linked directly to forms, while other commands lead to a group of second-level commands that appear to the right of the primary command list. All the buttons can be followed sequentially except for the Radon pathway button; it can be turned on only after a radon precursor has been selected from the Source form. The forms that are linked to these command buttons are discussed in Section 4.

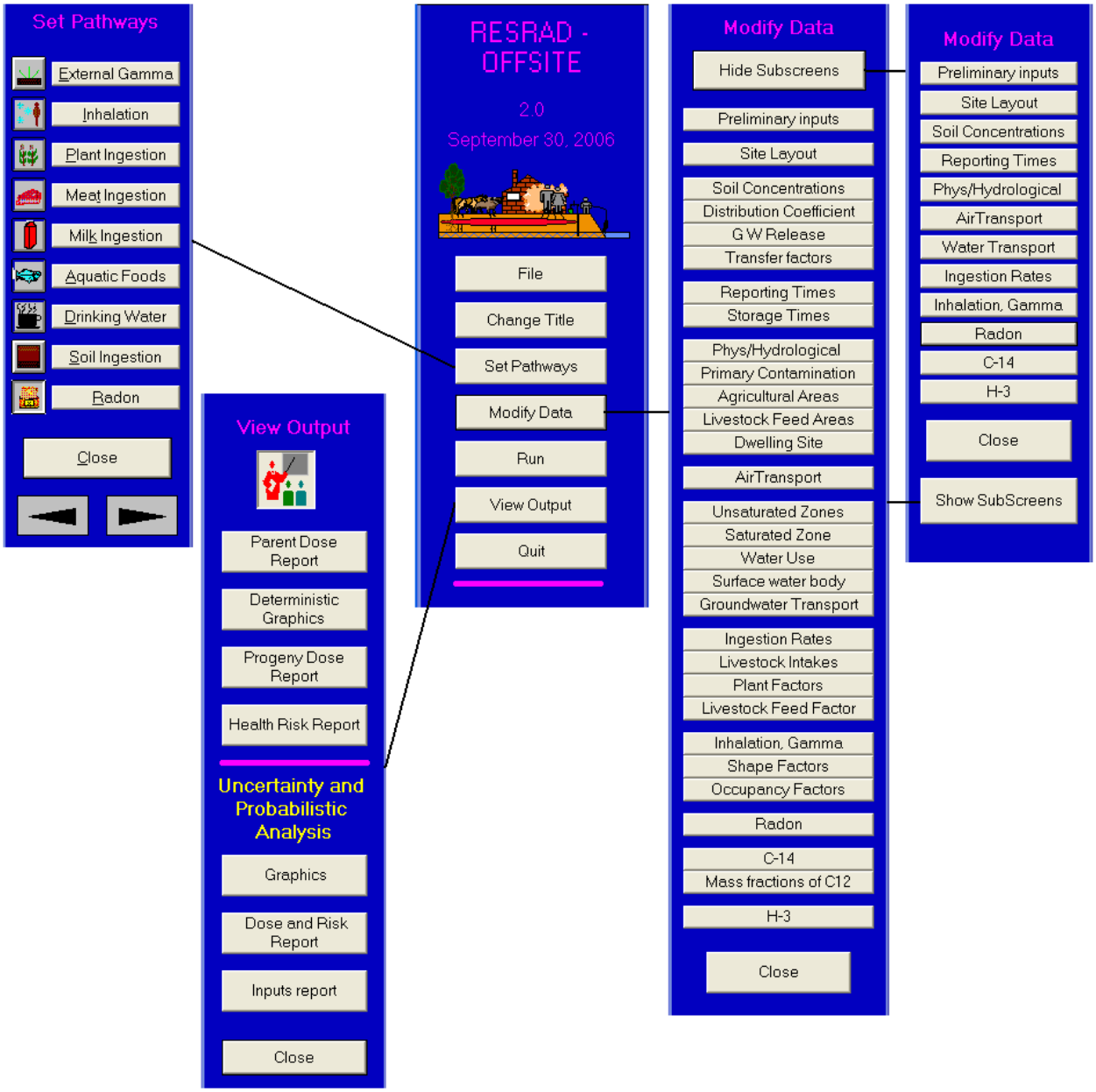

If the screen resolution is not sufficient to display the expanded modify data command buttons (1024x768 pixels), a compact version can be displayed by clicking on the "Hide Subscreens" command button.

3.3 ICONIC NAVIGATOR WINDOW

The Iconic Navigator window will be displayed if that user preference has been set by using the View submenu (the default preference is to display this window). It has four tabs. The first Problem tab gives the broad outline of the sequence to be adopted to perform the analysis. Buttons on the tab lead to the second Pathways/Input tab for specifying the site-specific scenario

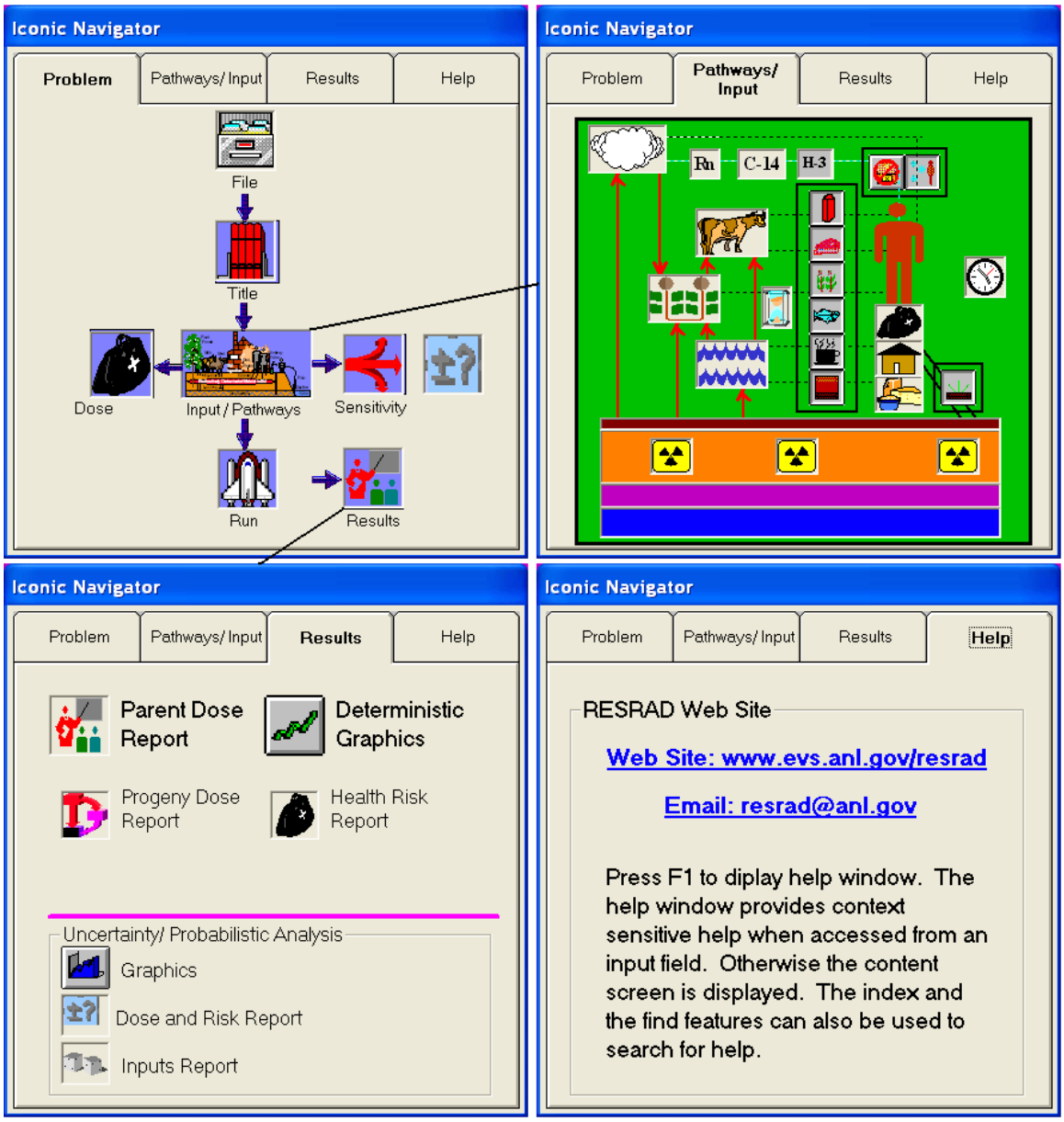

being analyzed and to the third Results tab for viewing the results. The forms that are accessed by these buttons are described in Section 1.3. Prompts displaying a descriptive name will appear as the cursor lingers over the buttons on the Pathways/Input tab. This feature is turned on by using the Button Prompts option from the View submenu (prompts are displayed by default).

- **Problem:** This tab guides the user to set up a case in RESRAD-OFFSITE. Each button brings up windows or forms to continue with the process.

- **Pathways/Input:** This tab allows the user to view and activate pathways. Buttons for the pathways are in the three black boxes. Inhalation pathways are above the person. Ingestion pathways are to the left. The single external pathway is at the lower right. Input windows are accessed by clicking on icons. Prompts appear to display what the icon means if the Button Prompts option was selected from the View submenu.

- **Results:** The top two buttons give access to the main deterministic results in report and graphical formats. The next two buttons open supplementary reports. If an uncertainty analysis was run, three more buttons appear below the purple line to provide access to the two reports and set of graphics.

- **Help:** If connected to the Internet, this tab gives the user access to the RESRAD Web site and to the address to which users can e-mail questions to the RESRAD team.

3.4 LINKED INPUT FORMS

All the input forms that are relevant to the current analysis can be displayed in sequence by using the forward and backward arrows in each form. The linked sequence begins in the About RESRAD-OFFSITE window, which is displayed each time RESRAD-OFFSITE is launched. This window is also accessible from the Help submenu (Alt h, a). The last form in the sequence has the run command instead of a forward arrow, and it issues the command to perform the RESRAD-OFFSITE analysis using the current set of inputs. The sequence of the forms is as follows: Title, Preliminary Inputs, Site Layout (and Map Interface), Source, Source Release and Deposition Velocity, Distribution Coefficients, Dose Conversion and Slope Factors, Transfer Factors, Set Pathways, Reporting Times, Storage Times, Physical and Hydrological, Primary Contamination, Agricultural Areas, Livestock Feed Growing Areas, Offsite Dwelling Area, Atmospheric Transport, Unsaturated Zone Hydrology, Saturated Zone Hydrology, Water Use, Surface Water Body, Groundwater Transport, Ingestion Rates, Livestock Intakes, Livestock Feed Factors, Plant Factors, Inhalation and External Gamma, External Radiation Shape and Area Factors, Occupancy, Radon, Carbon-14, Mass Fractions of Carbon-12, Tritium. The last 4 forms are displayed only if they are relevant to the current selection of nuclides. The forms are described in the linked sequence in Section 4.

4 INPUT FORMS

There are 31+ input forms for entering the parameters that define the site data, assumptions, site identification, and calculation specifications. Sections 4.1 through 4.31 describe each form in detail. Most input is entered by keying numbers into boxes, although some input is entered through list boxes, check boxes, and option boxes. Some features common to all input forms are described here.

Saving Information to Memory

There are two levels for saving information in RESRAD-OFFSITE. The first level is to temporarily save the information to memory. This is done with any of the following commands:

- **Command Buttons:** Click on the Save button, Forward button, or Backward button on the form.
- **Menu:** Select Form Options, then Save current form (Ctrl k).
- **Toolbar:** Click on the Folder button.

Saving Information to File

The second level is to save the settings to a disk file. This is done with any of the following commands:

- **DOS Emulator:** Press the File button on the DOS Emulator to activate the File Options form, then select Save or Save As.
- **Menu:** Select File, then either Save (Ctrl s) or Save As (Ctrl a).
- **Toolbar:** Press the Disk button to save to a file.
- **Run:** If any input form had been exited with a save operation (as opposed to a cancel operation), then the file will need to be saved to disk before calculations are performed. This will do a save, but not a save as.

Canceling Changes Made to a Form

The changes to the inputs in a form can be canceled if they have not yet been saved to memory as follows:

- **Function Keys:** Press the ESC key.
- **Command button:** Click on the Cancel button on the form.
- **Menu:** Select Form Options, then Cancel current form (Ctrl u).

- **Toolbar:** Click on the Canceled Folder button.

Saving Information to Memory and Opening Next or Previous Form

The information in a form can be saved to memory, and the next or previous form can be opened by pressing the forward arrow or the backward arrow, as appropriate.

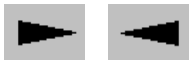

Entering Numbers

Some input boxes may be grayed out (disabled) because they are not applicable to the current case, either because some pathways have been turned off or because the pertinent radionuclide was not chosen. Values representative of the site should be entered in all input boxes that are active.

The default value and the bounds (upper and lower) of the selected parameter will be displayed in the variable information bar. The value in the input box may be set to the default value or to an upper or lower bound, as described below:

- **Defaults:** To set the selected parameter to its default, either select Form Options and then Default from the Main menu, or press the F6 function key. While some default values (e.g., ingestion rates, inhalation rates) are generally accepted values, others (e.g., field capacity, distribution coefficient) are merely placeholder values.

- **Bounds:** To set the selected parameter to its upper (or lower) bound, either select Form Options and then UpperBound (or LowerBound) from the Main Menu, or press the F7 (F5) function key. These may be a physical bound (i.e., the highest or lowest value that is applicable for the parameter because of physical considerations) or simply a numerical bound imposed to prevent the code from crashing.

Obtaining Help

Context-specific help will be shown anytime the F1 function key is pressed. For additional sources of help, refer to the Help section (Section 7) of this user's guide.

Selecting a Parameter for Probabilistic or Uncertainty Analysis

Input parameters can be selected for inclusion in a probabilistic or uncertainty analysis by pressing the F8 key while the cursor is in the input box for that parameter (see Section 6.2 on Uncertainty and Probabilistic Analysis). Some parameters are ineligible for uncertainty analysis, either because it does not make sense to perform the analysis on those parameters, or because of the unmanageable constraints imposed by interrelationships with other parameters.

Selecting a Parameter for One-Parameter-at-a-Time Sensitivity Analysis

Input parameters can be selected for one-parameter-at-a-time sensitivity analysis by pressing the F9 key while the cursor is in the input box for that parameter (see Section 6.1 on Sensitivity Analysis). Some parameters are ineligible for sensitivity analysis because it does not make sense to perform sensitivity analysis on those parameters.

Selecting a Parameter for Multi-parameter Sensitivity Analysis

Input parameters can be selected for inclusion in a multi-parameter sensitivity analysis by pressing the Shift + F8 key while the cursor is in the input box for that parameter. The selected parameters will be included in an uncertainty analysis, with a uniform distribution ranging from 0.9 to 1.1 of the current value (see Section 6.2 on Uncertainty and Probabilistic Analysis). Only the parameters that are eligible for uncertainty analysis can be included in the multi-parameter sensitivity analysis. The sensitive parameters can be ranked using the standardized regression coefficient or the standardized rank regression coefficient.

4.1 TITLE

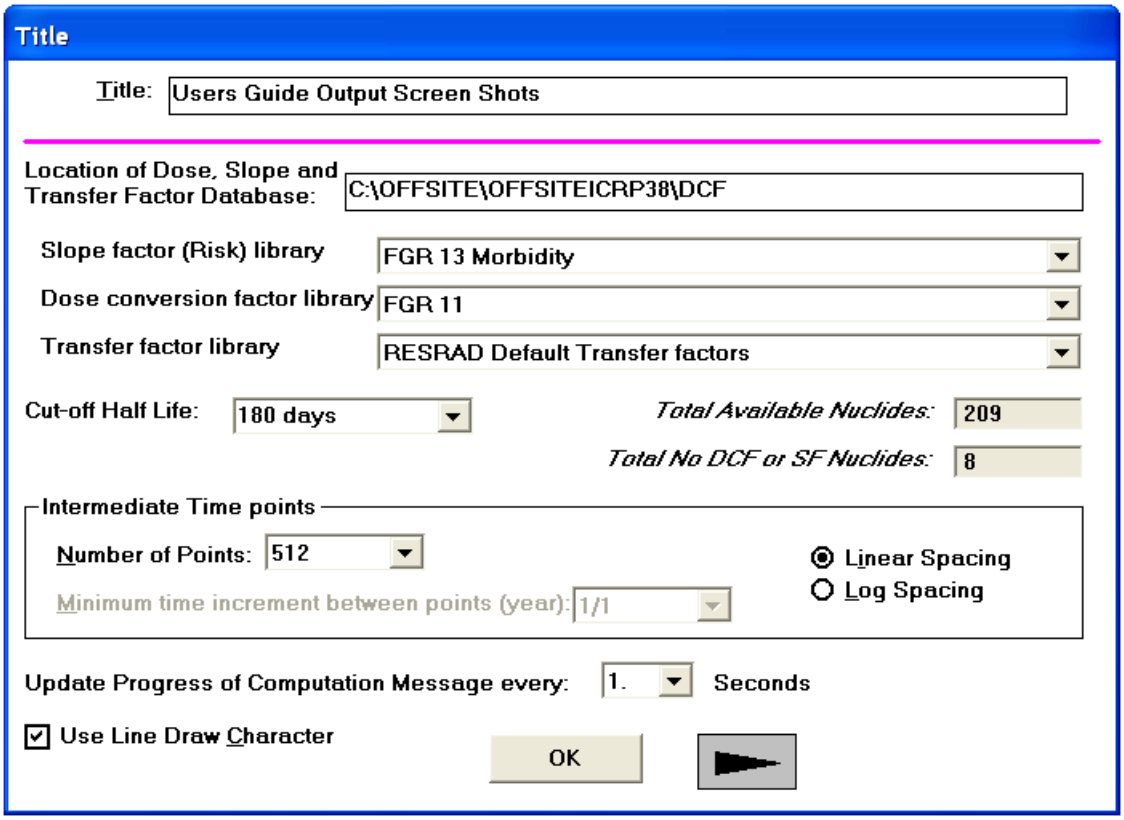

This form does not have a cancel feature. Any changes made to this form can be reversed only by re-entering the original inputs. None of the parameters in this form are eligible for uncertainty analysis or for one-at-a-time sensitivity analysis.

Title: This box shows the text that describes the site/scenario being modeled. This identification text will appear at the top of each textual report page.

Location of Dose, Slope and Transfer Factor Database Library: This is the directory in which the RESRAD dose, slope, and transfer factor database and editor are located. A common dose, slope, and transfer factor database can be used by many of the RESRAD codes (RESRAD, RESRAD-BUILD, RESRAD-OFFSITE), which makes any user-created library accessible to all the codes. As such, the database file need not reside in the OFFSITE directory but can be in a directory that is shared by the RESRAD family of codes. Double click on this input box to activate a file dialog form, then navigate to the directory in which the database that you want to use is located. Open the database that you want to use, and the libraries available in that database will be displayed in the appropriate drop down lists.

Slope Factor Library: The slope (risk) factors in this library will be used for the current analysis. Libraries of slope factors can be set up by using the RESRAD Dose Conversion Factors Editor, which is a stand-alone utility program common to the RESRAD family of codes. The libraries are stored in a database file. The dropdown list contains all the slope factor libraries that

are available in the current database — the FGR13 (Eckerman et al. 1999) morbidity, FGR13 mortality, the HEAST 2001morbidity libraries (EPA 2001), and any created by the user.

Dose Conversion Factor Library: The dose conversion factors in this library will be used for the current analysis. Libraries of dose conversion factors can be set up by using the RESRAD Dose Conversion Factors Editor, which is a stand-alone utility program common to the RESRAD family of codes. The libraries are stored in a database file. The dropdown list contains all the dose conversion factor libraries that are available in the current database — the FGR11 (Eckerman et al. 1988) and age-dependant ICRP72 (ICRP 1996) libraries and any created by the user.

Transfer Factor Library: The transfer factors in this library will be used for the current analysis unless the values are changed in the nuclide-specific transfer factor form (Section 4.9). Libraries of transfer factors can be set up by using the RESRAD Dose Conversion Factors Editor. The libraries are stored in a database file. The dropdown list contains all the dose conversion factor libraries that are available in the current database — the standard RESRAD default transfer factor library and any created by the user. The RESRAD transfer factor library contains only one soil to plant transfer factor for each nuclide, whereas the RESRAD-OFFSITE code can accept and use different factors for the vegetation in each of the four different agricultural and farmed areas. The transfer factors are site and species specific; the transfer factor form (Section 4.9) allows these values to be changed for each input file without having to create a different library for each site.

Cut-Off Half-Life: The fate and transport of nuclides with half-lives larger than the specified half-life are modeled explicitly by the code. Progeny nuclides with a half-life shorter than the specified value are assumed to be in secular equilibrium with their immediate parent. The user can select from the values in the list [180, 30, 7, or 1 day(s)] or type in any value that is not less than 10 minutes.

Informational Boxes There are two informational boxes in this form. The first shows the number of radionuclides in the current ICRP38 (ICRP 1983) database that have a half-live greater than or equal to the current cut-off half-life. The second show the number of such nuclides that are lacking at one or more dose conversion or slope factors.

Intermediate Time points

- **Number of Points:** This shows the number of time points at which concentrations, doses, and risks are computed. Because RESRAD-OFFSITE computes the concentration and fluxes at any time on the basis of the concentration and fluxes computed at preceding times, and because the code uses all the time points that fall within the appropriate exposure duration to perform time integration of dose and risk, this parameter determines the accuracy of the computed values. This is also the number of points that are used to generate the temporal graphics. Straight line segments connect the points in the curve. A larger number of times enables the code to compute off-site accumulation, groundwater transport, and time integration of dose and

risk more accurately and will result in smoother plots. But a larger number of points will also increase the execution time. For most radionuclides, a number of time points equal to about one-tenth to one-fifth of the prediction time horizon should give results of sufficient accuracy. A greater number of intermediate time points is required if the rate of release of a radionuclide changes rapidly over time. The number of points shown must be such that a linear approximation between the values of flux at those times is a good representation of the actual temporal variation of the flux. The interval of time between the intermediate time points must not exceed the travel time in any of the groundwater transport zones.

- **Linear Spacing or Log Spacing:** The spacing shows the manner in which the intermediate time points are distributed over the time horizon. The time horizon is the sum of the maximum user-specified reporting time (Section 4.11, reporting times form) and the exposure duration (Section 4.2, preliminary inputs form). The spacing may be linear or log:

  1. Linear**:** If linear is chosen, the intermediate time points are spaced uniformly (in an arithmetic series) between 0 and the time horizon.

  2. Log**:** If log is chosen, the intermediate time points are spaced in a geometric series (uniformly on a log scale) between the specified minimum time increment and the time horizon. The spacing in this case may be adjusted by the minimum time increment, as described below.

- **Minimum Time Increment:** In addition to being the first intermediate time point under the choice of log spacing, as described above, this is also the lower bound for spacing between intermediate time points of a geometric series. Depending on the time horizon and the number of points, the spacing between the intermediate time points can be very small at the beginning of the geometric series for the log option. In order to avoid unnecessary calculations, if the spacing is less than the specified minimum value, the sequence of time points will then be modified to a linear series with the minimum time increment, followed by a geometric series with a time increment that is never less than the specified minimum.

Update Progress of Computation Message: The time needed to perform the RESRAD-OFFSITE computations can range from a few minutes to a couple of hours, depending on the number of intermediate time points, number of radionuclides, length of the transformation chain, groundwater transport characteristics of the nuclides, and, in the case of probabilistic analysis, number of realizations that are chosen. The FORTRAN computational code periodically writes out a message indicating the progress of the computation in order to reassure the user that computations are being performed and, in the case of probabilistic analysis, to provide an estimate of the time required to finish the computations. This input box specifies the frequency at which this message will be updated by the computational code and the frequency at which it is sampled for display in the interface.

Writing the progress message can increase the total run time significantly. A “0.0” option is provided to turn off message writing by computational code. This can reduce the run time of probabilistic analysis. In this case, an estimate of the computation time will be made on the basis of the size of the output files.

Use Line Draw Character: It is recommended that the MS Line Draw Font be used for the reports. This font produces well-formatted tables and good lines. If another font is desired, it is suggested that this box be unchecked to substitute minus signs for the lines.

Forward arrow button: You can save the current values, hide the Title form, and open the next form (Section 4.2, preliminary inputs form), all with one click of this button (or Alt o). The same button appears on all input forms to facilitate rapid movement through all the relevant input forms.

OK button: Use this button to hide (i.e., minimize away from view) the Title form.

4.2 PRELIMINARY INPUTS

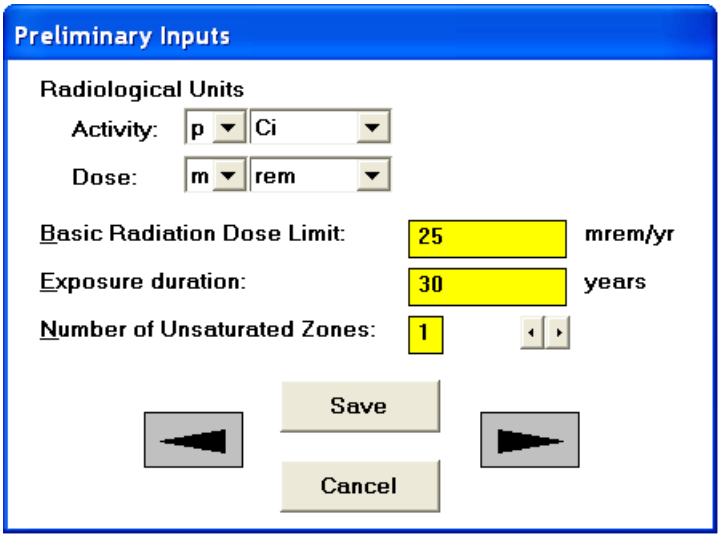

None of the parameters in this form are eligible for uncertainty analysis or for one-at-a-time sensitivity analysis.

Radiological Units

- **Activity:** The dropdown boxes allow the user to choose the desired unit of radiological activity. Available choices are curie (Ci), becquerel (Bq), disintegrations per second (dps), and disintegrations per minute (dpm); the first two can be combined with metric prefixes ranging from atto (10^{-18}) through exa (10^{18}).

- **Dose:** The dropdown boxes allow the user to choose the desired unit of radiological dose. Available choices are roentgen equivalent man (rem) and sievert (Sv); these can be combined with metric prefixes ranging from atto (10^{-18}) through exa (10^{18}).

Basic Radiation Dose Limit: This is the annual radiation dose limit used to derive all site-specific soil guidelines.

Exposure Duration: This is the length of time that the receptor is exposed to radiation at this site. Values reported for risk are time-integrated over this exposure duration. The risk is calculated by using the trapezoidal formula on contaminated intakes computed at all the intermediate time points falling within the exposure duration and at the intermediate time point that is just outside the exposure duration. Dose is time integrated over 1 year or the exposure duration, whichever is less. (Given the current lower bound of 1 year on the exposure duration, dose in currently integrated over a 1-year period.)

Number of Unsaturated Zones: This is the number of different partially saturated layers between the primary contamination and the saturated zone. The code has provisions for up to five different horizontal strata.

4.3 SITE LAYOUT

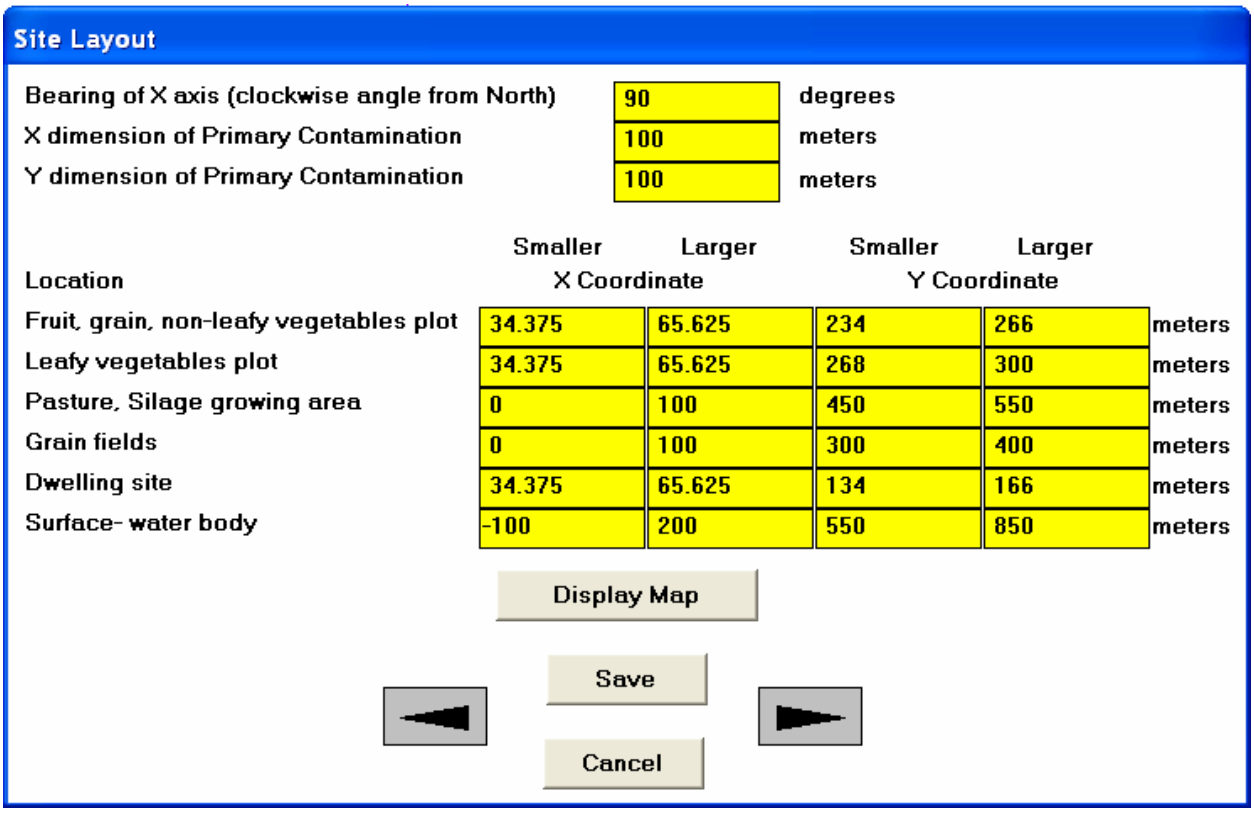

Uncertainty and sensitivity analysis can be performed on any parameter on this form. The map interface (Section 4.4) can be used to input the same information in a interactive graphical fashion. The site layout form is appropriate when measured or computed lengths are available. The interactive map interface is appropriate when visible features in the map are to be used to define the various areas.

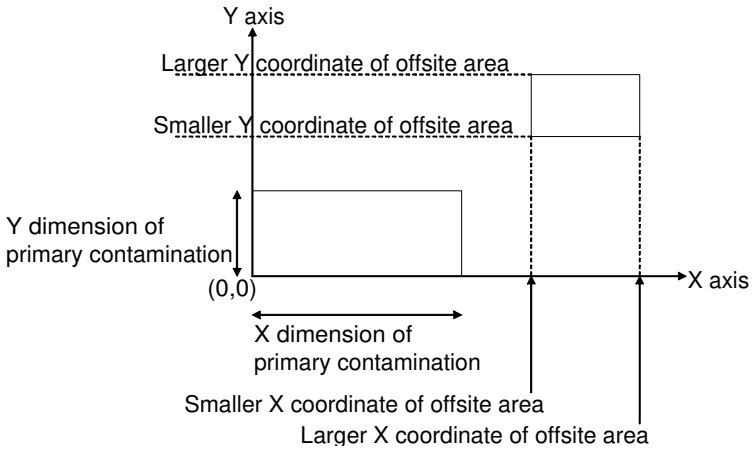

The inputs on this form are used by the atmospheric transport code and also used to compute the areas of the primary contamination and the offsite locations. The atmospheric transport model assumes that the primary contamination and the offsite locations are rectangular in shape and that a pair of sides of all the rectangles are oriented in the same direction. The two sides of the primary contamination that meet at the lower left corner are the axes of the coordinate system. Each offsite area is defined by the four coordinates as shown in the figure above. These can be thought of as the coordinates of the sides of the offsite area.

Bearing of X Axis: This is the clockwise angle from the north to the direction of the positive X axis.

X Dimension of the Primary Contamination: This is the length of the side of the idealized primary contamination that is parallel to the X axis, the length of the lower side.

Y Dimension of the Primary Contamination: This is the length of the side of the idealized primary contamination that is parallel to the Y axis, the length of the left side.

The X Coordinates of an Offsite Area: These are the X coordinates of the two sides that are parallel to the Y axis. When the save command or one of the form-linking arrow commands is issued, the code will compare the two X coordinates of each area and interchange them if the larger value is entered in the column for the smaller value and vise versa.

The Y Coordinates of an Offsite Area: These are the Y coordinates of the two sides that are parallel to the X axis. When the save command or one of the form-linking arrow commands is issued, the code will compare the two Y coordinates of each area and interchange them if the larger value is entered in the column for the smaller value and vise versa.

4.4 MAP INTERFACE

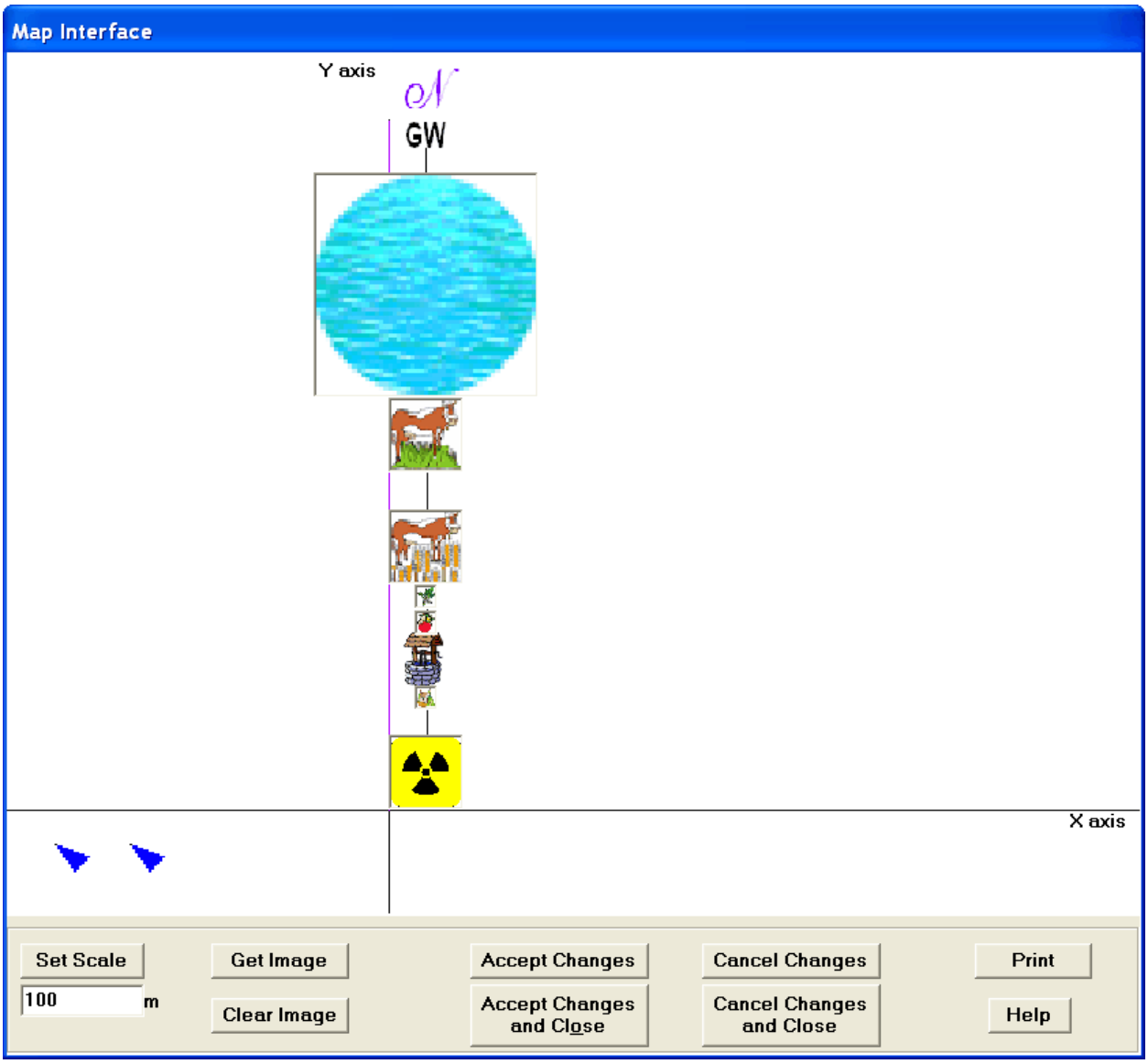

The map interface can be used to position and, where appropriate, size the objects and directions of interest in RESRAD-OFFSITE (primary contamination, offsite dwelling, well, surface water body, agricultural fields, the direction of groundwater flow and the direction of north), either by dragging and dropping or resizing the corresponding icons. Alternatively, it can be used to view the layout that was specified in the standard input forms (layout form, Section 4.3, and the ground water transport form, Section 4.22). It can also be used to access the forms specifying the details of the location represented by each icon, ***right*** clicking the icon opens the corresponding form. The forms that are linked to the icons are listed in the following table.

Icon	Form
N	Site layout, Section 4.3
Radioactivity	Primary Contamination, Section 4.14
Cow	Livestock Feed Growing Areas, Section 4.15
Leaf or fruits	Agricultural Areas, Section 4.15
House	Offsite Dwelling Area, Section 4.16
Well	Saturated Zone Hydrology, Section 4.19
Blue circle/ellipse	Surface Water Body, Section 4.21
GW	Groundwater Transport, Section 4.22

The process for using the map interface is as follows:

1. View map interface form.

2. Add a background image (a map of the site or a map from Web sites such as MapQuest, TopoZone, or TerraServer).

3. Set the scale on the basis of a known distance in the background map.

4. Move and size the radioactivity icon to define the location of the primary contamination.

5. Move and size the other icons to define the corresponding locations. The GW (groundwater flow direction) and N (north) icons indicate direction; they can not be resized because size has no meaning for the direction. The well can not be resized because the diameter of the well is not an input.

6. Click on the Accept Changes button.

7. The image location, scale, and object locations will be written to the input file when the RESRAD-OFFSITE file is saved. This information is used to display the map image and the icons when the input file is opened at a later time.

Details on Using Map Interface

Steps 2 through 5 and step 7 are described in greater detail below.

2. Click on the Get Image button and navigate to an image (bitmap, metafile, enhanced metafile, JPEG, or GIF file) on the site that is large enough to contain all the objects of interest. These images can be obtained from popular Web sites, such as MapQuest, TopoZone, or TerraServer. To get an image:

- Go to one of these sites.
- Navigate and zoom to a level such that the map would show all objects of interest.
- Right click on the image.
- Choose Save picture.
- Save the image in a folder, such as the User Files folder under the default RESRAD-OFFSITE installation folder.
- When prompted for the file after clicking on Get Image, specify the location of this file.

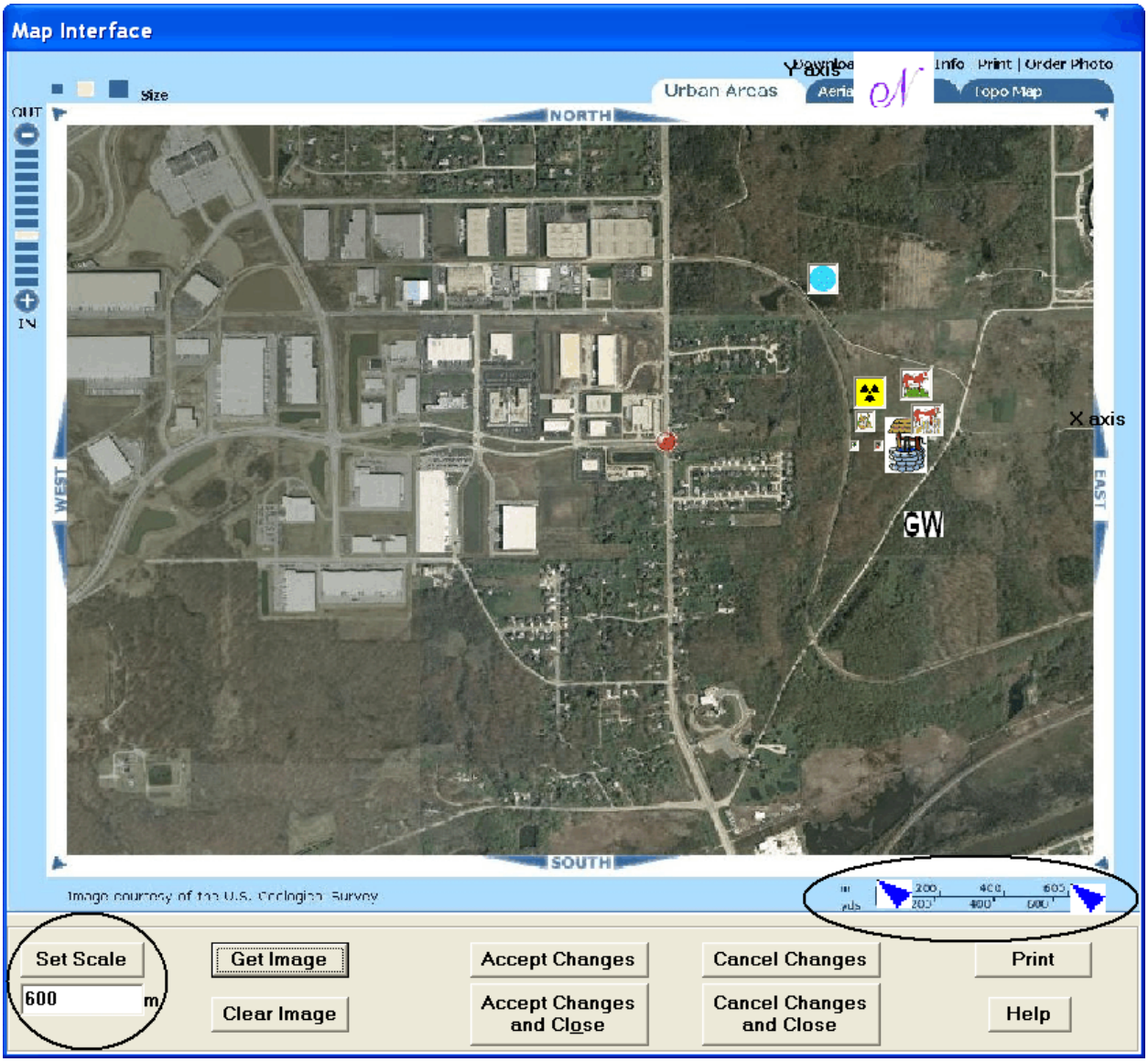

3. Find the scale on the map or find two points on the map for which the distance is known. Move the blue arrows to points on either end of the scale. Enter the distance (in meters) between the arrows in the entry box below the Set Scale button. For example, enter **600** if the scale says the distance between the two arrows represents 0.6 km. Then click on the Set Scale button.

4. Left click on the source icon (the yellow and black radionuclides symbol) and drag it to a new location. Move the sides of the icon to expand or shrink it to cover the entire primary contamination.

5. Left click on any other object and drag it to move it to a new location. Move the sides of the icon to expand or shrink it to cover the entire area that the icon represents. The GW icon indicates the direction of the groundwater flow from the source, and the N icon indicates north. If an icon does not appear on the

Map Interface, it can be moved into the map by specifying its location in the site layout form (Section 4.3).

7. The image location, scale, and object locations will be written to the input file when the RESRAD-OFFSITE file is saved. This information is used to display the map image and the icons when the input file is opened at a later time. If the input file is being sent to a different computer, the image files should also be sent in order for it to be displayed on that computer. The Get Image command may have to be used on the receiving computer after opening the input file if the structure and or the name of the RESRAD-OFFSITE directories are different on the two computers. If the image file is not sent, the image of the map cannot be displayed, but the icons will be in the specified locations and the analysis will yield the same results.

4.5 SOURCE (Initial Concentrations of Radionuclides at a Site)

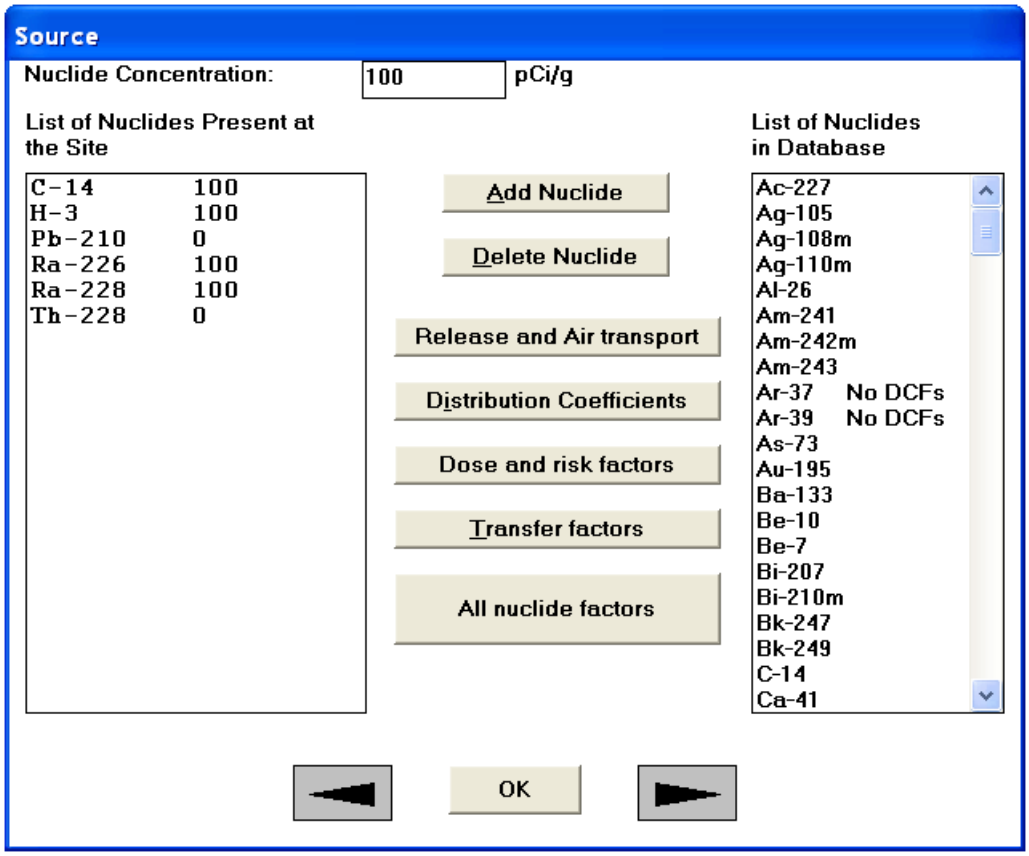

This form does not have a cancel feature. Any changes made to this form can be reversed only by re-inputting the original inputs.

An uncertainty analysis can be performed on the concentration of any nuclide that has a nonzero initial concentration. This is done by clicking on the nuclide in the left scroll box (list of nuclides present at the site) and then pressing the F8 key.

List of Nuclides in Database: This list in the right scroll box shows all the radionuclides in the database that have a half-life greater than the cutoff half-life selected in the Title form. Any nuclides that are lacking one or more of the dose or slope factors is flagged with a "No DCFs" comment on the side. This alerts the user that these nuclides can not be analyzed unless a library with a nonzero dose and slope factors is selected.

List of Nuclides Present at the Site: This list in the left scroll box shows radionuclides that will be explicitly considered in the current analysis. It includes all radionuclides that were specified to be initially present at the site and their principal nuclide progeny (see cutoff half-life in the Title form). Although the fate and transport of any associated radionuclides will not be modeled explicitly, their contribution to dose and risk will be included on the basis of the assumption that they are in secular equilibrium with their principal radionuclide parent.

Add Nuclide: To add a radionuclide, either click on its name in the right scroll box and then click on the Add Nuclide button, or just double click on its name in the right scroll box. The radionuclide will be added to the left scroll box with a concentration specified in the top center input box. All potential decay products will be added to the left scroll box with a default concentration of 0 if they are not already present.

Delete Nuclide: To delete a radionuclide, click on its name in the left scroll box and then click on the Delete Nuclide button. All potential decay products that arise only from the deleted radionuclide and have an initial concentration of zero will also be deleted automatically.

Nuclide Concentration: This is the radionuclide concentration averaged over an appropriate depth and area. See Section 3.3 of the RESRAD Manual and the RESRAD Data Collection Handbook for more details.

- *To change the concentration of a radionuclide that is in the left scroll box*: Click on the radionuclide in the left scroll box and type in the concentration.

- *To change the default concentration when adding new radionuclides:* Click on the right scroll box. Then enter the concentration in the top center box. To add radionuclides with this concentration, see above description.

Accessing Other Related Forms

The four command buttons on this form, which are listed below, provide access to the four forms that contain the radionuclide-dependent inputs. Alternatively, the first form can be opened by clicking on the forward arrow button on this form, then the other three forms can be accessed by continuing to use the forward arrow buttons on the successive forms. If the computer monitor is large enough (17 inches or more), all these forms can be viewed simultaneously by clicking on the All Nuclide Factors button. All four forms can also be accessed by double clicking on the radionuclide name in the left scroll box.

Release and Air transport: Use this button to specify the release mechanism and rate to groundwater (currently only one option is available) and the deposition velocity of the material with which the nuclide is being transported in the atmosphere. This opens the Source Release and Atmospheric Transport form (Section 4.6).

Distribution Coefficients: Use this button to open the Distribution coefficients form (Section 4.7).

Dose and risk factors: Use this button to display the Dose conversion and Slope Factors form (Section 4.8). The factors will be displayed on this form, but they cannot be changed directly on this form.

Transfer factors: Use this button to access the Transfer factors form (Section 4.9).

4.6 SOURCE RELEASE AND DEPOSITION VELOCITY

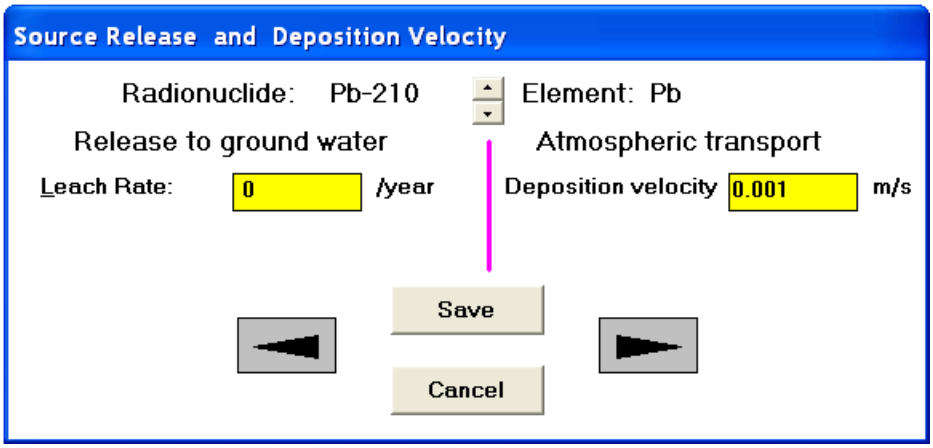

Uncertainty and sensitivity analysis can be performed on any parameter on this form.

RESRAD-OFFSITE currently uses a first-order, rate-controlled release model. If a nonzero release rate is specified, it will be used to compute the contaminant concentration in the region of primary contamination and the releases to groundwater. Because the contaminant concentration in the primary contamination contributes to the releases to the atmosphere and to surface runoff, the leach rate indirectly affects those two releases as well. If a zero is entered, the code will estimate a release rate on the basis of the equilibrium desorption concentration.

The deposition velocity of the material with which the nuclide is being transported is used by the code to account for loss from dry deposition along the atmospheric transport path and to compute the deposition flux at the offsite locations.

Click on the up or down arrow appearing next to the radionuclide name to save the inputs for the currently displayed radionuclide and to view the inputs for the next or previous radionuclide.

4.7 DISTRIBUTION COEFFICIENTS

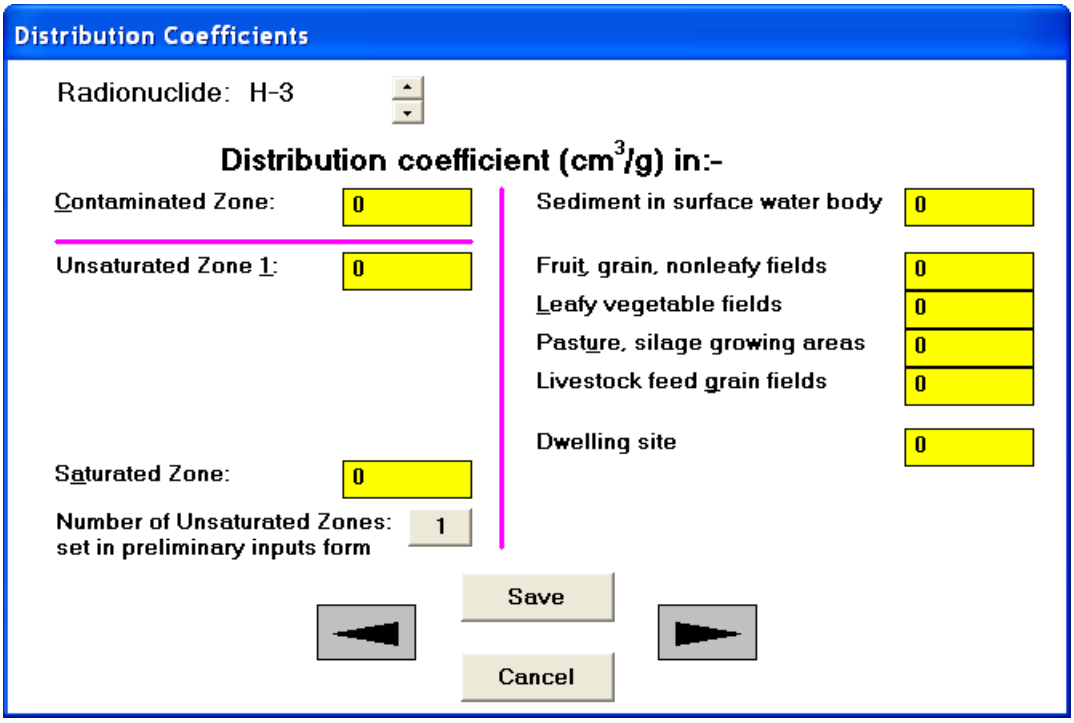

Uncertainty and sensitivity analysis can be performed on the distribution coefficients. Distribution coefficients are the ratios of the mass of solute that is adsorbed on or precipitated onto the soil (per unit of dry mass) to the solute concentration in the liquid phase at the different zones and locations. Default values are provided for each radionuclide; however, site-specific values can vary over many orders of magnitude, depending on the chemical form, soil type, pH, redox potential, and the presence of other ions.

Click on the up or down arrow next to the radionuclide name to save the distribution coefficients of the current radionuclide and to view the distribution coefficients of the next or previous radionuclide.

Contaminated Zone: This distribution coefficient is used to estimate a first-order release rate when the user does not specify a release rate.

Unsaturated Zone and Saturated Zone: These distribution coefficients are used to compute the radionuclide transport rate for groundwater transport calculations.

Sediment in Surface Water Body: This distribution coefficient is used to compute the concentration of the radionuclide in the surface water body.

Fruit, Grain, Nonleafy Fields; Leafy Vegetable Fields; Pasture, Silage Growing Areas; Livestock Feed Grain Fields; Dwelling Site: These five distribution coefficients for agricultural fields, pastures, and dwelling sites are used to account for leaching when accumulation in the fields, pastures, and dwelling sites is being computed.

Clicking on the button displaying the number of unsaturated zones causes the Preliminary inputs form (Section 4.2) to open, because the number of unsaturated zones can be changed only on that form.

4.8 DOSE CONVERSION AND SLOPE FACTORS

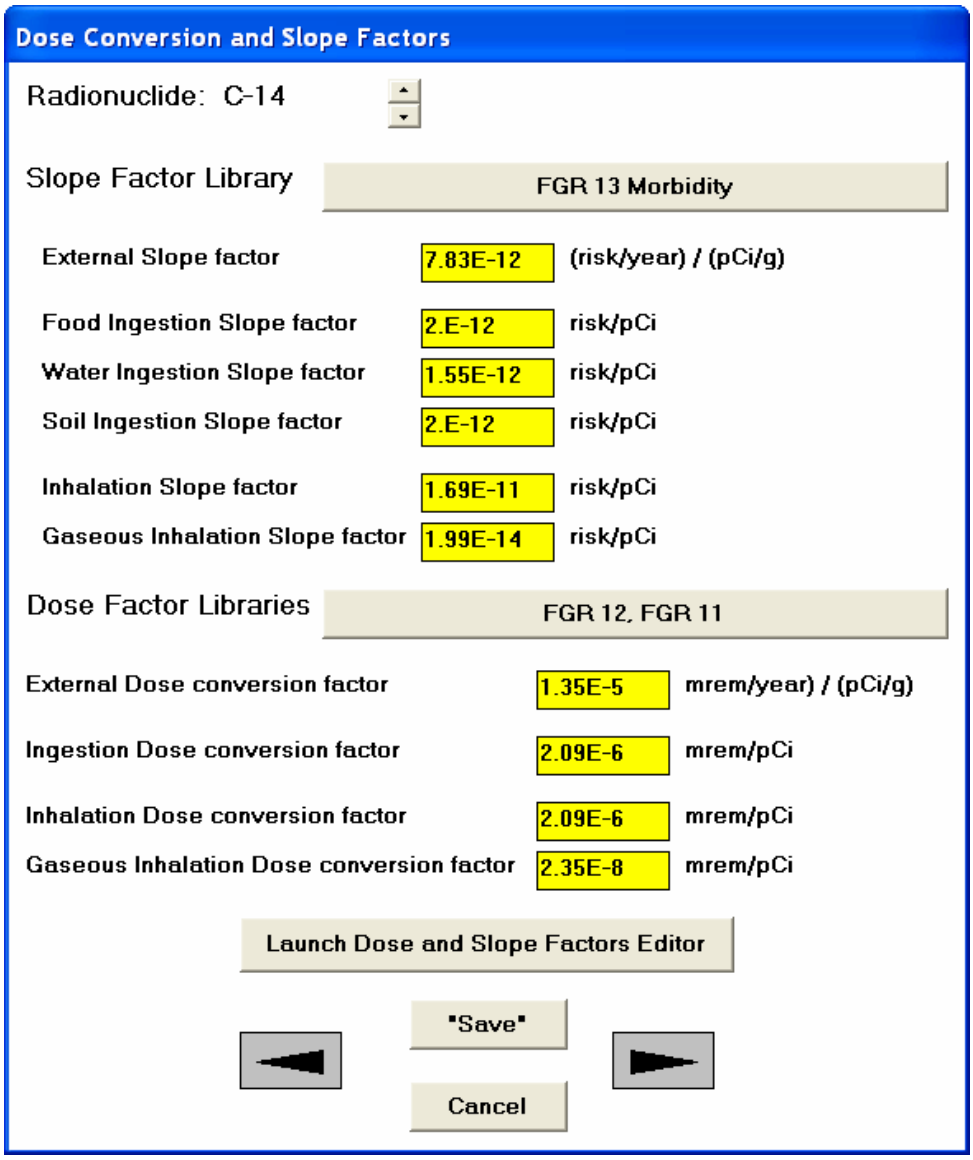

With the exception of the gaseous inhalation dose conversion factor for ^{14}C, the dose conversion and slope factors displayed on this form cannot be changed directly on the form. However, a different dose factor library or a different slope factor library may be selected by clicking on the corresponding button with name of the current library. A new library can be created by clicking on the Launch Dose and Slope Factors Editor button near the bottom of the screen. Neither uncertainty analysis nor sensitivity analysis can be performed on the dose conversion and slope factors in the current version of the code.

Radionuclide: The factors on the form pertain to the nuclide identified on the form. The factors for each radionuclide that was specified for the site can be viewed by clicking on the up or down button next to the radionuclide name.

Slope Factors: The slope factors for exposure by external radiation; ingestion of food, water, and soil; and inhalation are displayed.

Dose Conversion Factors: The dose conversion factors for exposure by external radiation, inhalation, and ingestion from the specified library are displayed on this form. In addition to the two factors mentioned above, the dose conversion factor for the inhalation of the gaseous form of C-14 will also be displayed when that radionuclide is selected.

Radon Dose Conversion Factors and Slope Factors

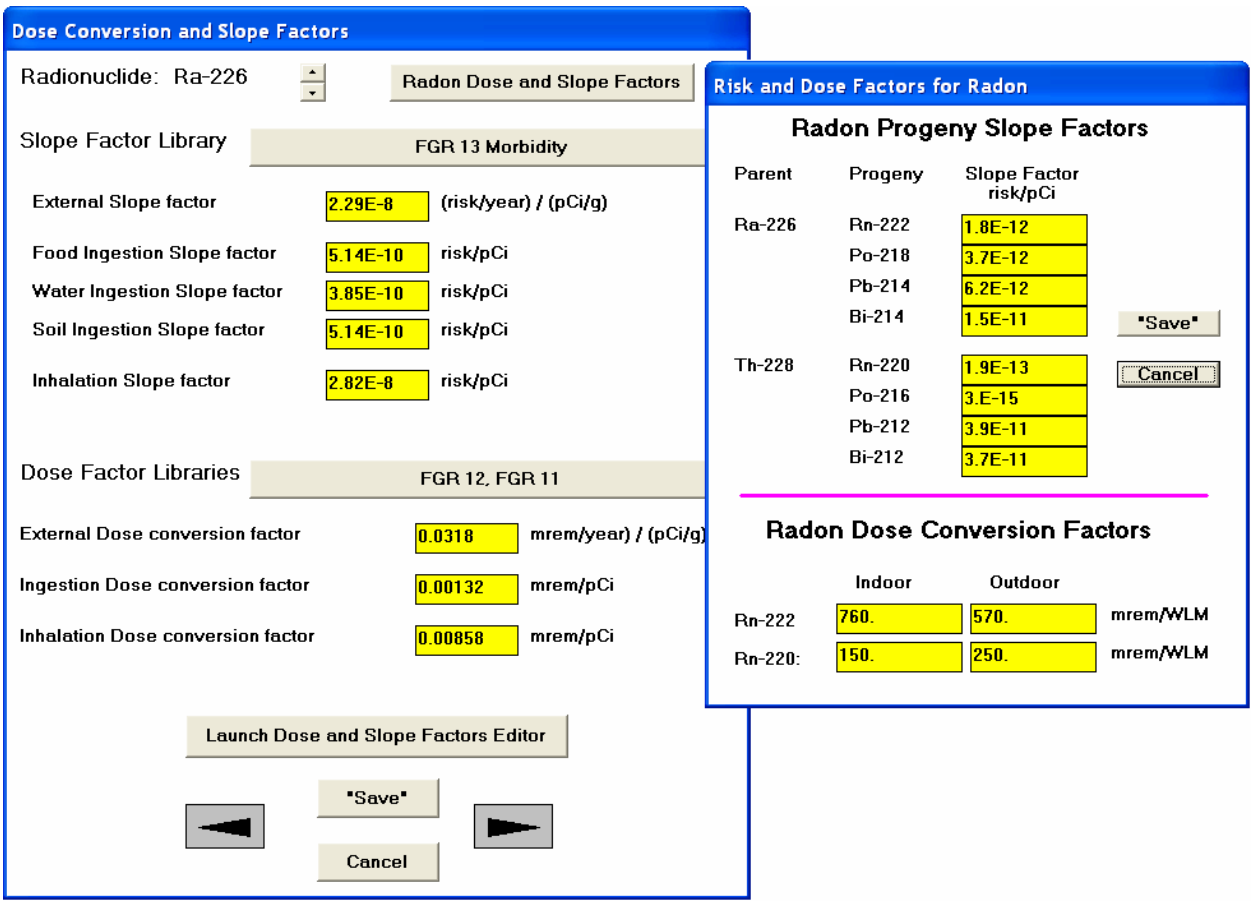

A button command to display the dose conversion and slope factors for the isotopes of radon and its short-lived progeny is displayed when an immediate radon precursor (Ra-226, Th-228) is selected and when the radon pathway is active.

4.9 TRANSFER FACTORS

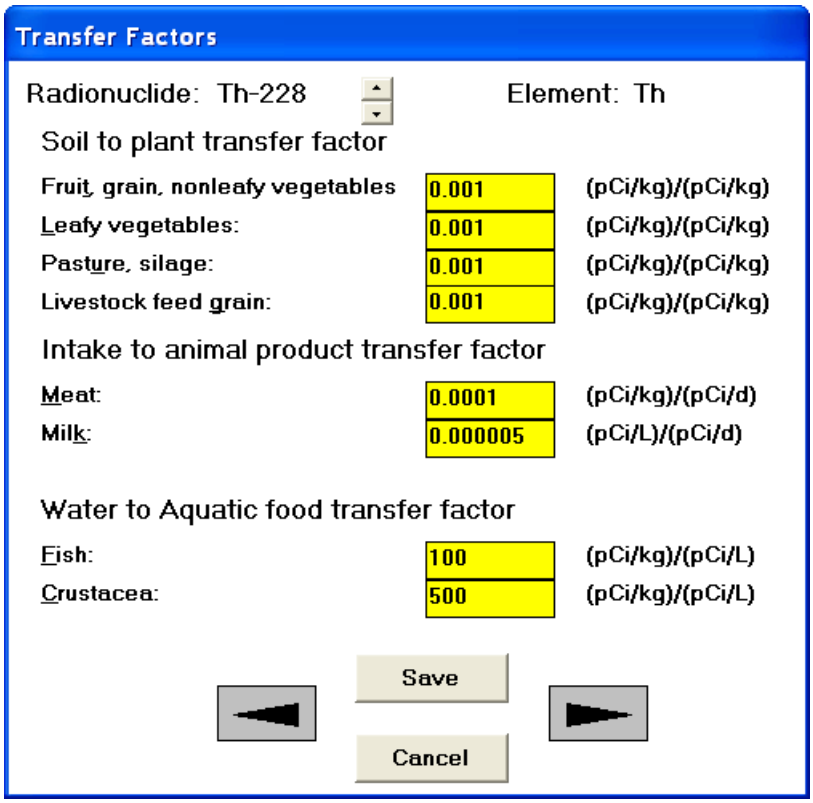

Uncertainty and sensitivity analysis can be performed on the transfer factors. This form is linked to the list of radionuclides specified to be present at the site. Therefore, it displays the transfer factors for each radionuclide that is specified to be present. However, the transfer factors are element-specific; thus, any changes made to the factors of an isotope will be used for all the isotopes of that element. The form displays the radionuclide name and the element name to remind the user that the transfer factors are element-specific. The factors for each element and radionuclide that were specified for the site can be viewed by clicking on the up or down button next to the radionuclide name.

Soil to Plant Transfer Factor: This is the root uptake transfer factor, which is the ratio between the contaminant concentration in the edible plant and that in the soil upon which the plant is grown. The RESRAD database contains only one default value for each element. Values appropriate for the site-specific vegetation must be entered in the four input boxes. Values are not displayed for H-3 and for C-14 because the transfer factors are computed by the code (see Appendix L of the RESRAD Manual).

Intake to Animal Product Transfer Factor: This is the ratio between the concentration of the radionuclide in meat or milk and the rate of intake of the radionuclide by livestock. Values are not displayed for H-3 and for C-14 because the transfer factors are computed by the code (see Appendix L of the RESRAD Manual).

Water to Aquatic Food Transfer Factor: This is the ratio between the radionuclide concentration in the edible parts of aquatic food and that in the water in which they live.

4.10 SET PATHWAYS

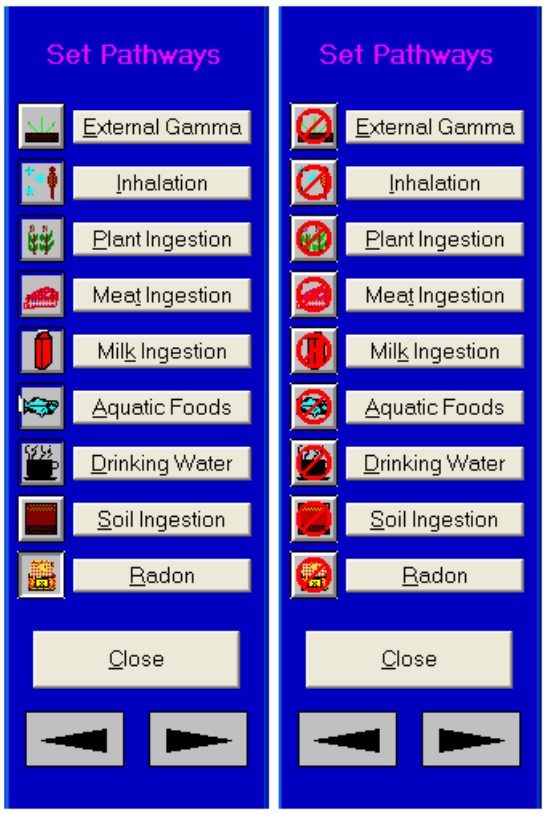

All pathways but the radon pathway are active by default. The radon pathway is inactive. The user can activate the radon pathway after selecting a radon precursor.

An inactive pathway can be activated by clicking on either the crossed-out icon corresponding to the pathway or the name of the pathway, or by using the hot key (Alt + underlined letter) corresponding to that pathway.

An active pathway can be deactivated by clicking on either the icon corresponding to the pathway or the name of the pathway, or by using the hot key (Alt + underlined letter) corresponding to that pathway.

4.11 REPORTING TIMES

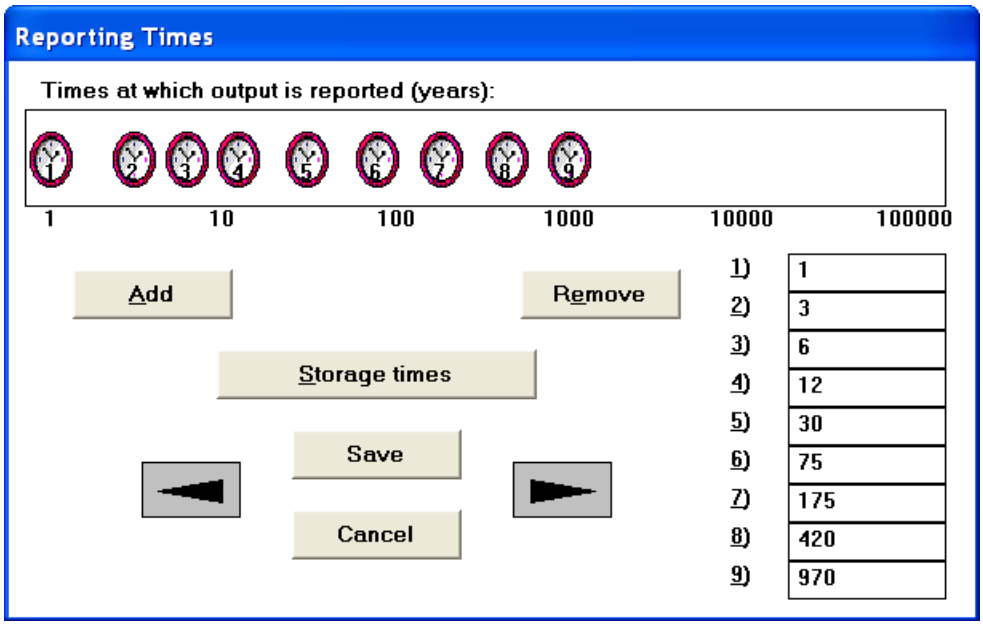

None of the inputs on this form are eligible for uncertainty analysis or for sensitivity analysis.

Times at which Output Is Reported: These are the times after the radiological survey when results are to be reported in the textual output. A time horizon of 1,000 years is commonly used; however, calculations can be carried out to longer periods to identify potential problems from delayed contributions from the groundwater or other pathways. The forecast time horizon is the sum of the last reporting time and the exposure duration. Results are always calculated and reported for year 0.

The code predictions are available at each of the intermediate time points generated by the specification in the Title form (Section 4.1). Interpolation is performed between those time points to produce the textual report at the times specified in this form.

Add: To add a time:

- Press the Add button and a new clock icon and time box will appear. Set the time following the change time procedure, or

- Click the right mouse button while the cursor is in the frame containing the clock icons.

Remove: To remove a time:

- Click on the appropriate time box or clock icon
- and then press the Remove button.

Change: To change a time:

- Click on the appropriate time box and enter new value, or
- Click on the appropriate clock icon and drag to desired time location.

Storage Times: The Storage Times form can be assessed by clicking on this button. Because the Storage Times form is the next linked form, the forward arrow can also be used to get to it.

4.12 STORAGE TIMES

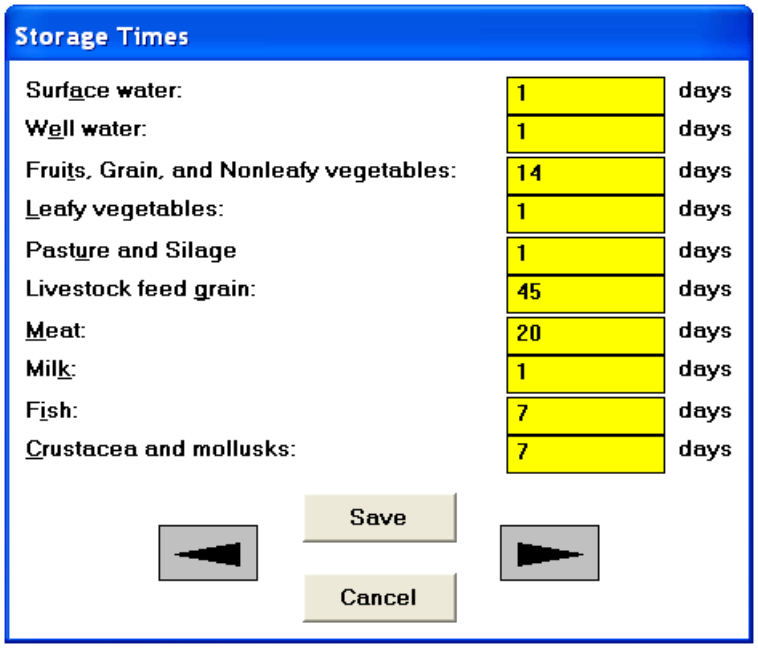

Uncertainty and sensitivity analysis can be performed on the storage times.

These are the times over which foodstuffs and water are stored before being consumed or used. The concentrations of radionuclides in food and water are adjusted for decay and ingrowth during this period. See Appendix D of the RESRAD Manual for more details.

4.13 PHYSICAL AND HYDROLOGICAL PARAMETERS

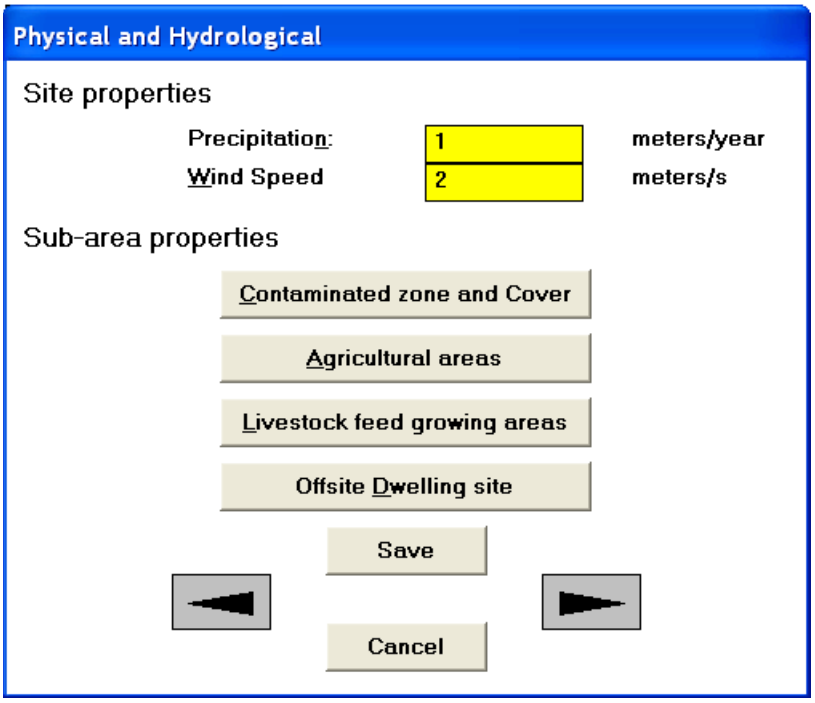

Uncertainty and sensitivity analysis can be performed on the two parameters on this form.

Precipitation: This the annual average value of precipitation at the site. It is used to compute the infiltration rate in the primary contamination, the leach rates in all areas, and the evapotranspiration of tritium. The leach rate is used to compute contaminant concentration in soil at the primary contamination site and in the agricultural, pasture, and dwelling areas. The infiltration rate affects the rate of transport through the unsaturated zone.

Wind Speed: This is the annual average wind speed used to calculate the area factor for inhalation and foliar deposition (see Appendixes B and D of the RESRAD Manual). It is also used for ingrowth calculations for the radon pathway (Appendix C) and in the tritium and C-14 models (Appendix L).

Accessing Other Related Forms

The four command buttons on this form — **Contaminated zone and Cover, Agricultural areas, Livestock feed growing areas, Offsite Dwelling site** — provide access to the four forms that provide physical and hydrological data on four subarea properties (see Sections 4.14, 4.15, and 4.16). Clicking on one of these four buttons opens the respective form. The current parent form will not be closed and will remain in the background, and it will appear again when the other form is exited. Alternatively, the first form can be opened by clicking on the forward arrow button on this form, then the other three forms can be accessed by continuing to use the forward arrow buttons in the successive forms.

4.14 PRIMARY CONTAMINATION (CONTAMINATED ZONE AND COVER): PHYSICAL AND HYDROLOGICAL DATA

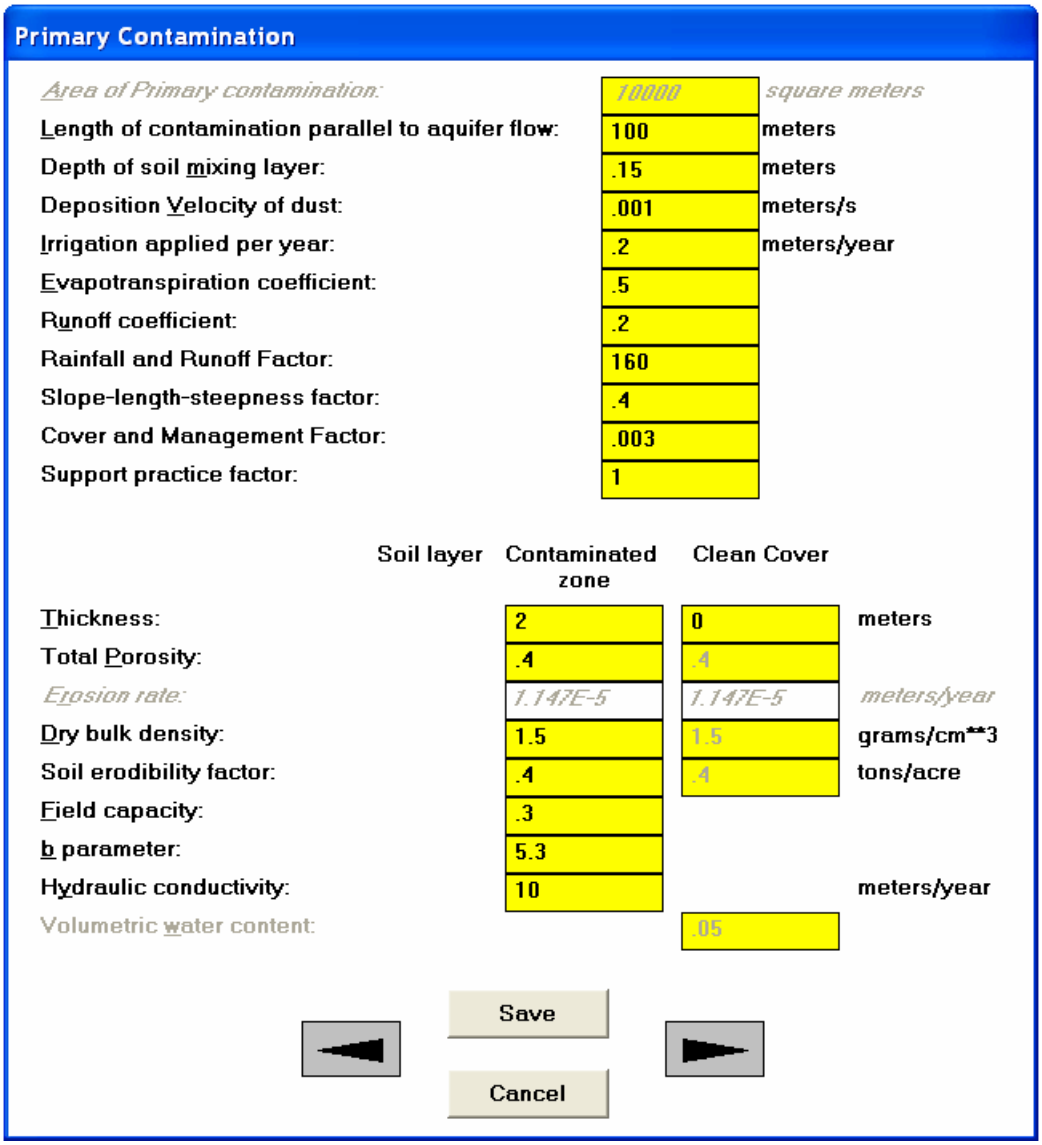

Uncertainty and sensitivity analysis can be performed on any parameter that is an input on this form. Parameters that are not inputs to the code are shown in gray italics for information only.

Area of Primary Contamination: This is not a direct input, but is computed using the information input in the site layout form. The primary contamination is a compact area that contains the location of all soil samples with radionuclide concentrations that are clearly (i.e., two standard deviations) above background.

Length of Contamination Parallel to Aquifer Flow: This is the distance between two parallel lines that are perpendicular to the direction of the aquifer flow — one at the upgradient edge of

the contaminated zone and the other at the downgradient edge. It is used in groundwater transport calculations.

Depth of Soil Mixing Layer: This is the thickness of the surface soil at the location of the primary contamination that may be assumed to be mixed uniformly from time to time as a result of anthropogenic or physical processes. It is used to calculate the concentration of contaminants in surface soil.

Deposition Velocity of Dust: This is the representative deposition velocity of dust at the location of primary contamination. It is used to compute the release to the atmosphere on the basis of the assumption that there is no net deposition of particulates at the site.

The next three inputs and the precipitation rate are used to compute the infiltration rate and also to compute the evapotranspiration of tritium from the primary contamination. They affect all releases from the primary contamination and also the transport rate through the unsaturated layers.

Irrigation Applied per Year: This is the volume of irrigation water that is applied over a period of 1 year per unit area of land. It is not the actual rate of irrigation during the growing season but the irrigation rate averaged over 1 year.

Evapotranspiration Coefficient: This is the fraction of precipitation and irrigation water that penetrates the topsoil that is lost to the atmosphere by evaporation and by transpiration by vegetation.

Runoff Coefficient: This is the fraction of precipitation that does not penetrate the topsoil but leaves the area of concern as surface runoff; no loss is assumed for irrigation water.

The next six inputs are used to compute the rate of erosion. Erosion rate is not an input in RESRAD-OFFSITE; it is displayed for the information of RESRAD users.

Rainfall and Runoff Index: This is a measure of the energy of the rainfall. It is used to compute the erosion rate.

Slope-Length-Steepness Factor: This factor accounts for the profile of the terrain on the erosion rate.

Cover and Management Factor: This factor (formerly called cropping-management factor) accounts for the effects of land use, vegetation, and management on the erosion rate.

Support Practice Factor: This factor (formerly called conservation practice factor) accounts for the effects of conservation practices on the erosion rate.

Dry Bulk Density (of soil in the contaminated zone and in clean cover): This is the mass of (dry) solids in a unit volume of soil in the respective layers of soil. In addition to being used to compute the erosion rate, this is also used to compute the exposure to external radiation. The

density in the contaminated zone is also used to compute the release to groundwater and thus the concentration in the primary contamination.

Soil Erodibility Factor: This is a measure of the susceptibility of the soil to erosion.

Thickness (of contaminated zone): This is the distance, in meters (m), between the uppermost and lowermost soil samples with radionuclide concentrations that are clearly (i.e., two standard deviations) above background.

Thickness (of clean cover): This is the distance from the ground surface to the location of the uppermost soil sample with radionuclide concentrations that are clearly above background.

Total Porosity (of contaminated zone and clean cover): This is the volume fraction of soil that is occupied by liquid and gaseous phases in the respective layers.

Field capacity (of contaminated zone): This is the volumetric moisture content of soil at which (free) gravity drainage ceases. This is the amount of moisture that will be retained in a column of soil against the force of gravity.

b Parameter (of contaminated zone): The soil-specific exponential b parameter relates the hydraulic conductivity of partially saturated soil to its moisture content.

Hydraulic Conductivity (of contaminated zone): This is the apparent flow velocity through the contaminated zone under a unit hydraulic gradient.

Volumetric Water Content (of clean cover): This is the volume fraction of soil that is occupied by water.

4.15 AGRICULTURAL AREAS AND LIVESTOCK FEED GROWING AREAS: PHYSICAL AND HYDROLOGICAL DATA

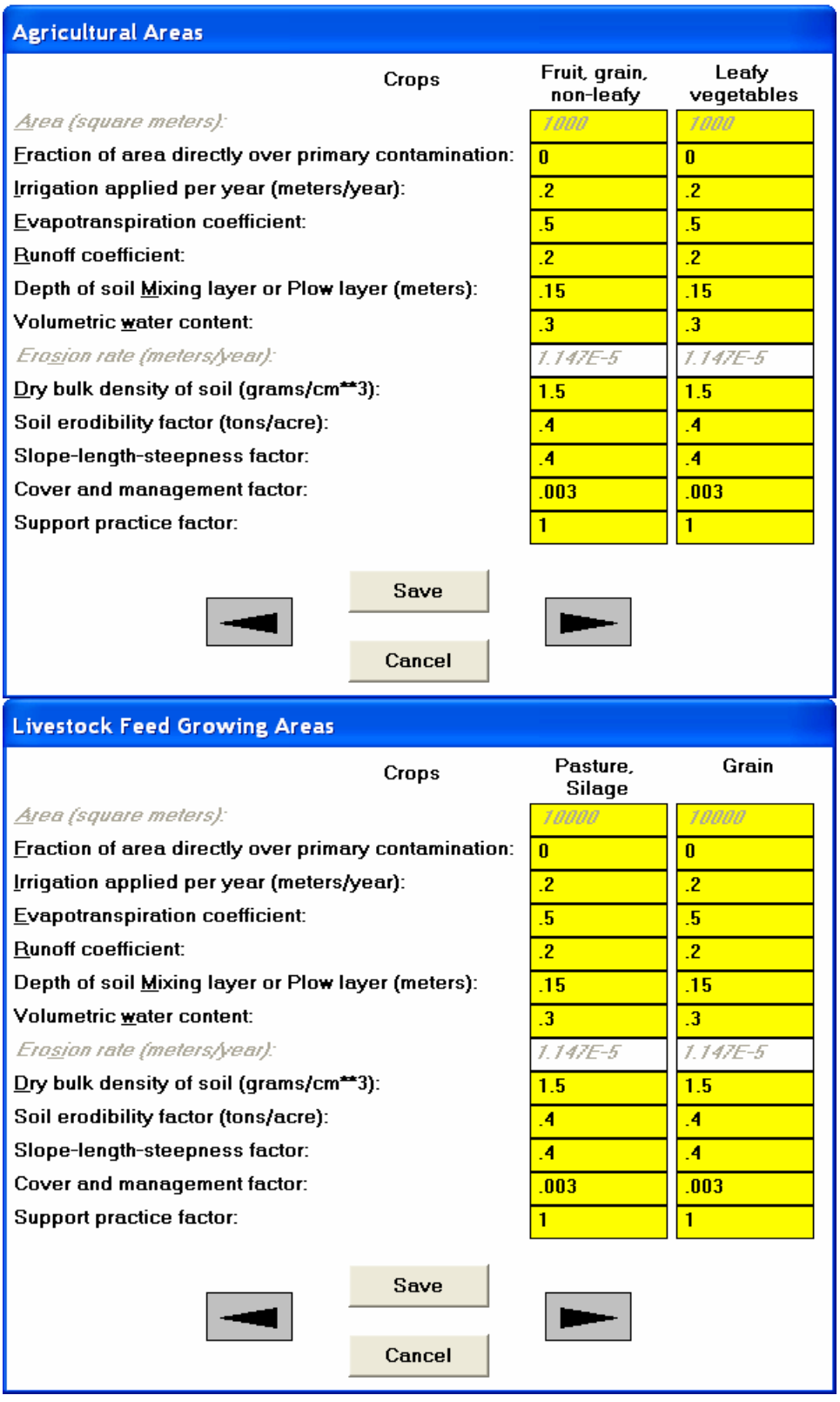

Uncertainty and sensitivity analysis can be performed on any parameter that is an input on these forms.

Area: This is the area of agricultural land on which the crop is cultivated or pasture land on which the livestock are allowed to feed. This is not a direct input, but is computed from the information input in the site layout form.

Fraction of Area Directly over the Primary Contamination: This is the areal fraction of the agricultural or pasture land that lies directly above the primary contamination. If the entire area is completely on the contamination, the fraction is one; if the entire area is away from the region of primary contamination, the fraction is zero. This fraction is used to account for direct root uptake of contaminants from the primary contaminated zone.

Irrigation Applied per Year: This is the volume of irrigation water that is applied over a period of 1 year per unit area of land. It is not the actual rate of irrigation during the growing season, but rather the irrigation rate averaged over 1 year.

Evapotranspiration Coefficient: This is the fraction of precipitation and irrigation water that penetrates the topsoil that is lost to the atmosphere by evaporation and by transpiration by vegetation.

Runoff Coefficient: This is the fraction of precipitation that does not penetrate the topsoil but leaves the area of concern as surface runoff; no loss is assumed for irrigation water.

Depth of Soil Mixing Layer or Plow Layer: This is the thickness of the surface soil that may be assumed to be mixed uniformly from time to time as a result of anthropogenic or physical processes. It is used to calculate off-site accumulation.

Total Water Filled Porosity of Soil: This is the volume fraction of soil.

Dry Bulk Density of Soil: This is the mass of solids in a unit volume of soil.

Soil Erodibility Factor: This is a measure of the susceptibility of the soil to erosion.

Slope-Length-Steepness Factor: This factor accounts for the profile of the terrain on the erosion rate.

Cover and Management Factor: This factor (formerly called cropping-management factor) accounts for the effects of land use, vegetation, and management on the erosion rate.

Support Practice Factor: This factor (formerly called conservation practice factor) accounts for the effects of conservation practices on the erosion rate.

4.16 OFFSITE DWELLING AREA: PHYSICAL AND HYDROLOGICAL DATA

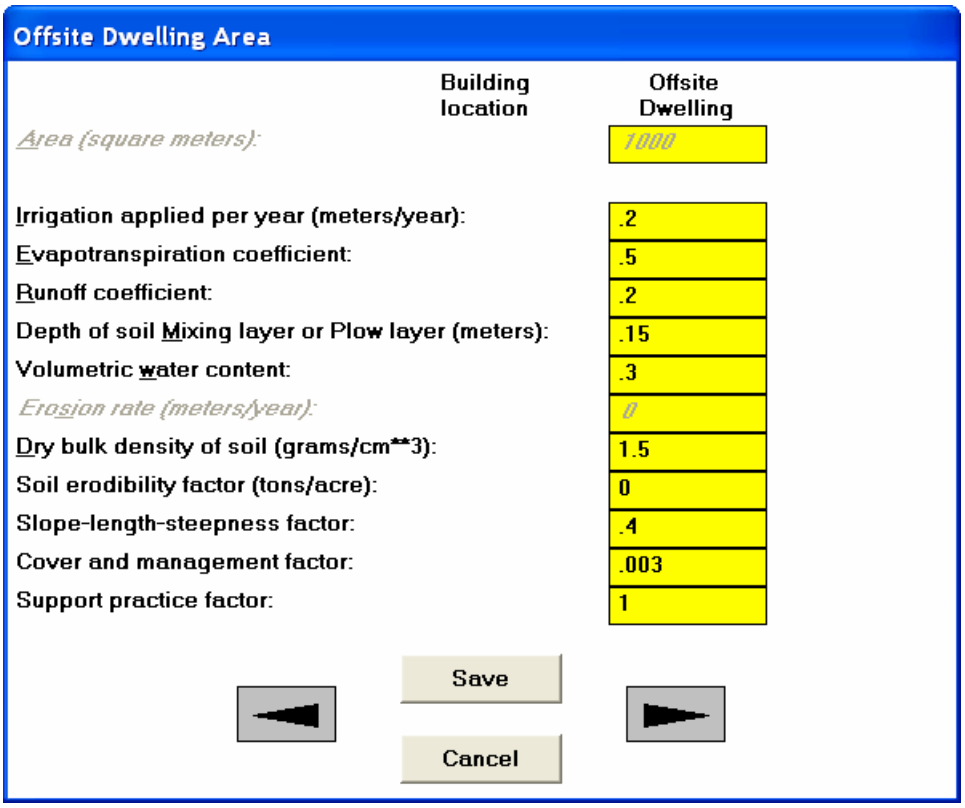

Uncertainty and sensitivity analysis can be performed on any parameter that is an input on this form.

Area: This is the area of the plot of land on which the offsite dwelling is located. This is not a direct input, but is computed from the information input in the site layout form.

Irrigation Applied per Year: This is the volume of irrigation water that is applied to the lawn or home garden over a period of 1 year per unit area of land.

Evapotranspiration Coefficient, Runoff Coefficient, Depth of Soil Mixing Layer or Plow Layer, Total Water Filled Porosity, Dry Bulk Density of Soil, Soil Erodibility Factor, Slope-Length-Steepness Factor, Cover and Management Factor, Support Practice Factor: The descriptions for these factors are the same as the preceding descriptions for the agricultural and pasture lands (Section 4.15).

4.17 ATMOSPHERIC TRANSPORT PARAMETERS

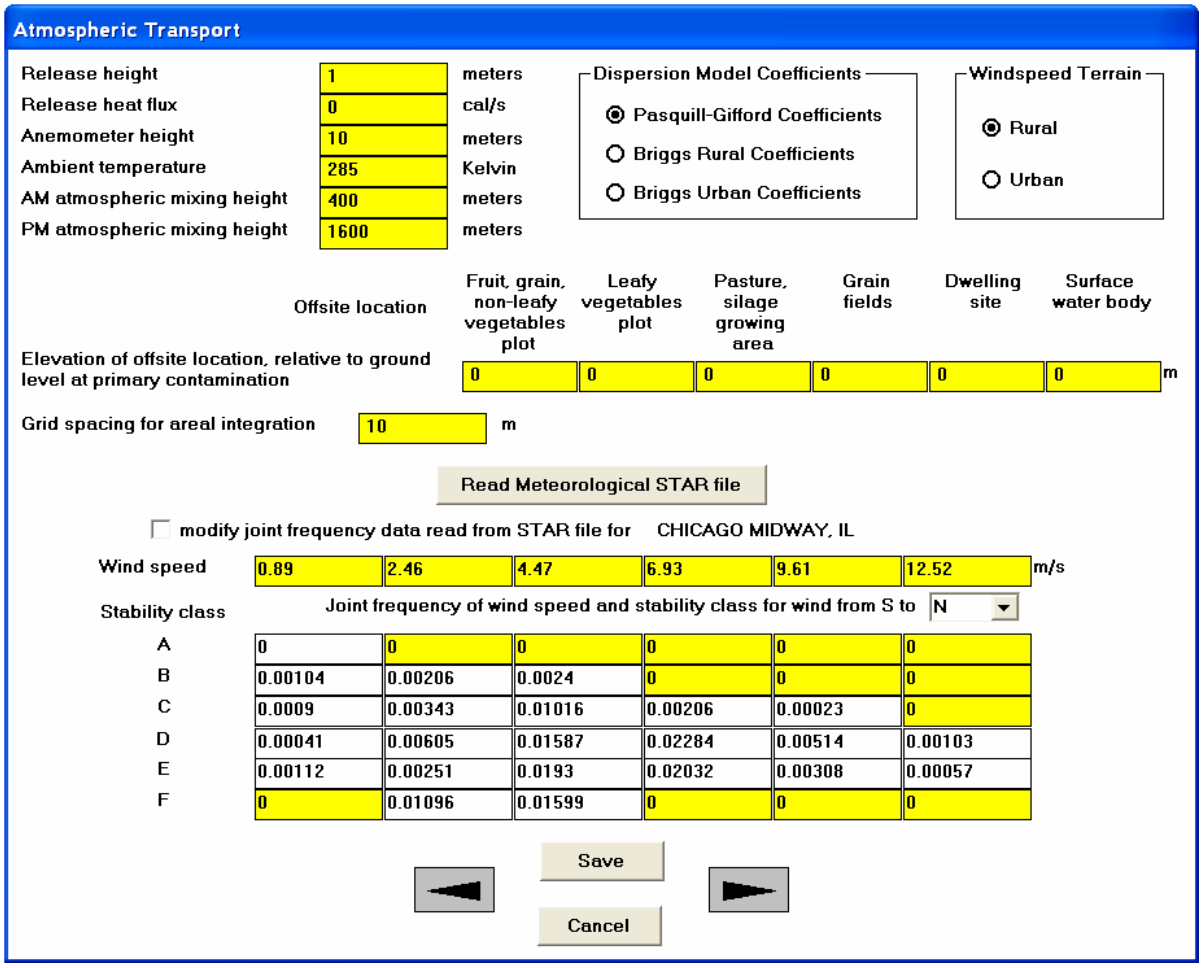

Uncertainty and sensitivity analysis can be performed on all but the following parameters on this form**:** grid spacing for areal integration, the joint frequency, and on the two parameters involving choices.

Release Height: This is the height of the release above the ground level at that location.

Release Heat Flux: This is the heat energy that accompanies the contaminant release. This factor is used to account for the rise of the plume.

Anemometer Height: This is the height at which the wind speed was measured.

Ambient Temperature: This is the temperature of the air at the location of release.

AM and PM Atmospheric Mixing Heights: The atmospheric mixing height is the thickness of the layer of air that is bounded by the ground surface and a layer of stable air above. The spreading of the contaminants is limited to the thickness of the mixing layer. AM and PM refer to the time of day.

Dispersion Model Coefficients: This is the formulation to be used to generate the dispersion coefficients for the atmospheric transport model.

Windspeed Terrain: The choice of terrain determines the relationship between the wind speed and the elevation above the ground surface.

Elevation, Relative to the Primary Contamination, of (the locations of off-site accumulation): When the ground level at the offsite location is above the ground level at the site of primary contamination, the code adjusts for the upward deflection of the wind. This is the difference between the height of the ground surface at the offsite location of contaminant accumulation and the height of the ground surface at the site of primary contamination.

Grid Spacing for Areal Integration: The primary contamination and the offsite receptor areas are assumed to be rectangular, as defined in Section 4.3, when modeling the atmospheric transport. Rather than use a single transport distance from the center of the source to the center of the receptor area, the code provides the option of subdividing the source and receptor areas into smaller squares or rectangles. The transport from each subdivision of the source to each subdivision of the offsite receptor area is computed, and these are summed to get a better estimate of the atmospheric transport. Smaller grid spacings improve the accuracy of the calculations, but require a longer computation time. This input is the maximum dimension of each subdivided rectangle.

Read Meteorological STAR File: This button is used to select the data file that contains the joint frequency distribution of the wind speed and stability class in STAR format.

- **Modify Joint Frequency Data Read from STAR File:** The data read from a STAR file is locked to prevent accidental alteration. This box must be check if the user wants to change the data (joint frequencies, wind speed) that were read.

Wind Speed: This is the average wind speed for the wind speed interval.

Joint Frequency (of wind speed, wind direction and stability class): This is the joint frequency distribution; that is, it is the fraction of the time during which the atmospheric conditions fall within each wind speed interval, wind direction, and stability class combination. There are 6 atmospheric stability classes (A through F), 6 wind speed intervals, and 16 wind directions. The from displays the joint frequency for the direction specified in *the dropdown box*. The information for each wind direction can be view and edited by selecting the desired direction from the dropdown box. Both the direction from which wind blows and the direction toward which it blows are shown in order to avoid confusion; customarily, wind is identified by the direction from which it blows rather than by the direction toward which it blows (e.g., a “north wind” means the wind is blowing from the north).

4.18 UNSATURATED ZONE HYDROLOGY

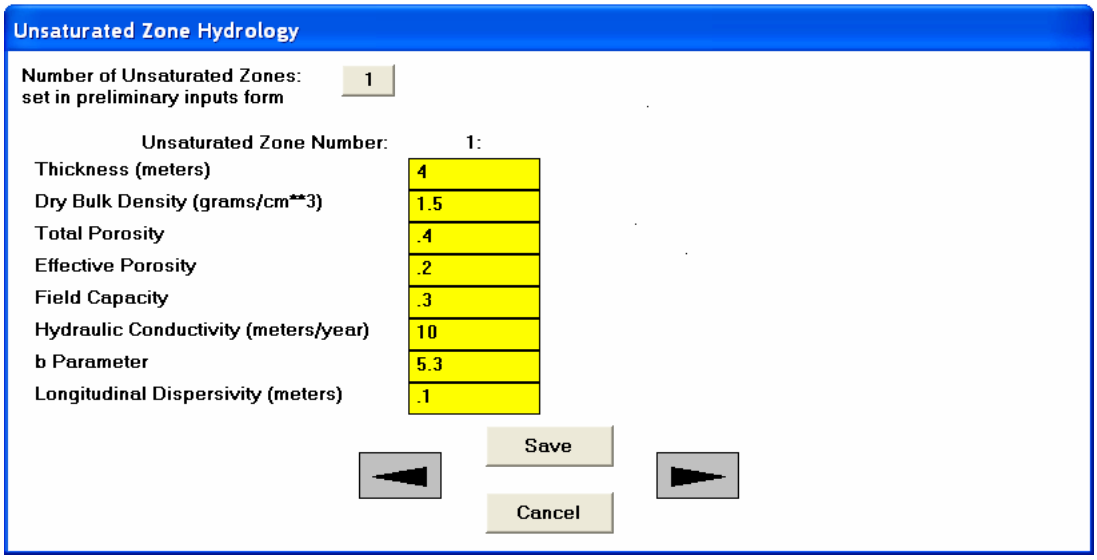

Uncertainty and sensitivity analysis can be performed on any parameter on this form except the number of unsaturated zones.

Number of Unsaturated Zones: This is the number of different partially saturated layers between the primary contamination and the saturated zone. The number of unsaturated zones can be changed only in the Preliminary Inputs form (Section 4.2). The code has provisions for up to five different horizontal strata. Clicking on the button displaying the number of unsaturated zones causes the Preliminary Inputs form to open. Because the distribution coefficients are likely to be different for each zone, the Distribution Coefficient form (Section 4.6) is also opened.

Thickness: This is the thickness of the specific unsaturated zone.

Dry Bulk Density: This is the mass of solids in a unit volume of soil in the specific unsaturated zone.

Total Porosity: This is the volume fraction of soil that is occupied by liquid and gaseous phases.

Effective Porosity: This is the volume fraction of soil through which water flows. Part of the soil moisture may not contribute to the movement of contaminants.

Field Capacity: This is the volumetric moisture content of soil at which (free) gravity drainage ceases, or the amount of moisture that will be retained in a column of soil against the force of gravity. This is the minimum moisture content of the unsaturated layer in the absence of evapotranspiration and root uptake.

Hydraulic Conductivity: This is the apparent flow velocity through the contaminated zone under a unit hydraulic gradient.

b Parameter: The soil-specific exponential b parameter relates the hydraulic conductivity of partially saturated soil to its moisture content.

Longitudinal Dispersivity: This is the ratio between the longitudinal dispersion coefficient and pore water velocity. It has the dimension of length. This parameter depends on the thickness of the zone and ranges from one one-hundredth of the thickness to the order of the thickness.

4.19 SATURATED ZONE HYDROLOGY

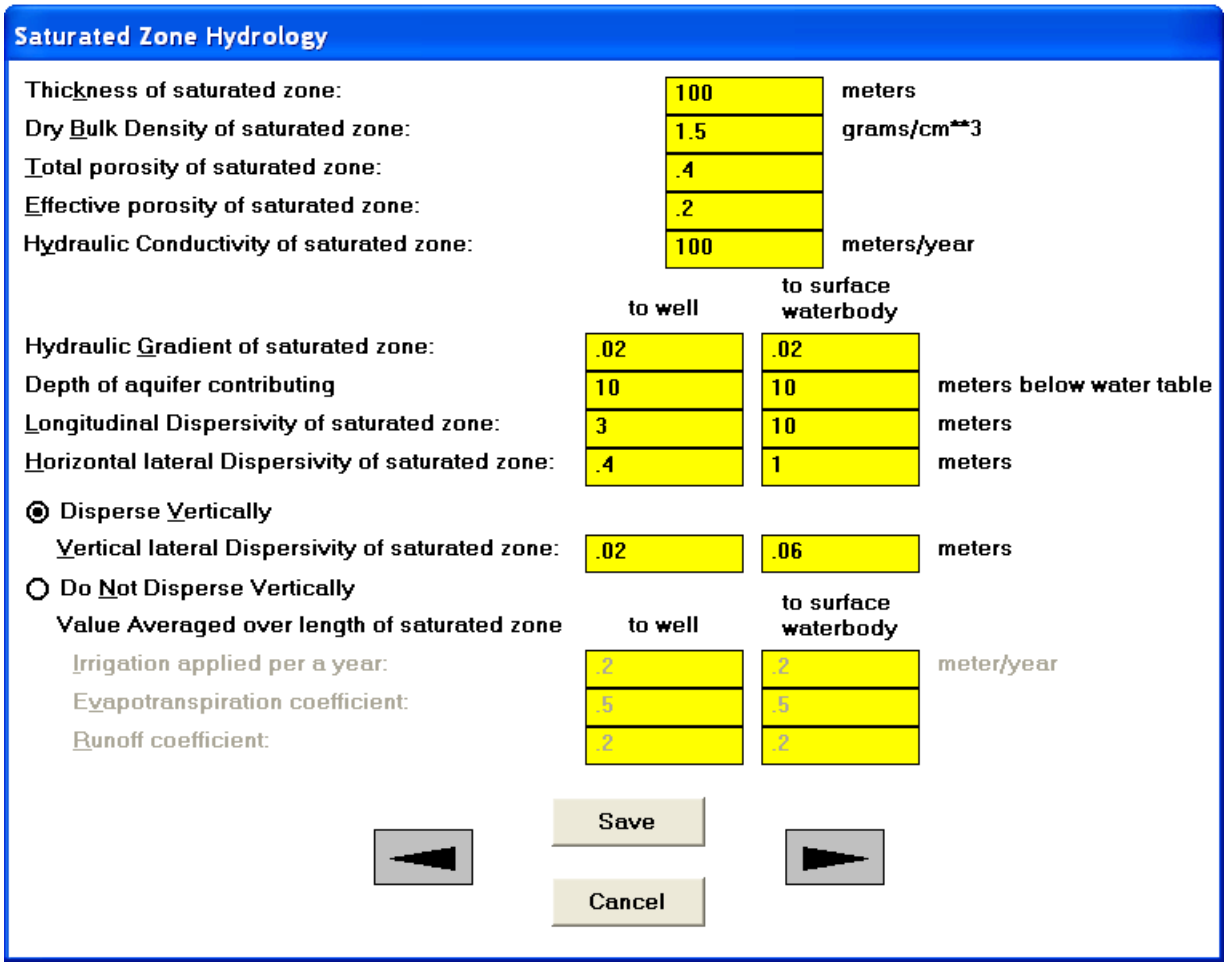

Uncertainty and sensitivity analysis can be performed on any parameter whose value can be input on this form.

Thickness of Saturated Zone: This parameter is used when dispersion in the vertical direction in the saturated zone is being modeled. It is also used to check that the total groundwater flow under primary contamination exceeds the inflow from infiltration through the primary contamination.

Dry Bulk Density of Saturated Zone: This is the mass of solids in a unit volume of soil in the specific unsaturated zone.

Total Porosity of Saturated Zone: This is the volume fraction of soil that is occupied by liquid and gaseous phases.

Effective Porosity of Saturated Zone: This is the volume fraction of soil through which water flows. Part of the soil moisture may not contribute to the movement of moisture and contaminants.

Hydraulic Conductivity of Saturated Zone: This is the apparent flow velocity through the contaminated zone under a unit hydraulic gradient.

There are two columns for the remaining properties specified in the form, the first for transport from the primary contamination to the well and the second for transport to the surface water body.

Hydraulic Gradient of Saturated Zone: This is the slope of the surface of the water table.

Depth of Aquifer Contributing: Water flowing through the specified depth of the aquifer is assumed to be intercepted by the well or surface water body. This parameter is used to calculate the contaminant concentration in well water or the contaminated flux into the surface water body.

Longitudinal Dispersivity of Saturated Zone: This is the ratio between the longitudinal dispersion coefficient and pore water velocity. It has the dimension of length. This parameter depends on the length of the saturated zone.

Horizontal Lateral Dispersivity of Saturated Zone: This is the ratio between the horizontal lateral dispersion coefficient and pore water velocity. It has the dimension of length.

Disperse Vertically: The user may choose to model (1) vertical dispersion of contaminants in the saturated zone and ignore the effects of any clean infiltration along the length of the saturated zone or (2) the effects of clean infiltration along the length of the saturated zone and ignore dispersion in the vertical direction.

Vertical Lateral Dispersivity of Saturated Zone: This is the ratio between the vertical lateral dispersion coefficient and pore water velocity. It has the dimension of length.

Irrigation Rate: This is the average annual irrigation rate, in meters/year (m/y), applied to the land overlying the saturated zone through which contaminants are transported to the water source. It is the amount of irrigation water that is applied over a period of 1 year and is not the actual rate of irrigation applied during the growing period. It is used when the effects of uncontaminated infiltration on the contaminated plume are being modeled.

Evapotranspiration Coefficient: This is the evapotranspiration coefficient averaged over the land overlying the saturated zone through which contaminants are transported to the water source. The evapotranspiration coefficient is the fraction of precipitation and irrigation water that penetrates the topsoil that is lost to the atmosphere by evaporation and by transpiration by the vegetation. It is used when the effects of uncontaminated infiltration on the contaminated plume are being modeled.

Runoff Coefficient: This is the runoff coefficient averaged over the land overlying the saturated zone through which contaminants are transported to the water source. The runoff coefficient is the fraction of precipitation that does not penetrate the topsoil but leaves the area of concern as

surface runoff; no loss is assumed for irrigation water. It is used when the effects of uncontaminated infiltration on the contaminated plume are being modeled.

4.20 WATER USE

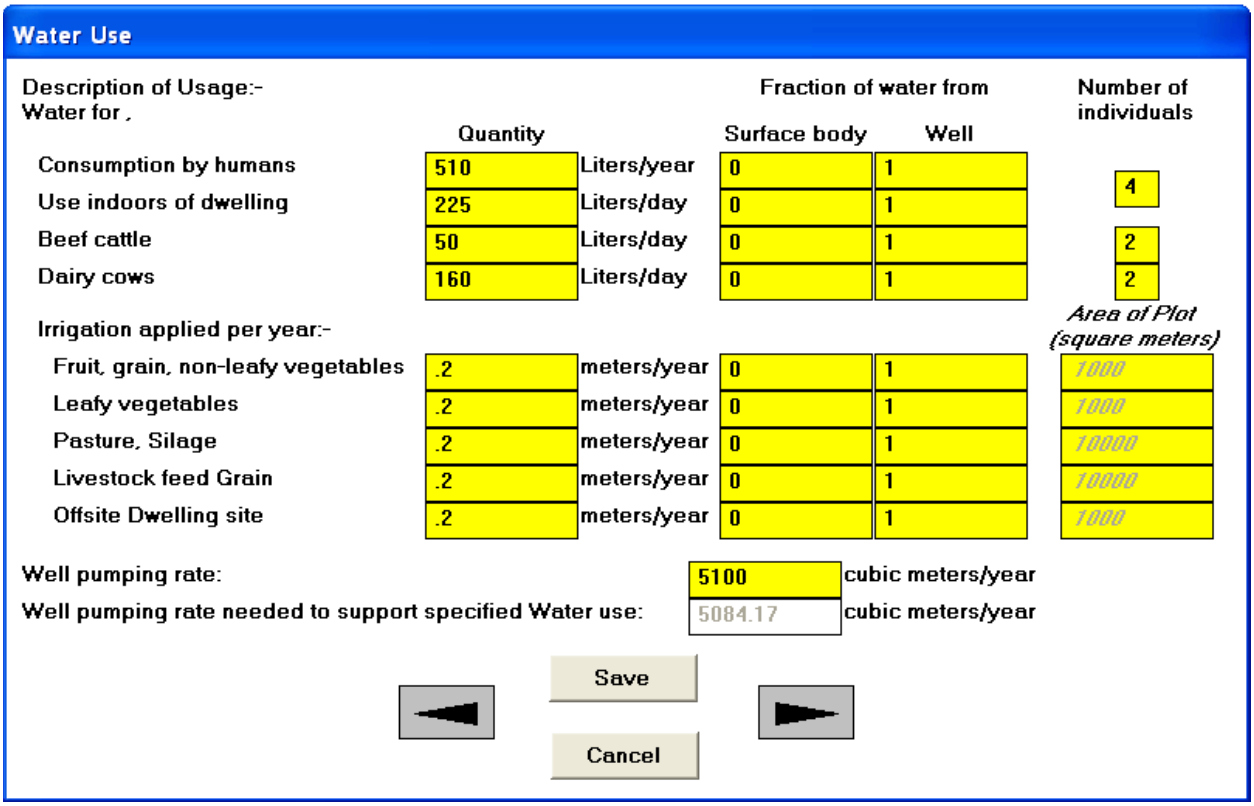

The quantities of water obtained from the two sources of water are the focus of this form. The water requirements of humans and livestock and for irrigation are in the first column. The water requirements also appear in other input forms, and if they are changed in one form, the other will automatically be updated immediately.

The second and third columns are the fractions of these water requirements that are obtained from the contaminated surface water body and contaminated well. These fractions can add up to less than one if water from uncontaminated sources is also used. Uncertainty and sensitivity analysis can be performed on any parameter that is input on this form except the number of individuals, as noted below. The user must ensure that the sum of the pair of fractions does not exceed unity when performing uncertainty analysis.

Water Consumed by Humans: This is the total amount of water consumed by an individual; it includes water that is used in the preparation of or is consumed with food.

Water Used in Dwelling: This is the total amount of water used in the house. It includes water used for cleaning, washing, showering/bathing, etc. It is used to compute the dose from waterborne radon.

Water for Beef Cattle: This is the amount of water consumed by each head of cattle raised for meat.

Water for Dairy Cows: This is the amount of water consumed by each cow raised for milk production.

Number of Individuals: This is the number of humans or livestock that obtain the specified water needs from the water source. These values are used only to compute the required minimum well pumping rate; they are not used by the computational code. These inputs are not eligible for uncertainty analysis.

Irrigation Applied per Year: This is the volume of irrigation water that is applied over a period of 1 year per unit area of land. It is not the actual rate of irrigation during the growing season, but rather the irrigation rate averaged over 1 year.

Well Pumping Rate Needed to Support Specified Water Use: This is the total volume of water that needs to be withdrawn from the well to satisfy the demand described in this form. It is provided to help the user select an appropriate well pumping rate. This value is computed every time a change is made to an input in this form. The well pumping rate is increased automatically so it will never be less than this minimum required rate.

Well Pumping Rate: This is the rate at which water is extracted from the well. The interface will not accept a well pumping rate that is insufficient to meet the needs specified in this form. While the code performs this check for the deterministic case, the user is responsible for ensuring that this condition is not violated when performing sensitivity or probabilistic/uncertainty analysis.

4.21 SURFACE WATER BODY

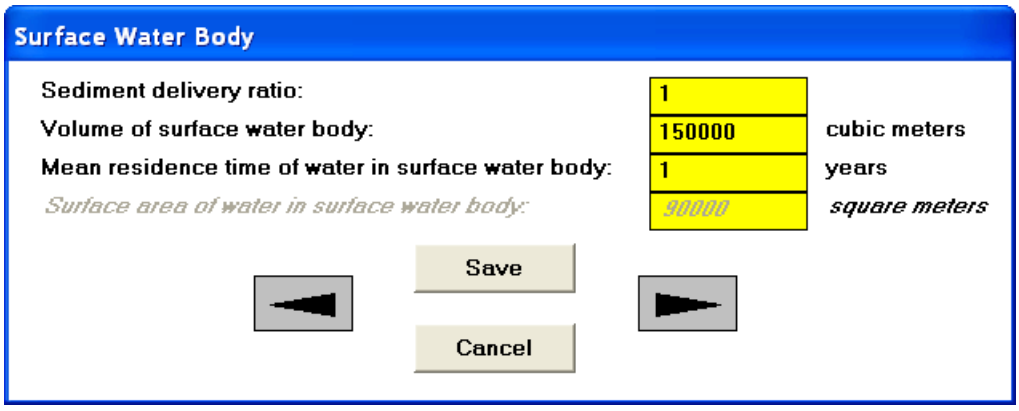

Uncertainty and sensitivity analysis can be performed on any parameter that is an input on this form.

Sediment Delivery Ratio: This is the fraction of the contaminated soil that was eroded from the primary contamination that reaches the surface water body. This parameter is used to compute the contaminant flux from surface erosion.

Volume of Surface Water Body: This is the volume of water in the surface water body.

Mean Residence Time of Water in Surface Water Body: This is the average time that water spends in the surface water body. It is obtained by dividing the volume of the surface water body by the quantity of water that flows into it each year.

Surface Area of Water in Surface Water Body: This is the area of the surface water body. This is not a direct input, but is computed f the information input in the site layout form. It is used to compute the contaminant flux from atmospheric deposition.

4.22 GROUNDWATER TRANSPORT PARAMETERS

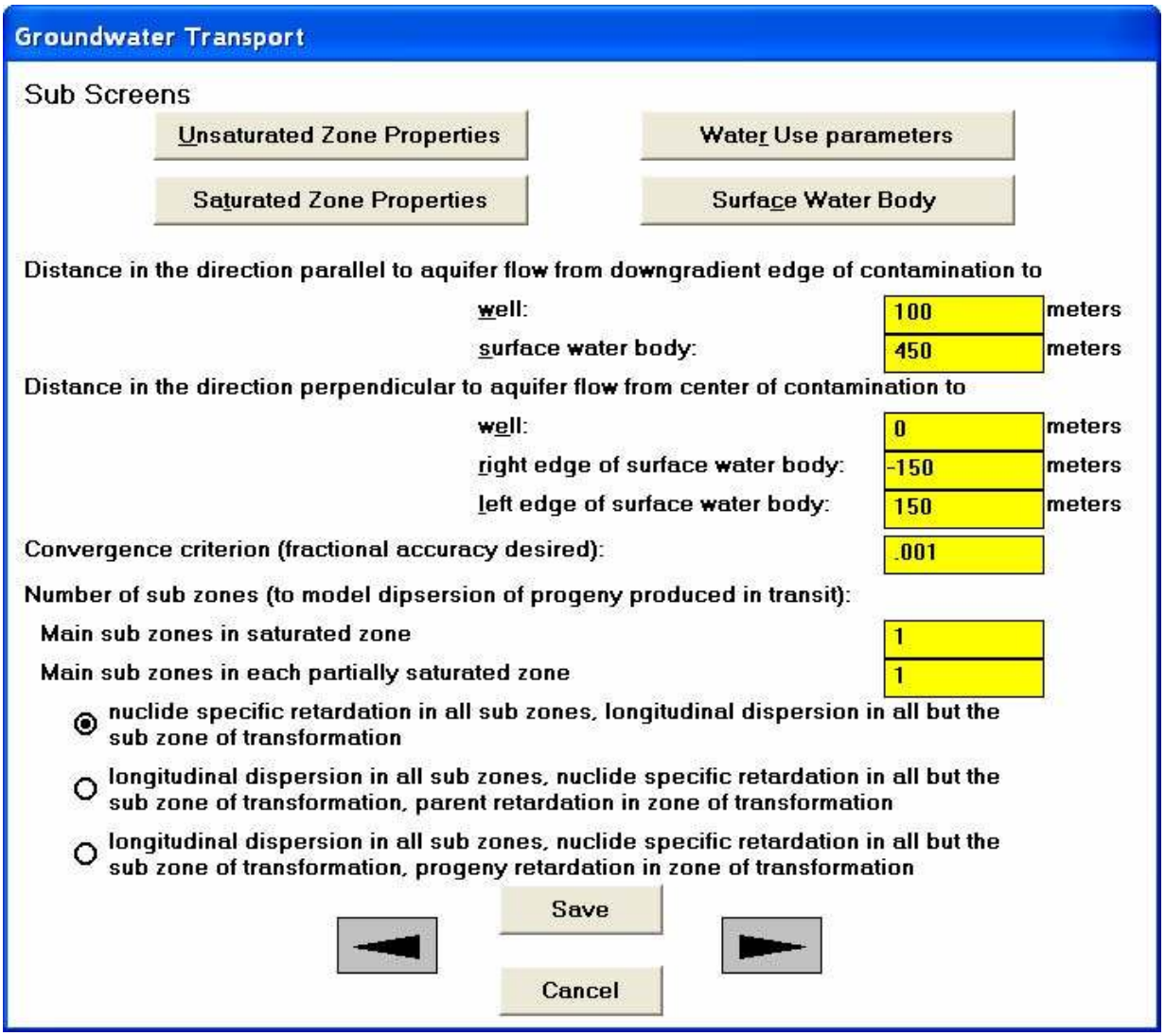

Sub Screens (accessing other related forms): Four forms can be accessed by using the four buttons listed. If the forward arrow buttons are being used to access each form in turn, the forms would have been accessed before this form and need not be revisited from here:

- **Unsaturated Zone Properties, Saturated Zone Properties, Water Use parameters, Surface Water Body:** Use these buttons to open the respective forms. The current parent form will not be closed and will remain in the background. It will reappear when the other forms are exited.

Uncertainty and sensitivity analysis can be performed on the distances that are inputs on this form. One-at-a-time sensitivity analysis can also be performed on the number of subzones.

Distance in the Direction Parallel to Aquifer Flow from Contamination to Well: This is the distance, in meters (m), along a groundwater flow line from the downgradient edge of the

primary contamination to the well. It is used in the computation of transport in the saturated zone to the well. A negative value indicates that the well is either upgradient of or within the primary contamination. If this value is negative or if the combination of water and land usage and exposure pathways indicates that well water has no influence on dose, the computational code will skip the well water concentration computations.

Distance in the Direction Parallel to Aquifer Flow from Contamination to Surface Water Body: This the distance, in meters (m), along a groundwater flow line from the downgradient edge of the primary contamination to the upgradient edge of the surface water body. It is used in the computation of transport in the saturated zone to the surface water body. A negative value indicates that the surface water body is upgradient of the primary contamination. If this value is negative or if the combination of water and land usage and exposure pathways indicates that water from the surface water body has no influence on dose, the computational code will skip the surface water computations.

Distance in the Direction Perpendicular to Aquifer Flow from Contamination to Well: This the distance, in meters (m), between two groundwater flow lines, one through the center of the contamination and the other thorough the well. It is used in the computation of dilution due to dispersion in the saturated zone, and it applies to water extracted from a well.

Distance in the Direction Perpendicular to Aquifer Flow from Contamination to Near Edge of Surface Water Body: This is the distance, in meters (m), between two groundwater flow lines, one through the center of the contamination and the other through the near edge of the surface water body. It is used to compute the contamination flux from the groundwater into the surface water body.

Distance in the Direction Perpendicular to the Aquifer Flow from Contamination to Far Edge of Surface Water Body: This is the distance, in meters (m), between two groundwater flow lines, one through the center of the contamination and the other thorough the far edge of the surface water body. It is used to compute the contamination flux from the groundwater into the surface water body.

Convergence Criterion: This is the fractional accuracy desired in the Romberg integration used to calculate the contaminant flux or concentration in groundwater. A lower value will likely require the use of a larger number of points in this numerical integration technique and thus a longer computation time. For each Romberg refinement or cycle number, the number of integrand function evaluations is 2^N, where N is the cycle number. Thus, if the convergence criterion is set too low, the computation time becomes excessive, and convergence may not be achieved. If convergence is not achieved, RESRAD will indicate the failure in the QRFAIL.LOG file, and the last estimate of the integral using 32,769 points will be used. If the convergence criterion is set at zero, Simpson's rule with 32 integration intervals will be used.

Modeling Transport of Progeny Produced in Transit

RESRAD-OFFSITE has two groundwater transport algorithms. One models the effects of the differences in the water-to-soil interaction of the parent nuclide and the progeny nuclides, and the other models the longitudinal dispersion. When one of these processes is clearly dominant, the user can choose the appropriate algorithm to model the transport of the progeny produced in transit. When both the longitudinal dispersion and the differences in the water-to-soil interaction are of comparable importance, the prediction of progeny nuclides produced in transit in the (un)saturated zone can be improved by breaking up the transport zone into a number of subzones. Then both processes will be modeled over most of the transport path. Additional run time will be needed to do this.

Main Sub Zones in Saturated Zone: This is the number of subzones into which the saturated zone is to be divided in order to improve the predictions of progeny nuclides produced in transit.

Main Sub Zones in Each Partially Saturated Zone: This is the number of subzones into which the partially saturated zone is to be divided in order to improve the predictions of progeny nuclides produced in transit.

Modeling Progeny-Specific Retardation or Dispersion

The two transport algorithms give rise to three choices for the algorithm to be used in the zones where the specific atom undergoes transformations. One of three options can be selected to:

- Model the effects of the progeny-specific distribution coefficient in the zone of transformation and ignore the effects of longitudinal dispersion,

- Model the effects of longitudinal dispersion and use the distribution coefficient of the parent nuclide for the progeny produced in that zone, or

- Model the effects of longitudinal dispersion and use the distribution coefficient of the progeny nuclide for the progeny produced in that zone.

4.23 INGESTION RATES

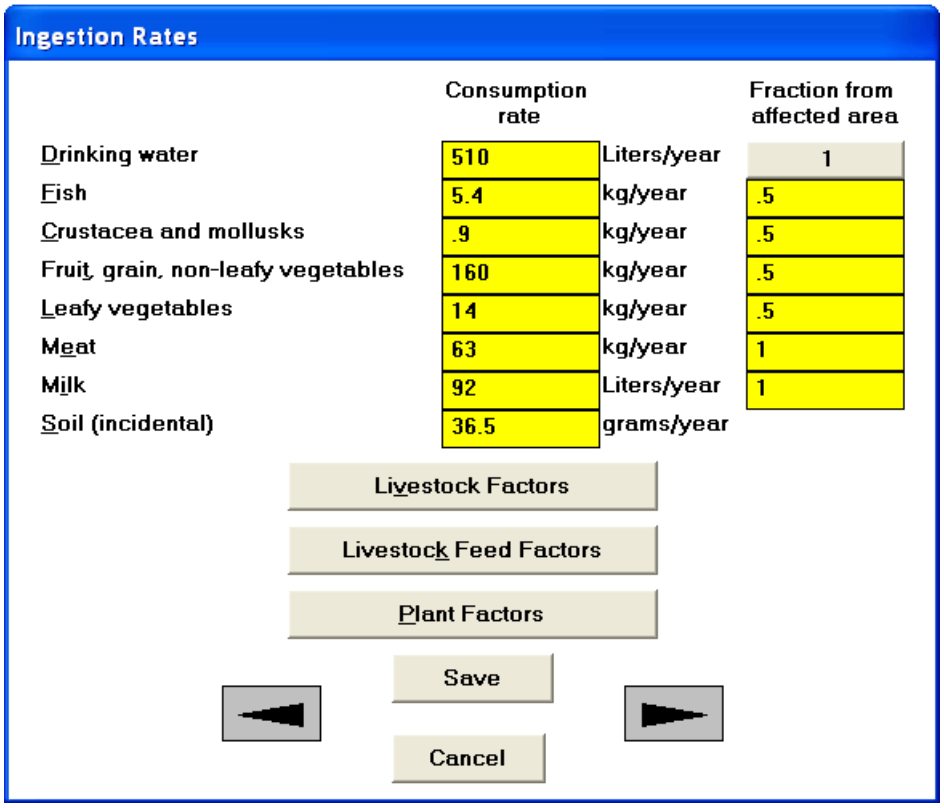

Uncertainty and sensitivity analysis can be performed on any parameter that is an input on this form.

Consumption Rate: Consumption rates are national averages that are usually site independent. Adjustments for regional differences in diet may sometimes be appropriate.

Fraction from Affected Area: This is the fraction of the consumption rate that is obtained from any area that is affected by the primary contamination. The entry for drinking water is the sum of the fraction obtained from the contaminated well and from the contaminated surface water body. Clicking on the entry for drinking water will open the Water Use form (Section 4.20); the fractions from each water source can be changed in that form.

Accessing Other Related Forms

Three forms can be accessed by using the three buttons listed below. Alternatively, the first form can be opened by clicking on the forward arrow button on this form, then the other forms can be opened by continuing to use the forward arrow buttons on the successive forms.

Livestock Factors, Livestock Feed Factors, Plant Factors: Use these buttons to open the respective forms. The current parent form will not be closed and will remain in the background; it will reappear when the form is exited.

4.24 LIVESTOCK INTAKES (FACTORS)

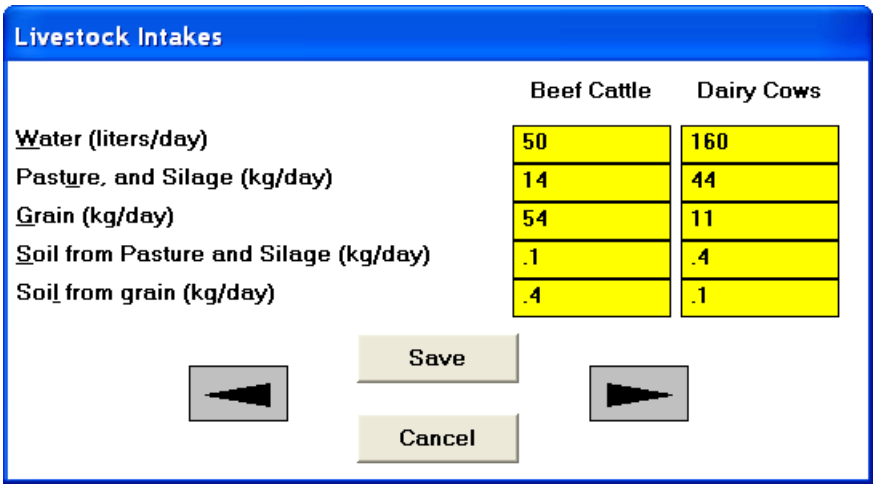

Livestock intake (i.e., ingestion) rates are national averages that are usually site independent. Adjustments for regional differences in animal husbandry practices are necessary. The first column is the intake rates for each head of livestock raised for meat, while the second column is for each head of livestock raised for milk production. The incidental ingestion of soil associated with the ingestion of the two types of feed (grain or pasture/silage) must be specified separately because the contaminant concentrations in the soils could be different. Uncertainty and sensitivity analysis can be performed on any parameter on this form.

4.25 LIVESTOCK FEED FACTORS AND PLANT FACTORS

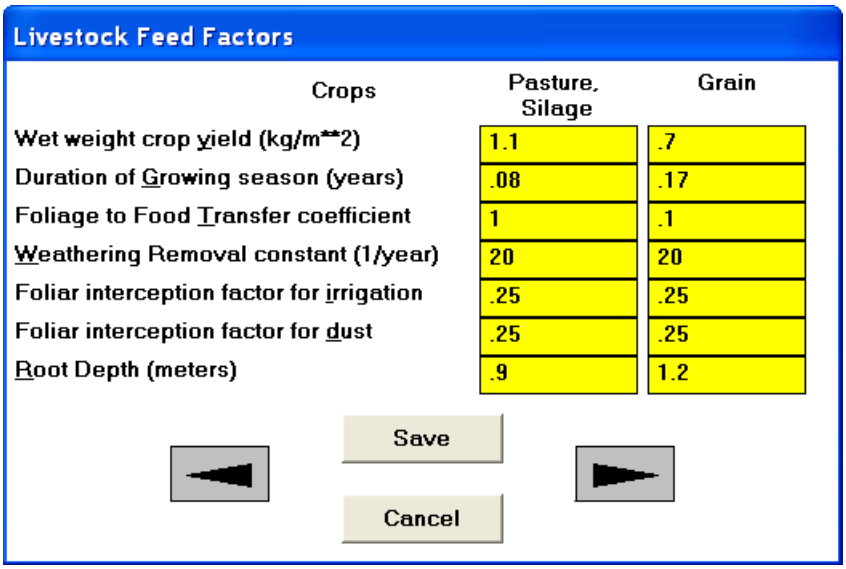

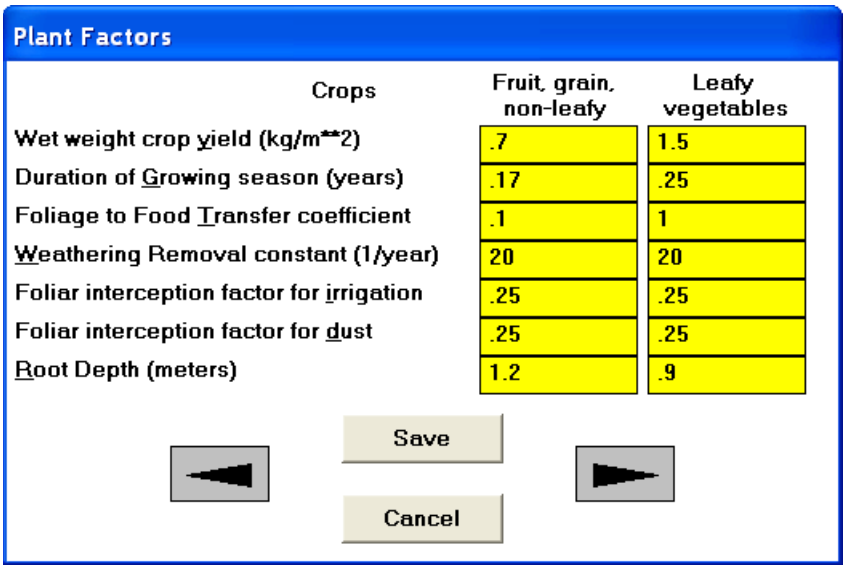

Plant (i.e., vegetables and livestock feed) factors are related to growth and contaminant transfer. They depend on the mix of crops and on regional farming practices. Uncertainty and sensitivity analysis can be performed on any parameter that is an input on this form.

4.26 INHALATION AND EXTERNAL GAMMA

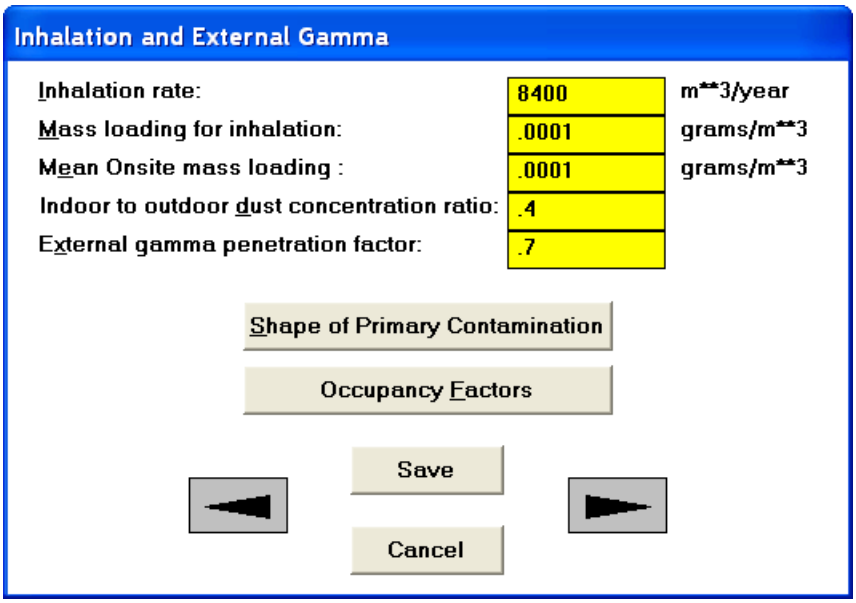

Uncertainty and sensitivity analysis can be performed on any parameter on this form.

Mass Loading for Inhalation: This is the average mass of respirable particulate in a unit volume of air when humans are present at the site (includes the effects of human activity). It is used in the inhalation pathway computations.

Mean Onsite Mass Loading: This is the average mass loading of airborne contaminated soil particles above the primary contamination. It is used to estimate the contaminant release rate to the atmosphere.

Indoor to Outdoor Dust Concentration Ratio: This parameter accounts for the effect of the building structure on the level of contaminated dust indoors. It is the fraction of outdoor contaminated dust that is present indoors.

External Gamma Penetration Factor: This factor accounts for the effect of the building structure on the level of gamma radiation indoors. It is the fraction of outdoor gamma radiation that penetrates the building.

Accessing Other Related Forms

Two forms can be accessed by using the two buttons listed below. Alternatively, the first form can be opened by clicking on the forward arrow button on this form, then the other form can be opened by continuing to use the forward arrow button on the first form.

- **Shape of Primary Contamination, Occupancy Factors:** Use these buttons to open the respective forms. The current parent form will not be closed and will remain in the background; it will reappear when the form is exited.

4.27 EXTERNAL RADIATION SHAPE AND AREA FACTORS

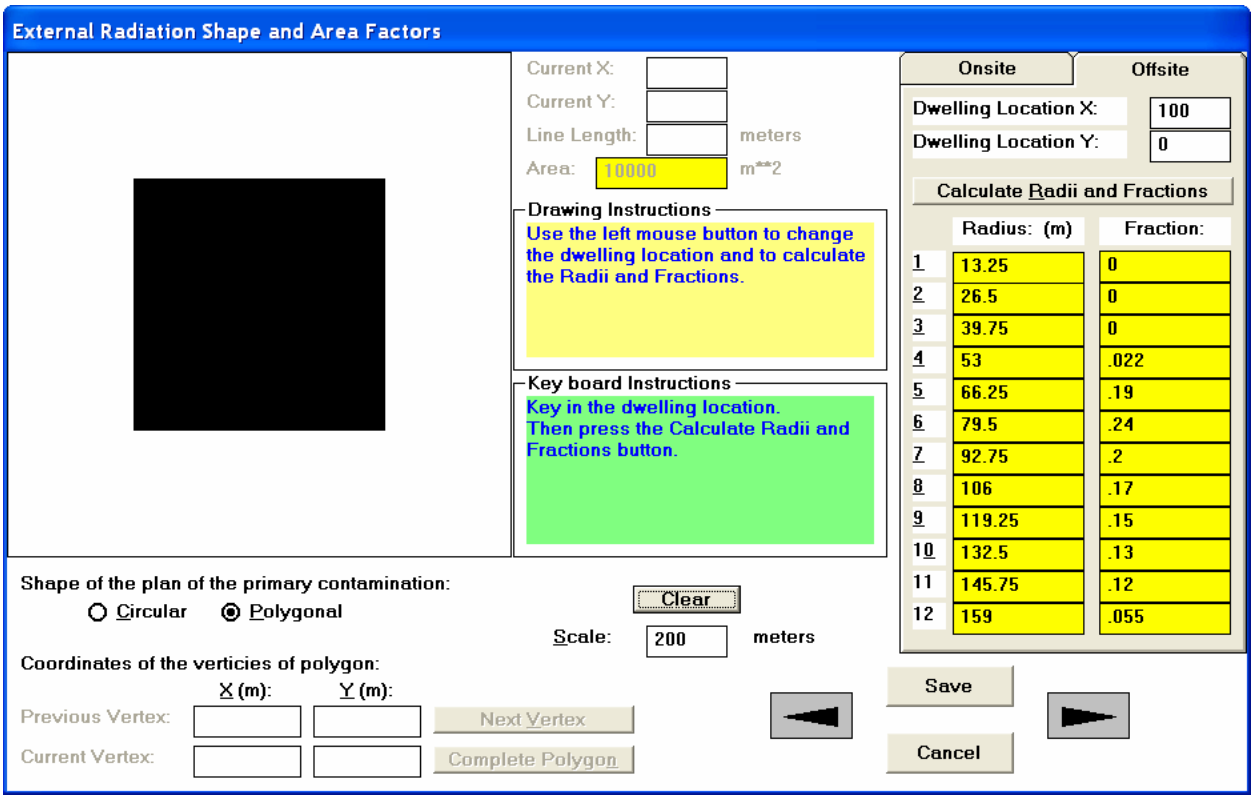

The primary contamination is shown in black against a white backdrop in the picture box at the top left corner of the form. The primary contamination will change to pink if the Calculate Radii and Fractions button near the top of the right side is pressed.

Shape of the Plan of the Primary Contamination: As a default, the shape of the primary contamination and the centroid of the offsite dwelling specified in the site layout/map interface form are used to calculate the shape and area factors for the external radiation pathway. The onsite dwelling is assumed to be located in the center of the primary contamination. This form can be used to specify different locations for the dwellings and also to define a polygonal shape for the primary contamination.

Changing the Location of the Dwellings

If the primary contamination is not completely within the picture box, change the number in the box next to Scale (in the middle near the bottom of the form) until it is visible in its entirety. At the top right, select the tab (Onsite tab or Offsite tab) corresponding to each dwelling in turn and specify its location, either by inputting the coordinates or by clicking on the location in the picture box. If the coordinates of the location are keyed in, the Calculate Radii and Fractions button must be pressed to compute the area fractions. This must be done before proceeding to the other tab (Onsite tab or Offsite tab). The coordinates of the position of the cursor are shown in

the Current X and Current Y information boxes at the top center of the form; this information is helpful when the cursor is being used to click on the location of the dwelling.

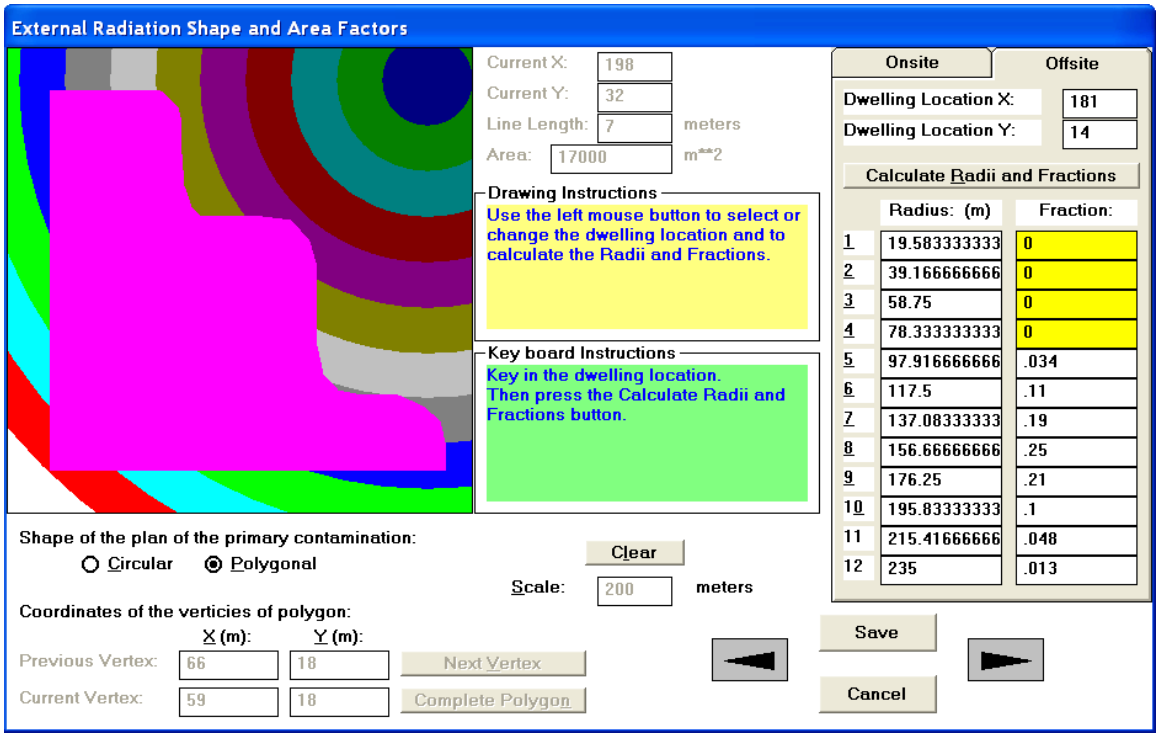

Changing the Shape of the Primary Contamination

Set the number in the box next to Scale to the length of the square enclosing the primary contamination and the two dwelling locations. Choose the Polygonal option. The polygon can be "drawn" by using the mouse and following the drawing instructions given in the yellow information box on the form. Alternatively, the vertices of the polygon can keyed in by following the instructions given in the green instructions box. After the polygon is completed, the location of the onsite and offsite dwellings must be specified, as described in the previous paragraph. The area of the polygon will be computed when the radii and area fractions are computed. The area is displayed in the box at the top center of the form.

Because the fraction of each annular area that is contaminated is computed graphically in the interface, it is not possible to perform uncertainty or sensitivity analysis on any of the parameters on this form.

4.28 OCCUPANCY FACTORS

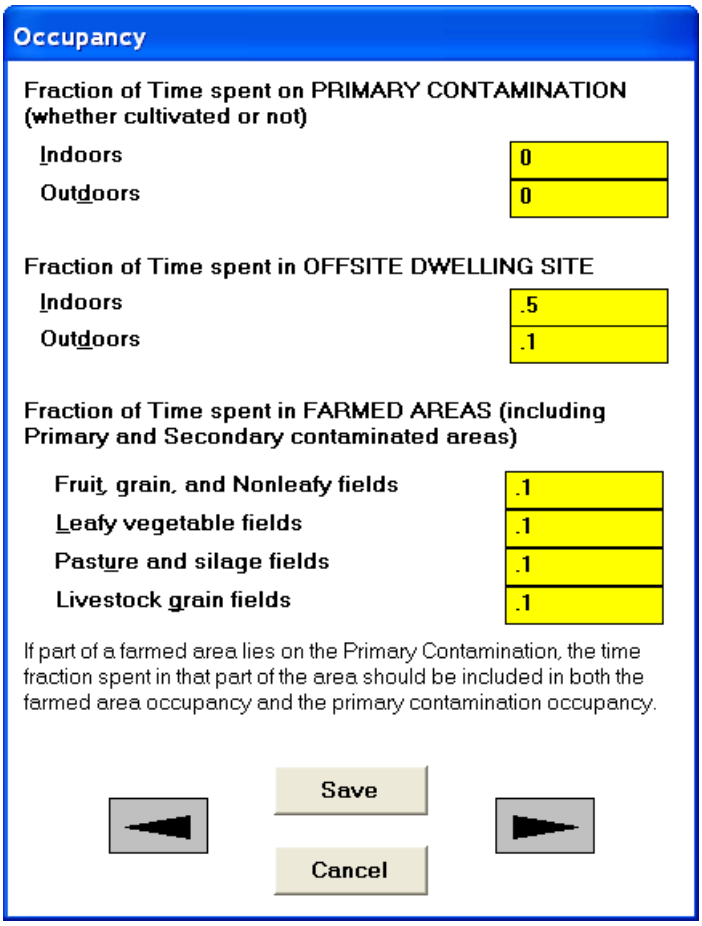

Fraction of Time spent on Primary Contamination

- **Indoors:** This is the fraction of time that the receptor spends in a building situated on top of the primary contamination.

- **Outdoors:** This the fraction of time that the receptor spends outdoors on top of the primary contamination. If any agricultural or pasture land lies over the primary contamination, the time spent in that common area should be included here and also in the entry for that agricultural or pasture land.

Fraction of Time Spent in Offsite Dwelling Site

- **Indoors:** This is the fraction of time that the receptor spends in a building situated away from the primary contamination.

- **Outdoors:** This the fraction of time that the receptor spends outdoors of the offsite dwelling that is located away from the primary contamination.

Fraction of Time Spent in Farmed Areas: This is the fraction of time that the receptor spends outside in agricultural land and pasture land contaminated by irrigation or by atmospheric deposition. If any agricultural or pasture land overlies the primary contamination, the time spent in that common area should be included in the entry for the agricultural or pasture land and also in the outdoor time fraction above the primary contamination.

[Note: The sum of the time fractions spent indoors and outdoors on the primary contamination and in the offsite dwelling site cannot exceed unity. Because of the way that the time fractions are defined here, it is possible for the sum of all the time fractions of a single individual to exceed unity. But the sum of the time fractions will not exceed 2. (The sum will equal 2 if an individual spends all the time outdoors in an agricultural or pasture land that overlies the primary contamination.) Also, the time fractions spent indoors on the primary contamination and indoors and outdoors in the off-site dwelling site and in the farmed areas cannot exceed unity.

Uncertainty and sensitivity analysis can be performed on any parameter on this form. The user must ensure that the combined occupancy limits discussed in the preceding paragraph are not violated during uncertainty analysis.]

4.29 RADON DATA

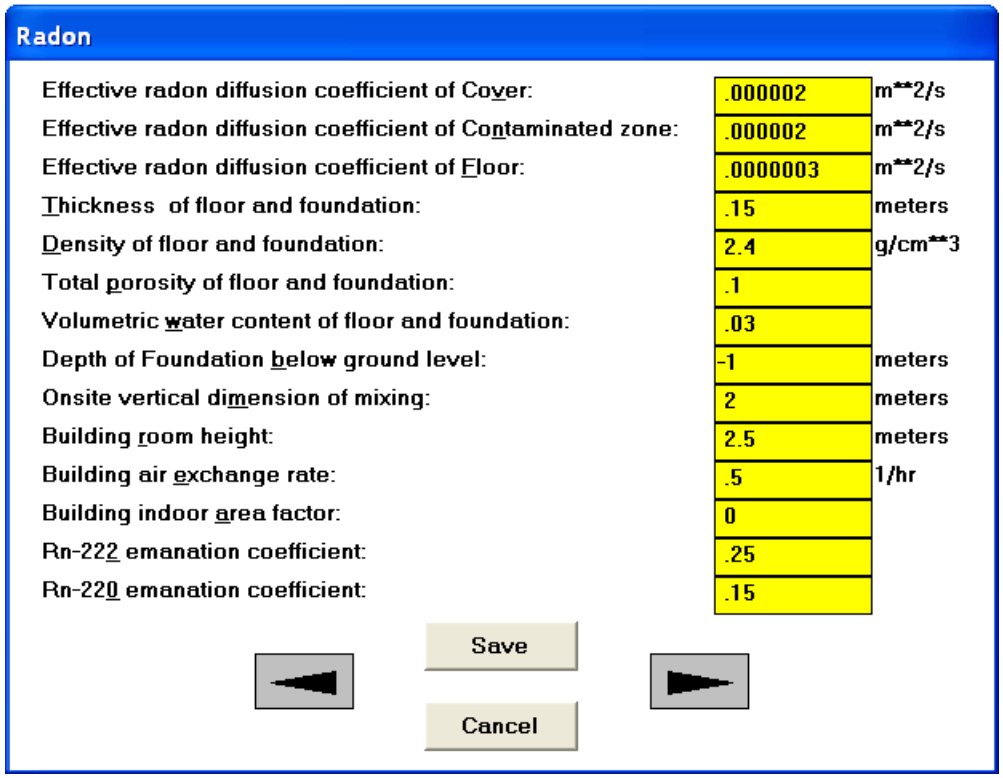

The radon model is discussed in Appendix C of the RESRAD Manual. The radon parameters are activated only when the radon pathway is turned on. The radon pathway can be turned on only if a parent of either Rn-222 or Rn-220 is present as a contaminant. The wind speed found on the Physical and Hydrological Parameters form (Section 4.13) and the volumetric water content of the clean cover on the Primary Contamination form (Section 4.14) are also used for the outdoor radon dose component calculation. Uncertainty and sensitivity analysis can be performed on any parameter on this form.

Depth of Foundation Below Ground Level: This is the depth from the ground surface to the bottom of the basement slab. The default value of -1 indicates that the slab will be placed directly on top of the contaminated zone.

Onsite Vertical Dimension of Mixing: This is used to define the mixing volume used to compute the onsite concentrations of radon, C-14, and H-3.

Building Indoor Area Factor: This is the fraction of the floor area built on the contaminated area. Values greater than 1.0 indicate a contribution from walls penetrating the contaminated zone. The default value of 0 indicates that the time-dependent area factor is derived from an assumed floor area of 100 m^2 and the amount of wall extending into the contaminated zone.

4.30 CARBON-14 DATA

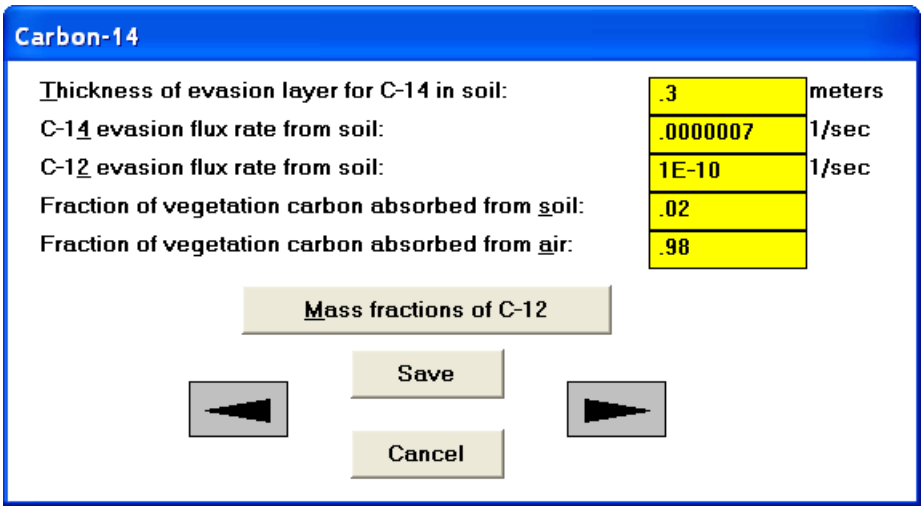

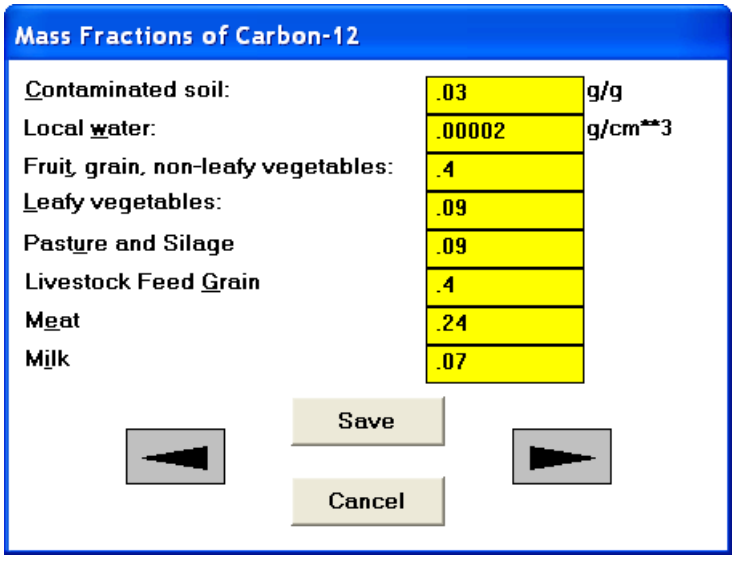

Appendix L of the RESRAD Manual contains a description of the C-14 parameters and their use in the C-14 model. The onsite vertical dimension of mixing parameter on the Radon Data form (Section 4.29) is also used to compute the onsite concentrations of C-14 and H-3. Uncertainty and sensitivity analysis can be performed on any parameter on these forms.

4.31 TRITIUM (H-3) DATA

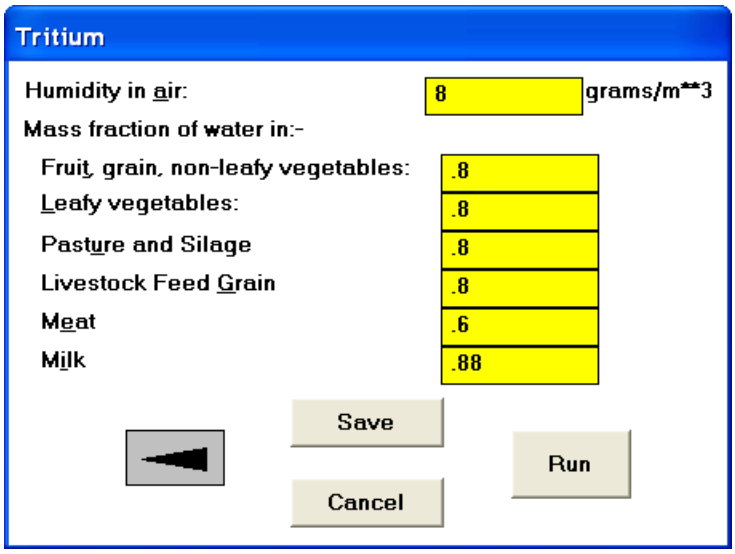

Appendix L of the RESRAD Manual contains a description of the H-3 parameters and their use in the H-3 model. It also contains a map of average U.S. humidity values. The onsite vertical dimension of mixing parameter on the Radon Data form (Section 4.29) is also used to compute the onsite concentrations of C-14 and H-3. Uncertainty and sensitivity analysis can be performed on any parameter on this form.

5 RESULTS

For each deterministic analysis, RESRAD-OFFSITE produces three text reports and a data file that can be viewed by using the RESRAD graphics interface. The first few pages of each report list the table of contents of the report. The RESRAD graphics interface provides many options for viewing the results.

Sensitivity analysis (one parameter at a time) results are also viewed by using the RESRAD graphics interface. Uncertainty analysis results are produced in a report and in a number of data files that can be graphed in the uncertainty interface. The contents of the reports are as outlined below.

- **Textual Reports**

  1. Parent Dose Report (.par)

  A. Inputs

  - Dose conversion factors
  - Transfer factors
  - Site characteristics

  B. Pathway selections

  C. Total dose

  - At user-specified reporting times
  - Peak and time of peak

  D. Pathway doses from transformation chain of initially present nuclides

  - At user-specified reporting times

  E. Guideline information

  - Dose/source ratios at user-specified reporting times, attributed to initially present nuclides
  - Single radionuclide soil guidelines at user-specified reporting times
  - Single radionuclide soil guidelines at time of peak dose from nuclide

- Radionuclide soil guidelines at time of peak dose from all nuclides

F. Run-time information

- Execution time
- Convergence failures of numerical integration (groundwater transport)

2. Progeny Dose Report (.pro)

A. Pathway doses from nuclides at point of exposure

- At user-specified reporting times

3. Cancer Risk Report (.rsk)

A. Cancer risk slope factors

B. Excess cancer risks

- Attributed to initially present nuclides
- Attributed to nuclides at point of exposure
- Radon and short-lived progeny contributions

- **Uncertainty and Probabilistic Analysis Reports**

1. Dose and Risk Report (.prb)

A. Inputs

- Summary of distribution of each input

B. Minimum, maximum, mean, and standard deviation at reporting times

- Total dose from each initially present nuclide
- Total risk from each initially present nuclide
- Pathway dose from each initially present nuclide

C. Cumulative distribution function

- Peak total dose

- Peak pathway dose
- Peak total risk
- Peak pathway risk

D. Correlation and regression coefficients (if requested by user)

- Peak total dose with inputs
- Peak pathway dose with inputs
- Peak nuclide dose with inputs
- Peak total risk with inputs
- Peak pathway risk with inputs
- Peak nuclide risk with inputs

2. Probabilistic Input Report (.smp)

A. Input specification

- Distribution of each input
- Rank correlation coefficients
- Warnings of incompatible input correlations

B. Input samples

- Input vectors
- Rank of input vectors
- Correlation coefficients of raw data
- Correlation coefficients of rank data

5.1 REPORT VIEWER

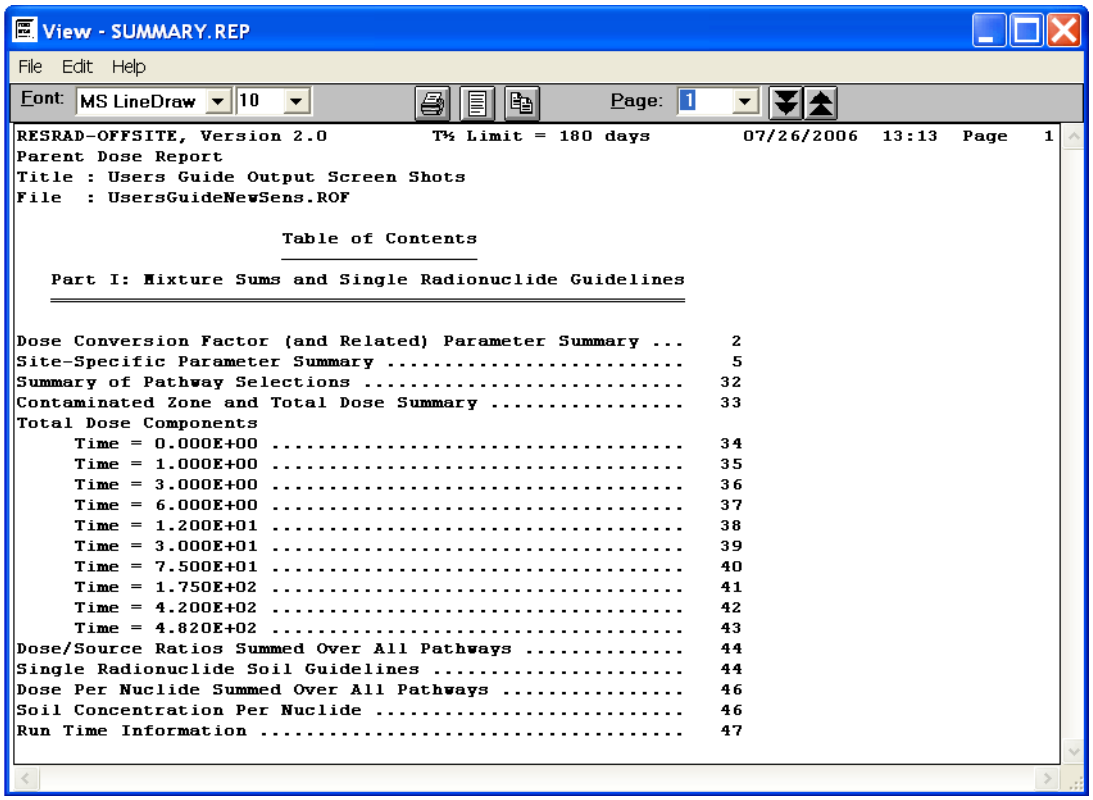

The Report Viewer is launched automatically at the end of each run to display the Parent Dose Report (summary.rep). The Report Viewer may also be accessed at any time from the Main Menu, toolbar, DOS Emulator, or Navigator to view any of the current reports or any reports from the past that were saved.

Getting to Report Viewer

- **Menu:** Click on Select View, Text Output, and then any of the available choices: Parent Dose Report, Risk Report, Progeny Dose Report, Uncertainty/Probabilistic Dose and Risk Report, Uncertainty/Probabilistic Inputs Report.

- **Toolbar:** Only the Parent Dose Report can be accessed from the toolbar. Click on the report page icon (the left button on the third cluster).

- **DOS Emulator:** Click on the View Output button and then the command button corresponding to the desired report.

- **Navigator:** Go to the Results tab and click on the command button corresponding to the desired report.

Viewing a Previously Saved Report

From within the Report Viewer, click on File and View another File (Ctrl f) from the Report Viewer main menu. Point to the subdirectory where the input files are located. Select the file that you want to view. The saved files have the same root name as the input file. Three-character extensions identify the five types of report files as follows:

- .par = parent dose report,
- .pro = progeny dose report,
- .rsk = cancer risk report,
- .prb = uncertainty and probabilistic dose and risk report, and
- .smp = uncertainty-probabilistic input report.

Moving Around

- **Pages:** To go to another page, choose one of the following methods:
  - Enter the page number in the page text box and hit return.
  - Pull down the page list and click on desired page.
  - Advance a page by pressing the "Page Down" key or by clicking on the double down arrows.
  - Go back a page by pressing the "Page Up" key or by clicking on the double up arrows.
- **Within a page:** Use scroll bars to position text.
- **Between reports:** Click on File and View another File (Ctrl f) from the Report Viewer main menu to view another report. You can also close the Report Viewer and go back to the Main menu to select a different file.

Saving Files

Every time a calculation is run, the previous reports and graphics files are overwritten. The results can be saved under different names, which allows their retrieval later.

- **Saving all files:** Click on File and Save All under the Report Viewer main menu. This will save all textual reports to files. If the input filename is xxxx.rad, the reports will be saved as xxxx.yyy, where the extension yyy

identifies the report as described in "Viewing a Previously Saved Report" above.

- **Saving the open report:** Click on File and Save under the Report Viewer main menu. This will prompt the user for a name under which to save the currently displayed report.

Copying Selections

- **Copy highlighted section:** Click on Edit/Copy under the Report Viewer main menu. The selected text will be placed on the Windows clipboard and can be placed into any document, such as a spreadsheet or word processing text.

- **Copy the current page:** Click on Edit/Select All, followed by Edit/Copy. Another option is to click on the icon that looks like two pages.

Printing

- **Setting up the printer:** RESRAD-OFFSITE uses the standard Windows printer. The setup for the printer can be accessed through the File/Printer/Setup menu option. Options that can be selected include printer, paper size, and orientation.

- **Setting up the report for printing:** Click on the icon that looks like a single page to automatically select the best font size that will fit the report to a single page width.

- **Printing:** Select the File/Print menu option or click on the printer icon button. A dialogue box will appear for printing the whole report, sets of pages, or the current highlighted text.

5.2 GRAPH VIEWER (DETERMINISTIC AND SENSITIVITY ANALYSIS)

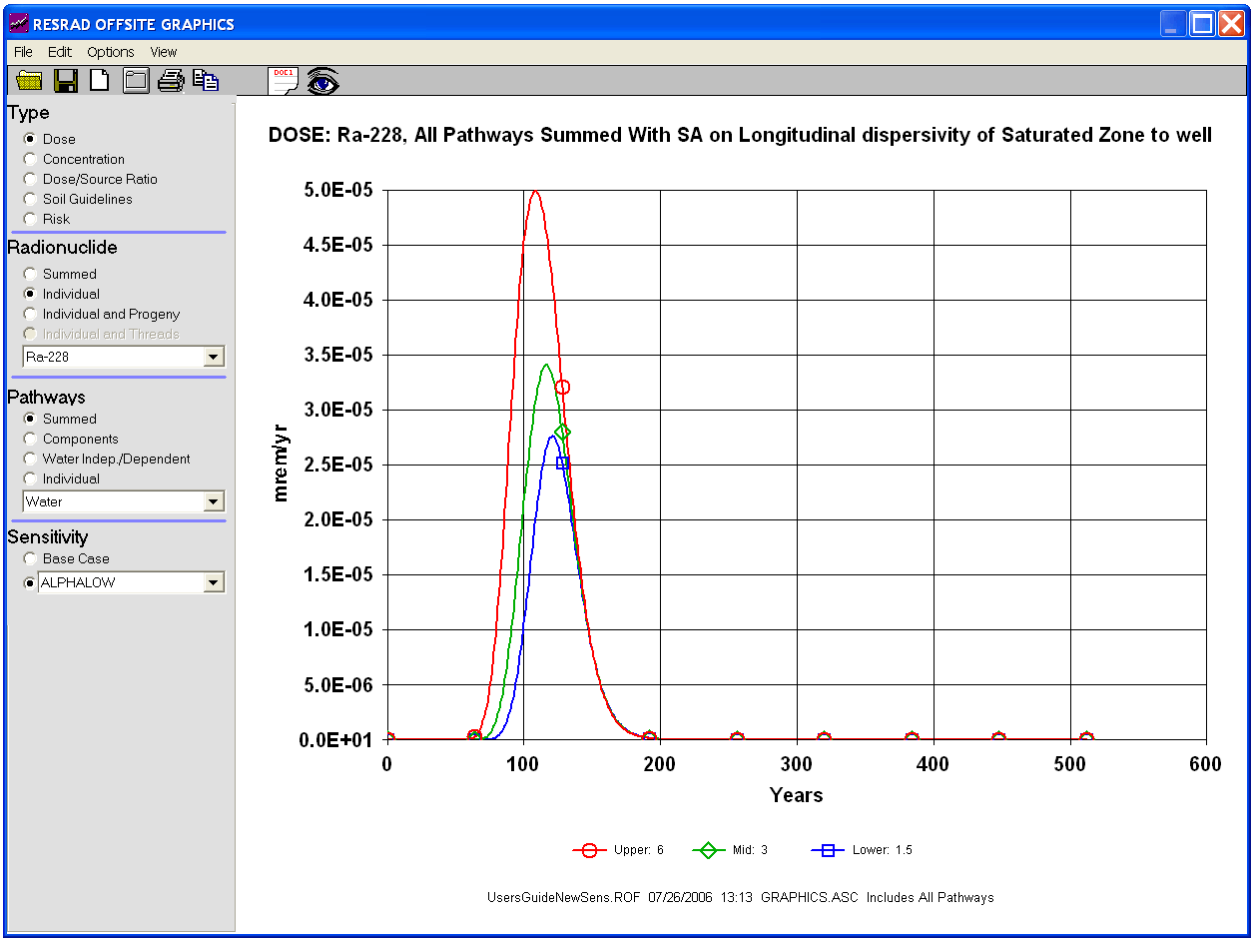

Getting to Graph Viewer

- **Menu:** Click on View on the RESRAD-OFFSITE menu, then select Deterministic Graphics.
- **Toolbar:** Click on the middle icon in the third cluster, the one with the button prompt saying "View Deterministic Graphics."
- **DOS Emulator:** Click on View Output to bring up the output form. Click on Deterministic Graphics.
- **Windows Navigator:** Click on the Results tab, then click on the Deterministic Graphics icon.

Choosing from the Plot Selection Pallet

All dose, risk, and concentration data produced by RESRAD-OFFSITE for each radionuclide and pathway or media combination are available to the Graph Viewer. Thus, a wide choice of plots is available. The plots are selected by specifying the following:

- **Type (of Plot)**

  - **Dose:** Select Dose to view a graphical representation of the radiological dose over the user-specified time horizon.

  - **Concentration:** This displays a plot of the concentration of the selected radionuclide in various media over the user-specified time horizon.

  - **Dose/Source Ratio:** This displays a graph of the ratio of an individual radionuclide's dose contribution to its initial concentration in soil in the primary contamination.

  - **Soil Guidelines:** Select Soil Guidelines to view a graph of the initial radionuclide concentration in soil that will produce the specified basic radiation dose limit at that specific time as a function of time.

  - **Risk:** Select Risk to view a graphical representation of the excess cancer risk over the user-specified time horizon.

- **Radionuclide**

  - **Summed:** This option is available for Dose and Risk plots; it displays the dose or risk due to all the radionuclides specified to be present at the site.

  - **Individual:** This option is available for all five types of plots, but its definition depends on the type of plot. Select the radionuclide by using the dropdown scroll box.

    a. When used with the concentration plots, it displays the concentration of the selected radionuclide (either an initially present nuclide or a progeny) in the selected media.

    b. When used with the other four types of plots, it displays the total quantity due to the selected radionuclide (initially present nuclide) and its progeny.

  - **Individual and Progeny:** This option is available for Dose, Dose/Source Ratio, and Risk plots. It displays the individual dose, dose-to-source ratio, or risk due to the selected radionuclide (initially present nuclide) and each of its progeny.

  - **Individual and Threads:** This option is available for Dose, Dose/Source Ratio, and Risk plots. It displays the individual dose, dose-to-source ratio, or risk due to each of the transformation chains of the initially present radionuclide. Threads for each principal radionuclide are listed in the "Condensed Threads in Decay Chain" section of the .chn file. The .chnfile can be viewed with any text editor such as Notepad.

- **Pathways:** Options are available for Dose, Dose/Source Ratio, and Risk plots.

  - **Summed:** This sums the selected quantity over all pathways and plots the sum.

  - **Components:** This plots the selected quantity from each pathway in one plot.

  - **Water Indep./Dependent:** This plots two lines on the graph. One plot shows the waterborne contribution, and the other shows the airborne and any direct contribution from the selected quantity.

  - **Individual:** This plots a single selected pathway. The pathway is selected by using the dropdown scroll box.

- **Media:** This appears in place of the Pathways options when concentration plots are selected. Select the medium by using the dropdown scroll box.

- **Sensitivity:** This is displayed when a sensitivity analysis is performed.

  - **Base Case:** This shows only the results of the deterministic run.

  - **Dropdown list of parameters:** Select a parameter from the dropdown list to see the sensitivity of the output to that parameter.

Selecting from the Graph Viewer Menu

- **File**

  - **Open:** This command is used to open the deterministic graphics data file from a previous run. The deterministic graphics data file is stored in the same directory as the input files at the end of each run. These files have the same root name as their input files but end with the extension .grp.

  - **New Window:** This command displays another Graph Viewer window. Two plots from the same data file can be viewed. Plots from two different graphics data files cannot be viewed in the different windows.

  - **Save Plot Data:** This command writes the x and y values used in the plot that is displayed in columns in an ASCII file. If multiple lines are displayed in the plot, a pair of columns is output for each line that is displayed. The "DOC1" icon is a shortcut to generate this file. The "eye" icon is a shortcut to view and/or print the file.

  - **Print:** This command is used to produce a hard copy of the current plot.

  - **Print Setup:** This opens a window displaying the list of available printers and the printing specifications.

  - **Close Window:** When multiple Graph Viewer windows are open, this command is used to close an individual window.

  - **Exit:** This closes all Graph Viewer windows.

- **Edit**

  - **Copy:** This command saves the plot in a metafile. The print screen (Print Scrn) key on the keyboard produces a much better quality image.

  - **Export to Excel:** This command opens a new Excel file and transfers the x and y values used in the plot. If multiple lines are displayed in the plot, a pair of columns is output for each line that is displayed. The first three rows contain the plot title, plot footer, and column headers.

- **Options:** This menu is used to change the appearance of the plot. The following choices can be made: display either axis in linear or logarithmic scale, display or suppress grid lines, use different colors for different plots or use black for all plots, use the same or different line styles for the different plots. This menu is also used to hide or show the prompts for the buttons on the toolbar.

- **View:** This menu is used to view the plot data. The plot data must have been saved previously by using the Save Plot Data command described above under the first option, File.

6 ENHANCEMENTS

The influence of each input on RESRAD-OFFSITE predictions can be investigated by using two independent features available in the code. The *sensitivity analysis option* can be used to observe the independent influence of each individual parameter. The *uncertainty and probabilistic analysis option* can be used to study the variation in the prediction and the importance of each individual parameter when a number of parameters are varied simultaneously over their likely range.

6.1 ONE-PARAMETER-AT-A-TIME SENSITIVITY ANALYSIS

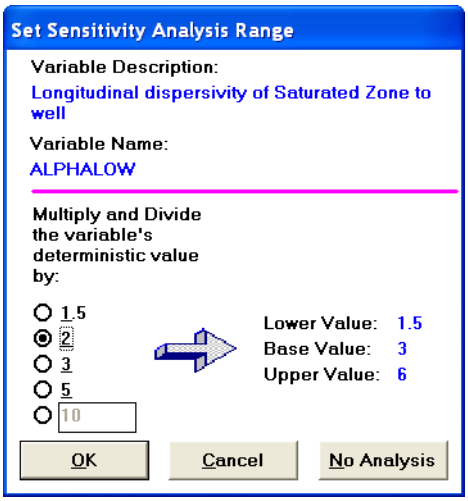

Purpose

One-parameter-at-a-time sensitivity analysis is used to study the independent influence of each individual parameter on the predicted dose, risk, and concentrations. Each of the selected parameters is varied in turn by a factor that is first higher than its deterministic (base) value and then lower. Thus, two additional runs of the code are performed for each parameter selected for sensitivity analysis. Three curves are plotted to show the variation of the predictions over time for the three values (low, base, high) of the parameter, while all the other parameter are held at their base values.

Displaying the Sensitivity Analysis Range

- **Menu:** First click on the input box of the parameter of interest to put it in focus. Then click on Form Options on the RESRAD-OFFSITE menu and Sensitivity Analysis (F9 key).

- **Toolbar:** First click on the input box of the parameter of interest to put it in focus. Then click on the Set Sensitivity button (fourth button in the second cluster on the toolbar).

- **Input Window:** First click on the parameter of interest, then press the F9 key.

- **Sensitivity Input Summary Bar:** If a sensitivity has already been set for a parameter, the sensitivity input summary bar (shown if Sensitivity Input Summary under the View option is checked) will include a button for each parameter selected for sensitivity analysis. The title of the button includes the variable name, the symbols */, and the factor by which to multiply and divide. Right click on any of these buttons to review, change, or remove a sensitivity analysis on the corresponding parameter.

Selecting a Parameter for Sensitivity Analysis

First display the Set Sensitivity Analysis Range form while the cursor is in the input box corresponding to the desired parameter. Then set the multiplication and division factor as described below.

Choose one of the options for the multiplication and division factor. The resultant values for the two sensitivity runs will be shown at the right along with the base value. If you choose the last option, you can enter any value greater than 1 or accept the value of 10. If the selected factor causes a parameter value to exceed its bounds, a warning message will be displayed with the option to set the factor to the maximum allowable value. If the base value specified for any variable selected for sensitivity analysis is changed, the sensitivity button corresponding to that factor should be revisited to ensure that the values for the sensitivity analysis will still be within the bounds.

Click on the OK button to include the parameter in the sensitivity analysis. A button for this parameter will be added on the sensitivity input summary bar, and the parameter will be selected for sensitivity analysis.

Removing a Parameter from Sensitivity Analysis

If a parameter has already been selected for sensitivity analysis, the button corresponding to it will be on the sensitivity input summary bar. Either right click on that button, or left click and choose No Analysis to remove the sensitivity analysis. Clicking on Cancel will not remove the parameter from the sensitivity analysis in this case.

If the parameter has not yet been selected, simply click on Cancel on the Set Sensitivity Analysis Range form to disregard the information in the form.

Viewing Results of Sensitivity Analysis

Sensitivity analysis results are shown only in a graphic format, not in any textual report. Launch the deterministic Graph Viewer after performing a sensitivity analysis on the selected parameters; the Sensitivity option will be displayed at the bottom of the plot selection pallet (Section 5.2). Select a parameter from the dropdown box to see the sensitivity of the output to that parameter.

6.2 UNCERTAINTY AND PROBABILISTIC ANALYSIS

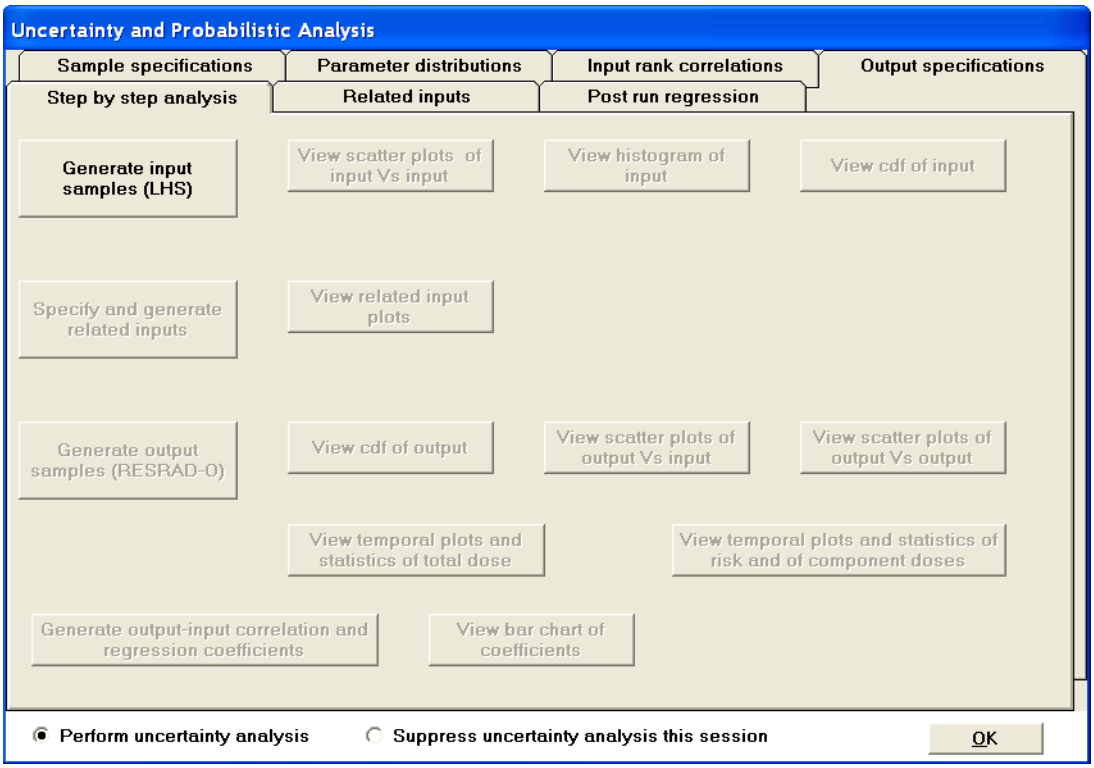

Purpose

Uncertainty and probabilistic analysis is used to determine the variation in the predictions (dose, risk, or media concentrations) due to the uncertainty in the values of some parameters and the probabilistic nature of other parameters. It can also be used to identify the input parameters that are responsible for the major part of the variation in the output (Multiparameter Sensitivity Analysis, Section 6.3). Then the resources can be focused on reducing any uncertainty in those parameters in order to most efficiently reduce the variation in the predicted dose, risk, or media concentration.

Selecting an Input Parameter for Uncertainty and Probabilistic Analysis

- **Menu:** First click on the input box of the parameter of interest to put it in focus. Then click on Form Options and Uncertainty/Probabilistic Analysis (F8 key).

- **Toolbar:** First click on the input box of the parameter of interest to put it in focus. Then click on the Uncertainty/Probabilistic Analysis button (farthest button on the right in the second cluster on the toolbar; it has a ±? symbol on it).

- **Input Window:** Press the F8 function key while the focus is on the input parameter to be included for uncertainty or probabilistic analysis.

The distribution of the selected variable is specified in the Parameter distributions tab (Section 6.2.1) of the Uncertainty and Probabilistic Analysis interface form.

Displaying the Uncertainty and Probabilistic Analysis (Interface) Form

- • **Menu:** Click on View and then Uncertainty/Probabilistic interface (Ctrl F8). This displays the form and also sets the user preference to always display the form when the RESRAD-OFFSITE interface is launched.

The methods just described (Selecting an Input Parameter for Uncertainty and Probabilistic Analysis) will also display the form if it is not already visible. They are not included here because they also select the input that is in focus at the time they were invoked for uncertainty or probabilistic analysis.

The Uncertainty and Probabilistic Analysis form currently has one tab (Related inputs) under development and six active tabs as follows:

1. **Parameter distributions:** The uncertainty in the value of an input or the probabilistic nature of an input is specified in the form of a probabilistic distribution on this tab.

2. **Sample specifications:** This is used to specify how the probabilistic input sets will be generated from the distributions specified in the previous tab.

3. **Input rank correlations:** This accepts the specification of correlations between pairs of uncertain/probabilistic inputs if the appropriate choice is made in the Sample specifications tab.

4. **Output specifications:** This describes the types of probabilistic display and analysis options that are available for the various outputs and is used to specify whether the component doses, risks, and concentrations for each realization of a probabilistic run need to be saved. It is also used to specify the desired output-input correlation and regression coefficients.

5. **Step-by-step analysis:** This allows the analysis to be carried out in sequence and provides an option to view the results of each step before proceeding to the next. It also allows viewing of the probabilistic graphics from a previous analysis.

6. **Post run regression:** This is used to obtain a specific selection of output-input correlation and regression coefficients.

These six tabs are described more fully in Sections 6.2.1 through 6.2.6.

6.2.1 Parameter Distributions Tab

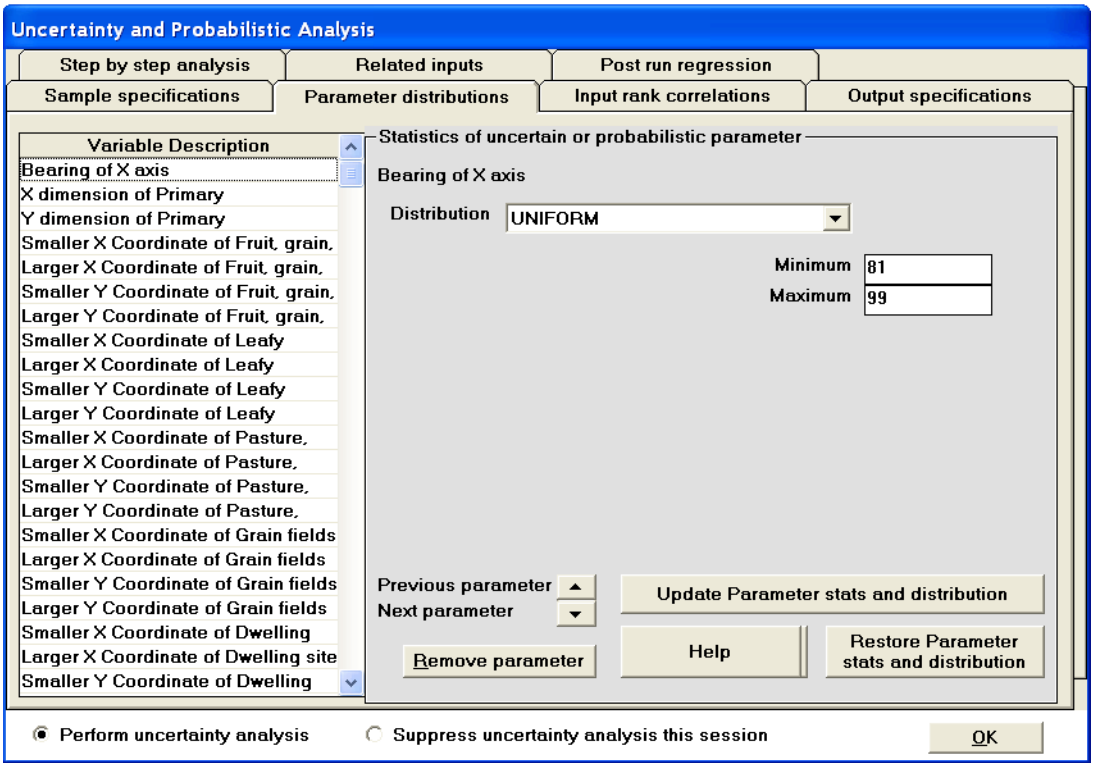

All the input parameters that are selected for uncertainty and probabilistic analysis are listed in the Variable Description box at the left of the tab. Click on any of the entries in that box to display the distribution specified for that input parameter. When an input parameter is selected for uncertainty and probabilistic analysis, it is added to the bottom of the list. The uncertainty in the value of the input parameter or the probabilistic nature of the input parameter can be specified on the right side of the tab. This is done as follows:

1. Select the type of distribution from the dropdown box.

2. Enter the statistics necessary to define the selected distribution in the input boxes below the dropdown box.

3. Save the distribution and its statistics by clicking on the Update Parameter stats and distribution button, the Previous parameter arrow, or the Next parameter arrow.

4. You can cancel any changes made to the distribution type or statistics if they have not yet been saved by clicking on the Restore Parameter stats and distribution button or by simply clicking on a different input parameter in the list on the left.

Clicking on the Help button on this tab displays the Help on Statistical distributions form for the selected distribution. This Help form displays the probability density function of the selected distribution in the brown box on the right side of the form. Interrelationships between alternative forms for specifying the same distribution, or the definitions of the distribution statistics, are also included in the same box, where appropriate. Any conditions that must be satisfied by the distribution statistics are in the gray box at the bottom of the form. The probability density function of the distribution is sketched on the left side of the form. The bounds of the input parameter are indicated by two red (vertical) lines if they fall within the sketch. If the red lines are visible, the statistics for the distribution need to be changed to confine the distribution within these bounds.

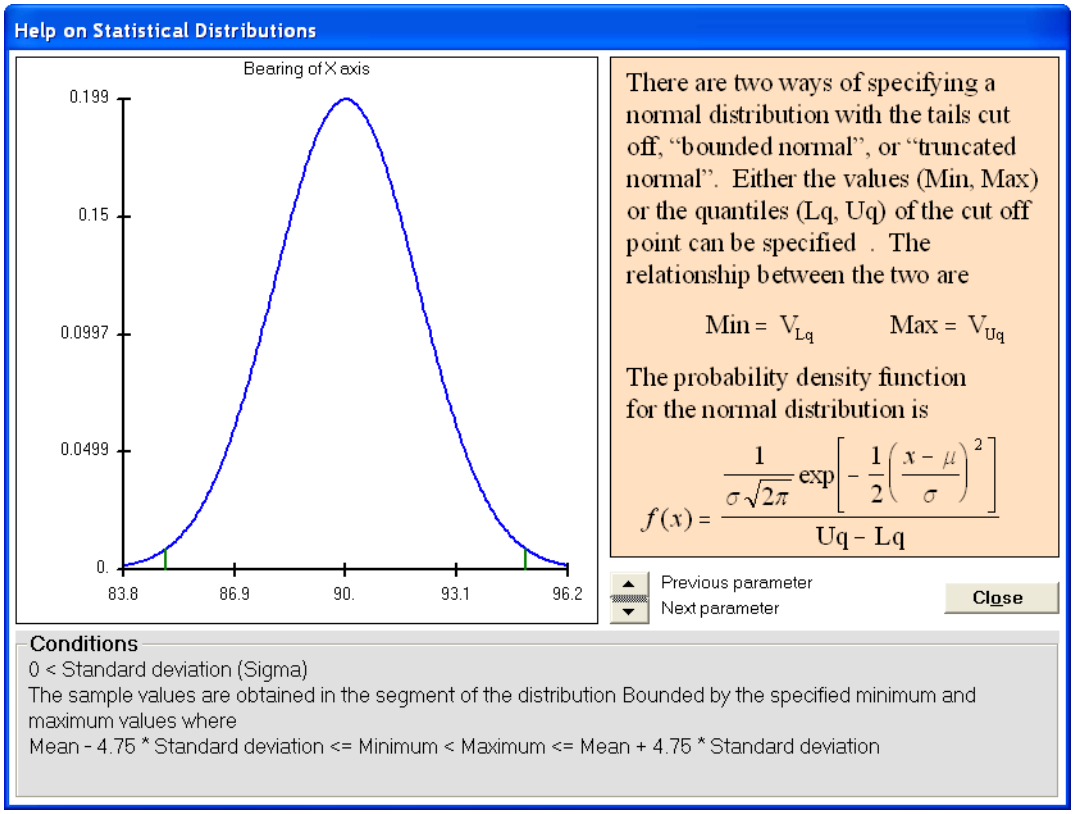

6.2.2 Sample Specifications Tab

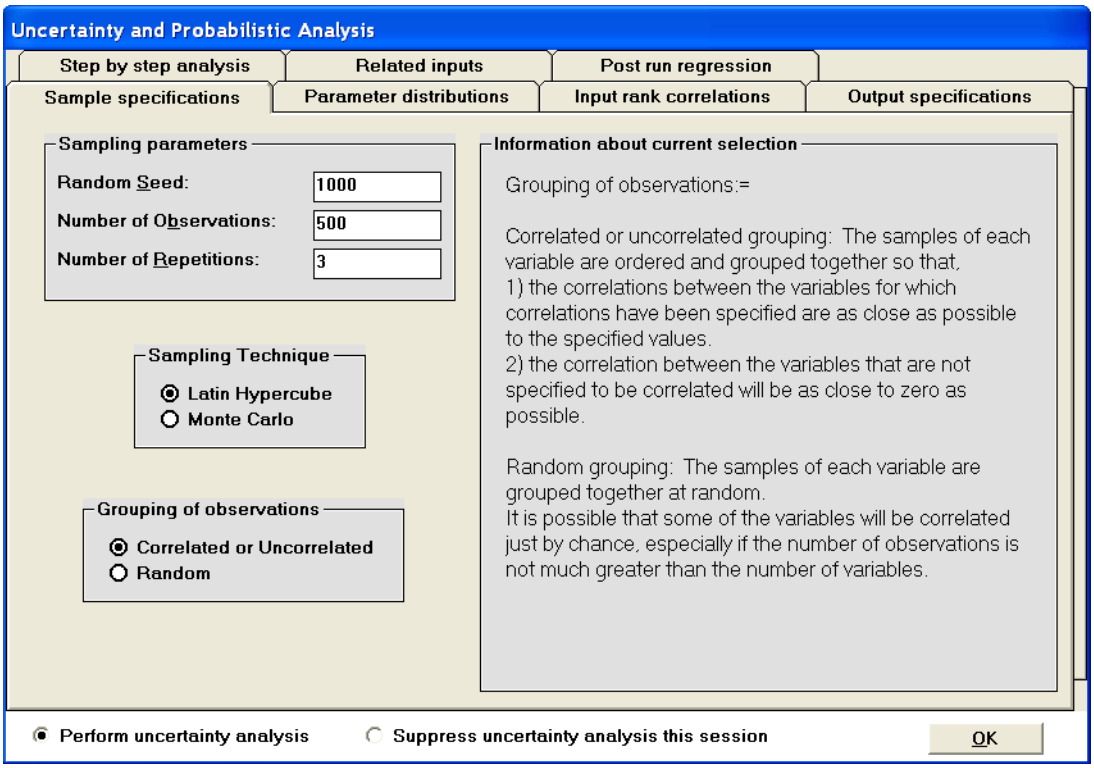

This tab selects how the distributions specified in the previous tab are sampled and how the samples for the different inputs are to be combined to produce the set of inputs. The frame on the right side of the tab describes the purpose and effect of each of the items on this tab:

- **Number of Observations:** This is the number of values that will be sampled from the distribution of each input parameter specified in the Parameter distributions tab. This must exceed the number of input parameters if correlations are specified between inputs or if regression statistics are to be produced. The accuracy of the probabilistic predictions can be improved by increasing the number of observations.

- **Sampling technique:** The code offers a choice of two sampling techniques: Latin hypercube sampling (LHS) or Monte Carlo. In the LHS technique, the distribution is divided into equally probable segments, equal in number to the desired number of observations. Then a value is picked at random from each segment according to the probability density function within that segment. This ensures that the sample covers the entire range of the distribution, even when the number of samples is relatively small. In the Monte Carlo technique, the desired observations are each picked at random from the entire distribution according to the probability density function. When the number of samples is small, the sampled values do not represent the distribution as well as the values obtained by using the LHS technique.

- **Random Seed:** Both sampling techniques choose the sample value from the appropriate part of the distribution at random according to the probability density function. The sampling code has a random number generator to produce the pseudo-random numbers needed to do the random sampling. The random number generator produces a random number on the basis of the seed it receives. It also increments the seed to the next integer every time a random number is generated. Thus, the sequence of random numbers that is generated to obtain the sample can be exactly reproduced if the same starting seed is used again. The Random Seed input is the starting seed; it allows the code to reproduce the same set of probabilistic inputs should there be a need to rerun the same analysis at a later time on a different computer.

- **Grouping of Observations:** After the code obtains the required number of samples for each input parameter, it produces the probabilistic set of inputs. Each element of the set of inputs will contain one sample from each of the input parameters. The code offers two choices on how the samples from each input parameter are combined to make the set of inputs: (1) random grouping or (2) correlated or uncorrelated grouping. If it is necessary to have correlations between some of the inputs, or if it is necessary to ensure that there is no correlation between some of the inputs (i.e., zero correlation), the correlated grouping must be used.

- **Number of Repetitions:** This is the number of times the analysis needs to be repeated in order to obtain a measure of the accuracy of the probabilistic predictions. Increasing the number of observations increases the accuracy of the probabilistic predictions, but a measure of the accuracy can be obtained only if the analysis is repeated. The closeness of the results, or the lack thereof, is an indication of the accuracy, or lack of accuracy, of the predictions.

6.2.3 Input Rank Correlations Tab

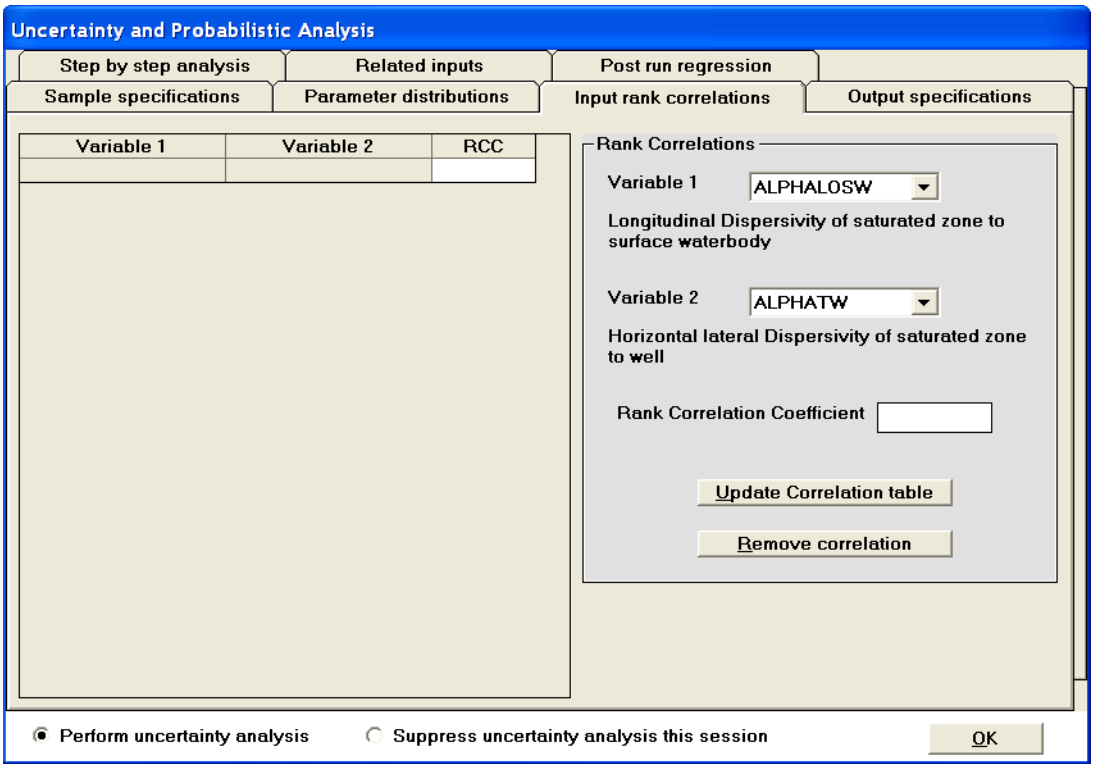

This tab becomes active to accept input only if the correlated or uncorrelated grouping option on the Sample specifications tab has been chosen. Correlations are specified between the ranks of the inputs, not the raw values of the inputs. The pair of inputs that are to be correlated are chosen from the two dropdown boxes, and the rank correlation coefficient is specified in the corresponding input box, all on the frame at the left.

The Update Correlation table button on the right frame saves the information in the correlation table at the left. Correlations that were saved can be deleted by first clicking on the corresponding line in the table at the left and then clicking on the Remove correlation button on the right. The correlations can also be edited by clicking on the appropriate row in the table and then changing the value of the rank correlation coefficient (RCC). The revised correlation must be updated for it to take effect. A pair of uncorrelated inputs (i.e., a pair with a zero correlation coefficient) need not be specified in the table because the correlation between any pair of inputs that are not included in the table is implicitly set to zero in the sampling code.

6.2.4 Output Specifications Tab

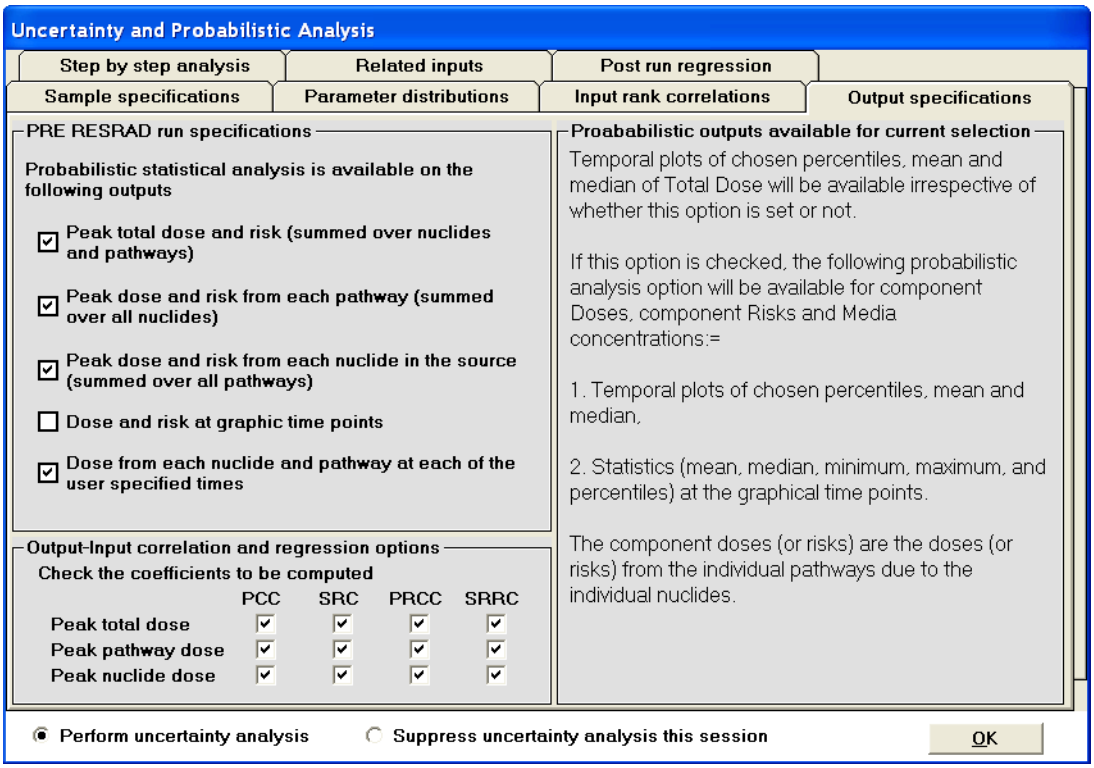

The frame at the top left shows the five categories of dose and risk for which probabilistic results can be obtained. Four of the five categories are always active, the user can choose whether to save on a file the dose, risk, and concentration at each graphical time for each realization (each observation of each repetition). The execution time increases when this option is checked. Clicking on the checkbox displays, in the frame at the right, the various forms of output that are available for each category. The frame at the lower left is used to select the output-input correlation coefficients to be computed during the analysis. Alternatively, these can be unselected before the run, and only the desired correlation and regression coefficients can be computed after the main computational code is run. This is done by using the Post run regression tab.

6.2.5 Step-by-Step Analysis Tab

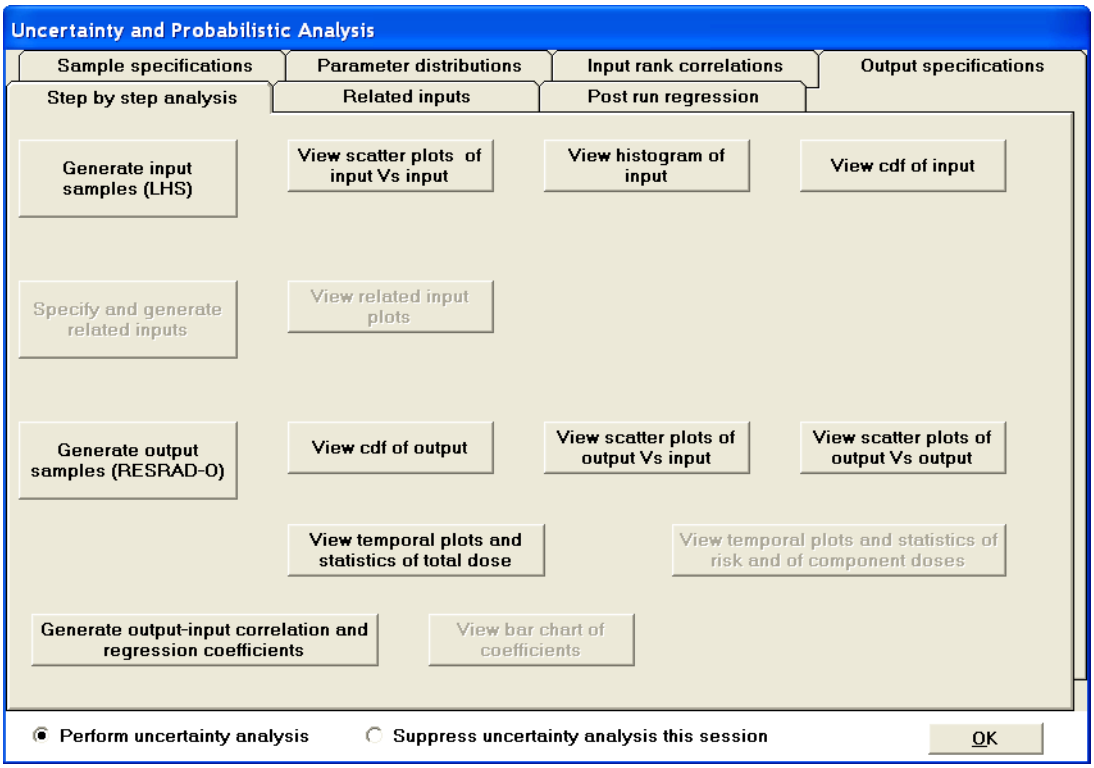

This tab fulfills three main functions: (1) permits a step-by-step approach to performing probabilistic analysis (2) serves as the starting point for viewing the probabilistic graphics, and (3) permits viewing of previously saved results. The different command buttons become active at the appropriate juncture.

The Generate input samples (LHS) command is the only button that is visible for a newly created uncertainty/probabilistic input file. Clicking on the button launches the probabilistic sample generating code (Latin hypercube sampling or LHS). The remaining three buttons in the upper active (first) row become active when the input samples have been generated. The Generate output samples (RESRAD-O) button is also activated at this time. The three buttons in the first row are used to view the corresponding plots and to check the statistics of the input distributions. These plots can be viewed to confirm that the samples accurately represent the specified distribution and to visualize any correlations that were specified between the inputs.

Clicking on the Generate output samples button launches the main computational code. The execution time can be significant for probabilistic analysis. While some simple cases might run in a few minutes, a typical analysis can run for hours. An estimate of the run time is displayed in the run time feedback form (Run form; Section 7.4). The remaining command buttons become active when the output samples have been produced.

The other three buttons in the third row are used to view the probabilistic plots pertaining to the output. These are discussed in more detail in the following paragraphs. The buttons on the fourth

row produce temporal plots. The left button produces temporal plots and statistics for the total dose; corresponding plots for the component doses, risks and concentration have not yet been developed. Instead, the right button will produce a deterministic plot file for each of the realizations; these can then be viewed in the deterministic Graph Viewer. Clicking on the Generate output-input correlation and regression coefficients button (bottom row) displays the Post run regression tab.

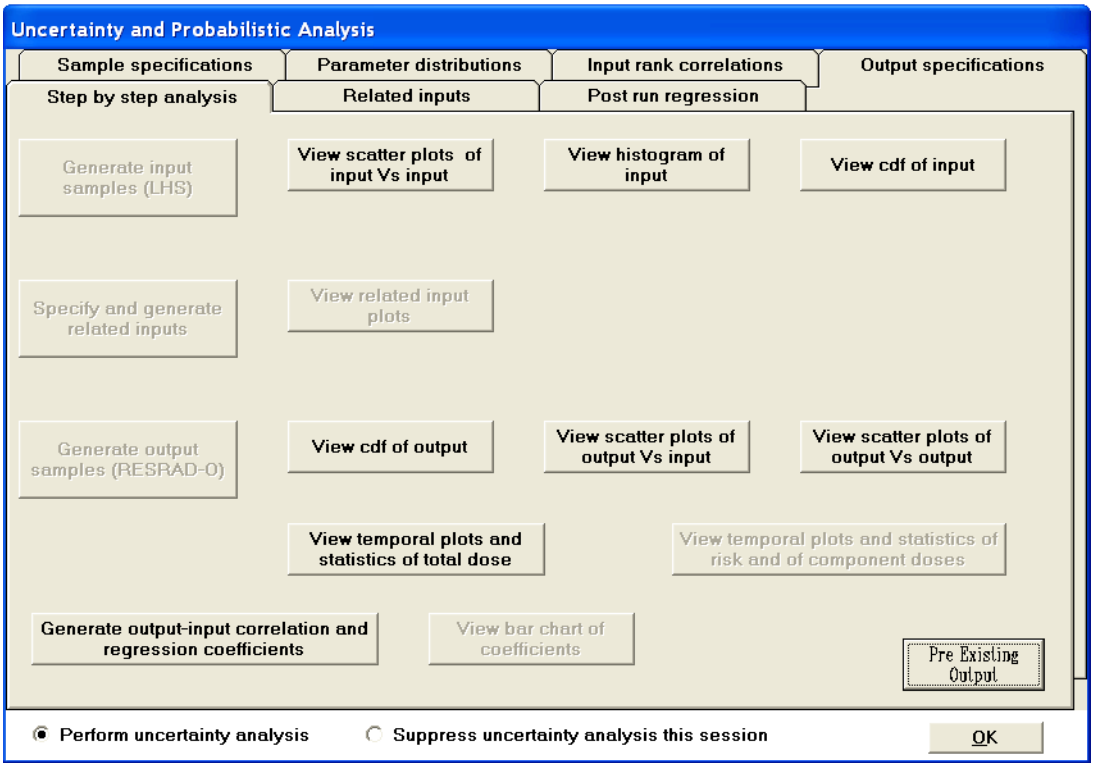

Plots from previous runs can also viewed from this tab by opening the corresponding input file. When a preexisting input file is opened, the code checks for an indication that the file has been executed previously. If it has and if probabilistic results are available, the Pre Existing Output button is displayed at the bottom right of the tab (see screen above). Click on this button to load the probabilistic input and output into the interface memory. This usually takes some time, so a Please Wait bar displays to ask for the user's patience. The seven view plot buttons can then be used to view the three input plots (scatter plots of input vs. input, histogram of input, and cumulative distribution function [cdf] of input), the three output plots (cdf of output, scatter plots of output vs. input, and scatter plots of output vs. output) and the temporal plots for total dose. Input-output regression analysis can also be performed.

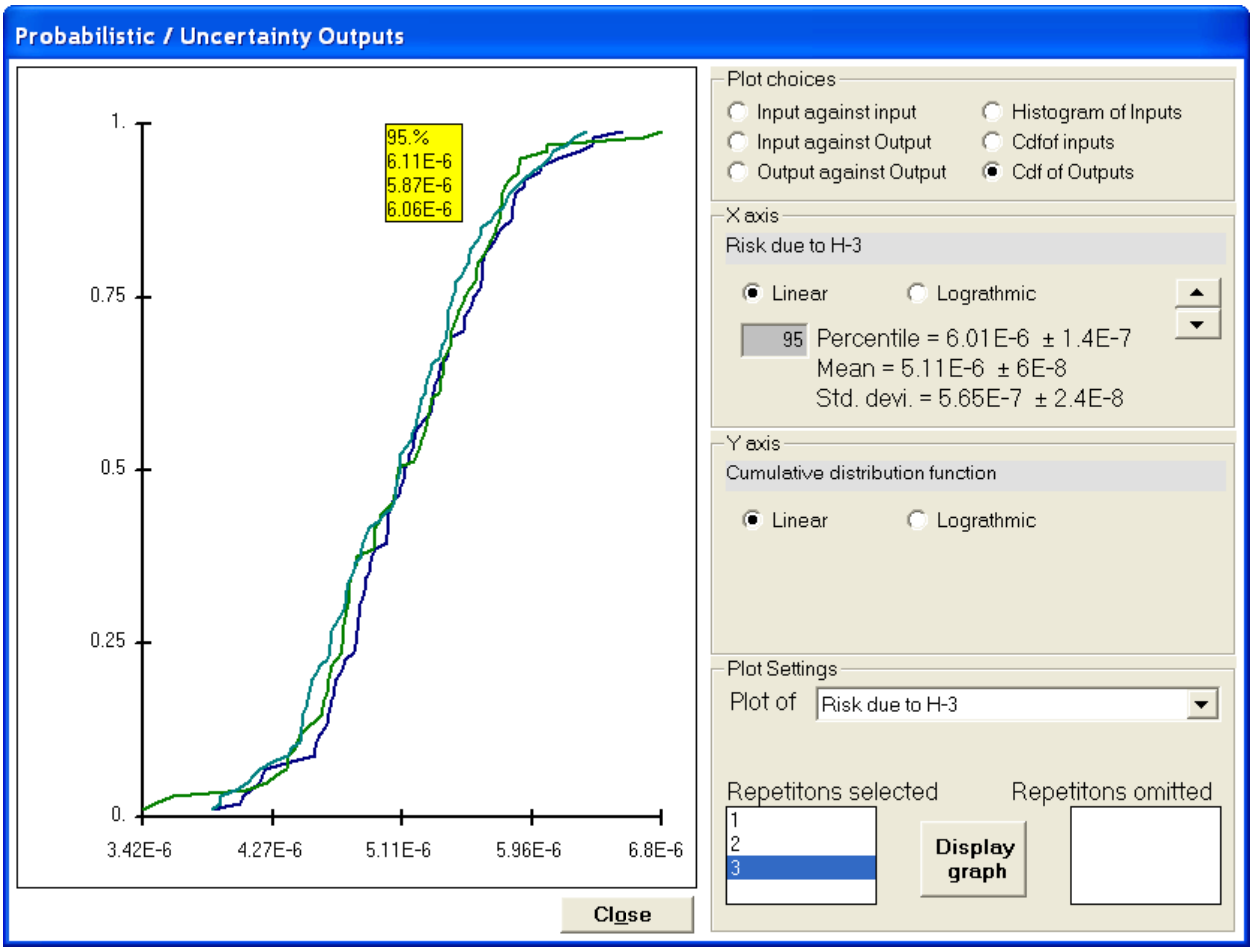

The cumulative distribution function (cdf) of the output can be used to obtain any desired percentile of the output (dose or risk). The value of the percentile can be obtained by keying in the desired percentile in the gray box in the X-axis frame on the right side of the Probabilistic/Uncertainty outputs screen. This frame also displays the mean and the standard deviation of the output. Error ranges are shown where appropriate after a plus/minus symbol (±). (If the error range is less significant than the number of significant figures in the output, it will not be shown.) The value of the percentile for the different repetitions can also be displayed by clicking on the location of the desired percentile on the plot. This value is shown in the yellow box that appears below the cursor. The box disappears when the cursor moves away from the box. The up or down arrow control can be used to cycle over all the probabilistic outputs. One or more repetitions can be omitted from the plot if needed to improve the clarity. At the bottom right of the screen, the Display graph button must be depressed to show the changes made in the Plot Settings frame. This form can be resized by expanding the sides or corners.

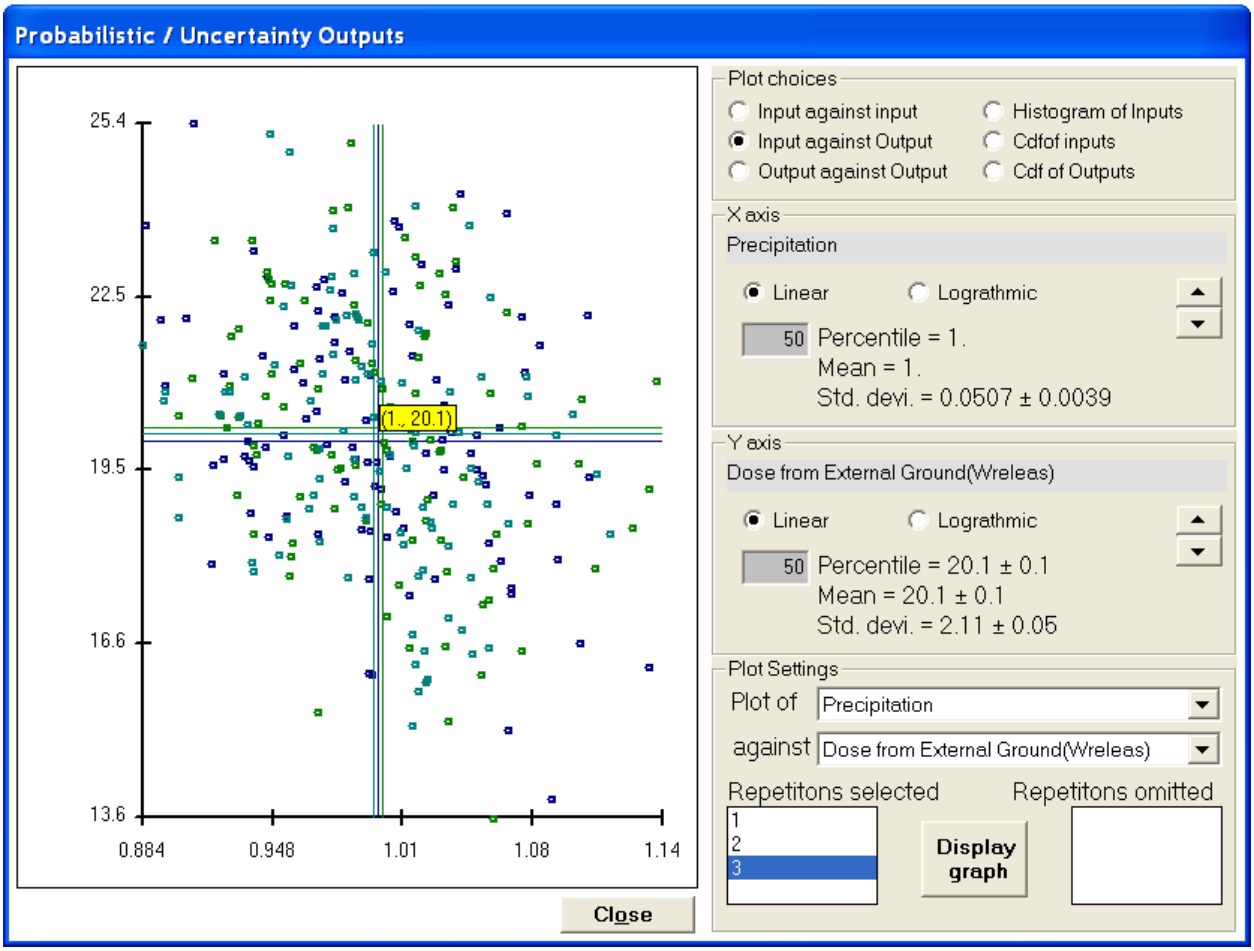

The scatter plots of output against input are helpful in identifying the input parameters that have a significant influence on the output, especially when there are a few significant input parameters. However, as the case illustrated in the above figure shows, it is not easy to visually pick out the important parameters when they are masked by the compounding effects (interference) of other equally important input parameters. The important parameters can be identified by using the regression coefficients, as was done in the case illustrated above.

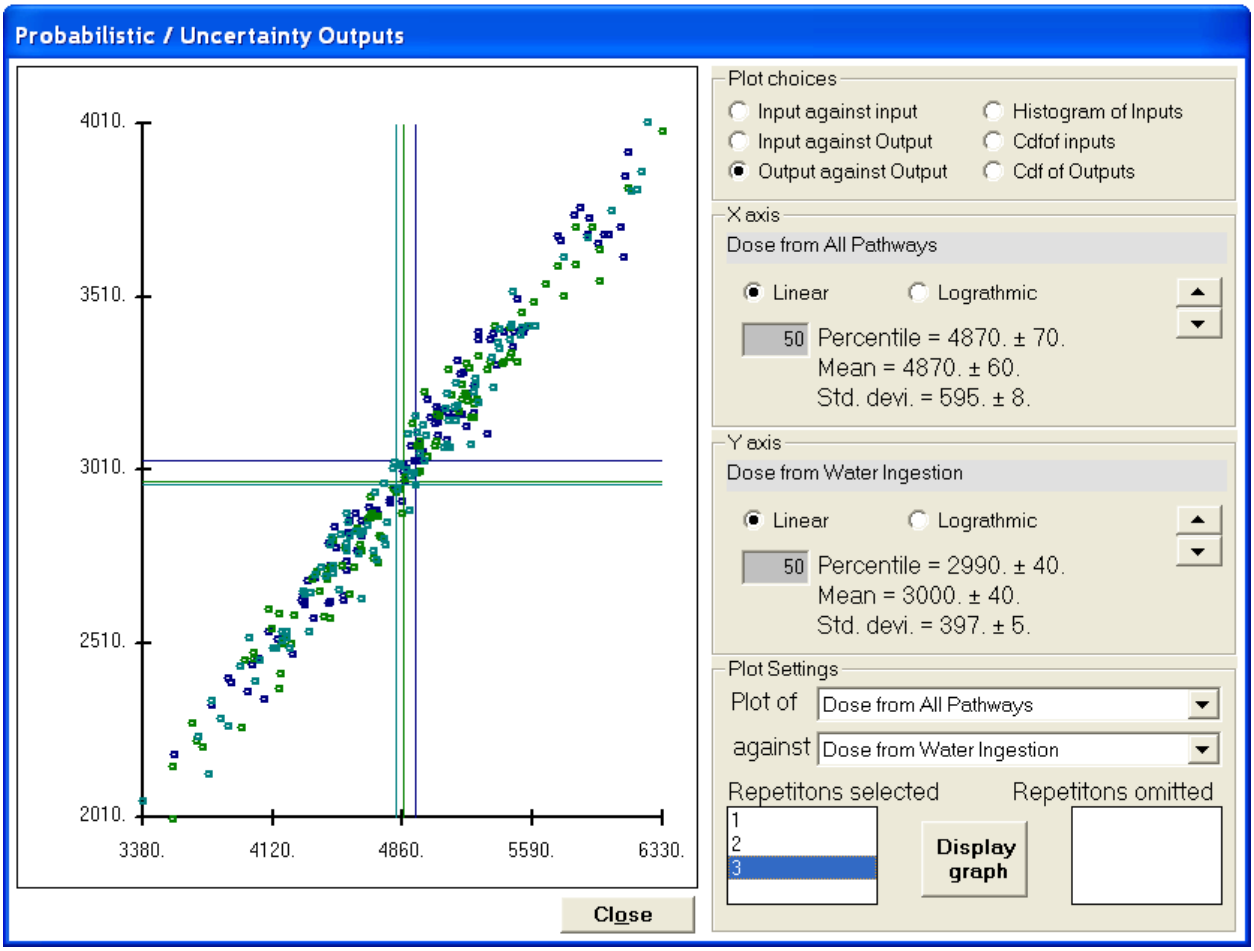

Scatter plots of output against output (see screen above) are useful for identifying the pathways and nuclides that make a significant contribution to the variation in the dose or risk. They can also point to the importance of common parameters that affect the significant pathways.

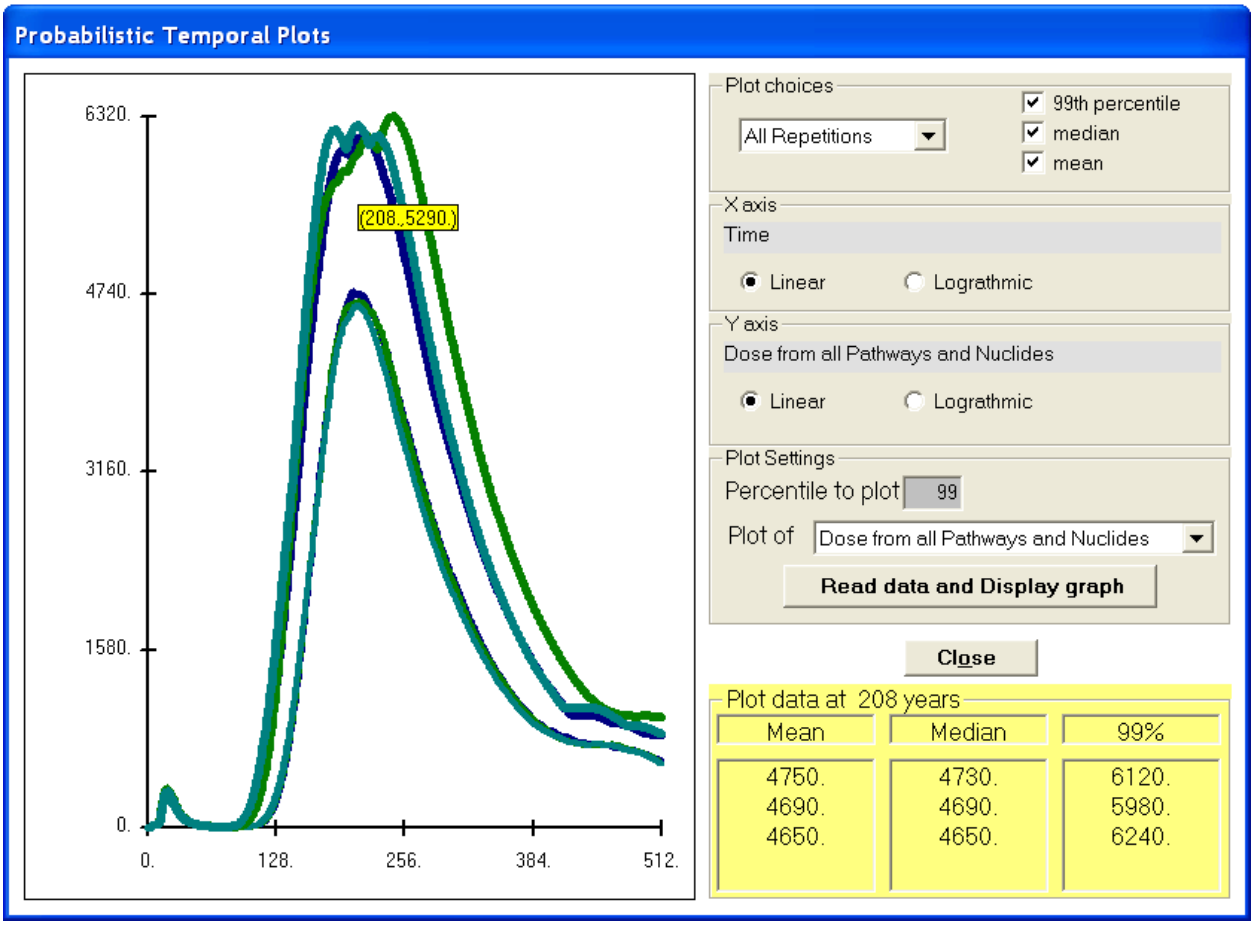

The temporal plot shows the variation of the mean, median and one other user-specifiable percentile of the total dose (dose summed over nuclides and pathways) with time. The plots for all repetitions can be displayed together, as shown above, to see the variation among repetitions; plots of each repetition can be displayed for clarity. The coordinates of any location on the plot can be displayed in the yellow box by moving the cursor to that point. The data from the plots for that corresponding year can be displayed by clicking the mouse; the data for each of the repetitions will be shown in the yellow box at the lower right of the form.

6.2.6 Post Run Regression Tab

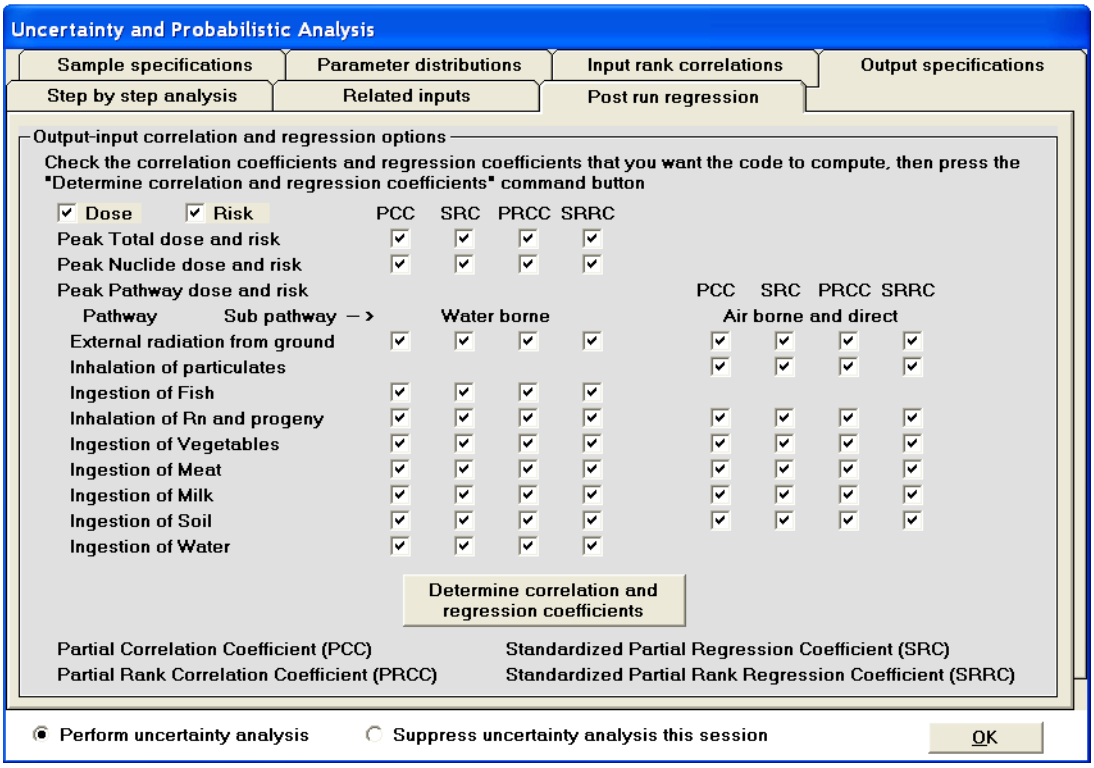

This is used to perform regression analysis between the desired outputs and the probabilistic inputs after RESRAD-OFFSITE's main computational code is run. Check the desired outputs (dose and/or risk and the pathways) and click on the Determine correlation and regression coefficients button. The results are appended to the probabilistic dose and risk report.

6.3 MULTIPARAMETER SENSITIVITY ANALYSIS

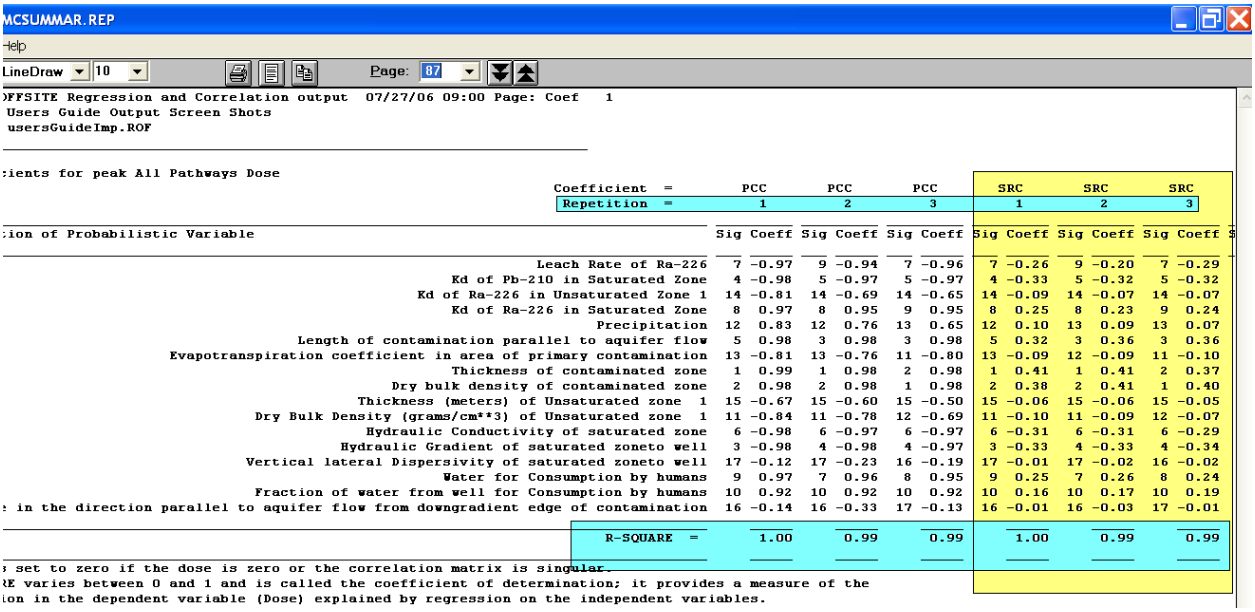

MCSUMMAR.REP

Help

LineDraw 10 Page: 87

OFFSITE Regression and Correlation output 07/27/06 09:00 Page: Coef 1
Users Guide Output Screen Shots
usersGuideImp.ROF

ients for peak All Pathways Dose

Coefficient =	PCC		PCC		PCC		SRC		SRC		SRC	
Repetition =	1		2		3		1		2		3	
ion of Probabilistic Variable	Sig	Coeff	Sig	Coeff	Sig	Coeff	Sig	Coeff	Sig	Coeff	Sig	Coeff
Leach Rate of Ra-226	7	-0.97	9	-0.94	7	-0.96	7	-0.26	9	-0.20	7	-0.29
Kd of Pb-210 in Saturated Zone	4	-0.98	5	-0.97	5	-0.97	4	-0.33	5	-0.32	5	-0.32
Kd of Ra-226 in Unsaturated Zone 1	14	-0.81	14	-0.69	14	-0.65	14	-0.09	14	-0.07	14	-0.07
Kd of Ra-226 in Saturated Zone	8	0.97	8	0.95	9	0.95	8	0.25	8	0.23	9	0.24
Precipitation	12	0.83	12	0.76	13	0.65	12	0.10	13	0.09	13	0.07
Length of contamination parallel to aquifer flow	5	0.98	3	0.98	3	0.98	5	0.32	3	0.36	3	0.36
Evapotranspiration coefficient in area of primary contamination	13	-0.81	13	-0.76	11	-0.80	13	-0.09	12	-0.09	11	-0.10
Thickness of contaminated zone	1	0.99	1	0.98	2	0.98	1	0.41	1	0.41	2	0.37
Dry bulk density of contaminated zone	2	0.98	2	0.98	1	0.98	2	0.38	2	0.41	1	0.40
Thickness (meters) of Unsaturated zone 1	15	-0.67	15	-0.60	15	-0.50	15	-0.06	15	-0.06	15	-0.05
Dry Bulk Density (grams/cm**3) of Unsaturated zone 1	11	-0.84	11	-0.78	12	-0.69	11	-0.10	11	-0.09	12	-0.07
Hydraulic Conductivity of saturated zone	6	-0.98	6	-0.97	6	-0.97	6	-0.31	6	-0.31	6	-0.29
Hydraulic Gradient of saturated zoneto well	3	-0.98	4	-0.98	4	-0.97	3	-0.33	4	-0.33	4	-0.34
Vertical lateral Dispersivity of saturated zoneto well	17	-0.12	17	-0.23	16	-0.19	17	-0.01	17	-0.02	16	-0.02
Water for Consumption by humans	9	0.97	7	0.96	8	0.95	9	0.25	7	0.26	8	0.24
Fraction of water from well for Consumption by humans	10	0.92	10	0.92	10	0.92	10	0.16	10	0.17	10	0.19
in the direction parallel to aquifer flow from downgradient edge of contamination	16	-0.14	16	-0.33	17	-0.13	16	-0.01	16	-0.03	17	-0.01
R-SQUARE =	1.00		0.99		0.99		1.00		0.99		0.99	

set to zero if the dose is zero or the correlation matrix is singular.
RE varies between 0 and 1 and is called the coefficient of determination; it provides a measure of the
ion in the dependent variable (Dose) explained by regression on the independent variables.

Multiparameter Sensitivity analysis can be performed using the uncertainty feature by allowing more than one parameter to vary at the same time. A parameter can be selected for this analysis by pressing the Shift+F8 key when the parameter is in focus. That parameter will be included in an uncertainty analysis with a uniform distribution ranging from 0.9 to 1.1 of its current deterministic value. The sensitivity of the dose or risk to the parameters is given by the standardized regression coefficient or the standardized rank regression coefficient.

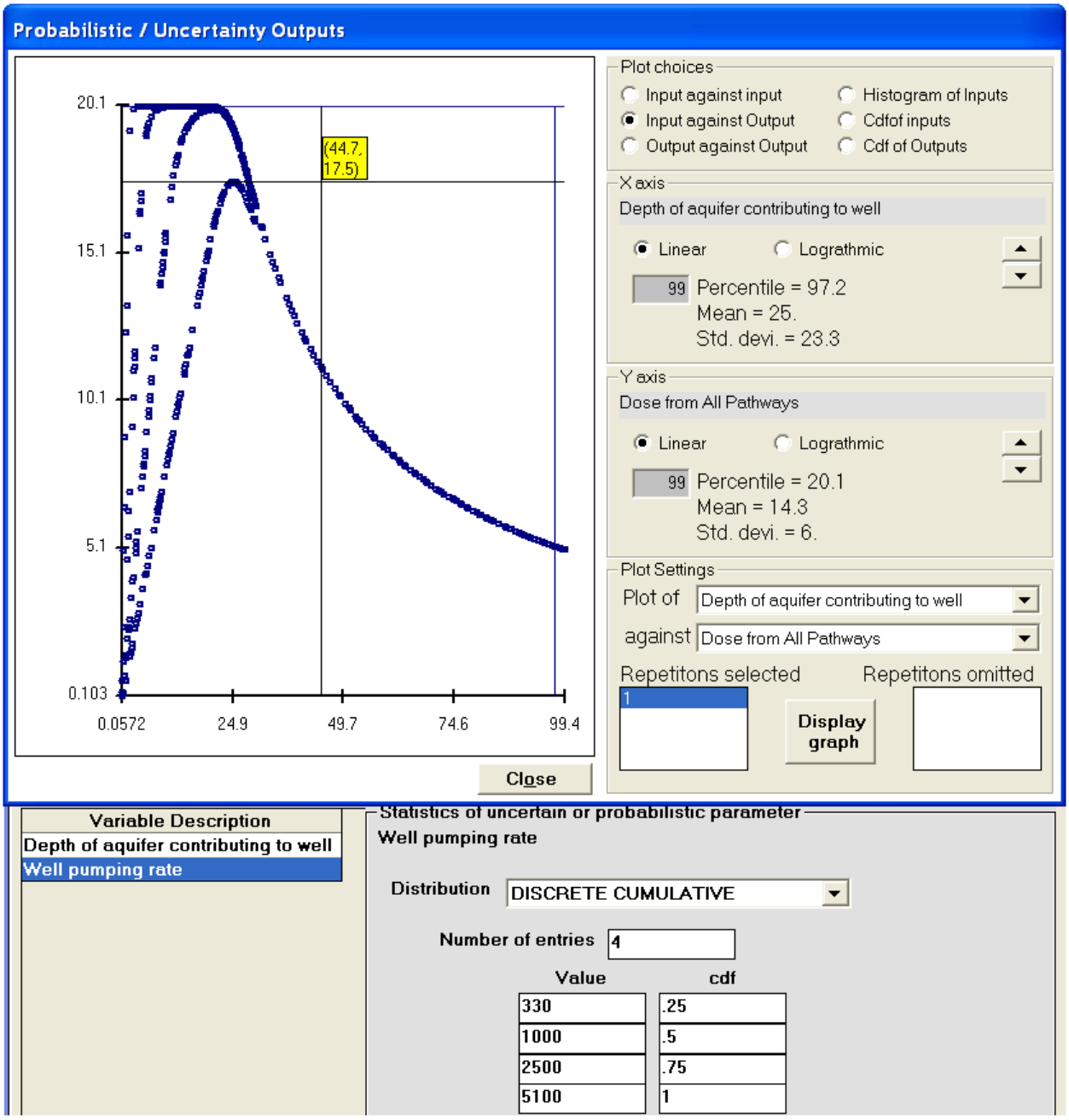

The uncertainty analysis feature can also be used to see the variation of dose over the range of one parameter at various levels of another parameter. The scatter plot of output against input is useful in seeing this variation and the interaction between the inputs as shown in the figure above. The coordinates of any point on the figure can be found by moving the cursor to that point; clicking the mouse will display the cross hair, which is useful in finding the peak of a curve.

7 HELP

Various levels of help are available in RESRAD-OFFSITE, as explained as follows:

- **Application Help Form:** A help file that is accessible from the code gives a description of each input and explains how the parameter is used in the code.

- **Message Log (View - OUTPUT.FIL) Form:** A message log that is produced during the execution of the computational code is useful for debugging if the code should terminate before completion.

- **RESRAD Web Site:** The RESRAD Web site has documents that relate to the RESRAD family of codes. The latest code is available for downloading from the site. The About RESRAD-OFFSITE form from the Help menu of the code contains a link to the RESRAD Web site and e-mail address of the RESRAD team.

- **Run Time Feedback Form:** This gives information about the progress of the computation and also a dynamic estimate of the run time for probabilistic cases.

- **Pdf Versions of the Users' Guide and the Users' Manual:** This guide and the technical manual can be accessed in pdf form.

7.1 APPLICATION HELP (ON INPUT PARAMETERS)

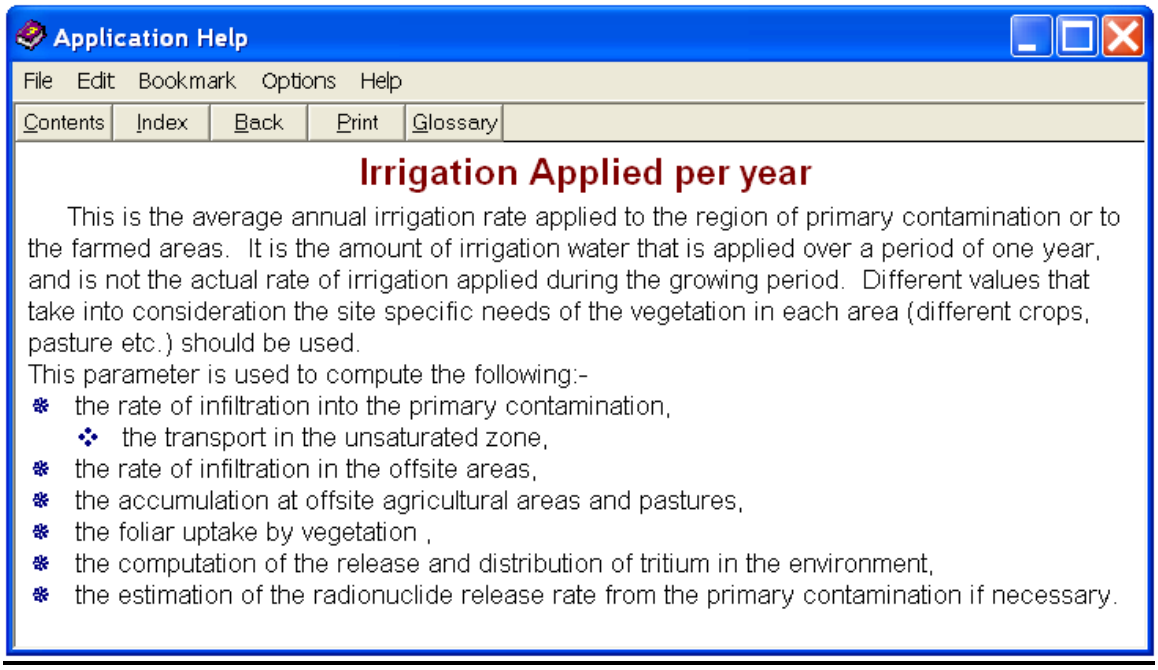

Getting Help

- **Menu:** when the desired parameter is in focus, select context help from the Help submenu (Alt h, c).
- **Input Window:** Press the F1 key.
- **From within the Help Window:**
  - Click on the desired parameter name on the Contents tab.
  - Look for a keyword in the Index tab.
  - Search for a word in the Find tab.

The Help file has a simple description of the input parameter selected by the user and explains how the parameter is used in the code. Refer to the *RESRAD Data Collection Handbook* for a more detailed description of the parameter and for information on how to obtain site-specific values.

7.2 MESSAGE LOG

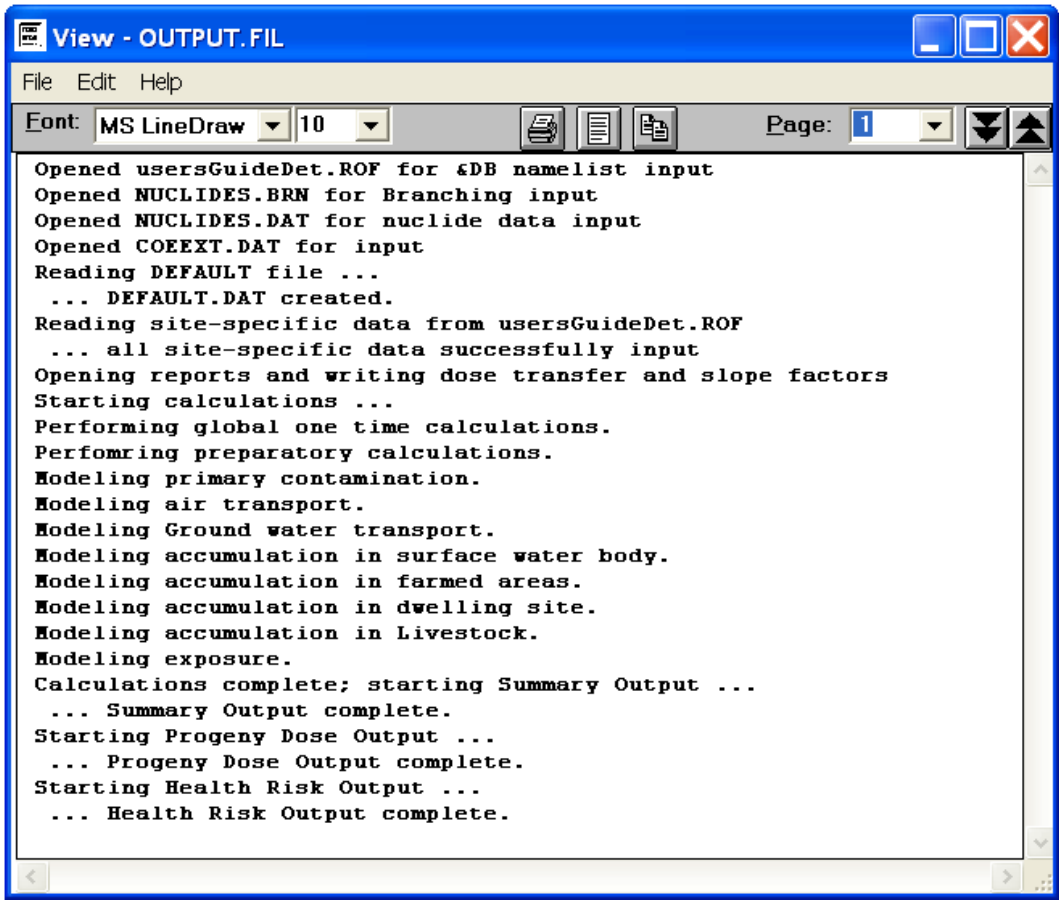

Getting to the Log

From the Main menu, choose View and Message Log. The message log will also be displayed if the computational code encounters an error.

Interpreting the Log

This file lists the progress of the computational code as it completes each phase of calculation and begins the next phase. If the computational code ended before completing the calculations, the file will contain an error message that should be reported to the RESRAD team.

Reporting on Problems

The e-mail address for communicating about problems and asking questions is resrad@anl.gov.

7.3 WEB SITE

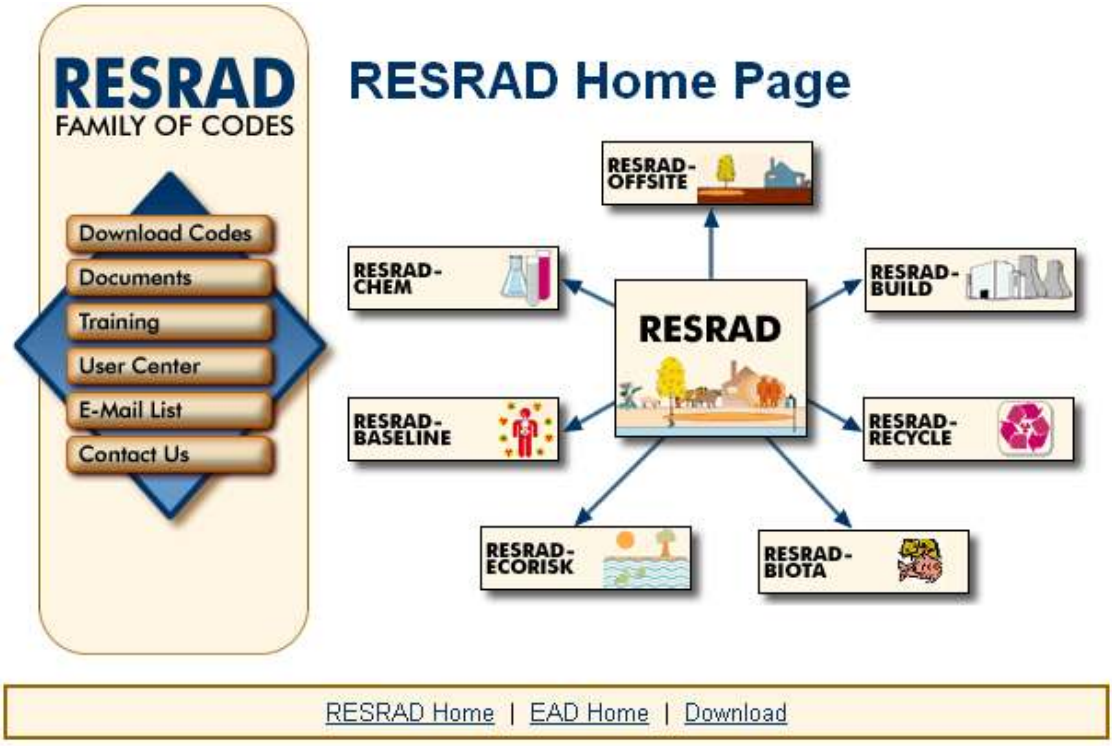

Getting to the Home Page

Type the RESRAD Web site address, http://www.evs.anl.gov/resrad, in your Web browser or click on the link to it in the code. The links are found on the About RESRAD-OFFSITE form (Alt h, a) and in the Help tab of the Navigator window.

The RESRAD Web site contains the following:

- Descriptions of the RESRAD family of codes
- Downloadable version of the latest code
- Table of current versions and release status
- Information on upcoming training workshops and pictures from previous workshops
- List of version releases and dates, along with a short description of the modifications included in the updated versions
- E-mail contact
- Documents related to the RESRAD family of codes

Getting to a RESRAD Document

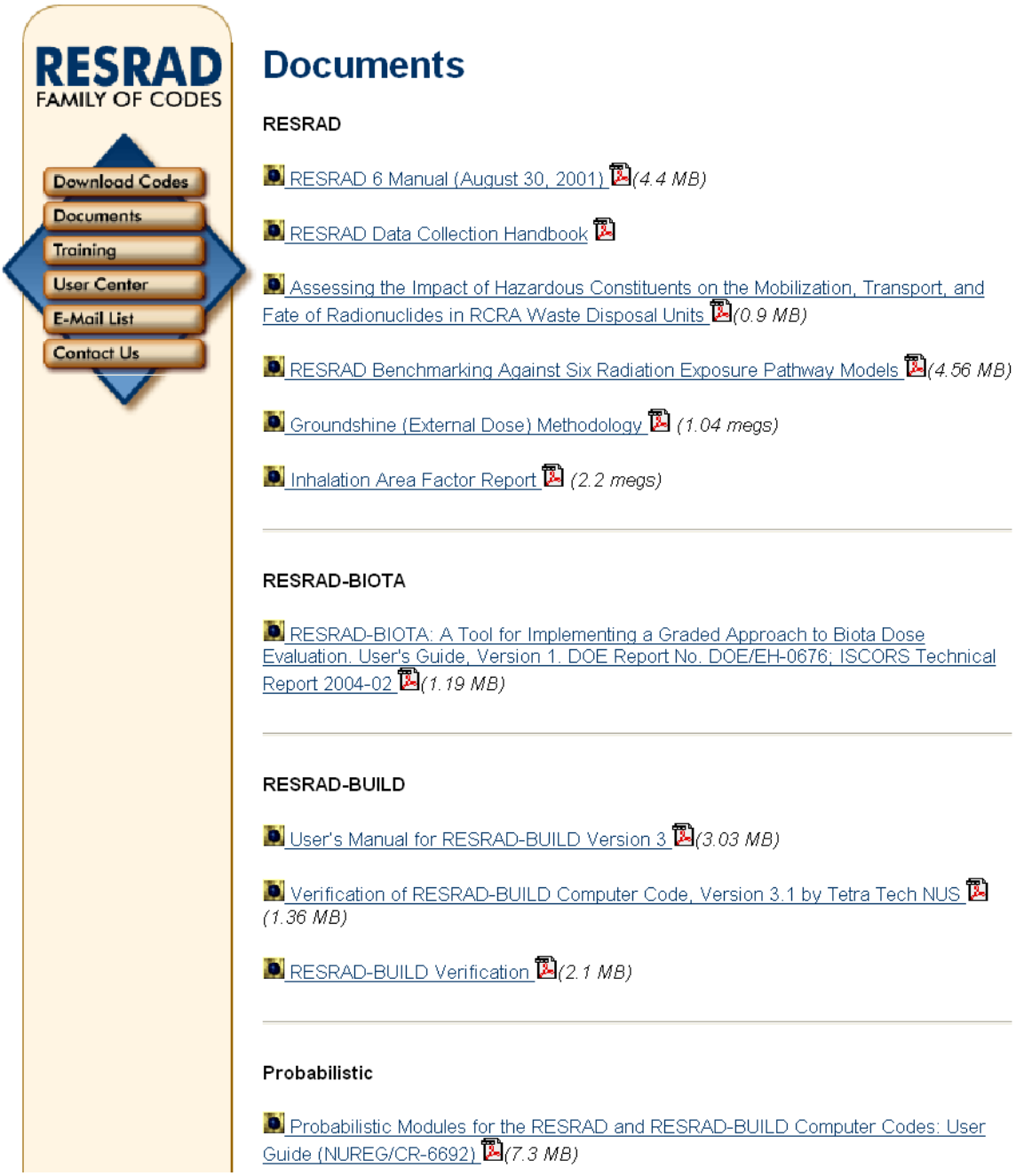

Go to the documents page of the Web site.

7.4 RUN TIME FEEDBACK FORM

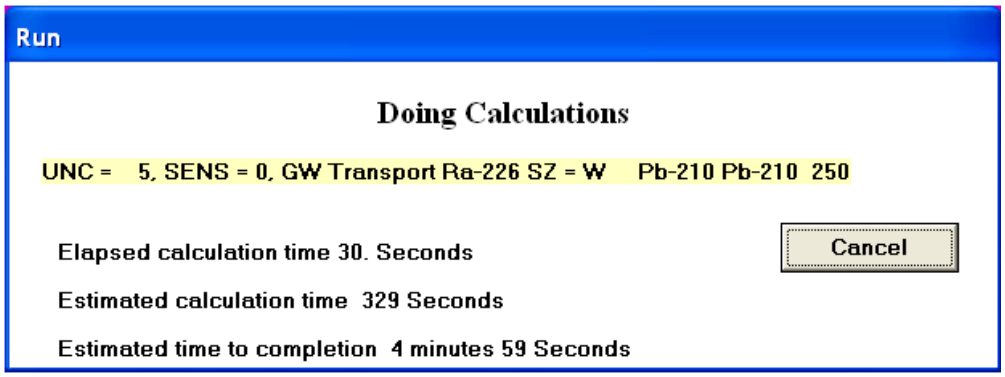

The colored highlighted information bar displays the progress of the computation. The information bar cycles through yellow, blue, and green as it checks the progress of the computational code. For a deterministic run, both UNC (uncertainty) and SENS (sensitivity) will equal zero. If a sensitivity analysis is being performed, the SENS counter will show the index of the current sensitivity run; there will be two sensitivity runs for each input parameter selected for sensitivity analysis. The UNC counter displays the index of the current uncertainty/probabilistic run. The remainder of the information bar shows the code module being executed, the primary contaminant being considered, the transport layer or location if appropriate, and, in the case of groundwater transport, the nuclides entering and leaving the transport layer and the current intermediate time. The frequency at which this information bar is updated can be changed in the Title form (Section 4.1). Frequent updates can increase the run time.

The time that elapsed since the run command was executed is shown in the first line below the information bar. This is followed by two more lines that are displayed only when an uncertainty/probabilistic analysis is performed. The second line shows the estimated calculation time. It includes the time that has elapsed and the time that the code is likely to continue running. This line should stabilize after the first few probabilistic runs. The stability of the calculation time is an indication of the reliability of the estimated time to completion, which is shown in the third line.

While obtaining frequent updates from the computational program can give the user a good idea of what the code is currently doing and how long it is likely to take before the run ends, that information can come at the cost of an increased run time. For probabilistic runs, it may be advantages to shut off message writing by the computational code as described in the paragraph titled **Update Progress of Computation Message** in Section 4.1. The interface will still be able to display the UNC counter of the index of the current uncertainty/probabilistic run and give estimates of calculation time and time to completion based on the size of the output files generated.

REFERENCES

Eckerman, K.F., et al., 1988, *Limiting Values of Radionuclide Intake and Air Concentration and Dose Conversion Factors for Inhalation, Submersion, and Ingestion*, EPA-520/1-88-020, Federal Guidance Report No. 11, prepared by Oak Ridge National Laboratory, Oak Ridge, Tenn., for U.S. Environmental Protection Agency, Office of Radiation Programs, Washington, D.C.

Eckerman, K.F., et al., 1999, *Cancer Risk Coefficients for Environmental Exposure to Radionuclides*, EPA-402-R-99-001, Federal Guidance Report No. 13, prepared by Oak Ridge National Laboratory, Oak Ridge, Tenn., for U.S. Environmental Protection Agency, Office of Radiation Programs, Washington, D.C.

EPA (U.S. Environmental Protection Agency), 2001, "Risk Assessment, Radionuclide Table Slope Factors Download Area," April 16. Available at http://www.epa.gov/radiation/heast/download.htm.

ICRP (International Commission on Radiological Protection), 1983, *Radionuclide Transformations: Energy and Intensity of Emissions*, ICRP Publication 38, Annals of the ICRP, Vols. 11−13, Pergamon Press, New York, N.Y.

ICRP, 1996, *Age-Dependent Doses to Members of the Public from Intake of Radionuclides: Part 5 — Compilation of Ingestion and Inhalation Dose Coefficients*, ICRP Publication 72, Annals of the ICRP, Vol. 26(1), Pergamon Press, New York, N.Y.

APPENDIX B:

PARAMETER DISTRIBUTIONS

COMPILATION OF PARAMETER DISTRIBUTION DATA FOR THE RESRAD-OFFSITE CODE

Prepared by

B.M. Biwer, S. Kamboj, J.-J. Cheng, C.R. Yuen,
E. Gnanapragasam, and C. Yu

Environmental Science Division
Argonne National Laboratory

CONTENTS

CONTENTS (Cont.)

FIGURES

FIGURES (Cont.)

TABLES

TABLES (Cont.)

TABLES (Cont.)

TABLES (Cont.)

NOTATION

ABBREVIATIONS/ACRONYMS

CDF	cumulative distribution function
DOE	U.S. Department of Energy
EPA	U.S. Environmental Protection Agency
EPACMTP	U.S. Environmental Protection Agency Composite Model for Leachate Migration
EPRI	Electric Power Research Institute
FAO	Food and Agriculture Organization
IAEA	International Atomic Energy Agency
ICRP	International Commission on Radiological Protection
NCDC	National Climatic Data Center
NCRP	National Council on Radiation Protection and Measurements
NRC	U.S. Nuclear Regulatory Commission
NRCS	Natural Resources Conservation Service
PM-2.5	particulates less than or equal to 2.5 micrometers in diameter
REUWS	Residential End Use of Water Study
TSP	total suspended particulates
USDA	U.S. Department of Agriculture
USLE	universal soil loss equation

UNITS OF MEASURE

°C	degree(s) Celsius	m	meter(s)
		m^3	cubic meter(s)
d	day(s)	mm	millimeter(s)
ft	foot (feet)	pCi	picocurie(s)
g	gram(s)	s	second(s)
in.	inch(es)	yr	year(s)
L	liter(s)	µg	microgram(s)
		µm	micrometer(s)

1 INTRODUCTION

1.1 PURPOSE AND SCOPE

The parameter distributions used in the probabilistic RESRAD (onsite) and RESRAD-BUILD codes have been documented in Yu et al. (2000), Biwer et al. (2002), and Yu et al. (2003). This report provides parameter distributions for those new parameters used in the RESRAD-OFFSITE code. Some parameters used in the RESRAD (onsite) code have additional data available now; therefore, their parameter distribution data are also compiled. However, the primary focus of this report is on the new parameters used in the RESRAD-OFFSITE code. A Letter Report listing the parameters and parameter types was previously prepared and submitted to the U.S. Nuclear Regulatory Commission (NRC). This Letter Report is included as Attachment A.

1.2 BRIEF DESCRIPTION OF RESRAD-OFFSITE CODE

The RESRAD-OFFSITE code is a computer code that evaluates the radiological dose and excess cancer risk to an individual who is exposed while residing and/or working in or near an area where the soil is contaminated by radionuclides. It is an extension of the RESRAD (onsite) code, which was designed for evaluation of radiological doses to an onsite receptor (Yu et al. 2001). The RESRAD-OFFSITE code couples an atmospheric dispersion model, groundwater transport model, and offsite accumulation model with the RESRAD (onsite) code to permit calculation of doses to persons located beyond the contaminated site boundary. It calculates radiation dose and excess lifetime cancer risk to a chronically exposed onsite/offsite resident for different land-use and exposure scenarios. The code focuses on radioactive contaminants in soil and their transport in air, water, and biological media to a single receptor. Nine exposure pathways are considered in RESRAD-OFFSITE: direct exposure; inhalation of particulates and radon; and ingestion of plant foods, meat, milk, aquatic foods, water, and soil. RESRAD-OFFSITE uses a pathway analysis approach in which the concentrations in environmental media that connect the source to the receptor are computed at a series of times. These concentrations are used to compute the exposure, dose, and excess cancer risk. Radiation doses, health risks, soil guidelines, and media concentrations of radionuclides are calculated at a series of user-specified times. The source is adjusted over time to account for radioactive decay and ingrowth, leaching, erosion, and mixing. The user can construct exposure scenarios by suppressing exposure pathways and adjusting the input parameters.

1.3 PARAMETER CLASSIFICATION

The parameters used in the RESRAD-OFFSITE code are classified into three types: physical, behavioral, or metabolic, as described in Attachment A. Some parameters may belong to more than one of these types (e.g., the mass loading factor). Additionally, if a parameter does not fit either the physical or metabolic definition, it is classified as a behavioral parameter. Many parameters used in the RESRAD-OFFSITE code are the same as those used in the RESRAD

(onsite) code (Yu et al. 2001); therefore, the same parameters are assigned the same parameter types (NRC 2000).

> ***Physical Parameter:*** Any parameter whose value would not change if a different group of receptors were considered is classified as a physical parameter. Physical parameters are determined by the source, its location, and the geological characteristics of the site (i.e., these parameters are source- and site-specific).
>
> ***Behavioral Parameter:*** Any parameter whose value depends on the receptor's behavior and the scenario definition is classified as a behavioral parameter. For the same group of receptors, a parameter value could change if the scenario changes (e.g., parameters for recreational use could be different from those for residential use).
>
> ***Metabolic Parameter:*** If a parameter represents the metabolic characteristics of the potential receptor and is independent of the scenario, it is classified as a metabolic parameter. The parameter values may be different in different population age groups. According to the recommendations of the International Commission on Radiological Protection, Report 43 (ICRP 1985), parameters that represent metabolic characteristics are defined by average values for the general population. These values are not expected to be modified for a site-specific analysis because the parameter values would not depend on site conditions.

1.4 PARAMETERS SELECTED FOR ASSIGNMENT OF DISTRIBUTIONS

The selection of parameters follows the general rule developed for the RESRAD (onsite) parameter distribution data collection effort (Yu et al. 2000). However, priority was given to those new parameters used in RESRAD-OFFSITE. Additional data were collected for several parameters (e.g., the depth of roots and transfer factors for plants) because of the way they are used in the RESRAD-OFFSITE code (e.g., different plants grown in different fields).

The parameters selected for assignment of distributions are listed in Table 1.2-1. These parameters are grouped in four categories according to their use in the exposure calculations. The assigned parameter distributions are presented in the following sections according to the following categories: soils and hydrology (Section 2), atmospheric (Section 3), agriculture (Section 4), and receptor (Section 5). The presentation of each parameter distribution gives a brief description of the parameter, its units, its assigned distributions, and input data. Also presented is a discussion on the available data and the reasoning used to determine the distribution assignment. A detailed description of the distribution functions is included in Attachment B.

TABLE 1.2-1 Parameters Selected for Assignment of Probability Density Functions

Parameter	Type[a]	Assigned Distribution Type	Report Section
Volumetric water content	P	Continuous linear	2.1
Dispersivity	P	Continuous linear	2.2
Rainfall erosion index	P	Continuous linear	2.3
Soil erodibility factor	P	Continuous linear	2.4
Slope length-steepness factor	P	Continuous linear	2.5
Cover and management factor	P, B	Continuous linear	2.6
Support practice factor	P, B	Continuous linear	2.7
Depth of soil mixing layer	P, B	Triangular	2.8
Evapotranspiration coefficient	P	Uniform	2.9
Mass loading	P, B	Continuous linear, or truncated lognormal-n	3.1
Deposition velocity	P	Loguniform	3.2
Wind speed	P	Bounded lognormal-n	3.3
Duration of growing season	P	Triangular	4.1
Depth of roots	P	Uniform	4.2
Transfer factors for plants	P	Truncated lognormal-n	4.3
Quantity of water for household purposes	B, M	Continuous linear	5.1
Outdoor time fraction	B	Continuous linear	5.2

[a] P = physical parameter, B = behavioral parameter, and M = metabolic parameter.

2 SOILS AND HYDROLOGY PARAMETER DISTRIBUTIONS

2.1 VOLUMETRIC WATER CONTENT

Applicable Code: RESRAD-OFFSITE

Description: The volumetric water content is the fraction of the total volume of porous medium that is occupied by water.

Units: unitless

Probabilistic Input:

Distribution: continuous linear

Defining Values for Distribution: See Table 2.1-1 for the input values.

Discussion: The volumetric water content of the cover material is used to calculate the radon flux from the primary contamination. In offsite receptor areas (dwelling location, and agricultural and livestock feed growing areas) it is used to calculate contaminant concentrations, and, for tritium, to calculate plant-to-soil transfer and the transfer to meat and milk.

The volumetric water content, as a measure of the soil water content (moisture content), will range between a minimum value represented by the residual water content (irreducible water content) and a maximum value given by the total porosity. A further discussion on these latter concepts is given in Sections 3.2 and 3.3 of Attachment C in Yu et al. (2000). The water content of a soil is influenced by a number of factors, including soil type (available pore space), local topology (drainage issues), and geographic location (weather issues). Thus, only a very generic distribution may be suggested in the absence of site-specific data. To be functional, the receptor areas modeled in RESRAD-OFFSITE are assumed to be in areas with relatively good drainage; that is, they are not part of water retention or detention areas and are not routinely flooded. As such, the volumetric water content is assumed to be equal to the field capacity for the development of a default parameter distribution. The field capacity "is generally interpreted as the water content at which drainage from a field soil becomes negligible" (Meyer et al. 1997). Equating the volumetric water content to the field capacity for use in RESRAD-OFFSITE is also reasonable because analysis periods are in the time frame of years. Over this period of time, the affected land is more often expected to be in some state where drainage has occurred. Variations will occur based on season, precipitation events/irrigation, and dry spells.

To address variations in soil type, Table 2.1-2 lists the distribution of volumetric water content (assumed to be equivalent to the field capacity) for different U.S. Department of Agriculture (USDA) soil classifications. The values in the table are taken from Meyer et al. (1997) and based on the work of Carsel and Parish (1988). These distributions are either normal or lognormal depending on soil type.

TABLE 2.1-1 Cumulative Distribution Function for Volumetric Water Content

Volumetric Water Content	Cumulative Probability	Volumetric Water Content	Cumulative Probability
0.025	0.000	0.375	0.897
0.030	0.0002	0.40	0.934
0.040	0.003	0.425	0.961
0.047	0.010	0.45	0.979
0.056	0.028	0.48	0.991
0.070	0.070	0.53	0.999
0.080	0.104	0.56	1.000
0.10	0.175		
0.115	0.226		
0.13	0.272		
0.15	0.329		
0.29	0.705		
0.325	0.793		
0.35	0.849		

TABLE 2.1-2 Distribution Values for Volumetric Water Content by Soil Type

Soil Type	Distribution	Mean	Standard Deviation	Lower Limit	Upper Limit
Sand	LN(-2.83,0.241)[a]	0.0466	0.0106	0.0228	0.0907
Loamy sand	LN(-2.55,0.281)	0.0809	0.0224	0.0327	0.186
Sandy loam	LN(-2.21,0.314)	0.116	0.0369	0.0417	0.291
Sandy clay loam	LN(-1.59,0.254)	0.212	0.0568	0.0933	0.449
Loam	LN(-1.68,0.300)	0.194	0.0609	0.0735	0.468
Silt loam	Normal	0.252	0.0776	0.0119	0.491
Silt	Normal	0.236	0.0578	0.0575	0.415
Clay loam	LN(-1.27,0.297)	0.292	0.0862	0.112	0.700
Silty clay loam	Normal	0.347	0.0710	0.127	0.566
Sandy clay	LN(-1.23,0.210)	0.299	0.0623	0.153	0.559
Silty clay	Normal	0.334	0.0678	0.124	0.543
Clay	Normal	0.340	0.0893	0.0638	0.615

[a] LN(m,s) = lognormal distribution; m and s are the mean and standard deviation of the underlying normal distribution.

Source: Meyer et al. (1997); Carsel and Parrish (1988).

The distribution to be used when the type of soil is not known (the selected default for RESRAD-OFFSITE) was calculated as the weighted average of the distributions for the individual soil classes. The weighting factor scheme was the same as that for the generic soil type discussed in Section 3.1 of Attachment C in Yu et al. (2000). The probability density function of the weighted average was plotted, and the parameters of a user-defined continuous function were chosen to represent the weighted average curve over the range of interest. Figure 2.1-1 displays the cumulative distribution function for the volumetric water content for this generic soil type. When a site-specific analysis is conducted, the distribution for the soil type present at the site should be used. For consistency, distributions corresponding to the same soil type selected for this parameter should also be selected for the following parameters: soil density, total porosity, effective porosity, hydraulic conductivity, and the soil b parameter.

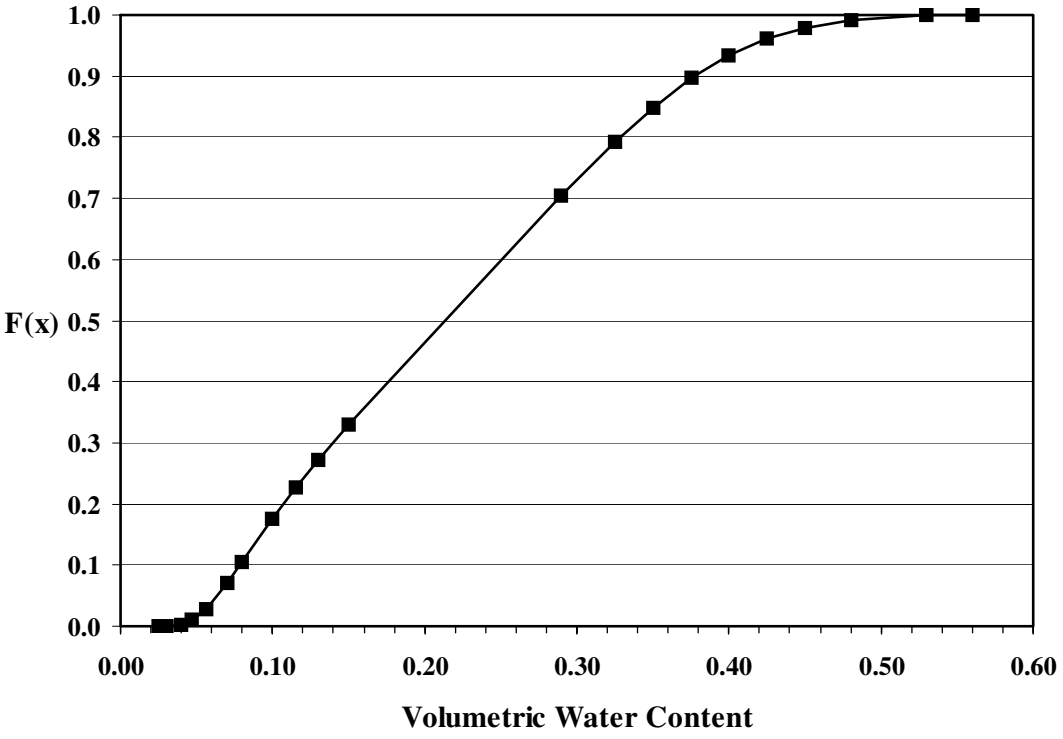

FIGURE 2.1-1 Volumetric Water Content Cumulative Distribution Function

2.2 DISPERSIVITY

Applicable Code: RESRAD-OFFSITE

Description: In a groundwater flow system modeled by the advection-dispersion equation, the dispersion of a contaminant in groundwater is characterized by the dispersion coefficient (or coefficient of hydrodynamic dispersion). The dispersion coefficient is composed of two components: mechanical mixing and diffusion. In coarse grain material such as sand, the dispersion caused by diffusion is relatively small and can be ignored. The dispersion caused by the mechanical mixing can be quantified by the dispersivity property (or dynamic dispersivity) of a porous medium.

Units: meters (m)

Probabilistic Input:

Distribution: continuous linear

Defining Values for Distribution: See Tables 2.2-1 through 2.2-3 for the input values.

Discussion: In the unsaturated zone, longitudinal dispersivity relates to the downward direction along the flow path. Preferential flow can occur through macropores in soil that are formed as aggregates of minerals, decayed root channels, cracks in clayey soils, and earthworm holes. These soil structures, though difficult to quantitatively define, can significantly affect various hydrogeological properties, including the dispersivity of soils (Vervoort et al. 1999).

Without direct site-specific measurements, a linear function may be used to derive the longitudinal dispersivity (EPA 2003):

$$\alpha_{LV} = 0.02 + 0.022 * D_u \,, \qquad (2.2\text{-}1)$$

where

D_u = total depth of the unsaturated zone (m).

This equation was based on a regression analysis of laboratory and field data presented by the Electric Power Research Institute (EPRI 1985), with a vertical scale of experiments ranging from 0.23 to 20 meters and has a correlation coefficient of 0.66. A similar approach of using a linear function to estimate the longitudinal dispersivity was applied by the MEPAS codes. In MEPAS, the longitudinal dispersivity is assumed to be one percent of the thickness of the unsaturated zone (Ho et al. 2002).

A default nationwide landfill modeling analysis using the regional site-based methodology was performed for the EPA's Composite Model for Leachate Migration with Transformation Products (EPACMTP) (EPA 2003). A distribution of values for longitudinal dispersivity was derived through Monte Carlo sampling of the unsaturated zone thickness from

TABLE 2.2-1 Cumulative Distribution for the Unsaturated Zone Longitudinal Dispersivity

Longitudinal Dispersivity (m)	Cumulative Probability
0.0267	0.00
0.057	0.10
0.107	0.25
0.154	0.50
0.354	0.75
0.423	0.80
0.665	0.85
0.959	0.90
1	0.95
1	1.00

Source: EPA (2003).

its Hydrogeologic Database for Groundwater Modeling. This distribution is summarized in Table 2.2-1, shown in Figure 2.2-1, and used in RESRAD-OFFSITE as the default distribution for longitudinal dispersivity for the unsaturated zone.

The dispersivity in the saturated zone is measured in three directions. The longitudinal dispersivity is along the preferred groundwater flow direction (the x direction), and the horizontal transverse (y direction) and the vertical transverse (z direction) dispersivities are perpendicular to the flow direction.

Most studies of dispersion reported in the literature have involved relatively homogeneous sandy materials under controlled conditions in the laboratory. Based on 2,500 column dispersion tests on disturbed and undisturbed samples of unconsolidated geological materials, Klotz and Moser (1974) found that dispersivity increases with the grain size and the uniformity coefficient of grain-size distribution of samples. Less uniform materials (with higher uniformity coefficient) have higher dispersivities. Other soil physical parameters, such as grain shape, grain roughness, grain angularity, and compactness can also affect the dispersivity, but to a lesser extent. Taking all of these parameters into consideration, the dispersion coefficient is a characteristic quantity of a soil and is independent of permeability.

Though laboratory studies are important in understanding various factors affecting saturated zone dispersivity, field studies on dispersivity find more practical uses. Neuman (1990) demonstrated that longitudinal dispersivity increases with distance scale in a variety of hydrogeologic settings. In laboratory studies, Gelhar et al. (1992) found that values of longitudinal dispersivity are typically in the range of 0.1-10 mm, with transverse dispersivity values normally lower by a factor of 5-20. In the fields, the values of longitudinal dispersivity as

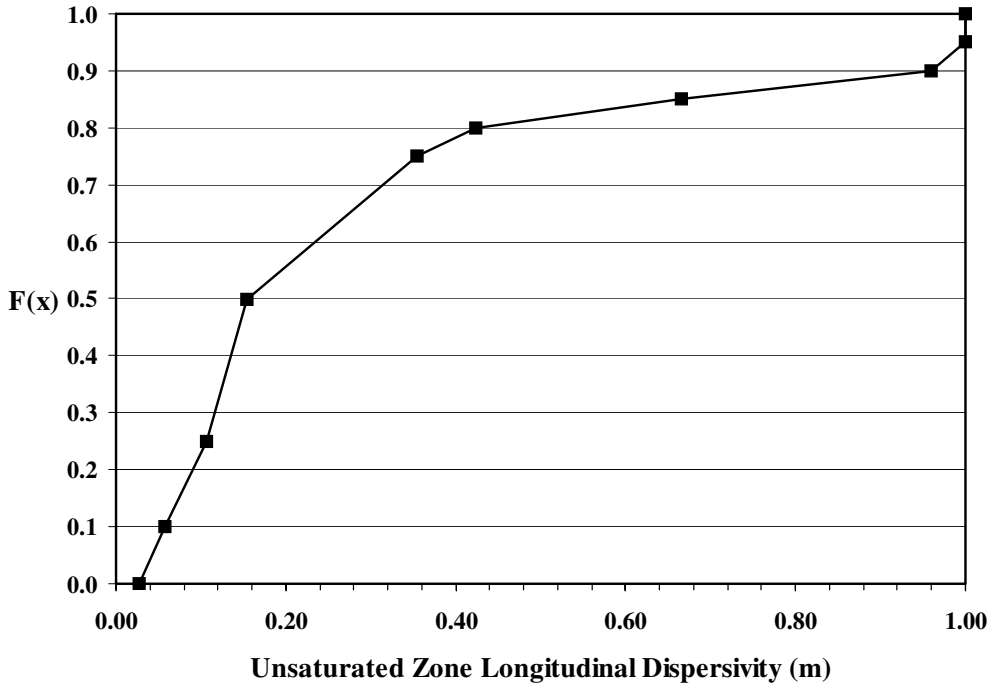

FIGURE 2.2-1 Cumulative Distribution Function for the Unsaturated Zone Longitudinal Dispersivity

large as 100 m and lateral dispersivity values as large as 50 m have been used in mathematical simulation studies of the migration of large contaminant plume in sandy aquifers (Gelhar et al. 1992). By using additional data and the data compiled by Gelhar et al. (1992), Schulze-Makuch (2005) suggested that the scaling relationship of longitudinal dispersivity can be described by the empirical power law:

$$\alpha_L = c(L)^m \ , \qquad (2.2\text{-}2)$$

where

α_L = longitudinal dispersivity,

L = flow distance, and

c, m = empirical fit constants,

with c and m varying with different geologic materials. In exploring the scaling effect of the longitudinal dispersivity, both Gelhar et al. (1992) and Schulze-Makuch (2005) emphasized the reliability of published data in their analyses. Eighty-eight high and immediate reliable category data compiled by Gelhar et al. (1992) and Schulze-Makuch (2005) for sediments were used to derive c and m (0.11 and 0.7 respectively). These values may be used in equation 2.2-2 to calculate the longitudinal dispersivity in saturated groundwater flow. The transverse

dispersivities may then be estimated assuming that the longitudinal dispersivity is 8 times larger than the horizontal traverse dispersivity and 160 times larger than the vertical traverse dispersivity (EPA 2003).

In the EPACMTP, a default modeling analysis, using the regional site-based modeling methodology, generated the CDF for longitudinal dispersivity for the saturated zone listed in Table 2.2-2 and shown in Figure 2.2-2. This distribution is the default for use in RESRAD-OFFSITE for general analyses. Site-specific analyses should employ site-specific data. The corresponding horizontal transverse and vertical transverse dispersivity distributions are provided in Tables 2.2-3 and 2.2-4 and shown in Figures 2.2-3 and 2.2-4, respectively.

TABLE 2.2-2 Cumulative Distribution for the Saturated Zone Longitudinal Dispersivity

Longitudinal Dispersivity (m)	Cumulative Probability
0.100	0.00
1.22	0.10
3.62	0.25
8.96	0.50
25.4	0.75
43.2	0.80
65.3	0.85
92.1	0.90
135	0.95
318	1.00

Source: EPA (2003).

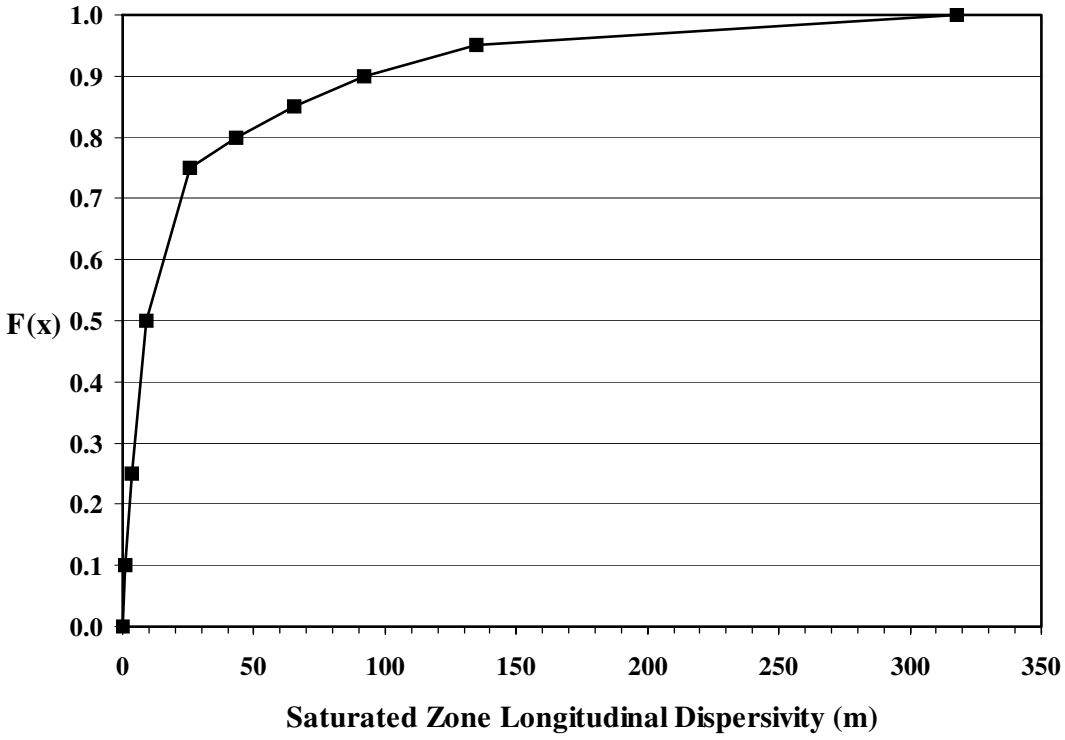

FIGURE 2.2-2 Cumulative Distribution Function for the Saturated Zone Longitudinal Dispersivity

TABLE 2.2-3 Cumulative Distribution for the Saturated Zone Horizontal Transverse Dispersivity

Horizontal Transverse Dispersivity (m)	Cumulative Probability
0.0125	0.00
0.153	0.10
0.452	0.25
1.12	0.50
3.17	0.75
5.40	0.80
8.16	0.85
11.5	0.90
16.9	0.95
39.7	1.00

Source: EPA (2003).

TABLE 2.2-4 Cumulative Distribution for the Saturated Zone Vertical Transverse Dispersivity

Vertical Transverse Dispersivity (m)	Cumulative Probability
0.0100	0.00
0.0100	0.10
0.0226	0.25
0.0560	0.50
0.158	0.75
0.270	0.80
0.408	0.85
0.576	0.90
0.845	0.95
1.99	1.00

Source: EPA (2003).

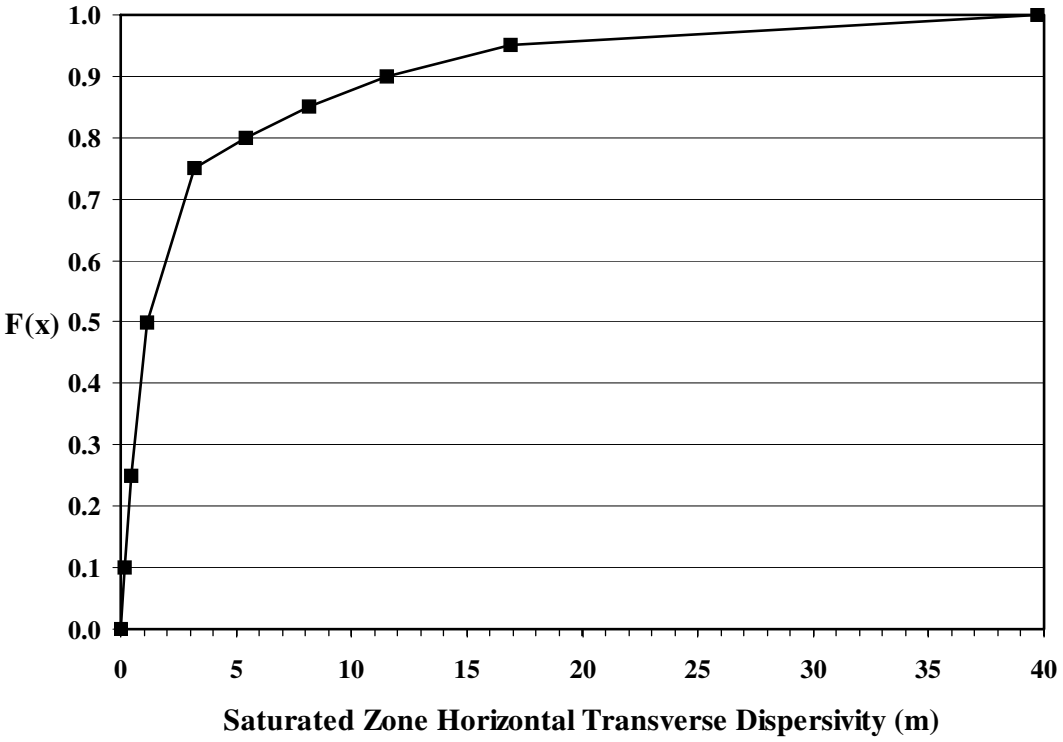

FIGURE 2.2-3 Cumulative Distribution Function for the Saturated Zone Horizontal Transverse Dispersivity

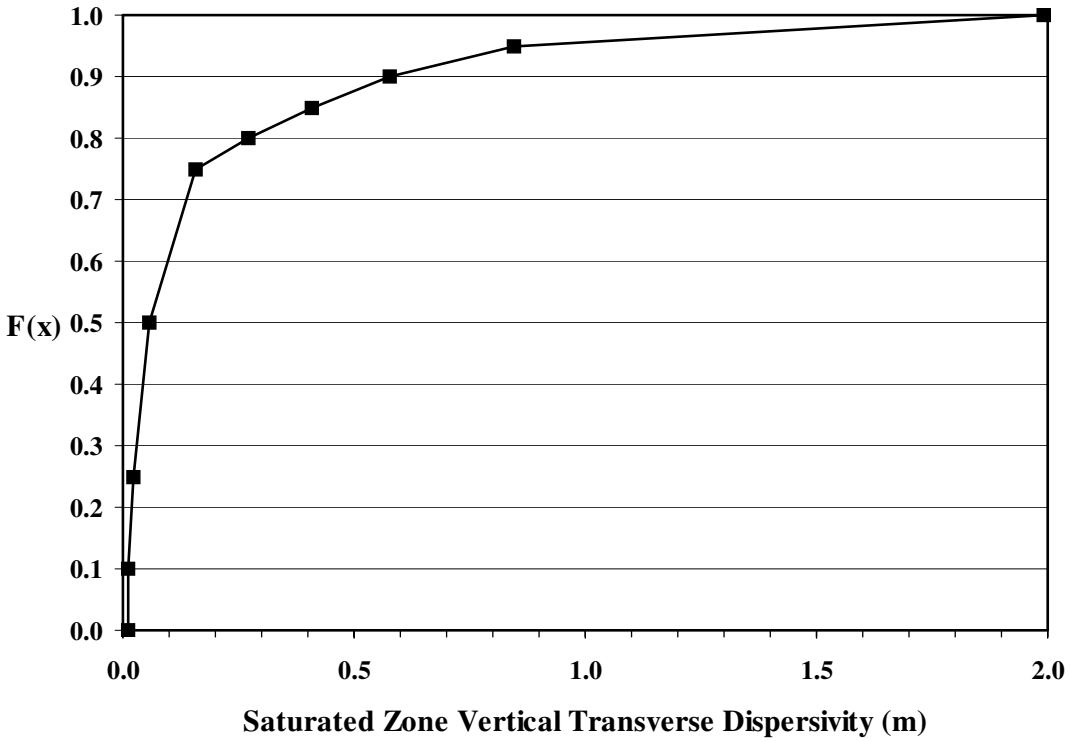

FIGURE 2.2-4 Cumulative Distribution Function for the Saturated Zone Vertical Transverse Dispersivity

2.3 RAINFALL EROSION INDEX

Applicable Code: RESRAD-OFFSITE

Description: The rainfall erosion index is a measure of soil erosion due to rainfall.

Units: unitless

Probabilistic Input:

Distribution: continuous linear

Defining Values for Distribution: See Table 2.3-1 for the input values.

Discussion: RESRAD-OFFSITE uses the soil erosion rate to estimate surface soil concentrations in the primary contamination area. These concentrations are used to estimate the release of radionuclide contaminants to the atmosphere and groundwater and are also used to calculate inhalation and soil ingestion doses to onsite receptors. The amount of contaminants released to the atmosphere is used to estimate the accumulation of the radionuclides downwind in the agricultural and livestock feed areas.

The universal soil loss equation (USLE) (Wischmeier and Smith 1978) is used in RESRAD-OFFSITE to estimate the erosion rate of soil in contaminated and agricultural areas. The USLE was developed over many years as a tool in water and soil conservation planning to estimate long-term average soil losses as a function of different cropping and management systems. The equation is written as:

$$A = RKLSCP\,, \tag{2.3-1}$$

where

A = the estimated soil loss per unit area, typically expressed in tons/acre per yr;

R = the rainfall and runoff factor;

K = soil erodibility factor;

LS = the slope length-steepness factor;

C = the cover and management factor; and

P = the support practice factor.

The soil erodibility factor, the slope length-steepness factor, the cover and management factor, and the support practice factor are discussed further in Sections 2.4 through 2.7, respectively.

TABLE 2.3-1 Cumulative Distribution for the Rainfall Erosion Index

Rainfall Erosion Index	Cumulative Probability
5	0.000777
65	0.177
123	0.341
200	0.683
315	0.863
400	0.967
475	0.991
600	1.00

The rainfall erosion index is used as the rainfall and runoff factor (R) in the USLE. The rainfall and runoff factor accounts for erosion due to rainfall and is defined as "the number of rainfall erosion index units, plus a factor for runoff from snowmelt or applied water where such runoff is significant" (Wischmeier and Smith 1978). The standard rainfall erosion index is a measure of the erosive forces due to rainfall and its runoff. An added term may be used to account for erosion due to surface thaws and snowmelt in northern sections of the United States. The suggested magnitude of the added term is 1.5 times the December through March precipitation measured as inches of water (Wischmeier and Smith 1978).

The rainfall erosion index can be evaluated on a storm by storm basis according to (Wischmeier and Smith 1978; Shen and Julien 1993):

$$R = 0.01 \sum EI \,, \tag{2.3-2}$$

where

E = the kinetic energy of the storm (foot-tons per acre-inch), and

I = the rainfall intensity (inches/hour),

with the summation performed over increments of the storm. The rainfall energy is directly related to the rainfall intensity:

$$E = 916 + 3311 \log_{10} I \,. \tag{2.3-3}$$

Soil erosion is highly dependent on site-specific parameters that are considered in the USLE. Local values for the rainfall erosion index can be estimated from Figure 1 in Wischmeier and Smith (1978), which provides isocontours of the index across the United States. This

reference also provides 50-, 20-, and 5-percent probability values for the erosion index at 181 locations across the United States in addition to single storm values for *EI*. Local values will also vary on an annual basis. However, longer-term averages are more appropriate for use in RESRAD-OFFSITE when considering impacts for years, decades, or more in the future.

The Natural Resources Conservation Service (NRCS) of the USDA has published the 1997 National Resources Inventory (USDA 2001), which contains a database with records for over 800,000 locations within the United States. Each record contains values for the parameters in the USLE. Because the database is designed for the statistical analysis of general conditions and trends involving soil, water, and related resources, individual farms and fields are not identified. From these data, a default distribution for the rainfall erosion index has been developed for RESRAD-OFFSITE that provides a national coverage. The distribution is listed in Table 2.3-1 and shown in Figure 2.3-1. The appropriate value or distribution of values for a site-specific soil erosion index are best determined in consultation with the expert at your local state agricultural extension office.

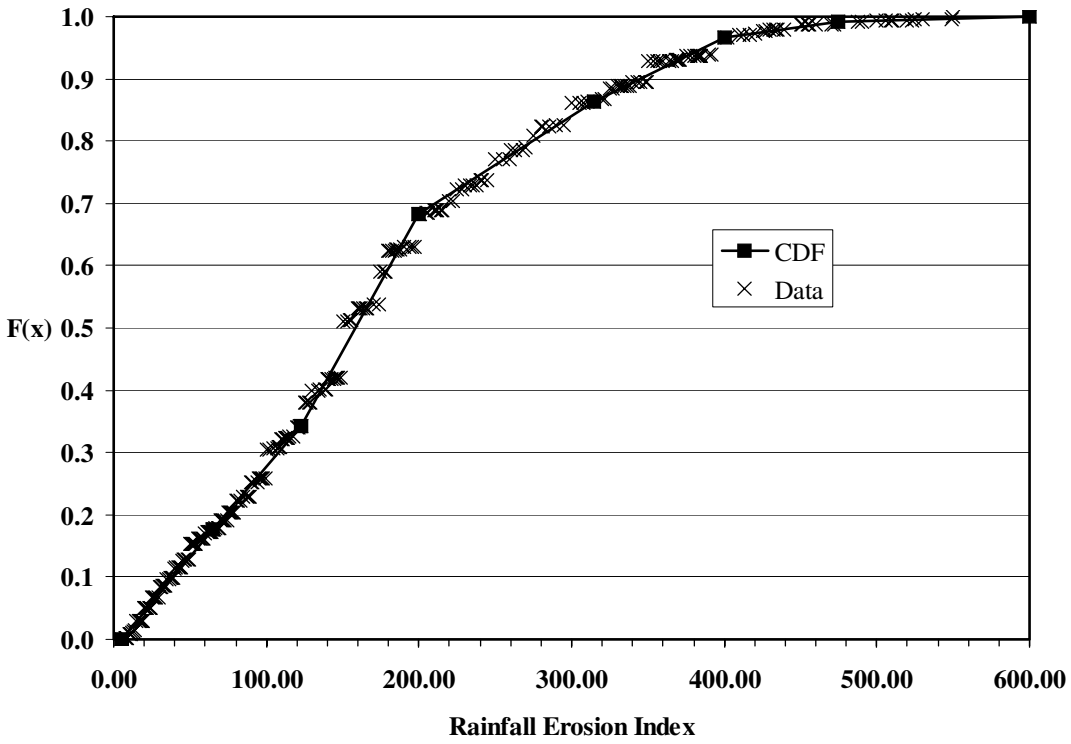

FIGURE 2.3-1 Cumulative Distribution Function for the Rainfall Erosion Index

2.4 SOIL ERODIBILITY FACTOR

Applicable Code: RESRAD-OFFSITE

Description: The soil erodibility factor quantifies the susceptibility of soil to erosion processes.

Units: tons/acre

Probabilistic Input:

Distribution: continuous linear

Defining Values for Distribution: See Table 2.4-1 for the input values.

Discussion: The soil erodibility factor (K) is part of the USLE, discussed previously in Section 2.3. As incorporated into RESRAD-OFFSITE, the USLE estimates the amount of soil erosion that occurs in the primary contamination area. The soil erosion rate is used to estimate surface soil concentrations in the primary contamination area. These concentrations are used to estimate the release of radionuclide contaminants to the atmosphere and groundwater and are also used to calculate inhalation and soil ingestion doses to onsite receptors. The amount of contaminants released to the atmosphere is used to estimate the accumulation of the radionuclides downwind in the agricultural and livestock feed areas.

The inherent properties of the soil at a given location influence the soil erosion rate in addition to such factors as land slope, cover, management practices, precipitation events, and runoff. Relevant soil properties characterized by the soil erodibility factor include grain size distribution, texture, permeability, and organic content (Shen and Julien 1993). Sample values for the erodibility factor are listed in Table 2.4-2 for two different levels of organic content. Further information on the soil erodibility factor, including a nomograph for determining its value, can be found in Wischmeier and Smith (1978). Additional discussion on the soil erodibility factor can be found in Renard et al. (1997).

TABLE 2.4-1 Cumulative Distribution for the Erodibility Factor

Erodibility Factor (tons/acre)	Cumulative Probability
0.01	1.99×10^{-6}
0.08	0.00495
0.15	0.107
0.25	0.364
0.37	0.869
0.43	0.961
0.49	0.996
0.64	1.00

TABLE 2.4-2 Soil Erodibility Factor (tons/acre)

	Organic Matter Content, %	
Textural Class	0.5	2
Fine sand	0.16	0.14
Very fine sand	0.42	0.36
Loamy sand	0.12	0.1
Loamy very fine sand	0.44	0.38
Sandy loam	0.27	0.24
Very fine sandy loam	0.47	0.41
Silt loam	0.48	0.42
Clay loam	0.28	0.25
Silty clay loam	0.37	0.32
Silty clay	0.25	0.23

Source: Shen and Julien (1993).

The NRCS of the USDA has published the 1997 National Resources Inventory (USDA 2001), which contains a database with records for over 800,000 locations within the United States. Each record contains values for the parameters in the USLE. Because the database is designed for the statistical analysis of general conditions and trends involving soil, water, and related resources, individual farms and fields are not identified. From these data, a default distribution for the soil erodibility factor has been developed for RESRAD-OFFSITE that provides a national coverage. The distribution is listed in Table 2.4-1 and shown in Figure 2.4-1. The appropriate value or distribution of values for a site-specific soil erodibility factor are best determined in consultation with the expert at your local state agricultural extension office.

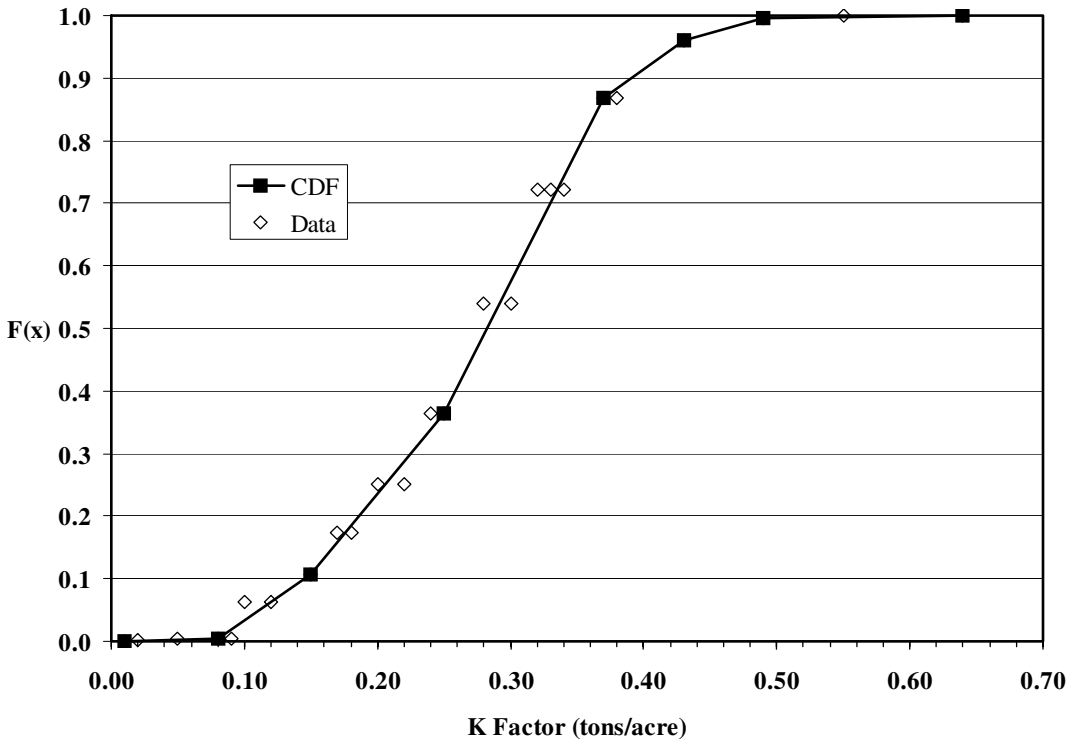

FIGURE 2.4-1 Soil Erodibility Factor Cumulative Distribution Function

2.5 SLOPE LENGTH-STEEPNESS FACTOR

Applicable Code: RESRAD-OFFSITE

Description: The slope length-steepness factor accounts for the effect of length and steepness of the land slope on erosion processes.

Units: unitless

Probabilistic Input:

Distribution: continuous linear

Defining Values for Distribution: See Table 2.5-1 for the input values.

Discussion: The slope length-steepness factor (LS) is part of the USLE, discussed previously in Section 2.3. As incorporated into RESRAD-OFFSITE, the USLE estimates the amount of soil erosion that occurs in the primary contamination area. The soil erosion rate is used to estimate surface soil concentrations in the primary contamination area. These concentrations are used to estimate the release of radionuclide contaminants to the atmosphere and groundwater and are also used to calculate inhalation and soil ingestion doses to onsite receptors. The amount of contaminants released to the atmosphere is used to estimate the accumulation of the radionuclides downwind in the agricultural and livestock feed areas.

The slope length-steepness factor is the ratio of soil loss per unit area from a field slope to that from a 72.6 ft length of uniform 9-percent slope under otherwise identical conditions (Wischmeier and Smith 1978). As the name implies, this factor is actually a combination of the slope length factor (L) and the slope steepness factor (S) which are often considered together as the single topographic factor, LS. The slope length factor is the ratio of field soil loss to the corresponding 72.6 ft slope length, given as (Wischmeier and Smith 1978):

$$L = \left(\frac{\lambda}{72.6} \right)^{m} , \qquad (2.5\text{-}1)$$

where

λ = the field slope length (ft); and

m = 0.2 when the slope percent slope < 1 percent, 0.3 for slopes of 1 to 3 percent, 0.4 for slopes of 3.5 to 4.5 percent, or 0.5 for slopes >= 5 percent;

and the slope percent is defined as vertical distance divided by the horizontal distance multiplied by 100 (i.e., rise/run × 100 for a given slope).

TABLE 2.5-1 Cumulative Distribution for the Slope Length-Steepness Factor

Slope Length-Steepness Factor	Cumulative Probability
0.0316	0.000206
0.15	0.301
0.30	0.566
0.60	0.745
1.5	0.893
5.00	0.978
20.0	0.998
49.2	1.00

The slope steepness factor (S) is evaluated by (Wischmeier and Smith 1978):

$$S = 65.41 sin^2\theta + 4.56 sin\theta + 0.065 , \tag{2.5-2}$$

where

$$\theta = angle\ of\ \ slope = \tan^{-1}\left(\frac{slope\ \ percent}{100}\right). \tag{2.5-3}$$

The slope length-steepness factor (LS) is then given by the combination of equations 2.5-1 and 2.5-2:

$$LS = \left(\frac{\lambda}{72.6}\right)^m \ (65.41 sin^2\theta + 4.56 sin\theta + 0.065). \tag{2.5-4}$$

Additional information about determining the proper values for L and S can be found in Wischmeier and Smith (1978) and Renard et al. (1997), including adjustments for irregular slopes or varying soil types. In addition, the values for m listed above for use in equation 2.5-1 are only average values. Renard et al. (1997) provide more detailed data on refining the value of m for a specific field slope.

The NRCS of the USDA has published the 1997 National Resources Inventory (USDA 2001), which contains a database with records for over 800,000 locations within the United States. Each record contains values for the parameters in the USLE. Because the database is designed for the statistical analysis of general conditions and trends involving soil, water, and related resources, individual farms and fields are not identified. From the values of slope length and slope percent from these data, a default distribution for the slope length-steepness factor has

been developed for RESRAD-OFFSITE, by using equation 2.5-3, that provides a national coverage. The distribution is listed in Table 2.5-1 and shown in Figure 2.5-1. The appropriate value or distribution of values for a site-specific slope length-steepness factor are best determined by using equation 2.5-3 or in consultation with the expert at your local state agricultural extension office.

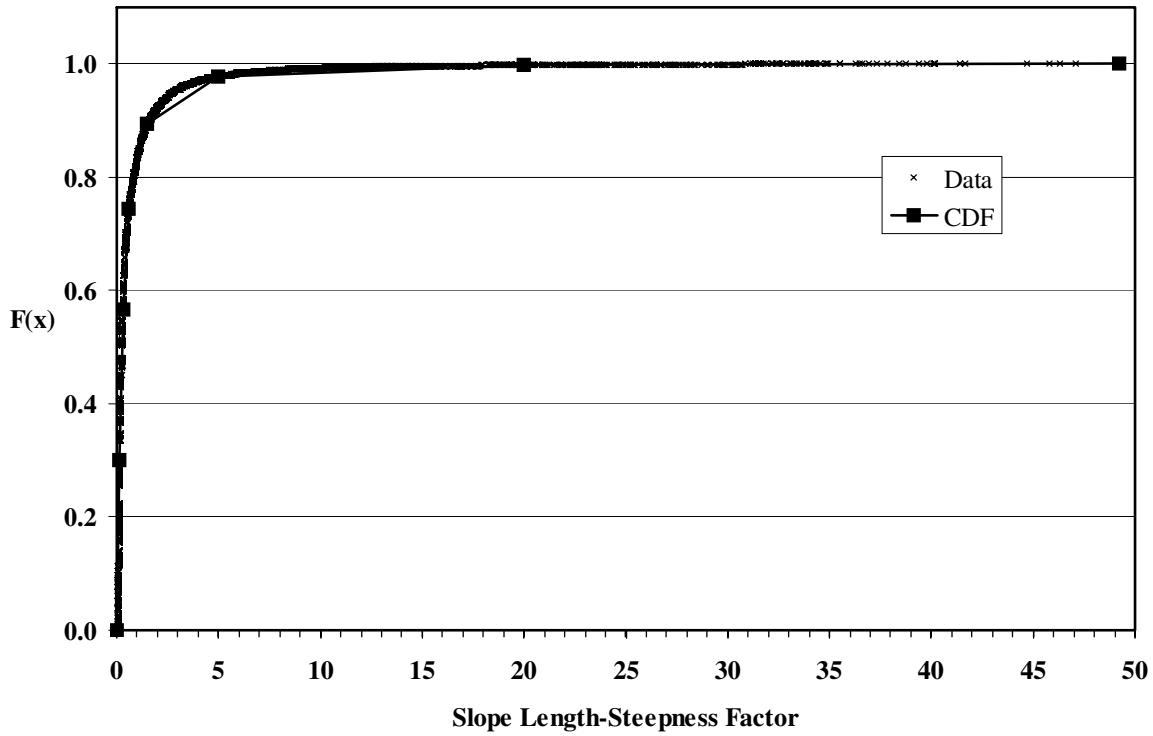

FIGURE 2.5-1 Slope Length-Steepness Factor Cumulative Distribution Function

2.6 COVER AND MANAGEMENT FACTOR

Applicable Code: RESRAD-OFFSITE

Description: The cover and management factor accounts for the effect of planting practices, crop rotations, management of crop residue, and canopy protection on soil erosion at the contaminated area.

Units: unitless

Probabilistic Input:

Distribution: continuous linear

Defining Values for Distribution: See Table 2.6-1 for the input values.

Discussion: The cover and management factor (C) is part of the USLE, discussed previously in Section 2.3. As incorporated into RESRAD-OFFSITE, the USLE estimates the amount of soil erosion that occurs in the primary contamination area. The soil erosion rate is used to estimate surface soil concentrations in the primary contamination area. These concentrations are used to estimate the release of radionuclide contaminants to the atmosphere and groundwater and are also used to calculate inhalation and soil ingestion doses to onsite receptors. The amount of contaminants released to the atmosphere is used to estimate the accumulation of the radionuclides downwind in the agricultural and livestock feed areas.

TABLE 2.6-1 Cumulative Distribution for the Cover and Management Factor

Cover and Management Factor	Cumulative Probability
0.00001	3.17×10^{-6}
0.020	0.327
0.085	0.421
0.149	0.519
0.284	0.845
0.400	0.961
0.550	0.991
1.00	1.00

Cover and management effects are closely intertwined because the type of cover present is dependent on how the land is managed. Crops can be grown in rotation, continuously, or the land can be laid fallow between crops. Seed bed preparation can involve various levels of previous crop or other plant residue left on the surface and various degrees of surface roughness due to tillage. Harvesting will also leave a certain amount of residue on the surface until the field is prepared for the next crop. Land may also be unmanaged and consist of open or forested areas.

The cover and management factor accounts for these effects and is defined as the ratio of soil loss from land cropped under certain conditions with the corresponding loss from clean-tilled continuous fallow conditions (Wischmeier and Smith 1978). Tables 2.6-2 and 2.6-3 present suggested values for the cover and management factor for pasture areas and forest land, respectively. More details on estimating this factor for farmed areas can be found in Wischmeier and Smith (1978) and Renard et al. (1997).

The NRCS of the USDA has published the 1997 National Resources Inventory (USDA 2001), which contains a database with records for over 800,000 locations within the United States. Each record contains values for the parameters in the USLE. Because the database is designed for the statistical analysis of general conditions and trends involving soil, water, and related resources, individual farms and fields are not identified. From these data, a default distribution for the cover and management factor has been developed for RESRAD-OFFSITE that provides a national coverage. The distribution is listed in Table 2.6-1 and shown in Figure 2.6-1. The appropriate value or distribution of values for a site-specific cover and management factor are best determined in consultation with the expert at your local state agricultural extension office.

TABLE 2.6-2 Cover and Management Factor C for Permanent Pasture, Range, and Idle Land[a]

Vegetative Canopy		Cover that Contacts the Soil Surface						
			Percent Ground Cover					
Type and Height[b]	Percent Cover[c]	Type[d]	0	20	40	60	80	95+
No appreciable canopy		G	0.45	0.20	0.10	0.042	0.013	0.003
		W	0.45	0.24	0.15	0.091	0.043	0.011
Tall weeds or short brush, with average drop fall height of 20 in.	25	G	0.36	0.17	0.09	0.038	0.013	0.003
		W	0.36	0.20	0.13	0.083	0.041	0.011
	50	G	0.26	0.13	0.07	0.035	0.012	0.003
		W	0.26	0.16	0.11	0.076	0.039	0.011
	75	G	0.17	0.10	0.06	0.032	0.011	0.003
		W	0.17	0.12	0.09	0.068	0.038	0.011
Appreciable brush or bushes, with average drop fall height of 6½ ft .	25	G	0.40	0.18	0.09	0.040	0.013	0.003
		W	0.40	0.22	0.14	0.087	0.042	0.011
	50	G	0.34	0.16	0.08	0.038	0.012	0.003
		W	0.34	0.19	0.13	0.082	0.041	0.011
	75	G	0.28	0.14	0.08	0.036	0.012	0.003
		W	0.28	0.17	0.12	0.078	0.040	0.011
Trees, but no appreciable low brush, with average drop fall height of 13 ft	25	G	0.42	0.19	0.10	0.041	0.013	0.003
		W	0.42	0.23	0.14	0.089	0.042	0.011
	50	G	0.39	0.18	0.09	0.040	0.013	0.003
		W	0.39	0.21	0.14	0.087	0.042	0.011
	75	G	0.36	0.17	0.09	0.039	0.012	0.003
		W	0.36	0.20	0.13	0.084	0.041	0.011

[a] The listed C values assume that the vegetation and mulch are randomly distributed over the entire area.

[b] Canopy height is measured as the average fall height of water drops falling from the canopy to the ground. Canopy effect is inversely proportional to drop fall height and is negligible if fall height exceeds 33 ft.

[c] Portion of total-area surface that would be hidden from view by the canopy in a vertical projection (a bird's-eye view).

[d] G: cover at surface is grass, grasslike plants, decaying compacted duff, or litter at least 2 in. deep.

W: cover at surface is mostly broadleaf herbaceous plants (as weeds with little lateral-root network near the surface) or undecayed residues or both.

Source: Wischmeier and Smith (1978).

TABLE 2.6-3 Cover and Management Factor C for Undisturbed Forest Land[a]

Percent of Area Covered by Canopy of Trees and Undergrowth	Percent of Area Covered by Duff at Least 2 in. Deep	Factor C[b]
100-75	100-90	.0001-.001
70-45	85-75	.002-.004
40-20	70-40	.003-.009

[a] Where effective litter cover is less than 40 percent or canopy cover is less than 20 percent, use Table 2.6-2. Also use Table 2.6-2 where woodlands are being grazed, harvested, or burned.

[b] The ranges in listed C values are caused by the ranges in the specified forest litter and canopy covers and by variations in effective canopy heights.

Source: Wischmeier and Smith (1978).

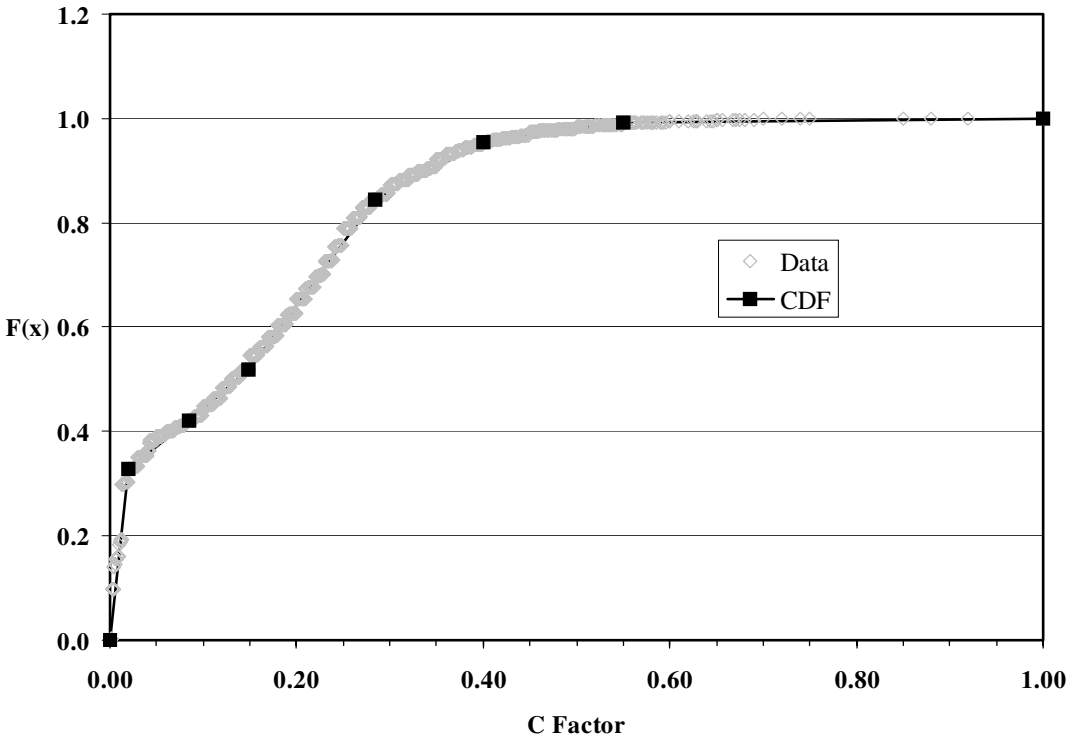

FIGURE 2.6-1 Cover and Management Factor Cumulative Distribution Function

2.7 SUPPORT PRACTICE FACTOR

Applicable Code: RESRAD-OFFSITE

Description: The support practice factor accounts for the effect of contouring, strip cropping, and terracing on soil erosion at the contaminated area.

Units: unitless

Probabilistic Input:

Distribution: continuous linear

Defining Values for Distribution: See Table 2.7-1 for the input values.

Discussion: The support practice factor (P) is part of the USLE, discussed previously in Section 2.3. As incorporated into RESRAD-OFFSITE, the USLE estimates the amount of soil erosion that occurs in the primary contamination area. The soil erosion rate is used to estimate surface soil concentrations in the primary contamination area. These concentrations are used to estimate the release of radionuclide contaminants to the atmosphere and groundwater and are also used to calculate inhalation and soil ingestion doses to onsite receptors. The amount of contaminants released to the atmosphere is used to estimate the accumulation of the radionuclides downwind in the agricultural and livestock feed areas.

The support practice factor is defined as the ratio of soil loss with a specific support practice to the corresponding loss with upslope and downslope tillage (Wischmeier and Smith 1978). Thus, the support practice factor equals a value of 1.0 for crop rows running straight up-and-down a slope. Specific support practices include contouring, strip cropping, or terracing. Crop rotations, the amount of plant residue material, and other tillage practices are not considered here because these practices are considered as part of the cover and management factor (Section 2.6).

TABLE 2.7-1 Cumulative Distribution for the Support Practice Factor

Support Practice Factor	Cumulative Probability
0.25	0.00170
0.45	0.00821
0.55	0.0379
0.6	0.0604
0.75	0.0715
0.99	0.0782
1.00	1.00

Tillage and planting on the contour has shown to be the most effective on slopes in the 3-8-percent range (Wischmeier and Smith 1978). For smaller slopes, the land slope approaches the contour slope, and for larger slopes, the contour row capacity decreases. The slope length has an impact on the effectiveness of contouring because of water detention characteristics (infiltration and surface capacity) during precipitation events. If contour rows are breached by excess water, more soil could be lost than if the rows are oriented up and down the slope to carry the water away. Table 2.7-2 lists some approximate support practice factors depending on land slope percent and slope length. Table 2.7-3 lists values for the support practice factor when strip cropping is employed. Strip cropping, a practice that is more effective than contouring alone, involves alternating strips of sod and row crops or small grains on the contour. Terracing can further reduce erosion and can be combined with other practices, such as those considered with the cover and management factor (Section 2.6). More details on estimating this factor for farmed areas can be found in Wischmeier and Smith (1978) and Renard et al. (1997).

TABLE 2.7-2 Support Practice Factor P Values and Slope-Length Limits for Contouring

Land Slope Percent	(P) Value	Maximum Length (ft)[a]
1 to 2	0.60	400
3 to 5	0.50	300
6 to 8	0.50	200
9 to 12	0.60	120
13 to 16	0.70	80
17 to 20	0.80	60
21 to 25	0.90	50

[a] Limit may be increased by 25 percent if residue cover after crop seedlings will regularly exceed 50 percent.

Source: Wischmeier and Smith (1978).

TABLE 2.7-3 Support Practice Factor P Values, Maximum Strip Widths, and Slope-Length Limits for Contour Stripcropping

Land Slope Percent	P Values[a] A	B	C	Strip Width (feet)[b]	Maximum Length (feet)
1 to 2	0.30	0.45	0.60	130	800
3 to 5	.25	.38	.50	100	600
6 to 8	.25	.38	.50	100	400
9 to 12	.30	.45	.60	80	240
13 to 16	.35	.52	.70	80	160
17 to 20	.40	.60	.80	60	120
21 to 25	.45	.68	.90	50	100

[a] P values:

A: for 4-year rotation of row crop, small grain with meadow seedings, and 2 years of meadow. A second row crop can replace the small grain if meadow is established in it.

B: for 4-year rotation of 2 years row crop, winter grain with meadow seeding, and 1-year meadow.

C: for alternate strips of row crop and small grain.

[b] Adjust strip-width limit, generally downward, to accommodate widths of farm equipment.

Source: Wischmeier and Smith (1978).

The NRCS of the USDA has published the 1997 National Resources Inventory (USDA 2001), which contains a database with records for over 800,000 locations within the United States. Each record contains values for the parameters in the USLE. Because the database is designed for the statistical analysis of general conditions and trends involving soil, water, and related resources, individual farms and fields are not identified. From this data, a default distribution for the support practice factor has been developed for RESRAD-OFFSITE that provides a national coverage. The distribution is listed in Table 2.7-1 and shown in Figure 2.7-1. The appropriate value or distribution of values for a site-specific support practice factor are best determined in consultation with the expert at your local state agricultural extension office.

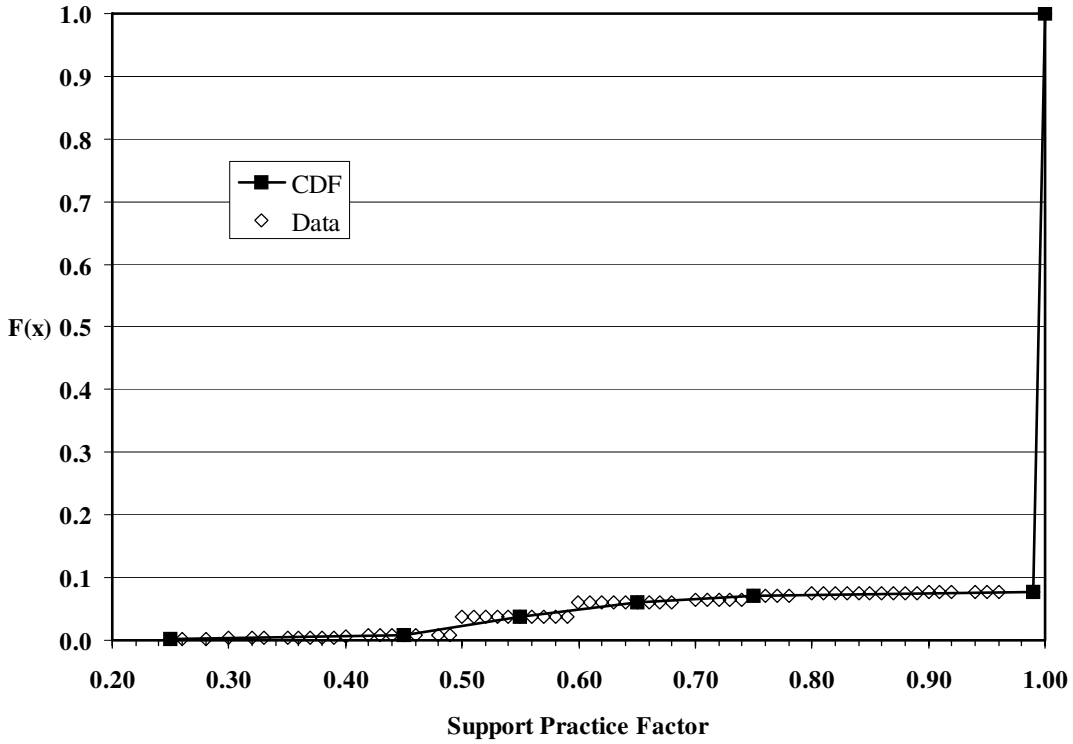

FIGURE 2.7-1 Support Practice Factor Cumulative Distribution Function

2.8 DEPTH OF SOIL MIXING LAYER

Applicable Code: RESRAD (onsite), RESRAD-OFFSITE

Description: The depth of soil mixing layer parameter is used in calculating the depth factor for the dust inhalation and soil ingestion pathways and for foliar deposition for the ingestion pathway.

Units: meters (m)

Probabilistic Input

Distribution: triangular

Defining Values for Distribution:

Minimum: 0.0 Maximum: 0.6 Most likely: 0.15

Discussion: The depth factor is the fraction of resuspendable soil particles at the ground surface that are contaminated. It is calculated by assuming that mixing of the soil with contamination will occur within the uppermost soil layer. The thickness of this layer is equal to the depth of the soil mixing layer.

Mixing of the upper soil layer can occur through atmospheric (wind or precipitation/runoff) and mechanical disturbances. For a residential farmer scenario, the greatest affected depths, on a routine basis, result from mechanical disturbances. Such disturbances include use of farm equipment (e.g., plowing) and foot and vehicle traffic. On relatively undisturbed portions of the land, a mixing layer depth close to 0 is expected. On the other hand, mixing of the soil to as deep as about 0.6 m (23 in.) is expected on the crop-producing portion of the land subjected to periodic plowing and other agricultural activities.

Tillage of the soil for crop production should be as shallow as possible and still meet the objectives of aerating the soil, removing stubble, controlling weeds, incorporating fertilizer, controlling erosion, and providing a suitable seedbed and rootbed (Buckingham 1984). Typical plow depths are on the order of 0.15-0.20 m (6-8 in.). However, a plow sole, or hardpan (compacted soil layer), can form when a field is plowed to the same depth each year (Buckingham 1984). This compacted layer should be broken up periodically by plowing to a deeper depth so as not to restrict air and water movement. Deeper tillage of this type, down to approximately 0.6 m (23 in.), can be routinely achieved with commercially available equipment. Thus, the soil mixing layer depth is expected to range from 0-0.6 m for the residential farmer scenario. A triangular distribution for the soil mixing layer between these two values, with 0.15 m (6 in.) as a most likely value, was selected for use in RESRAD as an approximation, because knowledge of the percentage of land used for crops and the crop types affect the amount of land and depth of plowing required, respectively. The probability density function for the soil mixing layer depth is shown in Figure 2.8-1.

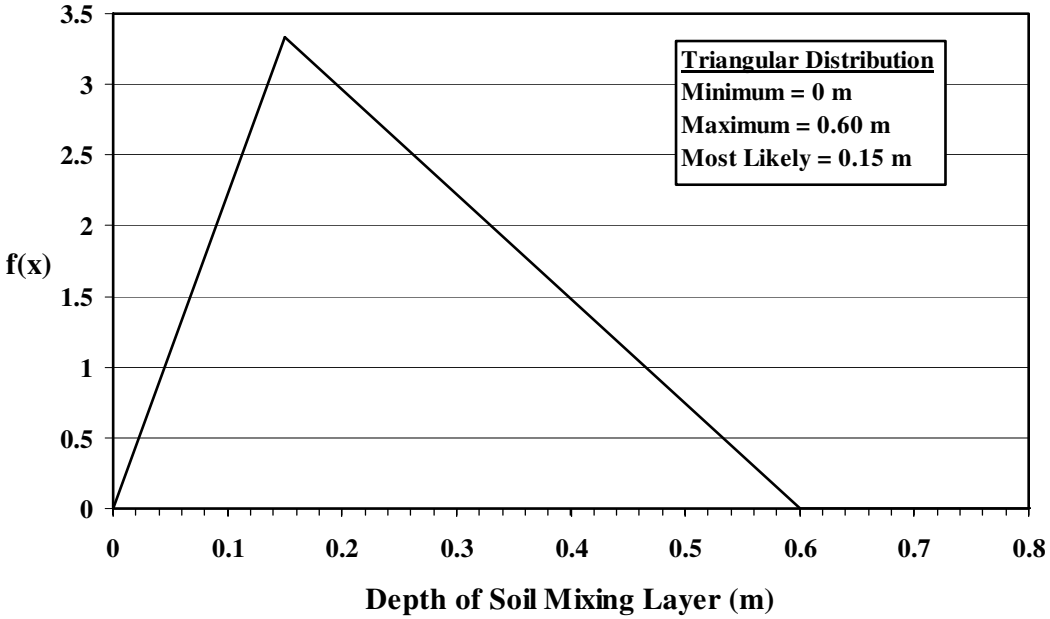

FIGURE 2.8-1 Depth of Soil Mixing Layer Probability Density Function

A site-specific value should be used when available. A minimum depth close to 0.0 m on an agricultural field could apply. Over the past two decades, the practice of no-till farming has gained increasing popularity. The benefits of no-till farming include reduced soil particulate emissions and erosion, improved soil organic content, increased moisture content available to plants, and reduced CO_2 emissions (USDA 2002).

Tillage deeper than 0.6 m is possible, but it is considered to be a nonstandard practice (Dunker et al. 1995; Allen et al. 1995). Commercial equipment capable of tillage down to depths of 1.2 m is available (Dunker et al. 1995). One of the countermeasures attempted, with mixed results, to reduce contamination of foodstuffs following the Chernobyl accident was deep plowing (Konoplev et al. 1993; Vovk et al. 1993). Deep plowing was considered a practical method for restoring large agricultural areas contaminated by radionuclides in the former USSR, with plow depths of approximately 0.6-0.75 m reported for different cases (Vovk et al. 1993).

2.9 EVAPOTRANSPIRATION COEFFICIENT

Applicable Code: RESRAD (onsite), RESRAD-OFFSITE

Description: The evapotranspiration coefficient is the ratio of the total volume of water vapor that is transferred to the atmosphere through evapotranspiration to the total volume of water available within the root zone of the soil.

Units*:* unitless

Probabilistic Input:

Distribution: uniform

Defining Values for the Distribution: None recommended (see the discussion for estimating site-specific values)

Discussion: The evapotranspiration coefficient, C_e, can be expressed as:

$$Ce = \frac{ET_r}{(1 - C_r)P_r + IR_r} \quad , \tag{2.9-1}$$

where

ET_r = the evapotranspiration rate (m/yr),

P_r = the precipitation rate (m/yr),

IR_r = the irrigation rate (m/yr), and

C_r = the runoff coefficient.

This parameter and certain other input parameters, such as precipitation rate, irrigation rate, and the runoff coefficient, are used in RESRAD-OFFSITE to determine the water deep percolation rate according to mass balance at the primary contaminated area, the two agricultural areas (i.e., fruit, grain, and nonleafy vegetables and leafy vegetables), the two livestock-feed growing areas (pasture and silage and grain), and the dwelling area. The water percolation rate in deep soil is ultimately used to calculate the radionuclide leaching rate from the topsoil in these areas and the subsequent contamination of the underlying groundwater system. RESRAD (onsite) looks only at the percolation rate at the primary contaminated area.

Evaporation is the process whereby liquid is converted to water vapor and removed from the evaporating surface (i.e., ground surface in this case). To change the state of the water molecules from liquid to vapor requires energy. Once water molecules evaporate, the difference of vapor pressure between the evaporating surface and the surrounding atmosphere would

remove the water vapor from the evaporating surface. Hence, solar radiation, air temperature, air humidity, and wind speed are climatological parameters to consider when assessing the evaporation process. In addition, the degree of shading of the crop canopy and the amount of water available at the evaporating surface also need to be considered when the evaporating surface is the soil surface.

Transpiration consists of the vaporization of liquid water contained in plant tissues and the vapor removal to the atmosphere. Nearly all water taken up is lost by transpiration and only a tiny fraction is used within the plant. Transpiration, like direct evaporation, depends on the energy supply, vapor pressure gradient, and wind. In addition, the soil water content and the ability of the soil to conduct water to the roots also determine the transpiration rate, as does water logging and soil water salinity. Different kinds of plants may have different transpiration rates. Not only the type of crop, but also the crop development, environment setting, and field management should be considered when assessing transpiration.

Evaporation and transpiration occur simultaneously and there is no easy way of distinguishing them. When the crop is small, water is predominantly lost by soil evaporation, but once the crop is well developed and completely covers the soil, transpiration becomes the main process. Evapotranspiration is the combination of evaporation from the soil surface and transpiration from vegetation. The evapotranspiration rate is normally expressed in length per unit time (e.g., mm/d and m/yr).

Owing to the difficulty of obtaining accurate field measurements, the evapotranspiration rate is commonly computed from weather data. Numerous equations have been developed by different researchers, but some of them are only valid under specific climatic and agronomic conditions. As a result of an Expert Consultation held in May 1990, the Food and Agriculture Organization (FAO) of the United Nations adopted the Penman-Monteith combination method to calculate the evapotranspiration rate for different types of crops under different growth and management conditions (Allen et al. 1998). The method involves the use of a reference evapotranspiration rate (ET_o) and a crop coefficient (K_c) to calculate the evapotranspiration rate for a specific crop (ET_c). The reference crop was defined as a hypothetical crop with an assumed height of 0.12 m, a surface resistance of 70 s/m, and an albedo of 0.23, closely resembling an extensive surface of green grass of uniform height, actively growing and adequately watered. ET_o is the evapotranspiration rate for the reference crop under standard, i.e., no stress, adequately watered, growing condition. K_c is a correction factor for ET_o and accounts for the aggregation of the physical and physiological differences between a specific crop and the reference crop. It can also include an adjustment to account for the deviation of actual growing condition from standard condition, such as water and salinity stress, low plant density, environmental factors, and management practices. The product of ET_o and K_c gives the value of ET_c.

Table 2.9-1 lists the average values of ET_o in different agroclimatic regions. The value of ET_o is expressed in mm/d and accounts for daily evapotranspiration rate during the growing season. Table 2.9-2 lists the crop coefficient K_c during different growing stages for different crops under nonstressed, well managed, i.e., standard conditions (Allen et al. 1998). The value of K_c during the middle growing stage, $K_{c,mid}$, is greater than that during the initial and

developmental stages, $K_{c,ini}$, and that during the late growing stage, $K_{c,end}$, because in the middle growing stage, crop is fully grown and transpires more water through foliage. The seasonal $K_{c,avg}$ listed in the last column is either the weighted average of K_c's obtained by considering the duration of different growing stages, when information on the duration of different stages is available, or simply the average of K_c's, when information on the duration of different stages is missing. Table 2.9-3 lists the ranges and mean values of K_c for the four different crop categories (leafy vegetables; fruit, grain, and nonleafy vegetables; forage; and grain) considered in RESRAD-OFFSITE during the growing season. They were obtained by aggregating the individual $K_{c,avg}$ over all the different crops listed under each crop category.

The values of K_c and $K_{c,avg}$ presented above are for standard growing conditions. In reality, the soil conditions in the field may differ from the standard conditions, because of unfavorable environmental settings or poor field management, such as soil salinity and water shortage. Therefore, an additional correction to the K_c values by a stress coefficient K_s is necessary to account for the real situation. Although no simple and direct method is provided by FAO (Allen et al. 1998) for estimating K_s, in general, a value between 0.5 and 1 can be selected, with 0.5 representing very poor soil conditions and 1 representing excellent, desirable conditions.

TABLE 2.9-1 Average ET_o (mm/d) for Different Agroclimatic Regions

	Mean Daily Temperature (°C)		
Regions	Cool ~10°C	Moderate 20°C	Warm > 30°C
Tropics and subtropics			
Humid and subhumid	2 - 3	3 - 5	5 - 7
Arid and semi-arid	2 - 4	4 - 6	6 - 8
Temperate region			
Humid and subhumid	1 - 2	2 - 4	4 - 7
Arid and semi-arid	1 - 3	4 - 7	6 - 9

Source: Allen et al. (1998), Table 2.

TABLE 2.9-2 Single, Time-Averaged Crop Coefficient, $K_{c,avg}$, for Nonstressed, Well-Managed Crops

				Length of Crop Development Stages (d)					
Crop	$K_{c,ini}$[a]	$K_{c,mid}$[b]	$K_{c,end}$[c]	Init. (L_{ini})	Dev. (L_{dev})	Mid (L_{mid})	Late (L_{late})	Total	$K_{c,avg}$[d]
Fruits and nuts									
Apple, cherry, and pear	1	1	1	23[e]	63[e]	113[e]	40[e]	239	0.86
Apricot, peach, stone fruits	*0.58*[f]	*1.03*	*0.76*	23[e]	63[e]	113[e]	40[e]	239	0.82
Banana, first year	0.5	1.1	1	120	90	120	60	390	0.76
Cantaloupe	0.5	0.85	0.6	20	52.5	30	17.5	120	0.6
Citrus fruits, no ground cover	*0.62*	*0.57*	*0.83*	60	90	120	95	365	0.66
Citrus fruits, active ground cover	*0.8*	*0.78*	*0.8*	60	90	120	95	365	0.79
Grape	0.3	0.78	0.45	22.5	50	81.25	55	209	0.53
Kiwi	0.4	1.05	1.05						0.83
Olive	0.65	0.7	0.7	30	90	60	90	270	0.68
Pineapple	0.5	0.4	0.4	60	120	600	10	790	0.42
Pistachio	0.4	1.1	0.45	20	60	30	40	150	0.58
Strawberry	0.4	0.85	0.75						0.67
Sweet melon	0.5	1.05	0.75	25	37.5	55	21.25	138.8	0.76
Watermelon	0.4	1	0.75	15	25	25	30	95	0.67
Walnut	0.5	1.1	0.65	20	10	130	30	190	0.93
Grain									
Barley	0.3	1.15	0.25	25	36.7	55.8	31.7	149	0.61
Maize, field (grain) *(field corn)*	*0.3*	1.2	*0.48*	26	40	48	35	148	0.63
Maize, sweet *(sweet corn)*	*0.3*	1.15	1.05	22	29	31	29	111	0.73
Millet	*0.3*	1	0.3	18	28	48	30	123	0.57
Oat	0.3	1.15	0.25	25	36.7	55.8	31.7	149.2	0.61
Sorghum	0.3	1.13	0.8	20	35	42.5	30	127.5	0.69
Spring wheat	0.3	1.15	0.33	25	36.7	55.8	31.7	149.2	0.62
Winter wheat	0.55	1.15	0.33	131	272	61.7	28.3	493	0.61
Nonleafy vegetables									
Artichoke	0.5	1	0.95	30	33	250	30	343	0.90
Asparagus	0.5	0.95	0.3	70	30	150	48	298	0.69
Bean, dry and pulses	0.4	1.15	0.35	*20*	*26.7*	*35*	*20*	101.7	0.65

TABLE 2.9-2 (Cont.)

Crop	$K_{c,ini}$[a]	$K_{c,mid}$[b]	$K_{c,end}$[c]	Length of Crop Development Stages (d)					$K_{c,avg}$[d]
				Init. (L_{ini})	Dev. (L_{dev})	Mid (L_{mid})	Late (L_{late})	Total	
Bean, green	0.5	1.05	0.9	*17.5*	*27.5*	*27.5*	*10*	82.5	0.73
Beets	0.5	1.05	0.95	*20*	*27.5*	*22.5*	*10*	80	0.71
Carrot	*0.7*	1.05	0.95	27	40	63	23	153	0.58
Cassava, year 1	*0.3*	0.8	0.3	20	40	90	60	210	0.51
Cassava, year 2	*0.3*	1.1	0.5	150	40	110	60	360	0.58
Chick pea	*0.4*	1	0.35						0.58
Cucumber	0.65	1	0.6	*22.5*	*32.5*	*45*	*17.5*	117.5	0.78
Eggplant	0.6	1.05	0.9	*30*	*42.5*	*40*	*22.5*	135	0.78
Fababean, fresh	0.5	1.15	1.1	90	45	40	0	175	0.65
Garlic	*0.7*	1	0.7						0.80
Grabanzo	0.4	1.15	0.35						0.63
Green gram and cowpea	*0.4*	1.05	0.48	20	30	30	20	100	0.61
Groundnut (peanut)	*0.4*	1.15	0.6	32	38	38	28	137	0.65
Lentil	*0.4*	1.1	0.3	23	33	65	40	160	0.66
Onion, green	*0.7*	1	1	25	43	28	18	115	0.41
Pea	*0.4*	*1.15*	*0.63*	23	27	33	17	100	0.69
Potato	0.5	1.15	0.75	31	32	*50.5*	27	140.5	0.78
Pumpkin	0.5	1	0.8	*22.5*	*32.5*	*32.5*	*22.5*	110	0.71
Radish	0.7	0.9	0.85	7.5	10	15	5	37.5	0.8
Soybean	*0.4*	1.15	0.5	18	13	58	23	113	0.81
Squash, zucchini	0.5	0.95	0.75	*22.5*	*32.5*	*25*	*15*	95	0.66
Sugar beet	0.35	1.2	0.7	*33.6*	*50*	*75.7*	*35.7*	195	0.74
Sweet pepper	0.6	1.05	0.9	*28.8*	*37.5*	*75*	*25*	166.25	0.85
Sweet potato	0.5	1.15	0.65	*17.5*	*30*	*55*	*35*	137.5	0.8
Tomato	0.6	1.15	0.8	31	41	53	29	154	0.83
Turnip	*0.5*	1.1	0.95						0.85
Leafy vegetables									
Broccoli	0.7	1.05	0.95	35	45	40	15	135	0.83
Brussel sprout	*0.7*	1.05	0.95	25	33	45	20	123	0.54

TABLE 2.9-2 (Cont.)

Crop	$K_{c,ini}$[a]	$K_{c,mid}$[b]	$K_{c,end}$[c]	Length of Crop Development Stages (d)					$K_{c,avg}$[d]
				Init. (L_{ini})	Dev. (L_{dev})	Mid (L_{mid})	Late (L_{late})	Total	
Cabbage	*0.7*	1.05	0.95	40	60	50	15	165	0.40
Cauliflower	0.7	1.05	0.95	35	50	40	15	140	0.83
Celery	0.7	1.05	1	*26.7*	*45*	*81.7*	*18.3*	171.7	0.90
Lettuce	0.7	1	0.95	*27.5*	*38.75*	*28.75*	10	105	0.81
Spinach	*0.7*	1	0.95	20	25	20	8	73	0.37
Forage									
Alfalfa	0.4	0.88	0.85	*7.5*	*20*	*16.25*	*8.75*	52.5	0.62
Bermuda grass	0.45	0.95	0.75	10	25	35	35	105	0.72
Clover	*0.4*	*1.03*	*0.98*						0.80
Grazing pasture	0.35	0.85	0.8						0.67
Sudan grass	*0.5*	*1.03*	*0.98*	28	40	27	17	112	0.70
Turf grass	0.85	0.9	0.9						0.88

[a] $K_{c,ini}$: K_c in the initial and developmental growing stages.

[b] $K_{c,mid}$: K_c in the middle growing stage.

[c] $K_{c,end}$: K_c in the late growing stage.

[d] $K_{c,avg}$: Average seasonal K_c value calculated by weighting K_c in a different growing stage with the duration of that growing stage, or by averaging the K_cs in a different growing stage, when the duration of different growing stages are not available.

[e] Values for deciduous orchard.

[f] Values in italic font are the average of the reported range.

Source: Allen et al. (1998), Tables 11 and 12.

TABLE 2.9-3 Range of $K_{c,avg}$ for Different Types of Crops under Nonstressed and Well-Managed Conditions

	Fruits, Nuts, Grains, and Nonleafy Vegetables	Leafy	Forage	Grain
Min.	0.41	0.37	0.62	0.57
Max.	0.93	0.90	0.88	0.73
Average	0.69	0.67	0.73	0.63

It should be pointed out that the literature values of K_c discussed in the previous paragraphs are valid for the growing season. However, the analysis performed by RESRAD (onsite) or RESRAD-OFFSITE requires the input of annual average value; therefore, the K_c value during the off-season should also be developed. It is considered that during the off-season, the cold weather restricts the growth of crops and minimizes farming activities; as a result, the agriculture fields are either barren or with little ground coverage. A low-end value of 0.3 was selected among the listed value in Table 2.9-2 for use during the off-season. The K_c values can be used together with E_o to obtain the annual evapotranspiration rate of a specific crop, E_c. E_c then can be plugged into Eq. (2.9-1) as the numerator and be divided by the amount of water delivered to the root zone $[(1 - C_r)P_r + IR_r]$, to obtain C_e, the evapotranspiration coefficient.

Because C_e is strongly influenced by climatic conditions (i.e., temperature and precipitation) and is highly site-specific, no recommendation is provided for its default distribution. Derivation of site-specific evapotranspiration coefficients are recommended when performing a RESRAD-OFFSITE calculation. The procedure of estimating site-specific distribution ranges for C_e is described in the following paragraphs.

Table 2.9-4 demonstrates the procedure that can be used in estimating site-specific evapotranspiration coefficients for different crop fields. First, the agroclimatic characteristics of the agricultural fields must be determined to select the most representative region from the four choices listed in Table 2.9-1 (humid and subhumid tropical or subtropical region, arid and semi-arid tropical or subtropical region, humid and subhumid temperate region, and arid and semi-arid temperate region). Then, the number of days in a year must be distributed to the four temperature ranges: ~0°C, ~10°C, ~20°C, and >30°C. With the daily ET_o (mm/d) listed in Table 2.9-1, the total amount of water lost through evapotranspiration for the reference crop can be calculated for each temperature range in a year. In Table 2.9-4, the fields were assumed to be in a semi-arid temperate region. (Note that the daily ET_o corresponding to the temperature range of ~0°C was not provided by FAO [Allen et al. 1998). A range of 0-1 mm/d was assumed in the example, by inference from the values for other temperature ranges.)

The amount of evapotranspiration, ET_o's, for the reference crop must be corrected by a crop coefficient, K_c, to determine the amount of evapotranspiration for different crop categories.

On the basis of the seasonal average, $K_{c,avg}$, for different crop categories (listed in Table 2.9-3) and a stress correction factor, K_s, the adjusted K_c for actual field conditions can be obtained (as the product of $K_{c,avg}$ and K_s). In Table 2.9-4, a stress correction factor of 1, 1, 0.75, and 0.75 was selected for the four crop fields, respectively, assuming the nonleafy vegetable and leafy vegetable fields receive more irrigation and care than the forage and grain fields. Because cultivation of crops would not be possible throughout the entire year due to low temperatures in the off-season, the adjusted K_c values calculated above were applied only during the growing period. In Table 2.9-4, the growing period was limited to the time when the temperature was in the range of ~10°C to >30°C. When the temperature dropped to ~0°C, crops were considered to wither and growth eventually stopped. An adjusted K_c value of 0.3 was used for the temperature range of ~0°C to account for the fact that the ground surface would be only partially covered by dead leaves and transpiration would not be active. The ET_o values calculated for different temperature ranges then were multiplied by the corresponding K_c values to obtain the ET_c values for actual crops. Table 2.9-4 lists the low and high bounds of ET_c for different temperature ranges and different crop categories. Finally, the annual evapotranspiration rate, ET_r (m/yr), can be calculated as the sum of ET_c from different temperature ranges.

The last portion of Table 2.9-4 presents estimates of the evapotranspiration coefficient calculated by using equation 2.9-1. The site-specific annual precipitation rate should be used in the calculation, and the values for the four different crop fields should be the same if they are located in the same region. The irrigation rate should reflect the stress conditions that crops experience in the fields. In Table 2.9-4, the irrigation rates assumed for nonleafy vegetables, leafy vegetable, forage, and grain fields were 0.5, 0.7, 0.2, and 0.2 m/yr, respectively. The irrigation rates for nonleafy vegetable and leafy vegetable fields were higher than for the forage and grain fields, reflecting the assumed stress correction factor (K_s) of 1 for the two vegetable fields and 0.75 for the two fodder fields. Site-specific runoff coefficients should also be obtained and used. In Table 2.9-4, a value of 0.25 was used for all the fields. The final calculation results for the evapotranspiration coefficient, E_c, showed a range of 0.41-0.78 for the nonleafy vegetable field, 0.34-0.65 for the leafy-vegetable field, 0.43-0.82 for the forage field, and 0.37-0.71 for the grain field. A uniform distribution with the calculated low and high bounds can then be assumed and used as site-specific input to run the RESRAD-OFFSITE code.

For comparison, Palmer (1993) gives a range of 0.6 to 0.75 for irrigation efficiency, which is the percentage of irrigation water that is delivered to the root zone and is available for evapotranspiration. A very small fraction of water is actually used for plant growth; the majority would be lost through evapotranspiration. The efficiency is influenced by the size of the irrigated area because of the effect of conveyance losses between the point of delivery to the crop fields. The Water Atlas of the United States (Geraghty et al. 1973) states that 70 percent of the water that falls as precipitation on the conterminous United States is lost by evapotranspiration from nonirrigated lands.

TABLE 2.9-4 Example Calculations for the Evapotranspiration Coefficients for a Site Located in a Temperate Semi-Arid Region

Temperatures	Days per Year[a]	Range of ET_o (mm/d)[b] Low	Range of ET_o (mm/d)[b] High	Total ET_o (mm)[c] Low	Total ET_o (mm)[c] High
Mean temperature ~ 0°C	120	0	1	0	120
Mean temperature ~ 10°C	120	1	3	120	360
Mean temperature ~ 20°C	65	4	7	260	455
Mean temperature about > 30°C	60	6	9	360	540

Crop Category	$K_{c,avg}$[d]	K_s[e]	Adjusted K_c[f]	K_c at Different Temperature[g] ~ 0°C	~ 10°C	~ 20°C	> 30°C
Nonleafy vegetable	0.69	1	0.69	0.30	0.69	0.69	0.69
Leafy vegetable	0.67	1	0.67	0.30	0.67	0.67	0.67
Forage	0.73	0.75	0.55	0.30	0.55	0.55	0.55
Grain	0.63	0.75	0.47	0.30	0.47	0.47	0.47

	Total ET_c (mm) for Different Temperature[h] ~ 0°C		~ 10°C		~ 20°C		> 30°C		Annual Evapotranspiration Rate, ET_r (m/yr)[i]	
Crop Category	Low	High	Low	High	Low	High	Low	High	Low	High
Nonleafy vegetable	0	36	83	248	179	314	248	373	0.51	0.97
Leafy vegetable	0	36	80	241	174	305	241	362	0.50	0.94
Forage	0	36	66	197	142	249	197	296	0.41	0.78
Grain	0	36	57	170	123	215	170	255	0.35	0.68

TABLE 2.9-4 (Cont.)

Crop Category	Annual Precipitation (m/yr)[j]	Annual Irrigation (m/yr)[k]	Runoff Coefficient[l]	Evapotranspiration Coefficient[m]	
				Low	High
Nonleafy vegetable	1	0.5	0.25	0.41	0.78
Leafy vegetable	1	0.7	0.25	0.34	0.65
Forage	1	0.2	0.25	0.43	0.82
Grain	1	0.2	0.25	0.37	0.71

[a] Values are the number of days of the specified temperature during a year.

[b] Range of ET_O was taken from Table 2.9-2 except for temperature ~ 0°C, for which 0 and 1 mm/d were assumed to be the bounding values.

[c] Total ET_o was obtained by multiplying the daily ET_o with the number of days of the specific temperature range.

[d] $K_{c,avg}$ is the seasonal average of K_c under standard, nonstressed conditions. The value was taken from Table 2.9-4.

[e] K_S is the correction factor to $K_{c,avg}$ for considering the deviation from the standard, nonstressed growing conditions.

[f] Adjusted K_C is the multiplication product of $K_{c,avg}$ and K_s, and is the crop correction factor during the growing period.

[g] K_c at different temperature was set to the adjusted K_c value when growth of crop was considered feasible under the specific temperature. Otherwise, it was set to a value of 0.3, a value assumed to reflect the condition when growth of crop is not possible, irrigation is discontinued, and the ground surface is covered with dead leaves or weeds. It was assumed that when the temperature drops to around 0°C or lower, growth of crop is not possible.

[h] "Total ET_c for different temperature" condition is the product of "K_c at different temperature" and the low or high end of "Total ET_o (mm)."

[i] ET_r is the sum of the "Total ET_c for different temperature," expressed in terms of m/yr.

[j] Annual precipitation rate was set to the same value for different crop fields, assuming the crop fields are located in the same region. Site-specific value should be used.

[k] Annual irrigation rate maybe different for different crop fields. The value is related to the K_s value used to consider deviation of the actual conditions from the standard, nonstressed conditions. Sufficient irrigation would provide enough water for plant growth, thereby reducing the deviation from standard conditions.

[l] The runoff coefficient can assume different values for different crop fields. In the example, the same value was used for all crop fields.

[m] The evapotranspiration coefficient was calculated by using equation 2.9-1. The value of the coefficient ranges from 0 to 1. Therefore, if the calculated value exceeds 1, it should be replaced with 1.

3 ATMOSPHERIC PARAMETER DISTRIBUTIONS

3.1 MASS LOADING

Applicable Code: RESRAD (onsite), RESRAD-OFFSITE

Description: This parameter represents the concentration of total contaminated airborne particulate matter (e.g., soil) over the primary contamination area (RESRAD-OFFSITE) or that amount which is respirable (RESRAD and RESRAD-OFFSITE).

Units: micrograms per cubic meter ($\mu g/m^3$)

Probabilistic Input:

Mass Loading for Inhalation (RESRAD (onsite), RESRAD-OFFSITE)

Distribution: continuous linear

Defining Values for Distribution: See Table 3.1-1 for the input values.

Mean Onsite Mass Loading (RESRAD-OFFSITE)

Distribution: truncated lognormal-n

Defining Values for Distribution:

Underlying mean value: 3.80	Lower quantile value: 0.001
Underlying standard deviation: 0.455	Upper quantile value: 0.999

Discussion: Resuspended contaminated soil and dust pose a radiological inhalation risk. The mass loading for inhalation input to RESRAD (onsite) and RESRAD-OFFSITE provides the time-averaged respirable concentration of contaminated soil and dust. The respirable portion of resuspended material can be represented by the PM-2.5 fraction of airborne particulate matter (particulates $\leq$ 2.5 μm in diameter). The PM-2.5 particles represent the fine particle fraction that poses the highest respiratory hazard (EPA 2004). Ambient PM-2.5 air concentrations were obtained from the EPA's AirData Web site (EPA 2005).

Resuspended soil and dust from the primary contaminated area can be dispersed downwind to contaminate other areas. The mean onsite mass loading for RESRAD-OFFSITE provides the concentration of contaminated airborne material used to calculate the contaminant release rate to the atmosphere. The amount of this material is represented by the amount of total suspended particulates (TSP). The TSP concentrations were also obtained from the EPA's AirData Web site (EPA 2005)

TABLE 3.1-1 Cumulative Distribution Function for Mass Loading for Inhalation (RESRAD [onsite], RESRAD-OFFSITE)

Mass Loading ($\mu g/m^3$)	Cumulative Probability	Mass Loading ($\mu g/m^3$)	Cumulative Probability	Mass Loading ($\mu g/m^3$)	Cumulative Probability
0	0.0000	18	0.9514	36	0.9989
1	0.0001	19	0.9664	37	0.9989
2	0.0005	20	0.9743	38	0.9990
3	0.0024	21	0.9801	>38	1.0000
4	0.0092	22	0.9842		
5	0.0237	23	0.9876		
6	0.0493	24	0.9899		
7	0.0870	25	0.9924		
8	0.1343	26	0.9940		
9	0.1946	27	0.9950		
10	0.2725	28	0.9959		
11	0.3666	29	0.9965		
12	0.4720	30	0.9967		
13	0.5815	31	0.9974		
14	0.6895	32	0.9980		
15	0.7929	33	0.9983		
16	0.8750	34	0.9985		
17	0.9223	35	0.9986		

Five years (2000 through 2004) of annual average ambient PM-2.5 and TSP air concentration measurements from approximately 1,690 (PM-2.5) or 345 (TSP) air monitoring stations across the United States and its territories were analyzed. The data are only indicative of what might be expected because the set of monitoring stations included is not representative of a uniform grid across the United States. Furthermore, the monitor sites are not always representative of all nearby areas because of differences in local weather patterns. Thus, site-specific data should be used when available.

Figure 3.1-1 presents a histogram of the data in conjunction with the cumulative distribution function (CDF) for the PM-2.5 data for inhalation. Table 3.1-1 lists the values used for the CDF. For the mean onsite mass loading, the TSP probability density function was fit reasonably well to a lognormal distribution by using nonlinear least squares regression analysis, as shown in Figure 3.1-2.

Both codes use the mass loading factor to estimate the annual inhalation dose. Therefore, use of a high, short-term loading will result in an overestimate of the annual dose. A time average mass loading factor should be used in RESRAD (onsite) and RESRAD-OFFSITE for a more realistic dose estimate. Similarly, the use of short-term loadings for the mean onsite mass loading in RESRAD-OFFSITE is also discouraged.

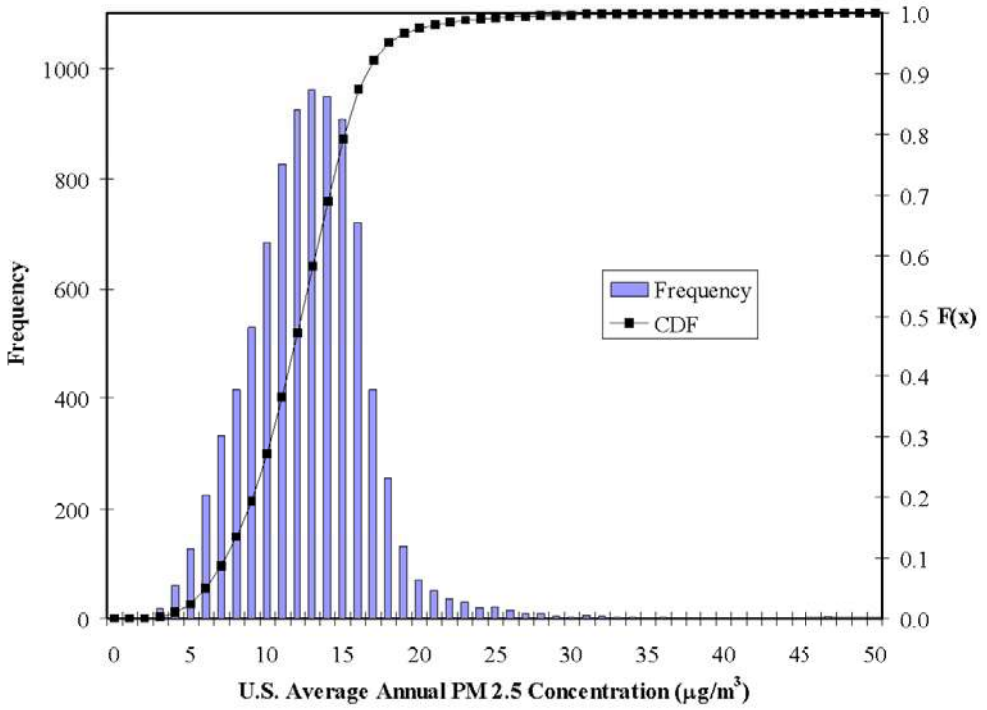

FIGURE 3.1-1 Mass Loading for Inhalation Histogram and Cumulative Distribution Function

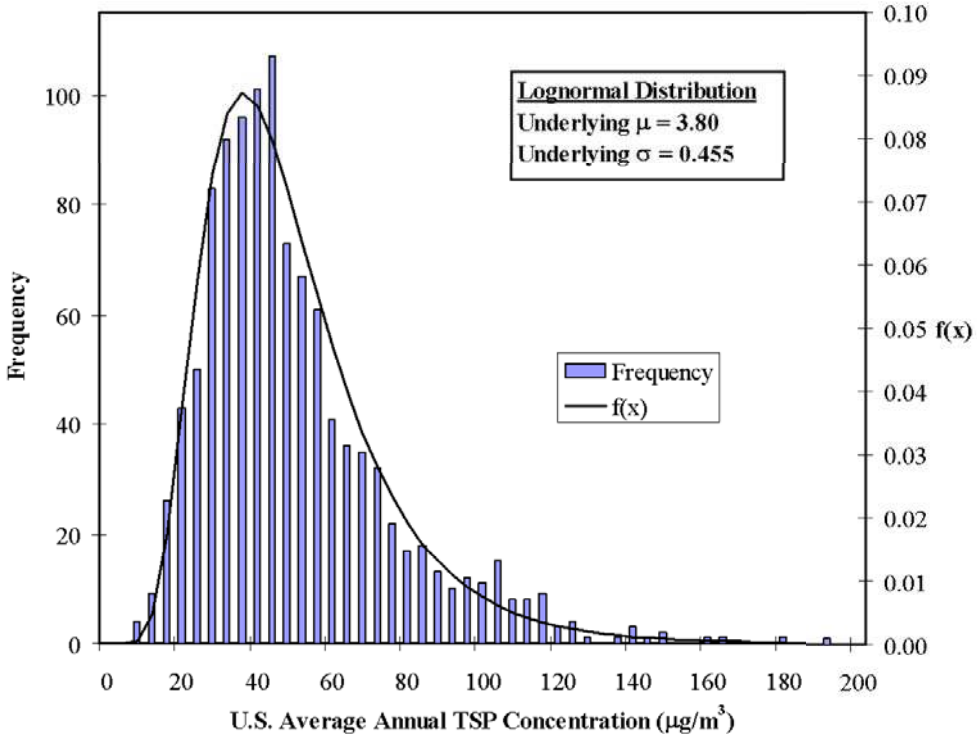

FIGURE 3.1-2 Mean Onsite Mass Loading Histogram and Probability Density Function

3.2 DEPOSITION VELOCITY

Applicable Code: RESRAD-BUILD, RESRAD-OFFSITE

Description: In RESRAD-BUILD, this parameter represents the indoor deposition velocity of contaminant particles in the building air. In RESRAD-OFFSITE, this parameter represents the outdoor deposition of airborne contaminant particles blown downwind from the contaminated area.

Units: meters per second (m/s)

Probabilistic Input:

RESRAD-OFFSITE

Distribution: loguniform

Defining Values for Distribution:

Minimum: 1.0×10^{-6} Maximum: 1.0

RESRAD-BUILD

Distribution: loguniform

Defining Values for Distribution:

Minimum: 2.7×10^{-6} Maximum: 2.7×10^{-3}

Discussion: The deposition velocity characterizes the rate at which particles in air deposit on a surface. In RESRAD-OFFSITE, the outdoor deposition velocity is used to calculate the resulting contaminant ground concentrations downwind of the contaminated area by multiplying the downwind air concentration by the deposition velocity at each location of interest. The deposition velocity, v_d, in outdoor air has traditionally been expressed as (Sehmel 1980):

$$v_d = \frac{-F}{\chi} \quad , \tag{3.2.-1}$$

where

F = the deposition flux, and

χ = the airborne concentration.

Thus, experimental determination of the deposition velocity involves the measurement of both the aboveground air concentration and the depositing flux. The air concentration at approximately 1 m from the ground surface has been historically used for this calculation.

The outdoor deposition velocity is a function of particle, meteorology, and ground surface properties (Sehmel 1980). Important particle properties include diameter, density, and shape; important meteorological properties include atmospheric stability and wind speed; and important surface properties include surface roughness and composition.

The decay rate, λ_d, of particles in indoor air due to deposition is often expressed as:

$$\lambda_d = \frac{v_d A_d}{V} \quad , \qquad (3.2.-2)$$

where

A_d = the surface area available for deposition, and

V = the volume of air.

For indoor deposition, the deposition velocity depends on particle and room properties. Important particle properties include diameter, density, and shape, as is the case for outdoor deposition. Room properties include air viscosity and density, turbulence, thermal gradients, and surface geometry.

Nazaroff and Cass (1989) have developed a relationship for the indoor deposition velocity of particulates as a function of particle size. Such theoretical calculations are not likely to produce satisfactory results because of lack of knowledge about near-surface flow conditions (Nazaroff et al. 1993), but they can provide insight into the general trend of deposition velocity as a function of particle size. Figure 3.2-1 presents an idealized representation of deposition velocity on a floor as a function of particle size on the basis of the methodology in Nazaroff and Cass (1989). A similar trend is observed and predicted for deposition of particles outdoors (Sehmel 1980).

Because deposition velocities depend on particle size, it is expected that the probability density function distribution of deposition velocities is dependent on the particle size distribution. The particle size distribution in the atmosphere typically exhibits three modes (Seinfeld and Pandis 1998). Fine particles (particles less than 2.5 μm in diameter) can be divided into two modes, the nuclei mode and the accumulation mode. The nuclei mode (particles approximately 0.005-0.1 μm in diameter) contains the largest number of particles in the atmosphere but represents only a few percent of the total mass of airborne particles (Seinfeld and Pandis 1998). Nuclei mode particles are formed from condensation of atmospheric gases, such as combustion products. Depletion of nuclei mode particles occurs primarily through coagulation with larger particles. The accumulation mode (particles approximately 0.1-2.5 μm in diameter) accounts for a large portion of the aerosol mass. Accumulation mode particles are formed through coagulation of particles in the nuclei mode and through condensation of gases

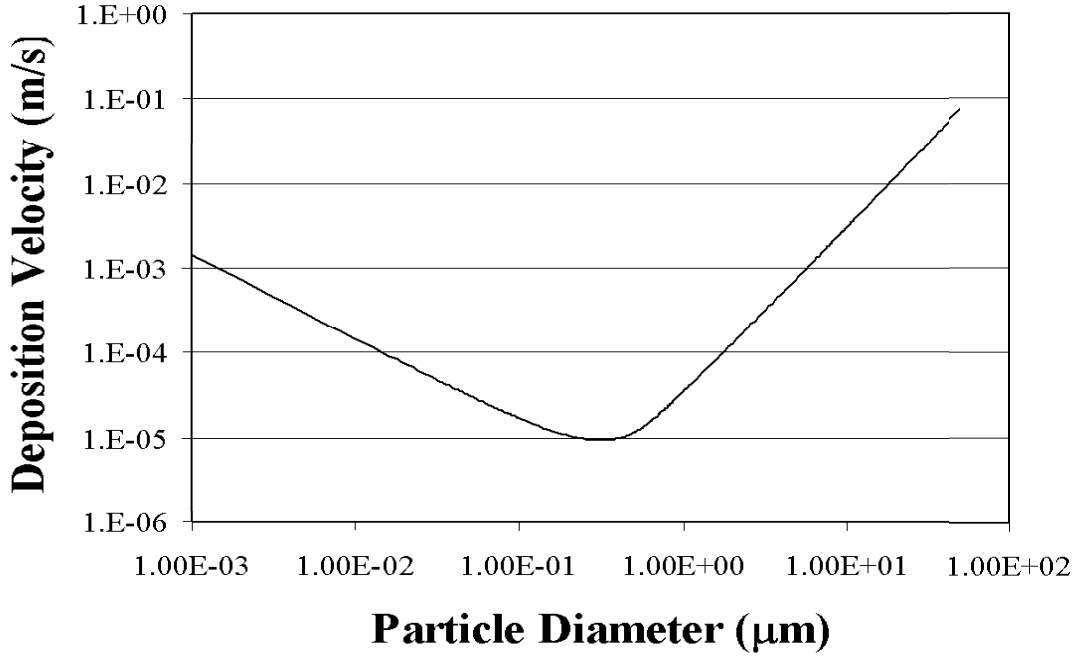

FIGURE 3.2-1 Estimated Indoor Deposition Velocities by Particle Size

onto smaller particles. Because removal mechanisms are not as efficient for this size range, particles tend to accumulate (hence the term "accumulation mode"). Coarse particles (diameters greater than 2.5 μm) constitute the third mode. Coarse mode particles are formed primarily from mechanical processes. Other sources of coarse particles include windblown dust and plant particles.

Each of the three particle size modes can be well characterized by lognormal distributions (John 1993). By using the means and standard deviations from Whitby and Sverdrup (1980), Figure 3.2-2 demonstrates the trimodal nature of the particle size distributions commonly found. Similar distributions are expected for indoor air concentrations, with the exception of some indoor source contributions, because the building shell has been shown to be an insignificant barrier to particle sizes under 10 μm (Yu et al. 2000).

A broad probability density function distribution is expected for the deposition velocity indoors and outdoors when comparing the trend in deposition velocity with the distribution of particles by size (Figures 3.2-1 and 3.2-2, respectively) and taking into consideration the variability of each. Indoor experimental estimates provide support for such an assumption, as shown in Tables 3.2-1 through 3.2-3. Also, because deposition is dependent on local airflow patterns (Nazaroff and Cass 1989), in conjunction with particle size and mass, a small difference in the local air handling system (such as changes due to climate or season) can easily cause a shift in deposition velocity. Because the deposition velocity input in RESRAD-BUILD is used for all particle sizes and species under a potential range of airflow conditions, a loguniform distribution is assigned, with minimum and maximum values of 2.7×10^{-6} m/s and

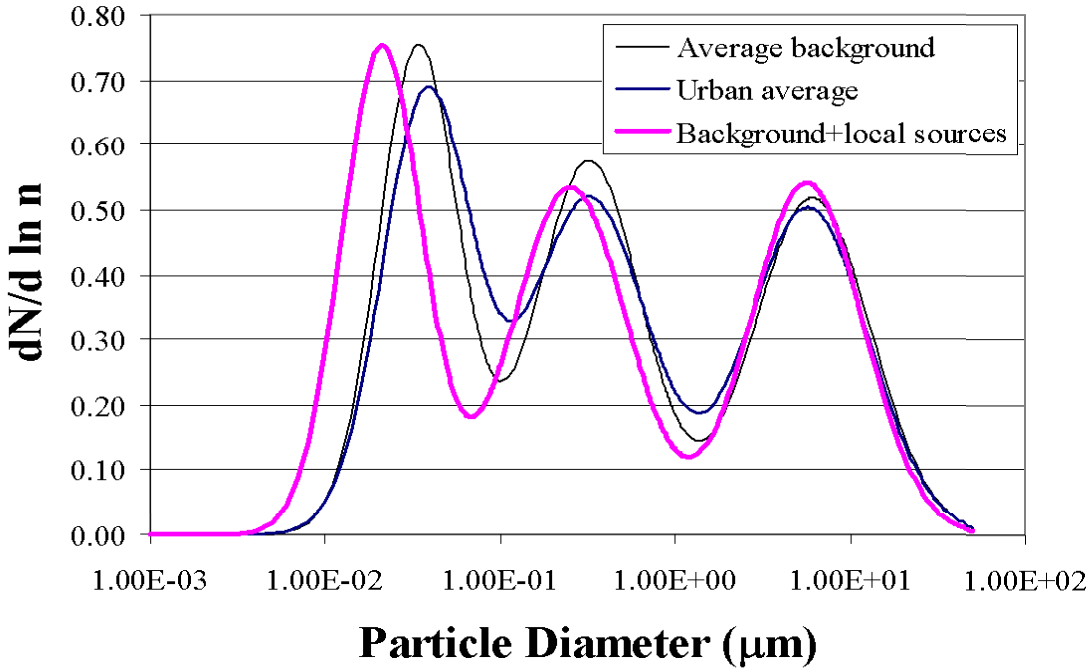

FIGURE 3.2-2 Trimodal Nature of Aerosol Particle Size Distribution

2.7×10^{-3} m/s, respectively, as found in Tables 3.2-1 through 3.2-3. This distribution is shown in Figure 3.2-3.

In addition to particle size, the deposition velocity of particulates outdoors is strongly influenced by wind speed, weather stability category, and surface roughness, among other effects (Sehmel 1980, 1984; Harper et al. 1995). Thus, the suggested parameter distribution for the outdoor deposition velocity is necessarily broad because the air dispersion model in RESRAD-OFFSITE does not explicitly account for particle size and surface roughness. An expert panel on deposition velocity was convened to provide suggested values for the range of outdoor deposition velocity under a variety of conditions for different particle sizes (Harper et al. 1995). For wind speeds of 2 and 5 m/s, estimated values for particle sizes 0.1, 0.3, 1.00, 3.00, and 10.00 μm were given for the 0, 5, 50, 95, and 100 quantiles for deposition on an urban area, meadow, forest, and human skin. The expert estimates generally varied by an order of magnitude or more on the low and high end of the deposition velocity range for most cases. Based primarily on the values for both wind speeds, particle sizes of 0.1 and 10 μm, and deposition on meadow and urban areas, a loguniform distribution with a minimum value of 1.0×10^{-6} m/s and a maximum value of 1.0 m/s were selected for RESRAD-OFFSITE. The corresponding probability distribution is shown in Figure 3.2-4.

TABLE 3.2-1 Estimated Indoor Deposition Velocities by Particle Size

Particle Size (μm)	Deposition Velocity (m/s)	Comments	Reference
0.71	1.7×10^{-5}	Be-7 with natural air exchange	Lang 1995
1.4	1.3×10^{-5}		
2.8	6.7×10^{-5}		
0.71	1.33×10^{-4}	Be-7 with forced air exchange	
1.4	2.66×10^{-4}		
2.8	3.88×10^{-4}		
1-2	1.7×10^{-4}	Data Set 1 (different sample dates using SF_6 tracer)	Thatcher and Layton 1995
2-3	3.7×10^{-4}		
3-4	5.1×10^{-4}		
4-6	1.1×10^{-4}		
1-2	1.9×10^{-4}	Data Set 2	
2-3	5.0×10^{-4}		
3-4	5.6×10^{-4}		
4-6	1.2×10^{-4}		
1-5	3.1×10^{-4}	Data Set 3	
5-10	9.1×10^{-4}		
10-25	1.6×10^{-4}		
>25	2.7×10^{-3}		
0.07	1.72×10^{-5}	Estimates based on data in Offermann et al. (1985) for cigarette combustion	Nazaroff and Cass 1989
0.10	2.7×10^{-6}		
0.12	3.8×10^{-6}		
0.17	3.8×10^{-6}		
0.22	4.7×10^{-6}		
0.26	8.9×10^{-6}		
0.35	8.2×10^{-6}		
0.44	8.7×10^{-6}		
0.56	9.8×10^{-6}		
0.72	1.51×10^{-5}		
0.91	1.3×10^{-4}		
<2.5	3×10^{-5} and 3×10^{-5}	Sulfate ion particulates at two locations	Sinclair et al. 1985
2.5-15	1×10^{-2} and 2×10^{-3}	Calcium ion particulates at two locations	

TABLE 3.2-2 Estimated Deposition Velocities by Particle Size in Residences with and without Furniture

Particle Size (μm)	Average Deposition Velocity (m/s)	
	Without Furniture	With Furniture
0.5	6.1×10^{-5}	8.2×10^{-5}
2.5	1.33×10^{-4}	1.73×10^{-4}
3.0	1.37×10^{-4}	2.25×10^{-4}
4.5	2.88×10^{-4}	2.88×10^{-4}
5.5	3.04×10^{-4}	3.24×10^{-4}

Source: Fogh et al. (1997).

TABLE 3.2-3 Estimated Indoor Deposition Velocities for Various Radionuclides

Isotope	Mean Deposition Velocity (m/s)
Cs-137	6.4×10^{-5}
Cs-134	6.2×10^{-6}
I-131 (particulate)	1.1×10^{-4}
Be-7	7.1×10^{-5}
Ru-103	2.0×10^{-4}
Ru-106	1.7×10^{-4}
Ce-141	3.1×10^{-4}
Ce-144	3.9×10^{-4}
Zr-95	5.8×10^{-4}
Nb-95	1.9×10^{-4}

Source: Roed and Cannell (1987).

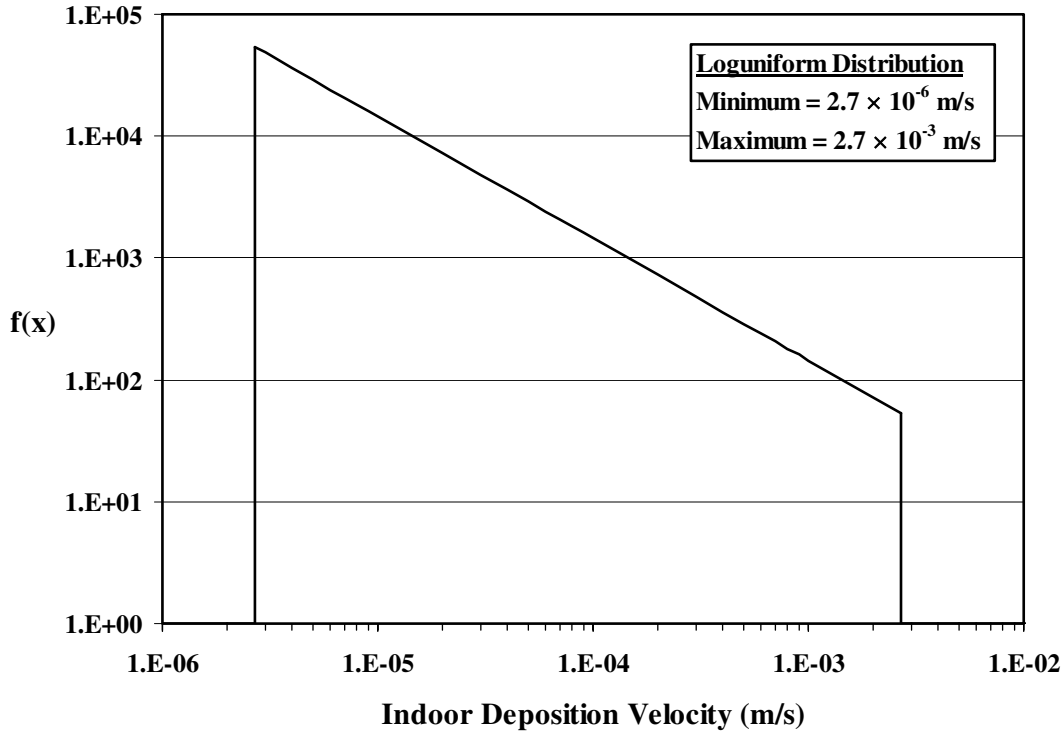

FIGURE 3.2-3 Indoor Deposition Velocity Distribution for RESRAD-BUILD

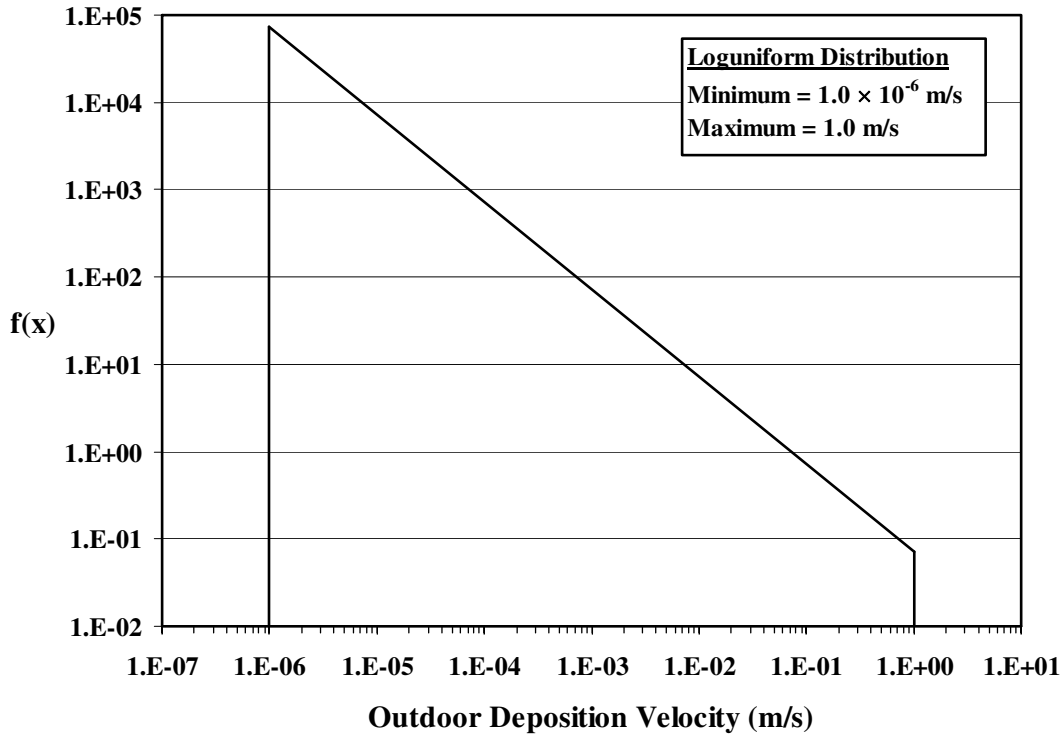

FIGURE 3.2-4 Outdoor Deposition Velocity Distribution for RESRAD-OFFSITE

3.3 WIND SPEED

Applicable Code: RESRAD (onsite), RESRAD-OFFSITE

Description: The wind speed represents the annual average wind speed at a site for RESRAD (onsite). For RESRAD-OFFSITE, the wind speed is divided into six intervals for use in a joint-frequency distribution with the atmospheric stability class when estimating air dispersion of contaminants. Each wind speed interval is characterized by a representative wind speed.

Units: meters per second (m/s)

Probabilistic Input:

RESRAD (onsite)

***Distribution*:** bounded lognormal-n

Defining Values for Distribution:

Underlying mean value:	1.445	Lower limit:	1.4
Underlying standard deviation:	0.2419	Upper limit:	13

RESRAD-OFFSITE

Distribution: uniform

Defining Values for Distribution: See Table 3.3-1.

Discussion: The wind speed at a given location varies by time of day and by season. Wind speed distribution at a given site has been characterized by both lognormal (Luna and Church 1974; Justus et al. 1976) and Weibull distributions (Justus et al. 1976). Annual average wind speed varies by location across the United States. For RESRAD (onsite), annual average wind speed data from 271 U.S. weather stations (NCDC 1999) were analyzed to obtain a reasonable estimate for a nationwide distribution for the United States. The average number of years of recorded data available for each station was 43 years.

The nationwide distribution was shown to be fit well by a lognormal distribution. Bayesian estimation was used to fit the probability density function shown in Figure 3.3-1 to a lognormal distribution. The maximum likelihood mean and standard deviation for the wind speed distribution were estimated to be 1.445 and 0.2419, respectively. Thus, the median (50th percentile) of the distribution corresponds to 4.2 m/s ($e^{1.445}$), near the national average wind speed of 4.1 m/s as determined by taking the arithmetic average of the 271 station annual averages. Lower and upper limits of 1.4 and 13 m/s imposed on the distribution correspond to the 0.000001 and 0.999999 quantiles, respectively.

TABLE 3.3-1 Uniform Distribution Limits for the Wind Speed Intervals in RESRAD-OFFSITE

Wind Speed Interval	Minimum (m/s)	Maximum (m/s)
1	0.514	1.80
2	1.81	3.34
3	3.35	5.40
4	5.41	8.49
5	8.50	11.1
6	11.2	14.1

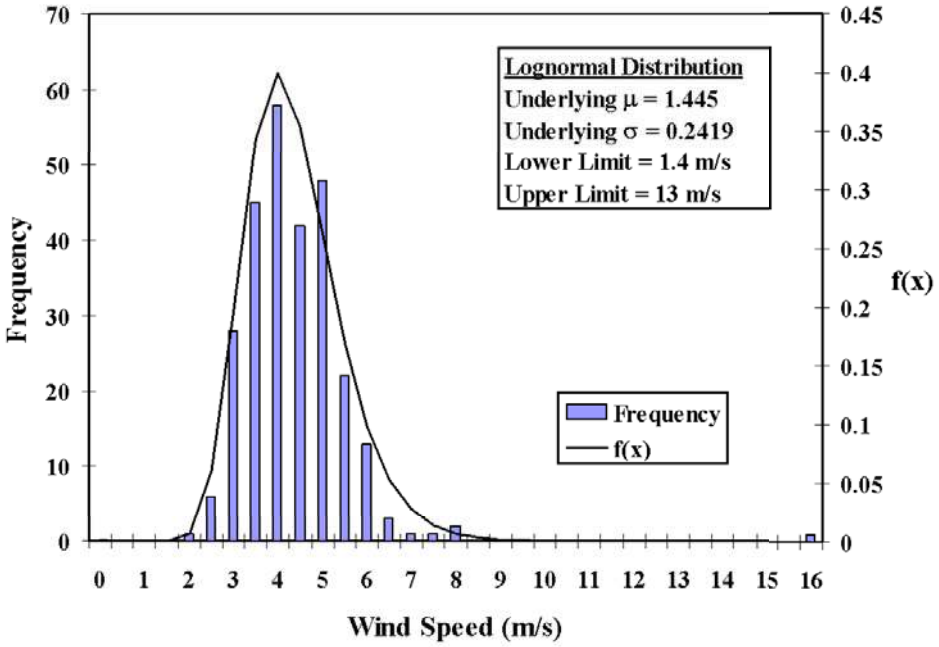

FIGURE 3.3-1 Wind Speed Histogram and the Fitted Probability Density Function for RESRAD (onsite)

This distribution is only indicative of what might be expected, because the sampling is of only limited size (271 data points) and is not representative of a uniform grid across the United States. Also, monitor sites are not always representative of all nearby areas because of differences in terrain over relatively short distances.

For RESRAD-OFFSITE, a joint frequency distribution of wind speed and atmospheric stability is used for each direction of a wind rose when estimating downwind contaminant concentrations. The frequency relates to the fraction of time that the atmospheric conditions in the specified sector (compass direction) fall within each wind speed interval and stability class combination. In keeping with the format of STAR joint frequency distribution data files, the code uses 6 wind speed intervals and 6 atmospheric stability classes for each of 16 sectors. In a STAR file, the wind speed intervals are defined as shown in Table 3.3-2. Each wind speed interval in RESRAD-OFFSITE is represented by an average value for use in the atmospheric dispersion calculations. For a probabilistic treatment, the wind speed can be assumed to have a uniform distribution across each interval, bounded by the limits for each interval for which the data is valid. The limits are shown in Table 3.3-1.

TABLE 3.3-2 STAR Wind Speed Intervals

Wind Speed Interval	Lower Bound[a] (knots [m/s])	Upper Bound[a] (knots [m/s])	RESRAD-OFFSITE (m/s)
1	1 (0.514)	3 (1.54)	0.89
2	4 (2.06)	6 (3.09)	2.46
3	7 (3.60)	10 (5.14)	4.47
4	11 (5.66)	16 (8.23)	6.93
5	17 (8.75)	21 (10.80)	9.61
6	>21 (10.80)		12.52

[a] Source: Parks (1992).

4 AGRICULTURE PARAMETER DISTRIBUTIONS

4.1 DURATION OF THE GROWING SEASON

Applicable Code: RESRAD-OFFSITE

Description: The growing season is the period of time during which a plant is exposed to contamination by foliar deposition and root uptake.

Units: days

Probabilistic Input:

Distribution: triangular

Defining Values for Distribution: See Table 4.1-1.

Discussion: The growing period, as defined by the National Council on Radiation Protection and Measurements (NCRP), is the time of aboveground exposure of a crop to contamination during the growing season (NCRP 1984). The period varies with plant type and with the growing season for a particular region (Hoffman et al. 1982).

Many references use a growing period of 30 days for pasture grasses and 60 days for produce (NRC 1977; NCRP 1984; Whelan et al. 1987; DOE 1995). Thirty days for pasture grasses represents animal grazing habits (Whelan et al. 1987), and 60 days for produce represents the approximate growing time for vegetable crops.

The FAO of the United Nations studies different food crops (Allen et al. 1998) and provides information about the duration of the different stages of plant growth for different crops. The plant growth is divided into four stages: the initial stage, the crop development stage, the midseason stage, and the late season stage. The initial stage runs from the planting date to approximately 10 percent ground cover. For perennial crops, the planting date is replaced by the "green-up" date, which refers to the time when the initiation of new leaves occurs. The crop development stage runs from 10 percent ground cover to effective full cover. The midseason stage runs from effective full cover to the start of maturity. The late season stage runs from the start of maturity to harvest or full senescence. The data are provided for different vegetables, fiber crops, oil crops, grains, forages, and fruits.

Many species of grasses (e.g., orchard grass, canary grass, timothy, broome grass, rye grass, and fescue) and legumes (e.g., red clover, alfalfa, and trefoil) are used as forages. Multiple clippings of forages are possible in a growing season (Owensby and Anderson 1969; Baker 2002, 2003; Majewski 2004). Table 4.1-2 lists the data extracted from Allen et al. (1998) for different forages. In general, it takes longer to grow first cuttings compared with other cuttings. For forages, it is expected that foliar deposition during the time between initial crop development and the start of maturity (i.e., when the crop has emerged from the ground and is ready to be

TABLE 4.1-1 Triangular Distribution Values for Duration of the Growing Season (in days)

Probabilistic Input	Field Type			
	Forage	Grain	Fruit, Grain, and Nonleafy Vegetables	Leafy Vegetables
Minimum	20	60	30	40
Most likely	30	120	105	75
Maximum	55	210	320	180

TABLE 4.1-2 Time (Days) Taken by Different Forages during Four Stages of Growth

Forage	Time Taken During Different Stages of Plant Growth (in days)				
	Initial	Crop Development	Start of Maturity	Harvest	Total (from crop development to start of maturity)
Alfalfa, first cutting	10	20-30	20-25	10	40-55
Alfalfa, other cuttings	5	10-20	10	5-10	20-30
Bermuda for hay (multiple cuttings)	10	15	75	35	30
Sudan, first cutting	25	25	15	10	40
Sudan, other cuttings	3	15	12	7	27

grazed by animals) could contribute to the dose of contamination that is ingested when the forage is consumed. Therefore, the time taken from crop development to the start of maturity is used to develop a distribution for forages. The proposed growing period for forages (Figure 4.1-1) is represented by a triangular distribution with minimum = 20 days, most likely = 30 days, and maximum = 55 days.

The usual planting and harvesting dates for U.S. field crops are provided in Agricultural Handbook Number 628 (USDA 1997). The information on the duration of the growing season for grains is extracted from this handbook. Table 4.1-3 summarizes the average, minimum, and maximum growing period for different field crops in the United States. It also lists the number of states where the crop is grown, the total harvested acres, the largest producing state, and the most likely uses of the crop. In some cases, multiple crops may be harvested during the growing season. Corn and winter wheat are harvested in most states in the United States. The stored grains most commonly used as livestock feed are barley, oats, corn, and sorghum. The minimum time required to grow these crops is 70 days. The maximum time required for the spring crop is 190 days.

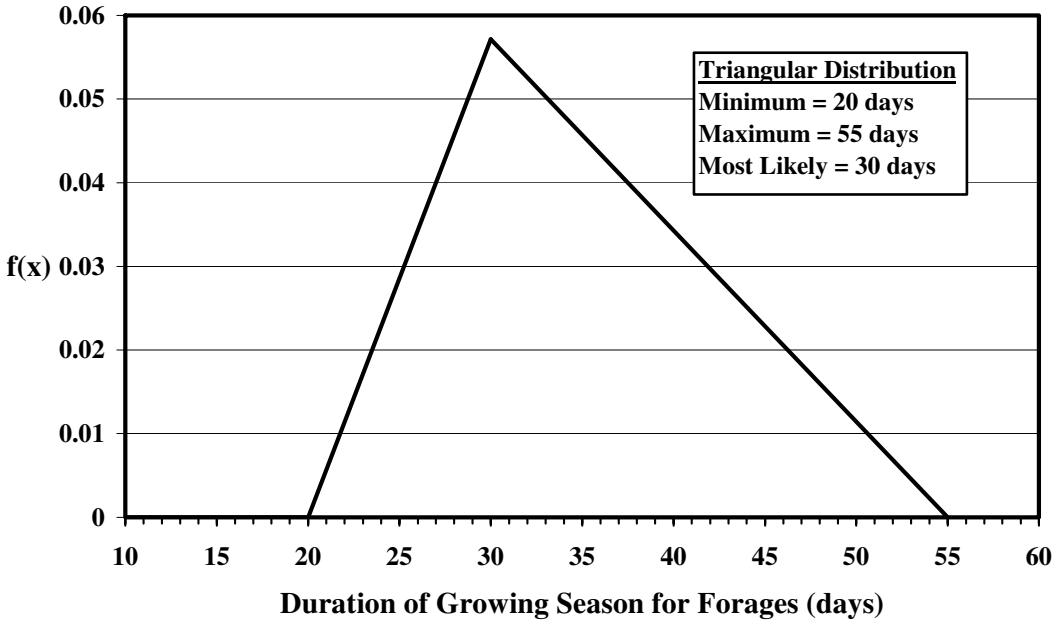

FIGURE 4.1-1 Probability Density Function for Forages for Duration of the Growing Season

TABLE 4.1-3 Growing Period (Days) for Different Grain Crops in the United States

Grains	Average	Minimum	Maximum	Number of States	Harvested Acres	Largest Producing States
Barley (spring)	1.1E+02	7.0E+01	1.8E+02	1.7E+01	6.4E+06	North Dakota
Barley (fall)	2.4E+02	1.1E+02	3.1E+02	1.4E+01	3.5E+02	Virginia and Pennsylvania
Wheat (spring)	1.2E+02	1.0E+02	1.5E+02	1.2E+01	2.0E+07	North Dakota
Wheat (winter)	2.7E+02	1.5E+02	3.4E+02	4.2E+01	4.0E+07	Kansas
Soybean	1.4E+02	1.2E+02	1.7E+02	2.9E+01	6.3E+07	Iowa and Illinois
Sorghum, grain, livestock	1.4E+02	9.4E+01	1.7E+02	1.8E+01	1.2E+07	Kansas
Rice	1.4E+02	1.2E+02	1.5E+02	6.0E+00	2.8E+06	Arkansas
Oat (fall)	2.3E+02	1.7E+02	2.7E+02	7.0E+00	2.5E+05	Texas
Oat (spring)	1.1E+02	8.4E+01	1.8E+02	2.4E+01	2.4E+06	North Dakota
Corn for grain	1.6E+02	1.3E+02	1.9E+02	4.1E+01	7.3E+07	Iowa and Illinois

Table 4.1-4 lists the data extracted from Allen et al. (1998) for different grains. In general, it takes longer to grow fall or winter crops compared with a spring crop. For grain, it is expected that foliar deposition during the time between initial crop development and the time of harvest could contribute to the dose of contamination that is ingested when the grain is consumed. Therefore, the total time taken from crop development to the start of harvest is used to develop a distribution for grains. The proposed growing period for grains (Figure 4.1-2) is represented by a triangular distribution with minimum = 60 days, most likely = 120 days, and maximum = 210 days.

TABLE 4.1-4 Time (Days) Taken by Different Grains during Four Stages of Growth

Grains	Initial	Crop Development	Start of Maturity	Harvest	Total (from crop development to harvest)
Barley/oats/spring wheat	15-40	25-60	40-60	20-40	90-160
Winter wheat	20-160	60-140	40-75	25-30	175-210
Small grains	20-25	30-35	60-65	40	130-140
Corn grain	20-30	35-50	40-60	30-50	105-150
Sweet corn	20-30	20-40	25-70	10-103	60-163
Millet	15-20	25-30	40-55	25-35	90-120
Sorghum	20	35	40-45	30	105-110
Rice	30	30	60-80	30-40	120-150

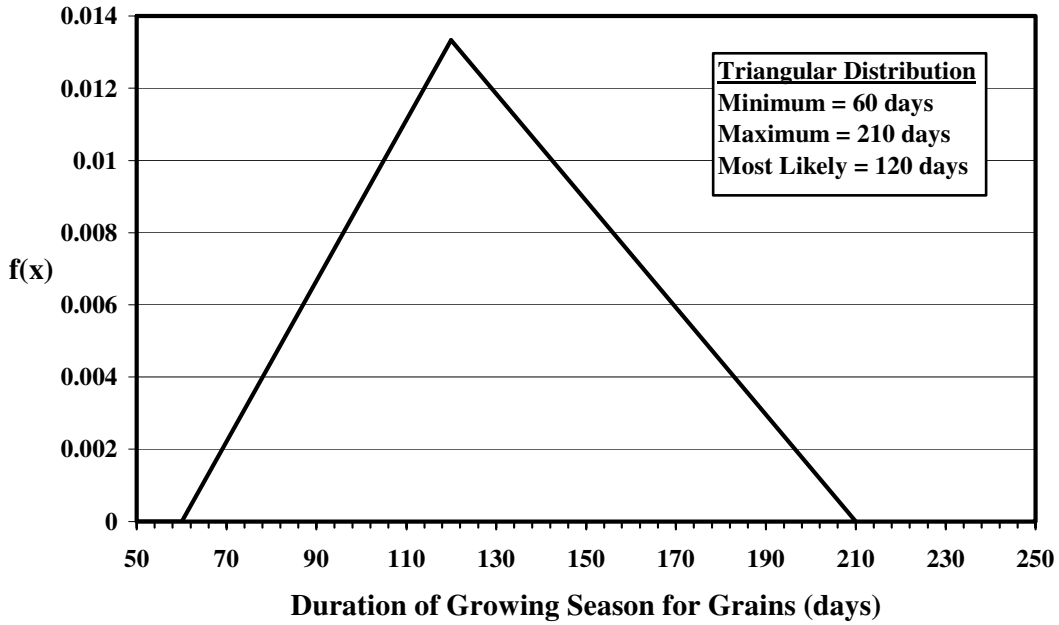

FIGURE 4.1-2 Probability Density Function for Grains for the Duration of the Growing Season

Table 4.1-5 lists the data extracted from Allen et al. (1998) for different fruits, nuts, grains, and nonleafy vegetables. For these plant food types, it is expected that foliar deposition during the time between initial crop development and the time of harvest could contribute to the dose of contamination that is ingested when the food is consumed. Therefore, the total time taken from crop development to the start of harvest is used to develop a distribution for fruits, grains, and nonleafy vegetables. The proposed growing period for fruits, grains, and nonleafy vegetables (Figure 4.1-3) is represented by a triangular distribution with minimum = 30 days, most likely = 105 days, and maximum = 320 days.

Table 4.1-6 lists the data extracted from Allen et al. (1998) for different leafy vegetables. For leafy vegetables, it is expected that foliar deposition during the time between initial crop development and the time of harvest could contribute to the dose of contamination that is ingested when the leafy vegetables are consumed. Therefore, the total time taken from crop development to the start of harvest is used to develop a distribution for leafy vegetables. The proposed growing period for leafy vegetables (Figure 4.1-4) is represented by a triangular distribution with minimum = 40 days, most likely = 75 days, and maximum = 180 days.

TABLE 4.1-5 Time (Days) Taken by Different Fruits and Nuts, Grains, and Nonleafy Vegetables during Four Stages of Growth

	Initial	Crop Development	Start of Maturity	Harvest	Total (from crop development to harvest)
Fruits and nuts					
Banana	120	60-90	120-180	5-60	245-270
Cantaloupe	10-30	45-60	25-40	10-25	90-110
Citrus	60	90	120	95	305
Grape	20-30	40-60	40-120	20-80	160-220
Olive	30	90	60	90	240
Pistachio	20	60	30	40	130
Sweet melon	15-30	30-45	40-65	15-30	95-130
Walnut	20	10	130	30	170
Watermelon	10-20	20-30	20-30	30	70-90
Grains					
Barley/oats/wheat	15-40	25-60	40-65	20-40	90-160
Corn (grain)	20-30	35-50	40-60	30-50	105-150
Grains (small)	20-25	30-35	60-65	40	130-140
Millet	15-20	25-30	40-55	25-35	90-120
Rice	30	30	60-80	30-40	120-150
Sorghum	20	35	40-45	30	105-110
Sweet corn	20-30	20-40	25-70	10-103	60-163
Winter wheat	20-160	60-140	40-75	25-30	160-210
Nonleafy vegetables					
Artichoke	20-40	25-40	250	30	305-320
Asparagus	50-90	30	100-200	45-50	180-275
Bean (dry)	15-25	25-30	30-40	20	75-90
Bean (green)	15-20	25-30	25-30	10	60-70
Beet	15-25	25-30	20-25	10	55-65
Bell pepper	25-30	35-40	40-110	20-30	95-180
Broad bean (dry)	90	45	40	60	145
Broad bean (green)	90	45	40	0	85
Carrot	20-30	30-50	30-90	20-30	80-170
Cassava	20-150	40	90-110	60	190-210
Cucumber	20-25	30-35	40-50	15-20	85-105
Eggplant	30	40-45	40	20-25	100-110
Faba bean	15-20	25-30	35	15	75-80
Green gram, coepea	20	30	30	20	80
Groundnut	25-35	35-45	35-45	25-35	105
Hops	25	40	80	10	130
Lentil	20-25	30-35	60-70	40	130-145
Onion	15-20	25-35	70-110	40-45	135-190

TABLE 4.1-5 (Cont.)

	Initial	Crop Development	Start of Maturity	Harvest	Total (from crop development to harvest)
Pea	15-35	25-30	30-35	15-20	75-80
Potato	25-45	30-35	30-70	20-30	90-120
Pumpkin	20-25	30-35	30-35	20-25	80-95
Radish	5-10	10	15	5	30
Soybean	15-20	15-35	40-75	15-30	70-130
Squash, zucchini	20-25	30-35	25	15	70-75
Sugar beet	25-50	30-75	50-100	10-65	130-230
Sweet potato	15-20	30	50-60	30-40	110-130
Tomato	25-35	40-45	45-70	25-30	105-145

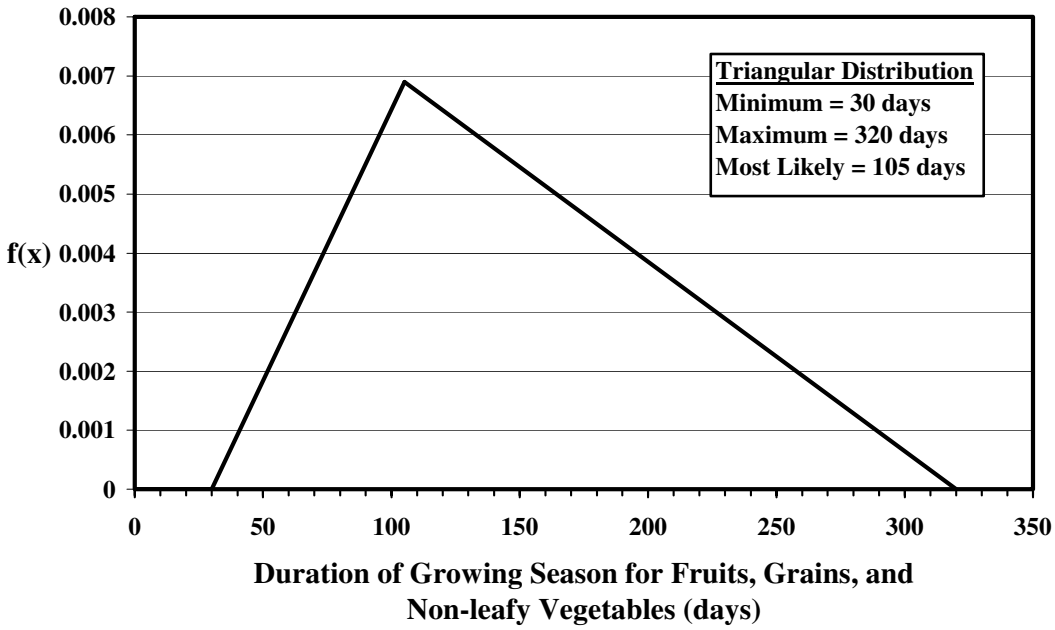

FIGURE 4.1-3 Probability Density Function for Fruits, Grains, and Nonleafy Vegetables for Duration of Growing Season

TABLE 4.1-6 Time (Days) Taken by Different Leafy Vegetables during Four Stages of Growth

Leafy Vegetables	Initial	Crop Development	Start of Maturity	Harvest	Total (from crop development to harvest)
Broccoli	35	45	40	15	100
Cabbage	40	60	50	15	125
Cauliflower	35	50	40	15	105
Celery	25-30	40-55	45-105	15-20	100-180
Crucifers	20-30	30-35	20-90	10-40	60-165
Lettuce	20-35	30-50	15-45	10	55-105
Onion (green)	20-30	30-55	10-55	5-40	45-150
Spinach	20	20-30	15-40	5-10	40-80

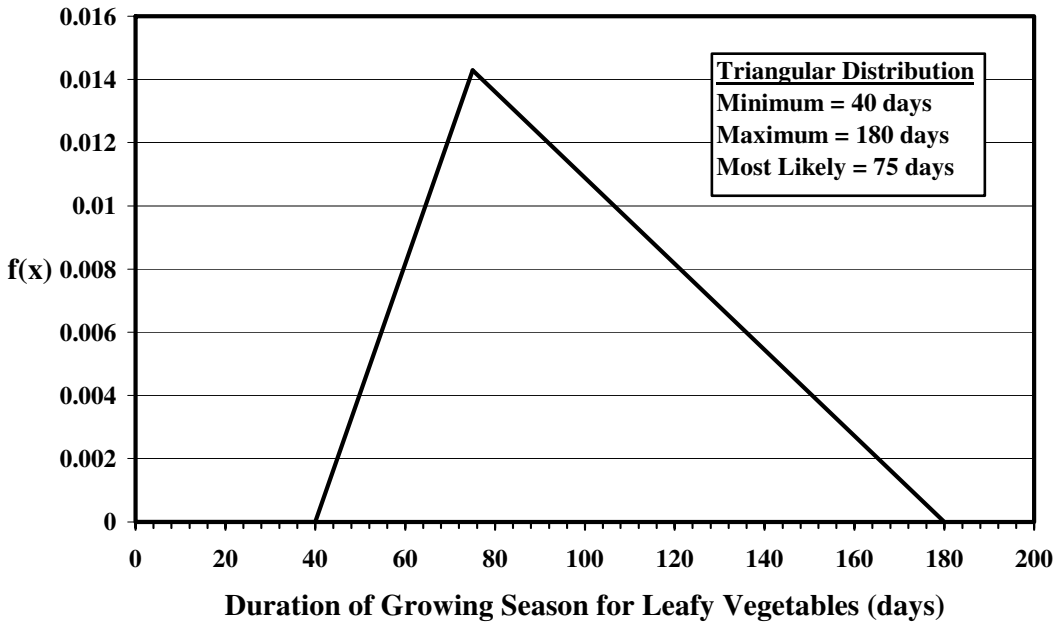

FIGURE 4.1-4 Probability Density Function for Leafy Vegetables for the Duration of Growing Season

4.2 DEPTH OF ROOTS

Applicable Code: RESRAD (onsite), RESRAD-OFFSITE

Description: This parameter represents the average root depth of various plant types grown in the contaminated zone. For RESRAD-OFFSITE, the plant types consumed by humans are divided in two categories: leafy vegetables; and fruit, grain, and nonleafy vegetables. The plant types consumed by livestock are also divided in two categories: pasture and silage, and grain.

Units: meters (m)

Probabilistic Input:

Distribution: uniform

Defining Values for Distribution: See Table 4.2-1.

Discussion: Root depth varies by plant type. For some plants (e.g., cabbage, spinach, lettuce, broccoli, and others) root depth does not extend below about 0.9 m. For other plants (e.g., fruit trees) the roots may extend 2 m below the surface. Tap roots for some crops (e.g., alfalfa) can extend to 4 m. Most of the plant roots from which nutrients are obtained, however, usually extend less than 1 m below the surface.

Root depth is used to calculate the cover and depth factor for the plant, meat, and milk exposure pathways, because edible plants become contaminated through root uptake of radionuclides. Uptake of radionuclides from plant roots is assumed possible only when the roots extend to the contaminated zone, and it is limited to the fraction of roots that have direct contact with contaminated soil.

Each crop has characteristic rooting habits that it will tend to follow if the soil is deep, uniform, and equally moist throughout. The depth of rooting increases during the growing

TABLE 4.2-1 Uniform Distribution Input for Depth of Roots

Field Type	Minimum	Maximum
RESRAD-OFFSITE		
Pasture and silage	0.3	3.6
Grain	0.5	2.4
Fruit, grain, and nonleafy vegetables	0.3	2.4
Leafy vegetables	0.3	0.9
RESRAD (onsite)		
Contaminated area	0.3	4.0

period. Crops that mature in 2 months usually penetrate only 0.6-0.9 m, and crops that require 6 months to mature may penetrate 1.8 to 3.0 m or more.

When the upper portion of the soil is kept moist, plants will obtain most of their moisture supply from near the surface. As the moisture content of the upper layers decreases, the plants draw more water from the lower layers, which encourages more root development in the lower levels. Fewer roots exist in the lower portion of the root zone because of the inability of the root system to extract enough moisture from the lower levels. Generally, the average root-zone depths are reached by the time the foliage of the plant has reached its maximum size. Root-zone depths are limited to the soil depth above the water table.

Table 4.2-2 lists rooting depths for a variety of forages that can be used for livestock consumption. Growing conditions (e.g., amount of rainfall or temperature) vary annually and geographically across United States, and the type of forage consumed by livestock is uncertain. Therefore, for forages, a uniform distribution with a minimum of 0.3 m and a maximum of 3.6 m (as shown in Figure 4.2-1) is suggested for use in RESRAD-OFFSITE. If specific conditions are known, values from Table 4.2-2 for a specific forage type may be used.

Table 4.2-3 lists rooting depths for a variety of grains that can be used for livestock consumption. In general, the grain crops grown during the spring season have less rooting depths compared with the crops grown during the winter season. The criteria cited for forage crops also apply to grain crops. Therefore, for grain, a uniform distribution with a minimum of 0.5 m and a maximum of 2.4 m (as shown in Figure 4.2-2) is suggested for use in RESRAD-OFFSITE. If specific conditions are known, values from Table 4.2-3 for a specific grain type may be used.

Table 4.2-4 lists rooting depths for fruits and nuts, grains, and nonleafy vegetables that can be consumed by humans. In general, the grain crops grown during the spring season have less rooting depths compared with the crops grown during the winter season. For fruit, grain, and nonleafy vegetables, a uniform distribution with a minimum of 0.3 m and a maximum of 2.4 m (as shown in Figure 4.2-3) is suggested for use in RESRAD-OFFSITE. If specific conditions are known, values from Table 4.2-4 for a specific plant type may be used.

Table 4.2-5 lists rooting depths for leafy vegetables that can be consumed by humans. For leafy vegetables, a uniform distribution with a minimum of 0.3 m and a maximum of 0.9 m (as shown in Figure 4.2-4) is suggested for use in RESRAD-OFFSITE.

If specific conditions are known, values from Table 4.2-5 for a specific leafy vegetable may be used.

Minimum and maximum values of 0.3 and 4.0 m for the root depth are suggested as input to RESRAD (onsite), which does not distinguish among the plant types. These values bound those presented in previous tables. However, site-specific minimum and maximum root depths should be used, based on the plant types present, and these may be obtained from Tables 4.2-2 through 4.2-5. Figure 4.2-5 presents the uniform probability density function for root depth for RESRAD (onsite).

TABLE 4.2-2 Root Depth of Forage from Different Sources

Forage Types	Depth (m)	Curwen and Massie (1994)	Weaver (1926)	Georgeson and Payne (1897)	Canadell et al. (1996)	Allen et al. (1998)
Alfalfa	0.6-3.6	0.6-1.2	3-3.6	1.5-1.8		1.0-3.0
Bermuda grass	1.0-1.5					1.0-1.5
Bluegrass	0.3-2.1		1.5-2.1	0.3-1.1		
Broome grass	1.1-2.0		1.7-2.0		1.1	
Canary grass	0.6-1.5			0.6-1.5		
Clover, ladino	1.5-2.4		1.5-2.4			
Clover, red	0.6-2.4	0.6	1.5-2.4	1.5		0.6-0.9
Fescue	0.6-1.2		0.6-1.2			
Orchard grass	0.9-1.3		0.9-1.3			
Rye grass	0.6-0.9		0.6-0.9			0.6-1.0
Trefoil	0.6-1.2	0.6-1.2				
Timothy	0.4-0.9		0.4-0.9			
Buffalo grass	0.6-1.9		0.6-0.9	0.9	1.9	
Pasture grasses	0.6-1.5	0.6-1.2				0.5-1.5
Bigbluestem	1.5-2.8		1.5-2.7		1.5-2.8	
Little bluestem	0.9-1.8		0.9-1.7		1.5-1.8	

Sources: Modified from Weaver (1926), Georgeson and Payne (1897), Canadell et al. (1996), Curwen and Massie (1994), Allen et al. (1998).

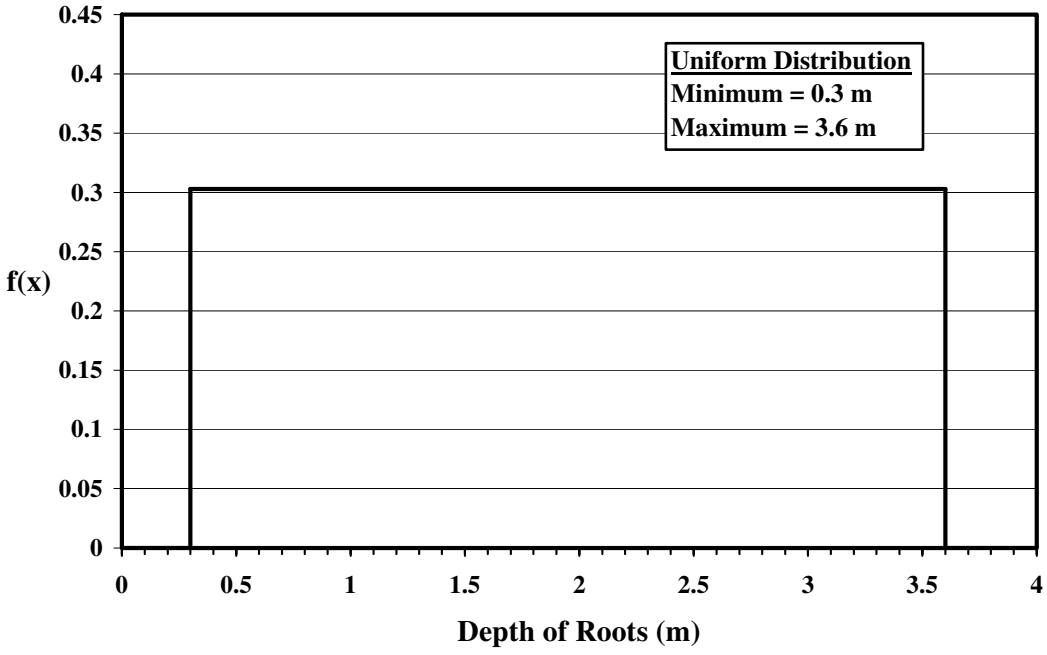

FIGURE 4.2-1 Root Depth Probability Density Function for Pasture and Silage

TABLE 4.2-3 Root Depth of Grains from Different Sources

Grain Plants	Range Root Depth (m)	Allen et al. (1998)	Weaver and Brunner (1927)	Curwen and Massie (1994)	Weaver (1926)
Barley	1.0-2.0	1.0-1.5			1.4-2.0
Corn	1.0-2.4	1.0-1.7	1.5-2.4	0.6-1.2	1.5-1.8
Millet	1.0-2.0	1.0-2.0			
Oat	1.0-1.5	1.0-1.5			1.2-1.5
Rice	0.5-1.0	0.5-1.0			
Sorghum	1.0-2.0	1.0-2.0			1.4-1.8
Spring wheat	1.0-1.5	1.0-1.5		0.6	
Winter wheat	1.5-2.1	1.5-1.8			1.5-2.1

Sources: Allen et al. (1998), Weaver and Brunner (1927), Curwen and Massie (1994), Weaver (1926).

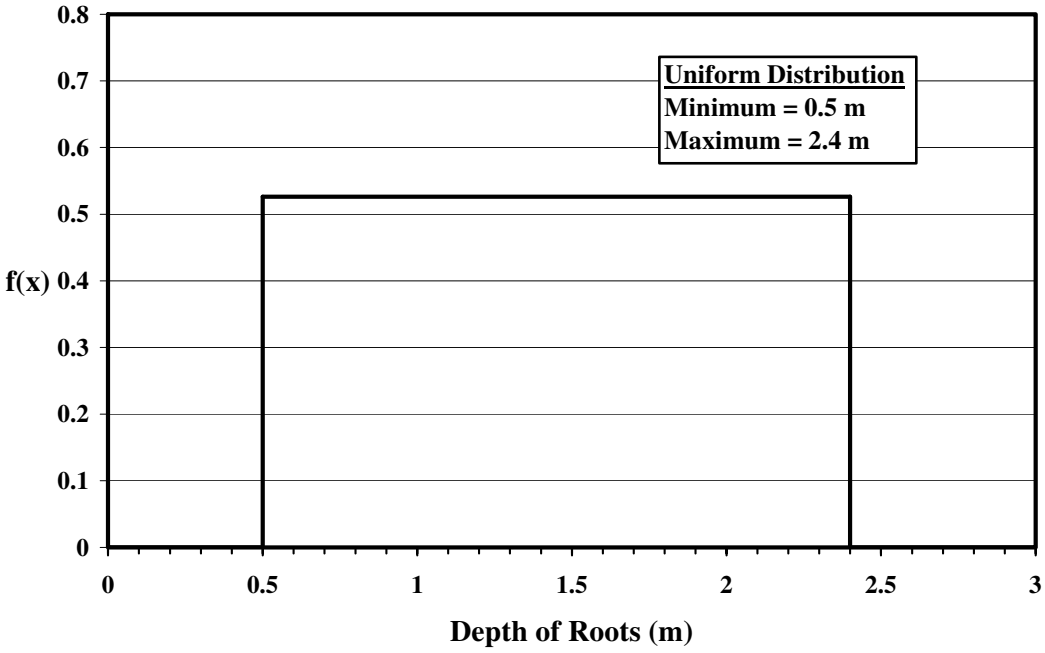

FIGURE 4.2-2 Root Depth Probability Density Function for Grains

TABLE 4.2-4 Root Depth of Fruits and Nuts, Grains, and Nonleafy Vegetables from Different Sources

Plant Type	Range Root Depth (m)	Allen et al. (1998)	Weaver and Brunner (1927)	Kemble and Sanders (2000)	Evans et al. (1996)	Curwen and Massie (1994)	Weaver (1926)
Fruit and nuts							
Almond, apple, apricot, cherry, grape, peach, and pear	1.0-2.0	1.0-2.0					
Avocado	0.5-1.0	0.5-1.0					
Banana	0.5-0.9	0.5-0.9					
Berries	0.6-1.2	0.6-1.2				0.6-1.2	
Cantaloupe	0.3-1.5	0.9-1.5	1.1	0.3-0.6			
Citrus fruits	1.2-1.5	1.2-1.5					
Kiwi	0.7-1.3	0.7-1.3					
Olive	1.2-1.7	1.2-1.7					
Pineapple	0.3-0.6	0.3-0.6					
Pistachio	1.0-1.5	1.0-1.5					
Strawberry	0.2-0.6	0.2-0.3	0.3-0.6		0.3	0.3	
Sweet melon, watermelon	0.8-1.5	0.8-1.5	1.1	>0.6		0.6-1.2	
Grain							
Barley	1.0-2.0	1.0-1.5					1.4-2.0
Corn	1.0-2.4	1.0-1.7	1.5-2.4			0.6-1.2	1.5-1.8
Millet	1.0-2.0	1.0-2.0					
Oat	1.0-1.5	1.0-1.5					1.2-1.5
Rice	0.5-1.0	0.5-1.0					
Sorghum	1.0-2.0	1.0-2.0					1.4-1.8
Spring wheat	1.0-1.5	1.0-1.5				0.6	
Winter wheat	1.5-2.1	1.5-1.8					1.5-2.1
Nonleafy vegetables							
Artichoke	0.6-0.9	0.6-0.9					
Asparagus	1.2-3.0	1.2-1.8	1.5-3.0	>0.6			
Carrot	0.3-2.0	0.5-1.0	0.6-2.0	0.3-0.6	0.5		
Chick pea	0.3-1.0	0.6-1.0	0.6-1.0	0.3-0.6	0.5	0.6	
Cucumber	0.3-1.2	0.7-1.2	1.1	0.3-0.6			
Eggplant	0.3-2.0	0.7-1.2	1.2-2.0	0.3-0.6			
Green bean	0.5-0.7	0.5-0.7		0.5-0.6	0.5		
Lima bean	0.6-1.2	0.8-1.2	0.9-1.2	>0.6		0.6	
Okra	0.5-1.2		0.5-1.2	>0.6			
Onion	0.3-1.0	0.3-0.6	0.5-1.0	0.3-0.5	0.3	0.5	
Potato	0.3-0.9	0.4-0.6		0.3-0.5	0.5	0.5	0.6-0.9
Pumpkin	0.6-1.8	1.0-1.5	1.8	>0.6		0.6-1.2	
Radish	0.3-0.9	0.3-0.5	0.6-0.9				
Squash, zucchini	0.3-1.8	0.6-1.0	1.8	0.3-0.6		0.6-1.2	
Sugar beet	0.5-2.0	0.7-1.2	1.2-2.0	0.5-0.6	0.5	0.5	1.5-1.8
Sweet pepper	0.3-1.2	0.5-1.0	0.9-1.2	0.3-0.6	0.3	0.6	
Sweet potato	0.6-1.5	1.0-1.5	1.2	>0.6			
Tomatoes	0.6-1.7	0.7-1.5	1.0-1.7	>0.6			
Turnip	0.5-1.5	0.5-1.0	1.5				

Sources: Allen et al. (1998), Weaver and Brunner (1927), Kemble and Sanders (2000), Evans et al. (1996), Curwen and Massie (1994), Weaver (1926).

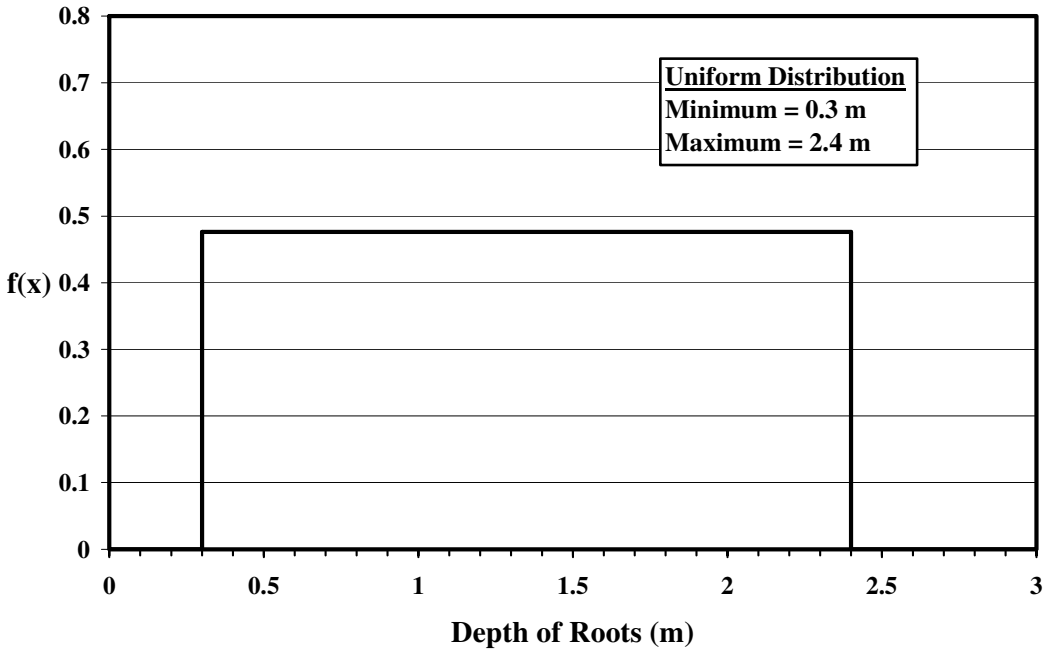

FIGURE 4.2-3 Root Depth Probability Density Function for Fruits, Grains, and Nonleafy Vegetables

TABLE 4.2-5 Root Depth of Leafy Vegetables from Different Sources

Leafy Vegetables	Root Depth (m)	Curwen and Massie (1994)	Allen et al. (1998)	Weaver and Brunner (1927)	Kemble and Sanders (2000)	Evans et al. (1996)
Spinach	0.3-0.5		0.3-0.5	0.3	0.3-0.5	0.3-0.5
Lettuce	0.3-0.9	0.5	0.3-0.5		0.6-0.9	0.3-0.5
Broccoli	0.3-0.6		0.4-0.6		0.3-0.5	0.3-0.5
Celery	0.3-0.5		0.3-0.5		0.3-0.5	
Cabbage	0.3-0.9		0.5-0.8	0.9	0.3-0.5	0.3-0.5
Cauliflower	0.3-0.9		0.4-0.7	0.9	0.3-0.5	0.3-0.5
Brussel sprout	0.3-0.6		0.4-0.6		0.3-0.5	
Mint	0.4-0.8		0.4-0.8			
Collard	0.3-0.5				0.3-0.5	
Mustard	0.3-0.6				0.5-0.6	0.3-0.5

Source: Curwen and Massie (1994), Allen et al. (1998), Weaver and Brunner (1927), Kevin and Sanders (2000), Evans et al. (1996).

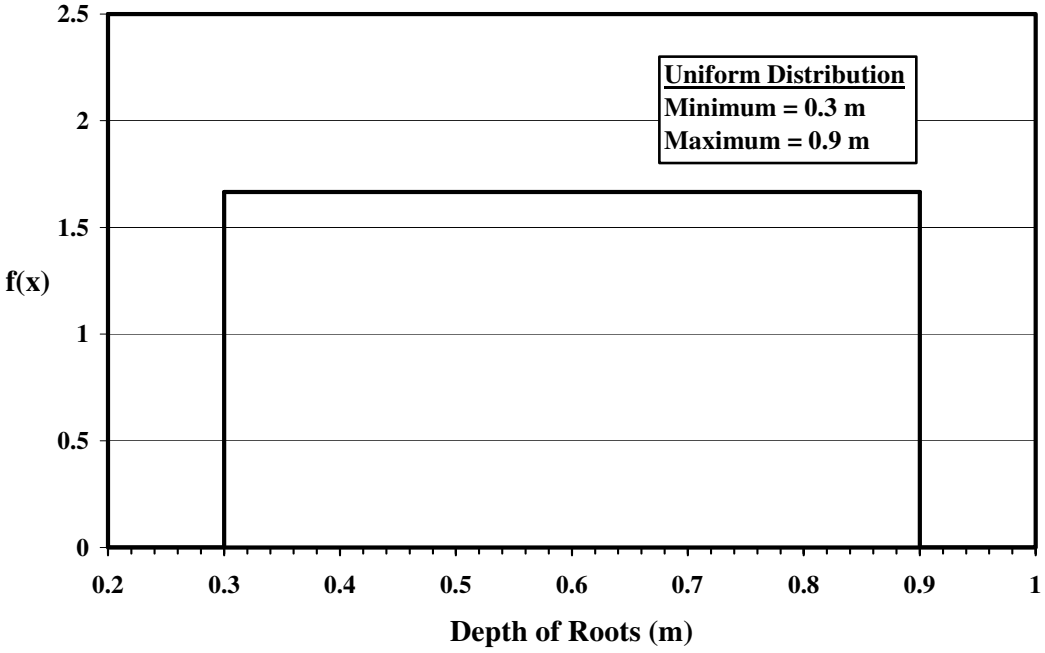

FIGURE 4.2-4 Root Depth Probability Density Function for Leafy Vegetables

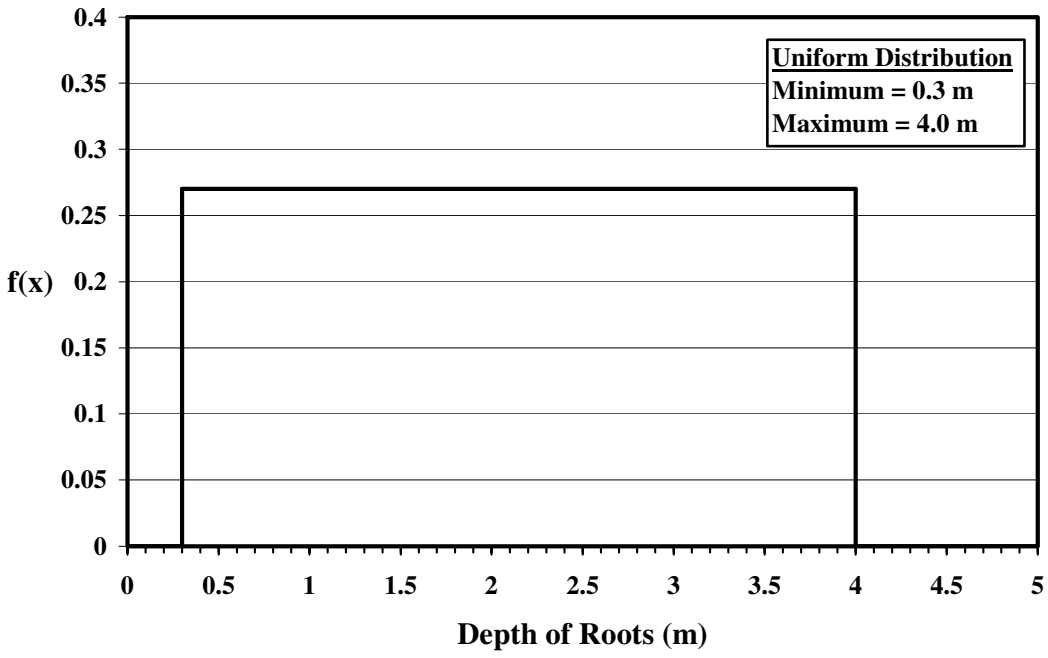

FIGURE 4.2-5 Root Depth Probability Density Function for RESRAD (onsite)

4.3 TRANSFER FACTORS FOR PLANTS

Applicable Code: RESRAD (onsite), RESRAD-OFFSITE

Description: The transfer factors for plants are the concentrations of the nuclide in vegetables, fruits, grains, and livestock feed products at the time of harvest (fresh weight basis) as a result of root uptake from soil that contains a unit concentration (dry weight basis) of the nuclide.

Units: pCi/g plant (wet) weight per pCi/g soil (dry)

Probabilistic Input:

Distribution: truncated lognormal-n

Defining Values for Distribution: Values are assigned according to the element of the radioactive isotope, as given in Table 4.3-1. The values in this table are for the fruits, grains, and vegetables consumed by humans (RESRAD [onsite] and RESRAD-OFFSITE) and the products consumed by livestock (RESRAD-OFFSITE). Lower and upper quantile input values are 0.001 and 0.999 for all elements.

Discussion: The soil-to-plant transfer factor is defined as the ratio of radionuclide concentration in vegetation to that of the soil. The soil-to-plant transfer factor of a radionuclide varies in a complex manner with soil properties and the geochemical properties of the radionuclide in the soil. The transfer factor for a given plant type can vary from site to site and season to season. In addition, management practices such as plowing, liming, fertilizing, and irrigating greatly affect the plant/soil transfer ratio (IAEA 1994). After entering the transpiration stream, radionuclides may not be uniformly distributed within a plant, but instead they tend to concentrate in certain plant organs (Grogan 1985). Sparse data exist for most radionuclides, and the data that do exist are restricted to only limited vegetation types (NCRP 1999). Even for the most studied radionuclides, the values of the soil-to-plant transfer factors can vary over several orders of magnitudes (IAEA 1994).

The RESRAD-OFFSITE code allows different soil-to-plant transfer factors for fruits, grains, nonleafy vegetables; leafy vegetables; pasture and silage; and livestock feed grain. The fruits, grains, nonleafy vegetables, and leafy vegetables are for human consumption. The pasture and silage and livestock feed grain are for livestock consumption. In other published radiological assessment reports, as discussed below for NUREG/CR-5512, the soil-to-plant transfer factors are also provided for different vegetation types and are given as the ratio of pCi per gram plant (dry)/pCi per gram soil (dry). To convert from the vegetation-specific dry plant/soil transfer factor to a composite wet plant/soil transfer factor, a dry-to-wet conversion factor must be determined for each vegetation type.

In addition, the vegetation-specific transfer factors must be weighted by the relative importance (measured in kilograms) of each vegetable category (Wang et al. 1993). Although the transfer factors may range over a couple of orders of magnitude for different radionuclides, the range among vegetation types for a given radionuclide is not as great (NCRP 1999).

TABLE 4.3-1 Lognormal Distribution Parameter Values for Soil-to-Plant Transfer Factors

	Human Consumption[a]		Livestock Feed[b]	
Element	μ_v	σ	μ_p	σ
Ac	-6.91	1.1	-6.91	1.1
Ag	-5.52	0.9	-3.69	0.9
Al	-5.52	1.1	-5.30	1.1
Am	-6.91	0.9	-6.91	0.9
As	-2.53	1.1	-3.00	1.1
Ba	-4.61	1.1	-3.69	0.9
Be	-5.52	1.1	-5.30	1.1
Bi	-2.3	1.1	-2.08	1.1
Br	-0.92	1.1	-0.69	1.1
C[c]	-0.36	0.9	-0.36	0.9
Ca	-0.69	1.1	0.22	1.1
Cd	-0.69	1.1	-1.39	1.1
Ce	-6.21	1	-4.38	1.0
Cf	-6.91	1.1	-6.91	1.1
Cl	3	1.1	3.22	1.1
Cm	-6.91	0.9	-6.91	0.9
Co	-2.53	0.9	-0.69	0.9
Cr	-4.61	1	-4.61	1.0
Cs	-3.22	1	-3.00	1.0
Cu	-3	1	-1.61	1.0
Eu	-6.21	1.1	-4.38	1.1
F	-3.91	1.1	-4.20	1.1
Fe	-6.91	0.9	-5.99	1.0
Gd	-6.21	1.1	-4.38	1.1
Ge	-0.92	1.1	0.00	1.1
H[c]	1.57	1.1	1.57	1.1
Hg	-1.2	1.1	-1.39	1.1
Ho	-6.21	1.1	-4.38	1.1
I	-3.91	0.9	-3.69	0.9
In	-5.81	1.1	-5.99	1.1
Ir	-3.51	1.1	-3.00	1.1
K	-1.2	1.1	-0.29	1.1
La	-6.21	0.9	-4.38	0.9
Mg	-3.5	1.1	-3.69	1.1
Mn	-1.2	0.9	0.92	0.9
Mo	-2.3	1.1	-2.30	1.0
N[c]	3.4	0.9	3.4	0.9
Na	-3	1	-3.00	1.0
Nb	-4.61	1.1	-3.69	1.0
Nd	-6.21	1	-4.38	1.1
Ni	-3	0.9	-1.39	0.9
Np	-3.91	0.9	-3.69	0.9
P	0	1.1	-0.29	1.1
Pa	-4.61	1.1	-4.38	1.1
Pb	-5.52	0.9	-3.79	0.9

TABLE 4.3-1 (Cont.)

	Human Consumption[a]		Livestock Feed[b]	
Element	μ_v	σ	μ_p	σ
Pd	-2.3	1.1	-2.08	1.1
Pm	-6.21	1.1	-4.38	1.1
Po	-6.9	0.9	-5.99	0.9
Pr	-6.21	1	-4.38	1.0
Pu	-6.91	0.9	-8.29	0.9
Ra	-3.22	0.9	-3.00	0.9
Rb	-1.61	1	-0.69	1.0
Rh	-3.51	1	-3.00	1.0
Ru	-3.51	0.9	-3.00	0.9
S	-0.51	1.1	-0.70	1.1
Sb	-4.61	1	-4.38	1.0
Sc	-6.21	1.1	-5.99	1.1
Se	-2.3	1.1	-2.08	1.1
Si	-3.9	1.1	-3.69	1.1
Sm	-6.21	1.1	-4.38	1.1
Sn	-1.2	1.1	-1.39	1.1
Sr	-1.2	1	0.00	1.0
Ta	-6.21	1.1	-5.30	1.1
Tb	-6.21	1.1	-4.38	1.1
Tc	1.61	0.9	2.30	0.9
Te	-2.3	1	-1.12	1.0
Th	-6.91	0.9	-8.29	0.9
Tl	-1.61	1.1	-1.90	1.1
U	-6.21	0.9	-3.69	0.9
W	-0.22	1	-0.29	1.0
Y	-6.21	1.1	-4.38	1.1
Zn	-0.92	0.9	-1.39	0.9
Zr	-6.91	1.1	-6.68	1.0

[a] Adopted from Bv(wet) values in NCRP (1999).

[b] Converted Bp(dry) values in NCRP (1999) to Bp(wet) by using a wet-to-dry conversion factor of 0.25 (average value from IAEA 1994).

[c] Derived from Yu et al. (2001).

Source: NCRP (1999), except as noted.

A lognormal distribution is consistently proposed as most appropriate for the plant/soil transfer factor (Beyeler et al. 1998). The soil-to-plant transfer factors were obtained from Appendix D of the National Council on Radiation Protection and Measurements Report 129 (NCRP 1999), except as noted. The report provides median and geometric standard deviations for composite wet soil-to-plant transfer factors for vegetations consumed by humans and the dry soil-to-plant transfer factors for fodder consumed by livestock for each element listed in

Table 4.3-1. A wet-to-dry conversion factor of 0.25 was used for the fodder. Table 4.3-2 provides the average dry-weight content of different fresh products. The values in this table are extracted from IAEA (1994). The parameters that describe the lognormal probability distribution of the soil-to-plant transfer factors for each element were estimated by setting the natural logarithm of the geometric standard deviation equal to σ and setting μ equal to the natural logarithm of the median value given in Appendix D of NCRP Report 129 (NCRP 1999).

RESRAD (onsite) and RESRAD-OFFSITE require the plant transfer factors to be expressed as the ratio of pCi per gram plant (wet)/pCi per gram soil (dry). Other studies, such as NUREG/CR-5512 (Kennedy and Strenge 1992), express the transfer factor for the four plant types as the ratio of pCi per gram plant type (dry)/pCi per gram soil (dry). A dry-to-wet weight conversion factor must therefore be applied to make proper comparisons between the transfer factors. An overall average conversion factor of 0.428 has been estimated by Baes et al. (1984). This average factor is based on several factors, including (1) calculation of the dry-to-wet weight conversion factors for exposed produce, protected produce, and grains on the basis of relative importance of various nonleafy vegetables in the United States; and (2) calculation of the average dry-to-wet conversion factor by weighting these calculated values by the relative importance (based on production, in kilograms) of each vegetable category grown in the United States. When an overall average dry-to-wet conversion factor of 0.428 is applied to the plant transfer factors given in Table 4.3-1, the values are in good agreement with the values presented in NUREG/CR-5512 (Kennedy and Strenge 1992), especially when the transfer factors can vary by a factor of 10 or more for the same vegetation type.

TABLE 4.3-2 Average Dry Weight Content of Different Fresh Products

Product	Dry Weight Content	Product	Dry Weight Content
Fodder		*Cereals*	
Alfalfa, clover	0.19	Barley, oat, rye, wheat	0.86
Maize	0.31	Corn (maize)	0.55
Grass	0.1	*Vegetables*	
Pea, bean	0.25	Cabbage	0.12
Soybean	0.31	Cauliflower	0.11
Root crops		Celery	0.06
Beet, sugar beet	0.22	Lettuce	0.08
Carrot	0.16	Spinach	0.08
Radish	0.09	Tomato	0.06
Turnip	0.12	Zuchini	0.05
Kohlrabi	0.06	Cucumber	0.05
Tapioca	0.38	Leek	0.11
Potato	0.21	Onion	0.11
Swede	0.11	Raspberry	0.16

Source: Extracted from IAEA (1994).

5 RECEPTOR PARAMETER DISTRIBUTIONS

5.1 QUANTITY OF WATER FOR HOUSEHOLD PURPOSES

Applicable Code: RESRAD-OFFSITE

Description: The quantity of water for household purposes is the average amount of water used indoors by an individual (per capita indoor water use).

Units: liters/day

Probabilistic Input:

Distribution: truncated lognormal-n

Defining Values for Distribution:

Underlying mean value: 5.51	Lower quantile value: 0.001
Underlying standard deviation: 0.407	Upper quantile value: 0.999

Discussion: The indoor water use at a residential dwelling typically comes from toilets, clothes washers, baths and showers, sinks, leaks, dishwashers, and other miscellaneous uses. The total amount of water used on a daily basis is dependent upon a number of variables including geographic location, time of year, the number of persons sharing the residence, and the water efficiency of the fixtures and appliances. Table 5.1-1 lists the average daily per capita water use in a residential setting for a number of past studies. Earlier work was also presented in Nazaroff et al. (1988), who summarized past work in the 1960s and 1970s, fitting a lognormal distribution to the available data with a geometric mean of 189 L/day for the per capita indoor use rate.

The latest study with the most extensive information available on residential water use is the Residential End Use of Water Study (REUWS) (Mayer et al. 1999). The study was funded by the American Water Works Association Research Foundation and 22 municipalities, water utilities, water purveyors, water districts, and water providers. The goals of the study included the development of predictive models of water use, discerning differences between geographic locations, disaggregating indoor and outdoor water use, and looking at variations in water usage by different fixtures and appliances. The REUWS looked at 12 different locations in North America, sampling approximately 100 single-family homes at each location for a continuous period of 2 weeks in the summer and 2 weeks in the winter. Sampling was accomplished by using data loggers connected to water flow meters in each residence. Table 5.1-2 lists the average per capita indoor water use at each site.

Figure 5.1-1 displays a histogram of the per capita water use frequency distribution from the REUWS (Mayer 2005) in conjunction with the probability distribution function for use in RESRAD-OFFSITE. The probability density function was fit well to a lognormal distribution by using nonlinear least squares regression analysis.

TABLE 5.1-1 Past Studies on Per Capita Indoor Water Use

Study	Number of Residences	Study Duration (months)	Average (liters/person/day)	Range (liters/person/day)
Brown & Caldwell (1984)	210		250.6	216.9 - 276.3
Anderson and Siegrist (1989)	90	3	268	249.4 - 289.9
Anderson et al. (1993)	25	3	191.9	98.9 - 322.5
Mayer et al. (1999)	1,188	1	262.3	216.1 - 316.1
Weighted average	153		259.7	

Source: EPA (2002).

TABLE 5.1-2 Per Capita Indoor Water Use for the 12 Sites in the REUWS

Study Site	Sample Size (Number of households)	Mean Persons per Household	Mean Daily per Capita Indoor Use (liters/person/day)	Median Daily per Capita Indoor Use (liters/person/day)	Standard Deviation of per Capita Indoor Use (liters/person/day)
Seattle, WA	99	2.8	216	204	108
San Diego, CA	100	2.7	221	205	88.6
Boulder, CO	100	2.4	245	228	97.7
Lompoc, CA	100	2.8	249	212	126
Tampa, FL	99	2.4	249	223	127
Walnut Valley Water District, CA	99	3.3	257	240	117
Denver, CO	99	2.7	262	246	132
Las Virgennes Metropolitan Water District, CA	100	3.1	263	231	146
Waterloo and Cambridge, ON	95	3.1	267	225	169
Phoenix, AZ	100	2.9	294	253	170
Tempe and Scottsdale, AZ	99	2.3	308	240	256
Eugene, OR	98	2.5	316	242	261
12 study sites	1188	2.8	262	229	150

Source: Mayer et al. (1999).

As seen in Tables 5.1-1 and 5.1-2, there is some variation in the per capita indoor water use. Some of this variation within and among sites can be attributed to regional personal use habits, additional individuals at home during the study period, or the prevalence of water-efficient appliances or reduced-flow fixtures (Mayer et al. 1999). Table 5.1-3 presents a breakdown of water use among fixture and appliance use for each of the 12 sites. Additional information on the presence of fixtures/appliances, usage events, flow rates, and the demographics of the study participants can be found in Mayer et al. (1999).

Further work using methods similar to those in the REUWS to monitor indoor water usage relevant to water-conserving fixtures has also been published for Seattle, Washington

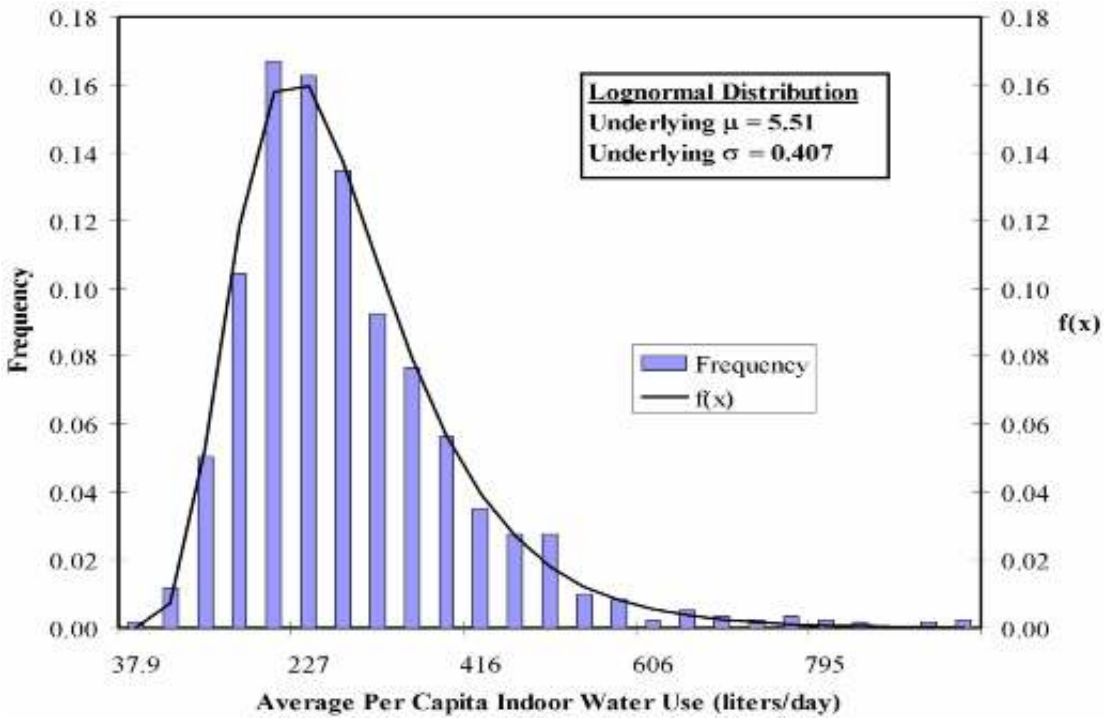

FIGURE 5.1-1 Quantity of Water for Household Purposes Probability Density Function

TABLE 5.1-3 Breakdown of Per Capita Indoor Water Use

Study Site	Toilet	Clothes Washer	Shower	Faucet	Leak	Other Domestic	Bath	Dishwasher
Seattle, WA	17.100	12.0	11.4	8.7	5.9	0.0	1.1	1.0
San Diego, CA	15.800	16.3	9.0	10.8	4.6	0.3	0.5	0.9
Boulder, CO	19.8	14.0	13.1	11.6	3.4	0.2	1.4	1.4
Lompoc, CA	16.6	15.3	11.1	9.9	10.1	0.9	1.2	0.8
Tampa, FL	16.700	14.2	10.2	12.0	10.8	0.3	1.1	0.6
Walnut Valley Water District, CA	18	14.1	11.7	12.3	7.6	2.3	1.0	0.8
Denver, CO	21.1	15.6	12.9	10.5	5.8	0.5	1.6	1.2
Las Virgennes Metropolitan Water District, CA	15.7	16.8	11.4	11.2	11.2	1.1	1.3	0.9
Waterloo and Cambridge, ON	20.3	13.7	8.3	11.4	8.2	6.0	1.9	0.8
Phoenix, AZ	19.6	16.9	12.5	9.6	14.8	2.2	1.2	0.8
Tempe and Scottsdale, AZ	18.4	14.5	12.6	11.2	17.6	5.0	0.9	1.1
Eugene, OR	22.9	17.1	15.1	11.9	13.6	0.1	1.5	1.4
12 study sites	18.5	15.0	11.6	10.9	9.5	1.6	1.2	1.0

Source: Mayer et al. (1999).

(Mayer et al. 2000); Tampa, Florida (Mayer et al. 2004); and the San Francisco Bay area (Mayer et al. 2003). More information on specific water fixture uses an be found in EPA (1997) for most indoor uses, and a more detailed analysis for specific uses can be found in Burmaster (1998) (showering) and Wilkes et al. (2005) (showering and bathing water use).

5.2 OUTDOOR FRACTION

Applicable Code: RESRAD (onsite), RESRAD-OFFSITE

Description: The outdoor fraction is the fraction of time an individual spends outside the residence (RESRAD [onsite], RESRAD-OFFSITE) or outside in the agricultural fields (RESRAD-OFFSITE).

Units: unitless

Probabilistic Input:

Distribution: continuous linear

Defining Values for Distribution: See Table 5.2-1 for the input values.

Discussion: In RESRAD (onsite) and RESRAD-OFFSITE, the outdoor fraction is used in the exposure calculations to calculate the amount of time spent outdoors at the residence or dwelling location. Actual exposure times at each location are estimated by multiplying the exposure duration by the outdoor fraction at the receptor location. In RESRAD-OFFSITE, an additional time fraction spent outdoors in farmed areas is used.

For RESRAD (onsite), the outdoor fraction is the fraction of time spent outside the residence where the receptor is exposed to external radiation from contaminated soil and resuspended contamination. This situation translates into the amount of time spent outdoors at a residence when evaluating the residential farmer scenario. The EPA's *Exposure Factors Handbook* (EPA 1997) contains a comprehensive review of human activity patterns, including time spent at home in the yard. That review extracts data for time spent at home from the most complete and current study on activity patterns (Tsang and Klepeis 1996). Table 5.2-1 summarizes a number of distributions, including distributions for time spent outdoors at home in the yard or other areas outside the house. The distribution chosen to represent the average members of the critical group (adult males) in the residential farmer scenario was that for the age group of 18-64 years. This distribution is almost identical to that for the male population group and close to those for all subjects and the female population group. Figure 5.2-1 presents the cumulative distribution function for the outdoor fraction parameter in RESRAD (onsite). This distribution function is also appropriate for the fraction of time spent outdoors at the offsite dwelling site in RESRAD-OFFSITE.

TABLE 5.2-1 Cumulative Distribution Functions for the Outdoor Fraction

	Outdoor Fraction	
Cumulative Probability	Residence/ Dwelling	Farmed Area
0	0.000174	0.000868
0.05	0.00694	0.00347
0.25	0.0278	0.0139
0.5	0.0625	0.0399
0.75	0.125	0.0868
0.9	0.222	0.11
0.95	0.292	0.127
0.98	0.396	0.162
0.99	0.458	0.166
1	0.896	0.166

The fraction of time spent outdoors in farmed areas in RESRAD-OFFSITE can be approximated by the amount of time spent outdoors on a farm (EPA 1997). Because RESRAD-OFFSITE models four different fields, the fraction of time spent in each field is assumed to be one-quarter the value of the total fraction of time spent farming. The distribution function values for this fraction are given in Table 5.2-1. Again, the values used are for the age group of 18-64 years, but these values are similar to those for all receptors, or for male or female receptors, as shown in Table 5.2-2. The cumulative distribution function for the fraction of time spent outdoors in a farm field is shown in Figure 5.2-2. For a true site-specific analysis, the fraction of time spent in each of the farm fields must be adjusted to account for the actual number of fields affected as well as the activities to be performed in each field.

For other scenarios using RESRAD (onsite) or RESRAD-OFFSITE that involve the fraction of time spent outdoors, EPA (1997) also contains information on the time spent outdoors at work (other than on farms). This distribution is shown in Table 5.2-2.

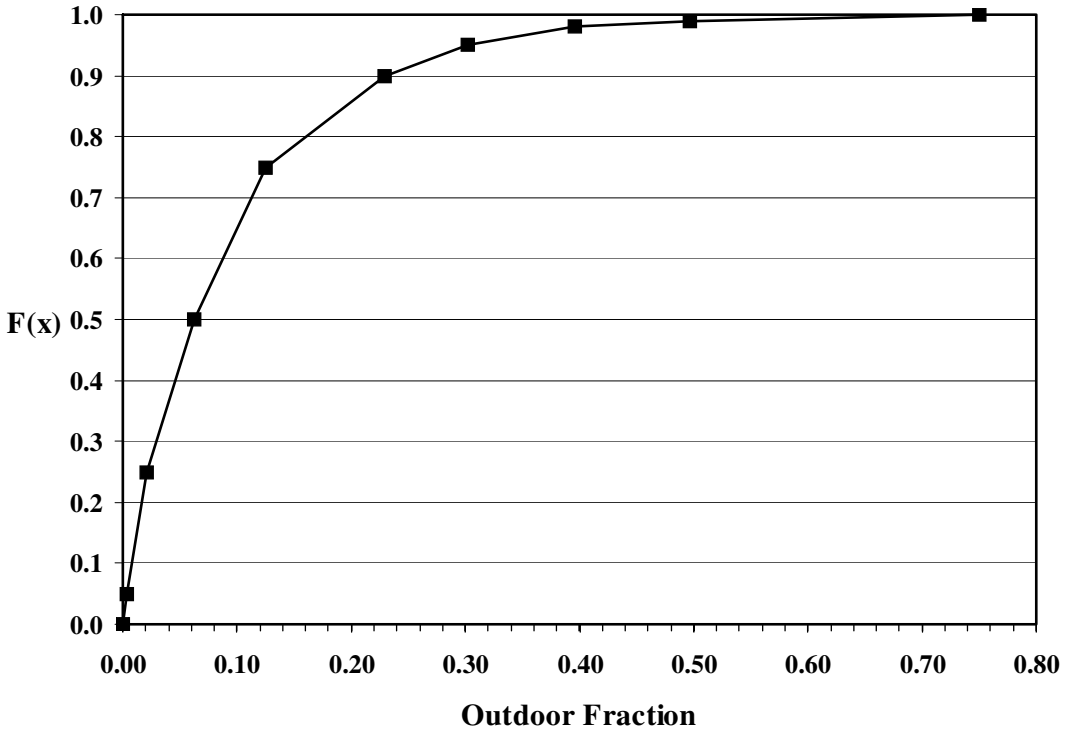

FIGURE 5.2-1 Outdoor Time Fraction Cumulative Distribution Function for the Residence (RESRAD [onsite]) or Dwelling (RESRAD-OFFSITE)

TABLE 5.2-2 Statistics for Fraction of Time Spent Outdoors per Day

Category	Population Group	N[a]	Min.	Max.	Percentiles							
					5	25	50	75	90	95	98	99
Fraction per Day Outdoors at Home or Other Areas outside the House												
All		2308	0.001	0.896	0.00694	0.0278	0.0625	0.125	0.222	0.292	0.396	0.458
Gender	Male	1198	0.001	0.896	0.00694	0.0417	0.0833	0.138	0.250	0.347	0.435	0.507
Gender	Female	1107	0.001	0.740	0.00347	0.0208	0.0521	0.104	0.198	0.250	0.313	0.389
Age (years)	18-64	1301	0.001	0.750	0.00347	0.0208	0.0625	0.125	0.229	0.302	0.396	0.497
Fraction per Day Outdoors on a Farm Field												
All		128	0	0.166	0.003	0.013	0.031	0.074	0.104	0.127	0.148	0.162
Gender	Male	86	0.001	0.166	0.005	0.016	0.040	0.087	0.115	0.135	0.162	0.166
Gender	Female	42	0.001	0.104	0.003	0.009	0.018	0.036	0.046	0.084	0.104	0.104
Age (years)	18-64	91	0.001	0.166	0.003	0.014	0.040	0.087	0.110	0.135	0.162	0.166
Fraction per Day Spent Outdoors at Work												
All		4891	0.000	0.000	0.000	0.000	0.000	0.000	0.000	0.001	0.021	0.035
Gender	Male	2463	0.000	0.000	0.000	0.000	0.000	0.000	0.000	0.011	0.029	0.042
Gender	Female	2428	0.000	0.000	0.000	0.000	0.000	0.000	0.000	0.000	0.001	0.008
Age (years)	18-64	4621	0.000	0.000	0.000	0.000	0.000	0.000	0.000	0.001	0.021	0.035

[a] Number of subjects in the survey.

Source: Derived from cumulative minutes per day spent outdoors listed in EPA (1997).

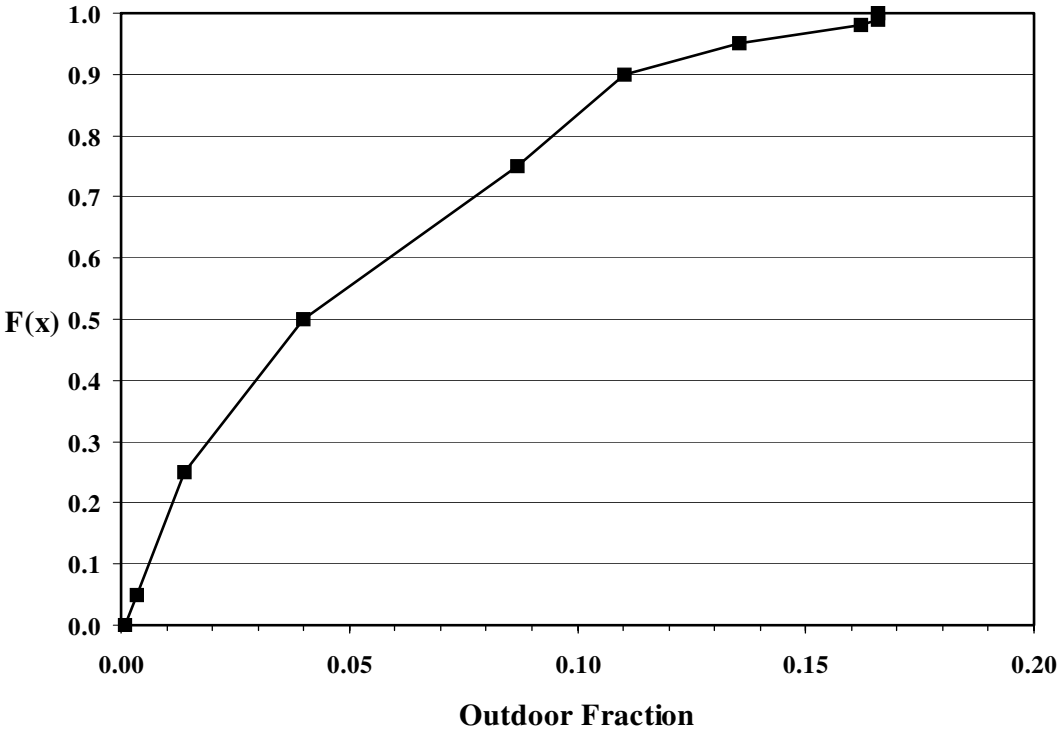

FIGURE 5.2-2 Outdoor Time Fraction Cumulative Distribution Function for the Time Spent in a Farm Field

6 REFERENCES

Allen, R.G., et al., *Crop Evapotranspiration — Guidelines for Computing Crop Water Requirements*, FAO Irrigation and Drainage Paper 56, Food and Agriculture Organization of the United Nations, Rome, Italy, http://www.fao.org/docrep/X0490E/x0490e00.htm, 1998.

Allen, R.R., et al., "Residual Deep Plowing Effects on Irrigation Intake for Pullman Clay Loam," *Soil Sci. Soc. Am. J.* 59:1424-1429, 1995.

Anderson, D.L. and R.L. Siegrist, "The Performance of Ultra-Low Volume Flush Toilets in Phoenix," *Journal of the American Water Works Association*, 81(3):52-57, 1989.

Anderson, D.L., et al., "The Impact of Water Conserving Water Fixtures on Residential Water Use Characteristics in Tampa, Florida," in *Proceedings of the Conserv93 Conference*, December 12-16, Las Vegas, Nev., 1993.

Baes, C.F., III, et al., *A Review and Analysis of Parameters for Assessing Transport of Environmentally Released Radionuclides Through Agriculture*, ORNL-5786, Health and Safety Division, Oak Ridge National Laboratory, Oak Ridge, Tenn., 1984.

Baker, J., *Forage Variety Production Notes*, http:/www.noble.org/Ag/Research/Articles/ ForageVariety2002/index.htm, 2002.

Baker, J., *Forage Yields from Burmudagrass, Varieties and Strains*, Jerry L. Baker, The Samuel Roberts Noble Foundation Inc., 2510 Sam Noble Parkway, Ardmore, Okla. 73401, NF-FO-04-02, 2003.

Beyeler, W.E., et al., "Review of Parameter Data for the NUREG/CR_5512 Residential Farmer Scenario and Probability Distributions for the DandD Parameter Analysis," letter report prepared by Sandia National Laboratories for U.S. Nuclear Regulatory Commission, January 1998.

Biwer, B.M., et al., *Technical Basis for Calculating Radiation Doses for the Building Occupancy Scenario Using the PROBABILISTIC RESRAD-BUILD 3.0 Code,* NUREG/CR-6755, ANL/EAD/TM-02-1, prepared by Argonne National Laboratory, Argonne, Ill., for the U.S. Nuclear Regulatory Commission, Office of Nuclear Regulatory Research, Division of Systems Analysis and Regulatory Research, Washington, D.C., February 2002.

Brown and Caldwell, *Residential Water Conservation Projects*, Research Report 903 (HUD-PDR-903), U.S. Department of Housing and Urban Development, Office of Policy Development, Washington, D.C., 1984.

Buckingham, F., *Tillage*, Deere & Company, Moline, Ill., 1984.

Burmaster, D.E., "A Lognormal Distribution for Time Spent Showering," *Risk Analysis,* 18(1):33-35, 1998.

Canadell, J., et al., "Maximum Rooting Depth of Vegetable Types at the Global Scale," *Oecologia*, 108:583-595, 1996.

Carsel R.F. and R.S. Parrish, "Developing Joint Probability Distributions of Soil Water Retention Characteristics," *Water Resources Research*, 24:755-769, May 1988.

Curwen, D. and L.R. Massie, "Irrigation Management in Wisconsin — the Wisconsin Irrigation Scheduling Program (WISP)," A3600, I-01-94-2M-90-MSC, 1994.

DOE — See U.S. Department of Energy.

Dunker, R.E., et al., "Deep Tillage Effects on Compacted Surface-Mined Land," *Soil Sci. Soc. Am. J.*, 59:192-199, 1995.

Electric Power Research Institute, *A Review of Field Scale Physical Solute Transport Processes in Saturated and Unsaturated Porous Media*, Palo Alto, Calif., as referenced in EPA (2003), 1985.

EPA — U.S. Environmental Protection Agency.

EPRI — See Electric Power Research Institute.

Evans, et al., "Soil, Water, and Crop Characteristics Important to Irrigation Scheduling," published by North Carolina Cooperative Extension Service, publication number AG 452-1, http://www.bae.ncsu.edu/programs/extension/evans/ag452-1.htm, June 1996.

Fogh, C.L., et al., "Size Specific Indoor Aerosol Deposition Measurements and Derived I/O Concentrations Ratios," *Atmospheric Environment*, 31:2193-2203, 1997.

Gelhar, Lynn W., et al., "A Critical Review of Data on Field-Scale Dispersion in Aquifers," *Water Resources Research*, 28(7):1955-1974, 1992.

Georgeson, C.C. and J.E. Payne, "Investigation of the Root Development of Some Forage Plants," Experimental Station of the Kansas State Agricultural College, Manhatton, Bulletin No. 75, August 1897.

Geraghty, J., et al., *Water Atlas of the United States*, Plate 13, Water Information Center, Inc., Port Washington, N.Y., 1973.

Grogan, H.A., *Concentration Ratios for BIOPATH: Selection of the Soil-to-Plant Concentration Ratios Database*, Report EIR-Bericht Nr. 575, Swiss Federal Institute for Reactor Research, Geneva, Switzerland, 1985.

Harper et al., *Probabilistic Accident Consequence Uncertainty Analysis, Dispersion and Deposition Uncertainty Assessments, Appendices C,D,E,F, and G*, Vol. 3, NUREG/

CR-6244, EUR 15855EN, SAND94-1453, prepared for U.S. Nuclear Regulatory Commission Office of Nuclear Regulatory Research, Washington, D.C., and the Commission of the European Communities, Brussels, 1995.

Ho, C.K., et al., *Development of a Risk-Based Probabilistic Performance-Assessment Method for Long-Term Cover Systems – 2nd Edition*, SAND2002-3131, Sandia National Laboratories, Albuquerque, N.M., 2002.

Hoffman, F. O., et al., *Variability in Dose Estimates Associated with the Food Chain Transport and Ingestion of Selected Radionuclides*, NUREG/CR-2612, Oak Ridge National Laboratory, Oak Ridge, Tenn., 1982.

IAEA — See International Atomic Energy Agency.

ICRP — International Commission on Radiological Protection.

International Atomic Energy Agency, *Handbook of Parameter Values for the Prediction of Radionuclide Transfer in Temperate Environments*, Technical Reports Series No. 364, produced in collaboration with the International Union of Radioecologists, Vienna, 1994.

International Commission on Radiological Protection, *Principles of Monitoring for the Radiation Protection of the Population*, ICRP No. 43, New York, N.Y., 1985.

John, W., "The Characteristics of Environmental and Laboratory-Generated Aerosols," in *Aerosol Measurement, Principles, Techniques, and Applications*, Willeke, K. and P.A. Baron (eds.), John Wiley & Sons, Inc., New York, N.Y., pp. 54-76, 1993.

Justus, C.G., et al., "Nationwide Assessment of Potential Output from Wind-Powered Generators," *J. Appl. Meteor.*, 15(7):673-678, 1976.

Kemble, J.K. and D.C. Sanders, "Basics of Vegetable Crop Irrigation," ANR-1169, http://www.aces.edu, April 2000.

Kennedy, W.E. and D.L. Strenge, *Residual Radioactive Contamination from Decommissioning; A Technical Basis for Translating Contamination Levels to Annual Total Effective Dose Equivalent*, NUREG/CR-5512, PNL 7994, Vol. 1, prepared by Pacific Northwest Laboratory for U.S. Nuclear Regulatory Commission, 1992.

Klotz, D. and Moser, H., "Hydrodynamic Dispersion as Aquifer Characteristic: Model Experiments with Radioactive Tracers," *Isotope Techniques in Groundwater Hydrology*, Vol. 2, International Atomic Energy Agency, Vienna, p. 341-354, 1974.

Konoplev, A.V., et al., "Influence of Agricultural Countermeasures on the Ratio of Different Chemical Forms of Radionuclides in Soil and Soil Solution," *Sci. Total Environ.*, 137:147-162, 1993.

Lang, C., "Indoor Deposition and the Protective Effect of Houses Against Airborne Pollution," Ph.D Thesis Riso-R-780(en), ISBN 87-550-2024-0 (as cited in Fogh et al., 1997), 1995.

Luna, R.E. and H.W. Church, "Estimation of Long Term Concentrations Using a 'Universal' Wind Speed Distribution," *J. Appl. Meteor.*, 13:910-916, 1974.

Majewski, C., University of New Hampshire Extension educator, agricultural resources (forage, hay, and haylage production with selected forage species), 2004.

Mayer, P.W., et al., *Residential End Uses of Water*, AWWA Research Foundation and American Water Works Association, Denver, Colo., 1999.

Mayer, P., 2005, personal communication from P. Mayer, Aquacraft, Inc., Boulder, Colorado, to B. Biwer, Argonne National Laboratory, Argonne, Illinois, October 5.

Meyer, P.D., et al., "Uncertainty Analyses of Infiltration and Subsurface Flow and Transport for SDMP Sites," NUREG/CR-6565, Pacific Northwest National Laboratory, prepared for U.S. Nuclear Regulatory Commission, September 1997.

Mayer, P.W., et al., *Seattle Home Water Conservation Study, the Impacts of High Efficiency Plumbing Fixture Retrofits in Single-Family Homes*, prepared by Aquacraft, Inc., Water Engineering and Management, Boulder, Colo., for Seattle Public Utilities and the U.S. Environmental Protection Agency, December 2000.

Mayer, P.W., et al., *Residential Indoor Water Conservation Study: Evaluation of High Efficiency Indoor Plumbing Fixture Retrofits in Single-Family Homes in the East Bay Municipal Utility District Service Area*, prepared by Aquacraft, Inc., Water Engineering and Management, Boulder, Colo., for the East Bay Municipal Utility District and the U.S. Environmental Protection Agency, July 2003.

Mayer, P.W., et al., *Tampa Water Department Residential Water Conservation Study, the Impacts of High Efficiency Plumbing Fixture Retrofits in Single-Family Homes*, prepared by Aquacraft, Inc., Water Engineering and Management, Boulder, Colo., for the Tampa Water Department and the U.S. Environmental Protection Agency, January 2004.

National Climatic Data Center, "Comparative Climatic Data for the United States through 1998," National Oceanic and Atmospheric Administration, U.S. Department of Commerce, Washington, D.C., 1999.

National Council on Radiation Protection and Measurements, *Radiological Assessment: Predicting the Transport, Bioaccumulation, and Uptake by Man of Radionuclides Released to the Environment*, NCRP Rep. No. 76, Bethesda, Md., 1984.

National Council on Radiation Protection and Measurements, *Recommended Screening Limits for Contaminated Surface Soil and Review of Factors Relevant to Site-Specific Issues*, Report No. 129, 1999.

Nazaroff, W.W., et al., "Radon Entry via Potable Water," in *Radon and Its Decay Products in Indoor Air*, Nazaroff, W.W. and A.V. Nero, Jr. (eds.), John Wiley & Sons, New York, N.Y., 1988.

Nazaroff, W.W. and G.R. Cass, "Mass-Transport Aspects of Pollutant Removal at Indoor Surfaces," *Environ. Int.*, 15:567-584, 1989.

Nazaroff, W.W., et al., "Critique of the Use of Deposition Velocity in Modeling Indoor Air Quality," in *Modeling of Indoor Quality and Exposure*, Nagda, N.L. (ed.), ASTM STP 1205, American Society for Testing and Materials, Philadelphia, Penn., pp. 148-165, 1993.

NCDC — See National Climatic Data Center.

NCRP — See National Council on Radiation Protection and Measurements.

Neuman, Shlomo P., "Universal Scaling of Hydraulic Conductivities and Dispersivities in Geologic Media," *Water Resources Research*, 26:1749-1758, 1990.

NRC — See U.S. Nuclear Regulatory Commission.

Offermann, F.J., et al., "Control of Respirable Particles in Indoor Air with Portable Air Cleaners," *Atmos. Environ.*, 19:1761-1771, 1985.

Owensby, C.E. and K.L. Anderson, *Effect of Clipping Date on Loamy Upland Bluestem Range*, contribution No. 1069, Department of Agronomy, Kansas Agricultural Experiment Station, Manhattan, Kan., 1969.

Palmer, D.P., "Irrigation," in *Davis's Handbook of Applied Hydraulics*, Zipparro, V.J., et al. (eds.), 4th ed., McGraw Hill, New York, N.Y., 1993.

Parks, B.S., 1992, User's Guide for CAP88-PC, Version 1.0, EPA-402-B-92-001, U.S. Environmental Protection Agency, Las Vegas, Nev., 1992.

Renard, K.G., et al., *Predicting Soil Erosion by Water: A Guide to Conservation Planning with the Revised Universal Soil Loss Equation (RUSLE)*, Agricultural Handbook No. 703, U.S. Department of Agriculture, Agricultural Research Service, Tucson, Ariz., January 1997.

Roed, J. and R.J. Cannell, "Relationship between Indoor and Outdoor Aerosol Concentration Following the Chernobyl Accident," *Radiat. Prot. Dosim.*, 21:107-110, 1987.

Schulze-Makuch, D., "Longitudinal Dispersivity Data and Implications for Scaling Behavior," *Ground Water*, 43(3):443-456, 2005.

Sehmel, G.A., "Particle and Gas Dry Deposition: A Review," *Atmos. Environ.*, 14:983-1011, 1980.

Sehmel, G.A., "Deposition and Resuspension," in *Atmospheric Science and Power Production*, DE84-005177, DOE/TIC-27601, Randerson, D. (ed.), Weather Nuclear Support Office, National Oceanic and Atmospheric Administration, U.S. Department of Commerce, prepared for U.S. Department of Energy, Office of Energy Research, Office of Health and Environmental Research, Washington, D.C., 1984.

Seinfeld, J.H. and S.N. Pandis, *Atmospheric Chemistry and Physics*, John Wiley & Sons, Inc., New York, N.Y., 1998.

Shen, H.W. and P. Julien, "Erosion and Sediment Transport," in *Handbook of Hydrology*, Maidment, D.R. (ed.), McGraw-Hill, Inc., New York, N.Y., 1993.

Sinclair, J.D., et al., "Indoor/Outdoor Concentrations and Indoor Surface Accumulations of Ionic Substances," *Atmos. Environ.*, 19(2):315-323, 1985.

Thatcher, T.L. and D.W. Layton, "Deposition, Resuspension, and Penetration of Particles within a Residence," *Atmos. Environ.*, 29(13):1487-1497, 1995.

Tsang, A.M. and N.E. Klepeis, "Results Tables from a Detailed Analysis of the National Human Activity Pattern Survey (NHAPS) Response," draft report prepared for the U.S. Environmental Protection Agency by Lockheed Martin, Contract No. 68-W6-001, 1996.

U.S. Department of Agriculture, "Usual Planting and Harvesting Dates for U.S. Field Crops," Agricultural Handbook Number 628, December 1997.

U.S. Department of Agriculture, *1997 National Resources Inventory (revised December 2000)*, Natural Resources Conservation Service, Washington, D.C., and Statistical Laboratory, Iowa State University, Ames, Iowa, CD-ROM, Version 1, December 2001.

U.S. Department of Agriculture, National Agronomy Manual, 190-V-NAM, 3rd edition, National Resources Conservation Service, Washington, D.C., October 2002.

U.S. Department of Energy, *Preliminary Remediation Goals for Use at the U.S. Department of Energy Oak Ridge Operations Office*, ES/ER/TM-106, Environmental Restoration Division, Oak Ridge, Tenn., 1995.

U.S. Environmental Protection Agency, "Exposure Factors Handbook, Update to Exposure Factors Handbook, EPA/600/8-89/043 — May 1989," EPA/600/P-95/002Fa,b&c, National Center for Environmental Assessment, Office of Research and Development, Washington, D.C., August 1997.

U.S. Environmental Protection Agency, *Onsite Wastewater Treatment Systems Manual*, EPA/625/R-00/008, Office of Water, Office of Research and Development, Washington, D.C., February 2002.

U.S. Environmental Protection Agency, *EPA's Composite Model for Leachate Migration with Transformation Products (EPACMTP), Parameters/Data Background Document*, EPA530-R-03-003, Office of Solid Waste, Washington, D.C., April 2003.

U.S. Environmental Protection Agency, *Air Quality Criteria for Particulate Matter*, *Vols. I & II*, EPA/600/P-99/002aF and EPA/600/P-99/002bF, National Center for Environmental Assessment-RTP, Office of Research and Development, Research Triangle Park, N.C., 2004.

U.S. Environmental Protection Agency, Office of Air and Radiation, home page for the AirData Web site, http://www.epa.gov/air/data/index.html, 2005.

U.S. Nuclear Regulatory Commission, *Regulatory Guide 1.109: Calculation of Annual Doses to Man from Routine Releases of Reactor Effluents for the Purpose of Evaluating Compliance with 10 CFR Part 50, Appendix I*, Washington, D.C., 1977.

USDA — See U.S. Department of Agriculture.

Vervoort, R. W., et al., "Soil Structure Development and Preferential Solute Flow," *Water Resources Research* 35:913-928, 1999.

Vovk, I.F., et al., "Technical Approaches to Decontamination of Terrestrial Environments in the CIS (former USSR)," *The Science of the Total Environment*, 137:49-63, 1993.

Wang, Y.Y., et al., *A Compilation of Radionuclide Transfer Factors for the Plant, Meat, Milk, and Aquatic Food Pathways and the Suggested Default Values for the RESRAD Code*, ANL/EAIS/TM_103, Argonne National Laboratory, Argonne, Ill., prepared for the U.S. Department of Energy, August 1993.

Weaver, J.E., *Root Development of Field Crops*, first edition, McGraw-Hill Book Company, http://www.soilandhealth.org/01aglibrary/010139fieldcroproots/010139toc.html, 1926.

Weaver, J.E. and W.E. Bruner, *Root Development of Vegetable Crops*, first edition, Mcgraw-Hill Book Company, http://www.soilandhealth.org/01aglibrary/010137veg.roots/010137toc.html, 1927.

Whelan, G., et al., *The Remedial Action Priority System (RAPS): Mathematical Formulations*, DOE/RL/87-09, Pacific Northwest Laboratory, Richland, Wash., 1987.

Whitby, K.T. and G.M. Sverdrup, "California Aerosols: Their Physical and Chemical Characteristics," in *The Character and Origins of Smog Aerosols*, Hidy, G.M., et al. (eds.), John Wiley & Sons, Inc., New York, N.Y., pg. 495, 1980 (as cited in John, 1993).

Wilkes, C.R., et al., "Probability Distributions for Showering and Bathing Water-Use Behavior for Various U.S. Subpopulations," *Risk Analysis*, 25(2):317-337, 2005.

Wischmeier, W.H. and D.D. Smith, *Predicting Rainfall Erosion Losses — A Guide to Conservation Planning*, Agriculture Handbook No. 537, U.S. Department of Agriculture, Washington, D.C., December 1978.

Yu, C., et al., *Development of Probabilistic RESRAD 6.0 and RESRAD-BUILD 3.0 Computer Codes*, NUREG/CR-6697, ANL/EAD/TM-98, prepared by Argonne National Laboratory, Argonne, Ill., for the U.S. Nuclear Regulatory Commission, Office of Nuclear Regulatory Research, Division of Risk Analysis and Applications, Washington, D.C. November 2000.

Yu, C., et al., *User's Manual for RESRAD Version 6*, ANL/EAD-4, Argonne National Laboratory, Argonne, Ill., July 2001.

Yu, C., et al., *User's Manual for RESRAD-BUILD Version 3*, ANL/EAD/03-1, Argonne National Laboratory, Argonne, Ill., June 2003.

ATTACHMENT A:

PARAMETERS AND PARAMETER TYPES IN RESRAD-OFFSITE CODE VERSION 2

CONTENTS

TABLES

NOTATION

The following is a list of the acronyms, initialisms, and abbreviations (including units of measure) used in this document. Acronyms used only in tables are defined in the respective tables.

ACRONYMS, INITIALISMS, AND ABBREVIATIONS

DCF	dose conversion factor
EPA	U.S. Environmental Protection Agency
FGR	Federal Guidance Report
GI	gastrointestinal
HEAST	Health Effects Summary Tables
ICRP	International Commission on Radiological Protection
NRC	U.S. Nuclear Regulatory Commission

UNITS OF MEASURE

Bq	becquerel
cal	calorie(s)
Ci	curie
cm	centimeter(s)
d	day(s)
DCF	dose conversion factor
dpm	disintegrations per minute
dps	disintegrations per second
g	gram(s)
h	hour(s)
K	Kelvin
kg	kilogram(s)
L	liter(s)
m	meter(s)
mrem	millirem(s)
pCi	picocurie(s)
s	second(s)
Sv	Sievert
yr	year(s)

PARAMETERS AND PARAMETER TYPES IN RESRAD-OFFSITE CODE VERSION 2

1 INTRODUCTION

1.1 PURPOSE AND SCOPE

This report provides the descriptions and the default values of the parameters used in the RESRAD-OFFSITE code Version 2. Tables listing the parameters used in the RESRAD-OFFSITE computer code Version 2 and their current default values are provided in Section 2. The parameters are classified as physical, behavioral, or metabolic. Definitions applied in identifying parameter types are included in Section 1.3.

1.2 MODEL DESCRIPTIONS

The RESRAD-OFFSITE code Version 2 couples an atmospheric dispersion model, surface water transport model, groundwater transport model, and offsite accumulation model with the RESRAD code to permit calculation of doses to persons located beyond the contaminated site boundary. It calculates radiation dose and excess lifetime cancer risk to a chronically exposed onsite/offsite resident for different land-use and exposure scenarios. The code focuses on radioactive contaminants in soil and their transport in air, water, and biological media to a single receptor. Nine exposure pathways are considered in RESRAD-OFFSITE code Version 2: direct exposure, inhalation of particulates and radon, and ingestion of plant foods, meat, milk, aquatic foods, water, and soil. RESRAD-OFFSITE code Version 2 uses a pathway analysis approach in which the concentrations in environmental media connecting the source to the receptor are computed at a series of times. These concentrations are used to compute the exposure, dose, and excess cancer risk. Radiation doses, health risks, soil guidelines, and media concentrations of radionuclides are calculated at a series of user-specified times. The source is adjusted over time to account for radioactive decay and ingrowth, leaching, erosion, and mixing. The user can construct exposure scenarios by suppressing exposure pathways and by adjusting the input parameters.

1.3 PARAMETER CLASSIFICATION

This report classifies RESRAD-OFFSITE code Version 2 parameters into three types: physical, behavioral, or metabolic, as described below. Some parameters may belong to more than one of these types (e.g., the mass loading factor). Additionally, if a parameter does not fit either the physical or metabolic definition, it is classified as a behavioral parameter. Many parameters used in the RESRAD-OFFSITE code Version 2 are the same as those used in the RESRAD (onsite) code (Yu et al. 2001); therefore, same parameters are assigned the same parameter types (NRC 2000).

Physical Parameter: Any parameter whose value would not change if a different group of receptors were considered is classified as a physical parameter. Physical parameters are determined by the source, its location, and the geological characteristics of the site (i.e., these parameters are source- and site-specific).

Behavioral Parameter: Any parameter whose value depends on the receptor's behavior and the scenario definition is classified as a behavioral parameter. For the same group of receptors, a parameter value could change if the scenario changed (e.g., parameters for recreational use could be different from those for residential use).

Metabolic Parameter: If a parameter represents the metabolic characteristics of the potential receptor and is independent of scenario, it is classified as a metabolic parameter. The parameter values may be different in different population age groups. According to the recommendations of the International Commission on Radiological Protection, Report 43 (ICRP 1985), parameters representing metabolic characteristics are defined by average values for the general population. These values are not expected to be modified for a site-specific analysis because the parameter values would not depend on site conditions.

2 MODEL PARAMETERS IN RESRAD-OFFSITE

This section presents tables listing characteristics of the parameters used in RESRAD-OFFSITE code Version 2. These tables include parameter name, default value, code-accepted range of values for the parameter, parameter type (based on the definitions given in Section 1.3), and the general description of the parameter. Table 2-1[1] lists user-changeable parameters in the RESRAD-OFFSITE code Version 2. Parameters are arranged according to the input window in which they appear. The number of parameters that a user can change will depend on the pathways and radionuclides selected. In RESRAD-OFFSITE code Version 2, pathways can be turned on (active) or off (suppressed). Parameters pertaining only to suppressed pathways are blanked out in the data entry screens because they would not be used in the calculations. Radon parameters can be changed only if a radon precursor is selected in the radionuclide list and the radon pathway is turned on. Similarly, a user will have access to carbon-14 (C-14) or tritium (H-3) parameters only if C-14 or H-3 is selected as a contaminant. Some parameters are nuclide- or element-specific. Table 2-1 identifies that characteristic of the parameter but does not provide details. Separate tables listing nuclide- or element-specific parameters accompanied by more detailed discussion are provided in Tables 2-2 through 2-6. Table 2-1 also identifies the parameter types: physical (P), metabolic (M), and behavioral (B). For some parameters, more than one type is listed; the first one listed is the primary type and the next one is secondary. For example, the inhalation rate is identified as M, B, which indicates that it depends primarily on the metabolic characteristics of the potential receptor, but that it also depends on the receptor behavior or exposure scenario. The default values are the current defaults in the code.

Table 2-2 lists the default dose conversion factors (DCFs) for some radionuclides included in the RESRAD-OFFSITE code Version 2 database. The external DCF are taken from Federal Guidance Report (FGR) No. 12 (Eckerman and Ryman 1993), and inhalation and ingestion DCFs are from FGR-11 (Eckerman et al. 1988). The code also includes six age groups (infant, age 1, age 5, age 10, age 15, and adult) internal (inhalation and ingestion) DCFs from ICRP-72. There are 209 principal radionuclides currently in the database with cut-off half life of 30 days. For the inhalation dose conversion factor, the default inhalation class used is also listed. For the ingestion dose conversion factor, the default fraction of a stable element entering the gastrointestinal (GI) tract that reaches body fluid is also listed. Table 2-3 lists default slope factors used in the code for some radionuclides; the values were obtained from FGR-13 (Eckerman et al. 1999), except for californium-252 (Cf-252), curium-248 (Cm-248), and plutonium-244 (Pu-244) (see Table 2-3 footnote). The code also includes slope factors from the Health Effects Summary Tables (HEAST) (EPA 1995 and 2001). Table 2-4 provides default distribution coefficients used in the code for some radionuclides (values are nuclide-specific); Table 2-5 lists element-specific transfer factors for plants, meat, and milk. Although only one "default" value is available for the plant transfer factor in the database, the user can input 4 different root uptake transfer factors for the 4 different types of plants (leafy vegetables; grains, fruit, and nonleafy vegetables; pasture and silage for livestock; and grains for livestock)

---

[1] To maintain the continuity of the text, the tables have been placed at the end of the section.

considered in RESRAD-OFFSITE code Version 2. Table 2-6 provides element-specific bioaccumulation factors for fish and for crustacea and mollusks.

TABLE 2-1 Parameters and Their Default Values Used in RESRAD-OFFSITE Code Version 2[a]

Input Screen Title and Parameter Name	Units	Default Value[a]	Code-Accepted Values[b] Physical or Numerical[c] (N) Range		Type[d]	Description
Title						
Title	--[e]	RESRAD-OFFSITE code Version 2 Default Parameters	80 alphabetic or numeric characters		NA[f]	The TITLE is used to identify the run and can be up to 80 alphabetic or numerical characters long.
Location of dose, slope, and transfer factor	--	C:\Program files\RESRAD_ Family\DCF	80 alphabetic or numeric characters		NA	This parameter specifies the location of dose, slope, and transfer factor library on the computer.
Slope factor (risk) library	--	FGR-13 Morbidity	FGR-13 morbidity, FGR-13 mortality, or Heast 2001 morbidity		NA	This is the name of the slope factor library containing all slope factors for the RESRAD-OFFSITE code Version 2 pathways.
Dose conversion factor library	--	FGR-11	FGR-11, ICRP-72 - Adult, ICRP-72 - Infant, ICRP-72 - Age 1, ICRP-72 - Age 5, ICRP-72 - Age 10, ICRP-72 - Age 15		NA	This is the name of the internal dose conversion factor library for the RESRAD-OFFSITE code Version 2.
Transfer factor library	--	RESRAD default transfer factors	RESRAD default transfer factors, user specified		NA	This is the name of the transfer factor library for the RESRAD-OFFSITE code Version 2.
Number of intermediate time points	--	2048	32, 64, 128, 256, 512, 1024, 2048, 4096		NA	This parameter specifies the number of graphic points. It affects the precision of the computed results and the smoothness of the output graphic curves.
Spacing between intermediate time points	--	Linear	Linear/Log		NA	LINEAR or LOG is to specify the type of spacing (years) between the generated time points.
Minimum time increment between intermediate time points	--	1	½, ¼, 1/8, 1/16, 1/32, 1/64, 1/128, 1/256, 1/512, 1/1,024, 1/2,048, 1/4,096		NA	This is the lowest time interval allowed between two intermediate time points. It is also used to determine the secondary intermediate time point.

TABLE 2-1 (Cont.)

Input Screen Title and Parameter Name	Units	Default Value[a]	Code-Accepted Values[b] Physical or Numerical[c] (N) Range		Type[d]	Description
Dose and slope factor library	--	FGR-13 morbidity	FGR-13 morbidity / mortality or HEAST 1995 or 2001 morbidity		NA	This is the name of the dose factor library containing all effective dose conversion factors, slope factors, and transfer factors for the RESRAD-OFFSITE code Version 2 pathways.
Cutoff half-life	days	30 days	180 days, 30 days, 6 days, 1 day		NA	This is the cutoff half-life that is used to separate the "principal nuclides" from the "associated nuclides."
Update progress of computation message	s	0	0, 1, 2, 4, 15, 30, 60, 900		NA	An interface parameter that specifies how frequently the progress of computation is to be reported and displayed on the screen.
Use line draw character	--	Yes	Yes/No		NA	Use line-draw character set in the report files.
Preliminary Inputs						
Radiological units for activity	Ci, Bq, dps, dpm	pCi	Ci, Bq, dps, dpm		NA	Any of the four units of radioactivity: Curie (Ci), Becquerel (Bq), disintegrations per second (dps), or disintegrations per minute (dpm) can be selected. Any standard 1-character metric prefix can be used with Ci and Bq.
Radiological units for dose	rem and Sv	mrem	rem, Sv		NA	Both conventional and SI units may be selected for radiation dose. Any standard 1-character metric prefix can be used with rem and Sv.
Basic radiation dose limit	mrem/yr	25	1E-34 – 1E+34	N	NA	This is the annual radiation dose limit in mrem/yr used to derive all site-specific guidelines.
Exposure duration	yr	30	1 – 1,000		B	The exposure duration is the span of time, in years, an individual is expected to spend at the exposure location.
Number of unsaturated zone	--	1	0 – 5	N	P	Number of unsaturated zones. An unsaturated zone is defined as a horizontal uncontaminated layer located between the contaminated zone and the aquifer.

TABLE 2-1 (Cont.)

Input Screen Title and Parameter Name	Units	Default Value[a]	Code-Accepted Values[b] Physical or Numerical[c] (N) Range		Type[d]	Description
Site Layout						
Bearing of X axis	degrees	90	0 – 360	P	P	
X dimension of Primary contamination	m	100	-80,000 – +80,000		P	The primary contamination is modeled as a rectangle for atmospheric release and transport calculations. The lengths of the sides of the rectangle are used to define the rectangular region for the atmospheric transport calculations. The area is obtained as the product of these two perpendicular dimensions. The two sides of the rectangle that meet at the lower left corner serve as the axes of the coordinate system that is used to define the locations of the other receptor areas.
Y dimension of Primary contamination	m	100	-80,000 – +80,000		P	See above.
Smaller x coordinate of the fruit, grain, nonleafy vegetables plot	m	34.375	-80,000 – +80,000		P	The fruit, grain and nonleafy vegetable plot, the leafy vegetable plot, the pasture and silage growing area, the livestock feed grain fields, and the dwelling site are all approximated by rectangular shapes in the atmospheric transport model. The sides of these rectangles must be parallel to the sides of the primary contamination. The location and size of these rectangular areas are specified in the code by the coordinates of two opposite corners. The coordinates are specified with respect to a system of Cartesian axes on the left and lower sides of the primary contamination. The area is obtained as the product of these two perpendicular dimensions. The size and location of these receptor areas can also be specified in the map interface.
Larger x coordinate of the fruit, grain, nonleafy vegetables plot	m	65.625	-80,000 – +80,000		P	See above.
Smaller y coordinate of the fruit, grain, nonleafy vegetables plot	m	234	-80,000 – +80,000		P	See above.

TABLE 2-1 (Cont.)

Input Screen Title and Parameter Name	Units	Default Value[a]	Code-Accepted Values[b] Physical or Numerical[c] (N) Range		Type[d]	Description
Larger y coordinate of the fruit, grain, nonleafy vegetables plot	m	266	-80,000 – +80,000		P	See above.
Smaller x coordinate of the leafy vegetables plot	m	34.375	-80,000 – +80,000		P	See above.
Larger x coordinate of the leafy vegetables plot	m	65.625	-80,000 – +80,000		P	See above.
Smaller y coordinate of the leafy vegetables plot	m	268	-80,000 – +80,000		P	See above.
Larger y coordinate of the leafy vegetables plot	m	300	-80,000 – +80,000		P	See above.
Smaller x coordinate of the pasture, silage growing area	m	0	-80,000 – +80,000		P	See above.
Larger x coordinate of the pasture, silage growing area	m	100	-80,000 – +80,000		P	See above.
Smaller y coordinate of the pasture, silage growing area	m	450	-80,000 – +80,000		P	See above.
Larger y coordinate of the pasture, silage growing area	m	550	-80,000 – +80,000		P	See above.
Smaller x coordinate of the grain fields	m	0	-80,000 – +80,000		P	See above.
Larger x coordinate of the grain fields	m	100	-80,000 – +80,000		P	See above.

TABLE 2-1 (Cont.)

Input Screen Title and Parameter Name	Units	Default Value[a]	Code-Accepted Values[b] Physical or Numerical[c] (N) Range		Type[d]	Description
Smaller y coordinate of the grain fields	m	300	-80,000 – +80,000		P	See above.
Larger y coordinate of the grain fields	m	400	-80,000 – +80,000		P	See above.
Smaller x coordinate of the dwelling site	m	34.375	-80,000 – +80,000		P	See above.
Larger x coordinate of the dwelling site	m	65.625	-80,000 – +80,000		P	See above.
Smaller y coordinate of the dwelling site	m	134	-80,000 – +80,000		P	See above.
Larger y coordinate of the dwelling site	m	166	-80,000 – +80,000		P	See above.
Smaller x coordinate of the surface-water body	m	-100	-80,000 – +80,000		P	See above.
Larger x coordinate of the surface-water body	m	200	-80,000 – +80,000		P	See above.
Smaller y coordinate of the surface-water body	m	550	-80,000 – +80,000		P	See above.
Larger y coordinate of the surface-water body	m	850	-80,000 – +80,000		P	See above.
Source						
Nuclide concentration	pCi/g	100	0 – 1E+34	N	P	The radionuclide concentration in the contaminated zone. The contaminated zone is treated as a uniformly contaminated area with a single radionuclide concentration at every point.

TABLE 2-1 (Cont.)

Input Screen Title and Parameter Name	Units	Default Value[a]	Code-Accepted Values[b] Physical or Numerical[c] (N) Range		Type[d]	Description
Source Release and Deposition Velocity						
Release to groundwater, leach rate	1/yr	0	0 – 1E+34	N	P	The fraction of the available radionuclide leached out from the contaminated zone per unit of time.
Deposition velocity	m/s	0.001 0.01 (Cl, I) 0 (Xe)	0 – 1E+34	N	P	For nuclides that are transported by contaminated dust, it is the settling velocity of dust. If the nuclide is being transported in the form of a gas (water vapor, carbon dioxide, radon, etc.), a value of zero may be entered.
Distribution Coefficients		(Table 2-4)				This is the ratio of the concentration of the contaminant in adsorbed phase in soil to the concentration of the contaminant in the aqueous phase of soil, in cm^3/g.
Contaminated zone	cm^3/g	Nuclide-dependent	0 – 1E+34	N	P	
Unsaturated zone	cm^3/g	Nuclide-dependent	0 – 1E+34	N	P	
Saturated zone	cm^3/g	Nuclide-dependent	0 – 1E+34	N	P	
Sediment in surface water body	cm^3/g	Nuclide-dependent	0 – 1E+34	N	P	
Fruit, grain, nonleafy fields	cm^3/g	Nuclide-dependent	0 – 1E+34	N	P	
Leafy vegetable fields	cm^3/g	Nuclide-dependent	0 – 1E+34	N	P	
Pasture, silage growing areas	cm^3/g	Nuclide-dependent	0 – 1E+34	N	P	
Livestock feed grain fields	cm^3/g	Nuclide-dependent	0 – 1E+34	N	P	
Offsite dwelling site	cm^3/g	Nuclide-dependent	0 – 1E+34	N	P	

TABLE 2-1 (Cont.)

Input Screen Title and Parameter Name	Units	Default Value[a]	Code-Accepted Values[b] Physical or Numerical[c] (N) Range	Type[d]	Description
Dose Conversion and Slope Factors					
External dose conversion factors	(mrem/yr) per (pCi/g)	Nuclide-specific (Table 2-2)		M	Radionuclide-specific values from FGR-12. User is not allowed to change these values.
Inhalation dose conversion factors	mrem/pCi	Nuclide-specific (Table 2-2)		M	Radionuclide-specific values from FGR-11. Usually values for more than one inhalation class are listed per radionuclide. The three classes, D, W, and Y, correspond to retention half-times of less than 10 days, 10 to 100 days, and greater than 100 days, respectively. For some gaseous radionuclides (e.g., H-3, C-14, nickel-59 [Ni-59], and nickel-63 [Ni-63]), inhalation classes other than D, W, Y are also listed. The most conservative dose conversion factor is chosen as the default. The values can be changed if chemical forms are known or more appropriate data are available.
Ingestion dose conversion factors	mrem/pCi	Nuclide-specific (Table 2-2)		M	Radionuclide-specific values from FGR-11. Ingestion dose conversion factors depend on the chemical form, which determines the fraction of a radionuclide entering the gastrointestinal tract that reaches body fluids. The code lists these factions along with the dose conversion factor. The most conservative dose conversion factor is chosen as the default. The values can be changed if chemical forms are known or more appropriate data are available.
Slope factor –– external	(risk/yr) per (pCi/g)	Nuclide-specific (Table 2-3)		M	The ratio of cancer risk per year to the radionuclide concentration. The user has the option to choose slope factors from FGR-13 morbidity/mortality or HEAST 1995 or HEAST 2001 morbidity. The values from FGR-13 morbidity are provided in Table 2-3.
Slope factor –– inhalation	risk/pCi	Nuclide-specific (Table 2-3)		M	The ratio of cancer risk per year to the radionuclide activity inhaled. The user has the option to choose slope factors from FGR-13 morbidity/mortality or HEAST 1995 or HEAST 2001 morbidity. The values from FGR-13 morbidity are provided in Table 2-3.

TABLE 2-1 (Cont.)

Input Screen Title and Parameter Name	Units	Default Value[a]	Code-Accepted Values[b] Physical or Numerical[c] (N) Range		Type[d]	Description
Slope factor –– food ingestion	risk/pCi	Nuclide-specific (Table 2-3)			M	The ratio of cancer risk per year to the radionuclide activity ingested. The user has the option to choose slope factors from FGR-13 morbidity/mortality or HEAST 1995 or HEAST 2001 morbidity. The values from FGR-13 morbidity are provided in Table 2-3. FGR-13 has different slope factors for food and water ingestion. HEAST 2001 has different slope factors for food, water, and soil ingestion.
Slope factor –– water ingestion	risk/pCi	Nuclide-specific (Table 2-3)			M	The ratio of cancer risk per year to the radionuclide activity ingested. The user has the option to choose slope factors from FGR-13 morbidity/mortality or HEAST 1995 or HEAST 2001 morbidity. The values from FGR-13 morbidity are provided in Table 2-3. FGR-13 has different slope factors for food and water ingestion. HEAST 2001 has different slope factors for food, water, and soil ingestion.
Slope factor –– soil ingestion	risk/pCi	Nuclide-specific (Table 2-3)			M	The ratio of cancer risk per year to the radionuclide activity ingested. The user has the option to choose slope factors from FGR-13 morbidity/mortality or HEAST 1995 or HEAST 2001 morbidity. The values from FGR-13 morbidity are provided in Table 2-3. FGR-13 has different slope factors for food and water ingestion. HEAST 2001 has different slope factors for food, water, and soil ingestion.
Transfer Factors		(Table 2-5)				
Fruit, grain, nonleafy vegetables transfer factor	(pCi/kg)/ (pCi/kg)	Element-dependent	0 – 1E+34	N	P	The soil-to-plant transfer factor is the ratio of radionuclide concentration in edible portions of the plant at harvest time to the dry soil radionuclide concentration.
Leafy vegetables transfer factor	(pCi/kg)/ (pCi/kg)	Element-dependent	0 – 1E+34	N	P	
Pasture and silage transfer factor	(pCi/kg)/ (pCi/kg)	Element-dependent	0 – 1E+34	N	P	
Livestock feed grain transfer factor	(pCi/kg)/ (pCi/kg)	Element-dependent	0 – 1E+34	N	P	

TABLE 2-1 (Cont.)

Input Screen Title and Parameter Name	Units	Default Value[a]	Code-Accepted Values[b] Physical or Numerical[c] (N) Range		Type[d]	Description
Meat transfer factor	(pCi/kg)/ (pCi/d)	Element-dependent	0 – 1E+34	N	P	The meat/livestock-intake transfer factor is the ratio of radionuclide concentration in beef to the daily intake of the same radionuclide in livestock feed or water.
Milk transfer factor	(pCi/L)/ (pCi/d)	Element-dependent	0 – 1E+34	N	P	The milk/livestock-intake transfer factor is the ratio of radionuclide concentration in milk to the daily intake of the same radionuclide in livestock feed or water.
Bioaccumulation factor for fish	(pCi/kg)/ (pCi/L)	Element-dependent	0 – 1E+34	N	P	The bioaccumulation factor is the ratio of radionuclide concentration in aquatic food to the concentration of the same radionuclide in water.
Bioaccumulation factor for crustacea and mollusks	(pCi/kg)/ (pCi/L)	Element-dependent	0 – 1E+34	N	P	The bioaccumulation factor is the ratio of radionuclide concentration in aquatic food to the concentration of the same radionuclide in water.
Reporting Times						
Times at which output is reported	yr	1, 3, 6, 12, 30, 75, 175, 420, 970	0 – 1E+5		P	These are the times in years following the radiological survey for which tabular values for single-radionuclide soil guidelines and mixture sums can be obtained. The code calculates dose at time zero and up to nine user-specified times.
Storage Times						
Storage time for surface water	d	1	0 – 1E+34	N	B	The storage times are used to calculate radioactive ingrowth and decay adjustment factors for food and feed due to storage. The code has values for fruits, nonleafy vegetables, and grain (one category), leafy vegetables, pasture and silage, milk, well and surface water, livestock feed grain, meat, fish, and crustacea and mollusks.
Storage time for well water	d	1	0 – 1E+34	N	B	
Storage time for fruits, grain, and nonleafy vegetables	d	14	0 – 1E+34	N	B	
Storage time for leafy vegetables	d	1	0 – 1E+34	N	B	

TABLE 2-1 (Cont.)

Input Screen Title and Parameter Name	Units	Default Value[a]	Code-Accepted Values[b] Physical or Numerical[c] (N) Range		Type[d]	Description
Storage time for pasture and silage	d	1	0 – 1E+34	N	B	
Storage time for livestock feed grain	d	45	0 – 1E+34	N	B	
Storage time for meat	d	20	0 – 1E+34	N	B	
Storage time for milk	d	1	0 – 1E+34	N	B	
Storage time for fish	d	7	0 – 1E+34	N	B	
Storage time for crustacea and mollusks	d	7	0 – 1E+34	N	B	
Physical and Hydrological						
Precipitation	m/yr	1	0 – 10		P	The average volume of water in the form of rain, snow, hail, or sleet that falls per unit of area per unit of time at the site. It is used in a number of calculations including 1) radionuclide leaching from the contaminated zone, 2) accumulation of contaminants in the agricultural fields and pastures. Site-specific data should be used.
Wind speed	m/s	2	1E-4 – 20		P	It is the overall average of the wind speed, measured near the ground, in a one-year period. It is used to compute the onsite contaminant concentration in airborne dust and the atmospheric release rate.
Primary Contamination						
Area of primary contamination	m^2	10,000	Calculated		P	Total area of the site that is homogeneously contaminated. This is not user input but is calculated by the code from the x and y dimension of the primary contamination.

TABLE 2-1 (Cont.)

Input Screen Title and Parameter Name	Units	Default Value[a]	Code-Accepted Values[b] Physical or Numerical[c] (N) Range		Type[d]	Description
Length of contamination parallel to aquifer flow	m	100	1E-4 – 1E+6		P	The distance between two parallel lines perpendicular to the direction of aquifer flow, one at the upgradient edge of the contaminated zone and the other at the downgradient edge of the contaminated zone.
Depth of soil mixing layer (m)	m	0.15	0 – 1		P, B	This is the thickness of surface soil that may be assumed to be mixed uniformly from time to time due to anthropogenic or physical processes. It is used in calculating the depth factor for the onsite components of dust inhalation and soil ingestion pathways and for computing the release to the atmosphere. The depth factor is the fraction of resuspendable soil particles at the ground surface that are contaminated. It is calculated by assuming that mixing of the soil will occur within a layer of thickness (depth of mixing layer) at the surface.
Deposition velocity of dust (m/s)	m/s	0.001	0 – 0.01		P	This is the average velocity with which dust settles onto the contaminated zone. It is used to calculate the release to the atmosphere.
Irrigation applied per year (m/yr)	m/yr	0.2	0 – 10		B	This is the average annual irrigation rate, in meters/year, applied to the region of primary contamination. It is the amount of irrigation water that is applied over a period of one year, and is not the actual rate of irrigation applied during the growing period. It is one of the parameters used to calculate radionuclide leaching from the contaminated zone. Site-specific data should be used.
Evapotranspiration coefficient	--	0.5	0 – 0.999		P	This is the fraction of precipitation and irrigation water that penetrates the topsoil that is lost to the atmosphere by evaporation and by transpiration by the vegetation. The evapotranspiration coefficient is one of a number of parameters used to calculate radionuclide leaching from the contaminated zone.
Runoff coefficient	--	0.2	0 – 1		P	The fraction of the average annual precipitation that does not infiltrate into the soil and is not transferred back to the atmosphere through evapotranspiration. The runoff coefficient is one of a number of parameters used to calculate radionuclide leaching from the contaminated zone.

TABLE 2-1 (Cont.)

Input Screen Title and Parameter Name	Units	Default Value[a]	Code-Accepted Values[b] Physical or Numerical[c] (N) Range		Type[d]	Description
Rainfall and runoff	--	160	0 – 1,000		P	This is also known as the rainfall erosivity factor; it is a measure of the energy of the rainfall. The value entered is used to compute the erosion rate at all locations.
Slope-length- steepness factor	--	0.4	0 – 10		P	This factor accounts for the effect of the profile of the terrain (the slope of the land and the length of the slope) on the erosion rate.
Cover and management factor	--	0.003	0 – 1		B, P	This factor accounts for the effects of vegetation, mulching, etc., on the erosion rate.
Support practice factor	--	1	0 – 1		B, P	This factor accounts for conservation practices such as terracing, etc., on the erosion rate.
Contaminated zone						
Thickness of contaminated zone	m	2	1E-5 – 1,000		P	This is the distance between the uppermost and lowermost soil samples that have radionuclide concentrations clearly above background.
Total porosity of contaminated zone	--	0.4	1E-5 – 1		P	It is the ratio of the pore volume to the total volume of the contaminated zone.
Dry bulk density of contaminated zone	g/cm^3	1.5	1E-3 – 22.5		P	Bulk density of the contaminated zone.
Soil erodibility factor of contaminated zone	tons/acre	0.4	0 – 0.5		P	This quantifies the susceptibility of the soil to erosion.
Field capacity of contaminated zone	--	0.3	1E-5 – 1		P	It is the volumetric moisture content of soil at which (free) gravity drainage ceases. This is the amount of moisture that will be retained in a column of soil against the force of gravity. The field capacity is one of several hydrogeological parameters used to calculate water transport through the unsaturated part of the soil.
Soil b parameter of contaminated zone	--	5.3	0 – 15		P	It is an empirical and dimensionless parameter that is used to evaluate the saturation ratio (or the volumetric water saturation) of the soil according to a soil characteristic function called the conductivity function.

TABLE 2-1 (Cont.)

Input Screen Title and Parameter Name	Units	Default Value[a]	Code-Accepted Values[b] Physical or Numerical[c] (N) Range		Type[d]	Description
Hydraulic conductivity of contaminated zone	m/yr	10	1E-3 – 1E+10		P	It is the measure of the soil's ability to transmit water when subjected to a hydraulic gradient. The hydraulic conductivity depends on the soil grain size, the structure of the soil matrix, the type of soil fluid, and the relative amount of soil fluid (saturation) present in the soil matrix.
Clean cover						
Thickness of clean cover	m	0	0 – 100		P	Distance from the ground surface to the contaminated zone.
Total porosity of clean cover	--	0.4	1E-5 – 1		P	This is the volume fraction of soil that is occupied by liquid and gaseous phases. The total porosity is one of several hydrogeological parameters used to calculate water transport times.
Dry bulk density of clean cover	g/cm^3	1.5	1E-3 – 22.5		P	Bulk density of the cover material.
Soil erodibility factor of clean cover	tons/acre	0.4	0 – 0.5		P	See contaminated zone soil erodibility factor parameter.
Volumetric water content of clean cover	--	0.05	0 – 1		P	It is the volumetric water content in a porous medium that represents the fraction of the total volume of porous medium that is occupied by the water. The value should be less than the total porosity of the medium.
Agriculture Area Parameters						
Fruit, grain, and nonleafy vegetables field						
Area for fruit, grain, and nonleafy vegetables field	m^2	1,000	Calculated		B	Area for growing fruit, grain, and nonleafy vegetables. This is not user input but is calculated by the code from the x and y coordinates of the fruit, grain, and nonleafy vegetable field.

TABLE 2-1 (Cont.)

Input Screen Title and Parameter Name	Units	Default Value[a]	Code-Accepted Values[b] Physical or Numerical[c] (N) Range		Type[d]	Description
Fraction of area directly over primary contamination for fruit, grain, and nonleafy vegetables field	--	0	0 – 1		B, P	Fraction of the growing area directly over primary contamination.
Irrigation applied per year for fruit, grain, and nonleafy vegetables field	m/yr	0.2	0 – 10		B	See primary contamination area irrigation parameter.
Evapotranspiration coefficient for fruit, grain, and nonleafy vegetables field	--	0.5	0 – 0.999		P	See primary contamination area evapotranspiration coefficient parameter.
Runoff coefficient for fruit, grain, and nonleafy vegetables field	--	0.2	0 – 1		P	See primary contamination area runoff coefficient parameter.
Depth of soil mixing layer or plow layer for fruit, grain, and nonleafy vegetables field	m	0.15	0 – 1		P, B	See primary contamination area depth of soil mixing layer parameter.
Volumetric water content for fruit, grain, and nonleafy vegetables field	--	0.3	1E-5 – 1		P	This is the fraction of the total volume of porous medium that is occupied by water. The value should not exceed the total porosity of the medium.
Dry bulk density of soil for fruit, grain, and nonleafy vegetables field	g/cm^3	1.5	1E-3 – 22.5		P	See contaminated zone dry bulk density parameter.
Soil erodibility factor for fruit, grain, and nonleafy vegetables field	tons/acre	0.4	0 – 0.5		P	See contaminated zone soil erodibility factor parameter.

TABLE 2-1 (Cont.)

Input Screen Title and Parameter Name	Units	Default Value[a]	Code-Accepted Values[b] Physical or Numerical[c] (N) Range		Type[d]	Description
Slope-length-steepness factor for fruit, grain, and nonleafy vegetables field	--	0.4	0 – 10		P	See primary contamination area slope-length-steepness factor parameter.
Cover and management factor for fruit, grain, and nonleafy vegetables field	--	0.003	0 – 1		B, P	See primary contamination area cover and management factor parameter.
Support practice factor for fruit, grain, and nonleafy vegetables field	--	1	0 – 1		B, P	See primary contamination area support practice factor parameter.
Leafy vegetable field						
Area for leafy vegetable field	m^2	1,000	Calculated		B	Area for growing leafy vegetables. This is not user input but is calculated by the code from the x and y coordinates of the leafy vegetable field.
Fraction of area directly over primary contamination for leafy vegetable field	--	0	0 – 1		B, P	Fraction of the growing area directly over primary contamination.
Irrigation applied per year for leafy vegetable field	m/yr	0.2	0 – 10		B	See primary contamination area irrigation parameter.
Evapotranspiration coefficient for leafy vegetable field	--	0.5	0 – 0.999		P	See primary contamination area evapotranspiration coefficient parameter.
Runoff coefficient for leafy vegetable field	--	0.2	0 – 1		P	See primary contamination area runoff coefficient parameter.
Depth of soil mixing layer or plow layer for leafy vegetable field	m	0.15	0 – 1		P, B	See primary contamination area depth of soil mixing layer parameter.

TABLE 2-1 (Cont.)

Input Screen Title and Parameter Name	Units	Default Value[a]	Code-Accepted Values[b] Physical or Numerical[c] (N) Range		Type[d]	Description
Volumetric water content for leafy vegetable field	--	0.3	1E-5 – 1		P	See fruit, grain, and nonleafy field volumetric water content parameter.
Dry bulk density of soil for leafy vegetable field	g/cm^3	1.5	1E-3 – 22.5		P	See contaminated zone dry bulk density parameter.
Soil erodibility factor for leafy vegetable field	tons/acre	0.4	0 – 0.5		P	See contaminated zone soil erodibility factor parameter.
Slope-length-steepness factor for leafy vegetable field	--	0.4	0 – 10		P	See primary contamination area slope-length-steepness factor parameter.
Cover and management factor for leafy vegetable field	--	0.003	0 – 1		B, P	See primary contamination area cover and management factor parameter.
Support practice factor for leafy vegetable field	--	1	0 – 1		B, P	See primary contamination area support practice factor parameter.
Livestock Feed Growing Area Parameters						
Pasture and silage field						
Area for pasture and silage field	m^2	10,000	Calculated		B	Area for growing pasture and silage. This is not user input but is calculated by the code from the x and y coordinates of the pasture and silage field.
Fraction of area directly over primary contamination for pasture and silage field	--	0	0 – 1		B, P	Fraction of the growing area directly over primary contamination.
Irrigation applied per year for pasture and silage field	m/yr	0.2	0 – 10		B	See primary contamination area irrigation parameter.

TABLE 2-1 (Cont.)

Input Screen Title and Parameter Name	Units	Default Value[a]	Code-Accepted Values[b] Physical or Numerical[c] (N) Range		Type[d]	Description
Evapotranspiration coefficient for pasture and silage field	--	0.5	0 – 0.999		P	See primary contamination area evapotranspiration coefficient parameter.
Runoff coefficient for pasture and silage field	--	0.2	0 – 1		P	See primary contamination area runoff coefficient parameter.
Depth of soil mixing layer or plow layer for pasture and silage field	m	0.15	0 – 1		P, B	See primary contamination area depth of soil mixing layer parameter.
Volumetric water content for pasture and silage field	--	0.3	1E-5 – 1		P	See fruit, grain, and nonleafy field volumetric water content parameter.
Dry bulk density of soil for pasture and silage field	g/cm^3	1.5	1E-3 – 22.5		P	See contaminated zone dry bulk density parameter.
Soil erodibility factor for pasture and silage field	tons/acre	0.4	0 – 0.5		P	See contaminated zone soil erodibility factor parameter.
Slope-length-steepness factor for pasture and silage field	--	0.4	0 – 10		P	See primary contamination area slope-length-steepness factor parameter.
Cover and management factor for pasture and silage field	--	0.003	0 – 1		B, P	See primary contamination area cover and management factor parameter.
Support practice factor for pasture and silage field	--	1	0 – 1		B, P	See primary contamination area support practice factor parameter.
Grain field						
Area for grain field	m^2	10,000	Calculated		B	Area for growing grain. This is not user input but is calculated by the code from the x and y coordinates of the grain field.

TABLE 2-1 (Cont.)

Input Screen Title and Parameter Name	Units	Default Value[a]	Code-Accepted Values[b] Physical or Numerical[c] (N) Range		Type[d]	Description
Fraction of area directly over primary contamination for grain field	--	0	0 – 1		B, P	Fraction of the growing area directly over primary contamination.
Irrigation applied per year for grain field	m/yr	0.2	0 – 10		B	See primary contamination area irrigation parameter.
Evapotranspiration coefficient for grain field	--	0.5	0 – 0.999		P	See primary contamination area evapotranspiration coefficient parameter.
Runoff coefficient for grain field	--	0.2	0 – 1		P	See primary contamination area runoff coefficient parameter.
Depth of soil mixing layer or plow layer for grain field	m	0.15	0 – 1		P, B	See primary contamination area depth of soil mixing layer parameter.
Volumetric water content for grain field	--	0.3	1E-5 – 1		P	See fruit, grain, and nonleafy field volumetric water content parameter.
Dry bulk density of soil for grain field	g/cm^3	1.5	1E-3 – 22.5		P	See contaminated zone dry bulk density parameter.
Soil erodibility factor for grain field	tons/acre	0.4	0 – 0.5		P	See contaminated zone soil erodibility factor parameter.
Slope-length-steepness factor for grain field	--	0.4	0 – 10		P	See primary contamination area slope-length-steepness factor parameter.
Cover and management factor for grain field	--	0.003	0 – 1		B, P	See primary contamination area cover and management factor parameter.
Support practice factor for grain field	--	1	0 – 1		B, P	See primary contamination area support practice factor parameter.

TABLE 2-1 (Cont.)

Input Screen Title and Parameter Name	Units	Default Value[a]	Code-Accepted Values[b] Physical or Numerical[c] (N) Range		Type[d]	Description
Offsite Dwelling Area Parameters						
Area of offsite dwelling site	m^2	1,000	Calculated		B	Area for offsite dwelling site. This is not user input but is calculated by the code from the x and y coordinates of the offsite dwelling site.
Irrigation applied per year to home garden or lawn	m/yr	0.2	0 – 10		B	See primary contamination area irrigation parameter.
Evapotranspiration coefficient for dwelling site	--	0.5	0 – 0.999		P	See primary contamination area evapotranspiration coefficient parameter.
Runoff coefficient for dwelling site	--	0.2	0 – 1		P	See primary contamination area runoff coefficient parameter.
Depth of soil mixing layer for dwelling site	m	0.15	0 – 1		P, B	See primary contamination area depth of soil mixing layer parameter.
Volumetric water content for dwelling site	--	0.3	1E-5 – 1		P	See fruit, grain, and nonleafy field volumetric water content parameter.
Dry bulk density of soil for dwelling site	g/cm^3	1.5	1E-3 – 22.5		P	See contaminated zone dry bulk density parameter.
Soil erodibility factor for dwelling site	tons/acre	0	0 – 0.5		P	See contaminated zone soil erodibility factor parameter.
Slope-length-steepness factor for dwelling site	--	0.4	0 – 10		P	See primary contamination area slope-length-steepness factor parameter.
Cover and management factor for dwelling site	--	0.003	0 – 1		B, P	See primary contamination area cover and management factor parameter.
Support practice factor for dwelling site	--	1	0 – 1		B, P	See primary contamination area support practice factor parameter.

TABLE 2-1 (Cont.)

Input Screen Title and Parameter Name	Units	Default Value[a]	Code-Accepted Values[b] Physical or Numerical[c] (N) Range		Type[d]	Description
Atmospheric Transport						
Release height	m	0	0 – 100		P	Physical release height of escaped material.
Release heat flux	cal/s	0	0 – 1E+10			
Anemometer height	m	10	0 – 100		P	This is the height at which the value for wind speed is measured.
Ambient temperature	K	285	250 – 320		P	Ambient temperature used in the calculation of plume rise of escaped material.
AM atmospheric mixing height	m	400	0 – 3,000		P	This is the annual average morning mixing height. The annual average morning mixing height and annual afternoon mixing height are used to determine the mixing height for different Pasquill stability classes.
PM atmospheric mixing height	m	1,600	0 – 3,000		P	This is the annual afternoon mixing height.
Dispersion model coefficients	--	Pasquill-Gifford	Briggs rural/urban, Pasquill-Gifford		P	Controls which dispersion coefficients are used for the plume dispersion calculations. Pasquill-Gifford coefficients should be used for releases at or near ground level.
Windspeed Terrain	--	Rural	Rural, urban		P	Used to select the wind speed height relationship appropriate for the terrain.
Fruit, grain, nonleafy vegetable plot	m	10	0 – 100		P	This is the elevation of the fruit, grain, nonleafy vegetable plot relative to primary contamination.
Leafy vegetable plot	m	12	0 – 100		P	This is the elevation of the leafy vegetable plot relative to primary contamination.
Pasture, silage growing area	m	20	0 – 100		P	This is the elevation of the pasture, silage growing area relative to primary contamination.
Grain fields	m	14	0 – 100		P	This is the elevation of the grain fields relative to primary contamination.

TABLE 2-1 (Cont.)

Input Screen Title and Parameter Name	Units	Default Value[a]	Code-Accepted Values[b] Physical or Numerical[c] (N) Range		Type[d]	Description
Dwelling site	m	6	0 – 100		P	This is the elevation of the dwelling site relative to primary contamination.
Surface water body	m	26	0 – 100		P	This is the elevation of the surface water body relative to primary contamination.
Grid spacing for areal integration	m	100	0 – 500		P	The primary contamination and the offsite receptor areas are assumed to be rectangular in shape when modeling the atmospheric transport. Rather than use a single transport distance from the centers of the source and the receptor, the code provides the option to subdivide the source and receptor areas into smaller squares or rectangles. The transport from each subdivision of the source to each subdivision of the offsite receptor area is computed and summed together to get a better estimate of the atmospheric transport.
Joint frequency of wind speed and stability class for a 16 sector windrose	--	1 (S to N)	0 – 1		P	This is the fraction of the time that the atmospheric conditions in a specified sector (compass direction) fall within each wind speed interval and stability class combination.
Wind speed	m/s	0.89, 2.46, 4.47, 6.93, 9.61, 12.52	0.001 – 20		P	Wind speeds for the joint frequency data.
Unsaturated Zone Parameters						
Unsaturated zone thickness	m	4	0.01 – 10,000		P	This is the thickness of the specific unsaturated zone.
Unsaturated zone dry bulk density	g/cm^3	1.5	1E-3 – 22.5		P	See contaminated zone dry bulk density parameter.
Unsaturated zone total porosity	--	0.4	1E-5 – 1		P	See clean cover total porosity parameter.
Unsaturated zone effective porosity	--	0.2	1E-5 – 1		P	The effective porosity of the unsaturated zone is the ratio of the pore volume where water can circulate to the total volume of the unsaturated zone. It is used along with other hydrological parameters to calculate the water transport breakthrough times.

TABLE 2-1 (Cont.)

Input Screen Title and Parameter Name	Units	Default Value[a]	Code-Accepted Values[b] Physical or Numerical[c] (N) Range		Type[d]	Description
Unsaturated zone field capacity	--	0.3	1E-5 – 1		P	See contaminated zone field capacity parameter.
Unsaturated zone hydraulic conductivity	m/yr	10	1E-3 – 1E+6		P	See contaminated zone hydraulic conductivity parameter.
Unsaturated zone soil b parameter	--	5.3	0 – 15		P	See contaminated zone soil b parameter.
Unsaturated zone longitudinal dispersivity	m	0.1	0 – 100		P	This is the ratio between the longitudinal dispersion coefficient and pore water velocity. This parameter is dependent on the thickness of the zone.
Saturated Zone Hydrological Data						
Thickness of saturated zone	m	100	0 – 1,000		P	This is the thickness of the saturated zone. It is used to model dispersion in the saturated zone in the vertical direction.
Dry bulk density of saturated zone	g/cm^3	1.5	1E-3 – 22.5		P	See contaminated zone dry bulk density parameter.
Saturated zone total porosity	--	0.4	1E-5 – 1		P	See clean cover total porosity parameter.
Saturated zone effective porosity	--	0.2	1E-5 – 1		P	See unsaturated zone effective porosity parameter.
Saturated zone hydraulic conductivity	m/yr	100	1E-3 – 1E+10		P	See contaminated zone hydraulic conductivity parameter.
Saturated zone hydraulic gradient to well	--	0.02	1E-10 – 10		P	This is the slope of the surface of the water table. The hydraulic gradient is one of several hydrogeological parameters used in water transport calculations.
Saturated zone longitudinal dispersivity to well	m	3	0 – 1,000		P	See unsaturated zone longitudinal dispersivity parameter.

TABLE 2-1 (Cont.)

Input Screen Title and Parameter Name	Units	Default Value[a]	Code-Accepted Values[b] Physical or Numerical[c] (N) Range		Type[d]	Description
Saturated zone horizontal lateral dispersivity to well	m	0.4	0 – 1,000		P	This is the ratio between the horizontal lateral dispersion coefficient and pore water velocity. This parameter is usually about one-tenth to three-tenths of the longitudinal dispersivity.
Saturated zone vertical lateral dispersivity to well	m	0.02	0 – 1,000		P	This is the ratio between the vertical lateral dispersion coefficient and pore water velocity.
Irrigation rate (value averaged over length of saturated zone) contributing to well	m/yr	0.2	0 – 10		B	See primary contamination area irrigation rate parameter.
Evapotranspiration coefficient (value averaged over length of saturated zone) contributing to well	--	0.5	0 – 0.999		P	See primary contamination area evaporation coefficient parameter.
Runoff coefficient (value averaged over length of saturated zone) contributing to well	--	0.2	0 – 1		P	See primary contamination area runoff coefficient parameter.
Depth of aquifer contributing to well	m	10	1E-4 – 1,000		P	The well is assumed to be fully screened from the water table to the specified well screen depth.
Saturated zone hydraulic gradient to surface water body	--	0.02	1E-10 – 10		P	This is the slope of the surface of the water table. The hydraulic gradient is one of several hydrogeological parameters used in water transport calculations.
Saturated zone longitudinal dispersivity to surface water body	m	10	0 – 1,000		P	See unsaturated zone longitudinal dispersivity parameter.
Saturated zone horizontal lateral dispersivity to surface water body	m	1	0 – 1,000		P	This is the ratio between the horizontal lateral dispersion coefficient and pore water velocity. This parameter is usually about one-tenth to three-tenths of the longitudinal dispersivity.

TABLE 2-1 (Cont.)

Input Screen Title and Parameter Name	Units	Default Value[a]	Code-Accepted Values[b] Physical or Numerical[c] (N) Range		Type[d]	Description
Saturated zone vertical lateral dispersivity to surface water body	m	0.06	0 – 1,000		P	This is the ratio between the vertical lateral dispersion coefficient and pore water velocity.
Irrigation rate (value averaged over length of saturated zone) contributing to surface water body	m/yr	0.2	0 – 10		B	See primary contamination area irrigation rate parameter.
Evapotranspiration coefficient (value averaged over length of saturated zone) contributing to surface water body	--	0.5	0 – 0.999		P	See primary contamination area evaporation coefficient parameter.
Runoff coefficient (value averaged over length of saturated zone) contributing to surface water body	--	0.2	0 – 1		P	See primary contamination area runoff coefficient parameter.
Depth of aquifer contributing to surface water body	m	10	0 – 1,000		P	This is the depth of the aquifer that flows into the surface water body. If water flows in the opposite direction (from the surface water body into the aquifer) this depth would be zero. This depth is used to calculate the contaminant flux reaching the surface water body by way of the aquifer.
Surface Water Body Parameters						
Sediment delivery ratio	--	1	0 – 1		P	This is the fraction of the contaminated soil that was eroded from the area of primary contamination that reaches the surface water body.
Volume of surface water body	m^3	150,000	1 – 1E+34	N	P	This is the volume of water in a surface water body.

TABLE 2-1 (Cont.)

Input Screen Title and Parameter Name	Units	Default Value[a]	Code-Accepted Values[b] Physical or Numerical[c] (N) Range		Type[d]	Description
Mean residence time of water in surface water body	yr	1	1E-4 – 1E+34	N	P	This is the value obtained by dividing the volume of the surface water body by the volume of water that is extracted annually from it.
Groundwater Transport Parameters						
Distance from downgradient edge of contamination to:						
Well in the direction parallel to aquifer flow	m	100	-16,000 – +16,000		P, B	This is the distance between two parallel lines that are perpendicular to the direction of aquifer flow, one at the downgradient edge of the contaminated zone and the other at the well.
Surface water body in the direction parallel to aquifer flow	m	600	-16,000 – +16,000		P	This the distance between two parallel lines perpendicular to the direction of aquifer flow, one at the downgradient edge of the contaminated zone and the other at the closest point on the surface water body.
Distance from center of contamination to:						
Well in the direction perpendicular to aquifer flow	m	0	-16,000 – +16,000		P, B	This the distance between two parallel lines that are parallel to the direction of aquifer flow, one through the center of the contaminated zone and the other at the well.
Near edge of surface water body in the direction perpendicular to aquifer flow	m	−150	-16,000 – +16,000		P	This the distance between two parallel lines that are parallel to the direction of aquifer flow, one through the center of the contaminated zone and the other at the closest point on the surface water body.
Far edge of surface water body in the direction perpendicular to aquifer flow	m	150	-16,000 – +16,000		P	This the distance between two parallel lines that are parallel to the direction of aquifer flow, one through the center of the contaminated zone and the other at the farthest point on the surface water body.
Convergence criterion (fractional accuracy desired)	--	0.001	0 – 0.1		P	It is the fractional accuracy desired (convergence criterion) in the Romberg integration used to calculate the contaminant flux or concentration in groundwater.

TABLE 2-1 (Cont.)

Input Screen Title and Parameter Name	Units	Default Value[a]	Code-Accepted Values[b] Physical or Numerical[c] (N) Range		Type[d]	Description
Number of subzones (to model dispersion of progeny produced in transit)						
Main subzones in saturated zone	--	1	1 – 1024		NA	The saturated zone can be subdivided into subzones to improve the predictions for the transport of progeny nuclides.
Main subzones in each partially saturated zone	--	1	1 – 1024		NA	Each partially saturated zone can be subdivided into subzones to improve the predictions for the transport of progeny nuclides.
Retardation and dispersion treatment						
Nuclide-specific retardation in all subzones, longitudinal dispersion in all but the subzone of transformation?	--	Yes	Yes/No		NA	When the layer is subdivided, one must choose which process, longitudinal dispersion or nuclide-specific retardation, will be considered in the subzone in which each atom undergoes a transformation.
Longitudinal dispersion in all subzones, nuclide-specific retardation in all but the subzone of transformation, parent retardation in zone of transformation?	--	No	Yes/No		NA	See above.
Longitudinal dispersion in all subzones, nuclide-specific retardation in all but the subzone of transformation, progeny retardation in zone of transformation?	--	No	Yes/No		NA	See above.

TABLE 2-1 (Cont.)

Input Screen Title and Parameter Name	Units	Default Value[a]	Code-Accepted Values[b] Physical or Numerical[c] (N) Range		Type[d]	Description
Water Use Parameters						
Human consumption						
Quantity of water consumed by an individual	L/yr	510	0 – 1,000		M, B	This is the total amount of water consumed by an individual; it includes water that is used in the preparation of and consumed with food.
Fraction of water from surface body for human consumption	--	0	0 – 1		B, P	This is the fraction of water consumed by humans that is obtained from the surface water source.
Fraction of water from well for human consumption	--	1	0 – 1		B, P	This is the fraction of water consumed by humans that is obtained from the well.
Number of household individuals consuming and using water	--	4	0 – 1,000		B	Number of household individuals for calculating water use.
Use indoors of dwelling						
Quantity of water for use indoors of dwelling per individual	L/d	225	0 – 1,000		M, B	This is the total amount of water that is used indoors by an individual for bathing, laundry, washing, etc. This quantity is used to estimate the volume of water that needs to be extracted from the well to satisfy the specified needs.
Fraction of water from surface body for use indoors of dwelling	--	0	0 – 1		B, P	This is the fraction of water used in the dwelling that is obtained from the surface water source. This factor is used in the computation of indoor radon.
Fraction of water from well for use indoors of dwelling	--	1	0 – 1		B, P	This is the fraction of water used in the dwelling that is obtained from the well. This factor is used in the computation of indoor radon.

TABLE 2-1 (Cont.)

Input Screen Title and Parameter Name	Units	Default Value[a]	Code-Accepted Values[b] Physical or Numerical[c] (N) Range		Type[d]	Description
Beef cattle						
Quantity of water for beef cattle	L/d	50	0 – 500		M, B	This is the total amount of water that is used by beef cattle. This quantity is used to estimate the volume of water that needs to be extracted from the well to satisfy the specified needs.
Fraction of water from surface body for beef cattle	--	0	0 – 1		B, P	This is the fraction of water consumed by beef cattle raised for meat that is obtained from the surface water source.
Fraction of water from well for beef cattle	--	1	0 – 1		B, P	This is the fraction of water consumed by beef cattle raised for meat that is obtained from the well water source.
Number of cattle for beef cattle	--	2	0 – 10		B	Number of beef cattle for calculating water use.
Dairy cows						
Quantity of water for dairy cows	L/d	160	0 – 1,000		M, B	This is the total amount of water that is used by dairy cows. This quantity is used to estimate the volume of water that needs to be extracted from the well to satisfy the specified needs.
Fraction of water from surface body for dairy cows	--	0	0 – 1		B, P	This is the fraction of water consumed by dairy cows raised for milk that is obtained from the surface water source.
Fraction of water from well for dairy cows	--	1	0 – 1		B, P	This is the fraction of water consumed by dairy cows raised for milk that is obtained from the well water source.
Number of cows for dairy cows	--	2	0 – 10		B	Number of dairy cows for calculating water use.

TABLE 2-1 (Cont.)

Input Screen Title and Parameter Name	Units	Default Value[a]	Code-Accepted Values[b] Physical or Numerical[c] (N) Range		Type[d]	Description
Irrigation applied per year						
Fruit, grain, non-leafy vegetables						
Fraction of water from surface body for fruit, grain, and nonleafy vegetables	--	0	0 – 1		B, P	This is the fraction of irrigation water applied at fruit, grain, and nonleafy vegetable field that is obtained from the surface water source.
Fraction of water from well for fruit, grain, and nonleafy vegetables	--	1	0 – 1		B, P	This is the fraction of irrigation water applied at fruit, grain, and nonleafy vegetable field that is obtained from the well.
Leafy vegetables						
Fraction of water from surface body for leafy vegetables	--	0	0 – 1		B, P	This is the fraction of irrigation water applied at leafy vegetable field that is obtained from the surface water source.
Fraction of water from well for leafy vegetables	--	1	0 – 1		B, P	This is the fraction of irrigation water applied at leafy vegetable field that is obtained from the well.
Pasture and silage						
Fraction of water from surface body for pasture and silage	--	0	0 – 1		B, P	This is the fraction of irrigation water applied at pasture and silage field that is obtained from the surface water source.
Fraction of water from well for pasture and silage	--	1	0 – 1		B, P	This is the fraction of irrigation water applied at pasture and silage field that is obtained from the well.
Livestock feed grain						
Fraction of water from surface body for livestock feed grain	--	0	0 – 1		B, P	This is the fraction of irrigation water applied at livestock feed grain field that is obtained from the surface water source.

TABLE 2-1 (Cont.)

Input Screen Title and Parameter Name	Units	Default Value[a]	Code-Accepted Values[b] Physical or Numerical[c] (N) Range		Type[d]	Description
Fraction of water from well for livestock feed grain	--	1	0 – 1		B, P	This is the fraction of irrigation water applied at livestock feed grain field that is obtained from the well.
Offsite dwelling site						
Fraction of water from surface body for offsite dwelling site	--	0	0 – 1		B, P	This is the fraction of irrigation water applied at offsite dwelling site that is obtained from the surface water source.
Fraction of water from well for offsite dwelling site	--	1	0 – 1		B, P	This is the fraction of irrigation water applied at offsite dwelling site that is obtained from the well.
Well pumping rate	m^3/yr	5,100	0 – 100,000		B, P	This is the total volume of water withdrawn from the well for all purposes. It is used to estimate the dilution that occurs in the well.
Well pumping rate needed to specified water use for livestock feed grain	m^3/yr	5,084.17	Calculated		B, P	
Ingestion Rates						
Consumption rate						
Drinking water intake	L/yr	510	0 – 1,000		M, B	This is the amount of water that is consumed by a single individual in a year.
Fish consumption	kg/yr	5.4	0 – 1,000		M, B	This is the weight of fish that is consumed by a single individual in a year.
Other aquatic food consumption	kg/yr	0.9	0 – 100		M, B	This is the weight of other aquatic organisms that is consumed by a single individual in a year.
Fruit, grain, nonleafy vegetables consumption	kg/yr	160	0 – 1,000		M, B	This is the weight of nonleafy vegetables, fruits, or grain that is consumed by a single individual in a year.

TABLE 2-1 (Cont.)

Input Screen Title and Parameter Name	Units	Default Value[a]	Code-Accepted Values[b] Physical or Numerical[c] (N) Range		Type[d]	Description
Leafy vegetables consumption	kg/yr	14	0 – 100		M, B	This is the weight of leafy vegetables that is consumed by a single individual in a year.
Meat consumption	kg/yr	63	0 – 300		M, B	This is the weight of meat that is consumed by a single individual in a year.
Milk consumption	L/yr	92	0 – 1,000		M, B	This is the weight of milk that is consumed by a single individual in a year.
Soil (incidental) ingestion rate	g/yr	36.5	0 – 10,000		M, B	This is the quantity of soil ingested by a single individual in a year.
Fraction from affected area						
Drinking water intake from affected area	--	1	0 – 1		B, P	This is the fraction of drinking water consumed by an individual that is obtained from the contaminated area.
Fish consumption from affected area	--	0.5	0 – 1		B, P	This is the fraction of fish consumed by an individual that is obtained from the contaminated surface water body.
Other aquatic food consumption from affected area	--	0.5	0 – 1		B, P	This is the fraction of the other aquatic food consumed by an individual that is obtained from the contaminated surface water body.
Fruit, grain, nonleafy vegetables consumption from affected area	--	0.5	0 – 1		B, P	This is the fraction of fruit, nonleafy vegetables, or grain consumed by an individual that is obtained from contaminated agricultural areas.
Leafy vegetables consumption from affected area	--	0.5	0 – 1		B, P	This is the fraction of leafy vegetables consumed by an individual that is obtained from contaminated agricultural areas.
Meat consumption from affected area	--	1	0 – 1		B, P	This is the fraction of meat consumed by an individual that is produced using contaminated feed and water.
Milk consumption from affected area	--	1	0 – 1		B, P	This is the fraction of milk consumed by an individual that is produced using contaminated feed and water.

TABLE 2-1 (Cont.)

Input Screen Title and Parameter Name	Units	Default Value[a]	Code-Accepted Values[b] Physical or Numerical[c] (N) Range		Type[d]	Description
Livestock Intakes						
Beef cattle						
Water intake for beef cattle	L/d	50	0 – 500		M	This is the daily intake of water by meat cows kept for meat production.
Pasture and silage intake for beef cattle	kg/d	14	0 – 300		M	This is the daily intake of silage or pasture by meat cows kept for meat production.
Grain intake for beef cattle	kg/d	54	0 – 300		M	This is the daily intake of grain by meat cows kept for meat production.
Soil from pasture and silage intake for beef cattle	kg/d	0.1	0 – 10		M	This is the daily incidental intake of soil with silage or pasture by meat cows kept for meat production.
Soil from grain intake for beef cattle	kg/d	0.4	0 – 10		M	This is the daily incidental intake of soil with grain by meat cows kept for meat production.
Dairy cows						
Water intake for dairy cows	L/d	160	0 – 500		M	This is the daily intake of water by milk cows kept for milk production.
Pasture and silage intake for dairy cows	kg/d	44	0 – 300		M	This is the daily intake of silage or pasture by milk cows kept for milk production.
Grain intake for dairy cows	kg/d	11	0 – 300		M	This is the daily intake of grain by milk cows kept for milk production.
Soil from pasture and silage intake for dairy cows	kg/d	0.4	0 – 10		M	This is the daily incidental intake of soil with silage or pasture by milk cows kept for milk production.
Soil from grain intake for dairy cows	kg/d	0.1	0 – 10		M	This is the daily incidental intake of soil with grain by milk cows kept for milk production.

TABLE 2-1 (Cont.)

Input Screen Title and Parameter Name	Units	Default Value[a]	Code-Accepted Values[b] Physical or Numerical[c] (N) Range		Type[d]	Description
Livestock Feed Factors						
Pasture and silage						
Wet weight crop yield of pasture and silage	kg/m^2	1.1	0.01 – 3		P	This is the mass (wet weight) of the edible portion of pasture and silage that is consumed by livestock produced from a unit land area.
Duration of growing season of pasture and silage	yr	0.08	0.01 – 1		P	This is the period of time during which the pasture and silage that is consumed by livestock is exposed to contamination by foliar deposition and root uptake.
Foliage to food transfer coefficient of pasture and silage	--	1	0 – 1		P	This is the contaminant foliage-to-food transfer coefficient. A fraction of the contaminants that retains on foliage of the pasture and silage that will be absorbed and transferred to the edible portion of the pasture and silage that is consumed by livestock.
Weathering removal constant of pasture and silage	1/yr	20	1 – 40		P	The weathering process would remove contaminants from foliage of the pasture and silage that is consumed by livestock. The process is characterized by a removal constant and reduces the amount of contaminants on foliage exponentially during the exposure period.
Foliar interception factor for irrigation of pasture and silage	--	0.25	0 – 1		P	This is the fraction of deposited radionuclides from irrigation that retains on the foliage of the pasture and silage food that is consumed by livestock.
Foliar interception factor for dust of pasture and silage	--	0.25	0 – 1		P	This is the fraction of deposited radionuclides from mass loading that retains on the foliage of the pasture and silage food that is consumed by livestock.
Root depth of pasture and silage	m	0.9	0 – 3		P	This is the maximum root depth of the pasture and silage that is consumed by livestock.
Grain						
Wet weight crop yield of grain	kg/m^2	0.7	0.01 – 3		P	This is the mass (wet weight) of the edible portion of grain that is consumed by livestock produced from a unit land area.

TABLE 2-1 (Cont.)

Input Screen Title and Parameter Name	Units	Default Value[a]	Code-Accepted Values[b] Physical or Numerical[c] (N) Range		Type[d]	Description
Duration of growing season of grain	yr	0.17	0.01 – 1		P	This is the period of time during which the grain that is consumed by livestock is exposed to contamination by foliar deposition and root uptake.
Foliage to food transfer coefficient of grain	--	0.1	0 – 1		P	This is the contaminant foliage-to-food transfer coefficient. A fraction of the contaminants that retain on foliage of the grain that is consumed by livestock will be absorbed and transferred to the edible portion of the grain.
Weathering removal constant of grain	1/yr	20	1 – 40		P	The weathering process would remove contaminants from foliage of the grain that is consumed by livestock. The process is characterized by a removal constant and reduces the amount of contaminants on foliage exponentially during the exposure period.
Foliar interception factor for irrigation of grain	--	0.25	0 – 1		P	This is the fraction of deposited radionuclides from irrigation that retains on the foliage of the grain that is consumed by livestock.
Foliar interception factor for dust of grain	--	0.25	0 – 1		P	This is the fraction of deposited radionuclides from mass loading that retains on the foliage of the grain that is consumed by livestock.
Root depth of grain	m	1.2	0 – 10		P	This is the maximum root depth of the grain that is consumed by livestock.
Plant Factors						
Fruit, grain, nonleafy vegetables						
Wet weight crop yield of fruit, grain, and nonleafy vegetables	kg/m^2	0.7	0.01 – 3		P	This is the mass (wet weight) of the edible portion of fruit, grain, and nonleafy vegetables produced from a unit land area.
Duration of growing season of fruit, grain, and nonleafy vegetables	yr	0.17	0.01 – 1		P	This is the period of time during which the fruit, grain, and leafy vegetables are exposed to contamination by foliar deposition and root uptake.

TABLE 2-1 (Cont.)

Input Screen Title and Parameter Name	Units	Default Value[a]	Code-Accepted Values[b] Physical or Numerical[c] (N) Range		Type[d]	Description
Foliage to food transfer coefficient of fruit, grain, and nonleafy vegetables	--	0.1	0 – 1		P	This is the contaminant foliage-to-food transfer coefficient. A fraction of the contaminants that retain on foliage of the fruit, grain, and nonleafy vegetables will be absorbed and transferred to the edible portion of the pasture and silage.
Weathering removal constant of fruit, grain, and nonleafy vegetables	1/yr	20	1 – 40		P	The weathering process would remove contaminants from foliage of the fruit, grain, and nonleafy vegetables. The process is characterized by a removal constant and reduces the amount of contaminants on foliage exponentially during the exposure period.
Foliar interception factor for irrigation of fruit, grain, and nonleafy vegetables	--	0.25	0 – 1		P	This is the fraction of deposited radionuclides from irrigation that retains on the foliage of the fruit, grain, and nonleafy vegetables.
Foliar interception factor for dust of fruit, grain, and nonleafy vegetables	--	0.25	0 – 1		P	This is the fraction of deposited radionuclides from mass loading that retains on the foliage of the fruit, grain, and nonleafy vegetables.
Root depth of fruit, grain, and nonleafy vegetables	m	1.2	0 – 10		P	This is the maximum root depth of the fruit, grain, and nonleafy vegetables.
Leafy vegetables						
Wet weight crop yield of leafy vegetables	kg/m^2	1.5	0.01 – 3		P	This is the mass (wet weight) of the edible portion of leafy vegetables produced from a unit land area.
Duration of growing season of leafy vegetables	yr	0.25	0.01 – 1		P	This is the period of time during which the leafy vegetables are exposed to contamination by foliar deposition and root uptake.
Foliage to food transfer coefficient of leafy vegetables	--	1	0 – 1		P	This is the contaminant foliage-to-food transfer coefficient. A fraction of the contaminants that retain on foliage of the leafy vegetables will be absorbed and transferred to the edible portion of the pasture and silage.

TABLE 2-1 (Cont.)

Input Screen Title and Parameter Name	Units	Default Value[a]	Code-Accepted Values[b] Physical or Numerical[c] (N) Range		Type[d]	Description
Weathering removal constant of leafy vegetables	1/yr	20	1 – 40		P	The weathering process would remove contaminants from foliage of the leafy vegetables. The process is characterized by a removal constant and reduces the amount of contaminants on foliage exponentially during the exposure period.
Foliar interception factor for irrigation of leafy vegetables	--	0.25	0 – 1		P	This is the fraction of deposited radionuclides from irrigation that retains on the foliage of the leafy vegetables.
Foliar interception factor for dust of leafy vegetables	--	0.25	0 – 1		P	This is the fraction of deposited radionuclides from mass loading that retains on the foliage of the leafy vegetables.
Root depth of leafy vegetables	m	0.9	0 – 3		P	This is the maximum root depth of the leafy vegetables.
Inhalation and External Gamma Data						
Inhalation rate	m^3/yr	8,400	0 – 20,000		M, B	This is the annual air intake.
Mass loading for inhalation	g/m^3	0.0001	0 – 2		P, B	This is the mass loading of airborne contaminated soil particles.
Mean onsite mass loading	g/m^3	0.0001	0 – 2		P, B	This is the average mass loading of airborne contaminated soil particles, above the primary contamination. It is used to estimate the contaminant release rate to the atmosphere.
Indoor dust filtration factor (indoor to outdoor dust concentration)	--	0.4	0 – 1		P, B	The indoor dust filtration factor describes the effect of the building structure on the level of contaminated dust existing indoors. Specifically, the factor is the fraction of outdoor contaminated dust that will be available indoors.
External gamma shielding (penetration) factor	--	0.7	0 – 1		P	The shielding factor describes the effect of the building structure on the level of gamma radiation existing indoors. Specifically, the shielding factor is the fraction of outdoor gamma radiation that will be available indoors.

TABLE 2-1 (Cont.)

Input Screen Title and Parameter Name	Units	Default Value[a]	Code-Accepted Values[b] Physical or Numerical[c] (N) Range		Type[d]	Description
External Radiation Shape and Area Factors						
Dwelling location		Offsite	Onsite or offsite		P	The dwelling location could be on the primary contamination or it could be offsite.
Scale	m	200	>0 – 32,000		P	This sets the lengths of the sides of the square frame with in which the primary contamination is to be drawn. The scale should be chosen to fully encompass the primary contamination. If the mouse is to be used to specify the locations of the dwellings, the scale must be chosen so that the primary contamination and the dwellings can be located in the drawing frame.
Dwelling location coordinate in X-direction	m	100	-16,000 – +16,000		P	The point locations of the onsite and offsite dwellings can be specified either by inputting the coordinates or by clicking on the figure. First select the tab corresponding to the dwelling location (onsite or offsite). Then key in the coordinates of the dwelling location in these input boxes. Click the Calculate Radii and Fractions button after entering the coordinates of each dwelling location to compute the radii and fractions.
Dwelling location coordinate in y-direction	m	0	-16,000 – +16,000		P	See above.
Radius	m	13.25 26.5 39.75 53.0 66.25 79.5 92.75 106 119.25 132.5 145.75 159	Calculated		P	The radii and fraction is calculated by the code by drawing 12 concentric circles centered at the dwelling location. The radius of the outermost circle is such that it encloses the entire dwelling. The radius of the innermost circle is 1/12 of the radius of the outermost circle. The radii of the remaining 10 circles are in an arithmetic series between the radii of these two circles. The interface then estimates the fraction of each annular ring that is within the primary contamination displayed in the graphic. The radii of the 12 concentric circles and the fractional area of each annular ring that is within the primary contamination are displayed in the 12 radii and fraction input boxes in the tab corresponding to the receptor location. The user can directly input the radii and fraction information if it is available.

TABLE 2-1 (Cont.)

Input Screen Title and Parameter Name	Units	Default Value[a]	Code-Accepted Values[b] Physical or Numerical[c] (N) Range		Type[d]	Description
Fraction	--	0 0 0 0.024 0.19 0.24 0.2 0.17 0.15 0.13 0.12 0.052	Calculated		P	See above.
Shape of the primary contamination	--	Polygonal	Circular or polygonal		P	This defines the shape of the primary contamination.
X coordinate of the vertices of polygon of the primary contamination	m	none	-16,000 – +16,000		P	If the user has more information on the shape of the primary contamination they can press clear to clear the previous shape and draw the exact shape of the polygon or input x and y coordinates of the vertices of polygon. The polygon can be "drawn" using the mouse and following the drawing instructions given in the yellow information box on the form. Alternatively, the vertices of the polygon can keyed in by following the instructions given in the green Instructions box.
Y coordinate of the vertices of polygon of the primary contamination	m	none	-16,000 – +16,000		P	See above.
Occupancy Factors						
Fraction of time spent on primary contamination (whether cultivated or not)						
Indoor time fraction on primary contamination	--	0	0 – 1		B	This is the average fraction of time during which an individual stays inside a house that is built on top of the primary contamination.

TABLE 2-1 (Cont.)

Input Screen Title and Parameter Name	Units	Default Value[a]	Code-Accepted Values[b] Physical or Numerical[c] (N) Range		Type[d]	Description
Outdoor time fraction on primary contamination	--	0	0 – 1		B	This is the average fraction of a day during which an individual stays outdoors on the area of primary contamination. If part of the farmed area lies on the area of primary contamination, the time fraction spent in that part of the area should be included in both the primary-contamination and farmed-area occupancies. Thus, the total occupancy could exceed one, but cannot exceed 2.
Fraction of time spent offsite in offsite dwelling site						
Indoor time fraction on offsite dwelling site	--	0.5	0 – 1		B	This is the average fraction of time during which an individual stays inside a house that is built outside the area of primary contamination.
Outdoor time fraction on offsite dwelling site	--	0.1	0 – 1		B	This is the average fraction of a day during which an individual stays outdoors in the offsite dwelling site.
Fraction of time spent in farmed areas (including primary and secondary contaminated areas)						
Time fraction in fruit, grain, and nonleafy vegetable fields	--	0.1	0 – 1		B	This is the average fraction of a day during which an individual spends in the agricultural field or pasture (farmed area). If part of the farmed area lies on the area of primary contamination, the time fraction spent in that part of the area should be included in both the primary-contamination and farmed-area occupancies. If part of the farmed area lies outside the area of primary contamination, but within the range of direct radiation emanating from the primary contamination, the time fraction spent in that part of the area should be included in both near the primary contamination and the farmed-area occupancies. Thus, the total occupancy could exceed one, but cannot exceed 2.
Time fraction in leafy vegetable fields	--	0.1	0 – 1		B	
Time fraction in pasture and silage fields	--	0.1	0 – 1		B	
Time fraction in livestock grain fields	--	0.1	0 – 1		B	

TABLE 2-1 (Cont.)

Input Screen Title and Parameter Name	Units	Default Value[a]	Code-Accepted Values[b] Physical or Numerical[c] (N) Range		Type[d]	Description
Radon Parameters						
Effective radon diffusion coefficient of cover	m^2/s	2×10^{-6}	0 – 1 or -1		P	The effective (or interstitial) radon diffusion coefficient is defined as the ratio of the gradient of the radon activity concentration in the pore space to the diffusive flux density of radon activity across the pore area. Entering –1 for any diffusion coefficient will cause the code to calculate a diffusion coefficient based on the porosity and water content of the medium.
Effective radon diffusion coefficient of contaminated zone	m^2/s	2×10^{-6}	0 – 1 or -1		P	Same as above.
Effective radon diffusion coefficient of floor	m^2/s	3×10^{-7}	0 – 1 or -1		P	Same as above.
Thickness of floor and foundation	m	0.15	0 – 10		P	The building foundation thickness is defined as the average thickness of the building shell structure in the subsurface of the soil.
Density of floor and foundation	g/cm^3	2.4	0 – 22.5		P	The building foundation bulk density is defined as the ratio of the solid-phase mass to the total volume.
Total porosity of floor and foundation	--	0.1	1E-4 – 1		P	Total porosity is defined as the ratio of the void-space volume to the total volume of a porous medium.
Volumetric water content of floor and foundation	--	0.03	0 – 1		P	The volumetric water content in a porous medium represents the fraction of the total volume of porous medium that is occupied by the water contained in the porous medium. The value should be less than the total porosity of the porous medium.

TABLE 2-1 (Cont.)

Input Screen Title and Parameter Name	Units	Default Value[a]	Code-Accepted Values[b] Physical or Numerical[c] (N) Range		Type[d]	Description
Depth of foundation below ground level	m	-1	0 – 100 or -100		P	The foundation depth below ground surface is defined as the vertical distance in the soil immediately from the bottom of the basement floor slab to the ground surface. If a negative value is entered, the absolute value will be adjusted (if needed) so that the foundation depth will not extend into the contaminated zone. Thus, due to erosion of the cover and contaminated zones, the foundation depth could be time-dependent and less than the (absolute) specified value.
Onsite vertical dimension of mixing	m	2	1E-4 – 1,000		P	Radon vertical dimension of mixing is defined as the height into which the plume of radon is uniformly mixed in the outdoor air.
Building room height	m	2.5	1E-4 – 100		P	The building room height is defined as the average height of the rooms in the building.
Building air exchange rate	1/h	0.5	0 – 1,000		B	The building air exchange (or ventilation) rate is defined as the number of the total volumes of air contained in the building being exchanged with outside air per unit of time.
Building indoor area factor	--	0	0 – 100		P	The building indoor area factor is the fraction of the floor area built on the contaminated area. Values greater than 1.0 indicate a contribution from walls extending into the contaminated zone. A default value of 0.0 means the code will calculate automatically a time-dependent area factor on the basis of an assumed floor area of 100 m^2 and the amount of wall area extending into the contaminated zone.
Rn-222 emanation coefficient	--	0.25	1E-2 – 1		P	The radon emanation coefficient is defined as the fraction of the total radon generated by radium decay that escapes from the soil particles. The emanating power is dependent upon on many factors, such as mineralogy, porosity, particle size distribution, and moisture content.
Rn-220 emanation coefficient	--	0.15	1E-2 – 1		P	Same as above.

TABLE 2-1 (Cont.)

Input Screen Title and Parameter Name	Units	Default Value[a]	Code-Accepted Values[b] Physical or Numerical[c] (N) Range		Type[d]	Description
Carbon-Model Parameters						
Thickness of evasion layer for C-14 in soil	m	0.3	0 – 10		P	This is the maximum soil thickness layer through which C-14 can escape to the air by conversion to CO_2. C-14 below this depth is assumed trapped in the soil.
C-14 evasion flux rate from soil	1/s	7×10^{-7}	0 – 1		P	This is the fraction of the soil inventory of C-14 that is lost to the atmosphere per unit time.
C-12 evasion flux rate from soil	1/s	1×10^{-10}	0 – 1		P	This is the fraction of C-12 in soil that escapes to the atmosphere per unit time.
Fraction of vegetation carbon absorbed from soil	--	0.02	1E-4 – 1		P	This is the fraction of total vegetation carbon obtained by direct root uptake from the soil.
Fraction of vegetation carbon absorbed from air	--	0.98	0 – 1		P	This is the fraction of total vegetation carbon assimilated from the atmosphere through photosynthesis.
C-12 mass fraction in contaminated soil	g/g	0.03	1E-4 – 1		P	This parameter is the C-12 concentration in the contaminated zone in g/g.
C-12 mass fraction in local water	$g/cm3^3$	0.00002	0 – 100		P	This parameter is the C-12 concentration in the local water.
C-12 mass fraction in fruit, grain, nonleafy vegetables	--	0.4	0 – 1		P	This is the mass of C-12 in a unit mass of fruit, grain, and nonleafy vegetables.
C-12 mass fraction in leafy vegetables	--	0.09	0 – 1		P	This is the mass of C-12 in a unit mass of leafy vegetables.
C-12 mass fraction in pasture and silage	--	0.09	0 – 1		P	This is the mass of C-12 in a unit mass of pasture and silage.
C-12 mass fraction in grain	--	0.4	0 – 1		P	This is the mass of C-12 in a unit mass of grain.
C-12 mass fraction in meat	--	0.24	0 – 1		P	This is the mass of C-12 in a unit mass of meat.

TABLE 2-1 (Cont.)

Input Screen Title and Parameter Name	Units	Default Value[a]	Code-Accepted Values[b] Physical or Numerical[c] (N) Range		Type[d]	Description
C-12 mass fraction in milk	--	0.07	0 – 1		P	This is the mass of C-12 in a unit mass of milk.
Tritium Model Parameters						
Humidity in air	g/m^3	8	0 – 1,000		P	Air humidity is used for the computation of tritium concentration in air.
Mass fraction of water in:						
Water fraction in fruit, grain, and nonleafy vegetables	--	0.8	0 – 1		P	This is the mass of water in a unit mass of fruit, grain, and nonleafy vegetables.
Water fraction in leafy vegetable	--	0.8	0 – 1		P	This is the mass of water in a unit mass of leafy vegetables.
Water fraction in pasture and silage	--	0.8	0 – 1		P	This is the mass of water in a unit mass of pasture and silage.
Water fraction in grain	--	0.8	0 – 1		P	This is the mass of water in a unit mass of grain.
Water fraction in meat	--	0.6	0 – 1		P	This is the mass of water in a unit mass of meat.
Water fraction in milk	--	0.88	0 – 1		P	This is the mass of water in a unit mass of milk.

[a] The default values listed in this table are the default values in the RESRAD-OFFSITE code Version 2.

[b] Code-accepted values are not provided for element- or nuclide-specific parameters.

[c] Numerical range is the range defined in a program file to prevent code crashes.

[d] P = physical, B = behavioral, M = metabolic; when more than one type is listed, the first is primary and the next is secondary.

[e] Two hyphens indicate that the parameter is dimensionless.

[f] NA = not applicable.

TABLE 2-2 Default Dose Conversion Factors[a] (DCFs) for External, Inhalation, and Ingestion Pathways in RESRAD-OFFSITE Code Version 2

Radionuclide[b]	External DCFs (mrem/yr)/(pCi/g)	Class[c]	Inhalation DCFs (mrem/pCi)	f_1[d]	Ingestion DCF (mrem/pCi)
Ac-227	2.01E+00	D	6.72	1.00E-03	1.48E-02
Ag-108m+D	9.65E+00	Y	2.83E-04	5.00E-02	7.62E-06
Ag-110m+D	1.72E+01	Y	8.03E-05	5.00E-02	1.08E-05
Al-26	1.74E+01	D	7.96E-06	1.00E-02	1.46E-05
Am-241	4.37E-02	W	4.44E-01	1.00E-03	3.64E-03
Am-243+D	8.95E-01	W	4.40E-01	1.00E-03	3.63E-03
Au-195	2.07E-01	Y	1.30E-05	1.00E-01	1.06E-06
Ba-133	1.98E+00	D	7.86E-06	1.00E-01	3.40E-06
Be-7	2.88E-01	Y	3.21E-07	5.00E-03	1.28E-07
Bi-207	9.38E+00	W	2.00E-05	5.00E-02	5.48E-06
C-14	1.34E-05	(ORGANIC)	2.09E-06	1	2.09E-06
Ca-41	0.00E+00	W	1.35E-06	3.00E-01	1.27E-06
Ca-45	6.26E-05	W	6.62E-06	3.00E-01	3.16E-06
Cd-109	1.47E-02	D	1.14E-04	5.00E-02	1.31E-05
Ce-141	3.18E-01	Y	8.95E-06	3.00E-04	2.90E-06
Ce-144+D	3.24E-01	Y	3.74E-04	3.00E-04	2.11E-05
Cf-252	1.76E-04	W	1.57E-01	1.00E-03	1.08E-03
Cl-36	2.39E-03	W	2.19E-05	1	3.03E-06
Cm-243	5.83E-01	W	3.07E-01	1.00E-03	2.51E-03
Cm-244	1.26E-04	W	2.48E-01	1.00E-03	2.02E-03
Cm-245	3.40E-01	W	4.55E-01	1.00E-03	3.74E-03
Cm-246	1.16E-04	W	4.51E-01	1.00E-03	3.70E-03
Cm-247	1.86E+00	W	4.14E-01	1.00E-03	3.42E-03
Cm-248	8.78E-05	W	1.65	1.00E-03	1.36E-02
Co-57	5.01E-01	Y	9.07E-06	3.00E-01	1.18E-06
Co-60	1.62E+01	Y	2.19E-04	3.00E-01	2.69E-05
Cr-51	1.74E-01	Y	3.34E-07	1.00E-01	1.47E-01
Cs-134	9.47E+00	D	4.63E-05	1	7.33E-05
Cs-135	3.83E-05	D	4.55E-06	1	7.07E-06
Cs-137+D	3.41E+00	D	3.19E-05	1	5.00E-05
Eu-152	7.01E+00	W	2.21E-04	1.00E-03	6.48E-06
Eu-154	7.68E+00	W	2.86E-04	1.00E-03	9.55E-06
Eu-155	1.82E-01	W	4.14E-05	1.00E-03	1.53E-06
Fe-55	0.00E+00	D	2.69E-06	1.00E-01	6.07E-07
Fe-59	7.64E+00	D	1.48E-05	1.00E-01	6.70E-06
Gd-152	0.00E+00	D	2.43E-01	3.00E-04	1.61E-04
Gd-153	2.45E-01	D	2.38E-05	3.00E-04	1.17E-06
Ge-68+D	5.62E+00	W	5.19E-05	1	1.41E-06
H-3	0.00E+00	(H_2O)	6.40E-08	1	6.40E-08
I-125	1.66E-02	D	2.42E-05	1	3.85E-05
I-129	1.29E-02	D	1.74E-04	1	2.76E-04
I-131	2.17E+00	D	3.29E-05	1	5.33E-05
In-111	1.96E+00	W	8.40E-7	2.00E-02	1.33E-06
Ir-192	4.61E+00	Y	2.82E-05	1.00E-02	5.74E-06
K-40	1.04E+00	D	1.24E-05	1	1.86E-05

TABLE 2-2 (Cont.)

Radionuclide[b]	External DCFs (mrem/yr)/(pCi/g)	Class[c]	Inhalation DCFs (mrem/pCi)	f_1[d]	Ingestion DCF (mrem/pCi)
La-138	7.96E+00	D	1.37E-03	1.00E-03	5.88E-06
Mn-54	5.16E+00	W	6.70E-06	1.00E-01	2.77E-06
Na-22	1.37E+01	D	7.66E-06	1	1.15E-05
Nb-93m	1.04E-04	Y	2.92E-05	1.00E-02	5.21E-07
Nb-94	9.68E+00	Y	4.14E-04	1.00E-02	7.14E-06
Nb-95	4.69E+00	Y	5.81E-06	1.00E-02	2.57E-06
Ni-59	0.00E+00	(VAPOR)	2.70E-06	5.00E-02	2.10E-07
Ni-63	0.00E+00	(VAPOR)	6.29E-06	5.00E-02	5.77E-07
Np-237+D	1.10E+00	W	5.40E-01	1.00E-03	4.44E-03
Pa-231	1.91E-01	W	1.28	1.00E-03	1.06E-02
Pb-210+D	6.05E-03	D	1.38E-02	2.00E-01	5.37E-03
Pm-147	5.01E-05	Y	3.92E-05	3.00E-04	1.05E-06
Po-210	5.23E-05	W	9.40E-03	1.00E-01	1.90E-03
Pu-238	1.51E-04	W	3.92E-01	1.00E-03	3.20E-03
Pu-239	2.95E-04	W	4.29E-01	1.00E-03	3.54E-03
Pu-240	1.47E-04	W	4.29E-01	1.00E-03	3.54E-03
Pu-241+D	1.89E-05	W	8.25E-03	1.00E-03	6.85E-05
Pu-242	1.28E-04	W	4.11E-01	1.00E-03	3.36E-03
Pu-244+D	7.73E+00	W	4.03E-01	1.00E-03	3.32E-03
Ra-226+D	1.12E+01	W	8.60E-03	2.00E-01	1.33E-03
Ra-228+D	5.98E+00	W	5.08E-03	2.00E-01	1.44E-03
Ru-106+D	1.29E+00	Y	4.77E-04	5.00E-02	2.74E-05
S-35	1.49E-05	W	2.48E-06	8.00E-01	7.33E-06
Sb-124	1.17E+01	W	2.52E-05	1.00E-02	1.01E-05
Sb-125	2.45E+00	W	1.22E-05	1.00E-01	2.81E-06
Sc-46	1.27E+01	Y	2.96E-05	1.00E-04	6.40E-06
Se-75	1.98E+00	W	8.47E-06	8.00E-01	9.62E-06
Se-79	1.86E-05	W	9.84E-06	8.00E-01	8.70E-06
Sm-147	0.00E+00	W	7.47E-02	3.00E-04	1.85E-04
Sm-151	9.84E-07	W	3.00E-05	3.00E-04	3.89E-07
Sm-153	1.58E-01	W	1.96E-06	3.00E-04	2.99E-06
Sn-113+D	1.46E+00	W	1.07E-05	2.00E-02	3.19E-06
Sn-126	1.18E+01	W	1.01E-04	2.00E-02	2.11E-05
Sr-85	2.97E+00	Y	5.03E-06	3.00E-01	1.98E-06
Sr-89	9.08E-03	Y	4.14E-05	1.00E-02	9.25E-06
Sr-90+D	2.46E-02	Y	1.31E-03	3.00E-01	1.53E-04
Ta-182	7.94E+00	Y	4.48E-05	1.00E-03	6.51E-06
Tc-99	1.26E-04	W	8.33E-06	8.00E-01	1.46E-06
Tc-99m	5.51E-01	D	3.26E-08	8.00E-01	6.22E-08
Te-125m	1.51E-02	W	7.29E-06	2.00E-01	3.67E-06
Th-228+D	1.02E+01	Y	3.45E-01	2.00E-04	8.08E-04
Th-229+D	1.60E+00	W	2.16	2.00E-04	4.03E-03
Th-230	1.21E-03	W	3.26E-01	2.00E-04	5.48E-04
Th-232	5.21E-04	W	1.64	2.00E-04	2.73E-03
Tl-201	2.76E-01	D	2.35E-07	1	3.00E-07
Tl-202	2.50E+00	D	9.84E-07	1	1.47E-06

TABLE 2-2 (Cont.)

Radionuclide[b]	External DCFs (mrem/yr)/(pCi/g)	Class[c]	Inhalation DCFs (mrem/pCi)	f_1[d]	Ingestion DCF (mrem/pCi)
Tl-204	4.05E-03	D	2.41E-06	1	3.36E-06
U-232	9.02E-04	Y	6.59E-01	5.00E-02	1.31E-03
U-233	1.40E-03	Y	1.35E-01	5.00E-02	2.89E-04
U-234	4.02E-04	Y	1.32E-01	5.00E-02	2.83E-04
U-235+D	7.57E-01	Y	1.23E-01	5.00E-02	2.67E-04
U-236	2.15E-04	Y	1.25E-01	5.00E-02	2.69E-04
U-238+D	1.52E-01	Y	1.18E-01	5.00E-02	2.69E-04
Xe-131m	2.26E-02	D	0.00E+00	0.00E+00	0.00E+00
Zn-65	3.70E+00	Y	2.04E-05	5.00E-01	1.44E-05
Zr-93	0.00E+00	D	3.21E-04	2.00E-03	1.66E-06
Zr-95+D	4.52E+00	D	2.36E-05	2.00E-03	3.79E-06

[a] External dose conversion factors taken from Eckerman and Ryman (1993), and inhalation and ingestion dose conversion factors are from Eckerman et al. (1988).

[b] +D indicates that the dose conversion factors of associated radionuclides (half-life less than 30 days) are included along with the principal radionuclide.

[c] The three inhalation classes D, W, and Y correspond to retention half-times of less than 10 days, 10 to 100 days, and greater than 100 days, respectively. (H_2O) indicates water; (ORGANIC) indicates an organic material; and (VAPOR) indicates a gaseous material.

[d] Fraction of a stable element entering the GI tract that reaches body fluids.

TABLE 2-3 Radionuclide Slope Factors[a] for External, Inhalation, and Different Ingestion Pathways in RESRAD-OFFSITE Code Version 2

Radionuclide	External (Risk/yr)/(pCi/g)	Inhalation (Risk/pCi)	Ingestion–Food (Risk/pCi)	Ingestion–Water (Risk/pCi)	Ingestion–Soil (Risk/pCi)
Ac-227+D	1.47E-06	2.13E-07	6.51E-10	4.85E-10	6.51E-10
Ag-108m+D	7.19E-06	1.04E-10	1.12E-11	8.14E-12	1.12E-11
Ag-110m+D	1.30E-05	4.51E-11	1.37E-11	9.88E-12	1.37E-11
Al-26	1.33E-05	2.90E-10	2.49E-11	1.73E-11	2.49E-11
Am-241	2.76E-08	3.77E-08	1.34E-10	1.04E-10	1.34E-10
Am-243+D	6.35E-07	3.70E-08	1.41E-10	1.08E-10	1.41E-10
Au-195	1.38E-07	6.48E-12	2.19E-12	1.50E-12	2.19E-12
Ba-133	1.44E-06	3.25E-11	9.44E-12	6.81E-12	9.44E-12
Be-7	2.13E-07	2.13E-13	1.20E-13	8.66E-14	1.20E-13
Bi-207	7.08E-06	1.10E-10	8.14E-12	5.66E-12	8.14E-12
C-14	7.83E-12	1.69E-11	2.00E-12	1.55E-12	2.00E-12
Ca-41	0.00E+00	5.07E-13	4.37E-13	3.53E-13	4.37E-13
Ca-45	3.96E-11	1.28E-11	3.37E-12	2.47E-12	3.37E-12
Cd-109	8.73E-09	2.19E-11	6.70E-12	5.00E-12	6.70E-12
Ce-141	2.27E-07	1.35E-11	6.77E-12	4.63E-12	6.77E-12
Ce-144+D	2.41E-07	1.80E-10	5.19E-11	3.53E-11	5.19E-11
Cf-252	1.80E-11	2.60E-08	1.80E-10	1.80E-10	1.80E-10
Cl-36	1.74E-09	1.01E-10	4.44E-12	3.30E-12	4.44E-12
Cm-243	4.19E-07	3.67E-08	1.23E-10	9.47E-11	1.23E-10
Cm-244	4.85E-11	3.56E-08	1.08E-10	8.36E-11	1.08E-10
Cm-245	2.38E-07	3.81E-08	1.35E-10	1.04E-10	1.35E-10
Cm-246	4.57E-11	3.77E-08	1.31E-10	1.02E-10	1.31E-10
Cm-247+D	1.36E-06	3.49E-08	1.30E-10	1.00E-10	1.30E-10
Cm-248	1.50E-11	1.50E-07	1.30E-09	1.30E-09	1.30E-09
Co-57	3.55E-07	3.74E-12	1.49E-12	1.04E-12	1.49E-12
Co-60	1.24E-05	1.01E-10	2.23E-11	1.57E-11	2.23E-11
Cr-51	1.27E-07	1.67E-13	2.66E-13	1.85E-13	2.66E-13
Cs-134	7.10E-06	6.99E-11	5.14E-11	4.22E-11	5.14E-11
Cs-135	2.36E-11	2.49E-11	5.88E-12	4.74E-12	5.88E-12
Cs-137+D	2.55E-06	1.12E-10	3.74E-11	3.04E-11	3.74E-11
Eu-152	5.30E-06	1.90E-10	8.70E-12	6.07E-12	8.70E-12
Eu-154	5.83E-06	2.11E-10	1.49E-11	1.03E-11	1.49E-11
Eu-155	1.24E-07	1.91E-11	2.77E-12	1.90E-12	2.77E-12
Fe-55	0.00E+00	1.48E-12	1.16E-12	8.62E-13	1.16E-12
Fe-59	5.83E-06	1.47E-11	1.11E-11	7.88E-12	1.11E-11
Gd-152	0.00E+00	9.10E-09	3.85E-11	2.97E-11	3.85E-11
Gd-153	1.62E-07	8.58E-12	2.22E-12	1.52E-12	2.22E-12
Ge-68+D	4.17E-06	1.08E-10	1.03E-11	7.24E-12	1.03E-11
H-3	0.00E+00	8.51E-13	1.44E-13	1.12E-13	1.44E-13
I-125	7.24E-09	2.77E-11	6.29E-11	2.54E-11	6.29E-11
I-129 (vapor)	6.09E-09	1.60E-10	3.22E-10	1.48E-10	3.22E-10
I-131	1.59E-06	5.03E-11	1.34E-10	4.55E-11	1.34E-10
In-111	1.42E-06	8.58E-13	1.85E-12	1.29E-12	1.85E-12
Ir-192	3.40E-06	2.41E-11	1.07E-11	7.36E-12	1.07E-11
K-40	7.97E-07	2.22E-10	3.43E-11	2.47E-11	3.43E-11

TABLE 2-3 (Cont.)

Radionuclide	External (Risk/yr)/(pCi/g)	Inhalation (Risk/pCi)	Ingestion–Food (Risk/pCi)	Ingestion–Water (Risk/pCi)	Ingestion–Soil (Risk/pCi)
La-138	6.07E-06	3.05E-10	4.96E-12	3.53E-12	4.96E-12
Mn-54	3.89E-06	1.21E-11	3.11E-12	2.28E-12	3.11E-12
Na-22	1.03E-05	9.73E-11	1.26E-11	9.62E-12	1.26E-11
Nb-93m	3.83E-11	5.66E-12	1.17E-12	8.03E-13	1.17E-12
Nb-94	7.29E-06	1.35E-10	1.11E-11	7.77E-12	1.11E-11
Nb-95	3.53E-06	6.44E-12	3.50E-12	2.45E-12	3.50E-12
Ni-59	0.00E+00	1.27E-12	3.89E-13	2.74E-13	3.89E-13
Ni-63	0.00E+00	3.74E-12	9.51E-13	6.70E-13	9.51E-13
Np-237+D	7.96E-07	2.87E-08	9.10E-11	6.73E-11	9.10E-11
Pa-231	1.39E-07	7.62E-08	2.26E-10	1.73E-10	2.26E-10
Pb-210+D	4.17E-09	2.80E-08	1.19E-09	8.88E-10	1.19E-09
Pm-147	3.21E-11	1.61E-11	2.48E-12	1.69E-12	2.48E-12
Po-210	3.95E-11	1.45E-08	2.25E-09	1.77E-09	2.25E-09
Pu-238	7.22E-11	5.22E-08	1.69E-10	1.31E-10	1.69E-10
Pu-239	2.00E-10	5.51E-08	1.74E-10	1.35E-10	1.74E-10
Pu-240	6.98E-11	5.55E-08	1.74E-10	1.35E-10	1.74E-10
Pu-241+D	1.33E-11	8.66E-10	2.28E-12	1.77E-12	2.28E-12
Pu-242	6.25E-11	5.25E-08	1.65E-10	1.28E-10	1.65E-10
Pu-244	2.70E-08	2.70E-08	3.20E-10	3.20E-10	3.20E-10
Ra-226+D	8.49E-06	2.82E-08	5.14E-10	3.85E-10	5.14E-10
Ra-228+D	4.53E-06	4.37E-08	1.43E-09	1.04E-09	1.43E-09
Ru-106+D	9.66E-07	2.23E-10	6.11E-11	4.22E-11	6.11E-11
S-35	8.77E-12	6.55E-12	3.70E-12	2.72E-12	3.70E-12
Sb-124	8.89E-06	3.20E-11	1.85E-11	1.29E-11	1.85E-11
Sb-125	1.81E-06	4.00E-11	6.14E-12	4.37E-12	6.14E-12
Sb-126	1.28E-05	1.29E-11	1.59E-11	1.11E-11	1.59E-11
Sb-126m	6.94E-06	3.32E-14	9.21E-14	6.66E-14	9.21E-14
Sc-46	9.63E-06	2.47E-11	8.88E-12	6.22E-12	8.88E-12
Se-75	1.45E-06	5.00E-12	1.08E-11	8.14E-12	1.08E-11
Se-79	1.10E-11	1.99E-11	9.69E-12	7.29E-12	9.69E-12
Sm-147	0.00E+00	1.26E-08	4.77E-11	3.74E-11	4.77E-11
Sm-151	3.60E-13	9.18E-12	8.07E-13	5.55E-13	8.07E-13
Sm-153	1.06E-07	3.19E-12	7.10E-12	4.85E-12	7.10E-12
Sn-113	2.02E-08	1.45E-11	6.33E-12	4.33E-12	6.33E-12
Sn-126	8.83E-06	4.13E-11	3.92E-11	2.72E-11	3.92E-11
Sr-85	2.20E-06	3.23E-12	3.11E-12	2.26E-12	3.11E-12
Sr-89	7.19E-09	3.02E-11	1.84E-11	1.28E-11	1.84E-11
Sr-90+D	1.96E-08	4.34E-10	9.55E-11	7.40E-11	9.55E-11
Ta-182	6.04E-06	3.74E-11	1.15E-11	7.96E-12	1.15E-11
Tc-99	8.14E-11	3.81E-11	4.00E-12	2.75E-12	4.00E-12
Tc-99m	3.93E-07	6.07E-14	1.14E-13	7.96E-14	1.14E-13
Te-125m	6.98E-09	1.45E-11	4.70E-12	3.33E-12	4.70E-12
Th-228+D	7.79E-06	1.44E-07	4.22E-10	3.00E-10	4.22E-10
Th-229+D	1.17E-06	2.30E-07	7.14E-10	5.29E-10	7.14E-10
Th-230	8.18E-10	3.40E-08	1.19E-10	9.10E-11	1.19E-10
Th-232	3.42E-10	4.33E-08	1.33E-10	1.01E-10	1.33E-10

TABLE 2-3 (Cont.)

Radionuclide	External (Risk/yr)/(pCi/g)	Inhalation (Risk/pCi)	Ingestion–Food (Risk/pCi)	Ingestion–Water (Risk/pCi)	Ingestion–Soil (Risk/pCi)
Tl-201	1.88E-07	6.85E-13	5.00E-13	3.61E-13	5.00E-13
Tl-202	1.83E-06	1.34E-12	2.01E-12	1.49E-12	2.01E-12
Tl-204	2.76E-09	6.07E-11	8.25E-12	5.85E-12	8.25E-12
U-232	5.98E-10	9.25E-08	3.85E-10	2.92E-10	3.85E-10
U-233	9.82E-10	2.83E-08	9.69E-11	7.18E-11	9.69E-11
U-234	2.52E-10	2.78E-08	9.55E-11	7.07E-11	9.55E-11
U-235+D	5.43E-07	2.51E-08	9.73E-11	7.18E-11	9.73E-11
U-236	1.25E-10	2.58E-08	9.03E-11	6.70E-11	9.03E-11
U-238+D	8.66E-08	2.37E-08	1.20E-10	8.73E-11	1.20E-10
Xe-131m	1.41E-08	0	0	0	0
Zn-65	2.81E-06	7.59E-12	1.54E-11	1.17E-11	1.54E-11
Zr-93	0.00E+00	1.52E-11	1.44E-12	1.11E-12	1.44E-12
Zr-95	3.40E-06	2.11E-11	6.59E-12	4.59E-12	6.59E-12

[a] Values for slope factors were taken from FGR-13 (Eckerman et al. 1999) except for Cf-252, Cm-248, and Pu-244. These radionuclide values were obtained from Yu et al. (2001).

TABLE 2-4 Default Distribution Coefficients Used in RESRAD-OFFSITE Code Version 2

Radionuclide	Distribution Coefficient[a] (cm^3/g)	Radionuclide	Distribution Coefficient[a] (cm^a/g)
Ac-227	2.00E+01	La-138	5.00E+00
Ag-108m	0	Mn-54	2.00E+02
Ag-110m	0	Na-22	1.00E+01
Al-26	0	Nb-93m	0
Am-241	2.00E+01	Nb-94	0
Am-243	2.00E+01	Nb-95	0
Au-195	0	Ni-59	1.00E+03
Ba-133	5.00E+01	Ni-63	1.00E+03
Be-7	9.29E+02	Np-237	2.57E+02
Bi-207	0	Pa-231	5.00E+01
C-14	0	Pb-210	1.00E+02
Ca-41	5.00E+01	Pm-147	8.25E+02
Ca-45	5.00E+01	Po-210	1.00E+01
Cd-109	0	Pu-238	2.00E+03
Ce-141	1.00E+03	Pu-239	2.00E+03
Ce-144	1.00E+03	Pu-240	2.00E+03
Cf-252[a]	1.378E+03	Pu-241	2.00E+03
Cl-36	1.000E-01	Pu-242	2.00E+03
Cm-243[a]	1.378E+03	Pu-244	2.00E+03
Cm-244[a]	1.378E+03	Ra-226	7.00E+01
Cm-245[a]	1.378E+03	Ra-228	7.00E+01
Cm-246[a]	1.378E+03	Ru-106	0
Cm-247[a]	1.378E+03	S-35	0
Cm-248[a]	1.378E+03	Sb-124	0
Co-57	1.00E+03	Sb-125	0
Co-60	1.00E+03	Sc-46	0
Cr-51	1.03E+02	Se-75	0
Cs-134	1.00E+03	Se-79	0
Cs-135	1.00E+03	Sm-147[a]	8.25E+02
Cs-137	1.00E+03	Sm-151[a]	8.25E+02
Eu-152[a]	8.25E+02	Sm-153[a]	8.25E+02
Eu-154[a]	8.25E+02	Sn-113	0
Eu-155[a]	8.25E+02	Sn-126	0
Fe-55	1.00E+03	Sr-85	3.00E+01
Fe-59	1.00E+03	Sr-89	3.00E+01
Gd-152[a]	8.25E+02	Sr-90	3.00E+01
Gd-153[a]	8.25E+02	Ta-182	0
Ge-68	0	Tc-99[a]	0
H-3	0	Tc-99m[a]	0
I-125	1.00E-01	Te-125m[a]	0
I-129	1.00E-01	Th-228	6.00E+04
I-131	1.00E-01	Th-229	6.00E+04
In-111	1.58E+02	Th-230	6.00E+04
Ir-192	0	Th-232	6.00E+04

TABLE 2-4 (Cont.)

Radionuclide	Distribution Coefficient[a] (cm^3/g)	Radionuclide	Distribution Coefficient[a] (cm^a/g)
K-40	5.50E+00	Tl-201	0
Tl-202	0	U-236	5.00E+01
Tl-204	0	U-238	5.00E+01
U-232	5.00E+01	Xe-131m	0
U-233	5.00E+01	Zn-65	0
U-234	5.00E+01	Zr-93[a]	1.378E+03
U-235	5.00E+01	Zr-95[a]	1.378E+03

[a] RESRAD-OFFSITE code Version 2 does not have the root uptake transfer factor correlation as an option for estimating the distribution, as such −1 is not used in RESRAD-OFFSITE code Version 2. The values that RESRAD computes using the correlation are the default inputs for RESRAD-OFFSITE code Version 2.

Sources: Baes and Sharp (1983); Nuclear Safety Associates (1980); Isherwood (1981); NRC (1980); Gee et al. (1980); Staley et al. (1979); Yu et al. (2001).

TABLE 2-5 Transfer Factors for Plants, Meat, and Milk in RESRAD-OFFSITE Code Version 2

Element	Plant	Meat (pCi/kg)/(pCi/d)	Milk (pCi/L)/(pCi/d)
Ac	2.50E-03	2.00E-05	2.00E-05
Ag	1.50E-01	3.00E-03	2.50E-02
Al	4.00E-03	5.00E-04	2.00E-04
Am	1.00E-03	5.00E-05	2.00E-06
Au	1.00E-01	5.00E-03	1.00E-05
Ba	5.00E-03	2.00E-04	5.00E-04
Be	4.00E-03	1.00E-03	2.00E-06
Bi	1.00E-01	2.00E-03	5.00E-04
C	5.5	3.10E-02	1.20E-02
Ca	5.00E-01	1.60E-03	3.00E-03
Cd	3.00E-01	4.00E-04	1.00E-03
Ce	2.00E-03	2.00E-05	3.00E-05
Cf	1.00E-03	6.00E-05	7.50E-07
Cl	20	6.00E-02	2.00E-02
Cm	1.00E-03	2.00E-05	2.00E-06
Co	8.00E-02	2.00E-02	2.00E-03
Cr	2.50E-04	9.00E-03	2.00E-03
Cs	4.00E-02	3.00E-02	8.00E-03
Eu	2.50E-03	2.00E-03	2.00E-05
Fe	1.00E-03	2.00E-02	3.00E-04
Gd	2.50E-03	2.00E-03	2.00E-05
Ge	4.00E-01	2.00E-01	1.00E-02
H	4.8	1.20E-02	1.00E-02
I	2.00E-02	7.00E-03	1.00E-02
In	3.00E-03	4.00E-03	2.00E-04
Ir	3.00E-02	2.00E-03	2.00E-06
K	3.00E-01	2.00E-02	7.00E-03
La	2.50E-03	2.00E-03	2.00E-05
Mn	3.00E-01	5.00E-04	3.00E-04
Na	5.00E-02	8.00E-02	4.00E-02
Nb	1.00E-02	3.00E-07	2.00E-06
Ni	5.00E-02	5.00E-03	2.00E-02
Np	2.00E-02	1.00E-03	5.00E-06
Pa	1.00E-02	5.00E-03	5.00E-06
Pb	1.00E-02	8.00E-04	3.00E-04
Pm	2.50E-03	2.00E-03	2.00E-05
Po	1.00E-03	5.00E-03	3.40E-04
Pu	1.00E-03	1.00E-04	1.00E-06
Ra	4.00E-02	1.00E-03	1.00E-03
Ru	3.00E-02	2.00E-03	3.30E-06
S	6.00E-01	2.00E-01	2.00E-02
Sb	1.00E-02	1.00E-03	1.00E-04
Sc	2.00E-03	1.50E-02	5.00E-06
Se	1.00E-01	1.00E-01	1.00E-02
Sm	2.50E-03	2.00E-03	2.00E-05

TABLE 2-5 (Cont.)

Element	Plant	Meat (pCi/kg)/(pCi/d)	Milk (pCi/L)/(pCi/d)
Sn	2.50E-03	1.00E-02	1.00E-03
Sr	3.00E-01	8.00E-03	2.00E-03
Ta	2.00E-02	5.00E-06	5.00E-06
Tc	5	1.00E-04	1.00E-03
Te	6.00E-01	7.00E-03	5.00E-04
Th	1.00E-03	1.00E-04	5.00E-06
Tl	2.00E-01	2.00E-2	3.00E-03
U	2.50E-03	3.40E-04	6.00E-04
Xe	0	0	0
Zn	4.00E-01	1.00E-01	1.00E-02
Zr	1.00E-03	1.00E-06	6.00E-07

Source: Yu et al. (2001, Tables D.3 and D.4).

TABLE 2-6 Bioaccumulation Factors for Fish and Crustacea and Mollusks in RESRAD-OFFSITE Code Version 2

Element	Fish (pCi/kg)/(pCi/L)	Crustacea and Mollusks (pCi/kg)/(pCi/L)	Element	Fish (pCi/kg)/(pCi/L)	Crustacea and Mollusks (pCi/kg)/(pCi/L)
Ac	1.50E+01	1.00E+03	Nb	3.00E+02	1.00E+02
Ag	5	7.70E+02	Ni	1.00E+02	1.00E+02
Al	5.00E+02	1.00E+03	Np	3.00E+01	4.00E+02
Am	3.00E+01	1.00E+03	Pa	1.00E+01	1.10E+02
Au	3.50E+01	1.00E+03	Pb	3.00E+02	1.00E+02
Ba	4	2.00E+02	Pm	3.00E+01	1.00E+03
Be	1.00E+02	1.00E+01	Po	1.00E+02	2.00E+04
Bi	1.50E+01	1.00E+01	Pu	3.00E+01	1.00E+02
C	5.00E+04	9.10E+03	Ra	5.00E+01	2.50E+02
Ca	1.00E+03	3.30E+02	Ru	1.00E+01	3.00E+02
Cd	2.00E+02	2.00E+03	S	1.00E+03	2.40E+02
Ce	3.00E+01	1.00E+03	Sb	1.00E+02	1.00E+01
Cf	2.50E+01	1.00E+03	Sc	1.00E+02	1.00E+03
Cl	1.00E+03	1.90E+02	Se	2.00E+02	2.00E+02
Cm	3.00E+01	1.00E+03	Sm	2.50E+01	1.00E+03
Co	3.00E+02	2.00E+02	Sn	3.00E+03	1.00E+03
Cr	2.00E+02	2.00E+03	Sr	6.00E+01	1.00E+02
Cs	2.00E+03	1.00E+02	Ta	1.00E+02	3.00E+01
Eu	5.00E+01	1.00E+03	Tc	2.00E+01	5
Fe	2.00E+02	3.20E+03	Te	4.00E+02	7.50E+01
Gd	2.50E+01	1.00E+03	Th	1.00E+02	5.00E+02
Ge	4.00E+03	2.00E+04	Tl	1.00E+04	1.50E+04
H	1	1	U	1.00E+01	6.00E+01
I	4.00E+01	5	Xe	0	0
In	1.00E+04	1.50E+04	Zn	1.00E+03	1.00E+04
Ir	1.00E+01	2.00E+02	Zr	3.00E+02	6.7
K	1.00E+03	2.00E+02			
La	3.00E+01	1.00E+03			
Mn	4.00E+02	9.00E+04			
Na	2.00E+01	2.00E+02			

Source: Yu et al. (2001, Table D.5).

3 REFERENCES

Baes, C.F., and R.D. Sharp, 1983, "A Proposal for Estimation of Soil Leaching and Leaching Constants for Use in Assessment Models," *Journal of Environmental Quality* 12(1):17-28.

Eckerman, K.F., and J.C. Ryman, 1993, *External Exposure to Radionuclides in Air, Water, and Soil, Exposure to Dose Coefficients for General Application, Based on the 1987 Federal Radiation Protection Guidance*, EPA 402-R-93-081, Federal Guidance Report No. 12, prepared by Oak Ridge National Laboratory, Oak Ridge, Tenn., for U.S. Environmental Protection Agency, Office of Radiation and Indoor Air, Washington, D.C.

Eckerman, K.F., et al., 1988, *Limiting Values of Radionuclide Intake and Air Concentration and Dose Conversion Factors for Inhalation, Submersion, and Ingestion,* EPA-520/1-88-020, Federal Guidance Report No. 11, prepared by Oak Ridge National Laboratory, Oak Ridge, Tenn., for U.S. Environmental Protection Agency, Office of Radiation and Indoor Air, Washington, D.C.

Eckerman, K.F., et al., 1999, *Cancer Risk Coefficients for Environmental Exposure to Radionuclides,* EPA 402-R-99-001, Federal Guidance Report No. 13, prepared by Oak Ridge National Laboratory, Oak Ridge, Tenn., for U.S. Environmental Protection Agency, Office of Radiation and Indoor Air, Washington, D.C.

EPA: See U.S. Environmental Protection Agency.

Gee, G.W., et al., 1980, *Interaction of Uranium Mill Tailings Leachate with Soils and Clay Liners*, NUREG/CR-1494, PNL-3381, prepared by Pacific Northwest Laboratory, Richland, Wash., for U.S. Nuclear Regulatory Commission, Office of Nuclear Regulatory Research, Washington, D.C.

ICRP: See International Commission on Radiological Protection.

Isherwood, D., 1981, *Geoscience Data Base Handbook for Modeling a Nuclear Waste Repository*, NUREG/CR-0912, Vols. 1 and 2, U.S. Nuclear Regulatory Commission, Washington, D.C.

International Commission on Radiological Protection, 1985, *Principles of Monitoring for the Radiation Protection of the Population,* ICRP No. 43, New York, N.Y.

NRC: See U.S. Nuclear Regulatory Commission.

Nuclear Safety Associates, Inc., 1980, *Comparison of Alternatives for Long-Term Management of High-Level Radioactive Waste at the Western New York Nuclear Service Center*, prepared by Nuclear Safety Associates, Inc., Bethesda, Md., for Argonne National Laboratory, Argonne, Ill.

Staley, G.B., et al., 1979, "Radionuclide Migration from Low-Level Waste: A Generic Overview," in M.W. Carter et al. (eds.), *Management of Low-Level Radioactive Waste*, Pergamon Press, New York, N.Y., pp. 1041-1072.

U.S. Environmental Protection Agency, 1995, *Health Effects Summary Tables (HEAST)*, *FY-1995 Supplement*, EPA/540/R-95/142, Washington, D.C., Nov.

U.S. Environmental Protection Agency, 2001, *Update: Radionuclide Toxicity*, Washington, D.C., April 16.

U.S. Nuclear Regulatory Commission, 1980, *Final Generic Environmental Impact Statement on Uranium Milling*, NUREG-0706, Vols. 1-3, Office of Nuclear Material Safety and Safeguards, Washington, D.C.

U.S. Nuclear Regulatory Commission, 2000, *Development of Probabilistic RESRAD 6.0 and RESRAD-BUILD 3.0 Computer Codes*, NUREG/CR-6697, ANL/EAD/TM-98, Office of Nuclear Regulatory Research, Washington, D.C.

Yu, C., et al., 2001, *User's Manual for RESRAD, Version 6*, ANL/EAD-4, Argonne National Laboratory, Argonne, Ill., July.

ATTACHMENT B:

STATISTICAL DISTRIBUTIONS USED IN RESRAD-OFFSITE AND THEIR DEFINING PARAMETERS

ATTACHMENT B Statistical Distributions Used in RESRAD-OFFSITE and Their Defining Parameters

Statistical Distribution	Defining Parameters	Description, Conditions, and Probability Density/Mass Function[a]
Normal		
Normal	Mean (μ) Standard deviation (σ)	There are two ways of specifying the "complete" normal distribution. The sampling code actually cuts off the lower and upper 0.1% tails and samples between $V_{0.001}$ and $V_{0.999}$ in the latter case (Normal B). The relationship between the two sets of defining parameters follows: $\mu = (V_{0.999} + V_{0.001})/2$ and $\sigma = (V_{0.999} - V_{0.001})/2/3.09$.
Normal-B	Value of the 0.1% ($V_{0.001}$) Value of the 99.9% ($V_{0.999}$)	Conditions on inputs: $\sigma > 0$, $V_{0.001} < V_{0.999}$. Probability density function (pdf): $f(x) = \frac{1}{\sigma\sqrt{2\pi}} \exp\left[-\frac{1}{2}\left(\frac{x-\mu}{\sigma}\right)^2\right]$ for Normal and $f(x) = \frac{\frac{1}{\sigma\sqrt{2\pi}} \exp\left[-\frac{1}{2}\left(\frac{x-\mu}{\sigma}\right)^2\right]}{0.998}$ for Normal-B.

ATTACHMENT B (Cont.)

Statistical Distribution	Defining Parameters	Description, Conditions, and Probability Density/Mass Function[a]
Bounded Normal	Mean (μ) Standard deviation (σ) Minimum value (min) Maximum value (max)	Both distributions specify a normal distribution with the tails cut off. The lower cutoff is the minimum value or the lower quantile, and the upper cutoff is the maximum value or the upper quantile, which are related by min = V_{Lq} and max = V_{Uq}. Conditions on inputs: min < max, $0 < Lq < Uq < 1$.
Truncated Normal	Mean (μ) Standard deviation (σ) Lower quantile (Lq) Upper quantile (Uq)	pdf : $f(x) = \dfrac{\dfrac{1}{\sigma\sqrt{2\pi}}\, exp\left[-\dfrac{1}{2}\left(\dfrac{x-\mu}{\sigma}\right)^2\right]}{Uq - Lq}$.

ATTACHMENT B (Cont.)

Statistical Distribution	Defining Parameters	Description, Conditions, and Probability Density/Mass Function[a]
Lognormal		
Lognormal	Mean (M) Error factor (EF)	There are three ways of specifying the "complete" lognormal distribution. The sampling code actually cuts off the lower and upper 0.1% tails and samples between $V_{0.001}$ and $V_{0.999}$ in the second case. The relationship between the three sets of defining parameters follows: $\mu = (lnV_{0.999} + lnV_{0.001})/2 = lnM - \sigma^2/2$ and $\sigma = (lnV_{0.999} - lnV_{0.001})/2/3.09 = lnEF/1.645$. The error factor (EF) is the ratio between the 95th percentile value and the median (50th percentile) value. It is also the ratio between the median value and the 5th percentile value.
Lognormal-B	Value of the 0.1% ($V_{0.001}$) Value of the 99.9% ($V_{0.999}$)	
Lognormal-N	Mean (μ) of the underlying normal distribution Standard deviation (σ) of the underlying normal distribution	Conditions on inputs: $M > 0$, $EF > 1$, $\sigma > 0$, $V_{0.001} < V_{0.999}$. pdf: $f(x) = \frac{1}{x\sigma\sqrt{2\pi}} \exp\left[-\frac{1}{2}\left(\frac{\ln x - \mu}{\sigma}\right)^2\right]$ for Lognormal and Lognormal-N $f(x) = \frac{1}{x\sigma\sqrt{2\pi}} \exp\left[-\frac{1}{2}\left(\frac{\ln x - \mu}{\sigma}\right)^2\right] \Big/ 0.998$ for Lognormal-B.

ATTACHMENT B (Cont.)

Statistical Distribution	Defining Parameters	Description, Conditions, and Probability Density/Mass Function[a]
Bounded Lognormal	Mean (M) Error factor (EF) Minimum value (min) Maximum value (max)	These four distributions specify a lognormal distribution with the tails cut off. The lower cutoff is the minimum value or the lower quantile, and the upper cutoff is the maximum value or the upper quantile, which are related by min = V_{Lq} and max = V_{Uq} .
Bounded Lognormal-N	Mean (μ) of the underlying normal distribution Standard deviation (σ) of the underlying normal distribution Minimum value (min) Maximum value (max)	Conditions on inputs: min < max, $0 < Lq < Uq < 1$. pdf: $f(x) = \frac{\frac{1}{x\sigma\sqrt{2\pi}} exp\left[-\frac{1}{2}\left(\frac{ln\, x - \mu}{\sigma}\right)^2\right]}{Uq - Lq}$.
Truncated Lognormal	Mean (M) Error factor (EF) Lower quantile (Lq) Upper quantile (Uq)	
Truncated Lognormal-N	Mean (μ) of the underlying normal distribution Standard deviation (σ) of the underlying normal distribution Lower quantile (Lq) Upper quantile (Uq)	
Uniform	Minimum value (min) Maximum value (max)	Conditions on inputs: min < max pdf: $f(x) = \frac{1}{max - min}$.

ATTACHMENT B (Cont.)

Statistical Distribution	Defining Parameters	Description, Conditions, and Probability Density/Mass Function[a]
Loguniform	Minimum value (min) Maximum value (max)	Conditions on inputs: $0 < \min < \max$. pdf: $f(x) = \frac{1}{x(\ln max - \ln min)}$.
Uniform*	Number of subintervals (N_{int}) Limits of subintervals (L_i) $i = 0$ to N_{int} Number of observations in subinterval (O_{int})	This is a collection of adjacent uniform distributions. Conditions on inputs: $N_{int} > 1, L_{i-1} < L_i, O_i > 0, 0, N_{obs} = \sum_{i=1}^{N_{int}} O_i$ pdf: $f_i(x) = \frac{1}{L_i - L_{i-1}} \frac{O_i}{N_{obs}}$.
Loguniform*	Number of subintervals (N_{int}) Limits of subintervals (L_i) $i = 0$ to N_{int} Number of observations in subinterval (O_{int})	This is a collection of adjacent loguniform distributions. Conditions on inputs: $N_{int} > 1, 0 < L_o, L_{i-1} < L_i, i > 0, N_{obs} = \sum_{i=1}^{N_{int}} O_i$. pdf: $f_i(x) = \frac{1}{x(\ln L_i - \ln L_{i-1})} \frac{O_i}{N_{obs}}$.

ATTACHMENT B (Cont.)

Statistical Distribution	Defining Parameters	Description, Conditions, and Probability Density/Mass Function[a]
Continuous Linear	Number of points (N_{pts}) Values of points (V_i) i = 1 to N_{pts} cdf of points (cdf_i) i = 1 to N_{pts}	The cumulative distribution function (cdf) of a number of points is specified, and the cdf of intermediate points is obtained by linear interpolation. Conditions on inputs: $N_{pts} > 2$, $V_i < V_{i+1}$, $cdf_1 = 0$, $cdf_{Npts} = 1$, $cdf_{i-1} < cdf_i$. pdf: $f_i(x) = \frac{cdf_i - cdf_{i-1}}{V_i - V_{i-1}}$.
Continuous Frequency	Number of points (N_{pts}) Values of points (V_i) i = 1 to N_{pts} Frequency of points (f_i) i = 1 to N_{pts}	The cdf of a number of points is first computed from the user-specified frequencies. Then the cdf of intermediate points is obtained by linear interpolation. The cdf is computed from the frequencies as follows: $cdf_1 = 0$. $cdf_i = cdf_{i-1} + \frac{f_{i-1} + f_i}{2} \div \sum_{i=2}^{N_{pts}} \frac{f_{i-1} + f_i}{2}$. Conditions on inputs: $N_{pts} > 2$, $V_i < V_{i+1}$, $f_i > 0$. pdf: $f_i(x) = \frac{cdf_i - cdf_{i-1}}{V_i - V_{i-1}}$

ATTACHMENT B (Cont.)

Statistical Distribution	Defining Parameters	Description, Conditions, and Probability Density/Mass Function[a]
Continuous Logarithmic	Number of points (N_{pts}) Values of points (V_i) i = 1 to N_{pts} cdf of points (cdf_i) i = 1 to N_{pts}	The cdf of a number of points is specified, and the cdf of intermediate points is obtained by logarithmic interpolation. Conditions on inputs: $N_{pts} > 2$, $0 < V_1$, $V_i < V_{i+1}$, $cdf_1 = 0$, $cdf_{Npts} = 1$, $cdf_{i-1} < cdf_i$. pdf: $f_i(x) = \frac{cdf_i - cdf_{i-1}}{x(\ln V_i - \ln V_{i-1})}$
Triangular	Minimum (min) Mode or most likely (mod) Maximum (max)	Conditions on inputs: min $\leq$ mod $\leq$ max, min < max. pdf: $f(x) = \frac{2}{max - min}\frac{x - min}{mod - min}$ when $x \leq mod$. $f(x) = \frac{2}{max - min}\frac{max - x}{max - mod}$ when $x \geq mod$.

ATTACHMENT B (Cont.)

Statistical Distribution	Defining Parameters	Description, Conditions, and Probability Density/Mass Function[a]
Logtriangular	Minimum (min) Mode or most likely (mod) Maximum (max)	Conditions on inputs: $0 < \min \leq \text{mod} \leq \max$, $\min < \max$. pdf: $f(x) = \frac{2}{\ln max - \ln min} \frac{1}{x} \frac{\ln x - \ln min}{\ln mod - \ln min}$ *when* $x \leq mod.$ $f(x) = \frac{2}{\ln max - \ln min} \frac{1}{x} \frac{\ln max - \ln x}{\ln max - \ln mod}$ *when* $x \geq mod.$
Pareto	Alpha (α) Beta (β)	Make sure that the values entered for α and β correspond to the definition used for the pdf below. Conditions on inputs: $\alpha < 2$, $\beta > 0$. pdf: $f(x) = \frac{\alpha \beta^{\alpha}}{x^{\alpha+1}}$ *when* $x \geq \beta$.

ATTACHMENT B (Cont.)

Statistical Distribution	Defining Parameters	Description, Conditions, and Probability Density/Mass Function[a]
Exponential		
Exponential	Lambda (λ)	Conditions on inputs: λ < 0. pdf: $f(x) = \lambda \exp(-\lambda x)$.
Bounded Exponential	Lambda (λ) Minimum value (min) Maximum value (max)	Both distributions specify an exponential distribution with the two ends cut off. The lower cutoff is the minimum value or the lower quantile, and the upper cutoff is the maximum value or the upper quantile, which are related by $1 - \exp(-\lambda \min) = V_{Lq}$ and $1-\exp(-\lambda \max) = V_{uq}$.
Truncated Exponential	Lambda (λ) Lower quantile (*Lq*) Upper quantile (*Uq*)	Conditions on inputs: $0 < \min < \max$, $0 < Lq < Uq < 1$. pdf: $f(x) = \frac{\lambda \exp(-\lambda x)}{Uq - Lq}$.

ATTACHMENT B (Cont.)

Statistical Distribution	Defining Parameters	Description, Conditions, and Probability Density/Mass Function[a]
Weibull	Alpha (α) Beta (β)	Make sure that the values entered for α and β correspond to the definition used for the pdf below. Conditions on inputs: $\alpha > 0$, $\beta > 0$. pdf: $f(x)\frac{\alpha}{\beta}\left(\frac{x}{\beta}\right)^{\alpha-1} exp\left(-\frac{x}{\beta}\right)^{\alpha}$.
Inverse Gaussian	Mean (μ) Lambda (λ)	Conditions on inputs: $\mu > 0$, $\lambda > 0$. pdf: $f(x) = \sqrt{\frac{\lambda}{2\pi x^3}}\, exp\left[-\frac{\lambda}{2\mu^2 x}(x-\mu)^2\right]$.

ATTACHMENT B (Cont.)

Statistical Distribution	Defining Parameters	Description, Conditions, and Probability Density/Mass Function[a]
Gamma	Alpha (α) Beta (β)	Make sure that the values entered for α and β correspond to the definition used for the pdf below. Conditions on inputs: $\alpha > 0$, $\beta > 0$. pdf: $f(x) = \frac{\beta(\beta x)^{\alpha-1} exp(-\beta x)}{\Gamma(\alpha)}$.
Beta	P Q Minimum value (min) Maximum value (max)	Conditions on inputs: min < max, $0.001 \leq P \leq 10^7$, $0.001 \leq Q \leq 10^7$. pdf: $f(x) = \frac{(P+Q-1)!(x-\min)^{P-1}(\max-x)^{Q-1}}{(P-1)!(Q-1)!(\max-\min)^{P+Q-1}}$.

ATTACHMENT B (Cont.)

Statistical Distribution	Defining Parameters	Description, Conditions, and Probability Density/Mass Function[a]
Poisson	Mean (λ)	Conditions on inputs: $\lambda > 0$. Probability mass function (pmf)[a]: $p(n) + \frac{\lambda^n \exp(-\lambda)}{n!}$, where $n = 0, 1, 2, \ldots \infty$.
Geometric	Probability of success (p)	Conditions on inputs: $0 < p < 1$. pmf: $p(n) = (1-p)^{n-1} p$, where $n = 0, 1, 2, \ldots \infty$.
Binomial	Probability of success (p) Number of trials (N)	Conditions on inputs: $0 < p < 1$, $N > 1$. pmf: $p(n) = \frac{N!\, p^n (1-p)^{N-n}}{n!(N-n)!}$, where $n = 0, 1, 2, \ldots N$.

ATTACHMENT B (Cont.)

Statistical Distribution	Defining Parameters	Description, Conditions, and Probability Density/Mass Function[a]
Negative Binomial	Probability of success (p) Number of successes sought (N)	Conditions on inputs: $0 < p < 1$, $N > 1$. pmf: $p(n) = \frac{(n-1)!\, p^N (1-p)^{n-N}}{(N-1)!(n-N)!}$, where $n = N, N+1, \ldots \infty$.

ATTACHMENT B (Cont.)

Statistical Distribution	Defining Parameters	Description, Conditions, and Probability Density/Mass Function[a]
Hypergeometric	Size of population (N_{pop}) Sample size (N_{samp}) Successes in population (N_{succ})	The second input has to be the smaller of N_{samp}, N_{succ}. The third input is the larger of the two. Conditions on inputs: $N_{pop} > N_{samp} > 0$, $N_{pop} > N_{succ} > 0$. pmf: $$p(n) = \frac{\binom{N_{succ}}{n}\binom{N_{pop} - N_{succ}}{N_{samp} - n}}{\binom{N_{pop}}{N_{samp}}},$$ where $$\binom{M}{m} = \frac{M!}{m!(M-m)!}$$ and $n = \max(0, N_{succ} + N_{samp} - N_{pop}), \ldots \min(N_{succ}, N_{samp})$
Discrete Cumulative	Number of points (N_{pts}) Values of points (V_i) $i = 1$ to N_{pts} cdf of points (cdf_i) $i = 1$ to N_{pts}	Conditions on inputs: $N_{pts} > 2$, $V_i < V_{i+1}$, $cdf_1 > 0$, $cdf_{Npts} = 1$, $cdf_{i-1} < cdf_i$. pmf: $p(n) = cdf_n - cdf_{n-1}$.

ATTACHMENT B (Cont.)

Statistical Distribution	Defining Parameters	Description, Conditions, and Probability Density/Mass Function[a]
Discrete Histogram	Number of points (N_{pts}) Values of points (V_i) i = 1 to N_{pts} Frequency of points (f_i) i = 1 to N_{pts}	$cdf_i = f_i \; / \sum_{i=1}^{N_{pts}} f_i$ Conditions on inputs: $N_{pts} > 2$, $V_i < V_{i+1}, f_i > 0$. pmf: $p(n) = cdf_n - cdf_{n-1}$.

[a] Probability density function (pdf) is for continuous distributions; probability mass function (pmf) is for discrete distributions.

APPENDIX C:

REDUCING RUN TIME

REDUCING RUN TIME FOR THE RESRAD-OFFSITE PROBABILISTIC ANALYSIS

Prepared by

E. Gnanapragasam and C. Yu

Environmental Science Division
Argonne National Laboratory

CONTENTS

1 INTRODUCTION

1.1 PURPOSE AND SCOPE

This report describes the processes and code options that affect the execution time when performing probabilistic analysis using the RESRAD-OFFSITE code. The information provided will help the user to select the conditions and code options that will produce all the desired outputs in the shortest time. The execution time depends on the number of calculations to be performed and on the amount of information that is to be written to various output files. It also depends on the speed of the processor and on the amount of memory available for temporary storage of the calculation results that are performed by the code.

The probabilistic sampling code used for RESRAD-OFFSITE is very similar to that used for the RESRAD (onsite) and RESRAD-BUILD codes. Likewise, the codes used to perform the output-input linear regression analysis are very similar. Therefore, the discussion on reducing run time for RESRAD-OFFSITE is generally applicable to the RESRAD (onsite) and RESRAD-BUILD codes. However, the structures of the three codes are quite different. Thus, the information provided in this report for RESRAD-OFFSITE may not always be applicable to the other two codes. RESRAD-OFFSITE was designed to take into account the run time issue and allows users to control some parameters to reduce run time. These features are described in this report.

1.2 IMPLEMENTATION OF PROBABILISTIC ANALYSIS IN RESRAD-OFFSITE

RESRAD-OFFSITE is a computer code that evaluates the radiological dose and excess cancer risk to an individual who is exposed while situated within or outside the area of initial (primary) contamination. RESRAD-OFFSITE has a large number of input parameters that define the situation being modeled. In a deterministic analysis, a single value is specified for each parameter, resulting in a single set of input parameters. The model computations are performed once using this single set of inputs to produce a single set of deterministic outputs. A set of outputs consists of radiological dose and excess cancer risk from each nuclide via each exposure pathway at each graphical time point and the concentration of each nuclide in each medium at each graphical time point.

Probabilistic distributions are specified for the input parameters in a probabilistic analysis. The number of input sets to be developed from these distributions and the manner in which they are to be developed are also specified. The sampling program produces the specified number of sets of inputs for the RESRAD-OFFSITE code. The model computations are performed by using each of these sets of inputs, in turn, to produce an equal number of sets of outputs. While the code will compute all the outputs described previously for each set of inputs, the user can specify which of these outputs are to be saved for later use. The computational code of RESRAD-OFFSITE provides feedback on its progress; the RESRAD-OFFSITE interface uses this feedback to provide the user with an estimate of the execution time. The probabilistic results can be viewed graphically, and a linear regression analysis can be performed to identify the significant (sensitive) probabilistic inputs.

2 FACTORS AFFECTING THE EXECUTION TIME OF RESRAD-OFFSITE

Probabilistic analysis in RESRAD-OFFSITE involves the following sequence of steps, which contribute to or influence the total execution time:

- Specifying the probabilistic inputs and the desired probabilistic outputs in the interface,
- Executing the sampling code (Latin Hypercube Sampling [LHS]) to produce the specified number of sets of input parameters,
- Executing the computational code (RESRAD-OFFSITE) by using each set of input parameters while,
  - Saving in memory the temporary output (dose and risk) that is needed to produce some of the information for the probabilistic report,
  - Writing to files the output needed for regression or graphical analysis and for the probabilistic report,
  - Writing to file the feedback information that indicates the progress of computation and gives an estimate of the time to complete the probabilistic computations,
- Displaying graphics of the probabilistic analysis, and
- Performing regression analysis between the desired probabilistic output and the probabilistic inputs.

While the first step, specification of inputs and desired outputs is an interactive procedure and is not part of the execution, it is included in the list because the specifications affect the time spent executing the subsequent steps. The execution time of the sampling code (LHS) is very small in relation to the execution time of the RESRAD-OFFSITE computational code. The sampling code is therefore not considered any further in this report. The influence of each of the other steps on the execution time is discussed in the following sections.

2.1 RESRAD-OFFSITE COMPUTATIONAL CODE

The execution time of the RESRAD-OFFSITE computational code consists of three components: (1) time spent reading inputs, (2) time spent performing calculations, and (3) time spent writing outputs and progress of computation messages. Of these three, the amount of time spent reading the input files is much smaller than the amount of time spent on the other two. The time spent writing the progress of computation messages and the time spent writing the probabilistic output to files can be a significant part of the execution time.

2.1.1 Progress of Computation Message

The execution time of even a single deterministic run of the RESRAD-OFFSITE computational code can be significant, depending on the situation being modeled (Section 2.1.3 of this appendix). The progress of computation message was developed to indicate the computation that was being performed. It is a single line describing the submodule, nuclide, and graphical time for which calculations are currently being performed, and any additional information pertaining to the submodule. The first part of the message indicates whether it is a deterministic, sensitivity, or probabilistic calculation, and also the run number for the latter two types of calculations. The computational code writes this information to a file; the interface reads the file and displays the information in the run time feedback form. The time spent writing these messages can be significant, even for computers with fast microprocessors; as microprocessors evolve, the computational time has been decreasing much more rapidly than the time to write to a file. The user can control the frequency of this message by using the corresponding input in the title form.

The interface uses the probabilistic run number in the progress of computation message to estimate the execution time. When preforming a probabilistic analysis, it is usually sufficient to know just how many runs have been completed rather than to know the progress within each run. The number of messages and thus the run time can be reduced by increasing the time interval between the messages. It is also possible to turn off the messages from the FORTRAN code by selecting the 0.0 option for the time interval between messages. This will give the shortest execution time, and the interface will still be able to display an estimate of the execution time. It monitors the progress of computations by using the size of the probabilistic output files, especially the file named “UNCGRPTO.BIN.” The size of this file will be four times the probabilistic run number times the number of graphical time points.

2.1.2 Choice of Probabilistic Outputs

The code writes to files two types of probabilistic results. One is the peak dose (or risk) from each probabilistic run, the other is the complete set of information necessary to produce the standard suite of temporal graphics for each of the probabilistic runs. The magnitude and the time of occurrence of the peak total dose, the peak pathway dose, and the peak nuclide dose are written to a file named UNCPEAK.ASC in the working directory and later copied to the user file directory with the extension “pds.” Similar information about peak risk is written to UNCPEAKR.ASC and copied to the user file directory with the extension “prk.” The data in these two files are used to generate the cumulative distribution function plots and the scatter plots and also in the regression analysis. These two files are always written because they contain the basic data obtained from a probabilistic analysis.

The data necessary to produce the standard suite of temporal plots for each probabilistic run are much larger and are appended to the deterministic graphics files named OFFSITE.RA, OFFSITE.RB, and OFFSITE.RC, which are for risk, dose, and concentration, respectively. It is unlikely that the typical user will choose to or even need to view the hundreds of temporal plots that can be produced. The user can choose whether or not to save the probabilistic data needed to

generate the standard suite of temporal plots of dose, risk, and concentration by checking or unchecking the "dose and risk at graphic time points" box in the "Output specifications" tab of the "Uncertainty and Probabilistic Analysis" form. The latter choice reduces the execution time, although not to the same extent as suppressing the progress of computation message does. There will be a noticeable pause between the end of the computations and the displaying of the dose report in the viewer, while the large graphics data files are being copied to the user file directory when the former choice is made. The data necessary to produce temporal plots of the total dose are saved to the file "UNCGRPTO.BIN" and later copied to the user file directory with extension "PTG," irrespective of the choice made for the standard suite of temporal plots.

2.1.3 Computational Choices and Specifications

RESRAD-OFFSITE uses a number of parameters to improve the accuracy of the calculations. These include the spacing of the grid used in the areal integration of atmospheric transport formulations, the convergence criteria used for the numerical integrations in the groundwater transport formulations, and the number of subdivisions of the unsaturated and saturated zones used to improve the modeling of groundwater transport. The choices made for these inputs and also for the number and spacing of the graphical time points influence the computational time.

Spacing of the Grid Used in the Areal Integration of the Atmospheric Transport Formulations: The primary contamination and the offsite receptor areas are assumed to be rectangular in shape when modeling the atmospheric transport. Rather than use a single transport distance from the centers of the source and the receptor, the code provides the option of subdividing the source and receptor areas into smaller squares or rectangles. The transport from each subdivision of the source to each subdivision of the offsite receptor area is computed and summed together to get a better estimate of the atmospheric transport. A large number of subdivisions may be warranted in a deterministic run where a single value for each of the inputs yields a single value for the dose or risk. The value of each input parameter can vary over a range in probabilistic analysis. This results in a distribution of values for the dose or risk. In this case, it is reasonable to increase the grid spacing (and reduce the number of subdivisions of the source and receptor) to reduce the computational time as long as the resultant inaccuracy is of a lower order of magnitude than the probabilistic range of the dose or risk. A sensitivity analysis can be performed on the grid spacing to arrive at the appropriate site-specific single value to be used for the probabilistic runs.

Convergence Criteria Used for the Numerical Integrations in the Groundwater Transport Formulations: The groundwater transport calculations in which the water table is the contaminant input boundary and those that compute the concentration in the aquifer involve a convolution (a special type of integration) that is performed numerically. These numerical calculations are performed with increasing subdivisions until the specified convergence criteria are met or until a preset maximum number of subdivisions is reached. For a deterministic RESRAD-OFFSITE run the convergence criteria is set to 0.001, which is a reasonable limit if results that are precise to three significant figures are desired. A higher value may be used as the

convergence limit for probabilistic analysis, as long as the precision of the result is compatible with the range of the probabilistic output.

Number of Subdivisions of the Unsaturated and Saturated Zones: The groundwater transport predictions of progeny nuclides produced in transit can be improved by subdividing the unsaturated and saturated zones, particularly in situations that require the modeling of both longitudinal dispersion and the effects of nuclide-specific water-soil interaction (distribution coefficients). Subdividing the zones increases the run time, although fortunately not in direct proportion in the saturated zone, which is typically the zone that requires the most computational time. The transport zones should be subdivided when probabilistic analysis is performed only if both longitudinal dispersion and progeny-specific retardation are of comparable importance in the transport of progeny produced in transit. If the groundwater transport zones are to be subdivided in probabilistic analysis, it would be best to use linear spacing between graphic points for the reasons discussed in the following paragraph.

Number of Graphical Time Points: The graphical time points should be able to capture the temporal changes in all the fluxes and concentrations that the code deals with. These include the contaminant releases to the atmosphere, groundwater, and to surface erosion; the contaminant fluxes out of the unsaturated zone(s); the contaminant concentration in the well; the contaminant flux from the aquifer to the surface water body; and the contaminant concentrations in the offsite agricultural areas and in the surface water body. The code assumes that these quantities vary linearly between their values at the graphical time points. The number of graphical points should be large enough so that this linear variation is a good representation of the form of the releases and concentrations. Because the execution time increases with the number of points, the number of points selected should be no more than is necessary especially in probabilistic analysis. The size of the probabilistic data file for the temporal graphics is proportional to the number of graphics points. The code offers two choices for the spacing of the time points — linear and geometric (log). Linear spacing is preferable for probabilistic analysis because the groundwater transport factors computed for a pair of time points can be saved and used for all pairs of time points that have the same time difference (i.e., travel time). It is difficult to find the pairs of points that have the same spacing in a geometric series, if there happen to be any. For this reason, the transfer factors are computed for every pair of points in the geometric series, leading to a larger computational time, especially when the transport zones are subdivided.

2.2 SPECIFICATION OF PROBABILISTIC INPUTS AND OUTPUTS

The number of observations in a probabilistic analysis and the number of repetitions of the probabilistic analysis directly influence the execution time. The distributions specified for the probabilistic inputs can affect the execution time if they require a large number of observations to represent them.

2.2.1 Number of Observations in the Probabilistic Analysis

The probabilistic distributions specified for the parameters have to be sampled to produce a number of sets of inputs for use by the RESRAD-OFFSITE code. The number of observations sampled from each distribution must be sufficient to give a good representation of the distribution. If correlations are to be specified between the inputs, this includes "0" correlation (i.e., no correlation), then the number of observations must be greater than the number of probabilistic inputs. This condition must also be met if a regression analysis is to be performed between the outputs and the inputs. The accuracy of the probabilistic predictions increases with the number of observations until a point where the input sets produced are representative of the specified distributions and input correlations. Increasing the number of samples further will increase the execution time but will not increase the accuracy of the digits that are of practical significance. An indication of the accuracy of the predictions is obtained by repeating the analysis and comparing the predictions of the repetitions as described in Section 2.2.2.

2.2.2 Number of Repetitions in the Probabilistic Analysis

The accuracy of a probabilistic result is evaluated by repeating the probabilistic analysis with a different set of probabilistic samples. This is achieved by beginning the sampling with a different (random) seed. This procedure is automated in the code; all that needs to be done is to specify the number of repetitions that are desired. The execution time increases with the number of repetitions. Three to seven repetitions are usually sufficient. It is possible to run the different repetitions on different computers as discussed in Section 2.5.2. Even if this does not reduce the (total) execution time, it does produce the results more quickly.

2.2.3 Distributions Specified for the Probabilistic Inputs

The distributions specified for the input parameters are sampled to produce sets of inputs that can be used by RESRAD-OFFSITE. The accuracy of the probabilistic predictions depends on how well the observations represent the distributions. The number of observations that is necessary to achieve the desired accuracy depends on the range of the distributions. A probabilistic analysis that contains a number of distributions that span a wide range will require a larger number of samples and hence a larger execution time. The execution time can be reduced by using probabilistic distributions that are specific to local conditions, rather than the wider national distributions that encompass conditions at sites across the nation.

2.3 GRAPHICAL DISPLAY OF THE PROBABILISTIC ANALYSIS

The probabilistic plots and statistical measures are displayed by using the "step by step analysis" tab of the "uncertainty and probabilistic analysis form." The probabilistic input data and the probabilistic peak dose and peak risk data are read into the memory when any of the plot buttons (cdf, scatter, or histogram) is clicked. The time required to read and sort the data increases with the number of realizations, which is the product of the number of samples and the

number of repetitions, the number of probabilistic variables, and the number of initially present nuclides in the analysis. A “Please wait - reading probabilistic data” message is displayed during this time. These factors also affect the time it takes to display the plots.

2.4 OUTPUT-INPUT LINEAR REGRESSION ANALYSIS

Linear regression analysis can be performed between any of the peak doses and/or risks and the probabilistic inputs. This can be done automatically at the end of the execution of the computational code or at a later time by using the “step by step analysis” tab of the “uncertainty and probabilistic analysis form.” The time taken to perform this analysis depends on the number of realizations, the number of probabilistic inputs, and the number of probabilistic outputs selected for the regression analysis.

2.5 DISTRIBUTED (PARALLEL) COMPUTING

A probabilistic analysis can be performed faster if all the computers that are connected via a network can be utilized to perform some of the individual runs when their CPU is idle. This would be limited to those computers in the network that agree to participate in the distributed computation. Software would have to be developed to perform full-fledged automated distributed computing or parallel computing. A limited version of distributed computing can be performed manually as described in Section 2.5.2.

2.5.1 Software Requirements for Implementing Distributed Computing

The initiating computer would keep track of the runs that have already been performed and would send the input file with the run number of the next run that needs to be performed to the next available participating computer with an idle CPU. When that computer has executed its assigned run, the output data would be sent back to the initiating computer. The initiating computer would integrate the output data into the consolidated output data file. Meanwhile, the initiating computer would still be sending out information about the next run to be executed to computers with idle CPUs. It would also be performing probabilistic runs. The code also needs to be able to recognize whether there are multiple initiations on the network to handle this situation. The analysis that is currently performed by the computational code to write the probabilistic text report would have to be compiled into a separate executable that would be executed after all the probabilistic runs have been completed. Some of the probabilistic output that is saved in memory would need to be written to output files so that this separate executable will have the data it needs to produce the probabilistic text report.

2.5.2 Distributing the Repetitions to Different Computers

A limited form of distributed computing can be performed manually without the need to modify the software. All the runs belonging to the same repetition need to be performed on one

computer because the sampling code considers all the probabilistic samples that are generated for a repetition when deciding on how to group them together to produce the probabilistic input sets. Each repetition can be executed on a different computer provided the appropriate seed is used to generate the probabilistic inputs on the different computers. In theory, using a different seed for each repetition would produce statistically valid results. The aim, however, is to produce the same set of results as would have been produced if all the repetitions had been performed on the same computer in a single execution. This is achieved by using specific seeds for each of the repetitions and requires one additional step that does not significantly increase the run time. A complete set of probabilistic input samples for all the repetitions must first be produced using the "Generate input samples (LHS)" command button in the "step by step analysis" tab of the "Uncertainty and Probabilistic analysis form." Then the seed to be used for each repetition can be read from the "Uncertainty/Probabilistic inputs report." The seed for each repetition can be found at the beginning of the section of the report for that repetition. The input file can then be executed on different computers, each with a single repetition by using the appropriate seed. While this would result in a significant reduction in time to produce the outputs, it would come at the cost of not being able to combine the results of the repetitions in a single plot or report. The plots for each repetition would have to be viewed (or printed) separately. The results of the regression analysis for each repetition would also be on separate pages, rather than being on the same page for easier comparison.

3 SUMMARY CHECKLISTS FOR REDUCING RUN TIME

Two checklists are provided in this section. The first is a list of measures that can be taken to reduce the time to produce the probabilistic outputs. The second is a list of symptoms that might indicate insufficient memory for storing some of the temporary probabilistic outputs or excessive time being spent on writing information to the disk.

3.1 RUN TIME CHECKLIST

☐ Set the time interval between progress of computation messages to 0.0, unless there is a need to know detailed information about which module is being computed within a probabilistic run (Section 2.1.1 of this appendix).

☐ Decide whether a detailed study of the probabilistic results is going to be carried out and if so, whether it will involve viewing the temporal plots of dose, concentration, or risk of the individual runs. If not, uncheck the (probabilistic) “dose and risk at graphic time points” check box (Section 2.1.2 of this appendix).

☐ Make an educated estimate of the number of observations and the number of repetitions that might be needed. The number of observations influences the accuracy of the probabilistic results, while the number of repetitions quantifies the accuracy of the results. The run time increases with their product, that is, the number of realizations (Sections 2.2.1 and 2.2.2 of this appendix).

☐ Perform a sensitivity analysis on the grid spacing to be used for the areal integration of the atmospheric transport calculations prior to performing the probabilistic analysis. Be sure to use deterministic values that are representative of the distributions that will be used for the probabilistic/uncertain parameters (Section 2.1.3 of this appendix, first item).

☐ Decide on the level of convergence that is appropriate for the groundwater transport calculation (Section 2.1.3 of this appendix, second item).

☐ Use linear spacing between graphical time points, and set the number of time points to a value that is just sufficient to capture the variation of the fluxes and concentrations (Section 2.1.3 of this appendix, fourth item).

☐ Subdivide the groundwater transport zones only if the following three conditions are met: (1) the run includes transformation chains, (2) the progeny makes a significant contribution to the exposure pathways that involve groundwater transport, and (3) longitudinal dispersion and nuclide-specific soil-water interaction are both of comparable importance in the transport of progeny produced in transit (Section 2.1.3 of this appendix, third item).

☐ Use probabilistic distributions that are specific to the site rather than distributions that cover the entire spectrum of sites in the nation. This will reduce the number of observations necessary to achieve the desired accuracy of the probabilistic results (Section 2.2.3 of this appendix).

☐ Run the repetitions on different computers if more than one computer is available. Be aware that the results of each repetition will have to be viewed and printed separately and that combined plots and results cannot be produced in this case (Section 2.5.2 of this appendix).

3.2 EXECUTION CHECKLIST

☐ Monitor the estimated calculation time. A steady increase in the execution time might indicate insufficient physical memory to save the temporary data produced by the code. The temporary data are then written to virtual memory on the disk; this takes more time than saving these data in physical memory. Consider adding physical memory.

☐ Monitor the light indicating disk access. If the disk is being accessed over a major part of the execution, this might be an indication that writing information to disk is slowing the execution. Consider whether the information being written can be reduced.

NRC FORM 335 (9-2004) NRCMD 3.7

U.S. NUCLEAR REGULATORY COMMISSION

BIBLIOGRAPHIC DATA SHEET

(See instructions on the reverse)

1. REPORT NUMBER (Assigned by NRC, Add Vol., Supp., Rev., and Addendum Numbers, if any.)

ANL/EVS/TM/07-1
DOE/HS-0005
NUREG/CR-6937

2. TITLE AND SUBTITLE

User's Manual for RESRAD-OFFSITE Version 2

3. DATE REPORT PUBLISHED

MONTH	YEAR
June	2007

4. FIN OR GRANT NUMBER

JCN Y6467

5. AUTHOR(S)

C. Yu, E. Gnanapragasam, B.M. Biwer, S. Kamboj, J.-J. Cheng, T. Klett, D. LePoire, A.J. Zielen, S.Y. Chen, W.A. Williams, A. Wallo, S. Domotor, T. Mo, and A. Schwartzman

6. TYPE OF REPORT

Technical

7. PERIOD COVERED *(Inclusive Dates)*

8. PERFORMING ORGANIZATION - NAME AND ADDRESS *(If NRC, provide Division, Office or Region, U.S. Nuclear Regulatory Commission, and mailing address; if contractor, provide name and mailing address.)*

Argonne National Laboratory
Environmental Science Division
9700 South Cass Avenue
Argonne, IL 60439

9. SPONSORING ORGANIZATION - NAME AND ADDRESS *(If NRC, type "Same as above", if contractor, provide NRC Division, Office or Region, U.S. Nuclear Regulatory Commission, and mailing address.)*

Division of Fuel, Engineering, and Radiological Research
Office of Nuclear Regulatory Research
U.S. Nuclear Regulatory Commission
Washington, DC 20555-0001

Office of Environmental Management &
Office of Health, Safety and Security
U.S. Department of Energy
Washington, DC 20585-0119

10. SUPPLEMENTARY NOTES

11. ABSTRACT *(200 words or less)*

The RESRAD-OFFSITE code is an extension of the RESRAD (onsite) code, which has been widely used for calculating doses and risks from exposure to radioactively contaminated soils. The development of RESRAD-OFFSITE started more than 10 years ago, but new models and methodologies have been developed, tested, and incorporated since then. Some of the new models have been benchmarked against other independently developed (international) models. The databases used have also expanded to include all the radionuclides (more than 830) contained in the International Commission on Radiological Protection (ICRP) 38 database. This manual provides detailed information on the design and application of the RESRAD-OFFSITE code. It describes in detail the new models used in the code, such as the three-dimensional dispersion groundwater flow and radionuclide transport model, the Gaussian plume model for atmospheric dispersion, and the deposition model used to estimate the accumulation of radionuclides in offsite locations and in foods. Potential exposure pathways and exposure scenarios that can be modeled by the RESRAD-OFFSITE code are also discussed. A user's guide is included in Appendix A of this manual. The default parameter values and parameter distributions are presented in Appendix B, along with a discussion on the statistical distributions for probabilistic analysis. A detailed discussion on how to reduce run time, especially when conducting probabilistic (uncertainty) analysis, is presented in Appendix C of this manual.

12. KEY WORDS/DESCRIPTORS *(List words or phrases that will assist researchers in locating the report.)*

RESRAD-OFFSITE; RESRAD (onsite); dose; exposure pathways; risk; databases; radionuclides; User's Manual; model; code; Gaussian plume model; atmospheric dispersion; groundwater transport; deposition; probabilistic analyses; source term; technical basis; accumulation; concentration; meat; milk; fish; vegetation; ingestion; inhalation; absorption; adsorption; uptake

13. AVAILABILITY STATEMENT

unlimited

14. SECURITY CLASSIFICATION

(This Page) unclassified

(This Report) unclassified

15. NUMBER OF PAGES

16. PRICE

Environmental Science Division
Argonne National Laboratory
9700 South Cass Avenue, Bldg. 900
Argonne, IL 60439-4832

www.anl.gov

UChicago ▶
Argonne LLC

A U.S. Department of Energy laboratory
managed by UChicago Argonne, LLC